Design, synthesis and biological evaluation of TG2 transglutaminase inhibitors

Javier Fidalgo Lopez

▶ **To cite this version:**

Javier Fidalgo Lopez. Design, synthesis and biological evaluation of TG2 transglutaminase inhibitors. Organic chemistry. Université de Lyon, 2016. English. NNT : 2016LYSE1190 . tel-01546457

HAL Id: tel-01546457
https://theses.hal.science/tel-01546457

Submitted on 24 Jun 2017

HAL is a multi-disciplinary open access archive for the deposit and dissemination of scientific research documents, whether they are published or not. The documents may come from teaching and research institutions in France or abroad, or from public or private research centers.

L'archive ouverte pluridisciplinaire **HAL**, est destinée au dépôt et à la diffusion de documents scientifiques de niveau recherche, publiés ou non, émanant des établissements d'enseignement et de recherche français ou étrangers, des laboratoires publics ou privés.

N°d'ordre NNT : 2016LYSE1190

THESE de DOCTORAT DE L'UNIVERSITE DE LYON
opérée au sein de
l'Université Claude Bernard Lyon 1

Ecole Doctorale 206
Ecole Doctorale de Chimie de Lyon

Spécialité de doctorat : CHIMIE
Discipline : CHIMIE ORGANIQUE

Soutenue à huis clos le 23/11/2016, par :
Javier FIDALGO LOPEZ

DESIGN, SYNTHESIS AND BIOLOGICAL EVALUATION OF TG2 TRANSGLUTAMINASE INHIBITORS

Devant le jury composé de :

MOREAU Pascale	Professeure	Université Blaise Pascal–Clermont-Ferrand	Rapporteure
GALLET Olivier	Professeur	Université de Cergy-Pontoise	Rapporteur
RICARD-BLUM Sylvie	Professeure	Université Claude Bernard – Lyon 1	Examinatrice
DEMEUNYNCK Martine	Directeur de recherche	Université Joseph Fourier – Grenoble	Examinatrice
JOSEPH Benoît	Professeur	Université Claude Bernard – Lyon 1	Directeur de thèse
EL ALAOUI Saïd	Docteur	Covalab SAS	Invité

UNIVERSITE CLAUDE BERNARD - LYON 1

Président de l'Université	**M. le Professeur Frédéric FLEURY**
Président du Conseil Académique	M. le Professeur Hamda BEN HADID
Vice-président du Conseil d'Administration	M. le Professeur Didier REVEL
Vice-président du Conseil Formation et Vie Universitaire	M. le Professeur Philippe CHEVALIER
Vice-président de la Commission Recherche	M. Fabrice VALLÉE
Directeur Général des Services	M. Alain HELLEU

COMPOSANTES SANTE

Faculté de Médecine Lyon Est – Claude Bernard	Directeur : M. le Professeur J. ETIENNE
Faculté de Médecine et de Maïeutique Lyon Sud – Charles Mérieux	Directeur : Mme la Professeure C. BURILLON
Faculté d'Odontologie	Directeur : M. le Professeur D. BOURGEOIS
Institut des Sciences Pharmaceutiques et Biologiques	Directeur : Mme la Professeure C. VINCIGUERRA
Institut des Sciences et Techniques de la Réadaptation	Directeur : M. le Professeur Y. MATILLON
Département de formation et Centre de Recherche en Biologie Humaine	Directeur : Mme la Professeure A-M. SCHOTT

COMPOSANTES ET DEPARTEMENTS DE SCIENCES ET TECHNOLOGIE

Faculté des Sciences et Technologies	Directeur : M. F. DE MARCHI
Département Biologie	Directeur : M. le Professeur F. THEVENARD
Département Chimie Biochimie	Directeur : Mme C. FELIX
Département GEP	Directeur : M. Hassan HAMMOURI
Département Informatique	Directeur : M. le Professeur S. AKKOUCHE
Département Mathématiques	Directeur : M. le Professeur G. TOMANOV
Département Mécanique	Directeur : M. le Professeur H. BEN HADID
Département Physique	Directeur : M. le Professeur J-C PLENET
UFR Sciences et Techniques des Activités Physiques et Sportives	Directeur : M. Y. VANPOULLE
Observatoire des Sciences de l'Univers de Lyon	Directeur : M. B. GUIDERDONI
Polytech Lyon	Directeur : M. le Professeur E. PERRIN
Ecole Supérieure de Chimie Physique Electronique	Directeur : M. G. PIGNAULT
Institut Universitaire de Technologie de Lyon 1	Directeur : M. le Professeur C. VITON
Ecole Supérieure du Professorat et de l'Education	Directeur : M. le Professeur A. MOUGNIOTTE
Institut de Science Financière et d'Assurances	Directeur : M. N. LEBOISNE

RESUME en français

La transglutaminase tissulaire (TG2) est une enzyme de la famille des transglutaminases (EC 2.3.2.13) qui est exprimée de manière ubiquitaire chez les mammifères. Cette enzyme catalyse la formation d'une liaison amide intra- ou intermoléculaire entre un résidu glutamine et un résidu lysine. Ce processus biologique conduit à la modification post-traductionnelle des protéines. Un nombre croissant de publications associe la surexpression de cette enzyme et la déréglementation de son activité, avec un certain nombre de pathologiques humaines telles que les maladies neurodégénératives (maladie d'Alzheimer, maladie de Huntington, maladie de Parkinson), la fibrose tissulaire, certains cancers et la maladie cœliaque. Le développement d'inhibiteurs puissants et sélectifs de la TG2 est primordial pour identifier soit des outils pharmacologiques pour comprendre les processus biologiques dépendant de cette enzyme ou soit des candidats médicaments pour traiter les pathologies liées à la surexpression de la TG2. La majorité des composés inhibiteurs synthétisés jusqu'à présent agissent en bloquant de manière irréversible la réaction de transamidification de la TG2 en ciblant spécifiquement la cystéine 277 présente dans le site actif de la TG2.

L'objectif de ce travail a été d'identifier et de sélectionner des molécules de faible poids moléculaire inhibant de façon sélective et puissante l'activité de transamidification de la TG2. Nous présenterons l'optimisation de deux séries originales de composés (synthèse, études de relation de structure-activité) comportant un noyau aromatique central de type naphtalénique ou indolique et une fonction acrylamide comme accepteur de Michael pour piéger la fonction thiol de la cystéine 277. Un certain nombre de composés synthétisés montre une inhibition nanomolaire de la TG2 (IC_{50} = 1.7-6 nM) avec un excellent profil de sélectivité vis-à-vis de TG1, TG6 et FXIIIa (IC_{50} > 10 µM). Ces inhibiteurs inhibent efficacement la TG2 dans des extraits de tissus et de cellules. Aucune toxicité apparente n'a été observée pour des concentrations inférieures à 10 µM d'inhibiteur sur les lignées vSMCs et SH-SY5Y. Les valeurs de K_I, k_{inact} et k_{inact}/K_I ont été également déterminés sur deux inhibiteurs sélectionnés (**23b** et **78f**) pour leurs activités biologiques. La formation d'une liaison covalente entre la cystéine 277 de la TG2 et ces deux inhibiteurs a été prouvée par digestion trypsique suivie d'une analyse LC-MS/MS.

TITRE en anglais

"Design, synthesis and biological evaluation of TG2 transglutaminase inhibitors"

RESUME en anglais

Tissue transglutaminase (TG2) is a ubiquitously expressed enzyme of the mammalian transglutaminase (TG) family which catalyzes the formation of an intra- or inter-molecular isopeptide bond between a glutamine and a lysine, leading to the post-translational modification of proteins. An increasing number of literature has associated the over-expression of this enzyme, and the deregulation of its activity, with a number of human physio-pathological states like neurodegenerative disorders (Alzheimer's disease, Huntington's disease, Parkinson's disease),

tissue fibrosis, certain cancers, and celiac disease. The development of potent and selective TG2 inhibitors has become primordial to reach either a pharmacological probe, to understand the biological processes that depend on this enzyme, or a drug candidate, to treat the pathologies related with its overexpression. The majority of the inhibitory compounds synthesized so far act by irreversibly blocking the transamidation reaction of TG2. These TG2 inhibitors specifically target the cysteine 277 present in the TG2 active site.

The aim of this work was the identification and selection of new potent and selective small molecules to inhibit the TG2 transamidation activity. We present the optimization of two new series of compounds (synthesis, structure-activity relationship studies) bearing naphthalene or indole aromatic rings as the central backbone structure. Both series present an acrylamide group as the Michael acceptor in order to react with the thiol group of cysteine 277. Several of the synthesized compounds showed a nanomolar inhibition over TG2 (1.7-6 nM) with an excellent selectivity profile over TG1, TG6 and FXIIIa (IC_{50} > 10 μM). These inhibitors showed high specificity on inhibiting TG2 in tissue and cell extracts. No apparent toxicity up to 10 μM was observed in vSMCs and SH-SY5Y cell lines. Their K_I, k_{inact} et k_{inact}/K_I were also determined on two selected inhibitors (**23b** and **78f**) for their biological activities. The formation of a covalent bond between the cysteine 277 of TG2 and these two inhibitors was proven by tryptic digestion followed by LC-MS/MS analysis.

DISCIPLINE Chimie

MOTS-CLES

Transglutaminase tissulaire (TG2), transamidification, inhibiteurs covalents, accepteur de Michael, naphtalène, indole, relation de structure-activité (RSA), cinétiques enzymatiques, candidat médicament, outil pharmacologique.

KEY WORKDS

Tissue transglutaminase (TG2), transamidation, covalent inhibitors, Michael acceptor, naphthalene, indole, structure-activity relationship (SAR), enzyme kinetics, drug candidate, pharmacological probe.

INTITULE ET ADRESSE DU LABORATOIRE:

Institut de Chimie et Biochimie Moléculaires et Supramoléculaires (ICBMS) – UMR CNRS 5246

Université de Lyon, Université Claude Bernard – Lyon 1

43, Boulevard du 11 Novembre 1918

F-69622 Villeurbanne cedex

ACKNOWLEDGEMENTS

« *When any door closes, thousands of windows suddenly open… »,* This is a phrase I always say to myself. Sometimes, some people offer you to open that new door, and introduce you in a brand new world of opportunities, but also a world open to a new completely different knowledge. These opportunitties sometimes happen, and here, today, in this section is what I want to transmit to all the people who made this opportunity become real.

First of all, I would like to thank to the European FP7-PEOPLE - initial training network (ITN) Marie-Curie Actions programme (grant agreement 289964), which allowed me to be financed for carrying out this PhD during this period within the TRANSPATH project.

I would like to thank the support and involvement in this project of an unusual thesis director. He is young, and even when oddly enough, he also works in the lab. He always drives you to do your best, and be sure of yourself in every step of the research. For being demanding and for letting me learn and move forward with this thesis, Thank you very much Prof. Benoît JOSEPH.

I would also like to say thanks to Guy FOURNET,for his Radio Jazz, knowledge, kindness, good work, a source of experience and tricks. I could continue with more adjectives regarding his proffesional carrier, but above all, and the most important is the person…So, thank you for being always there Guy. (Muchísimas gracias!).

Special thanks to all the « Equipe GEMBAS » for an amazing working time for my biochemistry part of this PhD. Specially, I would like to highlight the work of Dr. Bastien DOUMECHE. He made possible, with their knowledge and good direction, that the enzymology part is nowdays included in this PhD dissertation.

I will be a pleasure to include Chérif, Sofiene, Matthieu, Cecile, and all the other M2 students, they made this PhD even more enjoyable.

I would also like to thank all the team from the department of anatomy and neuroscience, VUMC University (Amsterdam) where I have spent and awesome four months experience, learning and living science in a great atmosphere. From this department I would like to thank my supervisor of the TRANSPATH project, Prof. Anne-Marie VAN DAM., but also Prof. Micha M M WILHELMUS, Kees JONGENELEN, Navina CHROBOK, Claudia SESTITO, and the rest of its magnificent staff.

I would also say thank you to all the people from the société Covalab for being always kind to offer me his knowledge and experience in transglutaminases. Special thanks for Dr. Saïd EL ALAOUI, for alowing me to enter into this project.

Also many thanks to Dr. M. Medebielle, Dr. Lionel Perrin

Also many thanks to Éva, Gildas, and István, you are all great. Thank you for your special support. Good people, but above all, good friends.

Thanks to all the FF team from Vigo, without all of you, your sense of humor and your friendship, it will not be the same.

Dedicado a toda mi familia que siempre han estado apoyándome de manera incondicional a través de las dificultades, os quiero. Y a ti, mi cousiña más bonita, por ser mi mejor compañera en el camino y en las dificultades, te quiero.

LIST OF ABBREVIATIONS

ADME: absorption, distribution, metabolism and excretion

AIDS: acquired immune deficiency syndrome

BBB: blood-brain barrier

BCA: bicinchoninic acid

BCNU: carmustine; 1,3-bis(2-chloroethyl)-1-nitrosourea

br s: broad singlet

Cbz: benzyloxycarbonyl

DCE: 1,2-dichloroethane

d: doublet

dd: doublet of doublets

DHI: 4,5-dihydroisoxazole

DIPEA: *N*,*N*-diisopropylethylamine

DMAP: 4-dimethylaminopyridine

DMPK: drug metabolism and pharmacokinetics

DON: 6-diazo-5-oxo-norleucine

dt: doublet of triplets

DTT: dithiothreitol

EDTA: ethylenediaminetetraacetic acid

ESI: elecrospray ionization

FBS: fetal bovine serum

Fmoc: 9-fluorenylmethoxycarbonyl

FN: fibronectin

FXIIIa: coagulation factor XIII

GDH: glutamate dehydrogenase

GMP-PCP: guanosine-5'-[(β,γ)-methyleno]triphosphate

GTP: guanosin triphosphate

GTPɣS: guanosine-5'-O-(ɣ-thio)triphosphate

HRMS: high resolution mass spectra

HLA-DQ 2/8: cell surface receptor protein found on antigen presenting cells

IC_{50}: half maximal inhibitory concentration of a drug, the concentration of an inhibitor where the response (or binding) is reduced by half

***K_I*:** the dissociation constant of the enzyme-inhibitor complex

***k_{inact}*:** maximun (or limiting) inhibition rate of inhibition if the enzyme is saturated with inhibitor

***k_{inact}/K_I*:** efficiency of the enzyme inactivation by the inhibitor

MDCK-MDR1: madin Darby canine kidney cells with the gene MDR1 encoding for the efflux glycoprotein, P-glycoprotein

mLM: mouse liver microsomes

MOPS: 3-(N-morpholino)propanesulfonic acid

MTT: 3-(4,5-dimethyl-2-thiazolyl)-2,5-diphenyl-2H-tetrazolium bromide

NADH: nicotinamide adenine dinucleotide (reduced form)

$NAD(P)^+$: nicotinamide adenine dinucleotide phosphate (oxidized form)

NAD(P)H: nicotinamide adenine dinucleotide phosphate (reduced form)

m: multiplet

PDB: protein data bank

P-gp: permeability glycoprotein

$PLC\delta_1$: phospholipase C delta 1

PolyQ: polyglutamine tract

ppm: parts per million

q: quaternary carbon

R^2: square of the correlation coefficient in regression analysis

rhTG2 : recombinant human tissue transglutaminase

s: singlet

SAR: structure activity relationship

S.D.: standard deviation

SRB: sulforhodamine B

t: triplet

td: triplet of doublets

TG: transglutaminase

TG2: tissue transglutaminase

TG1: epidermal transglutaminase

TG3: keratinocyte transglutaminase

TG5: transglutaminase 5

TG6: neuronal transglutaminase

TG7: transglutaminase 7

TRIS: tris-buffered saline

tt: triplet of triplets

INDEX

INTRODUCTION 19

1. Transglutaminase family 20
   1.1. Definition 20
   1.2. Protein members of transglutaminase 22
   1.3. Transglutaminases' structure 22
   1.4. Regulation of the transglutaminases' activity 23
2. Tissue transglutaminase (TG2): a multifunctional enzyme 24
   2.1. Definition 24
   2.2. Tissue transglutaminase distribution 24
   2.3. Tissue transglutaminase structure 25
   2.4. Tissue transglutaminase and its implication in diseases 26
3. TG2 inhibitors: chemical tools for treatment and understanding 28
   3.1. TG2 inhibitors and biological functions 28
   3.2. TG2 inhibitors and diseases 28
4. Enzyme kinetics. Introduction to enzyme inhibition 29
   4.1. Reversible enzymatic inhibition 31
      4.1.1. Competitive reversible inhibitors 31
      4.1.2. Non-competitive reversible inhibitors 32
      4.1.3. Uncompetitive reversible inhibitors 33
   4.2. Irreversible enzymatic inhibitors 33
      4.2.1. Chemical labels (active-site directed inactivating reagents) 34
      4.2.2. Suicide inhibitors (mechanism-based inhibitors) 35
5. Kinetic assays employed for TG2 inhibition characterization 36
   5.1. TG2-GDH coupled assay 37
   5.2. Coumarin-based fluorimetric assay 38
   5.3. *p*-Nitrophenyl ester- based kinetic assay 38
   5.4. Colorimetric assay 39
   5.5. TG2 Kinetic parameters observed for the different assays 39

Bibliography 41

CHAPTER 1-Tissue transglutaminase inhibitors 49

1. Tissue transglutaminase (TG2) inhibitors 50
   1.1. TG2 reversible inhibitors 50

1.1.1. Competitive reversible inhibitors 50

1.1.1.1. Acyl acceptor inhibitors (competitive amine inhibitors) 50

1.1.1.2. Acyl donor inhibitors 52

- Cinnamoyl-based inhibitors 52

1.1.2. Non-competitive reversible inhibitors 53

- Guanosine nucleotides 53
- Hydrazide-based inhibitors 53
- Metals 54
- Oxindole-based inhibitors 54
- Tyrphostin 47 55

1.2. TG2 irreversible inhibitors 55

- α,β-unsaturated amide based inhibitors 56
- α,β-unsaturated carbonyl-based inhibitors 62
- Epoxide- and maleimide-based inhibitors 64
- 3-Halo-4,5-dihydroisoxazole-based inhibitors 65
- 6-diazo-5-oxo-norleucine (DON) - based inhibitors 68
- Halomethyl carbonyl-based inhibitors 70
- Sulfonium- and imidazolium- based inhibitors 72

1.3. Other TG2 inhibitors 74

- ZM39923 and its metabolite ZM449829 74
- *β*-Aminoethyl ketone-based inhibitors 74
- Targeting the fibronectin binding site 75

Bibliography 76

CHAPTER 2 - Naphthalene-based TG2 inhibitors 81

1. Objectives 82

2. Methodology to validate the inhibitory activity of potential TG2 inhibitors 83

2.1. Determination of the inhibitory potency (IC_{50} TGs) 83

2.2. Description of the methodology employed 84

3. Synthesis and biological evaluation of **1** 85

3.1 Synthesis of **1** 85

3.2. TG transamidation inhibition of **1** 86

4. Sulfonamide linker modulation 86

4.1. Synthesis of **4-8** 86

4.2. TG transamidation inhibition of **4-8** 87

5. Changing the position of sulfonamide chain on naphthalene ring 88
5.1. Synthesis of **9** and **10** 88
5.2. TG transamidation inhibition of **9** and **10** 89
6. Substituent at the C-5 position on naphthalene ring 89
6.1 Synthesis of 5-(di-*n*-butyl)amino and 5-acetylamino derivatives **15a-b** 89
6.2. TG transamidation inhibition of **15a-b** 90
7. Introduction of an acetylamino group at the C-4 position 91
7.1. Synthesis of the 4-(acetylamino)naphthalen-1-yl derivative 91
7.2. TG transamidation inhibition of **18** 92
8. Introduction of an arylamide at the C-5 position on naphthalene ring 92
8.1. Synthesis of 5-(arylamido)naphthalene-1-sulfonyl chlorides **22** 93
8.2. Synthesis of 5-(arylamido)naphthalene derivatives **23a-c** 94
8.3. Synthesis of 5-(arylamido)naphthalene derivatives **23d-s** 94
8.3.1. Synthesis of *N*-(piperidin-4-yl)acrylamide **27** 94
8.3.2. Synthesis of 5-(arylamido)naphthalen-1-yl derivatives **23d-s** 96
8.4. Benzamide at the C-4 position on naphthalene ring: synthesis of **28** 97
8.5. TG transamidation inhibition of **23a-s** and **28** 98
9. Extending the benzamide at meta position: introduction of an additional amide 100
9.1. Synthesis of **31a-b** 100
9.2. TG transamidation inhibition of **31a-b** 102
10. Acrylamide-piperidine linkage modifications 102
10.1. Homologation of the linker 103
10.2. Replacement by an (2-oxoethyl)piperazin-4-yl linker 104
10.3. Addition of a glycine amino acid to the linker 105
10.4. TG transamidation inhibition of **35-37** and **EB1-155** 106
11. Synthesis of naphthalenesulfonamide-based prodrugs 107
11.1. Design perspectives 107
11.2. Acrylamide prodrugs development 108
11.3. TG transamidation inhibition studies of **45** 109
12. Synthesis of the reference **EB1-155** 110
13. Conclusion 111

Experimental part 112

Bibliography 149

CHAPTER 3 - Indole-based TG2 inhibitors 153

1. Introduction and context of the work 154

2. *N*-substituted or not indolesulfonamide derivatives 155

2.1. Synthesis of 1-(benzenesulfonyl)indole **47** and 1*H*-indole **48** 156

2.2. TG transamidation inhibition of **47** and **48** 157

2.3. Different *N*-substituted indole inhibitors 157

2.3.1. Synthesis of the different *N*-substituted indole derivatives **53a-d** 157

2.3.2. TG transamidation inhibition of **53a-d** 159

3. Introduction of a benzamide group at C-5, C-6 or C-7 position on indole 160

3.1. Synthesis of the 5-(benzoylamino)-1-methylindole derivative **57** 160

3.2. Synthesis of the 6-(benzoylamino)-1-methylindole derivative **64** 161

3.3. Synthesis of the 7-(benzoylamino)-1-methylindole derivative **71** 163

3.4. TG transamidation inhibition of **57**, **64** and **71** 164

4. Introduction of different amides at C-7 position 165

4.1. Synthesis of compounds **78a-k** 165

4.2. Synthesis of the 7-(3,4-dimethoxybenzamido)-1*H*-indole derivative **81** 167

4.3. TG transamidation inhibition of **78a-k** and **81** 168

5. Introduction of an inverted amide at C-7 position 170

5.1. Synthesis of 7-substituted inverted amide indoles **87a-d** 170

5.2. TG transamidation inhibition of **87a-d** 172

6. Modulation of the warhead on **78f** 173

6.1. Synthesis of **94** and **95** 174

6.2. TG transamidation inhibition of **94** and **95** 174

7. Conclusion 175

Experimental part 176

Bibliography 217

CHAPTER 4 – Mechanism of inhibition of lead compounds 219

1. Optimization of a continuous TG2-GDH coupled enzymatic assay 220

1.1. Optimization and validation of the GDH-coupled assay conditions 220
1.2. Measuring the kinetic Michaelis-Menten kinetic constants:
V_{max}, K_m, and K_{cat}. 221
1.3. Validation of the of the assay: inter-assay repeatability 224
2. Inhibition study of derivatives **23b**, **78f** and reference **X** 224
2.1. Inhibition study of **23b** 225
2.2. Inhibition study of **78f** 231
2.3. Inhibition study of reference piperidine acrylamide **X** 236
3. Study of the chemical modification of Cys277 of TG2 by inhibitors
23b and **78f** 237
4. Conclusion 240
Experimental part 242
Bibliography 244

CHAPTER 5 – Inhibition studies in biological samples 245
1. Introduction and objectives 246
2. TG2 inhibition in tissue and cell extracts 247
2.1. TG2 inhibition in cell lysates 249
2.2. TG2 inhibition in tissue extracts 250
3. Toxicity of the inhibitory compounds in cell culture 250
3.1. cell viability of vSCMs and SH-SY5Y cells 251
3.1.1. MTT test 251
3.1.2. SRB test 253
4. TG2 inhibition in cell culture 254
4.1. *in situ* TG2 activity in cell culture models (BAP incorporation assay) 254
5. Conclusion 259
Experimental part 260
Bibliography 263

GENERAL CONCLUSION and FUTURE PERSPECTIVES 265

INTRODUCTION

1. Transglutaminase family

1.1. Definition

Transglutaminases (TG), also called protein-glutamine γ-glutamyltransferases (EC.2.3.213), are a family of enzymes that catalyze a calcium and thiol-dependent acyl transfer reaction, the formation of an isopeptide bond between the γ-carboxamide group from a glutamine (Gln, Q) and a ε-amine group of a lysine (Lys, K), giving rise to the crosslinking of proteins containing these two amino acids (**Figure 1**). This *N*-ε-(gamma-glutamyl) lysine bond can be also formed between a γ-carboxamide and a polyamine as the acyl acceptor, promoting incorporations of amines into proteins as well. This isopeptide bond formation, leading to the crosslinking of proteins, results in the post-translational modification of proteins.[1,2,3]

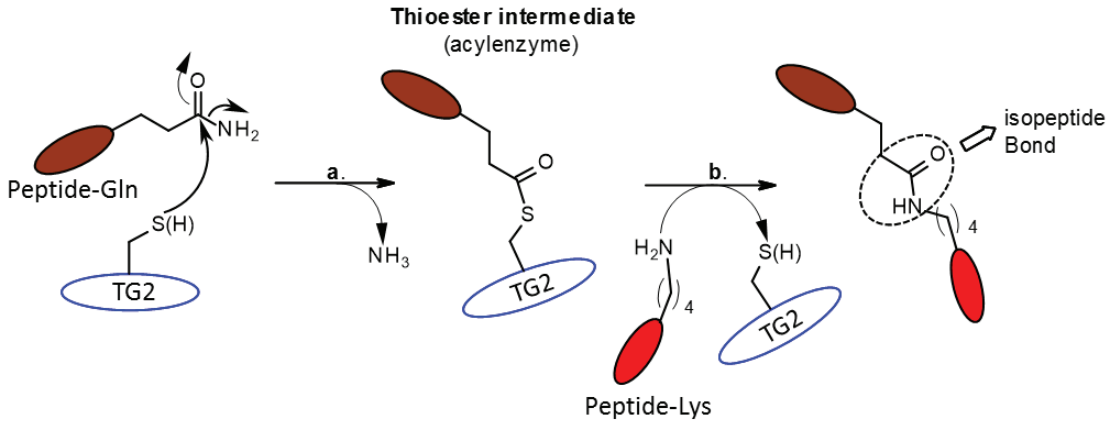

Figure 1. Translgutaminase transamidation activity between a glutamine-bearing peptide (acyl donor) and a Lysine-bearing peptide (acyl acceptor) from two different peptides. Step **a**: the activated thiol from the active-site Cys277 of TG will act as a nucleophile attacking the γ-carboxamide group of a glutamine, resulting in the release of ammonia and the formation of the acyl-enzyme intermediate. Step **b**: the ε-aminogroup of a lysine will attack the acylenzyme intermediate resulting in the formation of the final isopeptide bond between both peptides

Apart from their transamidation activity, transglutaminases can perform other 2 different enzymatic activities named as follows: hydrolysis (isopeptidase[4,5] and deamidation activities) and esterification (**Figure 2**).[6]

1) Hydrolysis:

- Isopeptide cleavage (isopeptidase activity): in the presence of water, the isopeptide bond between two proteins, formed by a glutamine and a lysine from two different proteins, will be attacked by the water molecule acting as the nucleophile, thus yielding glutamic acid and lysine.

- Deamidation: in the presence of water, either at low pH or in the absence of suitable amines donors, the acyl group from the acylenzyme intermediate will

be attacked by water molecules, acting as nucleophiles, thus yielding glutamic acid.

2) Esterification:

In the presence of an alcohol, acting as the nucleophile the acyl group from the acylenzyme intermediate will be attacked, resulting, in this case, in the formation of an ester.

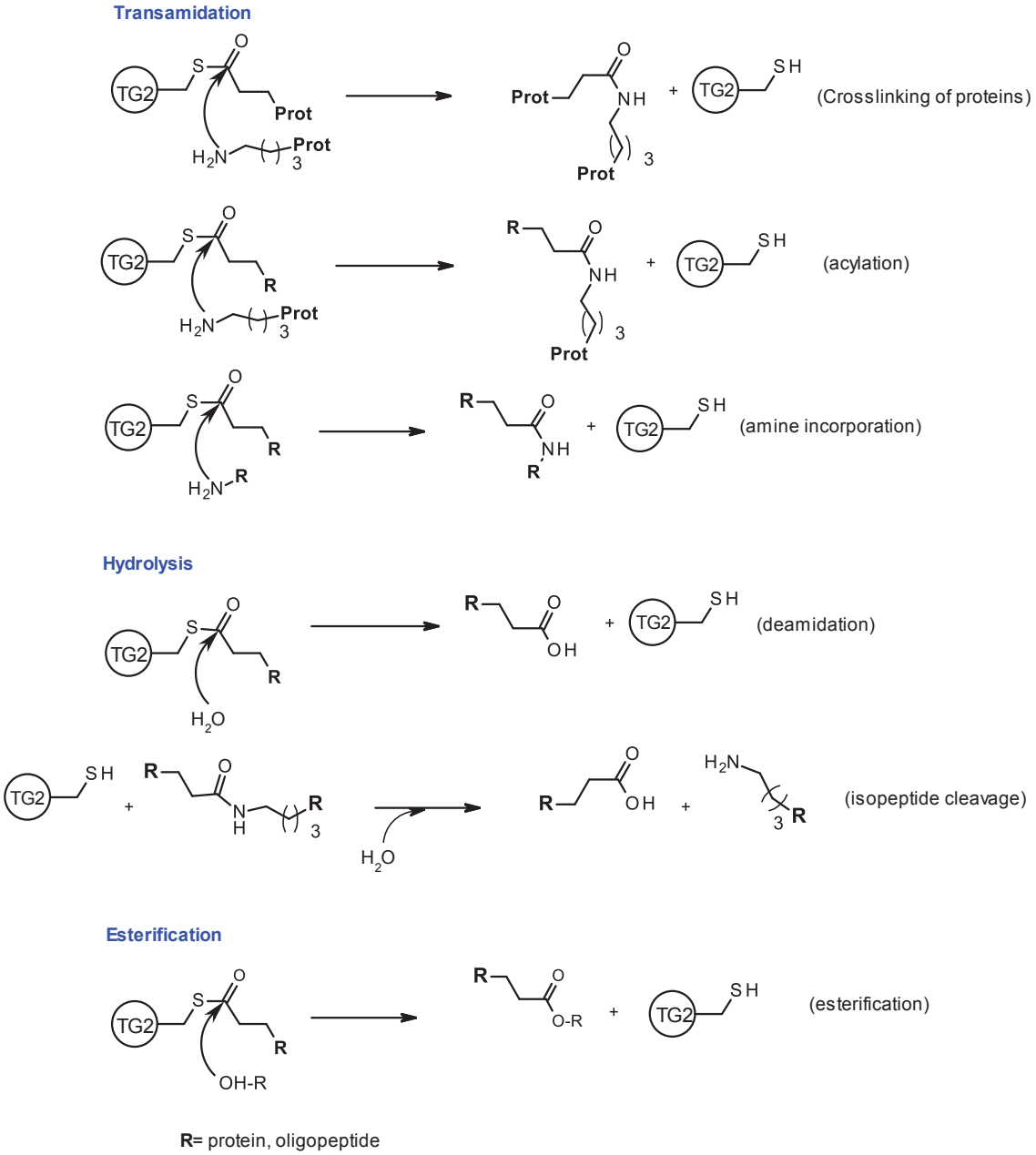

Figure 2. All the transglutaminases known catalytic activies described so far: transamidation, esterification, and hydrolysis (the last including the deamidation and isopeptidase activities)

1.2. Protein members of transglutaminase

This family of enzymes is composed by nine different isoforms, eight of them with enzymatic activity, from TG1-TG7 up to Factor XIIIa (FXIIIa). All these transglutaminase isoforms are implicated in different functions within different localizations of mammalian tissues catalyzing a variety of posttranslational protein modification reactions[2,7] (see **Table 1**). The exception within this family is the erythrocyte band 4.2. This protein has a high related amino acidic sequences when comparing with the other members of this family, but none of the four critical residues for the catalytic activity are conserved,[6] thus lacking of enzymatic activity. This band 4.2 protein is a major component of the erythrocyte skeletal network, and it regulates the erythrocyte shape, thus involved in mechanical properties.[8,9]

Protein	**Residues / Molecular Mass (KDa)**	**Tissue(s)**	**localization**	**Function(s)**
TG1 (keratinocyte TG)	814 / 90	Keratinocytes, brain	Membrane, cytosol	Cell envelope formation
TG2 (tissue TG)	686 / 80	Ubiquitous	Nuclei, cytosol, membrane, cell surface, and extracellular matrix	multiple
TG3 (epidermal TG)	692 / 77	Squamous epithelium, brain	cytosolic	Cell envelope formation
TG4 (prostate TG)	683 / 77	Prostate	/	Semen coagulation (particularly in rodents)
TG5	719 / 81	Ubiquitous, except for the CNS and lymphatic system	/	Epidermal differentiation
TG6 (neuronal TG)	706 / 79	CNS, skin	Cytosol, cell surface...	CNS development, and motor functions
TG7	710 / 80	Ubiquitous	/	/
FXIIIa (fibrin-stabilizing factor; coagulation factor XIII)	83	Platelets, dermal dendritic cells, placenta, chondrocytes, plasma, astrocytes, and synovial fluid	Cytosol, extracellular matrix	Blood coagulation, Bone growth

Table 1. The different charatcetistics of the different members of the transglutaminase family including their Molar Mass (KDa), number of aminoacidic residues, distribution (cell localization), tissue expression and function(s)

1.3. Transglutaminase structure

All of these proteins have four sequential and structurally distinct domains:[7]

1) One NH_2-terminal β-sandwich (FXIII-A and TG1 have an additional NH_2-terminal pro-peptide).

2) One α/β catalytic core (including the active site): Inside this region is located the active site. It contains four essential key amino acids for the catalytic activity of transglutaminases. This catalytic active site is composed by a cysteine, histidine, aspartate and a tryptophan. This tryptophan residue was found to stabilize the transition-state intermediates of the acylation activity of

transglutaminases.[10] These amino acidic residues are well conserved through the active site of all catalytically active members of this family of enzymes.

3) and 4) Two CO_2H-terminal β-barrel domains.

1.4. Regulation of the transglutaminases' activity

Transglutaminases assume also two different conformational states (**Figure 3**).[2,11,12]

1) Inactive conformation (*compact or closed conformation*). Transglutaminases domains assume a compact-close conformation in the absence of Ca^{2+}, when the protein binds to GTP (see **A** in **Figure 3**).[11-13]

2) Active conformation (*extended or open conformation*). Transglutaminases undergo a remarkably large conformational change, necessary to become an active protein. Therefore, this conformational change from compact conformation to an extended ellipsoid structure exposes the active site leading to an activation of transglutaminases. In the presence of certain levels of Ca^{2+} transglutaminases exhibit this open-active conformation.[9,14] Under physiological conditions, inside the cells, no transamidation activity is performed by transglutaminases, owing to the low existent Ca^{2+} levels required to its activation compared with the higher GTP concentration levels, staying in the closed-inactive conformation.[15,16] Furthermore, It has also been reported an stabilized open conformation when transglutaminase are bound to an inhibitor (PDB code 2Q3Z) (see **B** in **Figure 3**).[11]

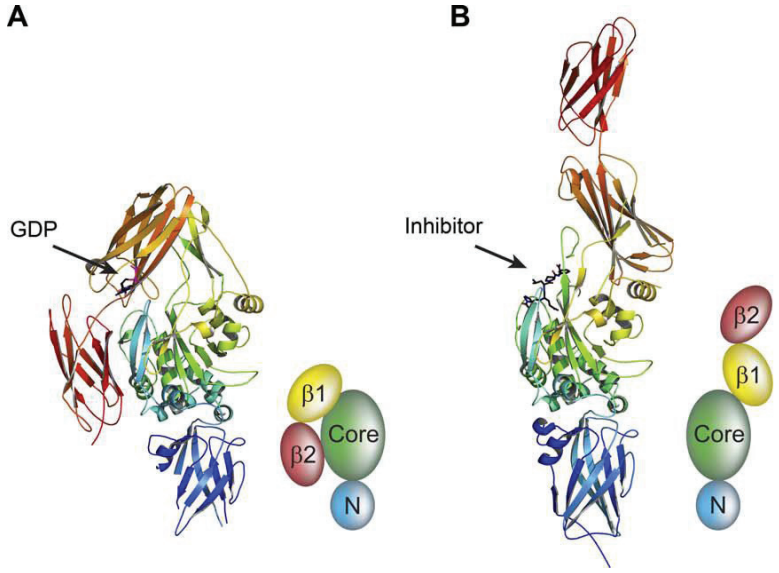

Figure 3. The two comformational states of transglutaminases. .Left image (**A**): a GDP-close (catalytically inactive) translgutaminase conformation (PDB code 1KV3); right image (**B**): inhibitor-open translgutaminase comformation (PDB code 2Q3Z) (figures taken from reference 11)

2. Tissue transglutaminase (TG2): a multifunctional enzyme

2.1. Definition

TG2 is an ubiquitously expressed member of the mammalian transglutaminase family, consisting of a 686 amino acidic sequence, with a molecular weight around 80 kDa. As described for the other catalytically active members of this family of proteins (TG1-TG7 and FXIIIa), tissue transglutaminase also has calcium-dependent transamidation, hydrolysis and esterification catalytic activities.[17,18] TG2 has also been discovered to be extracellularly regulated by redox conditions, in which reducing conditions are necessary to the complete activation of the open Ca^{2+}-bound TG2 enzymatic activity by avoiding the formation of Cys371- Cys370 and Cys230-Cys370 disulfide bonds.[19]

The calcium-dependent transamidation mechanisms of tissue transglutaminase (e.g., acylation, crosslinking and amine incorporation reactions) have been proposed for this enzyme,[3,20] as well as the negatively regulation of its transamidation activity by means of guanine nucleotides (GTP/GDP) in either the absence or low concentrations of Ca^{2+} ion.[12,13,21]

Apart from the general enzymatic functions also found in the other member from the transglutaminases family, tissue transglutaminase has also other enzymatic functions described so far. Between these proposed enzymatic functions are the following:

1) kinase activity,[22-24]

2) G-protein activity,[25-27]

3) GTPase/ATPase activity: tissue transglutaminase not only binds but also was discovered to hydrolyze GTP and ATP,[28,29]

4) protein disulfide isomerase[30]

2.2. Tissue transglutaminase distribution

Tissue transglutaminase is also widely distributed in mammalian tissues, and also located in the extracellular matrix (and cell surface) and in the different compartments at the cellular level: cellular membrane, cytosol, mitochondria, endolysosomes, and even in the nuclei.[31] Depending on where tissue transglutaminase is present, different biological functions are attributed to this enzyme. For instance, tissue transglutaminase can act as integrin-associated adhesion co-receptor for fibronectin on the cell surface affecting several key integrin functions promoting cell adhesion and spreading, as well as the activation of focal adhesion kinase thus activating different cell signaling cascades (Figure 4).[1,32-34] Furthermore, TG2 can activate the nuclear factor-kB, and also regulates the nuclei gene expression by means of the post-translational modification and/or interaction with transcription factors and related proteins like histones.[35,36]

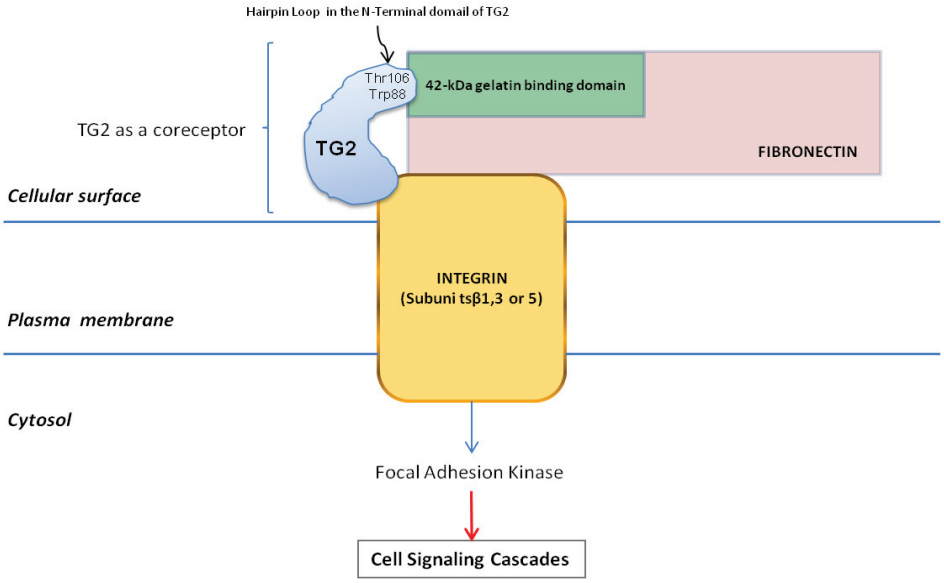

Figure 4. Representation of the cointeraction in the extracellular matrix of tissue transglutaminase with both, the 42-kDa gelatin binding domain from fibronectin and the integrin (subunits β1, β3, or β5). TG2 acts as an integrin-binding adhesion correceptor for fibronectin. This process will lead to different cell signaling cascades (e.g., RhoA/Rock and Focal adhesion kinase signaling cascades) and facilitates cell adhesion, spreading and migration

2.3. Tissue transglutaminase structure

Like all members of the transglutaminase family, tissue transglutaminase shares the same four structural domains. Nevertheless, in the case of TG2 within these domains it has been discovered different specific binding sites associated with different activities of this enzyme. The four TG2 structural domains are the followings (**Figure 5**):

1) NH_2-terminal β-sandwich domain: It includes the fibronectin and integrin binding sites,

2) catalytic core domain (with α-helices and β-sheets): It is the active site of the protein as the other enzymatically active transglutaminases includes the active site composed by the catalytic triad (Cys277, His355, Asp358) and a conserved Tryptophan 241,[10] as well as the Tryptophan 332, which stabilize the transition state of its catalytic enzymatic reaction. Within this catalytic core it could be found the six conserved Ca^{2+} binding sites of the protein, which are closer from each other in the closed-inactive TG2 conformation, whose distance increase considerably to be further apart from each other in the open conformation,[21]

3) one β-barrel domains: It includes the binding pocket for GTP and the interaction sites with the α_{1B} adrenergic receptor. GTP binding, negatively regulates the tissue transglutaminase transamidation activity in the absence or low concentration of Ca^{2+} ions,[13,37]

4) one CO_2H-terminal β-barrel domain: including a Phospholipase $C\delta_1$ interaction site

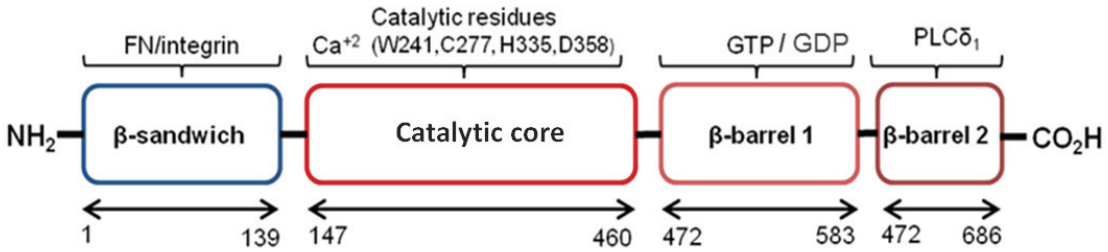

Figure 5. Representation of the four distinct domains of tissue transglutaminase and its different binding sites along the TG2 aminoacidic sequence

It has also been discovered within the structure of TG2 an heparin binding site composed by two clusters of basic aminoacids, RRWK (residues 262-265) and KQKRK (residues 598-602), which take part in the adhesion function of TG2 in the extracellular matrix.[38,39] Moreover, in the work from Simon-Vecsei et al.[40] it has been proposed an epitope were celiac antibodies directly bind to the TG2 surface delineated by three amino acids (Arg19, Glu153 and Met659) in the close-inactive conformation. This TG2 epitope involves different structural domains (*N*-terminal β-sandwich, core, and C-terminal β-barrel domains) (**Figure 6**).

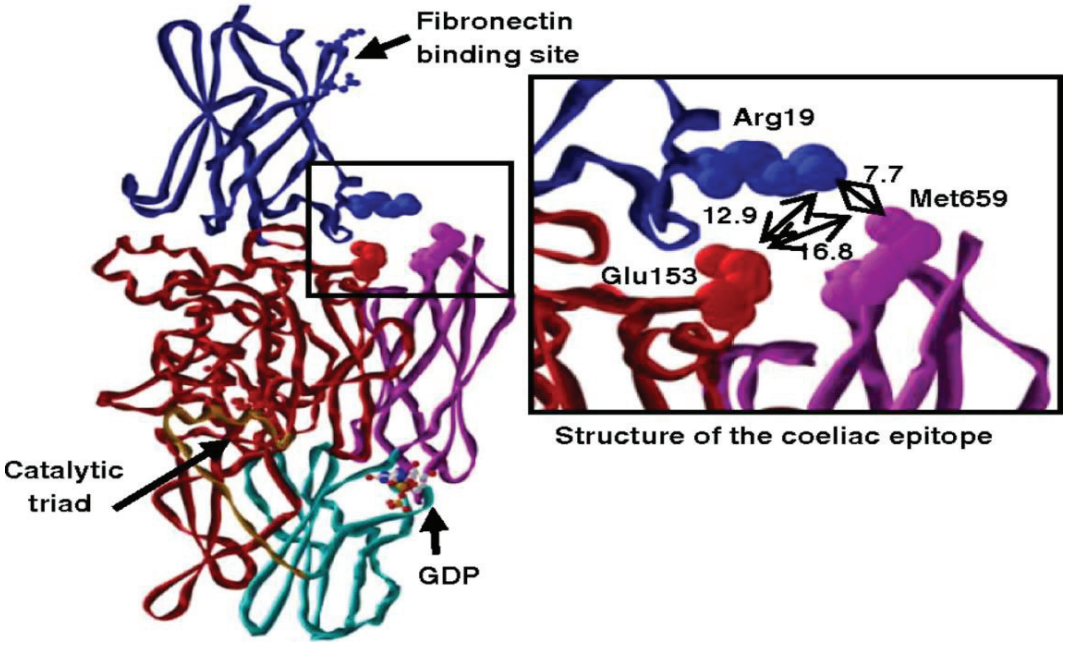

Figure 6. Image showing a GDP-close inactive conformation of TG2. The catalytic triad, and both, the fibronectin and the guanosin nucleotides (GDP) binding sites are indicated (black rows). It is also represented the proposed coeliac disease epitope formed by Arg19, Glu153 and Met659. (figure taken from reference 40)

2.4. Tissue transglutaminase and its implication in diseases

Taking into account that this enzyme is expressed in different tissues and that it has a wide variety of catalytic (e.g., transamidation and deamidation) and non-catalytic (e.g., GTPase/G-protein) enzymatic functions, it has been associated, directly or indirectly, with different pathologies such as some certain types of cancers,[41-44] neurodegenerative

diseases, such as Huntington's, Parkinson's and Alzheimer's disease,[15,45-48] celiac disease,[40,49-52] diabetes type 2,[53] and also related tissue fibrosis in lung, heart and kidney.[54-56]

Based on the cited references form the paragraph above, the implication of TG2 with celiac disease, neurodegenerative diseases and cancer, are briefly summarized:

Celiac disease

1. Regarding the T cell mediated response.

TG2 is implicated because of its deamidation enzymatic activity. The Q (glutamine) residues from glyadin peptides are deamidated by TG2 and transformed into glutamate. Owing to this modification, there is an increasing on the affinity for the disease associated HLA-DQ 2/8 proteins for this glutamate residue, resulting in a T cell response.

2. Regarding the humoral immune response.

There is a generation of an antibody autoimmune response against TG2, leading to the generation of anti-TG2 antibodies in the small intestine, and increased in the blood.

Neurodegenerative diseases

These diseases are characterized by the presence of intracellular and/or extracellular insoluble proteinaceous aggregates in different brain areas. The TG2 transamidation activity was observed to play a role in the formation of these aggregates owing to the covalent crosslinking of the pathogenic proteins involved in each of these neurodegenerative diseases. Huntington's disease is characterized by expanded polyQ repetitions in the N-Terminal Domain of the huntingtin Protein (htt) (over 40 consecutive Q residues), and this polyQ-bearing proteins can be incorporated into other proteins. In Alzheimer's disease, characterized by the amyloid β–proteins aggregates, TG2 transamidation activity could lead to the formation of extracellular senile plaques, and intracellularly, by the formation of intracellular neurofibrillary tangles (caused by the highly phosphorylated Tau protein).[15,45] In Parkinson's disease, caused by the formation of Lewy bodies, which are α–synuclein aggregates inside the cytoplasm of affected neurons, TG2 transamidation activity is also implicated.

Cancer

TG2 has been associated with some certain cancers as malignant melanoma[41] and glioblastomas[42] between others yet described in literature. The TG2 cell adhesion function to the extracellular matrix has also been associated with tumor dissemination and metastasis, and also with the activation of cell survival pathways in certain cancer cells.[57,58] It has also been studied that TG2 is involved in anti-apoptotic cell survival signaling,[43] and also in drug resistance.[59,60]

3. TG2 inhibitors: chemical tools for treatment and understanding

Knowing that TG2 has been associated with several diseases, the need of finding efficient treatments for these diseases would be of clinical value. The use of inhibitory compounds against TG2 as an alternative for the treatment of certain diseases has been described.[61] Not only would the inhibitors of such an important protein be beneficial for the treatment of TG2-associated diseases, but also will help us to deeply understand both, its biological/physiological functions and its implications in the several diseases this enzyme has been associated with.

3.1. TG2 inhibitors and biological functions

The use of inhibitors would provide useful informations about the biological functions, localization and mechanism of action of this multifunctional protein.

One example of the use of tissue transglutaminase inhibitors is the work carried out by Kahnna et al.,[57] in which a potent fibronectin (FN) binding domain TG2 inhibitor, ITP-79 (**Figure 7**), has been discovered to inhibit the binding of TG2 to a 42-kDa fragment of fibronectin in a dose-dependent manner. This finding allowed them to conclude the relationship between cancer and TG2-fibronectin interactions. Dansyl cadaverine (DC, amine competitive inhibitor), for instance, has been useful to elucidate the mode of action of this protein.[10] It is also relevant the work from Khosla et al.[62] in which labeled inhibitors has been described as a tool for TG2 visualization and distribution in cell cultures. Even, conformational change studies have been carried out in the presence of inhibitors, revealing an active site-exposed open conformation of TG2.[11] Even, the use of inhibitors, in the inhibition of intracellular TG2, has also been found to both have a protective effect against oxidative stress-cell death signaling.[63]

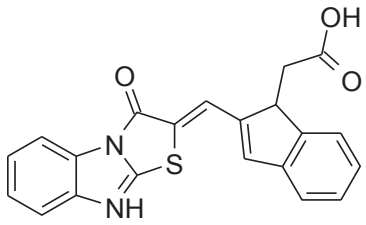

ITP-79

Figure 7. Chemical structure of the TG2 inhibitor ITP-79 employed as a pharmacological tool to discover the association between cancer and TG2-fibronectin interaction (ITP-79)[57]

3.2. TG2 inhibitors and diseases

The importance of the use of a TG2 inhibitor as a potential drug for the treatment of certain disease has been studied. Furthermore, recent studies affirmed that TG2 inhibitors must have some specific characteristic to be taken into account as desirable tools fot the treatment of diseases.[45] Desirable inhibitor characteristics are the following:

1) to be specific for TG2 without any effect on other members of the transglutaminase family (good selectivity profile),

2) to have *in vivo* efficacy,

3) to be safety (non-toxic),

4) to pass through the blood brain barrier (e.g.,in neurodegerative disorders)

One example of the therapeutical use of TG2 inhibitors was reported by Yuan et al, [42] in this case for the treatment of glioblastomas. In this study, the authors concluded that a combinatory treatment with two TG2 inhibitors induced apoptosis in a glioblastoma cell culture models, increasing sensitivity to the BCNU chemotherapy agent. In a different work, the same author confirmed this evidence using either KCC009 and dansylcadaverine as TG2 inhibitors (**Figure 8**), irreversible and reversible respectively, for the treatment of glioblastomas.[64] In addition, some examples of celiac disease treatments using TG2 inhibitors has also been proposed,[65,66] as well as for neurodegenerative diseases.[15,45,67] It also has been studied the effect of the non-expression of TG2 in murine models for Huntington's disease, reducing cell death and increasing life span,[68] this way opening a window to the treatment of these disease by inhibiting this enzyme.

Moreover, TG2 inhibitors were also employed to study the association of this enzyme with different diseases like: a) arterial stiffening by means of a isolated systolic hypertension (ISH) rat mode;[69] b) pulmonary hypertension disorder in a hypoxia-induced mousse model;[70] c) and celiac disease in a upper small intestine inflammation mousse model.[71]

To conclude, TG2 inhibitors are said to be a very promising alternative therapeutic agents for several diseases, as well as key agents to the discovery of the biological roles in which this multifunctional enzyme is involved in.

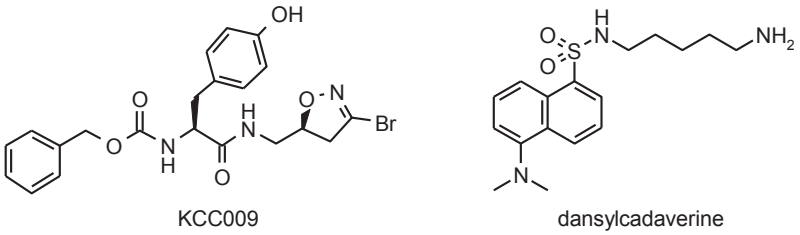

Figure 8. Chemical structure of theTG2 inhibitors KCC009 and dansylcadaverine as drug candidates for the treatment of glyoblastomas[64]

4. Enzyme kinetics. Introduction to enzyme inhibition

Many of pharmaceutical drugs alter the natural catalytic activity of enzymes. The understanding of the mechanism of inhibition of these drugs against an enzyme of interest is necessary to evaluate the potential therapeutic ability of any inhibitory compounds.

As shown in **Scheme 1**, in general terms, an enzyme E catalyzes the transformation of a substrate S into a product P, with the intermediate formation of a reversible ES complex, finally displaced to provide product P and free enzyme E. In the reversible equilibrium of formation and dissociation of the enzyme-substrate complex, ES, k_1 and k_{-1} are the association and dissociation rate constants respectively. On the other hand, k_{cat}, the turnover rate (maximal catalytic activity of an enzyme), is defined as the number of substrate molecules converted into product per enzyme molecule per unit of time, when the enzyme is saturated with substrate.

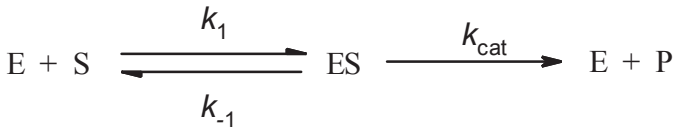

Scheme 1. Representation of an enzyme catalyzed reaction

In the steady-state hypothesis, using the Michaelis-Menten enzyme kinetics theory, the rate of formation of the ES complex from free enzyme and substrate is assumed to be balanced by the rate of conversion of ES into P as well as the dissociation of the ES complex into E and S (the change in concentration of ES in time is practically unchanged; assuming that $\frac{d\,[ES]}{dt} = 0$). In these conditions, the initial rates of the enzymatic reaction are obtained, when the initial substrate concentration ($[S_0]$) is assumed to be constant (few variations) and the initial substrate concentration ($[S_0]$) is much higher that the enzyme total concentration, ($[E_0]$). Considering this steady-state assumption, the Michaelis-Menten equation describes the relation between the initial rate (v) and the substrate concentration ([S]) following a rectangular hyperbola (see **Figure 9**) expressed in enzyme kinetics by the equation (1).

$$v = \frac{V_{max}\,[S]}{K_m + [S]} \qquad (1)$$

The typical parameters described in a Michaelis-Menten kinetics are the following:

- ✓ v is the initial rate of the enzymatic reaction. It is equal to the appearance of product P (or disappearance of substrate S) at the beginning of the enzymatic reaction per unit of time (d[P]/dt expressed in μM min^{-1}).
- ✓ V_{max} corresponds to the maximum rate of the reaction at saturating substrate concentrations, and it comes defined as $V_{max} = k_{cat}\,[E_0]$.
- ✓ K_m corresponds to the initial substrate concentration $[S]_0$ for which $v = V_{max} / 2$ (also called Michaelis constant), and it is defined in the Steady-State hypothesis as $K_m = \frac{(k_{-1} + k_{cat})}{k_1}$.

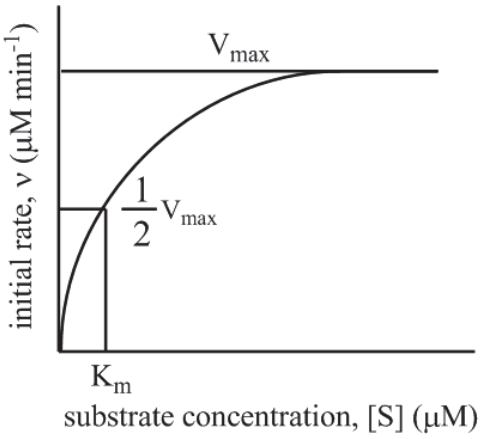

Figure 9. Plot of the initial reaction rate (v) *vs.* substrate concentrations [S]. V_{max} is represented as the maximal initial rate value from the enzymatic reaction, and K_m as the substrate concentration [S] where V_{max} is the half

Inhibitors, as modifiers of the enzymatic activity for the enzyme-substrate reaction, can be classified into different types, based on their mechanism of action. They are 1) reversible inhibitors, and 2) irreversible inhibitors.

An explanation of the different modes of inhibition will be given in the next paragraphs.

4.1. Reversible enzymatic inhibition

This kind of inhibition is caused by inhibitors that will reversibly block the catalytic activity of a given enzyme by non-covalent interactions with the enzyme. Depending the place where these compounds bound on the enzyme, it can be distinguished three types of reversible inhibitors: competitive, non-competitive, and uncompetitive inhibitors. For these compounds the dissociation constant of the enzyme-inhibitor complex, K_I, is indicative of the efficiency of their inhibition.

4.1.1. Competitive reversible inhibitors

The inhibitor competes with the enzyme substrate for the binding site via non-covalent interactions (see **Scheme 2**) forming the reversible enzyme-inhibitor complex, EI. K_I is the dissociation constante of the EI complex, and is expressed as K_I and defined as $K_I = \frac{[E]\,[I]}{[EI]} = \frac{k_{-i}}{k_i}$. This kind of compounds only modify the apparent K_m value ($K_{m\,app}$) which increases, but do not modify V_{max}. In this kind of inhibition, the equilibrium of the enzyme-inhibitor reversible complex can be displaced by rising the concentration of substrate. The equation for the initial rate (v) for this kind of reversible inhibition is defined in equation (2).

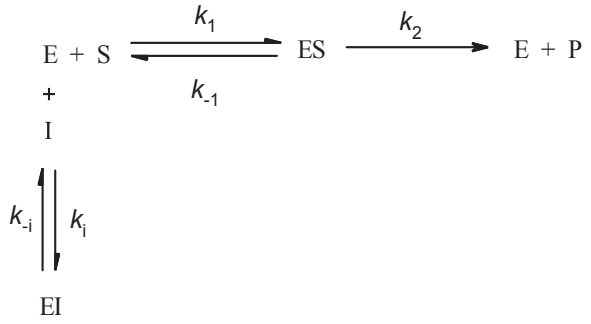

Scheme 2. Schematic representation of a reversible competitive inhibition

$$v = V_{max} \frac{[S]}{K_m \left(1 + \frac{[I]}{K_I}\right) + [S]} \qquad (2)$$

4.1.2. Non-competitive reversible inhibitors

This kind of inhibitors do not compete with the natural substrate of the enzyme because they bind at another site than the one of the substrate. As shown in **Scheme 3**, inhibitor can bind to the free enzyme E and to the ES complex, forming both the EI and ESI complexes, respectively. The dissociation constants for this inhibitors are K_I and K_I', where $K_I = \frac{[E]\,[I]}{[EI]} = \frac{k_{-i}}{k_i}$, and $K_I' = \frac{[ES]\,[I]}{[ESI]} = \frac{k'_{-i}}{k'_i}$, respectively. This kind of inhibition is called mixed non-competitive inhibition, and both inhibition constants K_I and K_I' are not equal. The equation for the initial rate (v) for this kind of inhibition is defined in equation (3). Both K_m and V_{max} are altered by the presence of I.

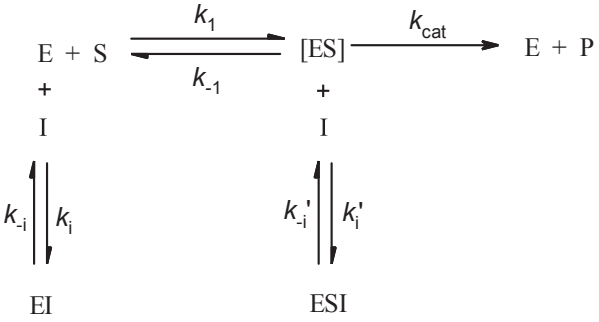

Scheme 3. Schematic representation of a reversible non-competitive inhibition

$$v = \frac{\frac{V_{max}\,[S]}{\left[1 + \frac{[I]}{K_I'}\right]}}{[S] + K_m \frac{\left[1 + \frac{[I]}{K_I}\right]}{\left[1 + \frac{[I]}{K_I'}\right]}} \qquad (3)$$

A special case of non-competitive inhibition is obtained when both inhibition constants K_I and K_I' are equal. This is called pure (simple) non-competitive inhibition. In this case the V_{max} value decreases (K_m is not affected). The equation for the initial rate (v) for this kind of inhibition is defined in equation (4).

$$v = \frac{V_{max}}{\left(1 + \frac{[I]}{K_I}\right)} \frac{[S]}{K_m + [S]} \qquad (4)$$

4.1.3. Uncompetitive reversible inhibitors

This type of inhibitors binds only to the ES complex as it is shown in **Scheme 4**, but not to the free enzyme E. The substrate binding to the enzyme modifies the enzyme structure, making binding site available for the inhibitor. In this case both kinetic parameters in the presence of inhibitor, K_m and V_{max}, decrease. The dissociation constant K_I can be described as $K_I = \frac{[ES]\,[I]}{[ESI]}$, where $K_I = \frac{k_{-i}}{k_i}$.

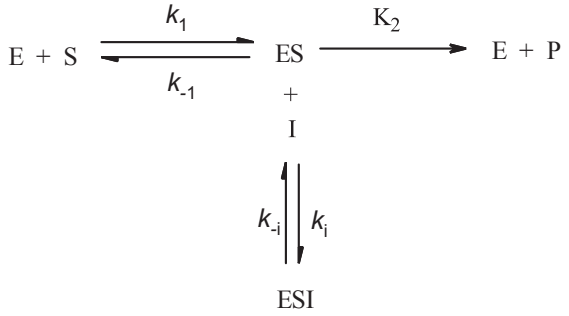

Scheme 4. Schematic representation of a reversible uncompetitive inhibition

The initial rate (v) for this kind of inhibition is defined in equation (5).

$$v = V_{max} \frac{[S]}{K_m + [S]\left(1 + \frac{[I]}{K_I}\right)} \qquad (5)$$

4.2. Irreversible enzymatic inhibitors

This class of inhibitors binds irreversibly to the enzyme, leading to the permanent inactivation of the enzyme. In the presence of the inhibitor, the enzyme forms a non-covalent EI complex, before permanently inactivate the enzyme (often covalently) forming an inactivated enzyme-inhibitor conjugate EI^*. Therefore, enzymatic activity cannot be restored since the inhibitor does not dissociate from the EI^* complex, even when dilution or dialysis experiments are carried out. These inhibitory compounds can

be classified at the same time in two differentiated groups: chemical labels (or active-site directed inactivating reagents), and suicide inhibitors (or mechanism-based inhibitors). For these inhibitors K_I and k_{inact} constants are both indicative of the efficiency of the inhibition.

4.2.1. Chemical labels (active-site directed inactivating reagents)

This kind of drugs shows specificity towards a certain functional group on amino acid residues within the active site of the enzyme; they are chemoselective. Usually, they are substrate analogs to favor their binding to the active site, bearing an additional reactive group (typically electrophiles; e.g., Michael acceptors, halomethyl ketones, diazo groups and epoxides), which will react with an active site nucleophile. The reactive group reacts stoichiometrically (1 mole of inhibitor per mole of active site). A schematic representation of this sort of inhibition and their kinetic parameters are shown in **Scheme 5**.

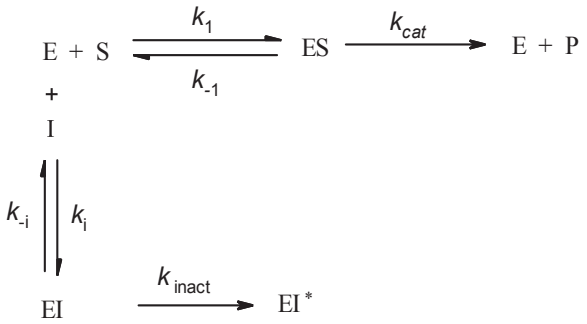

Scheme 5. Schematic representation of an irreversible inhibition

Kinetic constants K_I and k_{inact} are defined as follows:

K_I is the dissociation constant of the EI complex (or inhibition constant). It comes defined by $K_I = \frac{[E][I]}{[EI]}$, so, $K_I = \frac{k_{-i} + k_{inact}}{k_i}$. In the case where the inactivation rate constant, k_{inact}, is much lower than the dissociation rate constant k_{-i} ($k_{inact} << k_{-i}$), k_{inact} is negligible being $K_I = \frac{k_{-i}}{k_i}$ (resulting in competitive inhibition).

k_{inact} is the maximum (or limiting) inhibition rate if the enzyme is saturated with inhibitor. This is a first-order rate constant. It can be expressed substituting k_{inact} from equation (6) (min^{-1}).

k_{obs} is the observed pseudo-first order inhibition rate constant. It is the constant rate of the exponential decay of the loss of activity as a function of time, for a specific concentration of the inhibitor. It can be determined (for various concentration of inhibitor) from the slope of a semi-logarithmic plot of inhibitor, I, *vs.* time, or by fitting the kinetic data to an exponential rate equation (7). Moreover, in the absence of substrate, k_{obs} is defined by an hyperbolic equation (6) where values of K_I and k_{inact} can be obtained.[72]

$$k_{obs} = \frac{k_{inact}}{\left(1+\frac{K_I}{[I]}\right)} \quad (6)$$

$$A = A_0\, e^{-kobs\, t} \quad (7)$$

In equation (7), A is the residual enzyme activity, A_0 is the initial enzyme activity and t is the time at which enzymatic activity is measured at a defined inhibitor concentration.

The k_{inact}/K_I ratio represents the second-order rate constant for the reaction of the inhibitor with the target. (M^{-1} min^{-1}).[72] It is the efficiency of the enzyme inactivation by the inhibitor.

An example of these inhibitors is the phenylmethanesulfonyl fluoride (PMSF), a general inhibitor of serine proteases, such as α-chymotrypsin. (see **Scheme 6**). The mechanism of inhibition is described to happen when the nucleophilic oxygen of the hydroxyl group of the Ser195 active site residue reacts with the sulfur atom (the electrophile) of the sulfonyl moiety of PMSF. Elimination of the fluorine is carried out, yielding the final sulfonylenzyme derivative.[73]

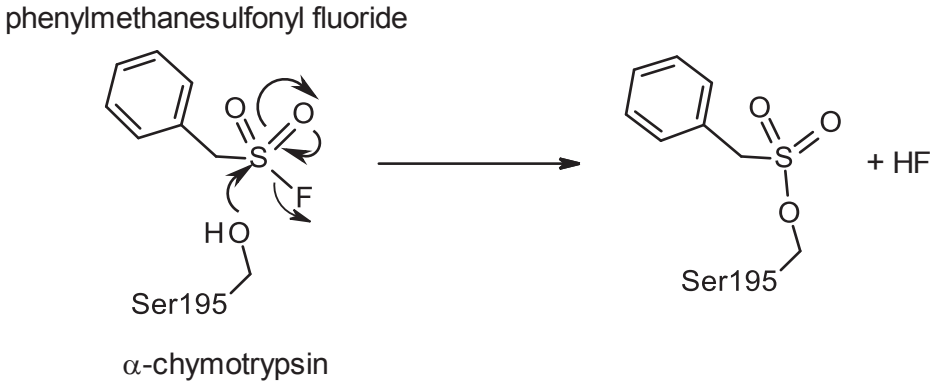

Scheme 6. Proposed sulfonylation mechanism of the active site Ser195 (in this case from the serine protease α-chymotrypsin) by the phenylmethanesulfonyl fluoride (PMSF)[73]

4.2.2. Suicide inhibitors (mechanism-based inhibitors)

These kind of compounds are chemical unreactive before being transformed by the enzyme into a reactive intermediate which can irreversibly modify the active site of the enzyme. The enzyme treats it as a substrate, starting the catalytic process with the inhibitor.[74] The inhibitor reversibly binds to the enzyme forming the EI reversible complex. As shown in **Scheme 7**, after the formation of the reversible complex EI, the inhibitor I is gradually transformed to a reactive intermediate I* by the enzyme giving the EI* complex. Then, it can happen that EI* dissociates yielding the reactive inhibitor I* and the free enzyme, or, on the contrary, the enzyme is being gradually inactivated forming a stable irreversible E-I* complex.[75,76]

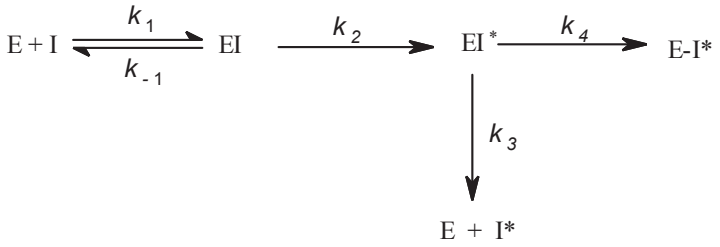

Scheme 7. Schematic representation of the mechanism-based inhibition[76,77]

Kinetic parameters K_I, k_{inact}, and k_{inact} / K_I are also employed to define the affinity and efficiency of inhibition for this kind of inhibitors,[78] but also the partition ratio r, which is the defined as the ratio of the product (I*) formation rate to the inactive enzyme formation rate ($r = \frac{k_{cat}}{k_{inact}} = \frac{k_3}{k_4}$).[77,79]

The rate of enzyme inactivation can be represented as equation (8).

$$\frac{d[E_t]}{dt} = \frac{k_{inact}[I]}{K_I + [I]} \qquad (8)$$

Where $[E_t]$ is the active enzyme concentration at time t; [I] the inhibitor concentration; k_{inact} the maximun inactivation rate constant, and K_I the inhibitor concentration that produces half-maximal rate of inactivation.

k_{inact} and K_I are complex functions of k_1, k_{-1}, k_2, k_3, and k_4 expressed in equations (9) and (10), respectively.

$$k_{inact} = \frac{k_2 k_4}{k_2 + k_3 + k_4} \quad (9)$$

$$K_I = \frac{k_{-1} k_2}{k_1} \frac{k_3 + k_4}{k_2 + k_3 + k_4} \quad (10)$$

Another kinetic parameter employed in this kind of irreversible inhibition is K_i. It represents the initial binding of the inhibitor to the enzyme, and it is represented in equation (11). It should be notice that K_i is not equivalent to K_I. It may be assumed that K_i and K_I have the same value if k_1 and k_{-1} are very large and k_2 is rate limiting.[77]

$$K_i = \frac{k_{-1} + k_2}{k_1} \quad (11)$$

5. Kinetic assays employed for TG2 inhibition characterization

The TG acyl transfer reaction, involving TG2, presented in the introductory chapter of this work (**Figure 1**) is known to occur via a modified ping-pong mechanism.[3,80,81] This kind of mechanism is common for enzymes with two (or more) substrates S_1 and S_2, where two different forms of enzymes, E and E', exist between the release of two different products, P_1 and P_2 (see **Scheme 8**).

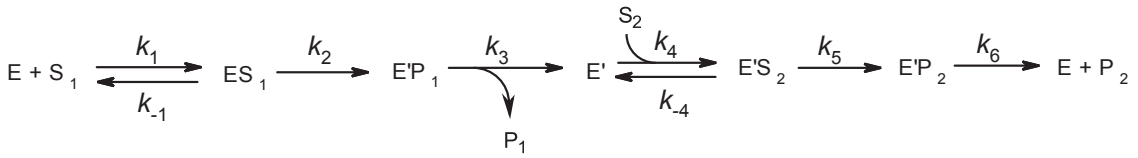

Scheme 8. Schematic representation of a general ping-pong kinetic mechanism for substrates S_1 and S_2 to form products P_1 and P_2 respectively

Both kinetic (initial velocity measurements and product inhibition) and isotope exchange studies from the work of Folk[81] demonstrated that TG family of enzymes have a ping-pong mechanism of action (see **Scheme 9**) in which: (1) glutamine substrate binds to enzyme in a binary complex; (2) ammonia dissociates with the formation of a thioester linkage (thioester intermediate), and (3) acyl group is transferred from enzyme either (3a) to an acceptor amine to form a ɣ-glutamyl-amine product (transamidation), or (3b) to water yielding glutamic acid as product (hydrolysis).

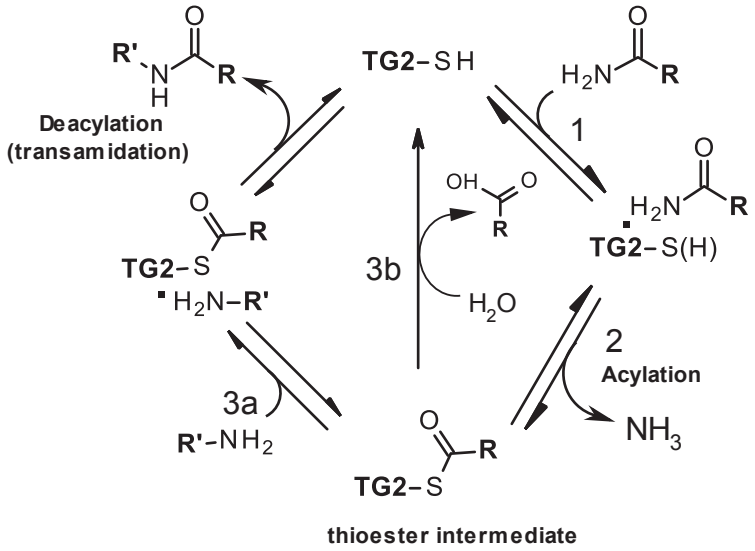

Scheme 9. Schematic representation of the ping-pong mechanism of TG2-catalyzed acylation

Several kinetic assays have been carried out for the characterization of reversible and irreversible TG2 inhibitors up to date. Although TG2 follows a ping-pong reaction mechanism, described methods employed so far for the determination of the different kinetics for its inhibition take advantage mostly in the first acylation step following less complicated Michaelis-Menten kinetic model. The different existing enzyme assays regarding TG2 kinetics will be described in the next paragraphs.

5.1. TG2-GDH coupled assay

A continuous spectrophotometric enzymatic assay based on a glutamate deshydrogenase coupled reaction was adapted for the kinetic study of TG2. The introduction of this methodology to the field of TG kinetics was carried out in the work of Day et al.[82] and Piper et al.[83] As shown in **Scheme 10,** the method is based in the release of 1 mole of

ammonia formed by the TG2 thiol acylation reaction. Consequently, this released ammonia will be used by the GDH coupled reaction. The α-ketoglutarate is reduced to L-glutamic acid while NAD(P)H is oxidized to $NAD(P)^+$. The decrease of NAD(P)H is monitored continuously as the decrease in absorbance at 340 nm. This approach was carried out to for the determination of the TG2 inhibition kinetics for reversible inhibitors[84], and irreversible inhibitors.[85-87,88]

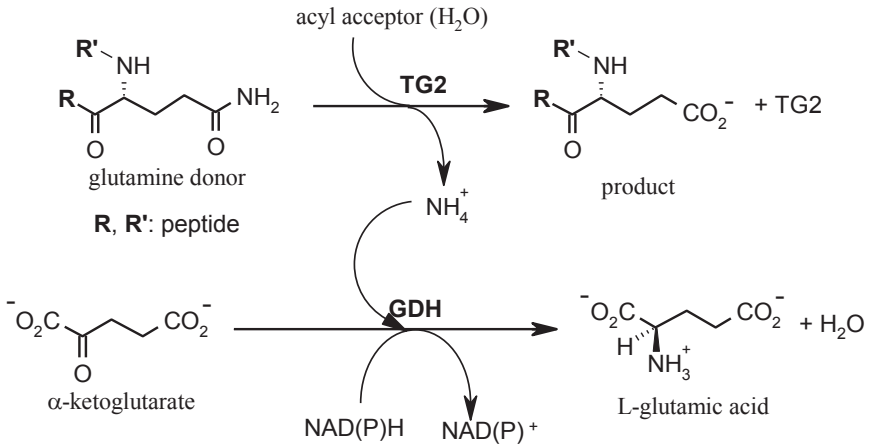

Scheme 10. Schematic representation of the two coupled reactions of the TG2-GDH assay. Assay is performed in 200 mM MOPS buffer (pH 7.2) at 25ºC

5.2. Coumarin-based fluorimetric assay

On the other hand, the use of a fluorogenic acyl donor substrate, the 4-(*N*-carbobenzyloxy-L-phenylalanylamino)-butyric acid coumarin-7-yl ester (CbzGBC), was optimized by Gillet et al.[89] This assay is based on the hydrolysis of the ester function by TG2 with the consequent release of the 7-hydroxycoumarin (see **Scheme 11**) which can be monitored as an increase in fluorescence (7-hydroxycoumarin is excited at 330 nm corresponding to an emission of fluorescence at 460nm).

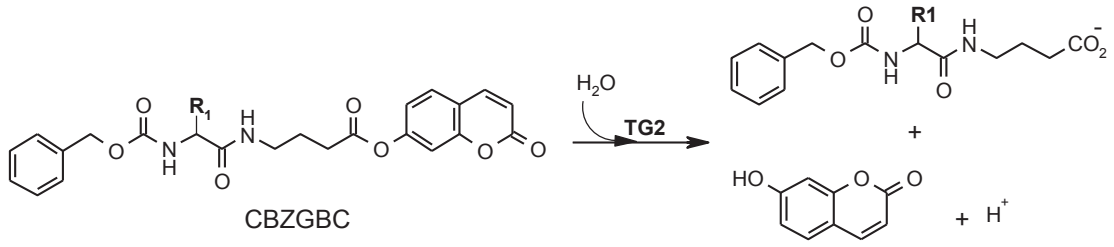

Scheme 11. Schematic representation of the ester hydrolysis reaction of the 4-(*N*-carbobenzyloxy-L-phenylalanylamino)butyric acid coumarin-7-yl ester (CbzGBC) catalyzed by TG2 in the presence of water. Water is used as acyl acceptor by TG2. Assay was performed in 200 mM MOPS buffer (pH 8.0) at 25ºC

5.3. *p*-Nitrophenyl ester-based kinetic assay

A different method to determine the TG2 kinetics in an inhibition assay was shown in the work from Pardin et al.[90] and Leblanc et al.,[80] where the hydrolysis of the chromogenic ester *N*-Cbz-L-glutamyl(*p*-nitrophenylester)glycine (see **Scheme 12**), as

the TG2 acyl donor substrate, releases *p*-nitrophenol. The increase of the *p*-nitrophenol produced by the TG2-catalyzed hydrolysis of the ester above can be measured as the absorbance at 400 nm.

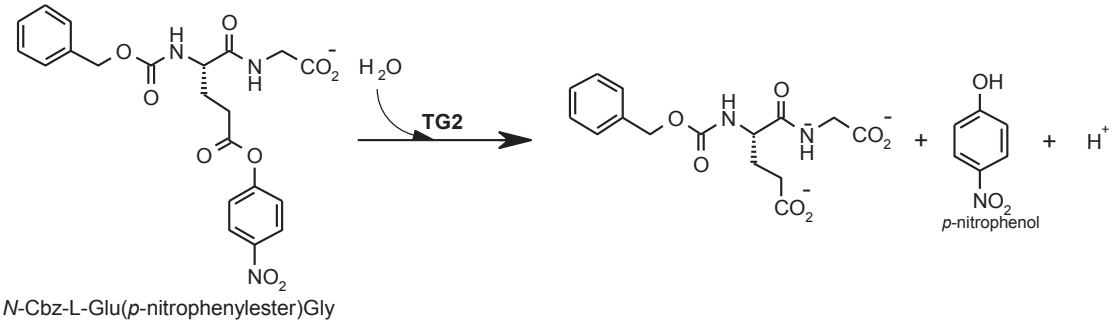

Scheme 12. Schematic representation of the TG2 catalyzed hydrolysis of the chromogenic substrate *N*-Cbz-L-Glu(*p*-nitrophenylester)Gly into *p*-nitrophenol. Assay was performed in 0.1 M MOPS buffer (pH 7.0) at 25ºC

5.4. Colorimetric assay

Another kinetic assay for the kinetic characterization of TG2 was performed by Marrano et al.[91] and de Macédo et al.[92] This assay is based on the TG2 transamidation reaction employing carbobenzyloxy-L-glutamylglycine (Cbz-Gln-Gly) and *N*,*N*-dimethyl-1,4-phenylenediamine (DMPDA) as the acyl donor and the acyl acceptor substrates, respectively. In this assay the resulting anilide product (the transamidated product), with a strong electron-donating group, is a chromophore that absorbs light at 278 nm (see **Scheme 13**).

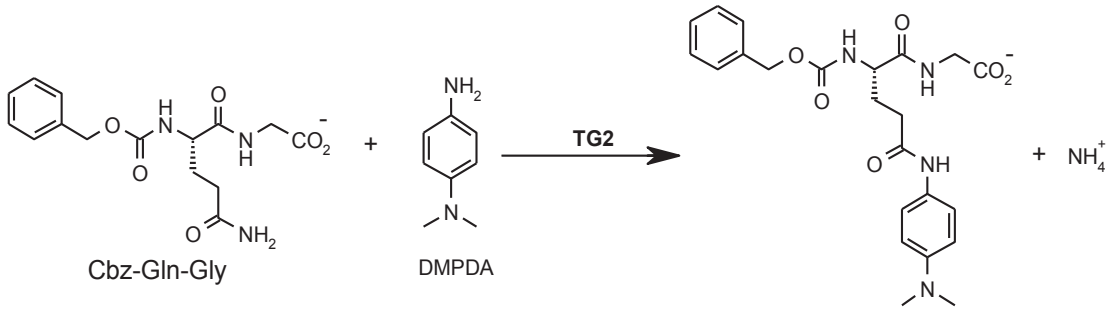

Scheme 13. Schematic representation of the TG-catalyzed DMPDA assay. In this method carbobenzyloxy-L-glutamylglycine (Cbz-Gln-Gly; acyl donor) and *N*,*N*-dimethyl-1,4-phenylenediamine (DMPDA) are transamidated forming an anilide product, the carbobenzyloxy-L-glutamyl-ɣ[4-(dimethylamino)anilido]glycine product. The TG2 transamidation activity is determined by measuring the absorbance at 278 nm. Assay was performed in 120 mM Tris-acetate buffer (pH 7.0) at 37ºC

5.5. TG2 Kinetic parameters observed for the different assays.

K_m and k_{cat} values from the different kinetic TG2 methods described above, and employed for the analysis of TG2 inhibitors, are summarized in **Table 2**.

Assay	Acyl donor	Acyl acceptor	K_m Acyl donor (mM)	K_m Acyl acceptor (mM)	k_{cat} (min^{-1})
GDH-coupled assay	Cbz-Gln-Gly	H_2O	6.8 ± 0.8	---------	17 ± 0.6
Coumarin-based assay	Cbz-Gly-BC	H_2O	$9\ 10^{-3}$ ± 2	---------	75 ± 5
p-nitrophenyl ester-based	N-Cbz-L-Glu(*p*-nitrophenylester)Gly	H_2O	0.02	---------	54.6
DMPDA colorimetric assay	Cbz-Gln-Gly	DMPDA	2.4 ± 0.05	0.25 ± 0.02	0.90 ± 0.06

Table 2. TG2 kinetic parameters (K_m and k_{cat}) for the different substrates (acyl acceptors and acyl donors) used in the different assays described so far for the study of the TG2 inhibition

Bibliography - Introduction

1. Mehta, K. Mammalian transglutaminases: a family portrait. *Prog. Exp. Tumor. Res*. **2005**, *38*, 1-18.
2. Griffin, M.; Casadio, R.; Bergamini, C. M. Transglutaminases: nature's biological glues. *Biochem. J*. **2002**, *368*, 377-396.
3. Keillor, J. W.; Clouthier, C. M.; Apperley, K. Y.; Akbar, Mulani, A. Acyl transfer mechanisms of tissue transglutaminase. *Bioorg. Chem*. **2014**, *57*, 186-197.
4. Király, R.; Thangaraju. K.; Nagy, Z.; Collighan, R.; Nemes, Z.; Griffin, M.; Fésüs, L. Isopeptidase activity of human transglutaminase 2: disconnection from transamidation and characterization by kinetic parameters. *Amino Acids* **2016**, *48*, 31-40.
5. Parameswaran, K. N.; Cheng, X. F.; Chen, E. C.; Velasco, P. T.; Wilson, J. H.; Lorand, L. Hydrolysis of gamma:epsilon isopeptides by cytosolic transglutaminases and by coagulation factor XIIIa. *J. Biol. Chem*. **1997**, *272*, 10311-10317.
6. Lorand, L.; Graham, R. M. Transglutaminases: crosslinking enzymes with pleiotropic functions. *Nat. Rev. Mol. Cell. Biol*. **2003**, *4*, 140-156.
7. Lismaa, S. E., Mearns, B. M.; Lorand, L.; Graham, R. M. Transglutaminases and disease: lessons from genetically engineered mouse models and inherited disorders. *Physiol. Rev*. **2009**, *89*, 991-1023.
8. Rybicki, A. C.; Schwartz, R. S.; Qiu, J. J.; Gilman, J. G. Molecular cloning of mouse erythrocyte protein 4.2: a membrane protein with strong homology with the transglutaminase supergene family. *Mamm. Genome* **1994**, *5*, 438-445.
9. Nemes, Z.; Petrovski, G.; Csosz, E.; Fésüs, L. Structure-function relationships of transglutaminases - a contemporary view. *Prog. Exp. Tumor. Res*. **2005**, *38*, 19-36.
10. Iismaa, S. E.; Holman, S.; Wouters, M. A.; Lorand, L.; Graham, R. M.; Husain A. Evolutionary specialization of a tryptophan indole group for transition state stabilization by eukaryotic transglutaminases. *Proc. Natl Acad. Sci. USA*. **2003**, *100*, 12636-12641.
11. Pinkas, D. M.; Strop, P.; Brunger, A. T.; Khosla, C. Transglutaminase 2 undergoes a large conformational change upon activation. *PLoS Biol*. **2007**, *5*, e327.
12. Begg, G. E.; Carrington, L.; Stokes, P. H.; Matthews, J. M.; Wouters, M. A.; Husain, A.; Lorand, L.; Iismaa, S. E.; Graham, R. M. Mechanism of allosteric

regulation of transglutaminase 2 by GTP. *Proc. Natl Acad. Sci. USA*. **2006**, *103*, 19683-19688.

13. Liu, S.; Cerione, R. A.; Clardy, J. Structural basis for the guanine nucleotide-binding activity of tissue transglutaminase and its regulation of transamidation activity. *Proc. Natl Acad. Sci. USA*. **2002**, *99*, 2743-2747.

14. Ahvazi, B.; Boeshans, K. M.; Idler, W.; Baxa, U.; Steinert, P. M. Roles of calcium ions in the activation and activity of the TG3 enzyme. *J. Biol. Chem*. **2003**, *278*, 23834-23841.

15. Ricotta, M.; Iannuzzi, M.; Vivo, G. D.; Gentile, V. Physio-pathological roles of tg-catalyzed reactions. *World. J. Biol. Chem*. **2010**, *1*, 181-187.

16. Smethurst, P. A.; Griffin, M. Measurement of tissue transglutaminase activity in a permeabilized cell system: its regulation by Ca2+ and nucleotides. *Biochem. J.* **1996**, *313*, 803-808.

17. Fésüs, L.; Piacentini, M. Transglutaminase 2: an enigmatic enzyme with diverse functions. *Trends. Biochem. Sci*. **2002**, *27*, 534-539.

18. Gundemir, S.; Colak, G.; Tucholski, J.; Johnson, G. V. Transglutaminase 2 a molecular swiss army knife. *Biochim. Biophys. Acta* **2012**, *1823*, 406-419.

19. Stamnaes, J.; Pinkas, D. M.; Fleckenstein, B; Khosla, C.; Sollid, L. M. Redox regulation of transglutaminase 2 activity. *J. Biol. Chem*. **2010**, *285*, 25402-25409.

20. Chica, R. A.; Gagnon, P.; Keillor, J. W.; Pelletier, J. N. Tissue transglutaminase acylation: proposed role of conserved active site Tyr and Trp residues revealed by molecular modeling of peptide substrate binding. *Protein Sci.* **2004**, *13*, 979-991.

21. Király, R.; Demény, M.; Fésüs, L. Protein transamidation by transglutaminase 2 in cells: a disputed Ca^{2+}-dependent action of a multifunctional protein. *FEBS J.* **2011**, *278*, 4717-4739.

22. Mishra, S.; Murphy, L. J. Tissue transglutaminase has intrinsic kinase activity: identification of transglutaminase 2 as an insulin-like growth factor-binding protein-3 kinase. *J. Biol. Chem*. **2004**, *279*, 23863-23868.

23. Mishra, S.; Melino, G.; Murphy, L. J. Transglutaminase 2 kinase activity facilitates protein kinase A-induced phosphorylation of retinoblastoma protein. *J. Biol. Chem*. **2007**, *282*, 18108-18115.

24. Mishra, S.; Murphy, L. J. The p53 oncoprotein is a substrate for tissue transglutaminase kinase activity. *Biochem. Biophys. Res. Commun*. **2006**, *339*, 726-730.

25. Nakaoka, H.; Perez, D. M.; Baek, K. J.; Das, T.; Husain, A.; Misono, K.; Im, M. J.; Graham, R. M. Gh: a GTP-binding protein with tranglutaminase activity and receptor signaling function. *Science* **1994**, *264*, 1901-1906.

26. Murthy, S. N.; Lomasney, J. W.; Mak, E. C.; Lorand, L. Interactions of Gh/transglutaminase with phospholipase Cd1 and with GTP. *Proc. Natl Acad. Sci. USA*. **1999**, *96*, 11815–11819.

27. Mhaouty-Kodja, S. Ghalpha/tissue transglutaminase 2: an emerging G protein in signal transduction. *Biol. Cell*. **2004**, *96*, 363–367.

28. Lai, T. S.; Slaughter, T. F.; Koropchak, C. M.; Haroon, Z. A.; Greenberg, C. S. C-terminal deletion of human transglutaminase enhances Magnesium-dependent GTP/ATPase activity. *J. Biol. Chem*. **1996**, *271*, 31191-31195.

29. Lismaa, S. E.; Chung, L.; Wu, M. J.; Teller, D. C.; Yee, V. C.; Graham, R. M. The core domain of the tissue transglutaminase Gh hydrolyzes GTP and ATP. *Biochemistry* **1997**, *36*, 11655–11664.

30. Hasegawa, G.; Suwa, M.; Ichikawa, Y.; Ohtsuka, T.; Kumagai, S.; Kikuchi, M.; Sato, Y.; Saito, Y. A novel function of tissue-type transglutaminase: protein disulfide isomerase. *Biochem. J*. **2003**, *373*, 793-803.

31. Nurminskaya, M. V.; Belkin, A. M. Cellular functions of tissue transglutaminase. *Int. Rev. Cell. Mol. Biol.* **2012**, *294*, 1–97.

32. Akimov, S. S.; Krylov, D.; Fleischman, L. F.; Belkin, A. M. Tissue transglutaminase is an integrin-binding adhesion coreceptor for fibronectin. *J. Cell. Biol*. **2000**, *148,* 825-838.

33. Akimov, S. S.; Belkin, A. M. Cell-surface transglutaminase promotes fibronectin assembly via integration with the gelatin-binding domain of fibronectin: a role in TGF-β dependent matrix deposition. *J. Cell Sci*. **2001**, *114*, 2989-3000.

34. Akimov, S. S.; Belkin, A. M. Opposing roles of Ras/Raf oncogenes and the MEK1/ERK signaling module in regulation of expression and adhesive function of surface transglutaminase. *J. Biol. Chem*. **2003***, 278,* 35609-35619.

35. Lee, J.; Kim, Y. S.; Choi, D. H.; Bang, M. S.; Han, T. R.; Joh, T. H.; Kim, S. Y. Transglutaminase 2 induces Nuclear Factor-kB activation via a Novel Pathway in BV-2 Microglia. *J. Biol. Chem*. **2004**, *279*, 53725-53735.

36. Kuo, T. F.; Tatsukawa, H.; Kojima, S. New insights into the functions and localization of nuclear transglutaminase 2. *FEBS J.* **2011**, *278*, 4756-4767.

37. Jang, T. H.; Lee, D. S.; Choi, K.; Jeong, E. M.; Kim, I. G.; Kim, Y. W.; Chun, J. N.; Jeon, J. H.; Park, H. H. Crystal structure of transglutaminase 2 with GTP complex and amino acid sequence evidence of evolution of GTP binding site. *PLoS One* **2014**, *9*, e107005.

38. Lortat-Jacob, H.; Burhan, I.; Scarpellini, A.; Thomas, A.; Imberty, A.; Vivès, R. R.; Johnson, T.; Gutierrez, A.; Verderio, E. A. Transglutaminase-2 interaction with heparin. Identification of a heparin binding site that regulates cell adhesion to fibronectin-transglutaminase-2 matrix. *J. Biol. Chem*. **2012**, *287*, 18005-18017.

39. Wang, Z.; Collighan, R. J.; Pytel, K.; Rathbone, D. L.; Li, X.; Griffin, M. Characterization of the heparin binding site of tissue transglutaminase: its importance in the enzyme's cell surface targeting, matrix deposition and cell signaling. *J. Biol. Chem*. **2012**, *287*, 13063-13083.

40. Simon-Vecsei, Z.; Király, R.; Bagossi, P.; Tóth, B.; Dahlbom, I.; Caja, S.; Csosz, É.; Lindfors, K.; Sblattero, D.; Nemes, É.; Mäki, M.; Fésüs, L.; Korponay-Szabó, I. R. A single conformational transglutaminase 2 epitope contributed by three domains is critical for celiac antibody binding and effects. *Proc. Natl Acad. Sci. USA*. **2012**, *109*, 431-436.

41. Fok, J. Y.; Ekmekcioglu, S.; Mehta, K. Implications of tissue transglutaminase expression in malignant melanoma. *Mol. Cancer Ther*. **2006**, *5*, 1493-1503.

42. Yuan, L.; Choi, K.; Khosla, C.; Zheng, X.; Higashikubo, R.; Chicoine, M. R.; Rich, K. M. Tissue transglutaminase 2 inhibition promotes cell death and chemosensitivity in glioblastomas. *Mol. Cancer Ther*. **2005**, *4*, 1293-1302.

43. Cao, L.; Petrusca, D. N.; Satpathy, M.; Nakshatri, H.; Petrache, I.; Matei, D. Tissue transglutaminase protects epithelial ovarian cancer cells from cisplatin-induced apoptosis by promoting cell survival signaling. *Carcinogenesis* **2008**, *29*, 1893-1900.

44. Mangala, L. S.; Mehta, K. Tissue transglutaminase (TG2) in cancer biology. *Prog. Exp. Tumor. Res*. **2005**, *38*, 125-138.

45. Grosso, H.; Mouradian, M. M. Transglutaminase 2: biology, relevance to neurodegenerative diseases and therapeutic implications. *Pharmacol. Ther.* **2012**, *133*, 392-410.

46. Wang, D. S.; Dickson, D. W.; Malter, J. S. Tissue transglutaminase, protein cross-linking and Alzheimer's disease: review and views. *Int. J. Clin. Exp. Pathol*. **2008**, *1*, 5-18.

47. Wilhelmus, M. M.; de Jager, M.; Bakker, E. N.; Drukarch, B. Tissue transglutaminase in Alzheimer's disease: involvement in pathogenesis and its potential as a therapeutic target. *J. Alzheimers. Dis.* **2014**, *42*, S289-303.

48. de Jager, M.; van der Wildt, B.; Schul, E.; Bol, J. G.; van Duinen, S. G.; Drukarch, B.; Wilhelmus, M. M.; Tissue transglutaminase colocalizes with extracellular matrix proteins in cerebral amyloid angiopathy. *Neurobiol. Aging* **2013**, *34*, 1159-1169.

49. León, F.; Sánchez, L.; Camarero, C.; Camarero, C.; Roy, G. Immunopathogenesis of celiac disease. *Immunology* **2005**, *24*, 313-325.

50. Qiao, S. W.; Piper, J.; Haraldsen, G.; Oynebråten, I.; Fleckenstein, B.; Molberg, O.; Khosla, C.; Sollid, L. M. Tissue transglutaminase-mediated formation and cleavage of histamine-gliadin complexes: biological effects and implications for celiac disease. *J. Immunol*. **2005**, *174*, 1657-1663.

51. Sakly, W.; Thomas, V.; Quash, G.; El Alaoui, S. A role for tissue transglutaminase in alpha-gliadin peptide cytotoxicity. *Clin. Exp. Immunol*. **2006**, *146*, 550-558.

52. Klöck, C.; Diraimondo, T. R.; Khosla, C. Role of transglutaminase 2 in celiac disease pathogenesis. *Semin. Immunopathol*. **2012**, *34*, 513-522.

53. Salter, N. W.; Ande, S. R.; Nguyen, H. K.; Nyomba, B. L.; Mishra, S. Functional characterization of naturally ocurring ransglutaminase 2 mutants implicated in early-onset type 2 diabetes. *J. Mol. Endocrinol*. **2012**, *48*, 203–216.

54. Small, K.; Feng, J. F.; Lorenz, J.; Donnelly, E. T.; Yu, A.; Im, M. J.; Dorn, G. W. II; Liggett, S. B. Cardiac specific overexpression of transglutaminase II (G(h)) results in a unique hypertrophy phenotype independent of phospholipase C activation. *J. Biol. Chem*. **1999**, *274*, 21291-21296.

55. Verderio, E. A.; Johnson, T.; Griffin, M. Tissue transglutaminase in normal and abnormal wound healing: review article. *Amino Acids* **2004**, *26*, 387–404.

56. Shweke, N.; Boulos, N.; Jouanneau, C.; Vandermeersch, S.; Melino, G.; Dussaule, J. C.; Chatziantoniou, C.; Ronco, P.; Boffa, J. J. Tissue transglutaminase contributes to interstitial renal fibrosis by favoring accumulation of fibrillar collagen through TGF-β activation and cell infiltration. *Am. J. Pathol*. **2008**, *173*, 631–642.

57. Khanna, M.; Chelladurai, B.; Gavini, A.; Li, L.; Shao, M.; Courtney, D.; Turchi, J. J.; Matei, D.; Meroueh, S. Targeting ovarian tumor cell adhesion mediated by tissue tansglutaminase. *Mol. Cancer Ther*. **2011**, *10*, 626-636.

58. Mangala, L. S.; Fok, J. Y.; Zorrilla-Calancha, I. R.; Verma, A.; Mehta, K. Tissue transglutaminase expression promotes cell attachment, invasion and survival in breast cancer cells. *Oncogene* **2007**, *26*, 2459-2470.

59. Budillon, A.; Carbone, C.; Di Gennaro, E. Tissue transglutaminase: a new target to reverse cancer drug resistance. *Amino Acids* **2013**, *44*, 63-72.

60. Han, J. A.; Park, S. C. Reduction of transglutaminase 2 expression is associated with an induction of drug sensitivity in the PC-14 human lung cancer cell line. *J. Cancer. Res. Clin. Oncol*. **1999**, *125*, 89-95.

61. Siegel, M.; Khosla, C. Transglutaminase 2 inhibitors and their therapeutic role in disease state. *Pharmacol. Ther*. **2007**, *115*, 232-245.

62. Dafik, L.; Khosla, C. Dihydroisoxazole analogs for labeling and visualization of catalytically active transglutaminase 2. *Chem. Biol*. **2011**, *18*, 58-66.

63. Basso, M.; Berlin, J.; Xia, L.; Sleiman, S. F.; Ko, B.; Haskew-Layton, R.; Kim, E.; Antonyak, M. A.; Cerione, R. A.; Iismaa, S. E.; Willis, D.; Cho, S.; Ratan, R. R. Oxidative stress-induced neuronal death downstream of pathological ERK activation. *J. Neurosci*. **2012**, *32*, 6561-6569.

64. Yuan, L.; Siegel, M.; Choi, K.; Khosla, C.; Miller, C. R.; Jackson, E. N.; Piwnica-Worms, D.; Rich, K. M. Transglutaminase 2 inhibitor, KCC009, disrupts fibronectin assembly in the extracellular matrix and sensitizes orthotopic glioblastomas to chemotherapy. *Oncogene* **2007**, *26*, 2563-2573.

65. Sollid, L. M.; Khosla, C. Novel therapies for coeliac disease. *J. Intern. Med*. **2011**, *269*, 604-613.

66. Rashtak, S.; Murray, J. A. Review article: Coeliac disease, new approaches to therapy. *Aliment. Pharmacol. Ther*. **2012**, *35*, 768-781.

67. Verhaar, R.; Jongenelen, C. A.; Gerard, M.; Baekelandt, V.; Van Dam, A. M.; Wilhelmus, M. M.; Drukarch, B. Blockade of enzyme activity inhibits tissue transglutaminase-mediated transamidation of α–synuclein in a cellular model of parkinson's disease. *Neurochem. Int*. **2011**, *58*, 785-793.

68. Mastroberardino, P. G.; Iannicola, C.; Nardacci, R.; Bernassola, F.; De Laurenzi, V.; Melino, G.; Moreno, S.; Pavone, F.; Oliverio, S.; Fésüs, L.; Piacentini, M. 'Tissue' transglutaminase ablation reduces neuronal death and Prolongs survival in a mouse model of Hungtington's disease. *Cell. Death. Differ*. **2002**, *9*, 873-880.

69. Chabot, N.; Moreau, S.; Mulani, A.; Moreau, P.; Keillor, J. W. Fluorescent probes of tissue transglutaminase reveal its association with arterial stiffening. *Chem. Biol*. **2010**, *17*, 1143-1150.

70. DiRaimondo, T. R.; Klöck, C.; Warburton, R.; Herrera, Z.; Penumatsa, K.; Toksoz, D.; Hill, N.; Khosla, C.; Fanburg, B. Elevated transglutaminase 2 activity is associated with hypoxia-induced experimental pulmonary hypertension in mice. *ACS Chem. Biol*. **2014**, *9*, 266-275.

71. Dafik, L.; Albertelli, M.; Stamnaes, J.; Sollid, L. M.; Khosla, C. Activation and inhibition of transglutaminase 2 in mice. *PLoS One* **2012**, *7*, e30.

72. Singh, J.; Petter, R. C.; Baillie, T. T.; Whitty, A. The resurgence of covalent inhibitors. *Nat. Rev. Drug Discov*. **2011**, *10*, 307-317.

73. Powers, J. C.; Asgian, J. L.; Ekici, O. D.; James, K. E. Irreversible inhibitors of serine, cysteine, and threonine proteases. *Chem. Rev*. **2002**, *102*, 4639-4750.

74. Metzler, D. E. Biochemistry: The Chemical reactions of living cells. 2nd Edition. **2003**. Elsevier (Academic Press).

75. Blobaum, A. L. Mechanism-based inactivation and reversibility: is there a new trend in the inactivation of cytochrome p450 enzymes? *Drug. Metab. Dispos*. **2006**, *34*, 1-7.

76. Sauvage, E.; Zervosen, A.; Dive, G.; Herman, R.; Amoroso, A.; Joris, B.; Fonzé, E.; Pratt, R. F.; Luxen, A.; Charlier, P.; Kerff, F. Structural basis of the inhibition of class A beta-lactamases and penicillin-binding proteins by 6-beta-iodopenicillanate. *J. Am. Chem. Soc*. **2009**, *131*, 15262-15269.

77. Yang, J.; Jamei, M.; Yeo, K. R.; Tucker, G. T. Rostami-Hodjegan A. Kinetic values for mechanism-based enzyme inhibition: assessing the bias introduced by the conventional experimental protocol. *Eur. J. Pharm. Sci*. **2005,** *26*, 334-340.

78. Malcomson, T.; Yelekci, K.; Borrello, M. T.; Ganesan, A.; Semina, E.; De Kimpe, N.; Mangelinckx, S.; Ramsay, R. R. cis-cyclopropylamines as mechanism-based inhibitors of monoamine oxidases. *FEBS J*. **2015** *282*, 3190-3198.

79. Sharma, U.; Roberts, E. S.; Kent, U. M.; Owens, S. M.; Hollenberg, P. F. Metabolic inactivation of cytochrome P4502B1 by phencyclidine: immunochemical and radiochemical analyses of the protective effects of glutathione. *Drug. Metab. Dispos*. **1997**, *25*, 243-250.

80. Leblanc, A.; Gravel, C.; Labelle, J.; Keillor, J. W. Kinetic studies of guinea pig liver transglutaminase reveal a general-base-catalyzed deacylation mechanism. *Biochemistry* **2001**, *40*, 8335-8342.

81. Folk, J. E. Mechanism of action of guinea pig liver transglutaminase. VI. Order of substrate addition. *J. Biol. Chem*. **1969**, *244*, 3707-3713.

82. Day, N.; Keillor, J. W. A continuous spectrophotometric linked enzyme assay for transglutaminase activity. *Anal. Biochem*. **1999**, *274*, 141-144.

83. Piper, J. L.; Gray, G. M.; Khosla, C. High selectivity of human tissue transglutaminase for immunoactive gliadin peptides: implications for celiac sprue. *Biochemistry* **2002**, *41*, 386-393.

84. Klöck, C.; Jin, X.; Choi, K.; Khosla, C.; Madrid, P. B.; Spencer, A.; Raimundo, B. C.; Boardman, P.; Lanza, G.; Griffin, J. H. Acylideneoxoindoles: a new class of reversible inhibitors of human transglutaminase 2. *Bioorg. Med. Chem. Lett*. **2011**, *21*, 2692–269.

85. Watts, R. E.; Siegel, M.; Khosla, C. Structure-activity relationships analysis of the selective inhibition of transglutaminase 2 by dihydroisoxazoles. *J. Med. Chem.* **2006***, 49,* 7493-7501.

86. Hausch, F.; Halttunen, T.; Mäki, M.; Khosla C. Design, synthesis, and evaluation of gluten peptide analogs as selective inhibitors of human tissue transglutaminase. *Chem. Biol*. **2003**, *10*, 225-231.

87. Choi, K.; Siegel, M.; Piper, J. .; Yuan, L.; Cho, E.; Strnad, P.; Omary, B.; Rich, K. M.; Khosla, C. Chemistry and biology of dihydroisoxazole derivatives: selective inhibitors of human transglutaminase 2. *Chem. Biol*. **2005**, *12*, 469-475.

88. Klöck, C.; Herrera, Z.; Albertelli, M.; Khosla, C. Discovery of potent and specific dihydroisoxazole inhibitors of human transglutaminase. *J. Med. Chem*. **2014**, *57*, 9042-64.

89. Gillet, S. M. F. G.; Pelletier, J. N.; Keillor, J. W. A direct fluorimetric assay for tissue transglutaminase. *Anal. Biochem*. **2005**, *347*, 221-226.

90. Pardin, C.; Gillet, S. M.; Keillor, J. W. Synthesis and evaluation of peptidic irreversible inhibitors of tissue transglutaminase. *Bioorg. Med. Chem*. **2006**, *14*, 8379-8385.

91. Marrano, C.; de Macédo, P.; Keillor, J. W. Evaluation of novel dipeptide-bound α,β-unsaturated amides and epoxides as irreversible inhibitors of Guinea pig liver transglutaminase. *Bioorg. Med. Chem*. **2001**, *9*, 1923-1928.

92. de Macédo, P.; Marrano, C.; Keillor, J. W. A direct continuous spectrophotometric assay for transglutaminase activity. *Anal. Biochem*. **2000**, 285, 16-20.

CHAPTER 1

Tissue transglutaminase inhibitors

1. Tissue transglutaminase (TG2) inhibitors

TG2 inhibitors can be included within two main groups:

1) Reversible inhibitors

2) Irreversible inhibitors

1.1. TG2 reversible inhibitors

These inhibitors have a temporarily action on enzyme activity, by not covalently blocking the active site of the enzyme, preventing the natural substrate to enter in it. Depending on both their chemical structure and the place where they act within the enzyme structure these inhibitors can be subdivided in two different series:

- competitive reversible inhibitors

- non-competitive reversible inhibitors

Both, competitive and non-competitive inhibitors, have different inhibition mechanism of action, and affect in a different way to the enzymatic activity.

1.1.1. Competitive reversible inhibitors

1.1.1.1. Acyl acceptor inhibitors (competitive amine inhibitors)

These sorts of inhibitors are probably the most used inhibitors of TG2 up to date. Some of the advantages that made them to be selected as useful inhibitors are the following: a) commercially available; b) chemically stable; and, c) non-toxic in living systems.[61]

These inhibitors are typically derivatives that include in their structure a medium to long saturated aliphatic chain bearing a terminal primary amine (**Figure 10**).[93]

Figure 10. General structure of competitive amine inhibitors

TG2 is inhibited by competition of these inhibitors with the natural amine substrates, such as lysine.[61] So, they block transamidation activity by acting as competitive primary amine substrates to finally being incorporated into the γ-glutamyl residue(s) of the peptide or protein substrate.[93]

Some of the mostly used amine competitive inhibitors are shown in **Figure 11**. Some shorter amines, such as hydroxylamine and methylamine, can also being used as amine substrates for the transamidation reaction of this enzyme.

Cystamine it is a very special inhibitor of TG2. It has been demonstrated to have different modes of inhibition. The structure of this diamine includes a sulfur bridge which can be reduced to its cysteamine form ($H_2NCH_2CH_2SH$ - 2-mercaptoethylamine), which has been shown to be a competitive TG2 inhibitor. Cystamine, has been shown to have time-dependent inhibition hypothesizing the formation of mixed disulfide bridges between active site Cysteine (Cys277) and cysteamine, but lucking at the same time of selectivity when applied to biological environments.[61,94]

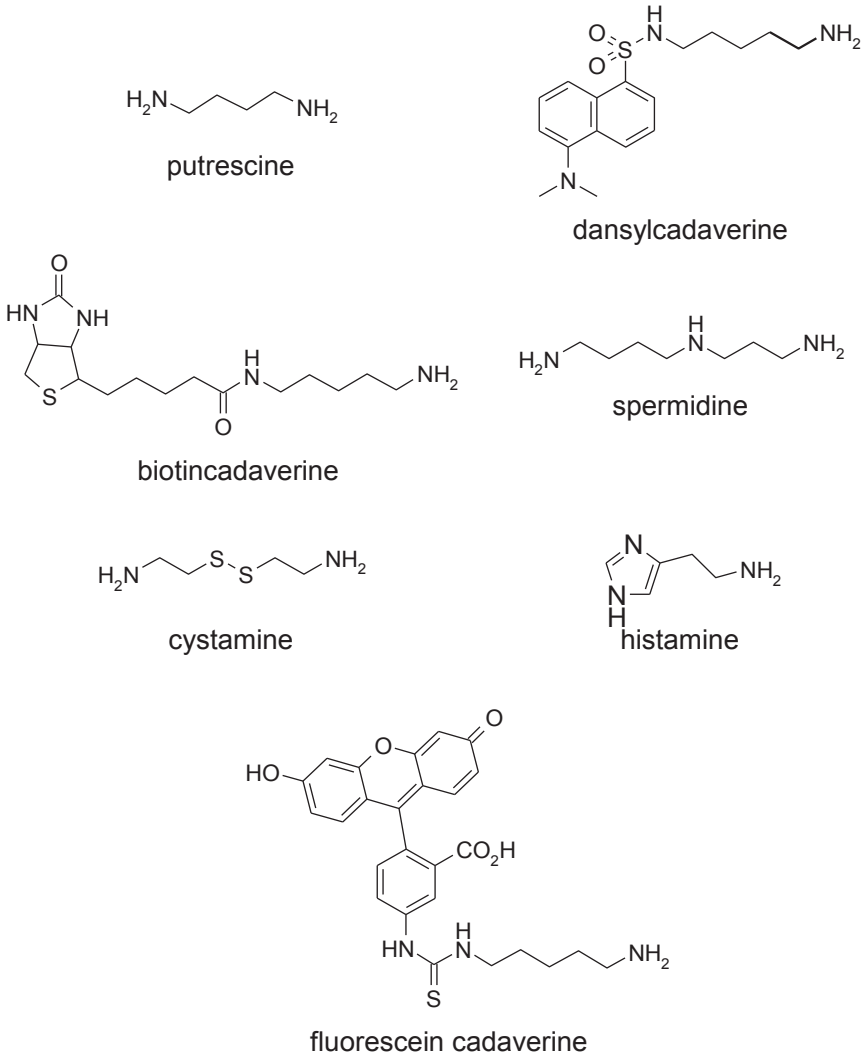

Figure 11. Structures for some of the existing acyl acceptor competitive inhibitors of TG2

Some of these acyl acceptor inhibitors of transglutaminases were extensively used as amine-competitive reversible inhibitors for the transamidation activity of transglutaminases including TG2. Their secondary substrate ability made them suitable to be included in detection systems for measuring the transglutaminase transamidation activity.[95-97] These transglutaminase reversible inhibitors have also been employed as

tools to understand the TG2 distribution and functions in biological systems in cell culture experiments.[98-100] It has also been reported the use of these inhibitors as lysine donors as tools for coagulation studies, such as dansylcadaverine and biotincadaverine, for the crosslinking of fusion plasma proteins, in this case, by the plasma protein FXIIIa.[101]

Furthermore, some of these inhibitors have intrinsic fluorescence; this is the case for dansylcadaverine and fluorescein cadaverine. Taking advantage of dansyl fluorescence property, Khosla et al.[102] introduced this moiety as part of the backbone structure in one inhibitor to understand the TG2 role in both normal and pathogenic conditions in mice. Dansylcadaverine has also being used as a permeable inhibitor with endocytic inhibition properties,[103] to study not only the in plasma pharmacokinetics transport of a drug, in a brain blood barrier cell culture model, but also to perform *in vivo* studies.

1.1.1.2. Acyl donor inhibitors

These kinds of inhibitors are competitive reversible inhibitors because they accommodate the acyl donor substrate-binding site, competing with the acyl donor substrate in the transamidation enzymatic reaction.[93]

- **Cinnamoyl-based inhibitors**

The synthesis of this kind of inhibitors was carried out from Pardin et al.[104] Different structure-activity relationship studies were carried out for this cinnamoyl derivatives, reaching low micromolar potency values, as for the compound **I** IC_{50} = 18 ± 1 μM (**Figure 12**).

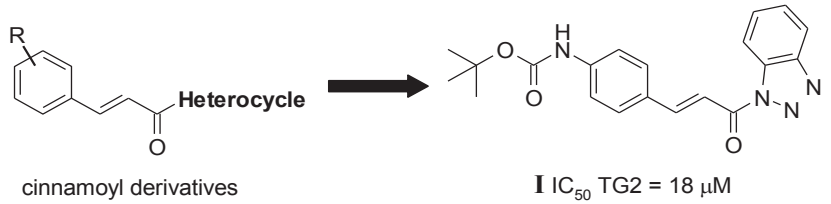

Figure 12. Cinnamoyl acyl donor competitive inhibitors scaffold structure, and the most potent derivative from this series, the cinnamoyl benzotriazolyl amide derivative **I** (TG2 IC_{50} = 18 μM)

Based on this cinnamoyl scaffold structure, novel inhibitors have been synthesized. Further studies[105] developed a photolabile derivative **II** with an IC_{50} of 28 μM, and the most potent inhibitor from these series, compound **CP4d**, with an IC_{50} of 2.1 ± 0.3 μM (K_I = 174 ± 48 nM), bearing a 4-nitrocinnamoyl scaffold (**Figure 13**).

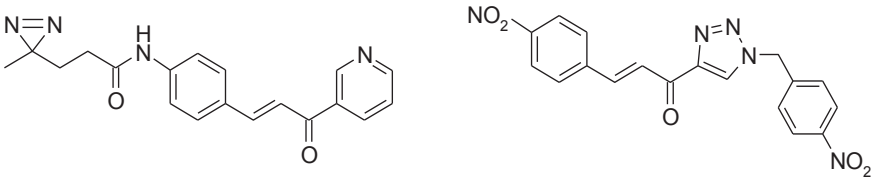

II IC_{50} TG2 = 28 μM

CP4d IC_{50} TG2 = 2.1 μM

Figure 13. Structures of the photolabile compound **II** and the **CP4d** cinnamoyl derivative, and their potencies (IC_{50}) for TG2 from the work of Pardin et al.[105]

1.1.2. Non-competitive reversible inhibitors

These inhibitors prevent enzyme activity by blocking substrate access to the active site without binding to the active site of the enzyme, but to the GTP binding site.[61] Many of the non-competitive inhibitors reported to date allosterically inactivate the enzyme by competing for the TG2 cofactor's binding sites (the guanosine nucleotides, GTP/GDP, and Ca^{2+} binding sites).

• Guanosine nucleotides

GTP (guanosine-5'- triphosphate) (**Figure 14**) is known to be a fundamental ligand of this protein, which allosterically regulates TG2 leading to a compact-close conformation of this protein, preventing its transamidation activity to happen.[12] The potency (IC_{50} value) of the guanine nucleotide on inhibiting the TG2 transamidase activity range from 300 nM to 6 μM.[18] Some non-hydrolysable GTP analogs, like GTPγS and GMP-PCP, have also been used as negative allosteric effectors for this enzyme. Based on the structure of the GTP guanine nucleotide, different substitutions in the tri-phosphate moiety will lead to the GTPγS and GMP-PCP analogs commented above (**Figure 13**).

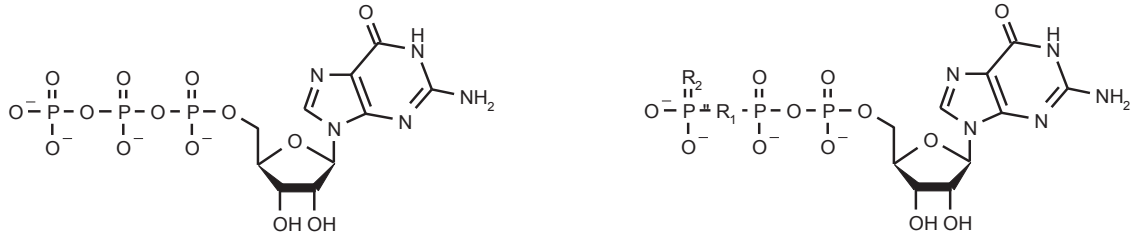

GTP

GTPγS R_1 = O, R_2 = S

GMP-PCP R_1 = CH_2, R_2 = O

Figure 14 Structure of the guanine nucleotide **GTP**, and the **GTP** analogs **GTPγS** and **GMP-PCP**

• Hydrazide-based inhibitors

Thieno[2,3-*d*]pyrimidinone acylhydrazide derivatives have been synthesized as allosteric non-competitive TG2 reversible inhibitors, based on a quinazolinone hydrazide scaffold.[106] As a representative of these inhibitors, the compound **LDN-27219** (**Figure 15**) have shown an IC_{50} of 0.6 μM ± 0.1 μM. In addition, Case and Stain[107] have kinetically analyzed this compound. These authors could conclude that

LDN-27219 has a slow binding mechanism of inhibition against TG2, and also that it competes with GTP for its binding site.[107]

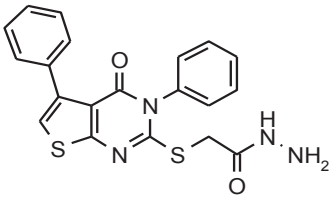

LDN-27219
IC_{50} TG2 = 0.6 μM

Figure 15. Structure of the acylhydrazine-based derivative **LDN–27219** and its potency (IC_{50}) for TG2

Nevertheless, it must be taken into account that this class of non-competitive reversible inhibitors can inhibit other members of the TG2 family (e.g. TG3 and TG5) by also binding to their guanine nucleotide binding site.[93,94]

• **Metals**

As it has been shown in the introduction, TG2 transamidation activity is also allosterically regulated by calcium ions. Divalent metals like Zinc (Zn^{2+}) can also compete for the Ca^{2+} binding site.[94]

• **Oxindole-based inhibitors**

Klöck et al.[84] designed a series of acylidene oxoindole derivatives based on the isatin structure (indoline-2,3-dione). Starting from the most simple acylidene oxoindole, compound **III** (IC_{50} = 11 μM), substitutions on the oxoindole ring and the ketone moiety lead to the most active compounds (compound **IV**, **V**, and **VI**) with IC_{50} values below 1 μM (**Figure 16**). Several kinetic studies were also carried out for some of these derivatives in order to study their mechanism of inhibition. The kinetic data suggested that these compounds have a non-competitive reversible mode of action against TG2 using a GHD-coupled enzymatic assay for some derivatives.[84] This non-competitive inhibition character, classifying these inhibitors as allosteric modulators of TG2 activity, was later observed by Yi et al.[108] employing the same enzymatic assay. K_I values for compounds **III**, **V** and **VI** were established in 10,[84] 47,[108] and 1.3 μM[84] respectively.

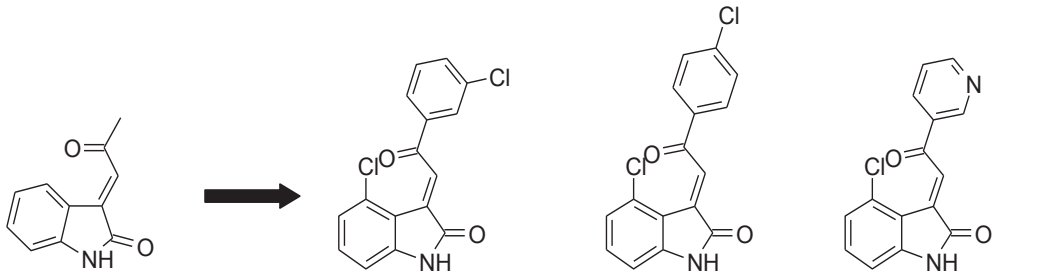

III IC_{50} TG2 = 11 μM
K_I= 10 μM

IV IC_{50} TG2 = 0.7 μM

V IC_{50} TG2 = 0.8 μM
K_I = 47 μM

VI IC_{50} TG2 = 0.9 μM
K_I= 1.3 μM

Figure 16. Structures of the acylidene oxoindole derivatives **III**, **IV**, **V** and **VI**, and their potencies (IC_{50}) and inhibition kinetic parameters (K_I) for TG2

• **Tyrphostin 47**

Studies to identify novel inhibitory compounds by the screening of libraries have been carried out by Lai et al.[109] High-throughput screening assays of two different libraries of pharmacologically active compounds, LOPAC (1,280 cpds, Sigma-Aldrich) and Preswick (880 cpds, Prestwick Chemical) have been performed. Several compounds were identified as TG2 inhibitors in vitro in the presence of Ca^{2+} (active site exposed TG2) and bioactive in vivo, suggesting that these inhibitors could serve as new scaffolds for the synthesis of new TG2 inhibitory compounds for the treatment of neurodegenerative disorders.

Among these compounds, **Tyrphostin 47** (T7540) was reported to compete for the GTP-binding, and the Tyrphostin 47-treated TG2 became protease resistant (partially protected from proteolysis) in a similar way as TG2 is when GTP is bound to its binding site (because of its TG2 closed-inactive conformation). **Tyrphostin 47** was reported to have an IC_{50} value of 3 μM. Nevertheless, the same compound was found to be 10-fold less potent (IC_{50} of 45 μM) in the work carried out by Schaertl et al.[110] when the reducing agent dithiotreitol (DTT) was present in the activity assay (**Figure 17**).

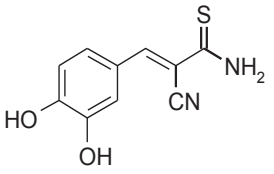

Tyrphostin 47 IC_{50} TG2 = 45 μM[110]

Figure 17. Structure of inhibitor **Tyrphostin 47**, and its potency (IC_{50}) for TG2 based in the assay conditions carried out in the work from Schaertl et al.[110]

1.2. TG2 irreversible inhibitors

A lot of efforts have been made for the synthesis of potent and selective TG2 irreversible inhibitors in the recent years. The main objectives for the synthesis of these irreversible derivatives are both, to reach at high potency levels against TG2 as well as a good selectivity profile for the other transglutaminases isoforms, thus not affecting the transamidation activity of the other catalytically active TG members. Based on the above mentioned objectives, different Cys277 active site-directed TG2 inhibitors with different electrophilic warheads were synthesized.[93,94]

Irreversible inhibitors will act by blocking the enzyme active site by formation of a covalent bond with the thiol group of Cys277 present in the TG2 active site, this way permanently avoiding TG2 transamidation activity to occur. For this purpose, the reactive warheads of these molecules can include α,β-unsaturated amide (acrylamide), epoxide, maleimide, 3-halo-4,5-dihydroisoxazole (DHI), 6-diazo-5-oxo-norleucine

(DON), halomethyl carbonyl, sulfonium, imidazolium and also α,β-unsaturated carbonyl moieties.

Herein the different TG2 irreversible inhibitors synthesized so far will be described in the next paragraphs from this chapter.

• α,β-unsaturated amides based inhibitors

Compounds bearing α,β-unsaturated amides have been described as irreversible inhibitors for cysteine proteases.[73] This warhead is a Michael acceptor, who will be attacked by the thiol group of the active-site cysteine undergoing a Michael Addition reaction (**Scheme 14**). Knowing that TG2 has a active site-cysteine residue (Cys277), a battery of compounds bearing an acrylamide group were synthesized as promising inhibitors for this enzyme.

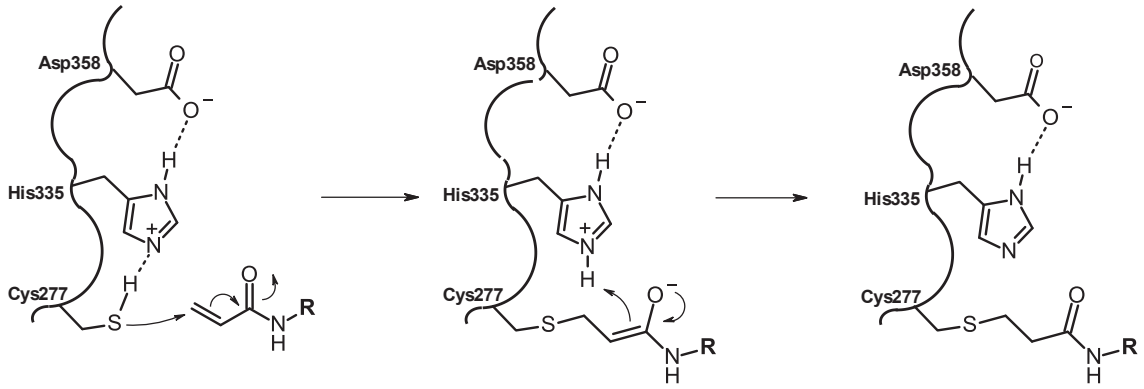

Scheme 14. The proposed mechanism of inactivation of the thiol from the active site Cys277 of TG2 by acrylamide-based inhibitors

TG2 inhibitors bearing this α,β-unsaturated amide can be subdivided in three groups: a) phenyl acrylamide-based inhibitors, b) piperidine acrylamide-based inhibitors, and c) alkyl acrylamide-based inhibitors.

a) Phenyl acrylamide-based inhibitors

Knowing the association of TG2 in Hungtington's disease,[15,45] the searching for a promising drug candidates for the treatment of this disease has been the objective in the work carried out by Wityak et al.[111] (CHDI Foundation-Evotec). Different SAR studies were carried out in order to achieve a desired inhibitor with: 1) high potency against TG2 (*in vitro* assays, inhibition tests for both recombinant TG2 and cellular lysates); 2) high selectivity against the other active isoforms from the transglutaminase family (TG1, TG3, and FXIIIa); 3) a good drug metabolism and pharmakokinetics (DMPK) profile; and 4) a good efficacity to pass through the Blood-Brain Barrier (BBB).

The starting point from this study was the SAR study of different substitutions on the phenyl moiety from a simple phenylacrylamide scaffold. From the different derivatives synthesized, the compound **VII** (**Figure 18**), possesed a key characteristic to continue

with the synthesis of the next series of derivatives (acrylamide CO-NH group was suggested by docking studies to interact via hydrogen bonding with the side chains of Trp241 (NH) and Gln276 (CO)). In addition, molecular docking studies also suggested that the sulfonyl moiety from this compound was observed to interact with the Asn333 from the TG2 active site. This interaction will place the inhibitor in a way that will allow it to enter and interact with the TG2 lipophilic region within its active site (also increasing the selectivity regarding the differences in aminoacid residues shared between the other TG within their lipophilic pocket).

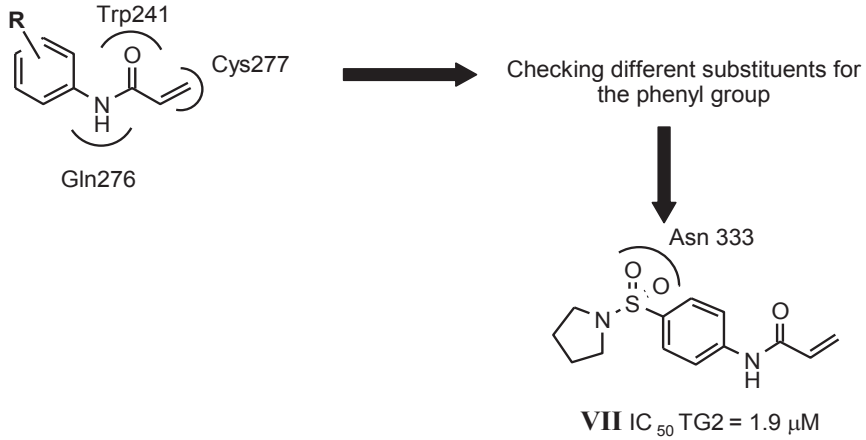

Figure 18. SAR strategy followed in the work of Wityak et al.[111]Structures for the starting point of this SAR studies, the phenylacrylamide scaffold, and compound **VII** from the same work[111] are represented. The interaction of the different chemical groups presented within these structures, with some key aminoacids within the active pocket from TG2 (acrylamide interactions with the Cys277, hydrogen bond interactions with Trp241, Gln276 and sulfonyl interaction with Asn333), based on docking studies in the work, are also represented

Based on these findings, Wityak et al.[111] carried out SAR studies by replacing the pyrrolidine heterocycle to a piperazine, leading to different sulfonamides substituted at the N-4 position of the piperazine in order to reach the lipophilic region within the TG2 active pocket. This SAR study finally lead to a highly potent compound **VIII** (**Figure 19**), with an IC_{50} of 10 nM against TG2, and a good selectivity of 3.4, > 80, and 0.18 μM for TG1, TG3 and FXIIIa, respectively. The compound **VIII** was also used in cell lysates inhibition studies (KET-TG2 cells), reaching an IC_{50} of 0.77 μM. Regarding the different DMPK studies, the compound **VIII** showed a low half-live ($t_{1/2}$) in mouse plasma of 248 min, a poor solubility in aqueous solution (0.01 mg/mL) and a poor to moderate permeability in Caco2 (human colon epithelial cancer cell line) bidirectional assay with an apparent permeability coefficient (P_{app}) (A-B) = 102 nm s^{-1} and a P_{app} (B-A) = 193 nm s^{-1}.

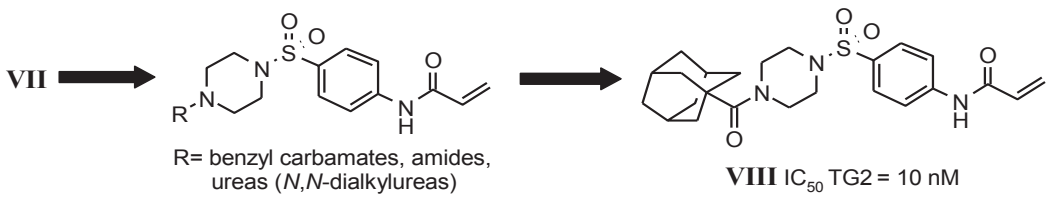

Figure 19. General scaffold for the next set of inhibitors derived from compound **VII** from the work of Wityal et al.[111] The most potent derivative of this series,compound **VIII**, and its potency (IC_{50}) over TG2, are also described

b) Piperidine acrylamide-based inhibitors

Owing to the poor plasma stability of the phenylacrylamide-based compounds,[111] a different approach for the development of TG2 inhibitory compounds was carried out by Wityak et al.[112] Therefore replacing the phenylacrylamide-based warhead[111] (**Figures 18** and **Figure 19**), by different heterocyclic-based warheads was performed. The starting point for the SAR study was then focused on a 4-aminopiperidinyl moiety whose shape and size seems appropriate to allow the acrylamide to reach the Cys277 within the TG2 catalytic tunnel, as well as replacing the benzylcarbamate moiety with different aryl alkylamides (and different arylamides) in order to reach the lipophilic pocket of TG2 (**Figure 20**).

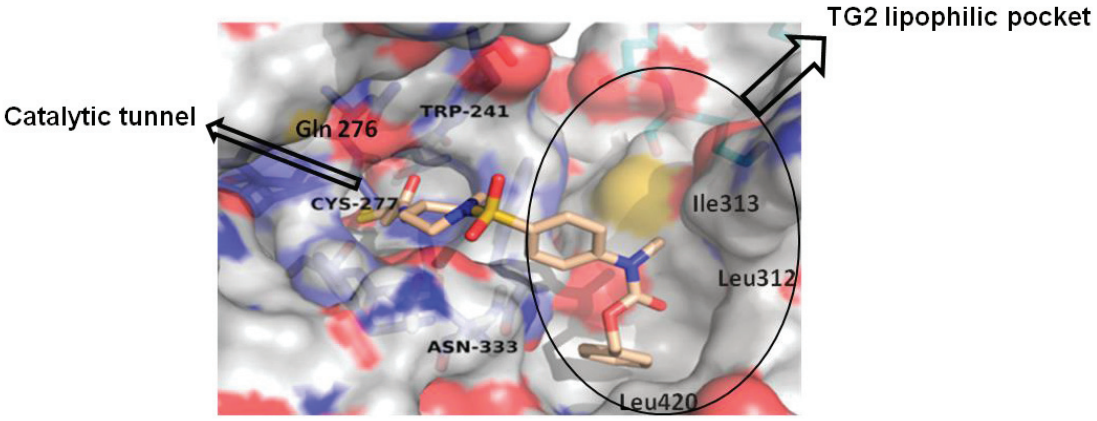

Figure 20. Image of the TG2 active site obtained from the docking studies of compound **IX**.[112] The acrylamide interaction with Cys277 within the catalytic tunnel of TG2 active site, and the orientation of the rest of the molecule within the lipophilic pocket (black circle) are represented. Key aminoacids are identified in bold characters, and compound **IX** is represented in cyan. The negatively charged residues of the TG2 active site surface are represented in red, and blue for the positively charged residues (Figure adapted from reference 112)

Furthermore, docking studies suggested aminopiperidine to be the best structure to help also the sulfonyl moiety to interact closely with Asn333 side chain in order to best fit the rest of the molecule within the TG2 lipophilic pocket, as in the case of compound **IX** (IC_{50} TG2 = 0.28 μM) (**Figure 21**).

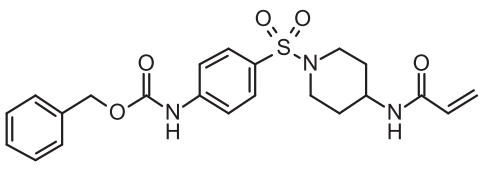

IX IC_{50} TG2 = 0.28 μM

Figure 21. Structure of derivative **IX** and its potency (IC_{50}) over TG2

SAR studies were focused on three different steps, regarding the inhibitor's structure (phenylacrylamides) from their previous work:[111] **a**) replacements at the level of the anilide moiety; **b**) substitutions at the phenethyl amide moiety; and **c**) substitutions around the benzene terminal ring (**Figure 22**). The TG2 inhibitors developed in this study are not as potent as the ones from their previous work,[111] since the IC_{50} TG2 from the best compound **X** is 0.110 μM (**Figure 22**). On the other hand, the majority of these new compounds synthesized were profiled in *in vivo* studies and showed good stability in both human and mouse plasma, with a half-life ($t_{1/2}$) > 6 h for compound **X (13)**, and a $t_{1/2}$ that exceeds 24 h for some others. Furthermore, when testing the molecules in the presence of the nucleophilic cellular antioxidant gluthatione (GSH) *in vitro* over a period of 120 h, compounds showed no evidence of conjugation (low GSH reactivity). On the contrary, compounds showed moderate permeability and a high P-gp active efflux, indicating that these molecules are not effective agents for the treatment of neurodegenerative disorders as they must pass through the BBB membrane to reach their target for *in vivo* purposes.

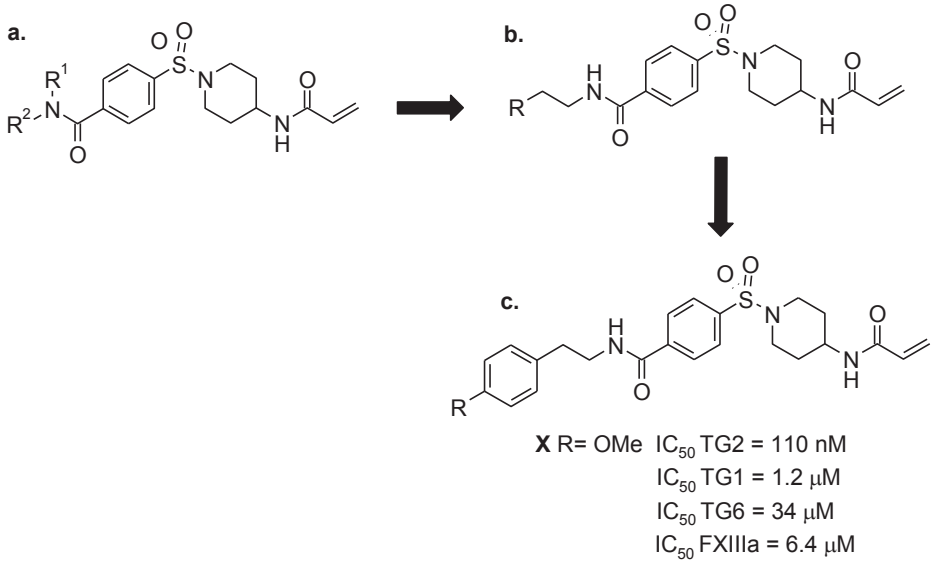

Figure 22. Different steps of the SAR studies conducted in the work of Wityak et al.[112]: **a**, replacements at the level of the anilide moiety; **b**, substitutions at the phenethyl amide moiety; and **c**) substitutions around the benzene terminal ring. The structure of compound **X,** its potency (IC_{50}) over TG2 and its selectivity profile for other TG are described

c) Alkyl acrylamide-based inhibitors

Based on the well-known structure from the dipeptide Cbz-GluGly, an acyl donor substrate for TGases, a new series of compounds has been synthesized by Keillor et al.[113] Glutamine was replaced by an alkyl chain ended in the acrylamide moiety. Efforts have been adressed to change the lenght (2 to 4 methylene units) of the alkyl side chain, to finally end up in the acrylamide group. Keillor et al.[91] observed an increase in the efficiency of the inhibitors related to an increase in the number of carbons of the alkyl

chain. It was also noteworthy that the removal of the bulky *tert*-butyl ester to yield the *tert*-butyl free glycine carboxylic acid, compound **XI**, results in the best inhibitory efficiency from all compounds of this serie (k_{inact}/K_I = 3000 $mM^{-1}min^{-1}$) (**Figure 23**).

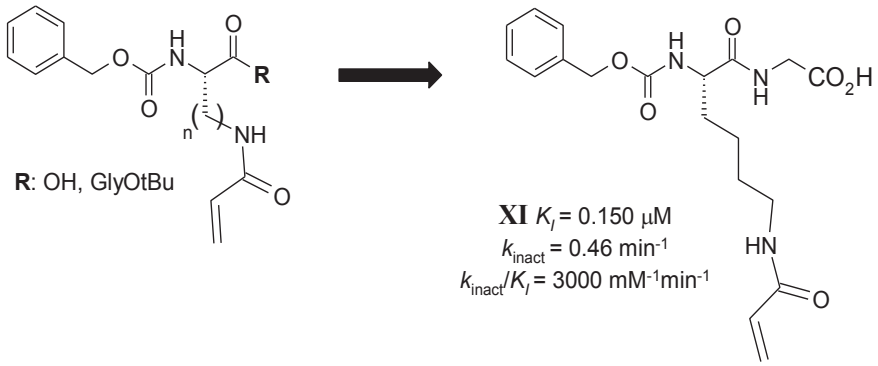

Figure 23. On the left, the general scaffold for the alkyl acrylamide derivatives developed in the work of Keillor et al.,[113] where differences in the lenght of the alkyl side chain (number of methylene units), and modifications in the carboxylic moiety were introduced. On the right, the structure of compound **XI** and its inhibition kinetic parameters (K_I, k_{inact}, and k_{inact}/K_I) for TG2[91]

Some other syntheses by Keillor et al.[90] were developed from a Cbz-phenylalanine moiety scaffold. An increase in carbon lenght of the alkyl linker between a phenylalanine and the inhibitor's acrylamide warhead was also related with an increase in the inhibitor's efficientcy against TG2. The best compounds **XII** and **XIII** have K_I and k_{inact}/K_I values of 4.5 μM and 0.080 $\mu M^{-1}min^{-1}$ and 3.5 μM and 0.109 $\mu M^{-1}min^{-1}$, respectively (**Figure 24**).

On the other hand, in a different work from Keillor et al.,[114] a dansyl labeled compound **NC9** was synthesized based on the Cbz-Lys(Acr)Gly scaffold already described before,[113] with a sustantially addition of a polyethylenglycol (PEG) moiety between dansyl and lysine residue. These changes will allow the fluorescence visualization of the probe in cell culture systems (e.g., to elucidate the role of TG2 and other TG isoforms in the production of collagenous extracellular matrix), but a loss of two orders of efficiency for TG2 inhibition (K_{inact}/K_I values decreased significantly from his parental molecule) was observed (**Figure 24**). This inhibitor was not only used for the localization of TG2 but it also demonstrated to target Factor XIIIa in MC3T3-E1 osteoblast cell cultures.[115]

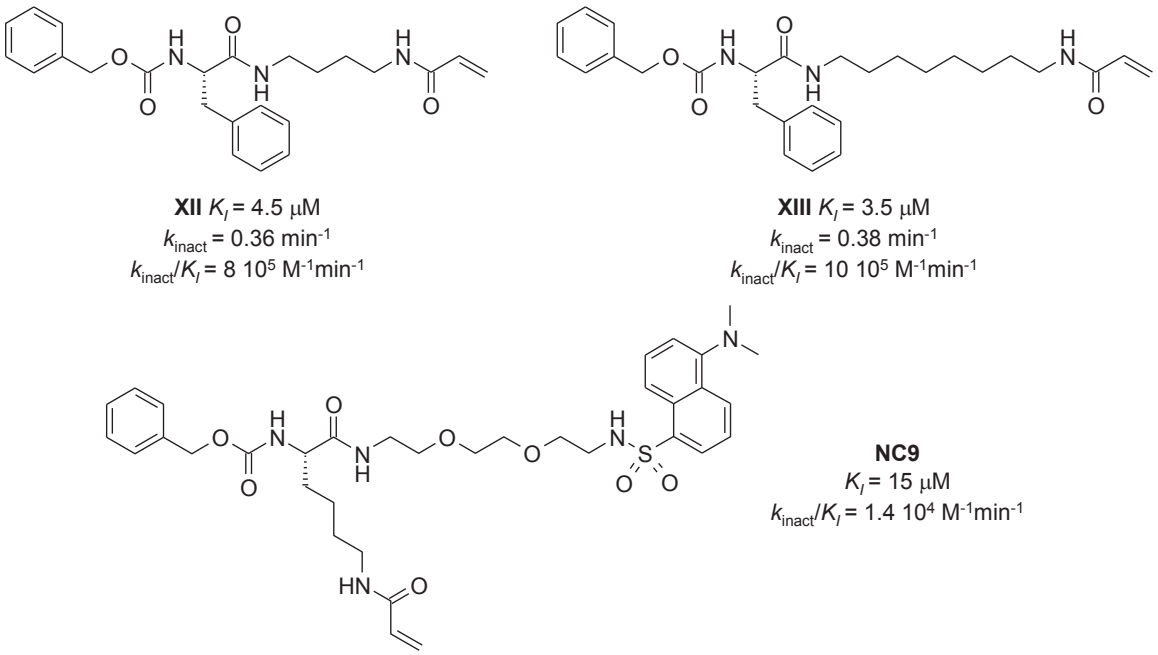

Figure 24. Structure of compounds **XII**,[90] **XIII**,[90] and **NC9**[114] and their respective inhibition kinetic parameters (K_I, k_{inact}, and k_{inact}/K_I) for TG2

With the objective of reaching a promising drug candidate for the treatment of Hungtington's disease, Wityak et al.[116] developed a series of lysine-based inhibitors. Using compound **XIV** as reference molecule,[91] SAR studies were performed (**Figure 25**). Efforts were adressed to improve the ADME profile focused on permeability, drug metabolism (mLM in mouse liver microsomes test), and potency of the drug candidate. In an attempt to reach these goals, the followed strategy consisted on lowering the polar surface area (PSA), the number of rotable bonds, and the number of hydrogen donors from the reference molecule structure.

ADME profile was first investigated for compound **XIV** (TG2 IC_{50} of 3.1 μM), demonstrating good solubility but also a low permeability potential with efflux, and rapid metabolism in mouse liver microsomes (mLM). These characteristics were observed as an impediment to pass through the Blood-Brain Barrier (BBB) for the *in vivo* purpose of treating Hungtington's disease. Further analysis of compound **XI** from the same work of reference[91] revealed lower PSA, equipotency relative to compound **XIV** (TG2 IC_{50} of 2.7 μM), in addition to its low molecular weight, making it a better starting point for te SAR studies than **XIV**. Keeping the Cbz of its structure (replacing Cbz lead to a loss of potency), they focused on replacing the carboxylic acid from **XI** with several tertiary amides.

Compound **XV** turned out to be the compound which best fits with the selected criteria of this study (**Figure 25**). Replacing the carboxylic acid with a 4-*N*-piperazinyl-2-chlorobenzyl moiety, this compound has a reasonable IC_{50} for TG2 of 0.062 μM, a good selectivity profile against other TG isoforms (IC_{50} values of 12.9, >80, 69, and 67 μM against TG1, TG3, TG6, and FXIIIa respectively), with good solubility and a good

plasma stability in both human and mouse plasma ($t_{1/2}$ = > 24 h). Furthermore, no conjugation to the natural thiol nucleophilic antioxidant gluthatione (GSH) when tested *in vitro* over a period of 68 h. This compound also has a high rate permeability, but its fast efflux rate (MDCK-MDR1 transfected cell lines P-gp eflux test) make it not suitable as an *in vivo* drug candidate for the treatment of Hungtington's disease.

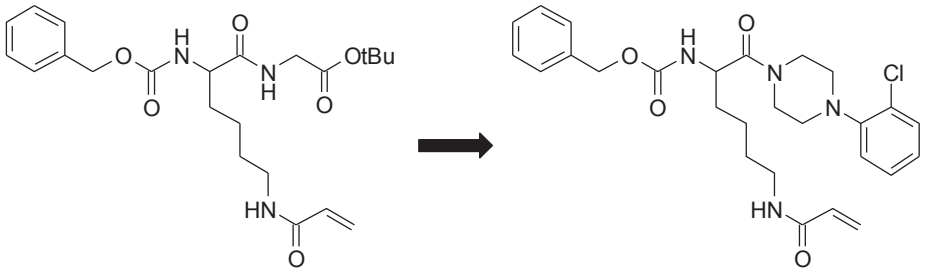

XIV IC_{50} TG2 = 3.1 μM **XV** IC_{50} TG2 = 0.062 μM

Figure 25. Structures of the reference compound **XIV**,[91] and compound **XV**, and their potencies (IC_{50}) over TG2 from the work of Wityak el at.[116]

Another series of acrylamide-based inhibitors have been synthesized, recently, by Griffin et al.[117] Based on a general structure bearing a *N*-(2-oxo-2-piperazin-1-yl-ethyl)prop-2-enamide scaffold, SAR studies have been developed introducing different substituents in its carbamate region (**Figure 26a**). At the **R** position different aralkyl, heterocyclic, cycloalkyl and alkyl groups were introduced in the inhibitors structure. The most potent inhibitor **EB1-155**, have an IC_{50} value in the low nanomolar range against TG2 (IC_{50} = 6.1 nM), and also showing a good selectivity profile against other TGs (**Figure 26b**).

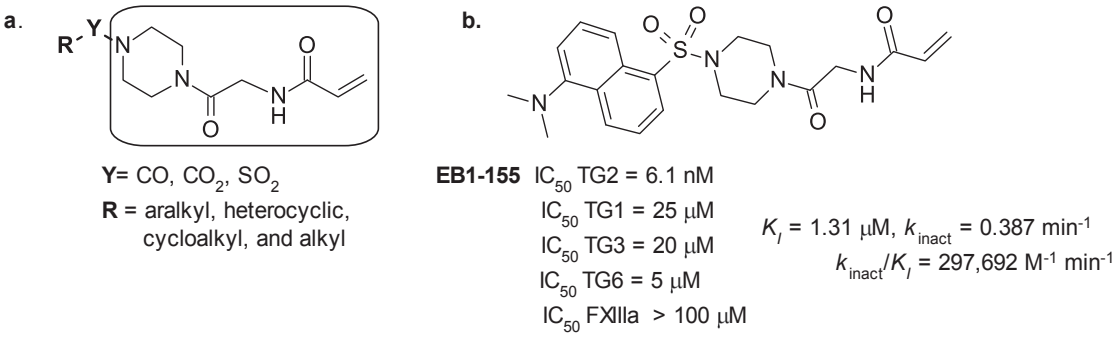

Figure 26. **a**, general scaffold for the SAR studies carried out by Griffin et al.[117]; and **b**, structure of derivative **EB 1-155**, its potency (IC_{50}) over TG2 and their selecivity profile over other TG

• α,β-unsaturated carbonyl-based inhibitors

Another kind of peptidic-based inhibitors bearing an α,β-unsaturated carbonyl warhead as electrophilic Michael acceptor have been developed by Zedira GmBH. As a representative of this serie the inhibitor **Z013** (also called **ZED754**), whose peptidic-based structure is shown in **Figure 27**, has an IC_{50} value of 200 nM over TG2. **Z013** has

been studied at the molecular level. By means of mass spectrometry studies, it was revealed a covalent mode of binding of the inhibitor with Cys277 in the TG2 active-site. Further co-cristallization (**Z013** and TG2) and X-ray analysis have demonstrated that **Z013** mimics the gluten peptide substrates on the way of interaction with the TG2 active site.[118]

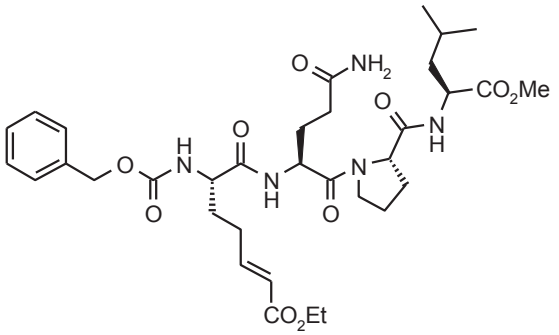

Figure 27. Structure of the TG2 inhibitor **Z013** from ZEDIRA GmbH[118] and its potency (IC_{50}) over TG2

From **Z103**, different inhibitors bearing the same warhead have been synthesized.[119] The best compounds **ZED1098**, **ZED1219**, and **ZED1227** (**Figure 28**) have IC_{50} values against TG2 of 32, 25, and 45 nM, respectively. The selectivity profile against other transglutaminases has also been calculated in terms of IC_{50} for these three compounds (**Table 3**). *In vivo* studies for these three compounds revealed no signs of toxicity in rat (50 mg drug/kg bodyweight), and moderate toxicologic effects in histopahology.[120]

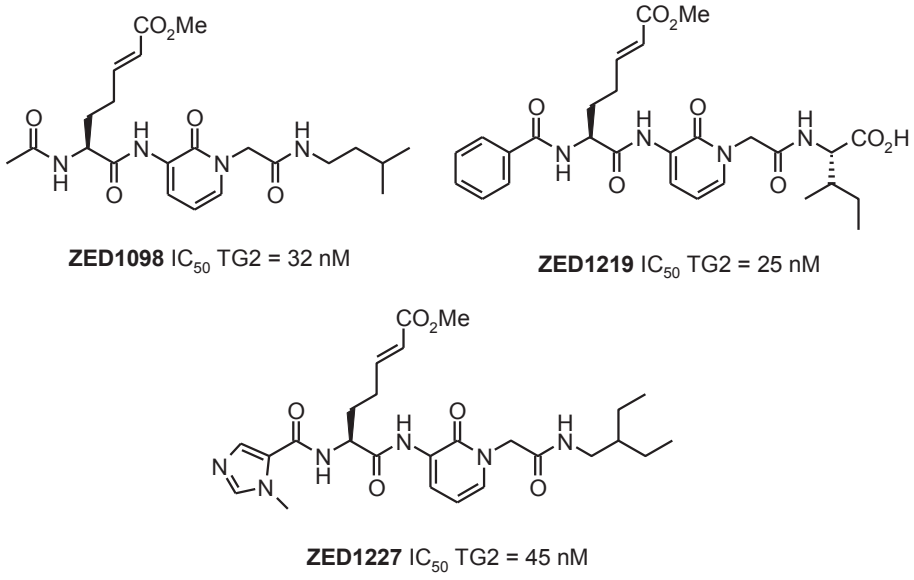

Figure 28. Structure of the TG2 inhibitors **ZED1098**, **ZED1219**, and **ZED1227,** and their potency (IC_{50}) over TG2

IC_{50} (nM)	TG1	TG3	TG6	FXIIIa
ZED1098	200	175	75	230
ZED1219	195	224	55	800
ZED1227	240	340	145	410

Table 3. Selectivity profile against TG1, TG3, TG6 and FXIIIa for TG2 inhibitors **ZED1098**, **ZED1219** and **ZED1227** from ZEDIRA GmbH[119,120]

• Epoxide- and maleimide-based TG2 inhibitors

Different maleimides and epoxide-based inhibitors were developed.[91,113,121] The mechanism of inhibition of cystein-active site enzymes with the electrophilic epoxide-based and the maleimide-based warheads leading to the inactive form of the enzyme are represented in **Scheme 15** (**a** and **b**, respectively).[73]

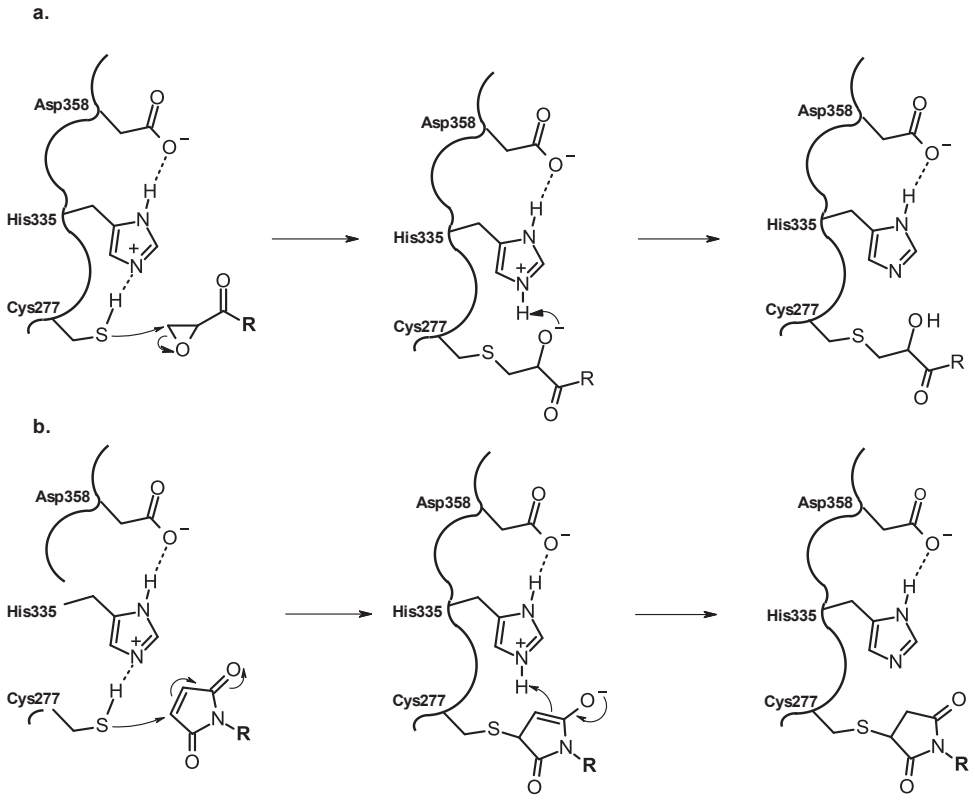

Scheme 15. Proposed mechanism of inactivation of the thiol from the active site Cys277 of TG2 by epoxide-, and maleimide-based inhibitors. **a**, representation of the mechanism of inhibition for the epoxide-based TG2 inhibitors; and **b**, representation of the mechanism of inhibition of maleimide-based TG2 inhibitors

These inhibitors were based on a Cbz-protected amino acid scaffold with variations on the carbon side chain lenght and different replacements at the carboxylic acid moiety (**Figure 29**). These dipeptides are analogs from the widely used transglutaminases substrate Cbz-Gln-Gly, already employed for the alkyl acrylamide-based inhibitors.[91,113]

The best efficiency against TG2 was observed with an increase in the methyl side chain for both series of inhibitors. Regarding the different replacements at the carboxylic acid moiety, Benzyl ester moiety resulted in a greater efficiency for the maleimide-based inhibitors, lossing up to 2-20-times the efficiency when an amino acid was included in their structures. The compound **XVI** was the most potent of the maleimides with an efficiency value (k_{inact}/K_I) of 17 mM^{-1} min^{-1} (**Figure 29**).

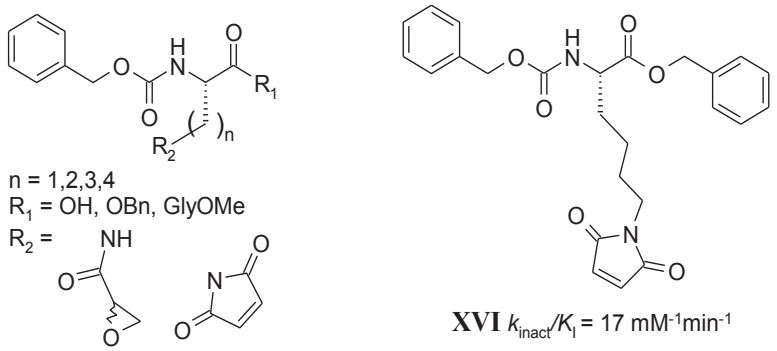

Figure 29. On the left, the general scaffold followed for the SAR studies of the epoxide-, and the maleimide-based inhibitors. On the right, the structure of the maleimide-based TG2 inhibitor **XVI,** and its eficiency on inactivating TG2 (k_{inact}/K_I)

On the other hand, epoxide-based inhibitors bearing either a C-terminal Boc protected Gly or a non C-terminal protected Gly increased affinity (K_I) of the inhibitors against TG2, even showing better specificity values when free-additional glycine amino acid structure was tested. The compound **XVII** was the most potent with K_I and k_{inact}/K_I values of 0.28 μM and 2.03 $\mu M^{-1}min^{-1}$, respectively (**Figure 30**).

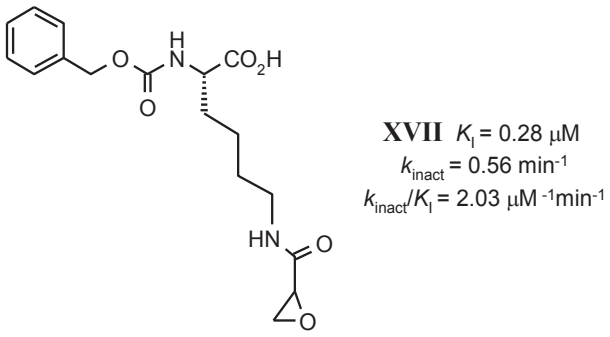

Figure 30. Structure of the epoxide-based TG2 inhibitor **XVII**, and its inhibition kinetic parameters (K_I, k_{inact}, and k_{inact}/K_I) for TG2

• 3-Halo-4,5-dihydroisoxazole-based inhibitors

Promising TG2 irreversible inhibitors have been synthesized bearing an electrophilic warhead based on the 4,5-dihydroisoxazole (DHI) ring (**Figure 31**). The discovery of the amino acid antibiotic acivicin, which mimics the glutamine donor and irreversibly inactivates another ɣ-glutamine transferase (anthranilate synthetase; also with an active-site cysteine), arouse interest in the synthesis of inhibitory compounds based on the DHI structure (**Figure 31**).[122]

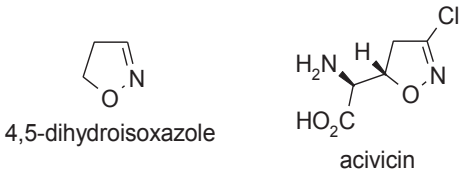

Figure 31. Structures of the 4,5-dihydroisoxazole ring (left) and the natural occurring aminoacid acivicin (right)

The mode of action of 3-halo-4,5-dihydroisoxazole inhibitor has been proposed to occur via the nucleophilic attack of thiol of Cys277 on electrophilic imino-halogen site of the dihydroisoxazole ring (**Scheme 16**), then displacement of the halogen (X) lead to the formation of the covalent bond (iminothioether adduct).[85] These inhibitors were demonstrated to covalently interact with the Cys277 form the TG2 active site by means of mass spectrometry in the work from Watts et al.[85]

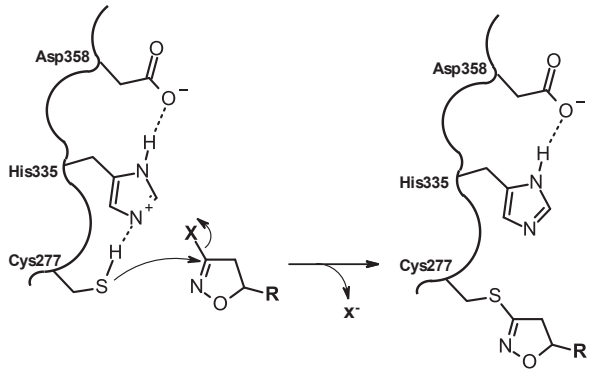

Scheme 16. Proposed mechanism of inactivation of the thiol from the active site Cys277 of TG2 by 3-halo-4,5-dihydroisoxazole-based inhibitors

Some of the efforts to synthesize derivatives bearing this warhead moiety were carried out by Hausch et al.[86] The peptidic sequence which have been used as scaffold in this work was the proteolitically resistant consensus sequence Pro-Gln-Pro-Gln-Leu-Pro-Tyr (highlighted the reactive glutamine), which is found in many gluten proteins, and also reported to be a exceptionally good substrate of human TG2 (**Figure 32**). These compounds were designed containing the inhibitory residue acivicin as warhead instead of the reactive Gln in their structure, thus becoming valuable probes of celiac disease pathogenesis (**Figure 27**).

The resulting inhibitors improved the specificity up to 100-fold over TG2 when compared to the natural occurring aminoacid acivicin, owing to the tripeptidic flanking sequences (Pro-Gln-Pro and Leu-Pro-Tyr). The compound **XVIII** is the most potent DHI-based inhibitor from this serie with an efficiency value (k_{inact}/K_I) of 18 $M^{-1}min^{-1}$ and a K_I value of 7.8 10^{-4} M (**Figure 32**).

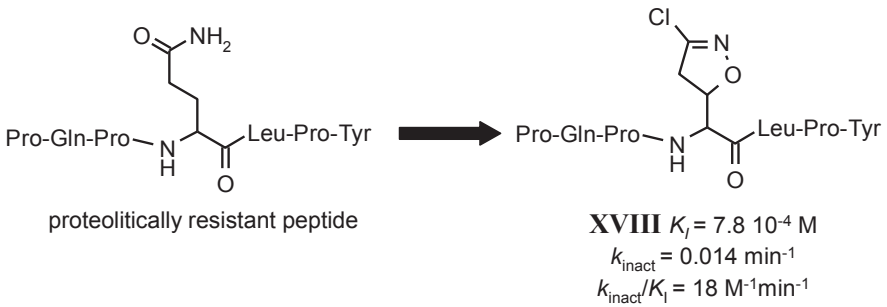

Figure 32. On the left, the proteolitically resistant consensus sequence found in gluten peptides used as scaffold for the development of TG2 inhibitors.[86] On the right, the structure of the TG2 inhibitor **XVIII**, and its inhibition kinetic parameters (K_I, k_{inact}, and k_{inact}/K_I) for TG2

In a separate work Choi et al.[87] developed a different series of DHI-based inhibitors with a dipeptide scaffold where the chlorine atom was substituted by a bromine on the 4,5-dihydroisoxazole ring. Optimization studies regarding the amino acid side chain, the dihydroisoxazole ring stereochemistry, and different variations at the carbamate group moiety led to the well-known TG2 inhibitor **KCC009** (**Figure 33**).[85,87] This inhibitor was also used in a murine glioblastoma tumor model,[42,64] improving the treatment in combination with the chemotherapeutic agent carmustine (BCNU), inducing apoptosis in glioblastoma cells, and also reducing the tumor size. It was also shown good oral bioavailability and low toxicity in *in vivo* studies.[85] **ERW1041E** has been prepared by Watts et al.[85], replacing both the tyrosine aminoacidic residue from the **KCC009** inhibitor by a (S)-proline and the Cbz-carbamoyl moiety by a quinolyl moiety (**Figure 33**). This compound was also tested *in vivo* and it could inhibit intestinal TG2 in mice.[70]

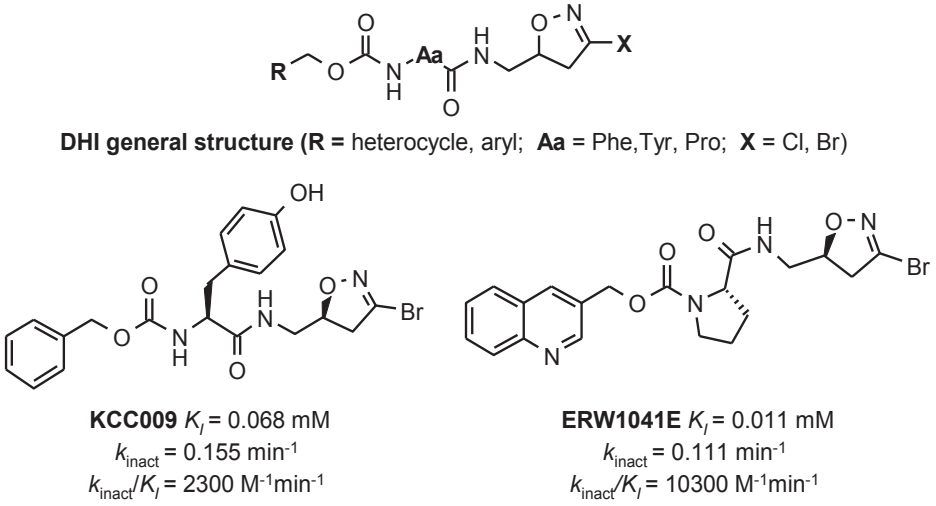

Figure 33. At the top, the dipeptidic general scaffold from the work of Choi et al.[87] At the bottom, the structures of the derivatives **KCC009**[85,87] (left) and **ERW1041E**[86] (right), and their respective inhibition kinetic parameters (K_I, k_{inact}, and k_{inact}/K_I) for TG2

Some other DHI ring-based derivatives conjugated with azide and alkynyl groups have been synthesized by Dafik et al.[62] The importance of these groups, is based on their ability to undergo click reactions inside living systems in order to be covalently modified with fluorophores. These features have allowed to visualize transiently

catalytically activated TG2 in cellular assays once the TG2 inhibitor covalently bonds to the enzyme active site (e.g., in WI-38 fibroblast scratch assay).

Finally, inhibitors including tryptophan in their structure seemed to be more potent that those which include a tyrosine. Regarding the bioorthogonal groups employed, in general, alkynyl-DHI inhibitors seemed moderately less potent that the ones with the azido group. The compound **XIX** is the most active TG2 inhibitor from this series (**Figure 34**).

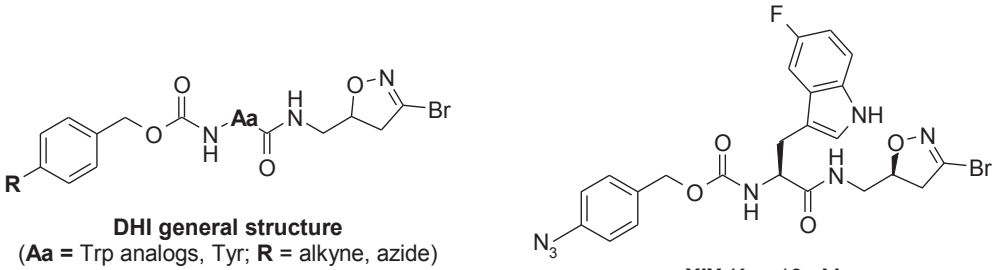

Figure 34. On the left, the general scaffold from the work of Dafik et al.[62]. On the right, the structure of alkynyl derivative **XIX**, and its inhibition kinetic parameters (K_I, k_{inact}, and k_{inact}/K_I) for TG2

• 6-Diazo-5-oxo-norleucine (DON) - based inhibitors

6-diazo-5-oxo-norleucine (DON) is a naturally occuring antibiotic isolated from Streptomices strains, that has the ability of potent inhibit ɣ-glutamyl traspeptidase (GGT), which catalyzed a similar transamidation reaction as TG2 does.[86] The diazoketone group has been well described as a inhibitory motif for cysteine proteases.[123] Providing a peptidic scaffold derived from a gluten peptide (Ac-Pro-Gln-Pro-Gln-Leu-Pro-Tyr-NH_2, reactive glutamine highlighted), reactive glutamine, flanked by leucine and proline aminoacids, was replaced by the DON moiety, yielding compound **XX** (Ac-Pro-Gln-Pro-DON-Leu-Pro-Phe-NH_2) (**Figure 35**). Affinity and efficiency values (K_I and k_{inact}/K_I) for TG2 were 70 nM and 2.9 10^6 $M^{-1}min^{-1}$, respectively. This new proposed warhead, the diazoketone group, from the DON moiety, is an electrophilic moiety for the nucleophilic thiol-Cys277 from the TG2 active site.

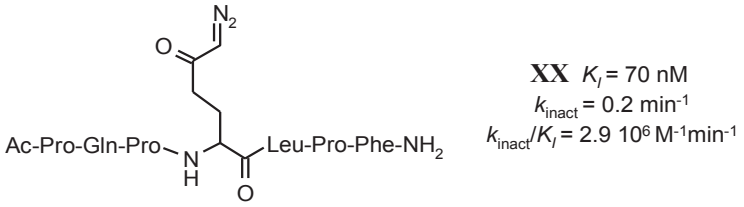

Figure 35. Structure of the TG2 inhibitor **XX**,[86] and its inhibition kinetic parameters (K_I, k_{inact}, and k_{inact}/K_I) for TG2

The proposed mechanism of inhibition for peptidic diazomethyl ketones with the cysteine active site residue of TG is shown in **Scheme 17**.[124]

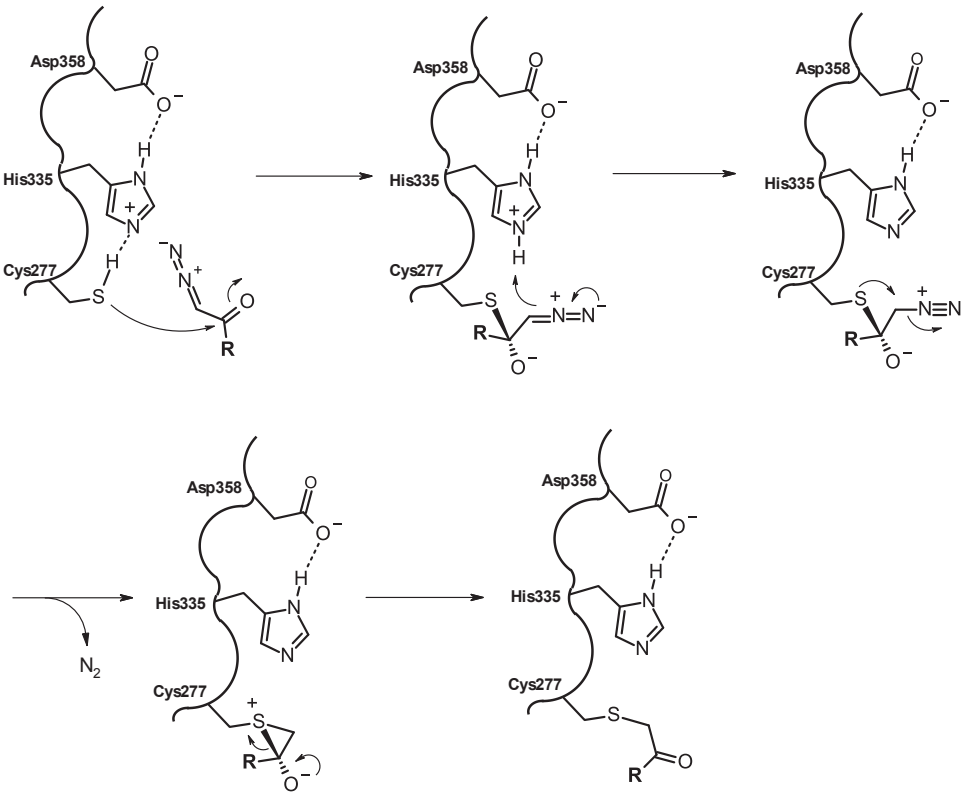

Scheme 17. Proposed mechanism of inactivation of the thiol from the active site Cys277 of TG2 by 6-diazo-5-oxo-norleucine (DON) - based inhibitors

It would involve the formation of a tetrahedral intermediate resulting from the Cys attack at the carbonyl group of the inhibitor's warhead. Then, abstraction of a proton of the His active site by the carbanion and the formation of a three-membered ring sulfonium intermediate would lead to a loss of N_2. Subsequentely, the rearrangement of sulfonium would rearrange to give the final thioether adduct.

Two other derivatives **Z006** and **B003** bearing the DON moiety were also synthesized by Zedira GmBH. These inhibitors have a peptidic structure, and they both differ, by the amine protecting group and the aminoacidic backbone. **Z006** and **B003** have a Cbz (benzyloxycarbonyl) and a Boc (*tert*-butyloxycarbonyl) protecting groups at the *N*-terminal position, respectively. Amino acid backbones are the following: Cbz-DON-Val-Pro-LeuOMe for **Z006**, and Boc-DON-Gln-Ile-ValOMe for **B003** (**Figure 36**).

The **Z006** compound was described as a cell permeable inhibitor,[70] inducing a near complete inhibition of intracellular TG2 at a concentration of 10 μM in neuroblastoma SH-SY5Y cells, with a measured potency value (IC_{50}) of 0.7 μM. The IC_{50} values for both derivatives *in vitro* vary from 0.020-0.040 μM for **Z006** and 0.3 μM for **B003**.[70,110]

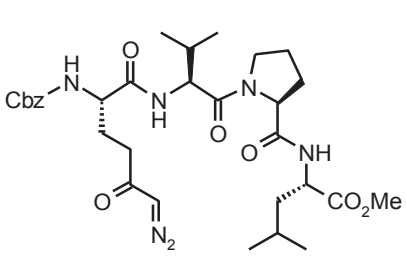

Z006 IC_{50} TG2 = 0.020-0.040 μM
IC_{50} intracellular TG2= 0.7 μM

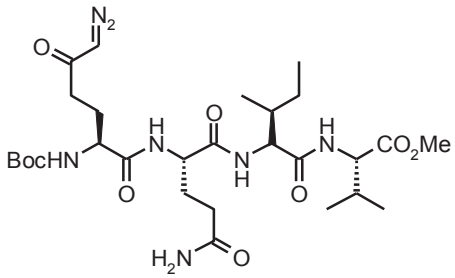

B003 IC_{50} TG2 = 0.3 μM

Figure 36. Structures of the TG2 inhibitors **Z006** and **B003** (ZEDIRA GmbH), and the respective potencies (IC_{50}) over TG2. In the case of compound **Z006**, both potencies for *in vitro* assays (recombinant human TG2 and cellular TG2) are reported

• Halomethyl carbonyl-based inhibitors

One of the structurally simplest TG2 inhibitor is iodoacetamide. In the work from Gillet et al.[89] kinetic parameters for iodoacetamide against TG2 were studied, obtaining K_I, k_{inact} and k_{inact}/K_I values of 0.075 μM, 0.90 min^{-1} and 1.2 10^7 $M^{-1}min^{-1}$ respectively (**Figure 37**). This simple halomethyl carbonyl inhibitor is based on iodine as a good leaving group that allows the thiol group from the cystein side chain to form a stable thioether bond with the inhibitor, making this molecule highly reactive. The disadvantage is that owing to its small structure becames a non-specific inhibitor for active-site cysteine. Another disadvantage is that iodoacetamide labels TG2 in a greater than 1:1 molar ratio, being highly probable that this compound will react with another different existing cysteine or nucleophilic residue around the TG2 structure.[125]

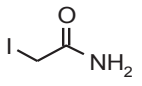

iodoacetamide K_I TG2 = 0.075 μM
K_{inact} = 0.90 min^{-1}
k_{inact}/K_I = 1.2 10^7 $M^{-1}min^{-1}$

Figure 37. Structure of iodoacetamide and its respective inhibition kinetic parameters (K_I, k_{inact}, and k_{inact}/K_I) for TG2[89]

Some other more complex structures of halomethyl carbonyl inhibitory compounds have been synthesized by Keillor et al.[90] In this work, different derivatives **XXI** bearing a Cbz-Phe scaffold were synthesized. In this case, iodine was substituted by a chlorine atom in all of the inhibitors. An alkyl spacer whose length varies form 2 up to 6 methylene groups has been introduced between the chloroacetamide and the phenylalanine moieties (**Figure 38**).

After studying the kinetic parameters for all inhibitors, the compound **XXIa** (n = 6; **Figure 38**), was found the best inhibitor (K_I = 6 μM, and k_{inact}/K_I = 5.3 10^5 $M^{-1}min^{-1}$). It has also been studied the increase of the efficiency of these inhibitors (k_{inact}/K_I) by increasing the carbon length of the alkyl spacer between the chloroacetamide and the phenylalanine.

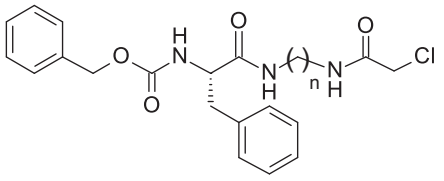

XXI General structure

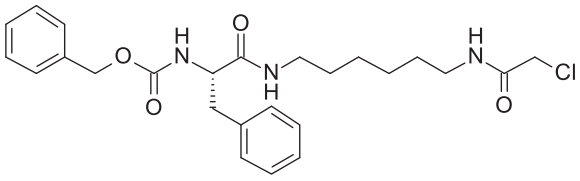

XXIa K_I TG2 = 6 μM
k_{inact} = 0.32 min^{-1}
k_{inact}/K_I = 5.3 10^5 $M^{-1}min^{-1}$

Figure 38. On the left, the general scaffold **XXI** for the synthesis of chloroacetamide-based TG2 inhibitors by Keillor et al.[90] On the right, the structure of derivative **XXIa**, and its inhibition kinetic parameters (K_I, k_{inact}, and k_{inact}/K_I) for TG2

Another series of halomethyl carbonyl compounds **XXII** have also been synthesized by Griffin et al.[117] In this case, the halogen from the warhead can be either a bromine or a chlorine atom. As in the case of the acrylamide-based compounds from the same authors, these derivatives are also based in a piperazine core, in this case either the 2-chloro-*N*-(2-oxo-2-piperazin-1-yl-ethyl)acetamide or the 2-bromo-*N*-(2-oxo-2-piperazin-1-yl-ethyl)acetamide were employed as scaffolds (**Figure 39**). Potencies from all inhibitors in terms of IC_{50} were calculated, resulting in a value of 0.0021 μM for the most potent compound **EB1-111**, and 0.0059 μM for compound **EB2-57**, the latter containing a fluorescence dansyl moiety within its structure (**Figure 39**).

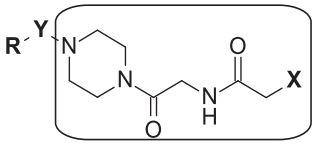

XXII X = Cl, Br; **Y** = CO, CO_2, SO_2
R = alkyl, heterocyclic and aralkyl

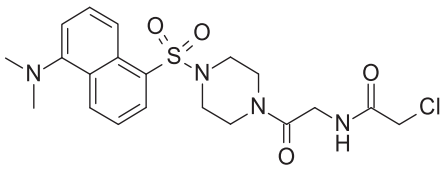

EB2-57 IC_{50} TG2 = 5.9 nM

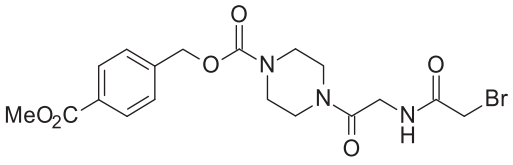

EB1-111 IC_{50} TG2 = 2.1 nM

Figure 39. At the top, the general scaffold **XXII** for the synthesis of halomethyl carbonyl inhibitors by Griffin et al.[117] At the bottom, the structures of derivatives **EB2-57** and **EB1-111** and their potencies (IC_{50}) over TG2

The proposed mechanism of action of these derivatives in the TG2 active site is shown in **Scheme 5**. Two possible mechanisms were proposed for the inhibition of cystein active site enzymes by compounds bearing this halomethyl ketone electrophilic warhead (**Scheme 18**).[73] Leading to the formation of a final stable thioether adduct, one proposed mechanism (**Scheme 18a**) involves a direct halogen displacement by the thiolate anion. The other mechanism (**Scheme 18b**) would involve a thiohemiketal formation and a

three-membered ring sulfonium intermediate, that would rearrange to give final thioether adduct.

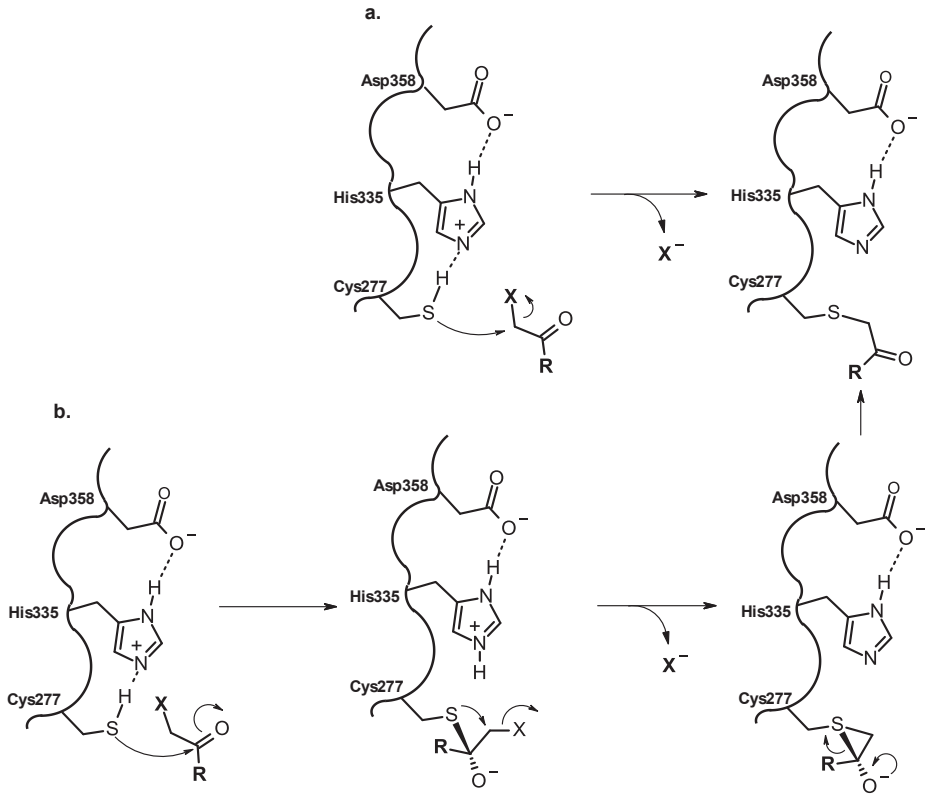

Scheme 18. Proposed mechanisms (**a** and **b**) of inactivation of the thiol from the active site Cys277 of TG2 by Halomethyl carbonyl - based inhibitors

• Sulfonium- and imidazolium- based inhibitors.

Based in the assumption that sulfonium peptidylmethylketones with a Cbz-Phe-$NH(CH_2)_nCOCH_2S^+(Me)_2$ structure have been found to be potent transglutaminase inhibitors,[126] Griffin has developed a new series of sulfonium-based compounds **XXIII**.[127] These derivatives are mentioned to have an increased solubility in aqueous solutions. This good solubility property in water was thought to be necessary to target extracellular TG2, whose been implicated in a varied number of diseases (yet described in other sections) like celiac disease, different fibrosis and cancer. The backbone structure of these derivatives consists on a peptidic Cbz-containing structure ending in dimethylsulfonium methylketone as the electrophilic warhead. Regarding to their aqueous solubility, the carboxylic acid and the dimethylsulfonium moieties are key groups that will increase the compound's solubility in water, due to the presence of charges at physiological pH.[127] The aminoacidic group was replaced in order to proceed to the SAR studies resulting in improved potencies when aminoacids proline or glycine are present within their structure resulting in compounds **XXIIIa** and **XXIIIb** (IC_{50} TG2 = 5 ± 1 and 8 ± 1 μM, respectively) (**Figure 40**). It has also proved that the Cbz protecting group has a positive effect in terms of inhibitor's potency (IC_{50}) when compared with Boc and Fmoc protecting groups.

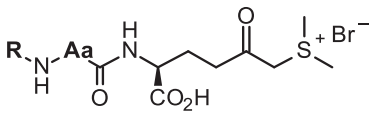

XXIII R = Cbz, Fmoc, Boc; **Aa** = Pro, Gly, Phe, Ala, Asp, Lys, Ile

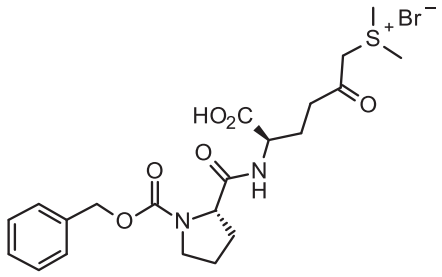

XXIIIa IC_{50} TG2 = 5 μM

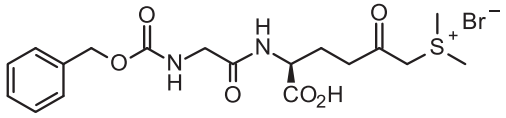

XXIIIb IC_{50} TG2 = 8 μM

Figure 40. At the top, the general scaffold for the development of sulfonium-based TG2 inhibitors by Giffin et al.[1278] At the bottom, the structures of derivatives **XXIIIa** and **XXIIIb** and their respective potencies (IC_{50}) over TG2

Another kind of inhibitors bearing a different warhead were synthesized by the same group.[128] Keeping the same scaffold **XXIII** from their previous work,[127] and replacing the dimethylsulfonium warhead by the polar imidazolium moiety a new serie of derivatives have been synthesized. The carboxylate group was preserved keeping the good aqueous solubility of these derivatives regarding the previous ones to target the extracellular TG2. SAR studies were performed at the level of the aminoacidic part of the inhibitor scaffold (Phe and Gly were employed) but also introducing different substituents on imidazolium nitrogens to test the tolerance relative to the warhead size in terms of inhibitory activity. Authors could conclude that the size of the imidazolium substituted ring was key in the potency from these derivatives, not being influenced by the aminoacidic moiety. The most potent inhibitors, compound **XXIVa** and **XXIVb**, bearing a methyl substituted nitrogen at the imidazolium ring and a Phe and a Gly respectively, reached TG2 potencies of 3 and 1 μM. These potencies at the low micromolar range are almost identically for compounds **XXIIIa-b** previously reported by Griffin et al.[127] against TG2. It is almost noteworthy, that both compounds **XXIVa-b** have also micromolar potencies against the plasma factor FXIIIa (IC_{50} = 5 and 2 μM respectively), so lacking of good selectivity (**Figure 41**).

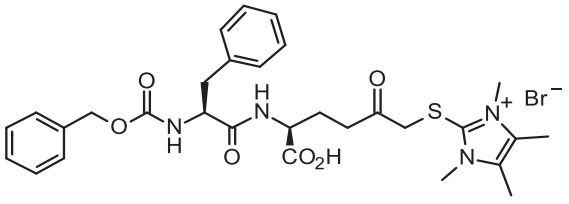

XXIVa IC_{50} TG2 = 3 μM

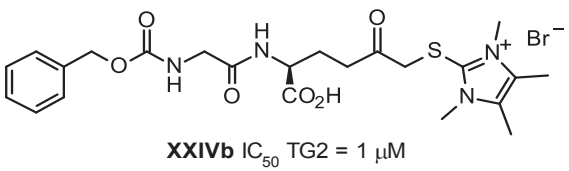

XXIVb IC_{50} TG2 = 1 μM

Figure 41. Structures of derivatives **XXIVa** and **XXIVb** and their respective potencies (IC_{50}) over TG2

1.3. Other TG2 inhibitors

This section is entitled "other TG2 inhibitors" because different compounds with a not well-defined mode of inhibition (either with a more complex inhibition mechanism or a unknown mechanism) for the TG2 enzymatic activity are described. It is also described a TG2 inhibitor affecting a different TG2 activity/function other than the transamidation activity as it has been described so far (e.g., TG2-Fibronectin interaction).

• ZM39923 and its metabolite ZM449829

From the work performed by Lai et al.,[109] the most potent hits found over TG2, by screening of two drug libraries, were the **ZM39923** derivative, designed to inhibit Janus Kinase 3, and its metabolite **ZM449829** (**Figure 42**). Both compounds reached low nanomolar IC_{50} values against TG2 (5-10 nM) in the presence of Ca^{2+} and in the absence of dithiothreithol (DTT). On the contrary, in the presence of DTT their potency values for **ZM39923** and **ZM449829** decrease, reaching values of 3 and 20 μM (decrease of 300- to 4,000-fold in potency). Regarding their inhibitory activity over FXIIIa in the presence of the same reducing agent (DTT), **ZM39923** and **ZM449829** showed IC_{50} values of 10 and >20 μM, respectively. In the absence of DTT, both inhibitors showed higher potencies of 0.025 and 0.006 μM for **ZM39923** and **ZM449829** respectively.

Authors concluded that the decrease in potency when employing the reducing agent DTT in the transamidation assay, suggested that these molecules target activated TG2 (they may react with the active-site Cys277 of TG2) and also the free thiol groups that are required for TG2 to become an active enzyme.[19] They also suggested that both are tight binding inhibitors and that they may participate in a complex mechanism of inhibition.

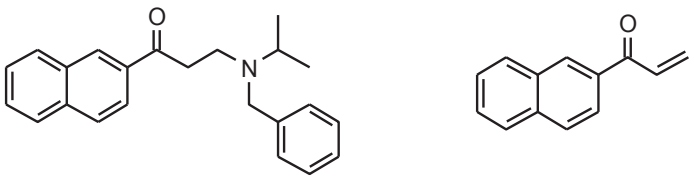

ZM39923 ZM449829

Figure 42. **S**tructures of the Janus kinase inhibitor **ZM39923** and its metabolite **ZM449829**

• β-Aminoethylketone-based inhibitors

A series of 200 derivatives of *N*,*N*-disubstituted β-aminoethyl ketone-based derivatives has been synthesized by Ozaki et al.[129] Starting from **ZM39923** (β-aminoethylketone building block),[109] different aryl and heteroaryl groups were introduced at the R_1 position (**Figure 43**). Heteroaryl substituents resulted in better potencies than aryls (naphthalenes and phenyls). Among the heteroaryl groups, thiophene ring turned out to give the best potencies. On the other side of the molecule different substituents were

introduced on the tertiary amine, from which the *t*-butyl and the benzyl groups resulted in the best activity (**Figure 43**). From all compounds synthesized, the compound **XXV** was found to be the most potent with an IC_{50} value of 0.081 μM against TG2 (**Figure 43**), although its mode of action is not confirmed.

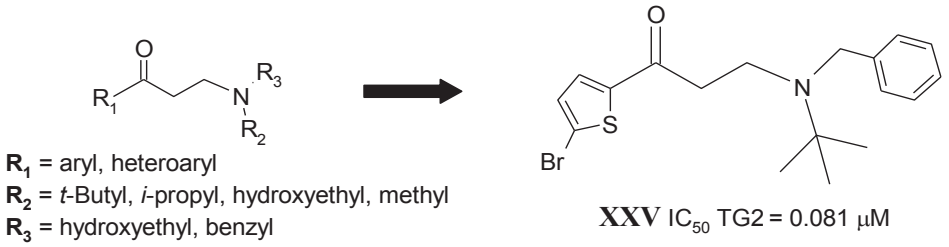

Figure 43. On the left, the general scaffold for the synthesis of *N*,*N*-disubstituted β-aminoethyl ketones derivatives.[129] On the right, the structure of derivative **XXV** and its potency (IC_{50}) over TG2

• Targeting the fibronectin binding site

A different perspective to inhibit TG2 was described by Yakubov et al.[130] focusing on inhibiting the TG2-fibronectin (TG2-FN) interaction knowing that TG2-FN interaction is associated with certain cancers and metastasis,[57,58] thus becoming a new valuable strategy for the treatment of these disease. A high throughput screening of 10,000 compounds from the ChemDiv Library (ChemDiv, inc, San Diego, CA) was performed in order to find small molecules inhibitors (SMIs), hits, able to inhibit this TG2-FN protein interaction. These SMIs were proposed to block this protein-protein interaction in particular because the interacting domains are not flat surfaces but comprise a relatively small TG2 hairpin inserting into a deep pocket of FN.

Compound **TG53** (see **Figure 44**), a diaminopyrimidine derivative, was the most active compound on inhibiting TG2 interaction with fibronectin, with an IC_{50} calculated at 10 μM. Furthermore, this compound was successfully employed to prevent TG2-FN interaction in SKOV3 AND IGROV1 ovarian cancer cells that endogenous express TG2, demonstrating a time-dependent inhibition of cell adhesion to fibronectin.

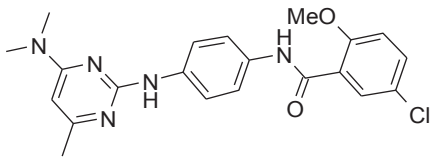

Figure 44. Structure of the most potent hit discovered in the screening of TG2 inihbitors against the fibronecting binding region of TG2, and its calculated potency (IC_{50})[130]

Bibliography - Chapter 1

93. Badarau, E.; Collighan, R. J.; Griffin, M. Recent advances in the development of tissue transglutaminase (TG2) inhibitors. *Amino Acids* **2011**, *44*, 119-127.

94. a) Keillor, J. W.; Apperley, K. Y.; Akbar, A. Inhibitors of tissue transglutaminase. *Trends Pharmacol. Sci*. **2015**, *36*, 32-40; b) Keillor, J. W. and Apperley, K. Y. Transglutaminase inhibitors: a patent review. *Expert. Opin. Ther. Pat*. **2016**, *26*, 49-63.

95. Perez Alea, M.; Kitamura, M.; Martin, G.; Thomas, V.; Hitomi, K.; El Alaoui, S. Development of an isoenzyme-specific colorimetric assay for tissue transglutaminase 2 cross-linking activity. *Anal. Biochem*. **2009**, *389*, 150-156.

96. Hitomi, K.; Kitamura, M.; Alea, M. P.; Ceylan, I.; Thomas, V.; El Alaoui, S. A specific colorimetric assay for measuring transglutaminase 1 and factor XIII activities. *Anal. Biochem*. **2009**, *394*, 281-283.

97. Wu, Y. W.; Tsai, Y. H. A rapid transglutaminase assay for high-throughput screening applications. *J. Biomol. Screen*. **2006**, *11*, 836-843.

98. Priglinger, S. G.; May, C. A.; Neubauer, A. S.; Alge, C. S.; Schönfeld, C. L.; Kampik, A.; Welge-Lussen, U. Tissue transglutaminase as a modifying enzyme of the extracellular matrix in PVR membranes. *Invest. Ophthalmol. Vis. Sci*. **2003**, *44*, 355-364.

99. Jeon, J. H.; Kim, C. W.; Shin, D. M.; Kim, Ki.; Cho, S. Y.; Kwon, J. C.; Choi, K. H.; Kang, H. S.; Kim, I. G. Differential incorporation of biotinylated polyamines by transglutaminase 2. *FEBS Lett*. **2003**, *534*, 180-184.

100. Hohl, D.; Aeschlimann, D.; Huber, M. In vitro and rapid in situ transglutaminase assays for congenital ichtyoses – a comparative study. *J. Invest. Dermatol*. **1998**, *110*, 268- 271.

101. Sheffield, W. P.; Eltringham-Smith, L. J.; Gataiance, S.; Bhakta, V. Addition of a sequence from alpha2-antiplasmin transforms human serum albumin into a blood clot component that speeds clot lysis. *BMC Biotechnol*. **2009**, *9*, 15.

102. Choi, K.; Siegel, M.; Piper, J. L.; Yuan, L.; Cho, E.; Strnad, P.; Omary, B.; Rich, K. M.; Khosla, C. Chemistry and biology of dihydroisoxazole derivatives: selective inhibitors of human transglutaminase 2. *Chem. Biol*. **2005**, *12*, 469-475.

103. Deguchi, Y.; Naito, Y.; Ohtsuki, S.; Miyakawa, Y.; Morimoto, K.; Hosoya, K.; Sakurada, S.; Terasaki, T. Blood-brain barrier permeability of novel [D-

Arg^2]dermorphin (1-4) Analogs: transport property is related to the slow onset of antinociceptive activity in the central nervous system. *J. Pharmacol. Exp. Ther*. **2004**, *310*, 177-184.

104. Pardin, C.; Pelletier, J. N.; Lubell, W. D.; Keillor, J. W. Cynnamoyl inhibitors of tissue transglutaminase. *J. Org. Chem.* **2008**, *73*, 5766-5775.

105. Pardin, C.; Roy, I.; Lubell, W. D.; Keillor, J. W. Reversible and competitive cinnamoyl triazole inhibitors of tissue transglutaminase. *Chem. Biol. Drug. Des*. **2008**, *72*, 189-196.

106. Duval, E.; Case, A.; Stein, R. L.; Cuny, G. D. Structure-activity relationship study of novel tissue transglutaminase inhibitors. *Bioorg. Med. Chem. Lett*. **2005**, *15*, 1885–1889.

107. Case, A.; Stein, R. L. Kinetic analysis of the interaction of tissue transglutaminase with a nonpeptidic slow-binding inhibitor. *Biochemistry* **2007**, *46*, 1106–1115

108. Yi, M. C.; Palanski, B. A.; Quintero, S. A.; Plugis, N. M.; Khosla, C. An unprecedented dual antagonist and agonist of human Transglutaminase 2. *Bioorg. Med. Chem. Lett.* **2015**, *25*, 4922-4926.

109. Lai, T. S.; Liu, Y.; Tucker, T.; kurt R. Daniel,K.R.; Sane, D. C.; Toone, E.; Burke, J. R.; Strittmatter, W. J.; Greenberg, C. S. Identification of chemical inhibitors to human tissue transglutaminase by screening existing drug libraries. *Chem. Biol*. **2008**, *15*, 969-978.

110. Schaertl. S.; Prime, M.; Wityak, J.; Dominguez, C.; Munoz-Sanjuan, I.; Pacifici, R. E.; Courtney, S.; Scheel, A.; Macdonald, D. A profiling platform for the characterization of transglutaminase 2 (TG2) inhibitors. *J. Biomol. Screen*. **2010**, *15*, 478-487.

111. Prime, M. E.; Andersen, O. A.; Barker, J. J.; Brooks, M. A.; Cheng, R. K.; Toogood-Johnson, I.; Courtney, S. M.; Brookfield, F. A.; Yarnold, C. J.; Marston, R. W.; Johnson, P. D.; Johnsen, S. F.; Palfrey, J. J.; Vaidya, D.; Erfan, S.; Ichihara, O.; Felicetti, B.; Palan, S.; Pedret-Dunn, A.; Schaertl, S.; Sternberger, I.; Ebneth, A.; Scheel, A.; Winkler, D.; Toledo-Sherman, L.; Beconi, M.; Macdonald, D.; Muñoz-Sanjuan, I.; Dominguez C.; Wityak, J. Discovery and structure-activity relationship of potent and selective covalent inhibitors of transglutaminase 2 for huntington's disease. *J. Med. Chem*. **2012**, *55*, 1021-1046.

112. Prime, M. E.; Brookfield, F. A.; Courtney, S. M.; Gaines, S.; Marston, R. W.; Ichihara, O.; Li, M.; Vaidya, D.; Williams, H.; Pedret-Dunn, A.; Reed, L.; Schaertl, S.; Toledo-Sherman, L.; Beconi, M.; Macdonald, D.; Muñoz-Sanjuan, I.; Dominguez, C.; Wityak, J. Irreversible 4-aminopiperidine transglutaminase 2 inhibitors for hungtington's disease. *ACS Med. Chem. Lett.* **2012**, *3*, 731–735.

113. de Macédo, P.; Marrano, C.; Keillor, J. W. Synthesis of dipeptide-bound epoxides and α-β, unsaturated amides as potential irreversible transglutaminase inhibitors. *Bioorg. Med. Chem*. **2002**, *10*, 355-360.

114. Keillor J. W.; Chica, R. A.; Chabot, N.; Vinci, V.; Pardin, C.; Fortin, E.; Gillet, S. M. F. G.; Nakano, Y.; Kaartinen, M. T.; Pelletier, J. N.; Lubell, W. D. The bioorganic chemistry of transglutaminase - from mechanism to inhibition and engineering. *Can. J. Chem*. **2008**, *86*, 271-276.

115. Al-Jallad, H. F.; Myneni, V. D.; Piercy-Kotb, S. A.; Chabot, N.; Mulani, A.; Keillor, J. W.; Kaartinen, M. T. Plasma membrane factor XIIIA transglutaminase activity regulates osteoblast matrix secretion and deposition by affecting microtubule dynamics. *PLoS One* **2011**, *6*, *e15893*.

116. Wityak, J.; Prime, M. E.; Brookfield, F. A.; Courtney, S. M.; Erfan, S.; Johnsen, S.; Johnson, P. D.; Li, M.; Marston, R. W.; Reed, L.; Vaidya, D.; Schaertl, S.; Pedret-Dunn, A.; Beconi, M.; Macdonald, D.; Muñoz-Sanjuan, I.; Dominguez, C. SAR development of lysine-based irreversible inhibitors of transglutaminase 2 for hungtington's disesase. *ACS Med. Chem. Lett.*, **2012**, *3*, 1024–1028.

117. a) Griffin, M.; Rathbone, D.; Badarau, L. E. Acylpiperazines as inhibitors of transglutaminase and their use in medicine. **2014**, WO 2014/057266 A1; Chem.Abstr., **160**, 559340; b) Badarau, E.; Wang, Z.; Rathbone, D. L.; Costanzi, A.; Thibault, T.; Murdoch, C. E.; El Alaoui, S.; Bartkeviciute, M.; Griffin, M. Development of potent and selective tissue transglutaminase inhibitors: their effect on TG2 function and application in pathological conditions. *Chem. Biol*. **2015**, *22*, 1347-1361.

118. Lindemann, I.; Böttcher, J.; Oertel, K.; Weber, J.; Hils, M.; Pasternack, R.; Linne, U.; Heine, A.; Klebe, G. Inhibitors of transglutaminase 2: a therapeutic option in celiac disease. *XXth International Symposium on Medicinal Chemistry EFMC-ISMC*. **2008**, Vienna, Austria. Poster session presentation.

119. Büchold, C.; Gerlach, U.; Hils, M.; Pasternack, R.; Weber, J. Pyridone derivatives as tissue transglutaminase inhibitors. **2014**, WO 2014/012858; *Chem. Abstr.*, **160**, 234406.

120. Pasternack, R.; Hils, M. Preclinical development of tissue transglutaminase blockers. *XXth International Symposium on Medicinal Chemistry EFMC-ISMC*. **2008**, Vienna, Austria. Poster session presentation.

121. Halim, D.; Caron, K.; Keillor, J. W. Synthesis and evaluation of peptidic maleimides as transglutaminase inhibitors. *Bioorg. Med. Lett*. **2007**, *17*, 305-308.

122. Rohloff, J. C.; Rubinsun III, J.; Gardner, J. O. Bromonitrile oxide [3+2] cycloadditions in water. *Tetrahedron Lett*. **1992**, *33*, 3113-3116.

123. Shaw, E. Peptidyl diazomethanes as inhibitors of cysteine and serine proteases. *Methods Enzymol*. **1994**, *244*, 649-656.

124. Sabo, T. M. Perturbations in protein dynamics associated with ligand binding to the blood coagulation enzymes thrombin and factor XIII (Doctoral dissertation). **2007**. Retrieved from *Electronic Theses and Dissertations*. Paper 1244. http://dx.doi.org/10.18297/etd/1244.

125. Folk, J. E.; Cole, P. W. Identification of a functional cysteine essential for the activity of guinea pig liver transglutaminase. *J. Biol. Chem*. **1966**, *241*, 3238-3240.

126. Pliura, D. H.; Bonaventura, B. J.; Pauls, H. W.; Killackey, J. F.; Krantz, A. Irreversible inhibition of transglutaminases by sulfonium methylketones: optimization of specificity and potency with omega-aminoacyl spacers. *J. Enz. Inhib. Med. Chem*. **1992**, *6*, 181-194.

127. Griffin, M.; Mongeot, A.; Collighan, R.; Saint, R. E.; Jones, R. A.; Coutts, I. G.; Rathbone, D. L. Synthesis of potent water-soluble tissue transglutaminase inhibitors. *Bioorg. Med. Chem. Lett*. **2008**, *18*, 5559-5562.

128. Badarau, E.; Mongeot, A.; Collighan, R.; Rathbone, D.; Griffin, M. Imidazolium-based warheads strongly influence activity of water-soluble peptidic transglutaminase inhibitors. *Eur. J. Med. Chem*. **2013**, *66*, 526-530.

129. Ozaki, S.; Ebisui, E.; Hamada, K.; Goto, J.; Suzuki, A. Z.; Terauchi, A.; Mikoshiba, K. Potent transglutaminase inhibitors, aryl beta-aminoethyl ketones. *Bioorg. Med. Chem. Lett.* **2010**, *20*, 1141-1144.

130. Yakubov, B.; Chen, L.; Belkin, A. M.; Zhang, S.; Chelladurai, B.; Zhang, Z.-Y.; Matei, D. Small molecule inhibitors target the tissue transglutaminase and fibronectin interaction. *PLoS One* **2014**, *9*, e89285.

CHAPTER 2

Naphthalene-based TG2 inhibitors

1. Objectives

In the recent years, the use of covalent inhibitors employed to block irreversibly the activity from enzymes has increased.[72,131,132] Even knowing the risk of using covalent inhibitors, the duration of the inhibition of covalent inhibitors have been described to yield a number of potential advantages.[133]

Different TG2 irreversible inhibitors based on electrophilic warheads have also been synthesized to date (see Chapter 1). The most widely employed group is the α,β-unsaturated amide which reacts with the thiol (Cys277) present in the TG2 active site.[91,111-114,116]

Acrylamide was selected as the warhead of choice because of its demonstrated low off-target reactivity,[134] thus being considered as an appropriate pharmacophore to be included in the structure of the new produced TG2 inhibitors of this dissertation.

Starting from the 4-(acrylamido)piperidine part of the TG2 inhibitor **X** (IC_{50} TG2 = 0.110 μM),[112] we have investigated the replacement of the benzenesulfonyl part by a naphthylsulfonyl ring found in the dansylcadaverine structure to reach new TG2 inhibitors. Dansylcadaverine has been selected for being a widely employed TG reversible inhibitor (reviewed in Chapter 1), possessing a different arylsulfonyl moiety (naphthylsulfonyl) to that found in reference compound **X** (benzenesulfonyl). A piperidine linker between sulfonyl and acrylamide moieties, as observed for compound **X**, was introduced in the inhibitor's structure. Based on this, a first chemical hybrid **1** was prepared in our laboratory (**Figure 45**).

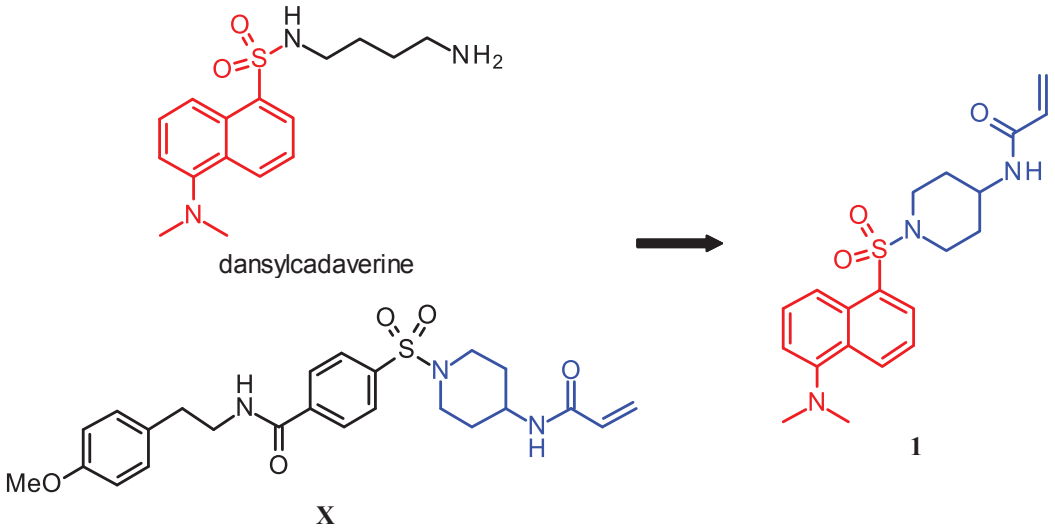

Figure 45. Structures of dansylcadaverine, the reference compound **X**,[112] and the resultant hybrid compound **1**

In addition, taking compound **1** as the reference molecule, different modulations were performed around the naphthyl moiety. The dimethylamino substituent was replaced with a substituent at the C-5 or C-4 positions of the naphthalene ring (**Figure 46**), R_2 being a hydrogen, acetylamino, dimethylamino or di-*n*-butylamino moiety, as well as

different substituted and non-substituted benzamides, in order to check whether extending these positions is tolerable within the active pocket of TG2. The importance of the sulfonamide position on the naphthalene has also been studied, giving rise to new compounds with sulfonamides at the C-2 or the C-1 position. It can be observed in **Figure 45** that different attempts at replacing the 4-aminopiperidine moiety have also been carried out, R_1 being different saturared heterocycles, such as piperazine or *N*-(1-acryloylpiperidin-4-yl)sulfonamide, in which the orientation of the 4-aminopiperidine group has been inverted, or R_1 being a diaminoalkyl chain from 2 to 4 carbons in length.

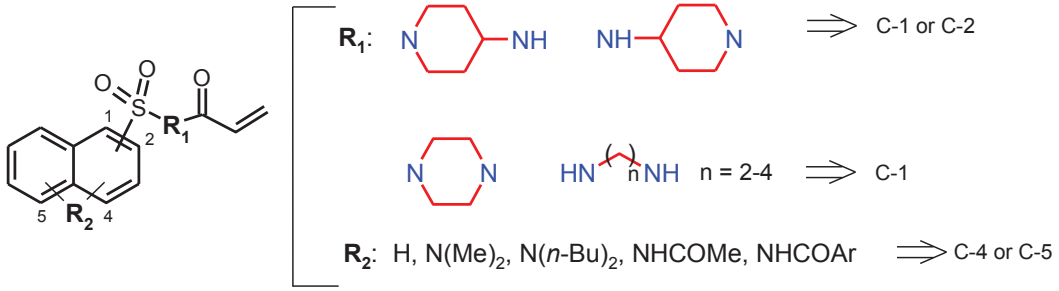

Figure 46. General structure of the naphthalenesulfonamide TG2 inhibitors from this chapter, and the different modulations carried out around the naphthalene ring. **R_1** represents different modifications introduced in the sulfonyl-acrylamide linker at both sulfonamide positions (C-1 or C-2); and **R_2,** represents different substituents introduced at C-4 or C-5 positions

To sum up, the development of new TG2 irreversible inhibitors is based on two main structural features:

a) an acrylamide group as the warhead (and covalent modifier) on a diamino linker to trap the sulfur atom of Cys277

b) a naphthalene core as the central aromatic ring

We can expect new TG2 inhibitors with low nanomolar potencies (IC_{50}) against TG2 and presenting a good selectivity profile against the other TG isoforms.

2. Methodology to validate the inhibitory activity of potential TG2 inhibitors

2.1. Determination of the inhibitory potency (IC_{50} TGs)

The inhibitory activity of many of the TG2 irreversible inhibitors has been measured in terms of the IC_{50} (see chapter 1). To define IC_{50} we can take a look to the work from Krippendorff,[135] who gave the following definition based on a fluorimetric assay regarding the control (non inhibited enzyme) of an enzymatic inhibition assay: "IC_{50} value is then defined as the inhibitor concentration at which the product concentration is half the concentration of the system without inhibitor". In other words, IC_{50} could be defined as the “half maximal inhibitory concentration”, or "the concentration needed to inhibit a biological or biochemical function by half".

In different structure-activity relationships studies, inhibitory activity of the compounds synthesized was referred in terms of IC_{50} for drugs designed to target enzymes others than transglutaminases like kinases,[136] histone deacetylases,[137] DNA topoisomerases,[138] and also for antitubulin agents.[139] Herein, they are presented structure-activity relationship studies for the new compounds synthesized against TG2, also based in their inhibitory potency in terms of IC_{50}, as well as their selectivity profiles against other TG isoforms.

2.2. Description of the methodology employed

For the inhibition of the different TG (TG1, TG2, TG6, and FXIIIa) with the compounds synthesized in this PhD, different TG specific transamidation assays developed by Covalab R&D (Lyon, France) were employed (opr-0038, opr-0030, opr-0037 kits for TG1,TG2 and FXIIIa respectively). In the case for the measurement of the TG6 transamidation activity, no Covalab test is commercially available so far. Therefore, in order to measure the TG6 transamidation activity, the same procedure and conditions were applied for its detection as perfomed for the other TG isoforms, but employing a different specific biotinylated peptide (see experimental section; page 148).

The general procedure carried out in the specific TG transamidation tests employed is summarized in **Figure 47**. This methodology is based in the crosslinking of a specific biotinylated peptide (a different specific biotinylated peptide for each of the TG isoforms; see experimental section in page 148) with an acyl acceptor substrate. TG are incubated in a TRIS buffer solution (pH 8.0) solution with the specific biotinylated peptide (the acyl donor substrate), which will be crosslinked to an acyl acceptor substrate coupled to the bottom of a microtiter plate (an immobilized amine donor substrate). After 30 minutes of incubation time, the crosslinked product is visualized by the ability of the biotin to couple with a Streptavidin-HRP (horse radish peroxidase) conjugate, and the ulterior colorimetric reaction by administration of H_2O_2 (peroxidase substrate) and the electro acceptor reagent 3,3',5,5'-Tetramethylbenzidine (TMB). Optical density is then measured at 450 nm after stopping the reaction with an acid solution (0.5 N H_2SO_4). The color development is directly related with the transamidation activity for the different TG. In the case of the TG inhibition, the different inhibitor solutions were incubated with the enzyme and the substrates in the same buffer conditions, observing a decrease in TG transamidation activity (see experimental part).

Thirty minutes was the time selected for the incubation time of the inhibitors and the enzyme within the assay conditions. **This incubation time was demonstrated optimal owing to the high correlation observed between IC_{50} and efficiency values for inhibition (k_{inact}/K_I) in the work of Wityak et al.[111] in a transamidation test. Thus, authors relied on the IC_{50} values to guide their medicinal chemistry study.** In addition, the inhibitory compounds tested in that

work also included an acrylamide[111] but also a 4-(acrylamido)piperidine[112] warheads in their structure as those presented in this manuscript.

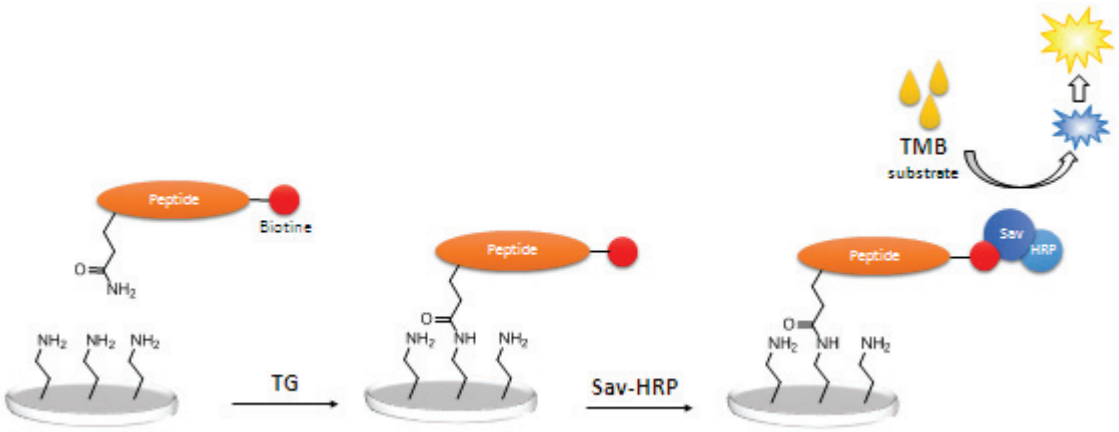

Figure 47. Schematic representation of the methodology employed in this work for the *in vitro* measurement of the TG transamidation activity

3. Synthesis and biological evaluation of 1

3.1. Synthesis of 1

Starting from the commercially available dansyl chloride (**Scheme 19**), the sulfonamide **2** was obtained in 99% yield by the reaction with the 4-(*N*-Boc-amino)piperidine, in the presence of the Hünig's base. After Boc hydrolysis in 20% TFA in CH_2Cl_2, the resulting ammonium salt **3** was treated with acryloyl chloride, in the presence of DIPEA, to provide the final product **1** in 70% yield. The global yield for this synthesis was 69% (3 steps).

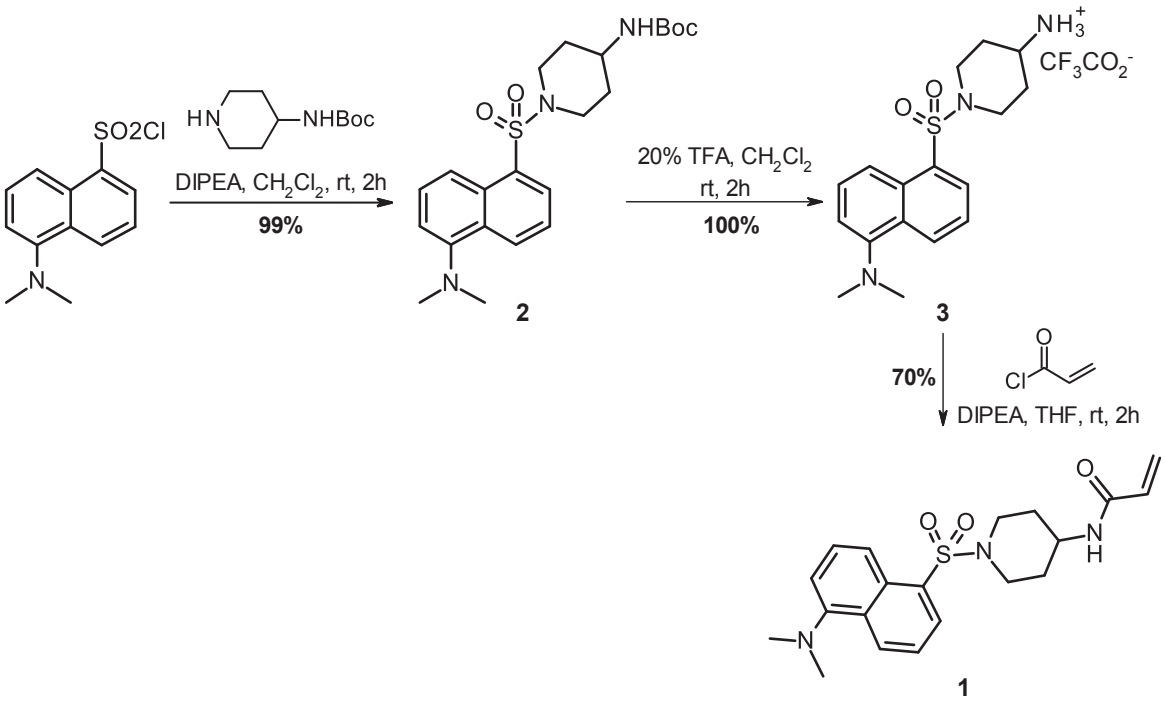

Scheme 19. Synthesis of the first inhibitor **1**

3.2. TG transamidation inhibition of 1

The inhibitory activity of **1** against TG1, TG2, TG6 and FXIIIa have been measured and reported in **Table 4**. IC_{50} TGs values are compared between **1**, and first our reference compound **X**, which has been synthesized in our laboratory following the authors procedure.[112] It can be observed that both TG2 inhibitors were found to have almost equipotent activity against TG2. These compounds also presented a good selectivity, especially compound **1** which was found to have an excellent selectivity profile with a loss of activity of more than 840-, 840-, and 420-fold against TG1, TG6, and FXIIIa, respectively, compared to TG2.

IC_{50} (μM)	TG2	TG1	TG6	FXIIIa
X	0.100 (0.110)[112]	> 6	NT	> 32
1	0.115 ± 0.009*	> 100	> 50	> 100

*Values accompanied by standard deviation were averaged from at least two independent experiments; they were otherwise obtained in a single determination. NT = not tested.

Table 4. TG2 inhibition and TG selectivity of **1** and reference inhibitor **X**[113]

4. Sulfonamide linker modulation

4.1. Synthesis of 4-8

Keeping dansyl as the central scaffold of the molecule, and following the same synthetic strategy employed for **1**, sulfonamide derivatives **4-8** bearing a 4-aminopiperidine (whose orientation has been inverted), a piperazine, or different diaminoalkyl chains as sulfonyl-acrylamide linkers were prepared (**Figure 48**). This was performed in order to check if any improvement in inhibitor's activity is observed by replacing the 4-aminopiperidine moiety (TG2 inhibitor **1**), by different sulfonamide linkers. The synthesis of **4-8** is not reported in this manuscript; however, a general schematic representation for their synthesis is presented in **Scheme 20**.

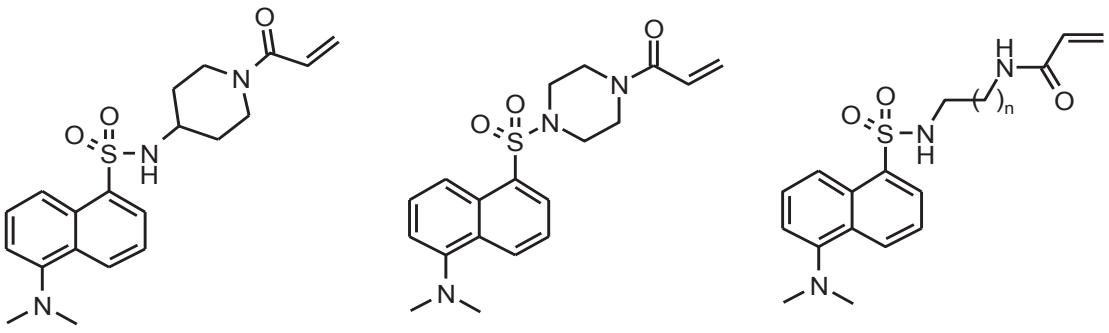

4 **5** **6** n = 1, **7** n = 2, **8** n = 3

Figure 48. Structure of **4-8**

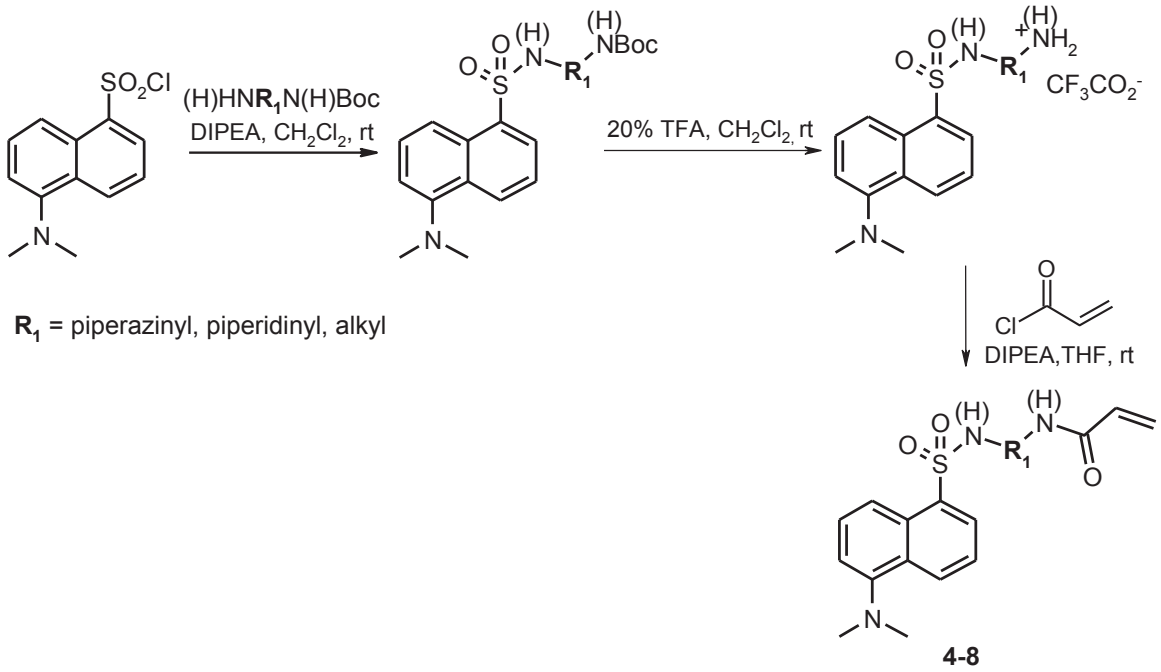

Scheme 20. General synthesis of inhibitors **4-8**

4.2. TG transamidation inhibition of 4-8

As shown in **Table 5**, all these TG2 inhibitors showed lower activity compared to TG2 inhibitor **1**. The compound **1** turned out to be from 101- to 160-fold more potent than its dansyl analogs **4** and **5** bearing the 4-aminopiperidine group (whose orientation has been inverted) and a piperazine, respectively. Regarding the diaminoalkyl based inhibitors (**6-8**), potency values also revealed lower inhibitory activities when compared to **1**, confirming the findings from the work from Wityak al.[112] where a 4-aminopiperidine-based warhead turned out to be the best options in order to get the best potencies against TG2.

IC_{50} (μM)	TG2	TG1	FXIIIa
1	0.12 ± 0.01*	> 100	> 100
4	19	> 20	> 20
5	12	> 10	> 10
6	14	> 10	> 10
7	4.9	> 10	> 10
8	10	> 10	> 10

*Values accompanied by standard deviation were averaged from at least two independent experiments; they were otherwise obtained in a single determination. NT = not tested.

Table 5. TG2 inhibition and TG selectivity of **1** and **4-8**

5. Changing the position of sulfonamide chain on naphthalene ring

Keeping the 4-aminopiperidine moiety, which resulted in the best inhibitory activity from all studied warheads, a change in the position of the sulfonyl chain on the naphthalene ring was also studied. This time the sulfonamide part was moved from C-1 to C-2 position on naphthalene ring, as shown in **Figure 49** for compounds **9** (C-2 position) and **10** (C-1 position).

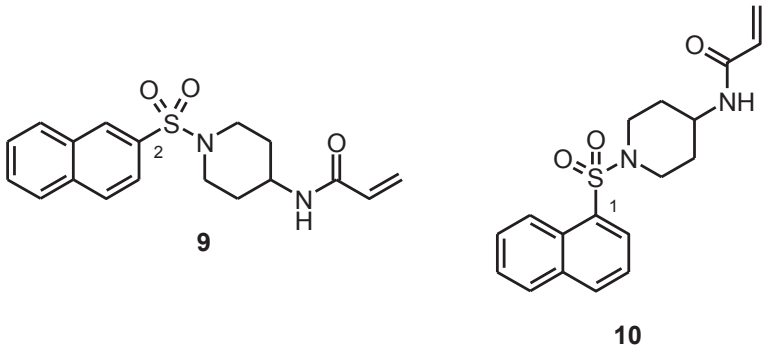

Figure 49. Structure of **9** and **10**

5.1. Synthesis of 9 and 10.

The sulfonamide **11** was obtained in 88% yield by treatment of the commercially available naphthalene-2-sulfonyl chloride with 4-(*N*-Boc-amino)piperidine in the presence of DIPEA. After Boc hydrolysis, the final C-2 substituted sulfonamide **9** was obtained in 90% yield by treatment of **12** with acryloyl chloride in the presence of Hünig's base (**Scheme 21**). The compound **9** was obtained with a global yield of 77% (3 steps).

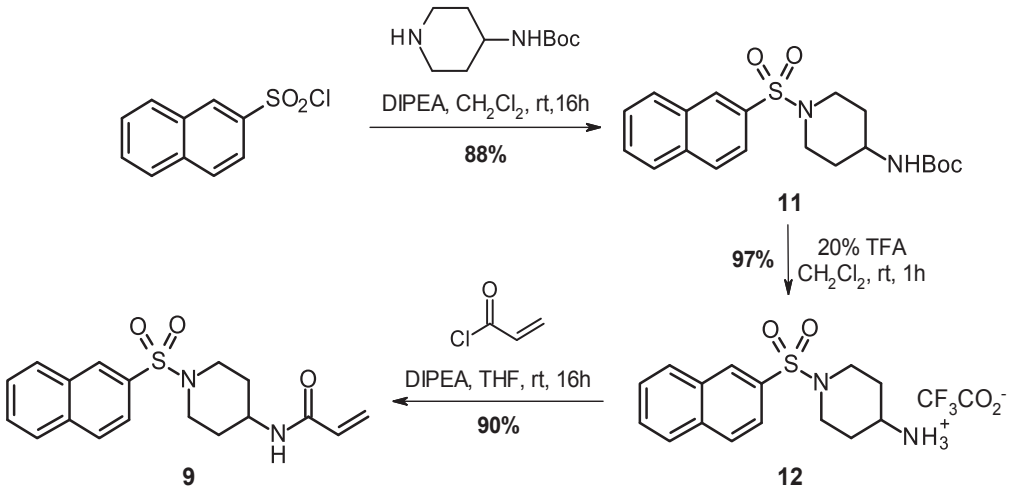

Scheme 21. Synthesis of inhibitor **9**

On the other hand, starting from the commercially available naphthalene-1-sulfonyl chloride, the C-1 substituted naphthalene **10** was obtained in 54% yield (3 steps) via the sulfonamide **13** (88% yield) and TFA salt **14** (95% yield) (**Scheme 22**).

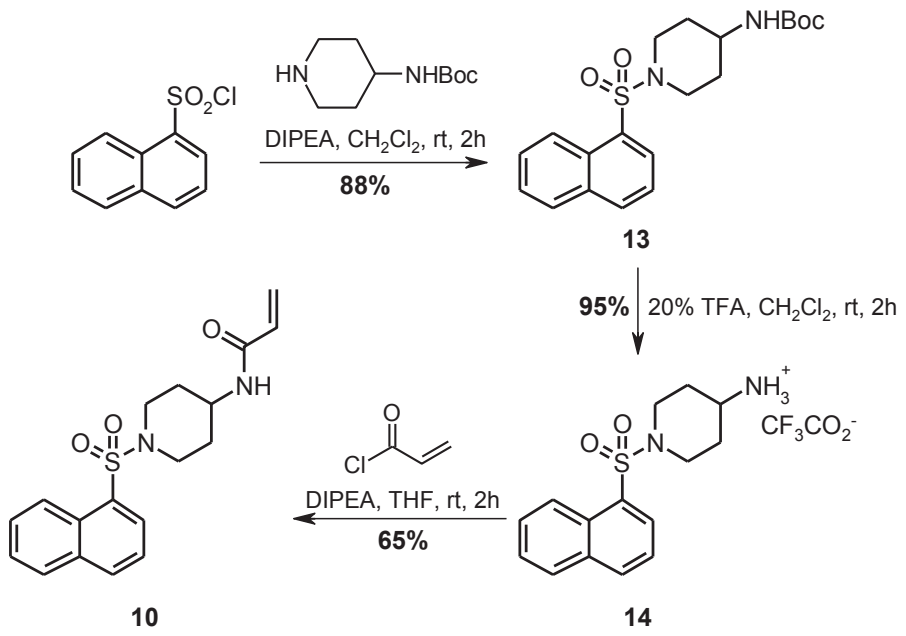

Scheme 22. Synthesis of inhibitor **10**

5.2. TG transamidation inhibition of 9 and 10

Sulfonamide at C-2 position (compound **9**) resulted in a loss of potency of 1.3-fold regarding its C-1 substituted analog **10** (**Table 6**). Both inhibitors, **9** and **10,** present a good selectivity profile over TG1, TG6, and FXIIIa (at least more than 10 μM of IC_{50} for all TG isoforms tested).

IC_{50} (μM)	TG2	TG1	TG6	FXIIIa
9	0.219	> 20	20	> 20
10	0.168 ± 0.03*	> 10	50	> 10

*Values accompanied by standard deviation were averaged from at least two independent experiments; they were otherwise obtained in a single determination.

Table 6. TG2 inhibition and TG selectivity of **9** and **10**

6. Substituent at the C-5 position on naphthalene ring

6.1. Synthesis of 5-(di-*n*-butyl)amino and 5-acetylamino derivatives 15a-b

Different amino substituents were introduced at the C-5 position on the naphthalene ring. A dibutylamino group was incorporated at the C-5 position to check the effect of a bulky dialkyl chain on the inhibitory activity. In the same way, an acetamide group at C-5 position was also tested.

Following the synthetic strategy described in sections 3 and 5 of this chapter, TG2 inhibitors **15a** and **15b** were prepared in three steps (**Scheme 23**). Both starting

materials (di-*n*-butylamino)naphthalene-1-sulfonyl chloride, and 5-(acetylamino)naphthalene-1-sulfonyl chloride, which are commercially available, were treated with 4-(*N*-Boc-amino)piperidine to give sulfonamides **16a-b**. After amine deprotection, compounds **15a-b** were obtained by acylation of ammonium salts **17a-b** in the presence of acryloyl chloride and Hünig's base (yields are reported in **Table 7**).

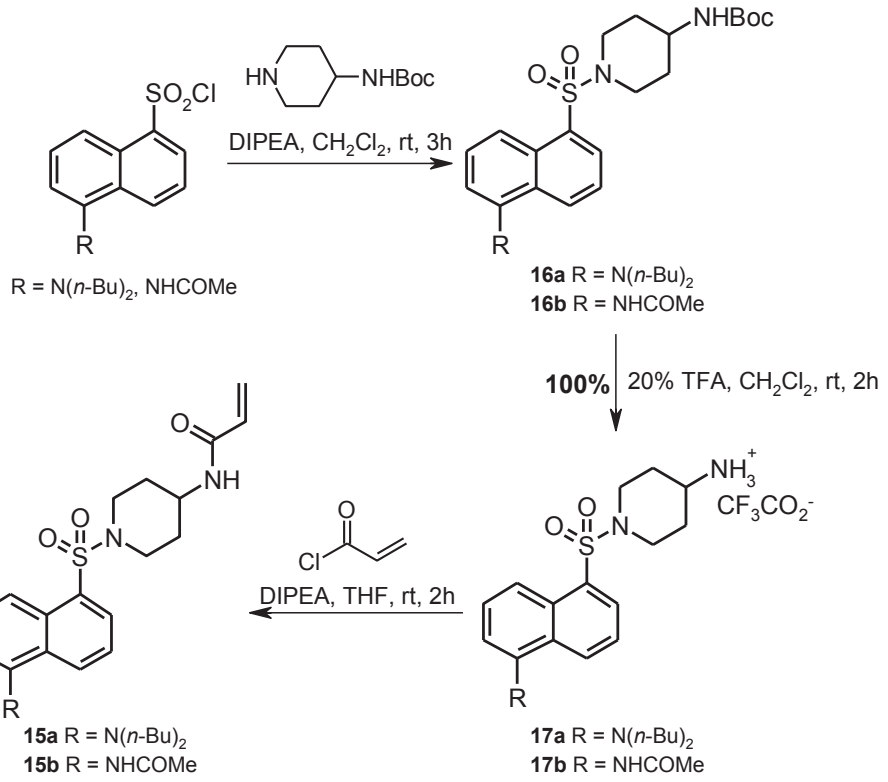

Scheme 23. General synthesis of **15a** and **15b**

R	**16** - Yield (%)	**17** - Yield (%)	**15** - Yield (%)
N(*n*-Bu)$_2$	**16a** - 97	**17a** - 100	**15a** - 50
NHCOMe	**16b** -100	**17b** - 100	**15b** - 64

Table 7. Isolated yields (%) for compounds **15** to **17**

6.2. TG transamidation inhibition of 15a-b

When comparing potencies from the different C-5 substituted naphthalenes synthesized (**Table 8**) with the non-substituted naphthalene **10** and the *N,N*-dimethylamino derivative **1**, the amino derivative **15a** resulted in a drastic decrease in the inhibitory activity, being this compound up to 100-fold less potent relative to **1**. A considerably improvement of potency up to 6- and 5-fold relative to **1** and **10**, respectively, was observed when acetamide group was introduced at C-5 position (**15b**, IC_{50} = 0.019 μM),

also presenting a good selectivity profile (IC_{50} of more than 10 μM) over TG1, TG6, and FXIIIa.

IC_{50} (μM)	R	TG2	TG1	TG6	FXIIIa
1	$N(Me)_2$	0.115 ± 0.009*	> 100	> 50	> 100
10	H	0.168 ± 0.030*	> 10	50	> 10
15a	$N(n\text{-}Bu)_2$	11.7	> 10	NT	> 10
15b	NHCOMe	0.019 ± 0.006*	> 10	> 50	> 10

*Values accompanied by standard deviation were averaged from at least two independent experiments; they were otherwise obtained in a single determination. NT = not tested.

Table 8. TG2 inhibition and TG selectivity of **1**, **10**, and **15a-b**

7. Introduction of an acetylamino group at the C-4 position

7.1. Synthesis of the 4-(acetylamino)naphthalen-1-yl derivative

Taking the compound **15b** as reference, introduction of an acetamide at C-4 position was desirable in order to check how the 4-acetamido-1-naphthyl scaffold would affect the inhibitory activity of compounds on TG2. Starting from the commercially available 4-(acetylamino)naphthalene-1-sulfonyl chloride, acetamide **18** was obtained, via isolated intermediates **19** and **20**, in a global yield (3 steps) of 48% (**Scheme 24**).

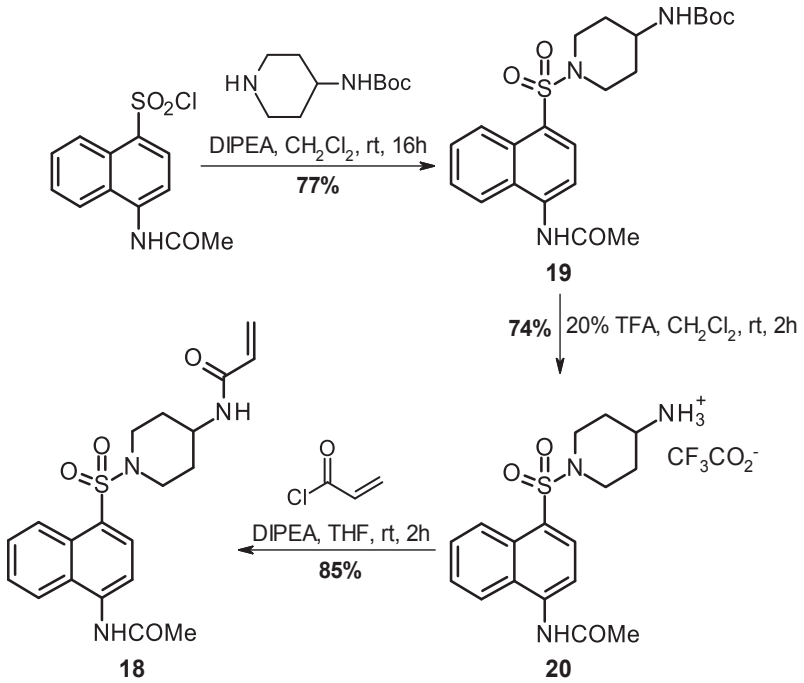

Scheme 24. Synthesis of **18**

7.2. TG transamidation inhibition of 18

When the compound **18** was assayed against TG2, its inhibitory activity slightly decreased compared with its C-5 analog **15b** (**Table 9**). The compound **18** was observed to be 1.6-fold less potent than **15b**. The introduction of an acetamide at the C-4 position did not improve the activity against TG2. Nevertheless, the compound **18** also presented a good selectivity profile over TG1, TG6, and FXIIIa (**Table 9**).

IC_{50} (μM)	TG2	TG1	TG6	FXIIIa
15b	0.019 ± 0.006*	> 10	> 50	> 10
18	0.030 ± 0.007*	> 50	> 20	> 50

*Values accompanied by standard deviation were averaged from at least two independent experiments; they were otherwise obtained in a single determination.

Table 9. TG2 inhibition and TG selectivity of **15b** and **18**

8. Introduction of an arylamide at the C-5 position on naphthalene ring

At this stage, the TG2 inhibitor **15b** was our lead compound with a nanomolar inhibitory activity against TG2 and a good selectivity over other transglutaminase isoforms. The next step was to modify the acetamido group through the replacement of the methyl by an aryl ring beginning by a phenyl (**Figure 50**). These aromatic rings at the C-5 position, varying from mono- to trisubstituted aryls with electron withdrawing groups (e.g., Cl, CF_3 and NO_2 groups), and electron-donating groups (e.g., methoxy, methyl groups), were introduced in order to check if bulky moieties are tolerable within the TG2 active pocket. Furthermore, the position of the substitutions around the benzene ring have also been modified, varying from meta to para positions, thus yielding a wide variety of substituted arylamides.

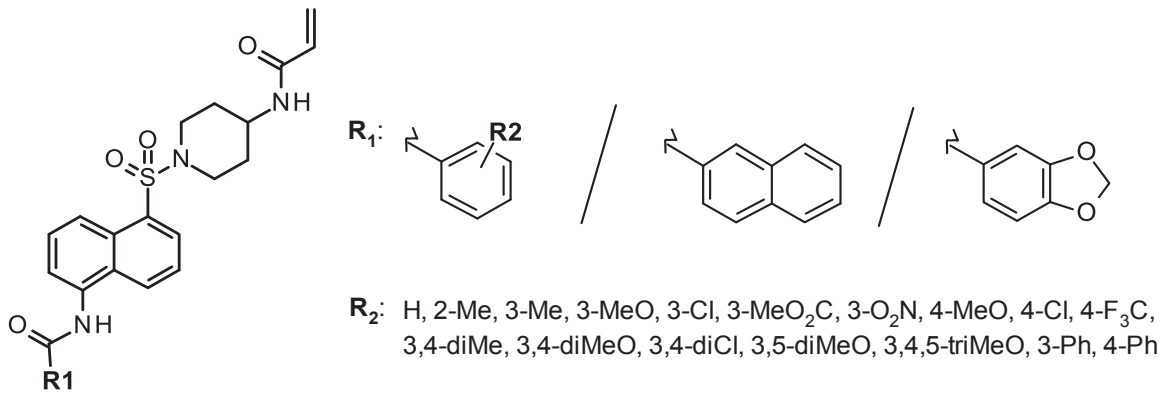

Figure 50. General structure of the 5-(arylamido)naphthalene TG2 inhibitors from this section, and the different aryl substituents introduced at R_1. R_1 represents the different aryl substituents introduced at this position; and R_2, represents the substituents introduced around the benzene ring

8.1 Synthesis of 5-(arylamido)naphthalene-1-sulfonyl chlorides 22

As described already, 5-(arylamido)naphthalene-1-sulfonyl chlorides are the starting materials of the synthesis but in this case, they are not commercially available or are sold at high cost. So, the preparation of these derivatives was realized according to a classical two-step strategy following the procedure carried out by Jenkins et al.[140] Therefore, acylation of 5-aminonaphthalene-1-sulfonic acid, commercially available, with different benzoyl chlorides gave 5-(arylamido)naphthalene-1-sulfonic pyridinium salts **21a-s** in fair yields (**Scheme 25**, **Table 10**), then chlorination of **21** was performed in the presence of thionyl chloride in DMF to afford the corresponding sulfonyl chlorides **22a-s** (**Scheme 25**, **Table 10**). The crude sulfonyl chlorides were ready used in the next step without further purification and characterisation.

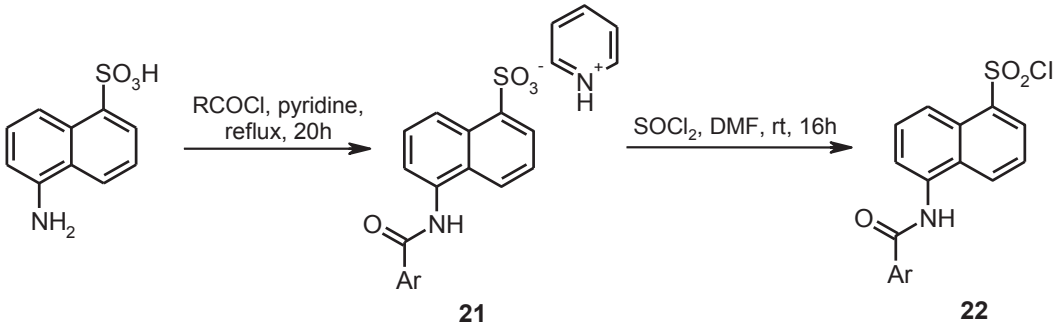

Scheme 25. General synthesis of 5–(arylamido)naphthalene-1-sulfonyl chlorides **22a-s**

Ar	**21** - Yield (%)	**22** - Yield (%)	Ar	**21** - Yield (%)	**22** - Yield (%)
Ph	**21a** - 52	**22a** - 46	3,4-diMePh	**21k** - 59	**22k** - 95
2-MePh	**21b** - 58	**22b** - 75	3,4-diMeOPh	**21l** - 56	**22l** - 87
3-MePh	**21c** - 26	**22c** - 66	3,4-diClPh	**21m** - 38	**22m** - 81
3-MeOPh	**21d** - 32	**22d** - 55	3,5-diMeOPh	**21n** - 48	**22n** - 71
3-ClPh	**21e** - 50	**22e** - 79	3,4,5-triMeOPh	**21o** - 49	**22o** - 75
3-MeO_2CPh	**21f** - 37	**22f** - 69	naphth-2-yl	**21p** - 45	**22p** - 88
3-O_2NPh	**21g** - 42	**22g** - 100	benzo[1,3]dioxol-5-yl	**21q** - 39	**22q** - 95
4-MeOPh	**21h** - 57	**22h** - 70	biphen-3-yl	**21r** - 41	**22r** - 78
4-ClPh	**21i** - 46	**22i** - 68	biphen-4-yl	**21s** - 46	**22s** - 86
4-F_3CPh	**21j** - 33	**22j** - 96			

Table 10. Isolated yields (%) for compounds **21a-s** and **22a-s**

8.2. Synthesis of 5-(arylamido)naphthalene derivatives 23a-c

Starting from 5-(benzamido-, 3,4-dimethoxybenzamido or 3-nitrobenzamido)naphthalene-1-sulfonyl chlorides **22a**, **22l** and **22g**, final compounds **23** were obtained by our three step synthetic pathway (sulfonylation (**24**), quantitative deprotection (**25**) and acylation). The reaction conditions and yields are reported in **Scheme 26** and **Table 11**, respectively.

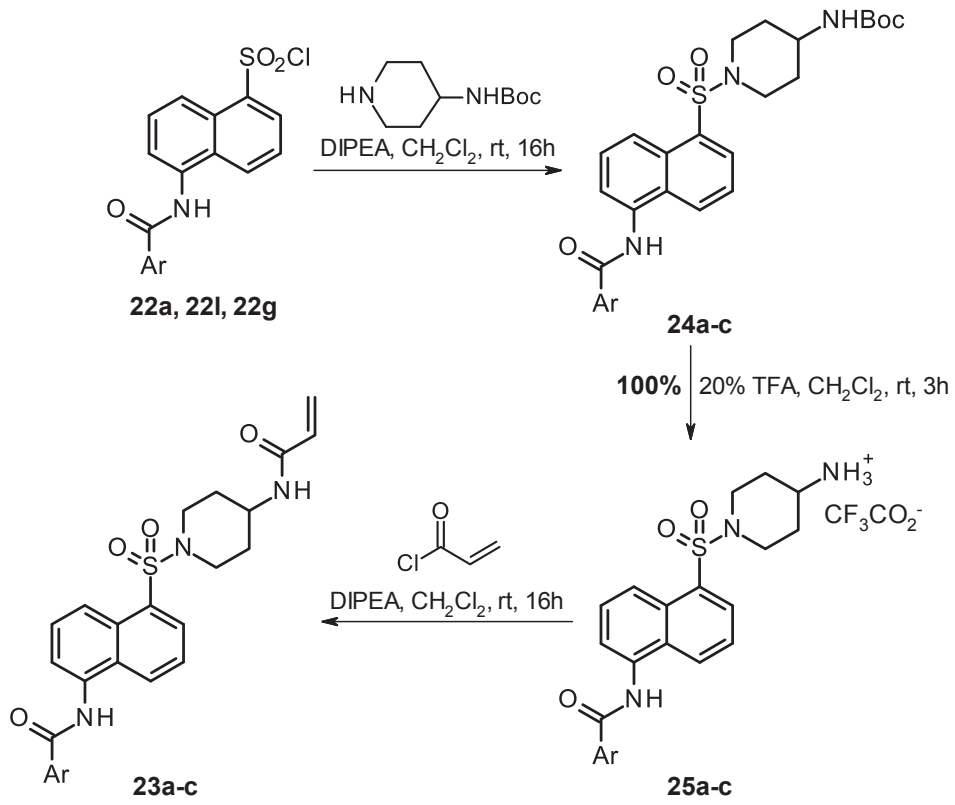

Scheme 26. General synthesis of 5-(arylamido)naphthalene inhibitors **23a-c**

22 - Ar	**24** - Yield (%)	**23** - Yield (%)
22a - Ph	**24a** - 84	**23a** - 65
22l - 3,4-diMeOPh	**24b** - 71	**23b** - 75
22g - 3-O_2NPh	**24c** - 56	**23c** - 57

Table 11. Isolated yields (%) for compounds **22** to **24**

8.3. Synthesis of 5-(arylamido)naphthalene derivatives 23d-s

8.3.1. Synthesis of *N*-(piperidin-4-yl)acrylamide 27

In this section the synthesis of the *N*-(piperidin-4-yl)acrylamide **27**, employed as starting material for the synthesis of the 5-(arylamido)naphthalene derivatives **23d-s**

presented in this section, was firstly carried out. This starting material was thought to save synthetic steps (with the consequent saving on reagents), but also to increase the global yields for the obtaining of the next set of TG2 inhibitors (**23d-s**), by only one more synthetic step starting from their corresponding 5-(arylamido)naphthalene-1-sulfonyl chlorides **22b-f**, **22h-k** and **22m-s** (Section 8.1, **Table 10**).

The synthesis of this compound is reported in **Scheme 27**. Treating the commercially available *tert*-butyl 4-amino-1-piperidinecarboxylate with acryloyl chloride in the presence of the Hünig's base furnished acrylamide **26** in 64% yield. Then, Boc hydrolysis in acidic conditions (TFA) afforded the *N*-(piperidin-4-yl)acrylamide **27** in quantitative yield.

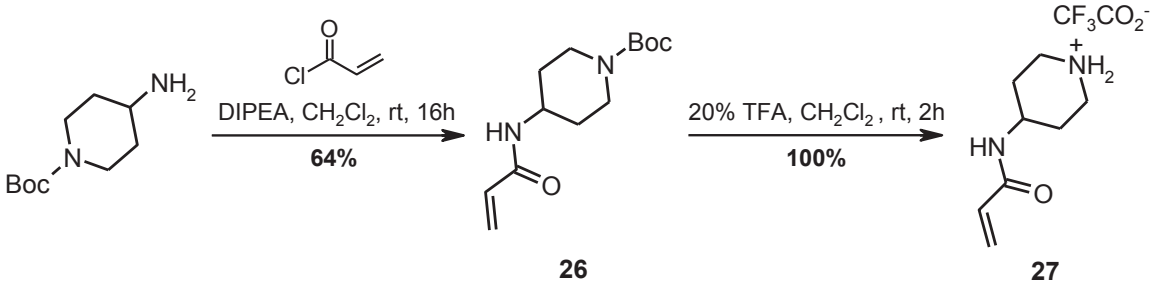

Scheme 27. Synthesis of the *N*-(piperidin-4-yl)acrylamide **27**

As a proof that this synthetic approach is advantageous, the synthesis of the 3,4-dimethoxybenzamido derivative **23b** is reported in **Scheme 28** (**b**), which is also compared with the three step strategy already reported in section 8.2 (**a** in **Scheme 28**). The global yield for the already described three step synthesis to afford compound **23b** from its sulfonyl chloride **22l** was 53%, while a higher global yield (64%) was obtained following the one step synthesis strategy. Thus, the next set of inhibitors was carried out following this new one-step synthetic approach.

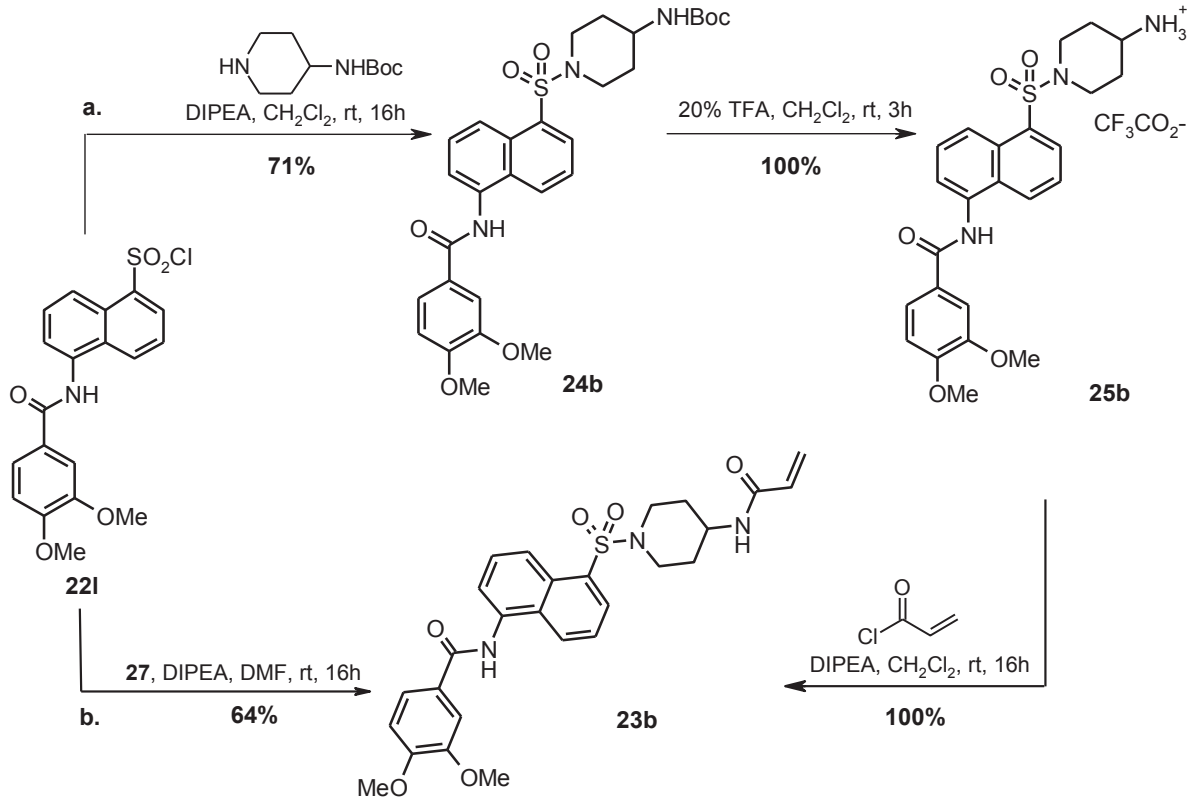

Scheme 28. Synthesis of inhibitor **23b** by the two proposed synthetic strategies (**a** and **b**)

8.3.2. Synthesis of 5-(arylamido)naphthalen-1-yl derivatives 23d-s

The final TG2 inhibitors described in this section are synthesized from their corresponding sulfonyl chlorides **22** in only one synthesis step (**Scheme 29**) as commented above. In order to yield the final 5-(arylamido)napththalen-1-yl derivatives **23d-s**, crude sulfonyl chlorides **22b-f**, **22h-k** and **22m-s** were treated with **27** in the presence of DIPEA in DMF. The non-optimized yields of the final compounds **23d-s** are reported in **Table 12**.

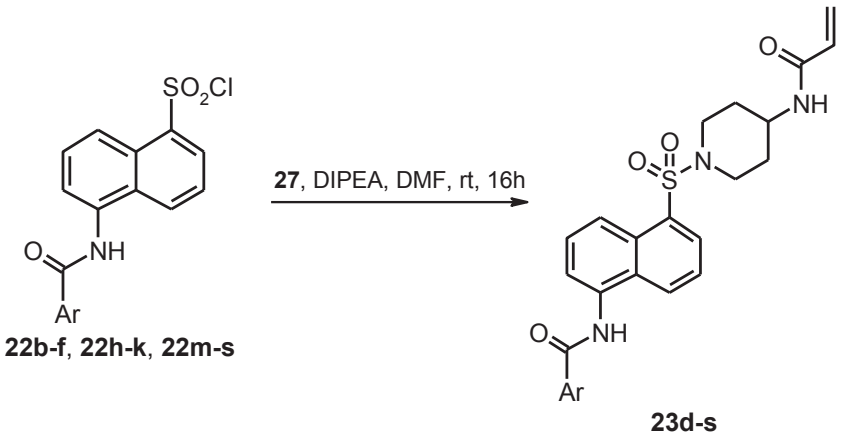

Scheme 29. General synthesis of 5-(arylamido)naphthalene inhibitors **23d-s**

22 - Ar	**23** - Yield (%)	**22** - Ar	**23** - Yield (%)
22b - 2-MePh	**23d** - 26	**22k** - 3,4-diMePh	**23l** - 43
22c - 3-MePh	**23e** - 63	**22m** - 3,4-diClPh	**23m** - 46
22d - 3-MeOPh	**23f** - 71	**22n** - 3,5-diMeOPh	**23n** - 75
22e - 3-ClPh	**23g** - 63	**22o** - 3,4,5-triMeOPh	**23o** - 52
22f - 3-MeO_2CPh	**23h** - 81	**22p** - naphth-2-yl	**23p** - 59
22h - 4-MeOPh	**23i** - 74	**22q** - benzo[1,3]dioxol-5-yl	**23q** - 56
22i - 4-ClPh	**23j** - 22	**22r** - biphen-3-yl	**23r** - 41
22j - 4-F_3CPh	**23k** - 22	**22s** - biphen-4-yl	**23s** - 78

Table 12. Isolated yields (%) for compounds **23d-s**

8.4. Benzamide at the C-4 position on naphthalene ring: synthesis of 28

Similar to the Section 7.1 of this chapter, a substitution at C-4 position on naphthalene ring was carried out, in this case, by introducing a benzamide at the same position (**Scheme 30**). The 4-(benzamido)naphthalene derivative **28** was synthesized from the commercially available 4-(amino)naphthalene-1-sulfonic acid, following the same three step synthetic strategy as described previously in this chapter for the synthesis of the final 5-(arylamido)naphthalene derivatives **23d-s** (section 8.3.). Therefore, starting from the commercially available 4-(amino)naphthalene-1-sulfonic acid and following the procedure carried out by Jenkins et al.,[140] treatment with benzoyl chloride in pyridine provided the 4-(benzamido)naphthalene-1-sulfonic pyridinium salt **29** in 64% yield, which was chlorinated with thionyl chloride to afford crude sulfonyl chloride **30**. Then, subsequent acylation with *N*-(piperidin-4-yl)acrylamide **27** in the presence of Hünig's base in DMF furnished the final compound **28**. The global yield for this synthesis was 13% (3 steps).

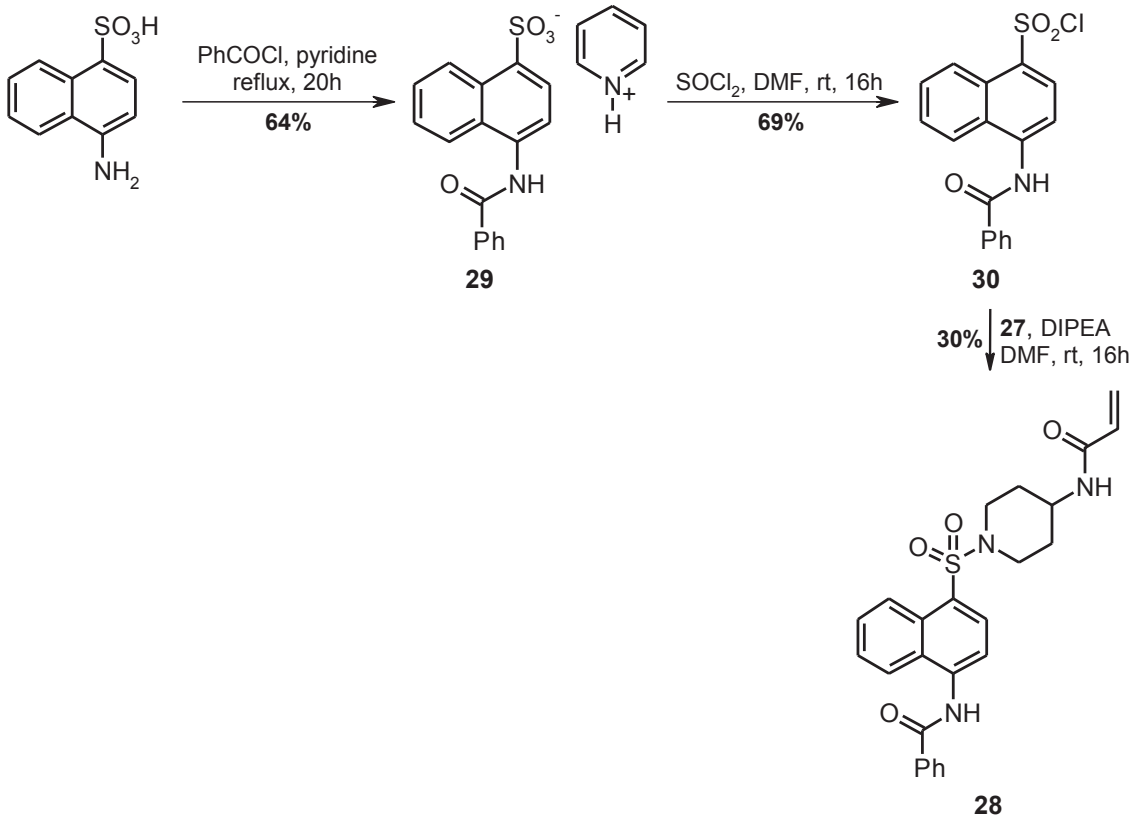

Scheme 30. Synthesis of **28**

8.5. TG transamidation inhibition of 23a-s and 28

The inhibition study of the 5-(arylamido)naphthalene derivatives **23a-s** was first investigated. The inhibition results against TG2 and the different TG isoforms tested are shown **Table 13**. Compared with acetamide **15b** at this position, the extension of the C-5 position on naphthalene with a phenyl (**23a**) resulted in almost equipotencies (IC_{50} = 0.018 μM). The study of different monosubstituted benzamides at 2-, 3-, and 4-positions was next investigated. Benzamides substituted at the *meta* position (**23c**, **23e-h**) resulted in improved activities over TG2 when comparing to those with substitutions at the *ortho* (**23d**) and *para* (**23i-k**) positions. The best monosubstituted benzamide was the 3-O_2NPh (**23c**), which improved potency values up to 3-fold compared with the simple benzamide **23a**. Furthermore, the di- and trisubstituted benzamides (**23b**, **23l-o**) also have improved activity over TG2, being the 3,4-diOMePh, compound **23b**, the most active between them (IC_{50} = 0.006 μM), but also the most active compound from this series of derivatives. On the contrary, when more bulky moieties were introduced the benzo[1,3]dioxol-5-yl derivative **23q** resulted in the most active compound over TG2 (IC_{50} = 7 nM) compared with biphenyl compounds **23s** and **23r**, but also compared with the naphthalen-2-yl compound **23p**. All compounds were found to have a good selectivity profile over TG1, TG6 and FXIIIa, with potency values of more than 10 μM for all these TG isoforms tested.

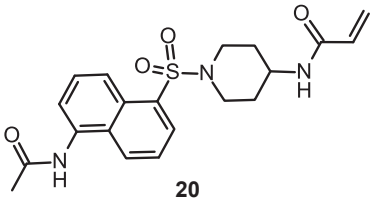

20

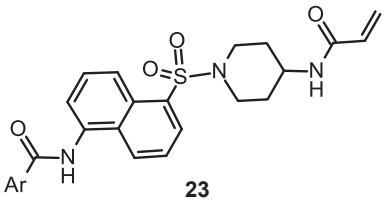

23

IC_{50} (μM)	TG2	TG1	TG6	FXIIIa
20	0.019 ± 0.006*	> 10	> 50	> 10
23a - Ph	0.018 ± 0.005*	> 50	> 50	> 50
23b - 3,4-diMeOPh	0.006 ± 0.001*	> 10	> 10	> 20
23c - 3-O_2NPh	0.007	NT	NT	NT
23d - 2-MePh	0.037	> 20	> 20	> 20
23e - 3-MePh	0.008	> 20	> 10	> 20
23f - 3-MeOPh	0.016	> 20	> 10	> 20
23g - 3-ClPh	0.011	> 20	> 10	> 20
23h - 3-MeO_2CPh	0.015	> 10	> 10	20
23i - 4-MeOPh	0.029	> 20	> 10	> 20
23j - 4-ClPh	0.027	> 20	> 10	> 20
23k - 4-F_3CPh	0.065	> 20	> 10	> 20
23l - 3,4-diMePh	0.010	NT	NT	NT
23m - 3,4-diClPh	0.012	NT	NT	NT
23n - 3,5-diMeOPh	0.009	> 10	> 10	> 20
23o - 3,4,5-triMeOPh	0.012	> 20	> 10	> 20
23p – naphth-2-yl	0.020	> 20	> 20	> 20
23q - benzo[1,3]dioxol-5-yl	0.007	> 20	> 10	> 20
23r - biphen-3-yl	0.028	> 20	> 10	> 20

23s - biphen-4-yl	0.500	> 20	>20	> 20

*Values accompanied by standard deviation were averaged from at least two independent experiments; they were otherwise obtained in a single determination. NT = not tested.

Table 13. TG2 inhibition and TG selectivity of **20** and **23a-d**

On the other hand, when a benzamide was introduced at C-4 position on naphthalene, the inhibitory activity of the derivative **28** also decreases in potency as it also happened for the 4-(acetylamino)naphthalene derivative **20** (**Table 14**). The compound **28** was found in this case to be 3-fold less potent than the C-5 substituted analog **23a**. Because of the decrease of the inhibitory activities the synthesis of compounds substituted at the C-4 on naphthalene was abandoned.

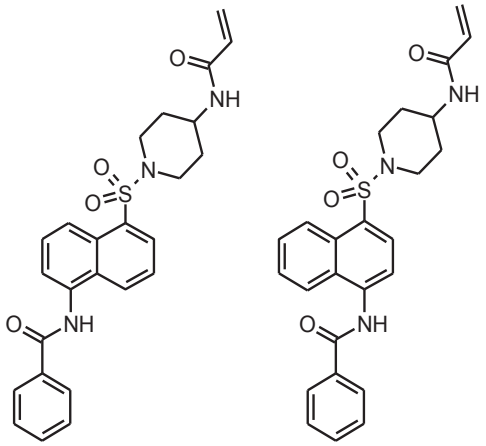

23a **28**

IC_{50} (μM)	TG2	TG1	TG6	FXIIIa
23a	0.018 ± 0.005*	> 50	> 50	> 50
28	0.058	> 50	> 50	> 50

*Values accompanied by standard deviation were averaged from at least two independent experiments; they were otherwise obtained in a single determination.

Table 14. TG2 inhibition and TG selectivity of **23a** and **28**

9. Extending the benzamide at meta position: introduction of an additional amide

In the attempt to further extend the benzamide at the C-5 on naphthalene to go further in the lipophilic pocket of the TG2 active site, compounds bearing an additional substituted amide at its meta position were synthesized.

9.1. Synthesis of 31a-b

For the synthesis of these two compounds the production of aniline derivative **32** was carried out. Reduction of its nitro compound **24c** with iron and NH_4Cl in $EtOH/H_2O$ (5:1) solution for 16h at reflux conditions, furnished **32** in 93% yield (**Scheme 31**).

Then, compound **32** was employed as the starting material for the synthesis of both compounds following a three steps synthesis strategy. First of all, an acylation step, to introduce the additional amide was carried out in the presence of the corresponding acyl chlorides in the presence of Hünig's base in CH_2Cl_2 to yield compounds **33a-b**. *N*-Boc deprotection step in acid solution (TFA) was carried out in order to yield their corresponding ammonium salts **34a-b**, followed by a second acylation step yielding the final derivatives **31a-b** (**Scheme 31**). The yields corresponding with the three synthesis steps for the synthesis of both compounds **31a-b**, and the different synthesis intermediates (**33a-b** and **34a-b**), are reported in **Table 15**.

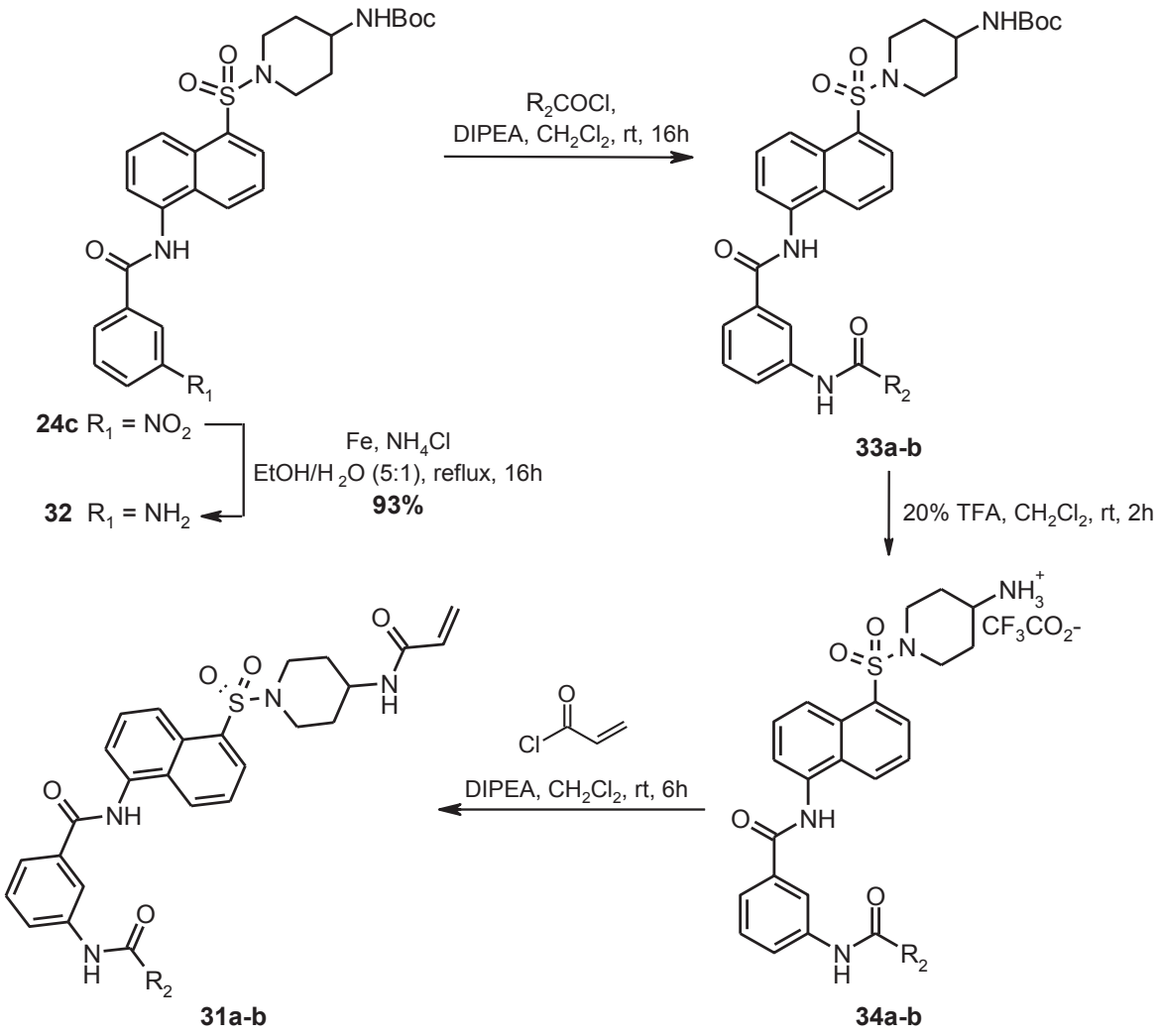

Scheme 31. General synthesis of **31a-b**

R_2	**33** - Yield (%)	**34** - Yield (%)	**31** - Yield (%)
Me	**33a** - 60	**34a** - 97	**31a** - 54
Ph	**33b** - 99	**34b** - 100	**31b** - 65

Table 15. Isolated yields (%) for compounds **31**, **33** and **34**

The global yields for the synthesis of the final naphthalenesulfonamides **31a-b** from the nitrobenzene **24c** (4 steps) are 29 % and 60% for acetamide **31a** and benzamide **31b**, respectively.

9.2. TG transamidation inhibition of 31a-b

Further inhibition tests for these meta-substituted benzamides, compounds **31a-b,** were carried out (**Table 16**). For the substituted acetamide at meta positon (**31a**) a 3-fold loss of activity was observed compared to the 3.4-dimethoxy substituted benzamide **23b**. On the contrary, a loss of potency of 4.3-times was observed when benzamide in compound **31b** was introduced at the same position. We can conclude that extension of benzamide with another amide at meta position have not improve inhibitory activity of compounds, even when both presented a good selectivity profile with IC_{50} values of more than 10 μM for all TG isoforms.

IC_{50} (μM)	TG2	TG1	TG6	FXIIIa
23b	0.006 ± 0.001*	> 10	> 10	> 20
31a	0.022	NT	NT	NT
31b	0.028	> 20	> 20	> 20

*Values accompanied by standard deviation were averaged from at least two independent experiments; they were otherwise obtained in a single determination. NT = not tested.

Table 16. TG2 inhibition and TG selectivity of **23b** and **31a-b**

10. Acrylamide-piperidine linkage modifications

Based on the most potent synthesized TG2 inhibitor, naphthalenesulfonamide **23b**, different derivatives based on its 3,4-dimethoxy-*N*-[5-(piperidine-1-sulfonyl)naphthalen-1-yl]benzamide moiety have been synthesized (**Figure 51**). Two classes of derivatives have been developed depending on both their chemical structure and their functionality. One of these inhibitors, compound **35**, is based on a methylene acrylamide warhead. Another two analogs from the naphthalenesulfonamide **23b**, compounds **36** and **37**, were also synthesized, being based on the warhead structure from the work of Griffin et al.,[117] a *N*-[(2-oxo-2-piperazin-1-yl)ethyl]prop-2-enamide warhead-based structure, as in the case of compound **EB1-155** taken as reference from the same work (**Figure 51**). *Compound **EB1-155** has been published during the achievement of this doctoral dissertation, and it has also been synthesized in our laboratory, in order to be compared with the TG2 inhibitors synthesized in this work, following the author's procedure*.[117]

The first inhibitor **35** will allow knowing if increasing the distance between acrylamide and piperidine, with one sp^3 carbon, will lead to an increase in potency (IC_{50}) against TG2 compared with its homologue, derivative **23b**. On the other hand, based on the warhead structure from **EB1-155**, piperazine and piperidine analogs based on this warhead, compounds **36** and **37** (**Figure 51**), will also allow us to know if this increase in length between sulfonyl and acrylamide moiety, as well as varying the heterocyclic moieties from their warhead moiety, will enhance the inhibitory activity of these compounds.

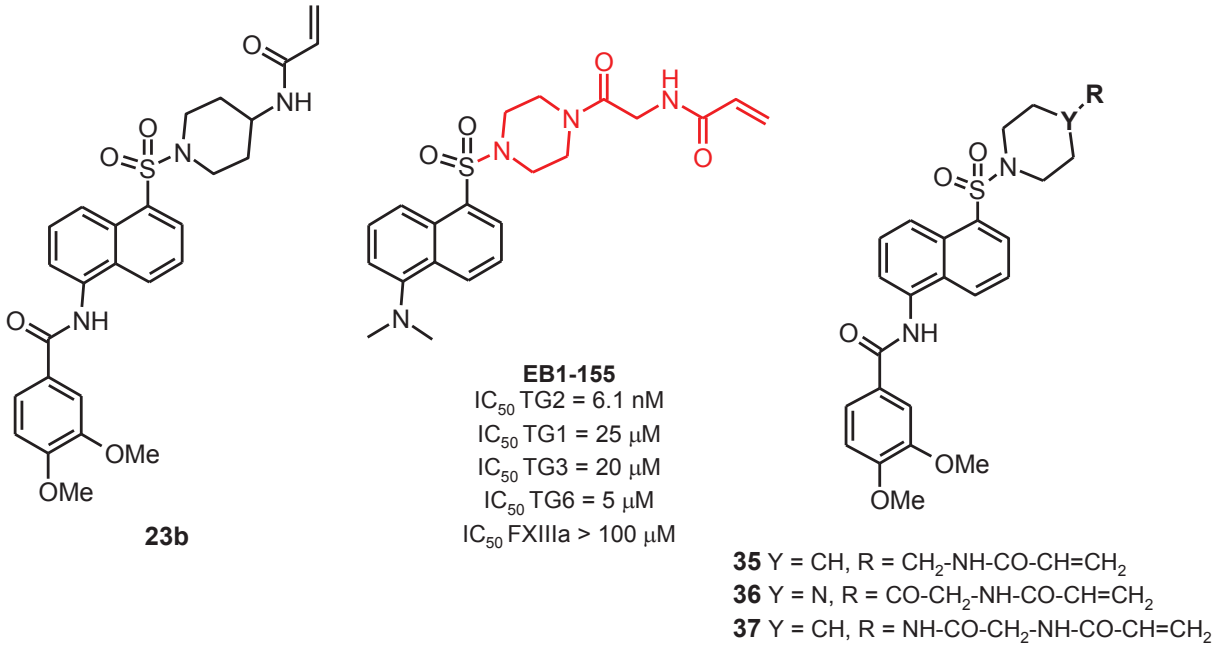

Figure 51. Structures of **23b**, reference compound **EB1-155**,[117] and general structure of **35**, **36**, and **37** synthesized in this section

10.1. Homologation of the linker

Compound **35** was synthesized starting from the sulfonyl chloride **22l** (**Scheme 32**). Firstly, sulfonamide formation by treating **22l** with the *tert*-butyl (piperidin-4-yl)methylcarbamate in the presence of DIPEA, yielded the sulfonamide **38**, which was deprotected in acidic medium to finally being acylated to furnish the compound **35** in 74% yield (33% three step yield).

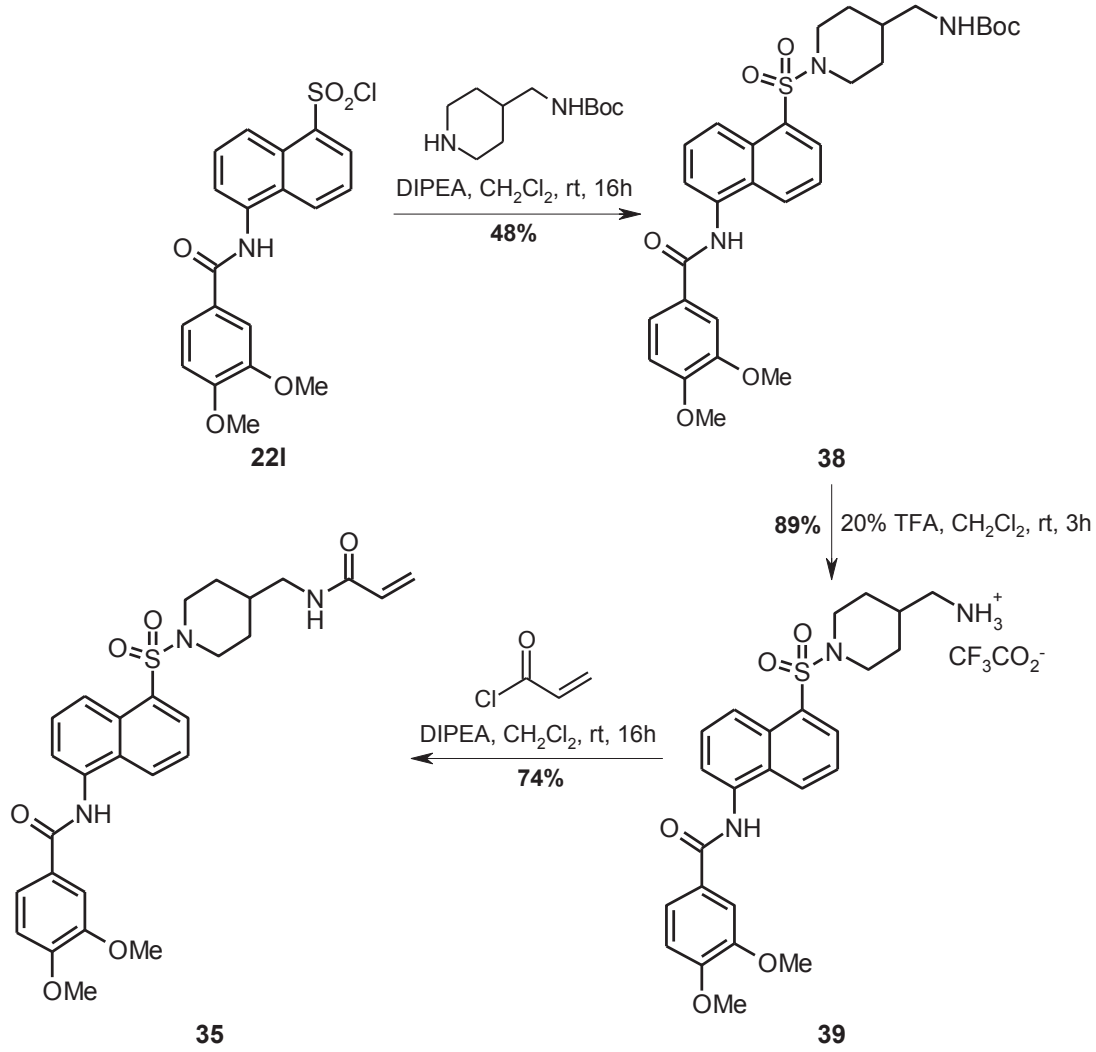

Scheme 32. Synthesis of **35**

10.2. Replacement by an (2-oxoethyl)piperazin-4-yl linker

Starting from sulfonyl chloride **22l**, treating it with the *tert*-butyl *N*-[(2-oxo-2-piperazin-1-yl)ethyl]carbamate in the presence of DIPEA provided **40** in 69% yield. After deprotection of the *tert*-butoxycarbonyl with TFA, the resulting ammonium salt **41** was then acylated with acryloyl chloride to furnish **36** in 80% yield (**Scheme 33**).

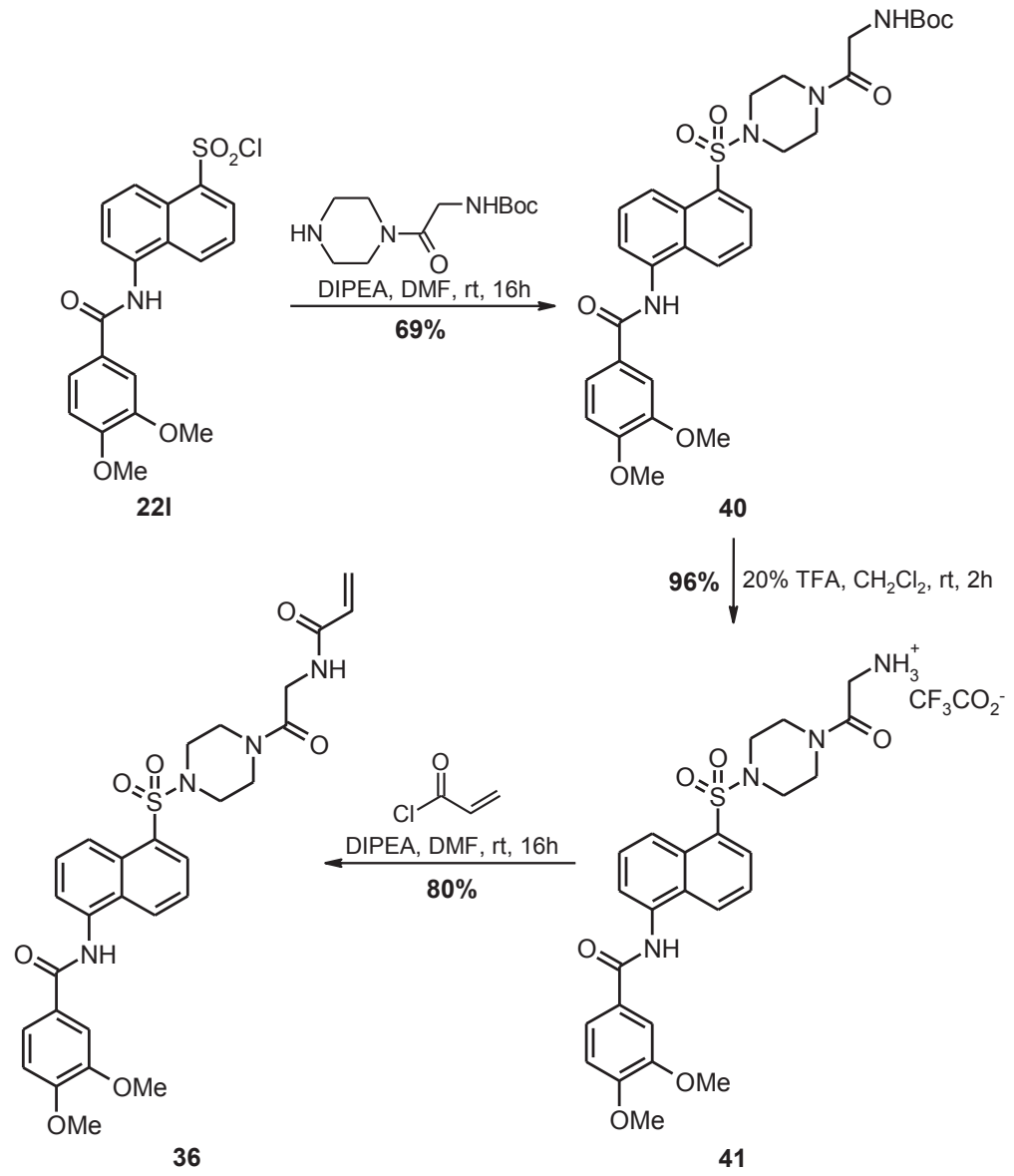

Scheme 33. Synthesis of **36**

10.3. Addition of a glycine amino acid to the linker

For the synthesis of compound **37**, amide formation with EDCI in the presence of DMAP was carried out for the ammonium salt **25b** by treatment with the *N*-(*tert*-butoxycarbonyl)glycine (**Scheme 34**) to yield **42** in 66% yield. Then, deprotection in acid conditions (TFA) provided ammonium salt **43** in 92% yield, whose acylation with acryloyl chloride in the presence of DIPEA furnished the final derivative **37** in 60% yield.

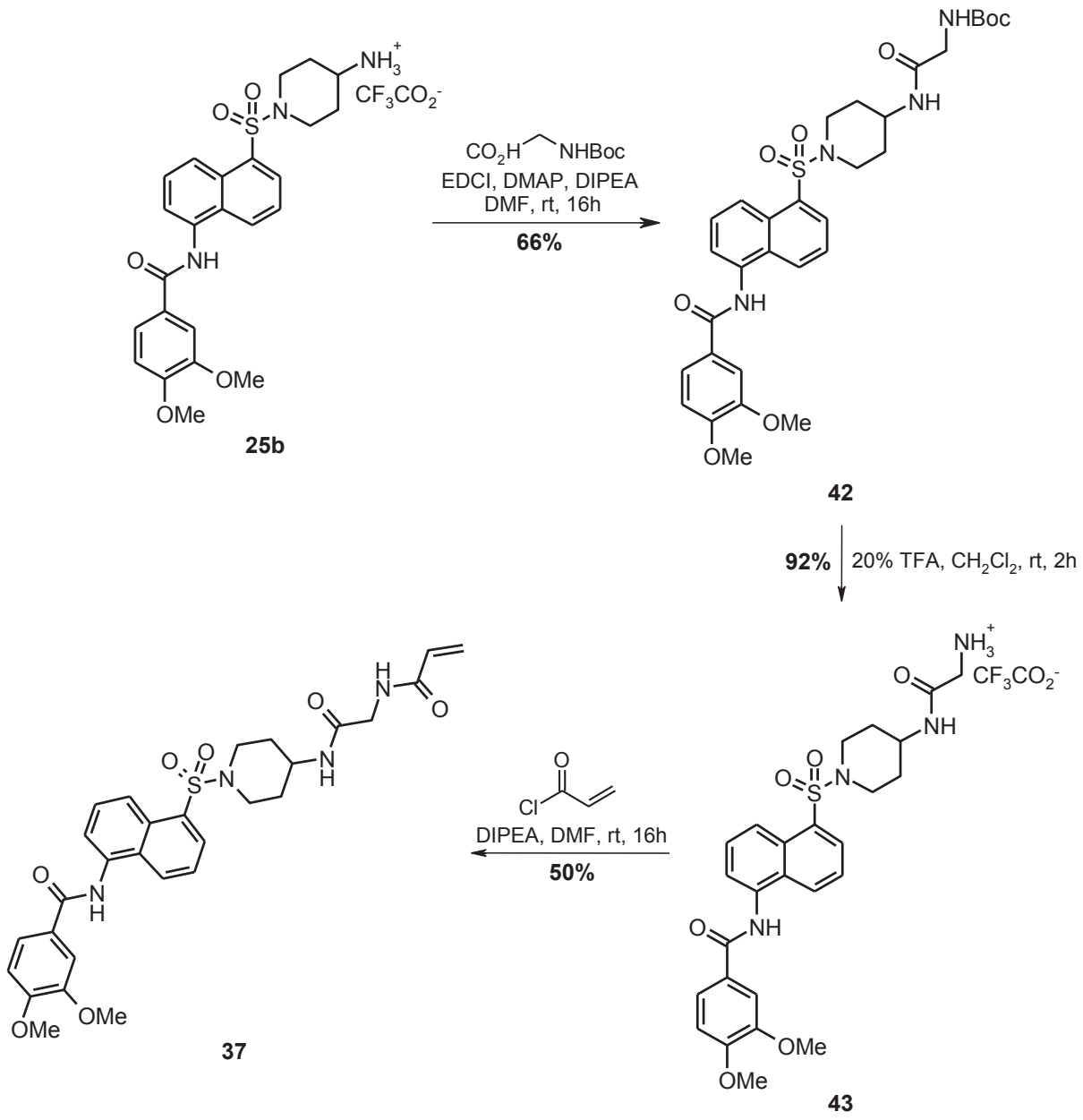

Scheme 34. Synthesis of **37**

10.4. TG transamidation inhibition of 35-37 and EB1-155

The inhibition potencies of derivatives **35**, **36**, and **37**, analogs of compound **23b**, are shown in **Table 17**. Regarding the homolog of compound **23b**, derivative **35**, resulted in a drastic reduction in potency of 77-times, possibly caused by the increase in length of the warhead and its additional sp3 carbon. When compounds **36** and **37** were tested, derivative **37** resulted in a drastically loss of activity (IC_{50} > 2 μM), while its piperazine analog **36** was 8-times less potent than compound **23b**. Derivative **36** showed less activity than compound **EB1-155**, even bearing the same warhead structures. In the same **Table 17**, it can also be compared the most active compound from the new TG2 inhibitors synthesized in this work, compound **23b,** with compound **EB1-155**. Within the same

assay conditions employed for the inhibition studies of this thesis dissertation, the reference **EB1-155** turned out to be around 3-times less active over TG2 (IC_{50} = 0.022 μM) than compound **23b**.

IC_{50} (μM)	TG2	TG1	TG6	FXIIIa
EB1-155	0.022 ± 0.001* (0.0061)***	NT (25)***	4.15 ± 0.35* (5)***	NT (>100)***
23b	0.006 ± 0.001*	> 10	> 10	> 20
35	0.5	> 20	> 20	> 20
36	0.050	> 20	> 10	> 5
37	> 2 (21%)**	> 20	> 20	> 5

*Values accompanied by standard deviation were averaged from at least two independent experiments; they were otherwise obtained in a single determination.** inhibition percentage at 2 μM.*** Values in the literature.[117]

Table 17. TG2 inhibition and TG selectivity of **23b**, **35-37**, and **EB1-155**

11. Synthesis of naphthalenesulfonamide-based prodrugs

11.1. Design perspectives

Acrylamide group is a known covalent Michael acceptor of thiol enzymes which was included in the reactive moiety of many drugs explained in this chapter (**Section 1**). As many covalent reactive groups, it may induce toxicity when reacting with an off-target molecule,[141] but also it will depend on both their dose of the drug employed (e.g., for *in vivo* purposes), and also on their reactivity with natural nucleophiles, such as amines and glutathione (GSH).[142,143] Knowing this, and in order to inhibit TG2 in complex biological systems, the synthesis of a prodrug was performed.

The term "prodrug", or "proagent" was first described by Albet et al.[144] Prodrugs are considered inactive and non-toxic derivatives from their corresponding parent active drugs. Prodrugs activation can occur via biotransformation (metabolic processing reactions) before exhibit their pharmacological actions, and once they reach their *in vivo* target.[145] One example of a prodrug design is the work from Ahn et al.,[146] in which pharmacologically selective “enone-like” pro-drugs for the treatment of cancer are described. These prodrugs were described to suffer bio-oxidative and bio-reductive metabolic processes inside the body. In a different publication, Rooseboom et al.[147] described the different prodrug activating in-cell mechanisms mediated by enzymes (e.g., lyases, kinases, reductases,…) which activate prodrugs into their active drugs.

To sum up the prodrug activity, in **Figure 52** is represented how the chemical stable drug-promoiety entity (the prodrug inhibitor) overcomes any limitation, or barrier, that the parent drug has, to be processed once it arrives to the desired target being transformed into the active drug, and releasing the promoiety as a by-product.[148]

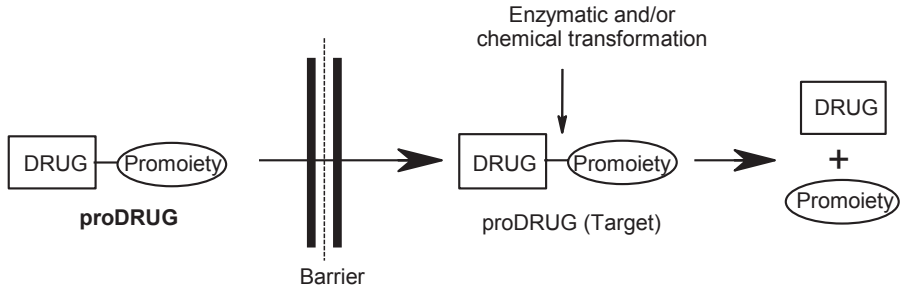

Figure 52. Representations of the ideally non toxic prodrug (pharmacologically inactive) passing through any barrier or limitation that its parental drug cannot overcome. After overcoming the barrier or limitation, the promoiety (any bioreversible group which is chemically or enzymatically labile) will be released from the prodrug, thus resulting in the active drug which will act on the desired target

11.2. Acrylamide prodrugs development

In the effort to develop acrylamide-like prodrugs, different works were taken into account. In the work from Carmi et al.,[149] prodrugs bearing an β-aminoethyl ketone moiety were developed. After bioconversion via β-elimination, these nonreactive compounds were transformed into their α,β-unsaturated carbonyl parent drugs, being able to covalently interact with the cysteine reactive group from the epidermal growth factor (EGF) receptor.

In a different work, from Maresso et al.,[150] the synthesis of different aryl (β-amino)ethyl ketone prodrugs was reported. Furthermore, in this work, an explanation of the mechanism for the β-elimination bioconversion of the β-diaminoethyl ketone to enone was described to happen in a two steps mechanism. As shown in **Scheme 35**, the first step involves deprotonation of α-acidic proton from the diaminoethyl ketone leading to the formation of an enolate. Then, elimination of the dimethylamine yields the active drug. This final enone-like drug was also studied to inhibit a cysteine active site from sortease. The **Figure 53** shows the prodrug herein synthesized and their corresponding acrylamide active drug synthesized in this work.

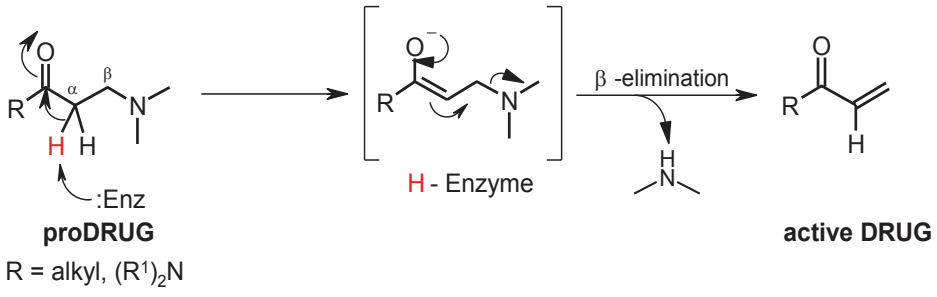

Scheme 35. Bioconversion mechanism of β-diaminoethyl ketone to enone

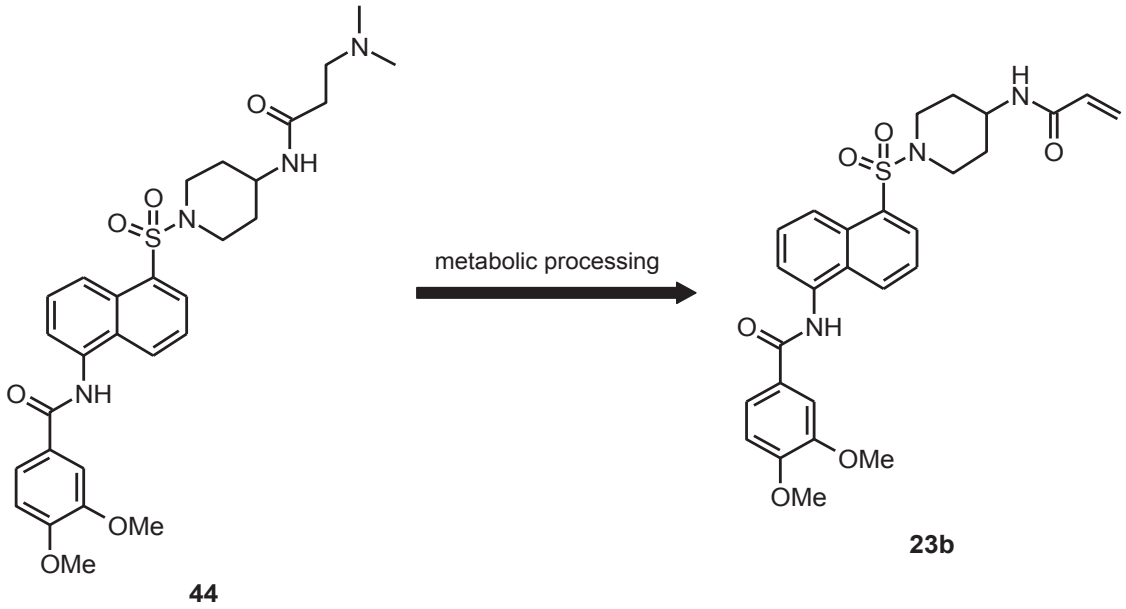

Figure 53. Structure of the pro-drug **44** synthesized in this work, and its corresponding acrylamide active drug **23b**, as a result of its metabolic processing

As shown in **Scheme 36**, amide formation with EDCI in the presence of DMAP was carried out with the ammonium salt **25b** by treating this with 3-(*N,N*-dimethylamino)propanoic acid in its hydrochloride salt form, providing the final prodrug **44** in 55% yield.

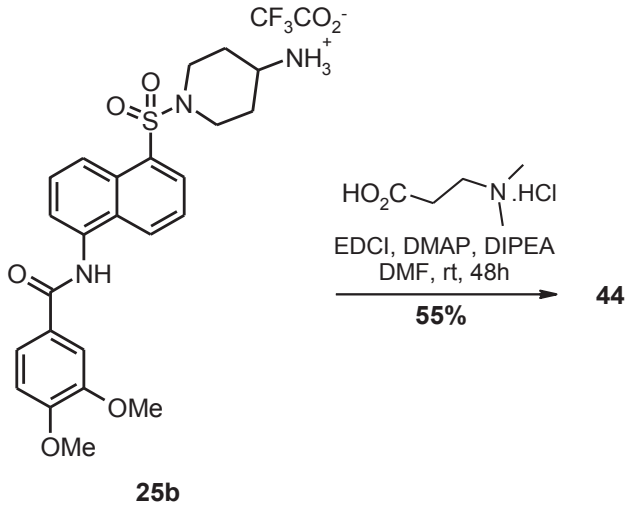

Scheme 36. Synthesis of pro-drug **44**

11.3. TG transamidation inhibition studies of 45

The prodrug **44** was also assayed in an enzymatic test without any influence of the cellular environment. As expected, its potency value, as shown in **Table 18**, was much weaker than their corresponding drug **23b**. An IC_{50} value of more than 1 μM was obtained with prodrug **44**, which is at least around 167-fold less active than compound **23b**.

IC_{50} (μM)	TG2
23b	0.006 ± 0.001*
44	> 1

*Values accompanied by standard deviation were averaged from at least two independent experiments; they were otherwise obtained in a single determination.

Table 18. TG2 inhibition of **23b** and its corresponding pro-drug **44**

12. Synthesis of the reference EB1-155

The compound **EB1-155** has been published in 2014 by Griffin et al.[117] This inhibitor was synthesized in this work to be used as a reference, in order to be compared, in terms of inhibitory activity (IC_{50}), with the new naphthalene-sulfonamide inhibitors synthesized in this work measured with the same TG transamidation method. The synthesis of compound **EB1-155** has been performed as described in the work of reference[117] (**Scheme 37**), with a global yield of 40% (3 steps).

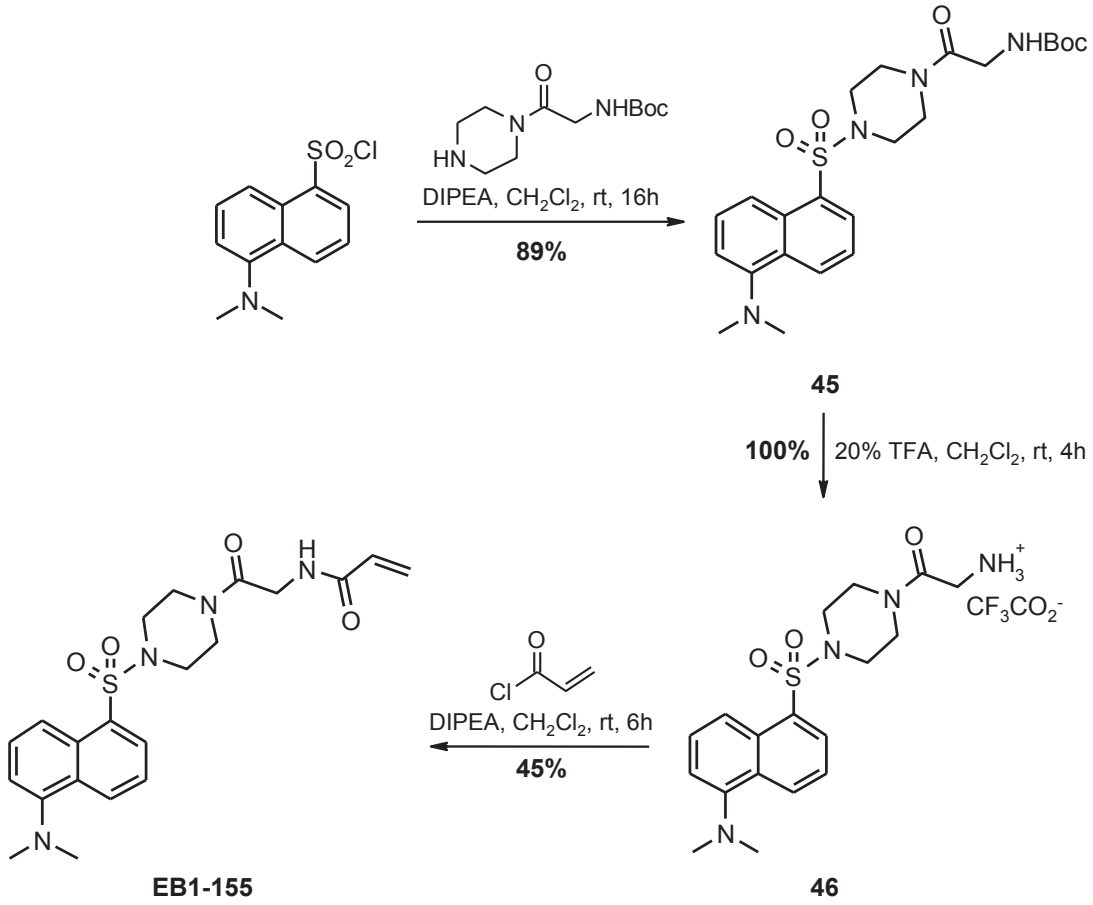

Scheme 37. Synthesis of **EB1-155**

13. Conclusion

With the aim of synthesizing a new series of naphthalene-based inhibitors, a wide range of inhibitors, all bearing a reactive acrylamide as the Michael acceptor for the thiol presented in the active site of TG2 were developed. After the development of different acrylamide-sulfonamide linkages, the 4-aminopiperidine was confirmed as the moiety of choice to be included based on the activity results.

Always with the intention of improving the activity of these compounds against TG2, but also their selectivity against the other isoforms from the transglutaminase family, naphthalene-sulfonamides bearing a substituted benzamide at C-5 position reached the best potencies, with IC_{50} values within the low nanomolar range as for compounds **23b-c**, **23n** and **23o** (**Table 12**), where different mono-, bi-, and tri-substituted methoxies and also a 3-nitro group were substituted at that position in a benzamide moiety. Benzamides substituted at *meta* position (**23c** and **23e-h**) yielded more active compounds (about twice the potency) compared with those with the same substituents at *para* position (**23i-k**), but also compared with the *ortho* position (**23d**). On the contrary, extending the benzamide moiety with another amide at *meta* position, and more bulky moieties like naphthalene (**23p**) and different biphenyls (**23r-s**) resulted in a loss of activity.

To conclude, the objectives from this chapter, which include the development of new potent naphthalene-based TG2 inhibitors, with also presenting a good selectivity profile against the other transglutaminases isoforms, were achieved. As a representative of this chapter, compound **23b** was taken as the lead compound from this serie with an IC_{50} value of 0.006 μM against TG2 and IC_{50} values of more than 10, 10, and 20 μM, over the other TG tested (TG1, TG6, and FXIIIa, respectively), therefore presenting the best activity against TG2, but also a good selectivity against the other TG tested. This compound was also more active over TG2 than reference molecules (compound **X** and **EB1-155**).

Experimental part - Chapter 2

Organic chemistry synthesis

Generalities

All reagents or solvents were purchased from Sigma-Aldrich, Fluorochem, Alfa-Aesar and Fisher Acros. All commercially solvents or reagents were used without purification. Regarding reactions requiring anhydrous conditions, solvents employed were either appropriately dried and distilled under calcium hydride, or purchased as already commercially available sure-sealed anhydrous solvents.

All reactions requiring anhydrous conditions were conducted in oven-dried apparatus under argon atmosphere.

All the reactions were monitored by Thin Layer Chromatography (TLC) analyses which were conducted on aluminium sheets silica gel Merck 60F254. The corresponding spots were followed under UV light (254 and 312 nm). For the non-ultraviolet material, spots were stained and heated with ninhydrin (as in the case of non aromatic amines).

Flash chromatography was carried out on silica gel 60 (40-63 μm, Merck) using the indicated solvents for the purification of compounds.

All the extracted organic layers were dried over Na_2SO_4.

The ^{1}H and ^{13}C NMR spectra were recorded on a Bruker Advance ALS300 and DRX400 MHz from Bruker. Chemical shifts are reported in ppm (δ) and were referenced to DMSO-d_6 (^{1}H, 2.50 ppm; ^{13}C, 39.52 ppm) or $CDCl_3$ (7.26 ppm). The coupling constants (*J*) were given in Hz.

The HRMS-ESI mass spectra were recorded in positive-ion mode on a hybrid quadrupole time-of-flight mass spectrometer (MicroTOFQ-II, Bruker Daltonics, Bremen) with an Electrospray Ionization (ESI) ion source. For the mass spectrometry of low resolution, LRMS-ESI mass spectra were recorded in a Thermo Finnigan MAT 95 XL spectrometer.

Melting points were determined using a Tottoli Büchi SMP-20 capillary instrument and are uncorrected.

To measure the enzymatic transamidation activity of the different transglutaminases employed in this work (TG1, TG2, TG6, and FXIIIa) different ELISA-LIKE microassays from Covalab R&D (Lyon, France), were employed. Opr-0030 kit assay (for TG2) and different TG-Cov tests (TG1, TG6, and FXIIIa) were used.

Recombinant human transglutaminases were purchased from Covalab R&D (Lyon, France). To activate FXIII and TG1 thrombin and dispase were used (Sigma-Aldrich, France).

Absorbance for transglutaminase transamidation assays was measured at 450 nm using a Multiskan Ascent microplate reader from Labsystems (Finland).

IC_{50} (half maximum inhibition; potency) values for each of the inhibitors, were calculated using the ED50 plus v1.0 online software.

General procedures

A. *Sulfonamide formation*

DIPEA (2 eq) was added to a solution of the amine (1 eq) dissolved in CH_2Cl_2 (0.4 M) or DMF (0.1 M), following by the addition of the corresponding sulfonyl chloride (1.1 eq) on ice-water (0ºC). The reaction was left to react under argon atmosphere at room temperature until completion (2 to 16 h).

Work-up 1: The reaction mixture was then extracted three times with water, and the recovered organic layer was then washed with saturated aqueous NaCl solution, and dried over Na_2SO_4. Then the solvent was evaporated and the resulting crude product was purified by flash column chromatography (MeOH in CH_2Cl_2), yielding the desired product.

Work-up 2: Addition of the reaction mixture (drop-wise manner) into a well stirred flask containing ice-water (10 mL) and the resulting suspension was filtered. Then, the solid was successively washed with cold water (10 mL), 1N aquous HCl solution (2 mL) and water (10 mL), to finally being dried in a P_2O_5 atmosphere under vacuum. After drying, a purification step by precipitation (solvent: MeOH/CH_2Cl_2) or flash column chromatography (solvent: MeOH in CH_2Cl_2) and/or precipitation furnished the final compound.

B. *Boc deprotection*

Addition of trifluoroacetic acid (1/5; v/v) to a solution containing the Boc-protected amine bearing compound dissolved in CH_2Cl_2 (4/5; v/v). Then, the reaction was left to proceed for 1 to 4 h. Solvent and excess TFA were evaporated under vacuum. The resulting dried residue was precipitated from Et_2O, filtrated, and washed with Et_2O. The final acetate salt was then recovered from the filter, and stored under vacuum with P_2O_5 until use.

C. *Acrylamide formation*

To a solution of the amine (1 eq) in solvent (THF or CH_2Cl_2 or DMF; 0.1 M) was added DIPEA (3 eq) at room temperature, followed by the addition of acyl chloride (1.1 eq) on ice-water (0ºC). After returning to room temperature the reaction mixture was allowed to proceed until completion (from 2 to 16 h) under argon atmosphere.

Work-up 1 *(THF as solvent)*: THF was removed under vacuum and the resulting crude extract dissolved in CH_2Cl_2 and extracted three times in water. The organic layer was

washed with saturated aqueous NaCl solution and dried over Na_2SO_4 before evaporating the solvent again

under vacuum. The resulting residue was purified by flash column chromatography (solvent: PE/EtOAc or MeOH/CH_2Cl_2) to yield the desired compound.

Work-up 2 *(CH_2Cl_2 as solvent)*: The reaction mixture was diluted in CH_2Cl_2 and extracted three times in water, the organic layer washed once with saturated aqueous NaCl solution and dried over Na_2SO_4 and the solvent concentrated to dryness. The resulting residue was purified using flash column chromatography (solvents: PE/EtOAc or MeOH/CH_2Cl_2) to yield the desired compound.

Work-up 3*(DMF as solvent)*: Addition of the reaction mixture (dropwise manner) into a flask containing water. Then, the precipitate formed was filtrated, washed with 1N aqueous HCl solution (2 mL), and washed again with water. The resulting solid was dried under vacuum in P_2O_5, to finally being purified by flash column chromatography (solvent: MeOH/CH_2Cl_2) and precipitated (solvents: EtOH, MeOH or CH_2Cl_2/Et_2O).

Work-up 4*(DMF as solvent)*: The crude material was concentrated to dryness, diluted in CH_2Cl_2 and extracted three times in water. The organic layer was then dried (Na_2SO_4), and evaporated. The resulting residue was purified using flash column chromatography (solvent: MeOH in CH_2Cl_2).

D. 4- *and 5-(Arylamido)naphthalene-1-sulfonic pyridinium salts synthesis*

To a solution of the commercially available 5-amino-1-naphthalenesulfonic acid (1 eq) in pyridine (0.67 M) was added the corresponding acyl chloride (1.2 eq) and the resultant solution was stirred at 100ºC for 20 h. After this time, the solvent was then removed under vacuum, and the crude material was precipitated from MeOH, filtrated and washed (2 x) with MeOH to afford the corresponding benzamide in a pyridinium salt form. The pyridinium salts obtained were dried in vacuo with P_2O_5.

E. *Chlorosulfonation*

To a solution of the pyridinium salt (1 eq) in DMF (0.59 M) was added thionyl chloride (1.5 eq). The reaction was stirred at room temperature for 16 h. At this point the reaction was quenched by pouring it into ice-water (10 mL) and then filtered and washed twice with cold water (10 mL) to afford the corresponding sulfonyl chloride. The freshly moisture sensitive crude sulfonyl chloride obtained was ready used in the next step without further purification and characterisation.

F. *Amide formation*

To a solution of the acid (1 eq) and the amine (1 eq) in DMF (0.1 M) was added at 0ºC, DMAP (0.1 eq). After 30 min of stirring at 0ºC, EDCI (1.1 molar eq) was added, and the reaction was left at room temperature until completion (from 16 to 48 h). The

solvent was then evaporated and the resulting crude material diluted with CH_2Cl_2 and the organic layer extracted three times in water and washed once with 10% aqueous Na_2CO_3 solution, dried (Na_2SO_4), and filtered. The resulting residue was purified by flash column chromatography (solvent: $CHCl_3$/MeOH/H_2O 65:25:4). Finally, the resultant purified product was precipitated from EtOH to give the final amide.

G. *Nitro reduction*

To a solution of the nitro compound (1 eq) in EtOH/H_2O (5:1) was added iron powder (2.5 eq) at room temperature followed by saturated aqueous NH_4Cl solution (1.8 mL). Then the reaction mixture was allowed to reach 80ºC, and allowed to proceed for 16 h. Once the reaction was finished, the crude material was filtered through a celite pad (first solvent: EtOAc/EtOH 5:1; second solvent: 100% CH_2Cl_2), and the solvents evaporated to dryness. Then, the resulting material was diluted in CH_2Cl_2, extracted three times with water, dried over Na_2SO_4, filtered, and the solvents evaporated to dryness providing the corresponding amine.

***Tert*-butyl 1-{[5-(Dimethylamino)naphthalene-1-sulfonyl]piperidin-4-yl}carbamate (2)**

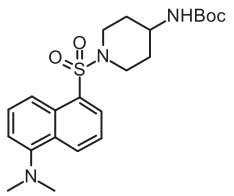

Following general procedure **A - work-up 1** (solvent: CH_2Cl_2; DIPEA (1.35 eq), sulfonyl chloride (1.35 eq); flash column chromatography solvent: MeOH/CH_2Cl_2 2:98), the compound **2** was obtained as a light-yellow solid. **Molecular Formula**: $C_{22}H_{31}N_3O_4S$; **MW**: 433.56 g/mol; **Yield**: 99%; **Mp**: 148-150ºC (washing Et_2O); **^{1}H NMR** (300 MHz, DMSO-*d_6*) δ 1.27-1.41 (m, 11H, $CH_{2piperidine}$ + 3 x CH_3), 1.68-1.80 (m, 2H, $CH_{2piperidine}$), 2.70-2.81 (m, 2H, $CH_{2piperidine}$), 2.83 (s, 6H, 2 x CH_3), 3.23-3.37 (m, 1H, $CH_{piperidine}$), 3.54-3.67 (m, 2H, $CH_{2piperidine}$), 6.87 (d, J = 7.3 Hz, 1H, NH), 7.27 (d, J = 7.4 Hz, 1H, H_{napht}), 7.60 (t, J = 7.0 Hz, 1H, H_{napht}), 7.66 (t, J = 6.9 Hz, 1H, H_{napht}), 8.10 (d, J = 7.3 Hz, 1H, H_{napht}), 8.25 (d, J = 8.5 Hz, 1H, H_{napht}), 8.50 (d, J = 8.6 Hz, 1H, H_{napht}); **^{13}C NMR** (75 MHz, DMSO-*d_6*) δ 154.7 (C=O), 151.4 (C), 133.6 (C), 130.0 (CH), 129.6 (C), 129.5 (CH), 129.2 (C), 128.0 (CH), 123.7 (CH), 119.0 (CH), 115.2 (CH), 77.6 (C), 46.2 (CH), 45.0 (2 x CH_3), 44.1 (2 x CH_2), 31.2 (2 x CH_2), 28.2 (3 x CH_3); **LRMS (ESI)**: *m/z* 434.2 $[M+H]^+$.

***N*-{[5-(Dimethylamino)naphthalene-1-sulfonyl]piperidin-4-yl}ammonium trifluoroacetate salt (3)**

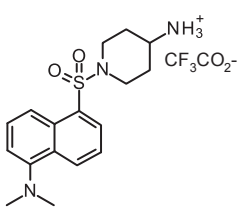

Following general procedure **B**, the compound **3** was obtained as a dark orange solid. **Molecular Formula**: $C_{19}H_{24}F_3N_3O_4S$; **MW**: 447.47 g/mol; **Yield**: 100%; **Mp**: 62-64ºC (washing Et_2O); **^{1}H NMR** (300 MHz, DMSO-*d_6*) δ 1.40-1.58 (m, 2H, $CH_{2piperidine}$), 1.87-1.97 (m, 2H, $CH_{2piperidine}$), 2.64-2.78 (m, 2H, $CH_{2piperidine}$), 2.84 (s, 6H, 2 x CH_3), 3.16 (m, 1H, $CH_{piperidine}$), 3.57-3.79 (m under HOD peak, 2H,

$CH_{2piperidine}$), 7.28 (d, J = 7.6 Hz, 1H, H_{napht}), 7.58-7.71 (m, 2H, H_{napht}), 7.80-7.93 (m, 3H, NH_3^+), 8.13 (d, J = 7.3 Hz, 1H, H_{napht}), 8.25 (d, J = 8.7 Hz, 1H, H_{napht}), 8.53 (d, J = 8.4 Hz, 1H, H_{napht}).

***N*-{1-[5-(Dimethylamino)naphthalene-1-sulfonyl]piperidin-4-yl}prop-2-enamide (1)**

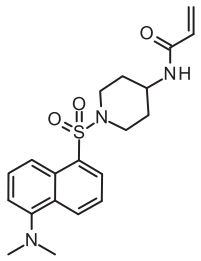

Following general procedure **C - work-up 1** (DIPEA (3.3 eq), acryloyl chloride (1.13 eq); flash column chromatography solvent: PE/EtOAc 1:1), the compound **1** was obtained as a light-yellow solid. **Molecular Formula**: $C_{20}H_{25}N_3O_3S$; **MW**: 387.50 g/mol; **Yield**: 70%; **Mp**: 170-172°C (washing Et_2O); **^{1}H NMR** (400 MHz, DMSO-*d*$_6$) δ 1.31-1.43 (m, 2H, $CH_{2piperidine}$), 1.75-1.85 (m, 2H, $CH_{2piperidine}$), 2.77-2.89 (m, 8H, 2 x CH_3 + $CH_{2piperidine}$), 3.57-3.77 (m, 3H, $CH_{piperidine}$ + $CH_{2piperidine}$), 5.55 (dd, J = 9.9, 2.4 Hz, 1H, CH_2= cis), 6.04 (dd, J = 17.1, 2.4 Hz, 1H, CH_2= trans), 6.15 (dd, J = 17.1, 9.9 Hz, 1H, CH=), 7.27 (d, J = 7.2 Hz, 1H, H_{napht}), 7.61 (dd, J = 8.7, 7.7 Hz, 1H, H_{napht}), 7.66 (dd, J = 8.5, 7.4 Hz, 1H, H_{napht}), 8.05 (d, J = 7.6 Hz, 1H, NH), 8.13 (dd, J = 7.3, 1.2 Hz, 1H, H_{napht}), 8.25 (d, J = 8.7 Hz, 1H, H_{napht}), 8.51 (d, J = 8.5 Hz, 1H, H_{napht}); **^{13}C NMR** (101 MHz, DMSO-*d*$_6$) δ 163.8 (C=O), 151.4 (C), 133.5 (C), 131.7 (CH), 130.1 (CH), 129.7 (CH), 129.6 (C), 129.2 (C), 128.1 (CH), 125.2 (CH_2=), 123.7 (CH), 118.9 (CH), 115.3 (CH), 45.1 (2 x CH_3), 44.8 (CH), 44.0 (2 x CH_2), 31.0 (2 x CH_2); **HRMS (ESI)** calcd for $C_{20}H_{26}N_3O_3S$ $[M+H]^+$, 388.1689; found, 388.1690.

***N*-{4-[5-(Dimethylamino)naphthalene-1-sulfonyl]piperidin-1-yl}prop-2-enamide (4)**

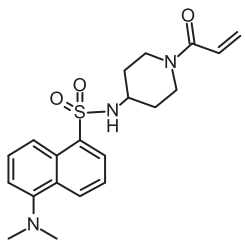

Following general procedure **C - work-up 1** (flash column chromatography solvent: PE/EtOAc 3:7 to 1:9), the compound **4** was obtained as a yellow foam. **Molecular Formula**: $C_{20}H_{25}N_3O_3S$; **MW**: 387.50 g/mol; **Yield**: 50%; **^{1}H NMR** (300 MHz, DMSO-*d*$_6$) δ 1.10-1.26 (m, 2H, $CH_{2piperidine}$), 1.43-1.57 (m, 2H, $CH_{2piperidine}$), 2.68-2.75 (m, 1H, $CH_{piperidine}$), 2.93-3.07 (m, 1H, $CH_{piperidine}$), 2.83 (s, 6H, 2 x CH_3), 3.19-3.30 (m, 1H, $CH_{piperidine}$), 3.73-3.86 (m, 1H, $CH_{piperidine}$), 3.97-4.11 (m, 1H, $CH_{piperidine}$), 5.59 (dd, J = 10.4, 2.5 Hz, 1H, CH_2= cis), 6.02 (dd, J = 16.7, 2.5 Hz, 1H, CH_2= trans), 6.71 (dd, J = 16.7, 10.4 Hz, 1H, CH=), 7.25 (d, J = 7.0 Hz, 1H, H_{napht}), 7.59 (t, J = 8.1 Hz, 1H, H_{napht}), 7.63 (t, J = 7.9 Hz, 1H, H_{napht}), 8.05 (d, J = 7.8 Hz, 1H, NH), 8.15 (dd, J = 7.3, 1.2 Hz, 1H, H_{napht}), 8.28 (d, J = 8.7 Hz, 1H, H_{napht}), 8.46 (d, J = 8.4 Hz, 1H, H_{napht}); **LRMS (ESI)**: *m/z* 388.2 $[M+H]^+$.

1-{4-[5-(Dimethylamino)naphthalene-1-sulfonyl]piperazin-1-yl}prop-2-enone (5)

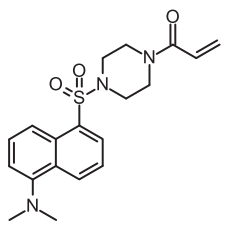

Following general procedure **C - work-up 1** (flash column chromatography solvent: PE/EtOAc 1:1 to 3:7), the compound **5** was obtained as an orange solid. **Molecular Formula**: $C_{19}H_{23}N_3O_3S$; **MW**: 373.48 g/mol; **Yield**: 85%; **Mp**: 198-199ºC; **^{1}H NMR** (300 MHz, DMSO-*d*$_6$) δ 2.82 (s, 6H, 2 x CH_3), 3.06-3.16 (m, 4H, 2 x $CH_{2piperazine}$), 3.51-3.63 (m, 4H, 2 x $CH_{2piperazine}$), 5.64 (d, J = 10.6, 2.3 Hz, 1H, CH_2= cis), 6.04 (d, J = 16.7, 2.3 Hz, 1H, CH_2= trans), 6.70 (d, J = 16.7, 10.6 Hz, 1H, CH=), 7.27 (d, J = 7.8 Hz, 1H, H_{napht}), 7.62 (t, J = 7.3 Hz, 1H, H_{napht}), 7.67 (t, J = 8.2 Hz, 1H, H_{napht}), 8.13 (d, J = 7,41 Hz, 1H, H_{napht}), 8.29 (d, J = 8.7 Hz, 1H, H_{napht}), 8.53 (d, J = 9.0 Hz, 1H, H_{napht}); **LRMS (ESI)**: *m/z* 374.2 $[M+H]^+$.

Tert-butyl *N*-[1-(Naphthalene-2-sulfonyl)piperidin-4-yl]carbamate (11)

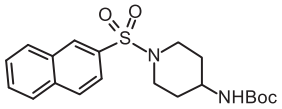

Following general procedure **A - work-up 1** (solvent: CH_2Cl_2; DIPEA (1.35 eq), sulfonyl chloride (1.35 eq), flash column chromatography solvent: MeOH/CH_2Cl_2 1-2/98-99), the compound **11** was obtained as a white solid. **Molecular Formula**: $C_{20}H_{26}N_2O_4S$; **MW**: 390.50 g/mol; **Yield**: 88%; **Mp**: 187-188ºC; **^{1}H NMR** (300 MHz, DMSO-*d*$_6$) δ 1.32 (s, 9H, 3 x CH_3), 1.36-1.48 (m, 2H, $CH_{2piperidine}$), 1.70-1.82 (m, 2H, $CH_{2piperidine}$), 2.56-2.69 (m, 2H, $CH_{2piperidine}$), 3.13-3.30 (m, 1H, $CH_{piperidine}$), 3.62-3.45 (m, 2H, $CH_{2piperidine}$), 6.84 (d, J = 8.1 Hz, 1H, NH), 7.76-7.66 (m, 3H, H_{napht}), 8.08 (d, J = 7.9 Hz, 1H, H_{napht}), 8.16 (d, J = 8.5 Hz, 1H, H_{napht}), 8.21 (d, J = 7.5 Hz, 1H, H_{napht}), 8.42 (d, J = 1.1 Hz, 1H, H_{napht}); **LRMS (ESI)**: *m/z* 391.2 $[M+H]^+$.

N-[1-(Naphthalene-2-sulfonyl)piperidin-4-yl]ammonium trifluoroacetate salt (12)

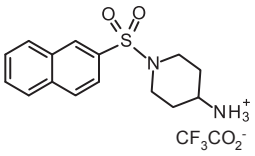

Following general procedure **B**, the compound **12** was obtained as a white solid. **Molecular Formula**: $C_{17}H_{19}F_3N_2O_4S$; **MW**: 404.40 g/mol; **Yield**: 97%; **Mp**: 185-186ºC (washing Et_2O); **^{1}H NMR** (300 MHz, DMSO-*d*$_6$) δ 1.44-1.62 (m, 2H, $CH_{2piperidine}$), 1.86-1.99 (m, 2H, $CH_{2piperidine}$), 2.45-2.35 (m, 2H, $CH_{2piperidine}$), 2.96-3.37 (m, 1H, $CH_{piperidine}$), 3.67-3.79 (m, 2H, $CH_{2piperidine}$), 7.67-7.80 (m, 2H, H_{napht}), 7.81-7.93 (m, 3H, NH_3^+), 8.09 (d, J = 8.8 Hz, 1H, H_{napht}), 8.18 (d, J = 8.5 Hz, 1H, H_{napht}), 8.21 (d, J = 7.4 Hz, 1H, H_{napht}), 8.44 (s, 1H, H_{napht}).

N-[1-(Naphthalene-2-sulfonyl)piperidin-4-yl]prop-2-enamide (9)

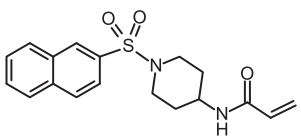

Following general procedure **C - work-up 1** (flash column chromatography solvent: PE/EtOAc 1:1 to 3.5:6.5), the compound **9** was obtained as a white solid. **Molecular Formula**: $C_{18}H_{20}N_2O_3S$; **MW**: 344.43 g/mol; **Yield**: 90%; **Mp**: 194-196ºC; **^{1}H NMR** (300 MHz, DMSO-*d*$_6$) δ 1.35-1.52 (m, 2H, $CH_{2piperidine}$),

1.76-1.89 (m, 2H, $CH_{2piperidine}$), 2.54-2.65 (m, 2H, $CH_{2piperidine}$), 3.51-3.68 (m, 3H, $CH_{piperidine}$ + $CH_{2piperidine}$), 5.53 (dd, J = 9.8, 2.6 Hz, 1H, CH_2= cis), 6.02 (dd, J = 17.0, 2.6 Hz, 1H, CH_2= trans), 6.14 (dd, J = 17.0, 9.8 Hz, 1H, CH=), 7.66-7.80 (m, 3H, H_{napht}), 8.02 (d, J = 7.4 Hz, 1H, NH), 8.09 (d, J = 7.7 Hz, 1H, H_{napht}), 8.17 (d, J = 8.7 Hz, 1H, H_{napht}), 8.21 (d, J = 8.3 Hz, 1H, H_{napht}), 8.44 (d, J = 1.1 Hz, 1H, H_{napht}); **LRMS (ESI)**: *m/z* 345.1 $[M+H]^+$.

Tert-butyl *N*-[1-(Naphthalene-1-sulfonyl)piperidin-4-yl]carbamate (13)

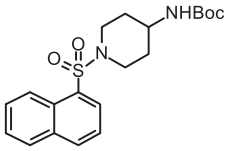

Procedure **A - work-up 1** was followed (DIPEA (1.35 eq), sulfonyl chloride (1.35 eq); flash column chromatography solvent: MeOH/CH_2Cl_2 1-2/98-99). The resultant purified product was precipitated from EtOH to give **13** as a white solid. **Molecular Formula**: $C_{20}H_{26}N_2O_4S$; **MW**: 390.50 g/mol; **Yield**: 88%; **Mp**: 138-140ºC (EtOH); **^{1}H NMR** (300 MHz, $CDCl_3$) δ 1.40 (s, 11H, $CH_{2piperidine}$ + 3 x CH_3), 1.85-2.01 (m, 2H, $CH_{2piperidine}$), 2.64-2.82 (m, 2H, $CH_{2piperidine}$), 3.35-3.51 (m, 1H, $CH_{piperidine}$), 3.71-3.84 (m, 2H, $CH_{2piperidine}$), 4.31-4.41 (m, 1H, NH), 7.51-7.69 (m, 3H, H_{napht}), 7.94 (d, J = 9.0 Hz, 1H, H_{napht}), 8.08 (d, J = 8.2 Hz, 1H, H_{napht}), 8.21 (d, J = 6.8 Hz, 1H, H_{napht}), 8.70 (d, J = 8.1 Hz, 1H, H_{napht}); **LRMS (ESI)**: *m/z* 391.2 $[M+H]^+$.

N-[1-(Naphthalene-1-sulfonyl)piperidin-4-yl]ammonium trifluoroacetate salt (14)

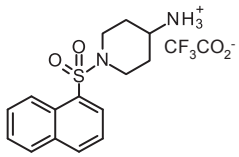

Following general procedure **B**, the compound **14** was obtained as a white solid. **Molecular Formula**: $C_{17}H_{19}F_3N_2O_4S$; **MW**: 404.40 g/mol; **Yield**: 95%; **Mp**: 202ºC (washing Et_2O); **^{1}H NMR** (300 MHz, DMSO-d_6) δ 1.40-1.55 (m, 2H, $CH_{2piperidine}$), 1.86-1.98 (m, 2H, $CH_{2piperidine}$), 2.67-2.77 (m, 2H, $CH_{2piperidine}$), 3.03-3.20 (m, 1H, $CH_{piperidine}$), 3.72-3.82 (m, 2H, $CH_{2piperidine}$), 7.64-7.77 (m, 3H, H_{napht}), 7.78-7.89 (m, 3H, NH_3^+), 8.14 (t, J = 6.9 Hz, 2H, H_{napht}), 8.31 (d, J = 8.6 Hz, 1H, H_{napht}), 8.62 (d, J = 9.0 Hz, 1H, H_{napht}).

N-[1-(Naphthalene-1-sulfonyl)piperidin-4-yl]prop-2-enamide (10)

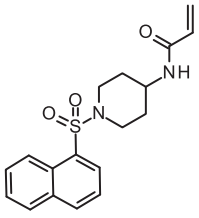

Following general procedure **C - work-up 1** (DIPEA (3.3 eq), acryloyl chloride (1.13 eq); flash column chromatography solvent: PE/EtOAc, 3:7 to 2:8), the compound **10** was obtained as a white solid. **Molecular Formula**: $C_{18}H_{20}N_2O_3S$; **MW**: 344.43 g/mol; **Yield**: 65%; **Mp**: 157ºC; **^{1}H NMR** (400 MHz, DMSO-d_6) δ 1.29-1.43 (m, 2H, $CH_{2piperidine}$), 1.75-1.85 (m, 2H, $CH_{2piperidine}$), 2.77-2.88 (m, 2H, $CH_{2piperidine}$), 3.58-3.76 (m, 3H, $CH_{piperidine}$ + $CH_{2piperidine}$), 5.54 (d, J = 9.9 Hz, 1H, CH_2= cis), 6.03 (d, J = 17.0 Hz, 1H, CH_2= trans), 6.15 (dd, J = 17.0, 9.9 Hz, 1H, CH=), 7.63-7.71 (m, 2H, H_{napht}), 7.74 (t, J = 7.7 Hz, 1H, H_{napht}), 8.04 (d, J = 7.3 Hz, 1H, NH), 8.11 (d, J = 8.1 Hz, 1H, H_{napht}), 8.15 (d, J = 7.3 Hz, 1H, H_{napht}), 8.29 (d, J = 8.1 Hz, 1H, H_{napht}), 8.63 (d, J =

8.6 Hz, 1H, H_{napht}); **^{13}C NMR** (101 MHz, DMSO-*d_6*) δ 163.8 (C=O), 134.5 (CH), 134.0 (C), 132.9 (C), 131.7 (CH), 129.9 (CH), 129.1 (CH), 128.2 (CH), 128.1 (C), 126.9 (CH), 125.2 (CH_2=), 124.7 (CH), 124.6 (CH), 44.8 (CH), 44.0 (2 x CH_2), 30.9 (2 x CH_2); **HRMS (ESI)** calcd for $C_{18}H_{21}N_2O_3S$ $[M+H]^+$, 345.1267; found, 345.1267.

***Tert*-butyl *N*-{1-[5-(Di-*n*-butylamino)naphthalene-1-sulfonyl]piperidin-4-yl}carbamate (16a)**

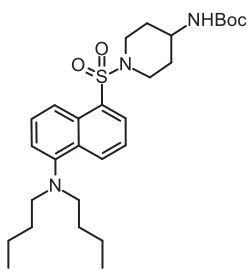

Following general procedure **A - work-up 1** (Solvent: CH_2Cl_2; DIPEA (1.35 eq), sulfonyl chloride (1.35 eq); flash column chromatography solvent: MeOH/CH_2Cl_2 1-2:98-99). The resultant product was precipitated from EtOH to give **16a** as a yellow solid. **Molecular Formula**: $C_{28}H_{43}N_3O_4S$; **MW**: 517.72 g/mol; **Yield**: 97%; **Mp**: 111ºC (EtOH); **^{1}H NMR** (300 MHz, DMSO-*d_6*) δ 0.80 (t, J = 7.2 Hz, 6H, 2 x CH_3), 1.15-1.47 (m, 19H, 3 x CH_3 + 4 x CH_2, $CH_{2piperidine}$), 1.68-1.81 (m, 2H, $CH_{2piperidine}$), 2.69-2.85 (m, 2H, $CH_{2piperidine}$), 3.09 (t, J = 7.3 Hz, 4H, 2 x CH_2), 3.25-3.40 (m, 1H, $CH_{piperidine}$), 3.55-3.69 (m, 2H, $CH_{2piperidine}$), 6.87 (d, J = 7.3 Hz, 1H, NH), 7.39 (d, J = 7.2 Hz, 1H, H_{napht}), 7.63 (t, J = 8.2 Hz, 1H, H_{napht}), 7.64 (t, J = 8.0 Hz, 1H, H_{napht}), 8.08 (t, J = 7.3 Hz, 1H, H_{napht}), 8.27 (t, J = 8.5 Hz, 1H, H_{napht}), 8.57 (t, J = 8.5 Hz, 1H, H_{napht}); **LRMS (ESI)**: *m/z* 518.3 $[M+H]^+$.

***Tert*-butyl *N*-{1-[5-(Acetylamino)naphthalene-1-sulfonyl]piperidin-4-yl}carbamate (16b)**

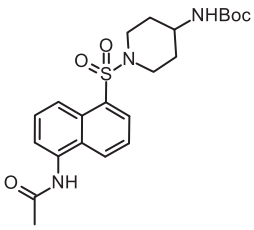

Following general procedure **A - work-up 1** (solvent: CH_2Cl_2 (0.2 M); DIPEA (1.3 eq), sulfonyl chloride (1.2 eq); after washing the organic layer, the crude extracts were crystallized in EtOAc/PE (1:9) and the resulting material purified by flash column chromatography, solvent: MeOH/CH_2Cl_2 5:95), the compound **16b** was obtained as a light-salmon colored solid. **Molecular Formula**: $C_{22}H_{29}N_3O_5S$; **MW**: 447.55 g/mol; **Yield**: 100%; **Mp**: > 210ºC; **^{1}H NMR** (300 MHz, DMSO-*d_6*) δ 1.25-1.43 (m, 2H, $CH_{2piperidine}$), 1.30 (s, 9H, 3 x CH_3), 1.68-1.80 (m, 2H, $CH_{2piperidine}$), 2.19 (s, 3H, CH_3), 2.70-2.84 (m, 2H, $CH_{2piperidine}$), 3.23-3.40 (m, 1H, $CH_{piperidine}$), 3.54-3.67 (m, 2H, $CH_{2piperidine}$), 6.86 (d, J = 7.6 Hz, 1H, NH), 7.65-7.79 (m, 3H, H_{napht}), 8.15 (dd, J = 7.3, 1.0 Hz, 1H, H_{napht}), 8.39 (d, J = 8.5 Hz, 1H, H_{napht}), 8.45 (d, J = 8.1 Hz, 1H, H_{napht}), 10.09 (s, 1H, NH); **LRMS (ESI)**: *m/z* 448.2 $[M+H]^+$.

***N*-{1-[5-(Di-*n*-butylamino)naphthalene-1-sulfonyl]piperidin-4-yl}ammonium trifluoroacetate salt (17a)**

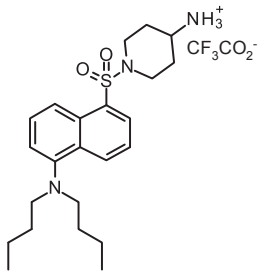

Following general procedure **B**, the compound **17a** was obtained as a dark-orange oil. **Molecular Formula**: $C_{25}H_{36}F_3N_3O_4S$; **MW**: 531.63 g/mol; **Yield**: 100%; **^{1}H NMR** (300 MHz, DMSO-*d*$_6$) δ 0.80 (t, J = 7.2 Hz, 6H, 2 x CH_3), 1.16-1.31 (m, 4H, 2 x CH_2), 1.33-1.58 (m, 6H, $CH_{2piperidine}$ + 2 x CH_2), 1.87-2.00 (m, 2H, $CH_{2piperidine}$), 2.68-2.82 (m, 2H, $CH_{2piperidine}$), 3.04-3.20 (m, 5H, 2 x CH_2 + $CH_{piperidine}$), 3.71-3.82 (m, 2H, $CH_{2piperidine}$), 7.40 (d, J = 7.8 Hz, 1H, H_{napht}), 7.61-7.69 (m, 2H, H_{napht}), 7.80-786 (m, 3H, NH_3^+), 8.11 (d, J = 7.4 Hz, 1H, H_{napht}), 8.26 (d, J = 9.4 Hz, 1H, H_{napht}), 8.59 (d, J = 7.5 Hz, 1H, H_{napht}).

_N_-{1-[(5-Acetylamino)naphthalene-1-sulfonyl]piperidin-4-yl}ammonium trifluoroacetate salt (17b)

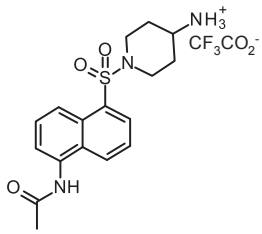

Following general procedure **B**, the compound **17b** was obtained as a white solid. **Molecular Formula**: $C_{19}H_{22}F_3N_3O_5S$; **MW**: 461.46 g/mol; **Yield**: 100%; **^{1}H NMR** (300 MHz, DMSO-*d*$_6$) δ 1.38-1.57 (m, 2H, $CH_{2piperidine}$), 1.85-1.99 (m, 2H, $CH_{2piperidine}$), 2.20 (s, 3H, CH_3), 2.65-2.80 (m, 2H, $CH_{2piperidine}$), 3.03-3.21 (m, 1H, $CH_{piperidine}$), 3.69-3.84 (m, 2H, $CH_{2piperidine}$), 7.65-7.79 (m, 3H, H_{napht}), 7.81-7.93 (m, 3H, NH_3^+), 8.18 (d, J = 6.8 Hz, 1H, H_{napht}), 8.41 (d, J = 8.6 Hz, 1H, H_{napht}), 8.46 (d, J = 7.6 Hz, 1H, H_{napht}), 10.12 (s, 1H, NH).

_N_-{1-[5-(Di-*n*-butylamino)naphthalene-1-sulfonyl]piperidin-4-yl}prop-2-enamide (15a)

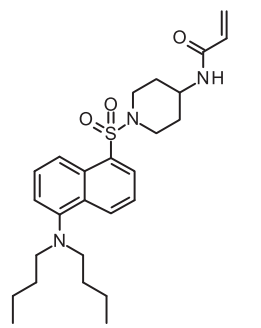

Following general procedure **C - work-up 1** (DIPEA (3.3 eq), acryloyl chloride (1.13 eq); flash column chromatography solvent: PE/EtOAc 1:1), the compound **15b** was obtained as a white solid. **Molecular Formula**: $C_{26}H_{37}N_3O_3S$; **MW**: 471.66 g/mol; **Yield**: 50%; **^{1}H NMR** (300 MHz, DMSO-*d*$_6$) δ 0.80 (t, J = 7.3 Hz, 6H, 2 x CH_3), 1.15-1.31 (m, 4H, 2 x CH_2), 1.32-1.49 (m, 6H, $CH_{2piperidine}$ + 2 x CH_2), 1.74-1.87 (m, 2H, $CH_{2piperidine}$), 2.78-2.93 (m, 2H, $CH_{2piperidine}$), 3.09 (t, J = 7.3 Hz, 4H, 2 x CH_2), 3.57-3.80 (m, 3H, $CH_{piperidine}$ + $CH_{2piperidine}$), 5.55 (dd, J = 9.7, 2.6 Hz, 1H, CH_2= cis), 6.04 (dd, J = 17.1, 2.6 Hz, 1H, CH_2= trans), 6.15 (dd, J = 17.1, 9.7 Hz, 1H, CH=), 7.39 (d, J = 7.3 Hz, 1H, H_{napht}), 7.64 (t, J = 8.1 Hz, 1H, H_{napht}), 7.65 (t, J = 8.0 Hz, 1H, H_{napht}), 8.05 (d, J = 7.2 Hz, 1H, NH), 8.11 (dd, J = 7.3, 1.1 Hz, 1H, H_{napht}), 8.27 (d, J = 8.6 Hz, 1H, H_{napht}), 8.58 (d, J = 8.4 Hz, 1H, H_{napht}); **LRMS (ESI)**: *m/z* 472.3 $[M+H]^+$.

_N_-{1-[5-(Acetylamino)naphthalene-1-sulfonyl]piperidin-4-yl}prop-2-enamide (15b)

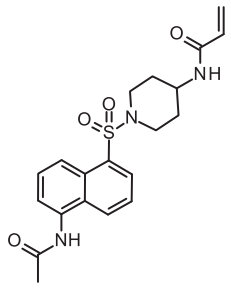

Following general procedure **C - work-up 2** (DIPEA (4 eq), acyl chloride (1.5 eq), CH_2Cl_2 (0.04 M); flash column chromatography solvent: MeOH/CH_2Cl_2 5:95), the compound **15b** was obtained as a white foam. **Molecular Formula**: $C_{20}H_{23}N_3O_4S$; **MW**: 401.48 g/mol; **Yield**: 64%; **^{1}H NMR** (300 MHz, DMSO-*d*$_6$) δ 1.27-1.45 (m, 2H, $CH_{2piperidine}$), 1.74-1.86 (m, 2H, $CH_{2piperidine}$), 2.20 (s, 1H, CH_3), 2.81-2.95 (m, 2H, $CH_{2piperidine}$), 3.56-3.80 (m, 3H, $CH_{piperidine}$ + $CH_{2piperidine}$), 5.54 (dd, J = 9.6, 2.7 Hz, 1H, CH_2= cis), 6.03 (dd, J = 17.1, 2.7 Hz, 1H, CH_2= trans), 6.14 (dd, J = 17.1, 9.6 Hz, 1H, CH=), 7.65-7.80 (m, 3H, H_{napht}), 8.04 (d, J = 7.6 Hz, 1H, NH), 8.18 (dd, J = 7.4, 1.0 Hz, 1H, H_{napht}), 8.40 (d, J = 8.5 Hz, 1H, H_{napht}), 8.46 (d, J = 8.3 Hz, 1H, H_{napht}), 10.10 (s, 1H, NH); **LRMS (ESI)**: *m/z* 402.1 $[M+H]^+$.

Tert-butyl _N_-{1-[(4-Acetylamino)naphthalene-1-sulfonyl]piperidin-4-yl}carbamate (19)

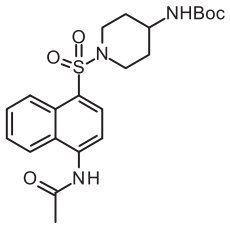

Following general procedure **A - work-up 1** (Solvent: CH_2Cl_2 (0.2 M); DIPEA (1.5 eq); flash column chromatography solvent: MeOH/CH_2Cl_2 5:95), the compound **19** was obtained as a light-brown solid. **Molecular Formula**: $C_{22}H_{29}N_3O_5S$; **MW**: 447.55 g/mol; **Yield**: 77%; **Mp**: > 210ºC; **^{1}H NMR** (300 MHz, DMSO-*d*$_6$) δ 1.22-1.43 (m, 2H, $CH_{2piperidine}$), 1.34 (s, 9H, 3 x CH_3), 1.68-1.82 (m, 2H, $CH_{2piperidine}$), 2.19 (s, 3H, CH_3), 2.70-2.86 (m, 2H, $CH_{2piperidine}$), 3.22-3.32 (m, 1H, $CH_{piperidine}$), 3.54-3.68 (m, 2H, $CH_{2piperidine}$), 6.86 (d, J = 7.4 Hz, 1H, NH), 7.64-7.80 (m, 3H, H_{napht}), 8.15 (d, J = 6.5 Hz, 1H, H_{napht}), 8.39 (d, J = 8.5 Hz, 1H, H_{napht}), 8.45 (d, J = 8.6 Hz, 1H, H_{napht}), 10.09 (s, 1H, NH); **LRMS (ESI)**: *m/z* 448.2 $[M+H]^+$.

_N_-{1-[(4-Acetylamino)naphthalene-1-sulfonyl]piperidin-4-yl}ammonium trifluoroacetate salt (20)

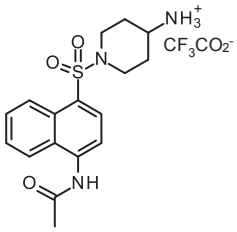

Following general procedure **B**, the compound **20** was obtained as a brown solid. **Molecular Formula:** $C_{19}H_{22}F_3N_3O_5S$; **MW**: 461.46 g/mol; **Yield**: 74%; **Mp**: 135-137ºC (washing Et_2O); **^{1}H NMR** (300 MHz, DMSO-*d*$_6$) δ 1.38-1.56 (m, 2H, $CH_{2piperidine}$), 1.86-1.98 (m, 2H, $CH_{2piperidine}$), 2.20 (s, 3H, CH_3), 2.64-2.79 (m, 2H, $CH_{2piperidine}$), 3.03-3.21 (m, 1H, $CH_{piperidine}$), 3.70-3.85 (m, 2H, $CH_{2piperidine}$), 7.65-7.79 (m, 3H, H_{napht}), 7.79-7.93 (m, 3H, NH_3^+), 8.18 (dd, J = 7.3, 1.0 Hz, 1H, H_{napht}), 8.41 (d, J = 8.6 Hz, 1H, H_{napht}), 8.46 (d, J = 8.3 Hz, 1H, H_{napht}), 10.11 (s, 1H, NH).

_N_-{1-[4-(Acetylamino)naphthalene-1-sulfonyl]piperidin-4-yl}prop-2-enamide (18)

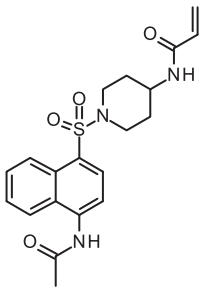

Following general procedure **C - work-up 2** (CH_2Cl_2 (0.17 M); flash column chromatography solvent: MeOH/CH_2Cl_2 5:95), the compound **18** was obtained as a white solid. **Molecular Formula:** $C_{20}H_{23}N_3O_4S$; **MW**: 401.48 g/mol; **Yield**: 85%; **Mp**: 118-120ºC; **^{1}H NMR** (300 MHz, DMSO-*d*$_6$) δ 1.28-1.46 (m, 2H, $CH_{2piperidine}$), 1.74-1.87 (m, 2H, $CH_{2piperidine}$), 2.20 (s, 3H, CH_3), 2.80-2.79 (m, 2H, $CH_{2piperidine}$), 3.56-3.80 (m, 3H, $CH_{piperidine}$ + $CH_{2piperidine}$), 5.54 (dd, J = 9.6, 2.7 Hz, 1H, CH_2= cis), 6.03 (dd, J = 17.0, 2.7 Hz, 1H, CH_2= trans), 6.15 (dd, J = 17.0, 9.6 Hz, 1H, CH=), 7.66-7.81 (m, 3H, H_{napht}), 8.03 (d, J = 7.5 Hz, 1H, NH), 8.18 (dd, J = 7.3, 1.0 Hz, 1H, H_{napht}), 8.40 (d, J = 8.5 Hz, 1H, H_{napht}), 8.46 (d, J = 8.1 Hz, 1H, H_{napht}), 10.10 (s, 1H, NH); **LRMS (ESI)**: *m/z* 402.1 $[M+H]^+$.

5-(Benzoylamino)naphthalene-1-sulfonate pyridinium salt (21a)

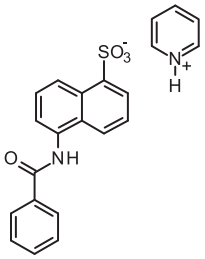

Following general procedure **D, the** compound **21a** was obtained as a pink solid. **Molecular Formula:** $C_{22}H_{18}N_2O_4S$; **MW**: 406.45 g/mol; **Yield**: 52%; **Mp**: > 210ºC (washing MeOH); **^{1}H NMR** (300 MHz, DMSO-*d*$_6$) δ 7.46 (dd, J = 8.5, 7.1 Hz, 1H, H_{napht}), 7.51-7.66 (m, 5H, H_{arom} + H_{napht}), 7.92-8.00 (m, 4H, H_{pyr} + H_{napht}), 8.06-8.13 (m, 2H, H_{arom}), 8.46 (tt, J = 1.6, 7.9, 1H, H_{pyr}), 8.78-8.90 (m, 3H, H_{napht} + H_{pyr}), 10.44 (s, 1H, NH).

5-(2-Methylbenzoylamino)naphthalene-1-sulfonate pyridinium salt (21b)

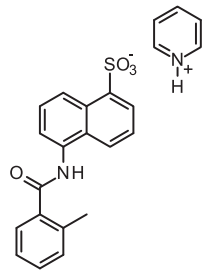

Following general procedure **D**, the compound **21b** was obtained as a pale pink solid. **Molecular Formula**: $C_{23}H_{20}N_2O_4S$; **MW**: 420.48 g/mol; **Yield**: 58%; **Mp**: > 210ºC (washing MeOH); **^{1}H NMR** (300 MHz, DMSO-*d*$_6$) δ 2.50 (s under solvent peak, 3H, CH_3), 7.34-7.62 (m, 6H, H_{napht} + H_{arom}), 7.89-8.13 (m, 5H, H_{napht} + H_{pyr} + H_{arom}), 8.53 (t, J = 7.8 Hz, 1H, H_{pyr}), 8.72-8.97 (m, 3H, H_{napht} + H_{pyr}), 10.33 (s, 1H, NH).

5-(3-Methylbenzoylamino)naphthalene-1-sulfonate pyridinium salt (21c)

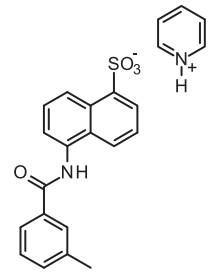

Following general procedure **D**, the compound **21c** was obtained as a pale pink solid. **Molecular Formula**: $C_{23}H_{20}N_2O_4S$; **MW**: 420.48 g/mol; **Yield**: 26%; **Mp**: > 210ºC (washing MeOH); **^{1}H NMR** (300 MHz, DMSO-*d*$_6$) δ 2.43 (s, 3H, CH_3), 7.39-7.49 (m, 3H, H_{napht} + H_{arom}), 7.50-7.58 (m, 2H, H_{napht}), 7.85-8.05 (m, 6H, H_{napht} + H_{pyr} + H_{arom}), 8.43-8.58 (m, 1H, H_{pyr}), 8.78-8.94 (m, 3H, H_{napht} + H_{pyr}), 10.40 (s, 1H, NH).

5-(3-Methoxybenzoylamino)naphthalene-1-sulfonate pyridinium salt (21d)

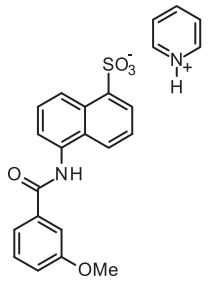

Following general procedure **D**, the compound **21d** was obtained as a pale pink solid. **Molecular Formula:** $C_{23}H_{20}N_2O_5S$; **MW**: 436.48 g/mol; **Yield**: 32%; **Mp**: > 210ºC (washing MeOH); **^{1}H NMR** (300 MHz, DMSO-*d*$_6$) δ 3.86 (s, 3H, CH_3, OCH_3), 7.18 (dd, J = 8.1, 2.1 Hz, 1H, H_{arom}), 7.39-7.58 (m, 4H, H_{napht} + H_{arom}), 7.59-7.74 (m, 2H, H_{arom}), 7.88-8.07 (m, 4H, H_{pyr} + H_{napht}), 8.40-8.55 (m, 1H, H_{pyr}), 8.76-8.93 (m, 3H, H_{pyr} + H_{napht}), 10.43 (s, 1H, NH).

5-(3-Chlorobenzoylamino)naphthalene-1-sulfonate pyridinium salt (21e)

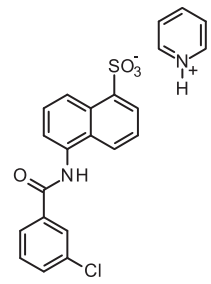

Following general procedure **D**, the compound **21e** was obtained as a pale pink solid. **Molecular Formula**: $C_{22}H_{17}ClN_2O_4S$; **MW**: 440.90 g/mol; **Yield**: 50%; **Mp**: > 210ºC (washing MeOH); **^{1}H NMR** (300 MHz, DMSO-*d*$_6$) δ 7.43-7.57 (m, 3H, H_{napht}), 7.60 (t, J = 7.8 Hz, 1H, H_{arom}), 7.70 (d, J = 8.1 Hz, 1H, H_{napht}), 7.93-8.09 (m, 5H, H_{napht} + H_{pyr} + H_{arom}), 8.14 (br s, 1H, H_{arom}), 8.50 (t, J = 7.5 Hz, 1H, H_{pyr}), 8.77-8.94 (m, 3H, H_{napht} + H_{pyr}), 10.56 (s, 1H, NH).

5-(3-Methoxycarbonylbenzoylamino)naphthalene-1-sulfonate pyridinium salt (21f)

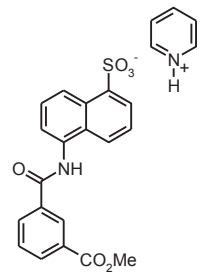

Following general procedure **D**, the compound **21f** was obtained as a pale pink solid. **Molecular Formula**: $C_{24}H_{20}N_2O_6S$; **MW**: 464.49 g/mol; **Yield**: 37%; **Mp**: > 210ºC (washing MeOH); **^{1}H NMR** (300 MHz, DMSO-*d*$_6$) δ 3.92 (s, 3H, CH_3), 7.43-7.58 (m, 4H, H_{napht} + H_{arom}), 7.73 (t, J = 7.7 Hz, 1H, $H_{5\ arom}$), 7.90-8.08 (m, 5H, H_{napht} + H_{pyr} + H_{arom}), 8.54 (t, J = 7.8 Hz, 1H, H_{pyr}), 8.70-8.96 (m, 4H, H_{napht} + H_{pyr} + H_{arom}), 10.67 (s, 1H, NH).

5-(3-Nitrobenzoylamino)naphthalene-1-sulfonate pyridinium salt (21g)

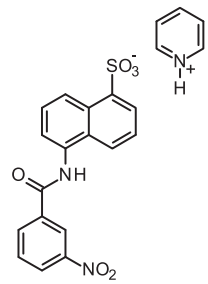

Following general procedure **D**, the compound **21g** was obtained as a pink solid. **Molecular Formula**: $C_{22}H_{17}N_3O_6S$; **MW**: 451.45 g/mol; **Yield**: 42%; **Mp**: > 210ºC (washing MeOH); **^{1}H NMR** (300 MHz, DMSO-*d*$_6$) δ 7.41-7.51 (m, 1H, H_{napht}), 7.52-7.63 (m, 2H, H_{napht}), 7.88 (t, J = 8.0 Hz, 1H, H_{arom}), 7.93-8.07 (m, 4H, H_{pyr} + H_{napht}), 8.43-8.60 (m, 3H, H_{napht} + H_{pyr} + H_{arom}), 8.81-8.97 (m, 4H, H_{pyr} + H_{arom}), 10.82 (s, 1H, NH).

5-(4-Methoxybenzoylamino)naphthalene-1-sulfonate pyridinium salt (21h)

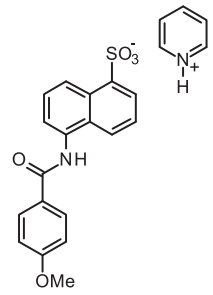

Following general procedure **D**, the compound **21h** was obtained as a light pink solid. **Molecular Formula**: $C_{23}H_{20}N_2O_5S$; **MW**: 436.48 g/mol; **Yield**: 57%; **Mp**: > 210ºC (washing MeOH); **^{1}H NMR** (300 MHz, DMSO-*d*$_6$) δ 3.82-3.90 (m, 3H, CH_3, OCH_3), 7.09 (d, J = 8.9 Hz, 2H, H_{arom}), 7.44 (dd, J = 8.5, 7.1 Hz, 1H, H_{napht}), 7.48-7.57 (m, 2H, H_{napht}), 7.90-8.00 (m, 4H, H_{napht} + H_{pyr}), 8.08 (d, J = 8.9 Hz, 2H, H_{arom}), 8.45 (t, J = 7.8 Hz, 1H, H_{pyr}), 8.76-8.90 (m, 3H, H_{napht} + H_{pyr}), 10.29 (s, 1H, NH).

5-(4-Chlorobenzoylamino)naphthalene-1-sulfonate pyridinium salt (21i)

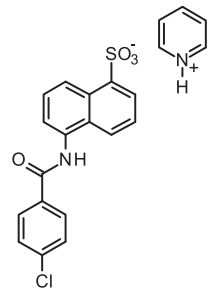

Following general procedure **D**, the compound **21i** was obtained as a pink solid. **Molecular Formula**: $C_{22}H_{17}ClN_2O_4S$; **MW**: 440.90 g/mol; **Yield**: 46%; **Mp**: > 210ºC (washing MeOH); **^{1}H NMR** (300 MHz, DMSO-*d*$_6$) δ 7.46 (dd, J = 8.5, 7.1 Hz, 1H, H_{napht}), 7.50-7.57 (m, 2H, H_{napht}), 7.64 (d, J = 8.6 Hz, 2H, H_{arom}), 7.90-8.02 (m, 4H, H_{napht} + H_{pyr}), 8.12 (d, J = 8.5 Hz, 2H, H_{arom}), 8.41-8.52 (m, 1H, H_{pyr}), 8.77-8.92 (m, 3H, H_{napht} + H_{pyr}), 10.52 (s, 1H, NH).

5-[4-(Trifluoromethyl)benzoylamino]naphthalene-1-sulfonate pyridinium salt (21j)

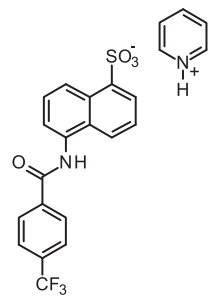

Following general procedure **D**, the compound **21j** was obtained as a pink solid. **Molecular Formula**: $C_{23}H_{17}F_3N_2O_4S$; **MW**: 474.45 g/mol; **Yield**: 33%; **Mp**: > 210ºC (washing MeOH); **^{1}HNMR** (300 MHz, DMSO-*d*$_6$) δ 7.42-7.64 (m, 5H, H_{napht} + H_{arom}), 7.92-8.08 (m, 5H, H_{arom} + H_{napht} + H_{pyr}), 8.29 (d, J = 7.9 Hz, 1H, H_{napht}), 8.47-8.56 (m, 1H, H_{pyr}), 8.78-8.86 (m, 2H, H_{pyr}), 8.89 (d, J = 6.1 Hz, 1H, H_{napht}), 10.67 (s, 1H, NH).

5-(3,4-Dimethylbenzoylamino)naphthalene-1-sulfonate pyridinium salt (21k)

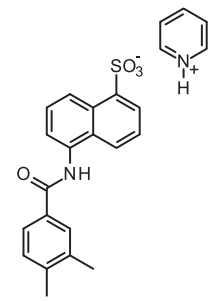

Following general procedure **D**, the compound **21k** was obtained as a pale pink solid. **Molecular Formula**: $C_{24}H_{22}N_2O_4S$; **MW**: 434.51 g/mol; **Yield**: 59%; **Mp**: > 210ºC (washing MeOH); **^{1}H NMR** (300 MHz, DMSO-*d*$_6$) δ 2.32 (s, 3H, CH_3), 2.33 (s, 3H, CH_3), 7.31 (d, J = 7.9 Hz, 1H, H_{arom}), 7.45 (dd, J = 8.5, 7.1 Hz, 1H, H_{napht}), 7.49-7.59 (m, 2H, H_{napht}), 7.78-8.03 (m, 6H, H_{napht} + H_{pyr} + H_{arom}), 8.41-8.52 (m, 1H, H_{pyr}), 8.77-8.91 (m, 3H, H_{napht} + H_{pyr}), 10.31 (s, 1H, NH).

5-(3,4-Dimethoxybenzoylamino)naphthalene-1-sulfonate pyridinium salt (21l)

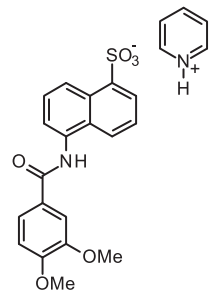

Following general procedure **D**, the compound **21l** was obtained as a pink solid. **Molecular Formula**: $C_{24}H_{22}N_2O_6S$; **MW**: 466.51 g/mol; **Yield**: 56%; **Mp**: > 210ºC (washing MeOH); **^{1}H NMR** (300 MHz, DMSO-*d*$_6$) δ 3.85 (s, 3H, OCH_3), 3.86 (s, 3H, OCH_3), 7.11 (d, J = 8.5 Hz, 1H, H_{arom}), 7.45 (dd, J = 8.5, 7.2 1H, H_{napht}) 7.48-7.57 (m, 2H, H_{napht}), 7.68 (d, J = 2.0 Hz, 1H, H_{arom}), 7.75 (dd, J = 8.4, 2.0 Hz, 1H, H_{arom}), 7.89-8.01 (m, 4H, H_{napht} + H_{pyr}), 8.41-8.51 (m, 1H, H_{pyr}), 8.81 (dd, J = 7.7, 1.5 Hz, 1H, H_{napht}), 8.84-8.91 (m, 2H, H_{pyr}), 10.30 (s, 1H, NH).

5-(3,4-Dichlorobenzoylamino)naphthalene-1-sulfonate pyridinium salt (21m)

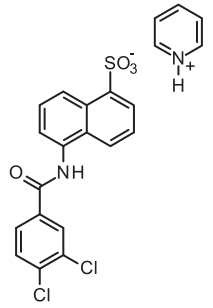

Following general procedure **D**, the compound **21m** was obtained as a pale pink solid. **Molecular Formula**: $C_{22}H_{16}Cl_2N_2O_4S$; **MW**: 475.34 g/mol; **Yield**: 38%; **Mp**: > 210ºC (washing MeOH); **^{1}H NMR** (300 MHz, DMSO-*d*$_6$) δ 7.42-7.61 (m, 3H, H_{napht}), 7.85 (d, J = 8.3 Hz, 1H, H_{napht}), 7.91-8.15 (m, 5H, H_{napht} + H_{pyr} + H_{arom}), 8.34 (s, 1H, H_{arom}), 8.45 (t, J = 7.7 Hz, 1H, H_{pyr}), 8.72-8.94 (m, 3H, H_{napht} + H_{pyr}), 10.61 (s, 1H, NH).

5-(3,5-Dimethoxybenzoylamino)naphthalene-1-sulfonate pyridinium salt (21n)

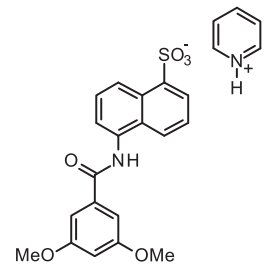

Following general procedure **D**, the compound **21n** was obtained as a pink solid. **Molecular Formula**: $C_{24}H_{22}N_2O_6S$; **MW**: 466.51 g/mol; **Yield**: 48%; **Mp**: > 210ºC (washing MeOH); **^{1}H NMR** (300 MHz, DMSO-*d*$_6$) δ 3.84 (s, 6H, 2 x OCH_3), 6.73 (t, J = 2.2 Hz, 1H, H_{arom}), 7.26 (d, J = 2.2 Hz, 2H, H_{arom}), 7.46 (dd, J = 8.5, 7.2 Hz, 1H, H_{napht}), 7.49-7.57 (m, 2H, H_{napht}), 7.89-8.00 (m, 4H, H_{napht} + H_{pyr}), 8.45 (t, J = 7.6 Hz, 1H, H_{pyr}), 8.82 (dd, J = 7.8, 1.9 Hz, 1H, H_{napht}), 8.85-8.90 (m, 2H, H_{pyr}), 10.33 (s, 1H, NH).

5-(3,4,5-Trimethoxybenzoylamino)naphthalene-1-sulfonate pyridinium salt (21o)

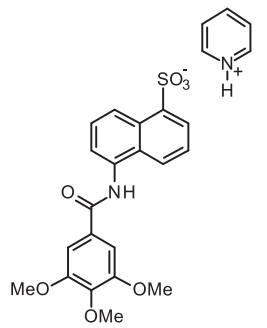

Following general procedure **D**, the compound **21o** was obtained as a light-pink solid. **Molecular Formula**: $C_{25}H_{24}N_2O_7S$; **MW:** 496.53 g/mol; **Yield**: 49%; **Mp**: > 210ºC (washing MeOH); **^{1}H NMR** (300 MHz, DMSO-*d*$_6$) δ 3.75 (s, 3H, OCH_3), 3.89 (s, 6H, 2 x OCH_3), 7.42-7.59 (m, 5H, H_{napht} + H_{arom}), 7.88-8.01 (m, 4H, H_{napht} + H_{pyr}), 8.38-8.52 (m, 1H, H_{pyr}), 8.79-8.91 (m, 3H, H_{napht} + H_{pyr}), 10.38 (s, 1H, NH).

5-(Naphth-2-ylcarbonylamino)naphthalene-1-sulfonate pyridinium salt (21p)

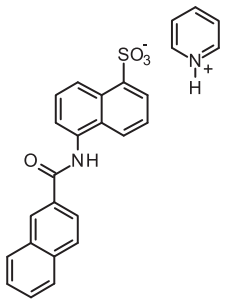

Following general procedure **D**, the compound **21p** was obtained as a light pink solid pyridinium salt. **Molecular Formula**: $C_{26}H_{20}N_2O_4S$; **MW**: 456.51 g/mol; **Yield**: 45%; **Mp**: > 210ºC (washing MeOH); **^{1}H NMR** (300 MHz, DMSO-*d*$_6$) δ 7.38-7.72 (m, 6H, H_{napht}), 7.91-8.17 (m, 7H, H_{napht} + H_{pyr}), 8.45 (t, J = 7.9 Hz, 1H, H_{pyr}), 8.72-8.92 (m, 4H, H_{napht} + H_{pyr}), 10.62 (s, 1H, NH).

5-(Benzo[1,3]dioxole-5-carbonylamino)naphthalene-1-sulfonate pyridinium salt (21q)

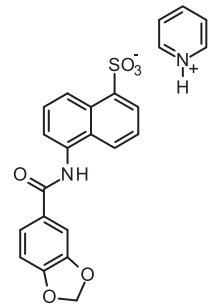

Following general procedure **D**, the compound **21q** was obtained as a pale pink solid. **Molecular Formula**: $C_{23}H_{18}N_2O_6S$; **MW**: 450.46 g/mol; **Yield**: 39%; **Mp**: > 210ºC (washing MeOH); **^{1}H NMR** (300 MHz, DMSO-*d*$_6$) δ 6.15 (s, 2H, CH_2), 7.08 (d, J = 8.1 Hz, 1H, H_{arom}), 7.45 (dd, J = 8.5, 7.1 Hz, 1H, H_{napht}), 7.49-7.57 (m, 2H, H_{napht}), 7.63 (d, J = 1.6 Hz, 1H, H_{arom}), 7.71 (dd, J = 8.1, 1.6 Hz, 1H, H_{arom}), 7.90-8.00 (m, 4H, H_{napht} + H_{pyr}), 8.40-8.51 (m, 1H, H_{pyr}), 8.81 (dd, J = 7.0, 2.6 Hz, 1H, H_{napht}), 8.83-8.91 (m, 2H, H_{pyr}), 10.27 (s, 1H, NH).

5-(3-Phenylbenzoylamino)naphthalene-1-sulfonate pyridinium salt (21r)

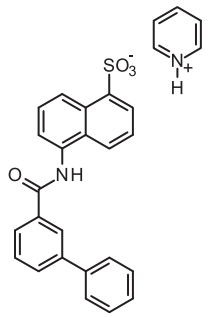

Following general procedure **D**, the compound **21r** was obtained as a pale pink solid. **Molecular Formula**: $C_{28}H_{22}N_2O_4S$; **MW**: 482.55 g/mol; **Yield**: 41%; **Mp**: > 210ºC (washing MeOH); **^{1}H NMR** (300 MHz, DMSO-*d*$_6$) δ 7.38-7.59 (m, 6H, H_{arom}), 7.66 (t, J = 7.7 Hz, 1H, H_{arom}), 7.83 (d, J = 7.3 Hz, 2H, H_{arom}), 7.88-8.02 (m, 5H, H_{pyr} + H_{arom}), 8.06 (d, J = 7.8 Hz, 1H, H_{arom}), 8.38-8.51 (m, 2H, H_{pyr} + H_{arom}), 8.79-8.93 (m, 3H, H_{pyr} + H_{arom}), 10.57 (s, 1H, NH).

5-(4-Phenylbenzoylamino)naphthalene-1-sulfonate pyridinium salt (21s)

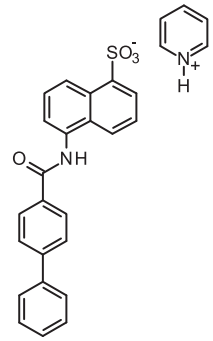

Following general procedure **D**, the compound **21s** was obtained as a pink solid. **Molecular Formula**: $C_{28}H_{22}N_2O_4S$; **MW**: 482.55 g/mol; **Yield**: 46%; **Mp**: > 210ºC (washing MeOH); **^{1}H NMR** (300 MHz, DMSO-*d*$_6$) δ 7.39-7.61 (m, 6H, H_{arom}), 7.79 (d, J = 7.2 Hz, 2H, H_{arom}), 7.84-8.03 (m, 6H, H_{pyr} + H_{arom}), 8.20 (d, J = 8.3 Hz, 2H, H_{arom}), 8.43 (t, J = 7.8 Hz, 1H, H_{pyr}), 8.79-8.90 (m, 3H, H_{pyr} + H_{arom}), 10.50 (s, 1H, NH).

Hydrolysis was always observed for all prepared sulfonyl chlorides **22** (general procedure **E**). These compounds were used rapidly in the next reaction without characterization (NMR spectra showed mixture of desired sulfonyl chlorides and derivatives from hydrolysis).

***Tert*-butyl *N*-{1-[5-(Benzoylamino)naphthalene-1-sulfonyl]piperidin-4-yl}carbamate (24a)**

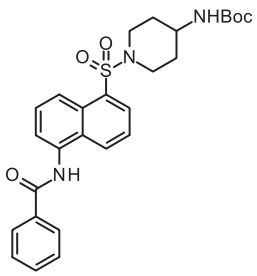

Following general procedure **A - work-up 1** (solvent: CH_2Cl_2; flash column chromatography solvent: MeOH/CH_2Cl_2 2:98), the compound **24a** was obtained as a white solid. **Molecular Formula**: $C_{27}H_{31}N_3O_5S$; **MW**: 509.62 g/mol; **Yield**: 84%; **Mp**: 194-195ºC; **^{1}H NMR** (300 MHz, DMSO-d_6) δ 1.35 (s, 9H, 3 x CH_3), 1.28-1.45 (m, 2H, $CH_{2piperidine}$), 1.69-1.83 (m, 2H, $CH_{2piperidine}$), 2.73-2.87 (m, 2H, $CH_{2piperidine}$), 3.25-3.42 (m, 1H, $CH_{piperidine}$), 3.57-3.70 (m, 2H, $CH_{2piperidine}$), 6.87 (d, J = 7.7 Hz, 1H, NH), 7.54-7.83 (m, 6H, H_{arom} + H_{napht}), 8.07-8.13 (m, 2H, H_{arom}), 8.17 (d, J = 6.4 Hz, 1H, H_{napht}), 8.34 (d, J = 8.6 Hz, 1H, H_{napht}), 8.56 (d, J = 7.2 Hz, 1H, H_{napht}), 10.59 (s, 1H, NH); ; **LRMS (ESI)**: *m/z* 510.2 $[M+H]^+$.

***Tert*-butyl *N*-{1-[5-(3,4-Dimethoxybenzoylamino)naphthalene-1-sulfonyl]piperidin-4-yl}carbamate (24b)**

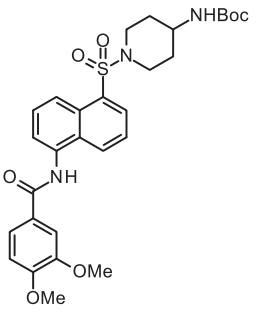

Procedure **A - work-up 2** was followed (solvent: CH_2Cl_2 (0.1 M); flash column chromatography solvent: PE/EtOAc 4:6). The resultant product was precipitated from EtOH to give **24b** as a white solid. **Molecular Formula**: $C_{29}H_{35}N_3O_7S$; **MW**: 569.67 g/mol; **Yield**: 71%; **Mp**: 173-175ºC (EtOH); **^{1}H NMR** (300 MHz, DMSO-d_6) δ 1.34 (s, 9H, 3 x CH_3), 1.37-1.45 (m, 2H, $CH_{2piperidine}$), 1.70-1.82 (m, 2H, $CH_{2piperidine}$), 2.70-2.85 (m, 2H, $CH_{2piperidine}$), 3.22-3.41 (m, 1H, $CH_{piperidine}$), 3.56-3.70 (m, 2H, $CH_{2piperidine}$), 3.86 (s, 6H, 2 x OCH_3), 6.87 (d, J = 7.4 Hz, 1H, NH), 7.13 (d, J = 8.5 Hz, 1H, H_{arom}), 7.63-7.82 (m, 5H, H_{napht} + H_{arom}), 8.17 (dd, J = 7.3, 1.0 Hz, 1H, H_{napht}), 8.30 (d, J = 8.5 Hz, 1H, H_{napht}), 8.55 (d, J = 8.4 Hz, 1H, H_{napht}), 10.44 (s, 1H, NH); **^{13}C NMR** (101 MHz, DMSO-d_6) δ 165.7 (C=O), 154.7 (C=O), 151.8 (C), 148.4 (C), 135.1 (C), 133.5 (C), 130.5 (C), 129.8 (2 x CH), 128.8 (C), 127.8 (CH), 126.2 (C), 125.2 (CH), 124.5 (CH), 122.9 (CH), 121.3 (CH), 111.1 (CH), 111.0 (CH), 77.6 (C), 55.7 (OCH_3), 55.6 (OCH_3), 46.2 (CH), 44.1 (2 x CH_2), 31.2 (2 x CH_2), 28.2 (3 x CH_3); **LRMS (ESI)**: *m/z* 570.2 $[M+H]^+$.

***Tert*-butyl *N*-{1-[5-(3-Nitrobenzoylamino)naphthalene-1-sulfonyl]piperidin-4-yl}carbamate (24c)**

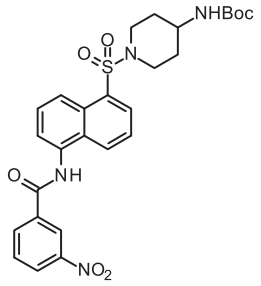

Following general procedure **A - workup 1** (solvent: CH_2Cl_2 (0.1 M); washing of the crude extract in MeOH; the filtrate was purified by flash column chromatography, solvent: MeOH/CH_2Cl_2 5:95), the compound **24c** was obtained as a white solid. **Molecular Formula**: $C_{27}H_{30}N_4O_7S$; **MW**: 554.61 g/mol; **Yield**: 56%; **Mp**: > 210ºC; **^{1}H NMR** (400 MHz, DMSO-*d*$_6$) δ 1.35 (s, 9H, 3 x CH_3), 1.33-1.43 (m, 2H, $CH_{2piperidine}$), 1.71-1.83 (m, 2H, $CH_{2piperidine}$), 2.73-2.87 (m, 2H, $CH_{2piperidine}$), 3.28-3.39 (m under HOD peak, 1H, $CH_{piperidine}$), 3.58-3.71 (m, 2H, $CH_{2piperidine}$), 6.89 (d, J = 7.4 Hz, 1H, NH), 7.68-7.84 (m, 3H, H_{napht}), 7.90 (t, J = 8.0 Hz, 1H, H_{arom}), 8.19 (d, J = 7.2 Hz, 1H, H_{napht}), 8.39 (d, J = 8.5 Hz, 1H, H_{napht}), 8.50 (dd, J = 8.4, 1.8 Hz, 1H, H_{arom}), 8.53 (d, J = 7.8 Hz, 1H, H_{napht}), 8.59 (d, J = 7.8 Hz, 1H, H_{arom}), 8.93 (s, 1H, H_{arom}), 10.96 (s, 1H, NH); **^{13}C NMR** (101 MHz, DMSO-*d*$_6$) δ 164.4 (C=O), 154.8 (C=O), 147.8 (C), 135.6 (C), 134.4 (CH + C), 133.6 (C), 130.3 (CH), 130.2 (C), 129.9 (CH), 129.7 (CH), 128.9 (C), 127.8 (CH), 126.4 (CH), 125.2 (CH), 124.7 (CH), 123.4 (CH), 122.7 (CH), 77.65 (C), 46.2 (CH), 44.1 (2 x CH_2), 31.3 (2 x CH_2), 28.2 (3 x CH_3); **LRMS (ESI)**: *m/z* 555.2 $[M+H]^+$.

***N*-{1-[5-(Benzoylamino)naphthalene-1-sulfonyl]piperidin-4-yl}ammonium trifluoroacetate salt (25a)**

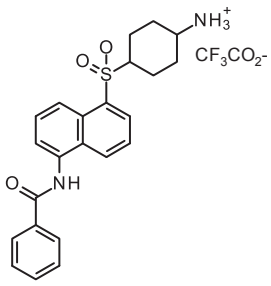

Following general procedure **B** compound **25a** was obtained as a white solid. **Molecular Formula**: $C_{24}H_{24}F_3N_3O_5S$; **MW**: 523.52 g/mol; **Yield**: 100%; **Mp**: > 210ºC (washing Et_2O); **^{1}H NMR** (300 MHz, DMSO-*d*$_6$) δ 1.41-1.60 (m, 2H, $CH_{2piperidine}$), 1.88-2.00 (m, 2H, $CH_{2piperidine}$), 2.67-2.82 (m, 2H, $CH_{2piperidine}$), 3.08-3.22 (m, 1H, $CH_{piperidine}$), 3.73-3.88 (m, 2H, $CH_{2piperidine}$), 7.53-7.93 (m, 9H, H_{arom} + H_{napht} + NH_3^+), 8.07-8.13 (m, 2H, H_{arom}), 8.20 (d, J = 7.3 Hz, 1H, H_{napht}), 8.36 (d, J = 8.3 Hz, 1H, H_{napht}), 8.57 (d, J = 7.9 Hz, 1H, H_{napht}), 10.61 (s, 1H, NH).

***N*-{1-[5-(3,4-Dimethoxybenzoylamino)naphthalene-1-sulfonyl]piperidin-4-yl}ammonium trifluoroacetate salt (25b)**

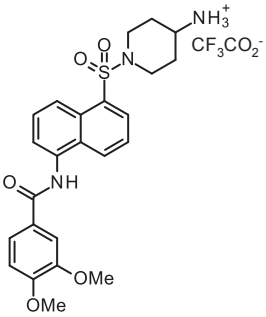

Following general procedure **B**, the compound **25b** was obtained as a white solid. **Molecular Formula**: $C_{26}H_{28}F_3N_3O_7S$; **MW**: 583.58 g/mol; **Yield**: 100%; **Mp**: 160-162ºC (washing Et_2O); **^{1}H NMR** (300 MHz, DMSO-*d*$_6$) δ 1.42-1.59 (m, 2H, $CH_{2piperidine}$), 1.88-2.00 (m, 2H, $CH_{2piperidine}$), 2.68-2.81 (m, 2H, $CH_{2piperidine}$), 3.05-3.22 (m, 1H, $CH_{piperidine}$), 3.75-3.84 (m, 2H, $CH_{2piperidine}$),

3.86 (s, 6H, 2 x OCH_3), 7.13 (d, J = 8.6 Hz, 1H, H_{arom}), 7.64-7.90 (m, 8H, H_{arom} + H_{napht} + NH_3^+), 8.20 (d, J = 7.4 Hz, 1H, H_{napht}), 8.32 (d, J = 8.4 Hz, 1H, H_{napht}), 8.55 (d, J = 8.5 Hz, 1H, H_{napht}), 10.46 (s, 1H, NH).

N-{1-[5-(3-Nitrobenzoylamino)naphthalen-1-sulfonyl]piperidin-4-yl}ammonium trifluoroacetate salt (25c)

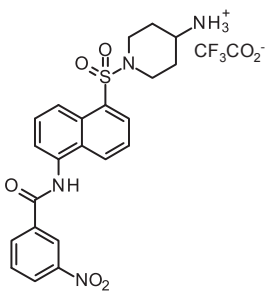

Following general procedure **B**, the compound **25c** was obtained as an orange solid. **Molecular Formula**: $C_{24}H_{25}F_3N_4O_5S$; **MW**: 538.54 g/mol; **Yield**: 100%; **Mp**: 122-124ºC (washing Et_2O); **^{1}H NMR** (300 MHz, DMSO-*d_6*) δ 1.41-1.60 (m, 2H, $CH_{2piperidine}$), 1.89-2.01 (m, 2H, $CH_{2piperidine}$), 2.67-2.83 (m, 2H, $CH_{2piperidine}$), 3.04-3.22 (m, 1H, $CH_{piperidine}$), 3.75-3.87 (m, 2H, $CH_{2piperidine}$), 7.66-7.95 (m, 8H, H_{arom} + H_{napht} + NH_3^+), 8.21 (dd, J = 7.3, 1.0 Hz, 1H, H_{napht}), 8.40 (d, J = 8.5 Hz, 1H, H_{napht}), 8.50 (dd, J = 7.6, 2.2 Hz, 1H, H_{arom}), 8.53 (d, J = 7.6 Hz, 1H, H_{napht}), 8.59 (d, J = 7.4 Hz, 1H, H_{napht}), 8.59 (d, J = 7.4 Hz, 1H, H_{arom}), 8.92 (t, J = 1.9 Hz, 1H, H_{arom}), 10.97 (s, 1H, NH).

N-{5-[4-(acryloylamino)piperidine-1-sulfonyl]naphthalen-1-yl}benzamide (23a)

Following general procedure **C - work-up 1** (flash column chromatography solvent: MeOH/CH_2Cl_2 1-2:98-99), the compound **23a** was obtained as a white solid. **Molecular Formula**: $C_{25}H_{25}N_3O_4S$; **MW**: 463.55 g/mol; **Yield**: 65%; **Mp**: > 210ºC; **^{1}H NMR** (400 MHz, DMSO-*d_6*) δ 1.32-1.47 (m, 2H, $CH_{2piperidine}$), 1.77-1.88 (m, 2H, $CH_{2piperidine}$), 2.83-2.97 (m, 2H, $CH_{2piperidine}$), 3.59-3.80 (m, 3H, $CH_{piperidine}$ + $CH_{2piperidine}$), 5.55 (dd, J = 9.9, 2.1 Hz, 1H, CH_2= cis), 6.05 (dd, J = 17.0, 2.1 Hz, 1H, CH_2= trans), 6.16 (dd, J = 17.0, 9.9 Hz, 1H, CH=), 7.53-7.84 (m, 6H, H_{arom} + H_{napht}), 8.04-8.16 (m, 3H, NH + H_{arom}), 8.21 (d, J = 7.2 Hz, 1H, H_{napht}), 8.36 (d, J = 8.5 Hz, 1H, H_{napht}), 8.58 (d, J = 8.3 Hz, 1H, H_{napht}), 10.61 (s, 1H, NH); **^{13}C NMR** (101 MHz, DMSO-*d_6*) δ 166.4 (C=O), 163.8 (C=O), 134.9 (C), 134.2 (C), 133.5 (C), 131.9 (CH), 131.7 (CH), 130.4 (C), 130.1 (CH), 129.8 (CH), 128.8 (2 x C), 128.5 (CH), 127.9 (2 x CH), 127.8 (CH), 125.3 (CH_2=), 125.2 (CH), 124.6 (CH), 123.1 (CH), 44.8 (CH), 44.0 (2 x CH_2), 31.0 (2 x CH_2); **HRMS (ESI)** calcd for $C_{25}H_{26}N_3O_4S$ $[M+H]^+$, 464.1639; found, 464.1627.

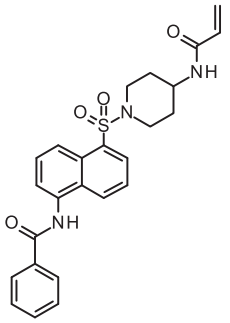

3,4-Dimethoxy-*N*-{5-[4-(acryloylamino)piperidine-1-sulfonyl]naphthalen-1-yl}benzamide (23b)

Following general procedure **C - work-up 3** (solvent: CH_2Cl_2/THF (1:1, 0.1 M); before work-up evaporation of solvents; flash column chromatography solvent: MeOH/CH_2Cl_2 2-5:98-95), the purified product was precipitated from EtOH to give **23b** as a pale white

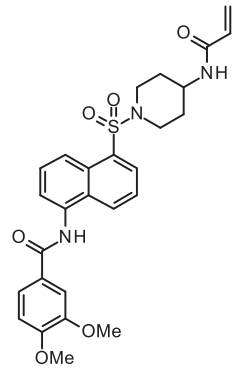

solid. **Molecular Formula:** $C_{27}H_{29}N_3O_6S$; **MW**: 523.60 g/mol; **Yield**: 75%; **Mp**: 125-128ºC (EtOH); **^{1}H NMR** (300 MHz, DMSO-*d_6*) δ 1.31-1.48 (m, 2H, $CH_{2piperidine}$), 1.76-1.88 (m, 2H, $CH_{2piperidine}$), 2.83-2.95 (m, 2H, $CH_{2piperidine}$), 3.59-3.79 (m, 3H, $CH_{piperidine}$ + $CH_{2piperidine}$), 3.87 (s, 6H, 2 x OCH_3), 5.55 (dd, J = 9.7, 2.7 Hz, 1H, CH_2= cis), 6.04 (dd, J = 17.1, 2.7 Hz, 1H, CH_2= trans), 6.16 (dd, J = 17.1, 9.7 Hz, 1H, CH=), 7.14 (d, J = 8.6 Hz, 1H, H_{arom}), 7.63-7.83 (m, 5H, H_{arom} + H_{napht}), 8.06 (d, J = 7.6 Hz, 1H, NH), 8.20 (d, J = 6.4 Hz, 1H, H_{napht}), 8.32 (d, J = 8.3 Hz, 1H, H_{napht}), 8.56 (d, J = 8.5 Hz, 1H, H_{napht}), 10.45 (s, 1H, NH); **^{13}C NMR** (101 MHz, DMSO-*d_6*) δ 165.7 (C=O), 163.8 (C=O), 151.8 (C), 148.4 (C), 135.1 (C), 133.5 (C), 131.7 (CH), 130.5 (C), 130.0 (CH), 129.9 (CH), 128.8 (C), 127.8 (CH), 126.2 (C), 125.3 (CH_2=), 125.2 (CH), 124.6 (CH), 122.9 (CH), 121.3 (CH), 111.1 (CH), 111.0 (CH), 55.7 (CH_3), 55.6 (CH_3), 44.8 (CH), 44.0 (2 x CH_2), 30.9 (2 x CH_2); **HRMS (ESI)** calcd for $C_{27}H_{30}N_3O_6S$ $[M+H]^+$, 524.1850; found, 524.1835.

3-Nitro-*N*-{5-[4-(acryloylamino)piperidine-1-sulfonyl]naphthalen-1-yl}benzamide (23c)

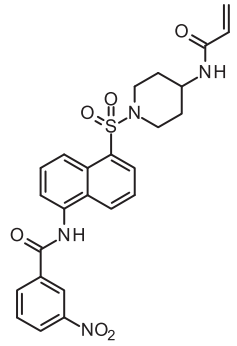

Following general procedure **C - work-up 2** (flash column chromatography solvent: MeOH/CH_2Cl_2 3:97), the purified product was precipitated from Et_2O to give **23c** as a white solid. **Molecular Formula**: $C_{25}H_{24}N_4O_6S$; **MW**: 508.55 g/mol; **Yield**: 57%; **Mp**: 150-152ºC (Et_2O); **^{1}H NMR** (300 MHz, DMSO-*d_6*) δ 1.31-1.48 (m, 2H, $CH_{2piperidine}$), 1.75-1.90 (m, 2H, $CH_{2piperidine}$), 2.83-2.98 (m, 2H, $CH_{2piperidine}$), 3.58-3.81 (m, 3H, $CH_{piperidine}$ + CH_2 $_{piperidine}$), 5.55 (dd, J = 9.7, 2.6 Hz, 1H, CH_2= cis), 6.04 (dd, J = 17.1, 2.6 Hz, 1H, CH_2= trans), 6.16 (dd, J = 17.1, 9.7 Hz, 1H, CH=), 7.68-7.85 (m, 3H, H_{napht}), 7.90 (t, J = 8.0 Hz, 1H, H_{arom}), 8.06 (d, J = 7.5 Hz, 1H, NH), 8.22 (dd, J = 7.3, 0.9 Hz, 1H, H_{napht}), 8.39 (d, J = 8.5 Hz, 1H, H_{napht}), 8.47-8.56 (m, 2H, H_{arom} + H_{napht}), 8.60 (dd, J = 7.9, 1.0 Hz, 1H, H_{arom}), 8.93 (t, J = 1.8 Hz, 1H, H_{arom}), 10.96 (s, 1H, NH); **^{13}C NMR** (75 MHz, DMSO-*d_6*) δ 164.4 (C=O), 163.8 (C=O), 147.8 (C), 135.6 (C), 134.4 (C), 134.3 (CH), 133.5 (C), 131.7 (CH), 130.3 (CH), 130.2 (C), 130.1 (CH), 129.8 (CH), 128.8 (C), 127.8 (CH), 126.4 (CH), 125.2 (CH + CH_2=), 124.7 (CH), 123.4 (CH), 122.7 (CH), 44.8 (CH), 44.0 (2 x CH_2), 30.9 (2 x CH_2); **HRMS (ESI)** calcd for $C_{25}H_{25}N_4O_6S$ $[M+H]^+$, 509.1489; found, 509.1492.

***Tert*-butyl 4-(Acryloylamino)piperidine-1-carboxylate (26)**

Following general procedure **C - work-up 2** (the crude residue was precipitated from Et_2O, filtered, and washed with Et_2O), the compound **26** was obtained as a white solid.

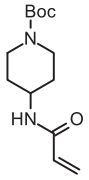

Molecular Formula: $C_{13}H_{22}N_2O_3$; **MW**: 254.32 g/mol; **Yield**: 64%; **Mp**: 96-98ºC (Et_2O); **^{1}H NMR** (300 MHz, DMSO-*d_6*) δ 1.16-1.32 (m, 2H, $CH_{2piperidine}$), 1.39 (s, 9H, 3 x CH_3), 1.66-1.79 (m, 2H, $CH_{2piperidine}$), 2.75-2.98 (m, 2H, $CH_{2piperidine}$), 3.72-3.92 (m, 3H, $CH_{piperidine}$ + $CH_{2piperidine}$), 5.57 (dd, J = 9.7, 2.6 Hz, 1H, CH_2= cis), 6.07 (dd, J = 17.1, 2.6 Hz, 1H, CH_2= trans), 6.19 (dd, J = 17.1, 9.7 Hz, 1H, CH=), 8.03 (d, J = 7.7 Hz, 1H, NH); **LRMS (ESI)**: *m/z* 255.2 $[M+H]^+$.

N-(Piperidinium-4-yl)prop-2-enamide trifluoroacetate salt (27)

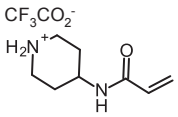

Following general procedure **B** (after first addition of Et_2O the supernatant was removed followed by three more washings with Et_2O, each time removing the supernatant), the compound **27** was obtained as a hygroscopic white solid. **Molecular Formula**: $C_{10}H_{15}F_3N_2O_3$; **MW**: 268.23 g/mol; **Yield**: 100%; **^{1}H NMR** (300 MHz, DMSO-*d_6*) δ 1.47-1.64 (m, 2H, $CH_{2piperidine}$), 1.85-1.99 (m, 2H, $CH_{2piperidine}$), 2.91-3.08 (m, 2H, $CH_{2piperidine}$), 3.20-3.34 (m, 2H, $CH_{2piperidine}$), 3.83-3.97 (m, 1H, $CH_{piperidine}$), 5.60 (dd, J = 9.7, 2.6 Hz, 1H, CH_2= cis), 6.09 (dd, J = 17.1, 2.6 Hz, 1H, CH_2= trans), 6.21 (dd, J = 17.1, 9.7 Hz, 1H, CH=), 8.21 (d, J = 7.2 Hz, 1H, NH), 8.27-8.66 (m, 2H, NH_2^+).

4-(Benzoylamino)naphthalene-1-sulfonate pyridinium salt (29)

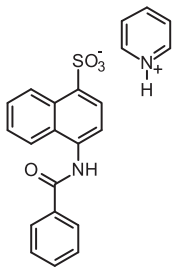

Following general procedure **D**, the compound **29** was obtained as a white solid. **Molecular Formula**: $C_{22}H_{18}N_2O_4S$; **MW**: 406.45 g/mol; **Yield**: 64%; **Mp**: > 210ºC (MeOH); **^{1}H NMR** (300 MHz, DMSO-*d_6*) δ 7.47-7.67 (m, 6H, H_{arom} + H_{napht}), 7.90-8.03 (m, 4H, H_{pyr} + H_{napht}), 8.10 (d, J = 8.1 Hz, 2H, H_{arom}), 8.40-8.54 (m, 1H, H_{pyr}), 8.82-8.94 (m, 3H, H_{napht} + H_{pyr}), 10.45 (s, 1H, NH).

Hydrolysis was observed for **30** (general procedure **E**). The compound was used rapidly in the next reaction without characterization (NMR spectra showed mixture of desired sulfonyl chloride and derivative from hydrolysis).

N-{4-[4-(Acryloylamino)piperidine-1-sulfonyl]naphthalen-1-yl}benzamide (28)

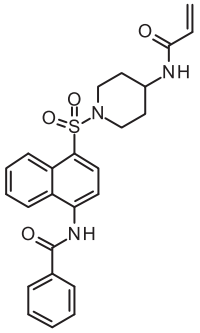

Following general procedure **A - work-up 1** (solvent: CH_2Cl_2; flash column chromatography solvent: $CHCl_3$/MeOH/H_2O 65:25:4), the compound **28** was obtained as a white solid. **Molecular Formula:** $C_{25}H_{25}N_3O_4S$; **MW**: 463.55 g/mol; **Yield**: 30%; **Mp**: > 210ºC; **^{1}H NMR** (300 MHz, DMSO-*d_6*) δ 1.30-1.48 (m, 2H, $CH_{2piperidine}$), 1.77-

1.88 (m, 2H, $CH_{2piperidine}$), 2.81-2.95 (m, 2H, $CH_{2piperidine}$), 3.59-3.79 (m, 3H, $CH_{piperidine}$ + $CH_{2piperidine}$), 5.55 (dd, J = 9.8, 2.7 Hz, 1H, CH_2= cis), 6.04 (dd, J = 17.1, 2.7 Hz, 1H, CH_2= trans), 6.16 (dd, J = 17.1, 9.8 Hz, 1H, CH=), 7.54-7.83 (m, 5H, H_{arom} + H_{napht}), 7.90 (d, J = 8.1 Hz, 1H, H_{napht}), 8.06 (d, J = 7.7 Hz, 1H, NH) 8.10 (d, J = 7.6 Hz, 2H, H_{arom}), 8.19-8.28 (m, 2H, H_{napht}), 8.66 (d, J = 8.2 Hz, 1H, H_{napht}), 10.70 (s, 1H, NH); **^{13}C NMR** (101 MHz, DMSO-*d*$_6$) δ 166.4 (C=O), 163.8 (C=O), 139.4 (C), 134.2 (C), 132.1 (CH), 131.7 (CH), 130.3 (C), 130.0 (CH), 129.2 (C), 129.0 (C), 128.6 (2 x CH), 128.2 (CH), 128.0 (2 x CH), 126.8 (CH), 125.3 (CH_2=), 124.9 (CH), 124.4 (CH), 121.3 (CH), 44.8 (CH), 44.0 (2 x CH_2), 30.9 (2 x CH_2); **HRMS (ESI)** calcd for $C_{25}H_{25}N_3NaO_4S$ $[M+Na]^+$, 486.1458; found, 486.1445.

2-Methyl-*N*-{5-[4-(acryloylamino)piperidine-1-sulfonyl]naphthalen-1-yl}benzamide (23d)

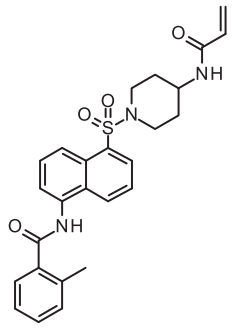

Following general procedure **A - work-up 2** (solvent: DMF; DIPEA (3 eq); flash column chromatography solvent: MeOH/CH_2Cl_2 5-10:90-95), the resultant product was precipitated from EtOH to give **23d** as a white solid. **Molecular Formula**: $C_{26}H_{27}N_3O_4S$; **MW**: 477.58 g/mol; **Yield**: 26%; **Mp**: > 210ºC (EtOH); **^{1}H NMR** (300 MHz, DMSO-*d*$_6$) δ 1.29-1.48 (m, 2H, $CH_{2piperidine}$), 1.72-1.90 (m, 2H, $CH_{2piperidine}$), 2.50 (s under peak solvent, 3H, CH_3), 2.81-3.00 (m, 2H, $CH_{2piperidine}$), 3.54-3.82 (m, 3H, $CH_{piperidine}$ + $CH_{2piperidine}$), 5.55 (dd, J = 9.7, 2.6 Hz, 1H, CH_2= cis), 6.04 (dd, J = 17.1, 2.6 Hz, 1H, CH_2= trans), 6.15 (dd, J = 17.1, 9.7 Hz, 1H, CH=), 7.30-7.50 (m, 3H, H_{arom}), 7.61-7.89 (m, 4H, H_{napht} + H_{arom}), 8.05 (d, J = 7.3 Hz, 1H, NH), 8.20 (d, J = 7.0 Hz, 1H, H_{napht}), 8.43 (d, J = 8.5 Hz, 1H, H_{napht}), 8.55 (d, J = 7.8 Hz, 1H, H_{napht}), 10.52 (s, 1H, NH); **^{13}C NMR** (101 MHz, DMSO-*d*$_6$) δ 168.9 (C=O), 163.8 (C=O), 136.7 (C), 135.5 (C), 134.6 (C), 133.5 (C), 131.7 (CH), 130.6 (CH), 130.1 (CH), 129.9 (C), 129.8 (CH), 129.6 (CH), 128.8 (C), 127.8 (CH), 127.5 (CH), 125.7 (CH), 125.3 (CH_2=), 124.6 (CH), 124.5 (CH), 122.8 (CH), 44.8 (CH), 44.0 (2 x CH_2), 31.0 (2 x CH_2), 19.6 (CH_3); **HRMS (ESI)** calcd for $C_{26}H_{28}N_3O_4S$ $[M+H]^+$, 478.1795; found, 478.1789.

3-Methyl-*N*-{5-[4-(acryloylamino)piperidine-1-sulfonyl]naphthalen-1-yl}benzamide (23e)

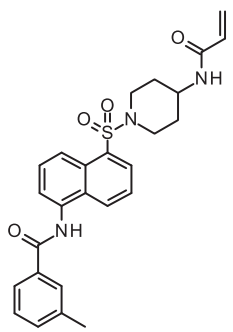

Following general procedure **A - work-up 2** (solvent: DMF; DIPEA (3 eq); flash column chromatography solvent: MeOH/CH_2Cl_2 5:95), the resultant product was precipitated from EtOH to give **23e** as a white solid. **Molecular Formula**: $C_{26}H_{27}N_3O_4S$; **MW**: 477.58 g/mol; **Yield**: 63%; **Mp**: > 210ºC (EtOH); **^{1}H NMR** (300 MHz, DMSO-*d*$_6$) δ 1.30-1.47 (m, 2H,

$CH_{2piperidine}$), 1.88-1.76 (m, 2H, $CH_{2piperidine}$), 2.43 (s, 3H, CH_3), 2.83-2.97 (m, 2H, $CH_{2piperidine}$), 3.56-3.82 (m, 3H, $CH_{2piperidine}$ + $CH_{piperidine}$), 5.55 (dd, J = 9.8, 2.4 Hz, 1H, CH_2= cis), 6.04 (dd, J = 17.0, 2.4 Hz, 1H, CH_2= trans), 6.16 (dd, J = 17.0, 9.8 Hz, 1H, CH=), 7.42-7.50 (m, 2H, H_{arom}), 7.66-7.81 (m, 3H, H_{napht}), 7.82-7.94 (m, 2H, H_{arom}), 8.06 (d, J = 7.5 Hz, 1H, NH), 8.20 (d, J = 7.5 Hz, 1H, H_{napht}), 8.34 (d, J = 8.7 Hz, 1H, H_{napht}), 8.56 (d, J = 8.3 Hz, 1H, H_{napht}),10.55 (s, 1H, NH); **^{13}C NMR** (101 MHz, DMSO-*d_6*) δ 166.5 (C=O), 163.8 (C=O), 137.9 (C), 134.9 (C), 134.2 (C), 133.5 (C), 132.4 (CH), 131.7 (CH), 130.4 (C), 130.0 (CH), 129.8 (CH), 128.8 (C), 128.4 (2 x CH), 127.8 (CH), 125.3 (CH_2=), 125.2 (CH), 125.0 (CH), 124.6 (CH), 123.0 (CH), 44.8 (CH), 44.0 (2 x CH_2), 31.0 (2 x CH_2), 21.0 (CH_3); **HRMS (ESI)** calcd for $C_{26}H_{28}N_3O_4S$ $[M+H]^+$, 478.1795; found, 478.1795.

3-Methoxy-*N*-{5-[4-(acryloylamino)piperidine-1-sulfonyl]naphthalen-1-yl}benzamide (23f)

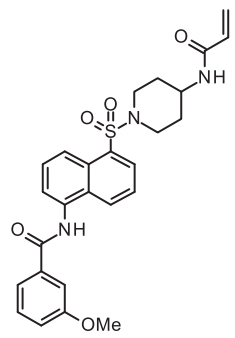

Following general procedure **A - work-up 2** (solvent: DMF; DIPEA (3 eq); flash column chromatography solvent: MeOH/CH_2Cl_2 5:95), the resultant product was precipitated from EtOH to give **23f** as a white solid. **Molecular Formula**: $C_{26}H_{27}N_3O_5S$; **MW**: 493.57 g/mol; **Yield**: 71%; **Mp**: 185-187ºC (EtOH); **^{1}H NMR** (300 MHz, DMSO-*d_6*) δ 1.30-1.47 (m, 2H, $CH_{2piperidine}$), 1.74-1.89 (m, 2H, $CH_{2piperidine}$), 2.82-2.97 (m, 2H, $CH_{2piperidine}$), 3.58-3.80 (m, 3H, $CH_{2piperidine}$ + $CH_{piperidine}$), 3.86 (s, 3H, OCH_3), 5.55 (dd, J = 9.7, 2.7 Hz, 1H, CH_2= cis), 6.04 (dd, J = 17.1, 2.7 Hz, 1H, CH_2= trans), 6.16 (dd, J = 17.1, 9.7 Hz, 1H, CH=), 7.21 (dd, J = 8.2, 1.8 Hz, 1H, H_{arom}), 7.50 (t, J = 7.9 Hz, 1H, H_{arom}), 7.60-7.83 (m, 5H, H_{napht} + H_{arom}), 8.06 (d, J = 7.5 Hz, 1H, NH), 8.20 (d, J = 6.9 Hz, 1H, H_{napht}), 8.33 (d, J = 8.5 Hz, 1H, H_{napht}), 8.57 (d, J = 8.4 Hz, 1H, H_{napht}), 10.58 (s, 1H, NH); **^{13}C NMR** (101 MHz, DMSO-*d_6*) δ 166.1 (C=O), 163.8 (C=O), 159.3 (C), 135.5 (C) 134.9 (C), 133.5 (C), 131.7 (CH), 130.4 (C), 130.1 (CH), 129.8 (CH), 129.7 (CH), 128.8 (C), 127.8 (CH), 125.3 (CH_2=), 125.2 (CH), 124.7 (CH), 123.1 (CH), 120.1 (CH), 117.8 (CH), 112.9 (CH), 55.4 (CH_3), 44.8 (CH), 44.0 (2 x CH_2), 31.0 (2 x CH_2); **HRMS (ESI)** calcd for $C_{26}H_{28}N_3O_5S$ $[M+H]^+$, 494.1744; found, 494.1727.

3-Chloro-*N*-{5-[4-(acryloylamino)piperidine-1-sulfonyl]naphthalen-1-yl}benzamide (23g)

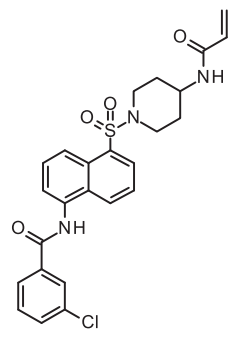

Following general procedure **A - work-up 2** (solvent: DMF; DIPEA (3 eq); flash column chromatography solvent: MeOH/CH_2Cl_2 5:95), the compound **23g** was obtained as a white solid. **Molecular Formula**: $C_{25}H_{24}ClN_3O_4S$; **MW**: 497.99 g/mol;

Yield: 63%; **Mp**: 194-196ºC; **^{1}H NMR** (300 MHz, DMSO-d_6) δ 1.32-1.46 (m, 2H, $CH_{2piperidine}$), 1.78-1.86 (m, 2H, $CH_{2piperidine}$), 2.84-2.94 (m, 2H, $CH_{2piperidine}$), 3.59-3.82 (m, 3H, $CH_{2piperidine}$ + $CH_{piperidine}$), 5.55 (dd, J = 9.9, 2.3 Hz, 1H, CH_2= cis), 6.05 (dd, J = 17.1, 2.3 Hz, 1H, CH_2= trans), 6.16 (dd, J = 17.1, 9.9 Hz, 1H, CH=), 7.62 (t, J = 7.9 Hz, 1H, H_{arom}), 7.67-7.83 (m, 4H, H_{napht} + H_{arom}), 7.92-8.10 (m, 2H, NH + H_{arom}), 8.16 (s, 1H, H_{arom}), 8.21 (d, J = 7.3 Hz, 1H, H_{napht}), 8.36 (d, J = 8.5 Hz, 1H, H_{napht}), 8.58 (d, J = 8.1 Hz, 1H, H_{napht}), 10.71 (s, 1H, NH); **^{13}C NMR** (101 MHz, DMSO-d_6) δ 165.0 (C=O), 163.8 (C=O), 136.2 (C), 134.6 (C), 133.5 (C), 133.4 (C), 131.7 (2 x CH), 130.5 (CH), 130.3 (C), 130.1 (CH), 129.8 (CH), 128.8 (C), 127.8 (CH), 127.7 (CH), 126.7 (CH), 125.3 (CH_2=), 125.2 (CH), 124.7 (CH), 123.2 (CH), 44.8 (CH), 44.0 (2 x CH_2), 31.0 (2 x CH_2); **HRMS (ESI)** calcd for $C_{25}H_{24}ClN_3NaO_4S$ $[M+Na]^+$, 520.1068; found, 520.1055.

Methyl 3-(*N*-{5-[4-(Acryloylamino)piperidin-1-sulfonyl]naphthalen-1-yl}carbamoyl)benzoate (23h)

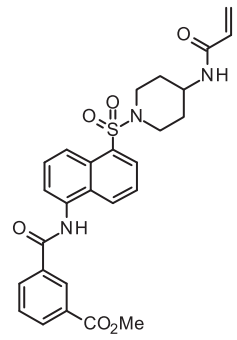

Following general procedure **A - work-up 2** (solvent: DMF; DIPEA (3 eq); flash column chromatography solvent: MeOH/CH_2Cl_2 5:95), the resultant product was precipitated from EtOH to give **23h** as a white solid. **Molecular Formula**: $C_{27}H_{27}N_3O_6S$; **MW**: 521.58 g/mol; **Yield**: 81%; **Mp**: 140-141°C (EtOH); **^{1}H NMR** (400 MHz, DMSO-d_6) δ 1.47-1.33 (m, 2H, $CH_{2piperidine}$), 1.75-1.89 (m, 2H, $CH_{2piperidine}$), 2.84-2.97 (m, 2H, $CH_{2piperidine}$), 3.57-3.81 (m, 3H, $CH_{2piperidine}$ + $CH_{piperidine}$), 3.93 (s, 3H, OCH_3), 5.55 (dd, J = 9.9, 2.2 Hz, 1H, CH_2= cis), 6.05 (dd, J = 17.1, 2.2 Hz, 1H, CH_2= trans), 6.16 (dd, J = 17.1, 9.9 Hz, 1H, CH=), 7.67-7.85 (m, 4H, H_{napht} + H_{arom}), 8.07 (d, J = 7.5 Hz, 1H, NH), 8.16-8.25 (m, 2H, H_{napht} + H_{arom}), 8.32-8.42 (m, 2H, H_{napht} + H_{arom}), 8.59 (d, J = 8.4 Hz, 1H, H_{napht}), 8.69 (s, 1H, H_{arom}), 10.83 (s, 1H, NH); **^{13}C NMR** (101 MHz, DMSO-d_6) δ 165.8 (C=O), 165.5 (C=O), 163.8 (C=O), 134.7 (C), 133.5 (C), 132.6 (CH), 132.3 (CH), 131.7 (CH, q), 130.4 (C), 130.1 (CH), 130.0 (C), 129.9 (CH), 129.2 (CH), 128.8 (C), 128.6 (CH), 127.8 (CH), 125.3 (CH + CH_2=), 124.7 (CH), 123.2 (CH), 52.5 (CH_3), 44.8 (CH), 44.0 (2 x CH_2), 31.0 (2 x CH_2); **HRMS (ESI)**: calcd for $C_{27}H_{28}N_3O_6S$ $[M+H]^+$, 522.1693; found, 522.1670.

4-Methoxy-*N*-{5-[4-(acryloylamino)piperidine-1-sulfonyl]naphthalen-1-yl}benzamide (23i)

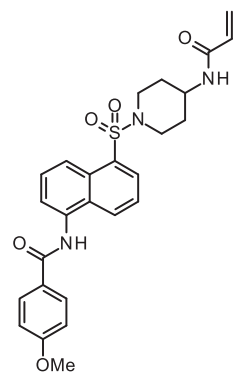

Following general procedure **A - work-up 2** (solvent: DMF; DIPEA (3 eq); crystallization solvent: MeOH/CH_2Cl_2 2:98), the compound **23i** was obtained as a white solid. **Molecular Formula**: $C_{26}H_{27}N_3O_5S$; **MW**: 493.57 g/mol; **Yield**: 74%; **Mp**: > 210ºC

(MeOH/CH_2Cl_2); **^{1}H NMR** (400 MHz, DMSO-*d_6*) δ 1.31-1.47 (m, 2H, $CH_{2piperidine}$), 1.76-1.88 (m, 2H, $CH_{2piperidine}$), 2.83-2.97 (m, 2H, $CH_{2piperidine}$), 3.59-3.79 (m, 3H, $CH_{piperidine}$ + $CH_{2piperidine}$), 3.86 (s, 3H, OCH_3), 5.55 (dd, J = 9.9, 2.2 Hz, 1H, CH_2= cis), 6.05 (dd, J = 17.1, 2.2 Hz, 1H, CH_2= trans), 6.16 (dd, J = 17.1, 9.9 Hz, 1H, CH=), 7.11 (d, J = 8.8 Hz, 2H, H_{arom}), 7.66-7.81 (m, 3H, H_{napht}), 8.03-8.13 (m, 3H, NH + H_{arom}), 8.20 (d, J = 7.1 Hz, 1H, H_{napht}), 8.33 (d, J = 8.5 Hz, 1H, H_{napht}), 8.56 (d, J = 8.5 Hz, 1H, H_{napht}), 10.45 (s, 1H, NH); **^{13}C NMR** (101 MHz, DMSO-*d_6*) δ 165.8 (C=O), 163.8 (C=O), 162.1 (C), 135.1 (C), 133.5 (C), 131.7 (CH), 130.5 (C), 130.0 (CH), 129.9 (CH), 129.8 (2 x CH), 128.8 (C), 127.8 (CH), 126.2 (C), 125.3 (CH_2=), 125.2 (CH), 124.6 (CH), 122.8 (CH), 113.7 (2 x CH), 55.5 (CH_3), 44.8 (CH), 44.0 (2 x CH_2), 31.0 (2 x CH_2); **HRMS (ESI)** calcd for $C_{26}H_{28}N_3O_5S$ $[M+H]^+$, 494.1744; found, 494.1738.

4-Chloro-*N*-{5-[4-(acryloylamino)piperidine-1-sulfonyl]naphthalen-1-yl}benzamide (23j)

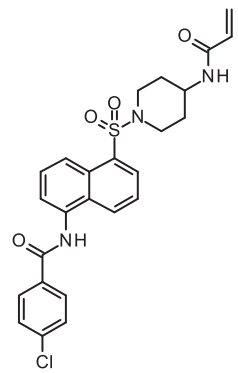

Following general procedure **2 - work-up 3** (solvent: DMF; DIPEA (3 eq); flash column chromatography solvent: MeOH/CH_2Cl_2 5:95), the resultant product was precipitated from EtOH to give **23j** as a white solid.

Molecular Formula: $C_{25}H_{24}ClN_3O_4S$; **MW**: 497.99 g/mol; **Yield**: 22%; **Mp**: > 210ºC (EtOH); **^{1}H NMR** (400 MHz, DMSO-*d_6*) δ 1.31-1.47 (m, 2H, $CH_{2piperidine}$), 1.73-1.90 (m, 2H, $CH_{2piperidine}$), 2.82-2.97 (m, 2H, $CH_{2piperidine}$), 3.55-3.81 (m, 3H, $CH_{piperidine}$ + $CH_{2piperidine}$), 5.55 (dd, J = 9.7, 2.6 Hz, 1H, CH_2= cis), 6.04 (dd, J = 17.0, 2.6 Hz, 1H, CH_2= trans), 6.16 (dd, J = 17.0, 9.7 Hz, 1H, CH=), 7.66 (d, J = 8.5 Hz, 2H, H_{arom}), 7.71-7.84 (m, 3H, H_{napht}), 8.06 (d, J = 7.7 Hz, 1H, NH), 8.12 (d, J = 8.5 Hz, 2H, H_{arom}), 8.20 (d, J = 6.7 Hz, 1H, H_{napht}), 8.35 (d, J = 8.5 Hz, 1H, H_{napht}), 8.57 (d, J = 8.3 Hz, 1H, H_{napht}), 10.67 (s, 1H, NH); **^{13}C NMR** (101 MHz, DMSO-*d_6*) δ 165.4 (C=O), 163.8 (C=O), 136.7 (C), 134.7 (C), 133.5 (C), 132.9 (C), 131.7 (CH), 130.3 (C), 130.1 (CH), 129.9 (2 x CH), 129.8 (CH), 128.8 (C), 128.6 (2 x CH), 127.8 (CH), 125.3 (CH_2=), 125.2 (CH), 124.7 (CH), 123.2 (CH), 44.8 (CH), 44.0 (2 x CH_2), 31.0 (2 x CH_2); **HRMS (ESI)** calcd for $C_{25}H_{24}ClN_3NaO_4S$ $[M+Na]^+$, 520.1068; found, 520.1048.

N-{5-[4-(Acryloylamino)piperidine-1-sulfonyl]naphthalen-1-yl}-4-(trifluoromethyl)benzamide (23k)

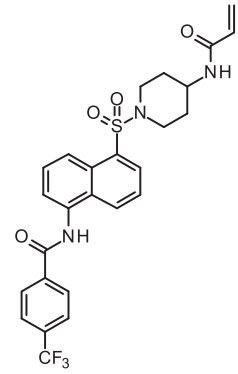

Following general procedure **A - work-up 2** (solvent: DMF; DIPEA (3 eq); flash column chromatography solvent: MeOH/CH_2Cl_2 2-3:97-98), the resultant product was precipitated from Et_2O to give **23k** as a white solid. **Molecular Formula**: $C_{26}H_{24}F_3N_3O_4S$; **MW**: 531.55 g/mol; **Yield**: 22%; **Mp**: > 210ºC

(Et_2O); **^{1}H NMR** (300 MHz, DMSO-d_6) δ 1.30-1.48 (m, 2H, $CH_{2piperidine}$), 1.74-1.88 (m, 2H, $CH_{2piperidine}$), 2.83-2.97 (m, 2H, $CH_{2piperidine}$), 3.60-3.80 (m, 3H, $CH_{piperidine}$ + $CH_{2piperidine}$), 5.56 (dd, J = 9.7, 2.6 Hz, 1H, CH_2= cis), 6.04 (dd, J = 17.0, 2.7 Hz, 1H, CH_2= trans), 6.16 (dd, J = 17.0, 9.7 Hz, 1H, CH=), 7.68-7.85 (m, 3H, H_{napht}), 7.97 (d, J = 8.2 Hz, 2H, H_{arom}), 8.05 (d, J = 7.5 Hz, 1H, NH), 8.21 (d, J = 7.3 Hz, 1H, H_{napht}), 8.30 (d, J = 8.2 Hz, 2H, H_{arom}), 8.38 (d, J = 8.5 Hz, 1H, H_{napht}), 8.58 (d, J = 8.4 Hz, 1H, H_{napht}), 10.82 (s, 1H, NH); **HRMS (ESI)** calcd for $C_{26}H_{25}F_3O_4S$ $[M+H]^+$, 532.1512; found, 532.1510.

3,4-Dimethyl-*N*-{5-[4-(acryloylamino)piperidine-1-sulfonyl]naphthalen-1-yl}benzamide (23l)

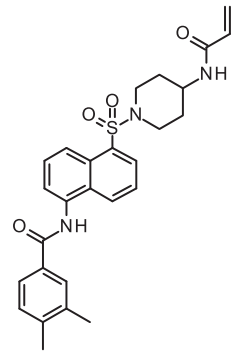

Following general procedure **A - work-up 2** (solvent: DMF; DIPEA (3 eq); flash column chromatography solvent: MeOH/CH_2Cl_2 5:95), the resultant product was precipitated from EtOH to give **23l** as a white solid. **Molecular Formula**: $C_{27}H_{29}N_3O_4S$; **MW**: 491.60 g/mol; **Yield**: 43%; **Mp**: > 210ºC (EtOH); **^{1}H NMR** (300 MHz, DMSO-d_6) δ 1.28-1.49 (m, 2H, $CH_{2piperidine}$), 1.72-1.90 (m, 2H, $CH_{2piperidine}$), 2.33 (s, 3H, CH_3), 2.34 (s, 3H, CH_3), 2.81-2.98 (m, 2H, $CH_{2piperidine}$), 3.57-3.84 (m, 3H, $CH_{2piperidine}$ + $CH_{piperidine}$), 5.55 (dd, J = 9.8, 2.6 Hz, 1H, CH_2= cis), 6.04 (dd, J = 17.1, 2.6 Hz, 1H, CH_2= trans), 6.16 (dd, J = 17.1, 9.8 Hz, 1H, CH=), 7.33 (d, J = 7.9 Hz, 1H, H_{arom}), 7.64-7.92 (m, 5H, H_{napht} + H_{arom}), 8.05 (d, J = 7.5 Hz, 1H, NH), 8.20 (d, J = 7.2 Hz, 1H, H_{napht}), 8.32 (d, J = 8.5 Hz, 1H, H_{napht}), 8.55 (d, J = 8.4 Hz, 1H, H_{napht}), 10.47 (s, 1H, NH); **^{13}C NMR** (101 MHz, DMSO-d_6) δ 166.4 (C=O), 163.8 (C=O), 140.6 (C), 136.5 (C) 135.1 (C), 133.5 (C), 131.7 (C + CH), 130.5 (C), 130.0 (CH), 129.9 (CH), 129.5 (CH), 128.9 (CH), 128.8 (CH), 127.8 (C), 125.4 (CH), 125.3 (CH_2=), 125.2 (CH), 124.6 (CH), 122.9 (CH), 44.8 (CH), 44.0 (2 x CH_2), 31.0 (2 x CH_2), 19.5 (CH_3), 19.5 (CH_3); **HRMS (ESI)** calcd for $C_{27}H_{30}N_3O_4S$ $[M+H]^+$, 492.1952; found, 492.1941.

3,4-Dichloro-*N*-{5-[4-(acryloylamino)piperidine-1-sulfonyl]naphthalen-1-yl}benzamide (23m)

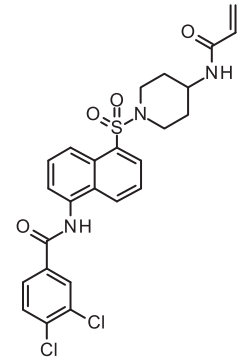

Following general procedure **A - work-up 2** (solvent: DMF; DIPEA (3 eq); flash column chromatography solvent: MeOH/CH_2Cl_2 5:95), the resultant product was precipitated from EtOH to give **23m** as a white solid. **Molecular Formula**: $C_{25}H_{23}Cl_2N_3O_4S$; **MW**: 532.44 g/mol; **Yield**: 46%; **Mp**: > 210ºC (EtOH); **^{1}H NMR** (400 MHz, DMSO-d_6) δ 1.30-1.48 (m, 2H, $CH_{2piperidine}$), 1.77-1.88 (m, 2H, $CH_{2piperidine}$), 2.85-2.96 (m, 2H,

$CH_{2piperidine}$), 3.56-3.81 (m, 3H, $CH_{2piperidine}$ + $CH_{piperidine}$), 5.55 (dd, J = 9.9, 2.2 Hz, 1H, CH_2= cis), 6.05 (dd, J = 17.0, 2.2 Hz, 1H, CH_2= trans), 6.16 (dd, J = 17.0, 9.9 Hz, 1H, CH=), 7.67-7.82 (m, 3H, H_{napht}), 7.87 (d, J = 8.3 Hz, 1H, H_{arom}), 8.00-8.13 (m, 2H, NH + H_{arom}), 8.21 (d, J = 7.1 Hz, 1H, H_{napht}), 8.33-8.43 (m, 2H, H_{napht} + H_{arom}), 8.59 (d, J = 8.4 Hz, 1H, H_{napht}), 10.77 (s, 1H, NH); **^{13}C NMR** (101 MHz, DMSO-*d*$_6$) δ 164.2 (C=O), 163.8 (C=O), 134.7 (C), 134.6 (C), 134.4 (C), 133.5 (C), 131.7 (CH), 131.4 (C), 130.9 (CH), 130.3 (C), 130.1 (CH), 129.9 (CH), 129.8 (CH), 128.8 (C), 128.2 (CH), 127.8 (CH), 125.3 (CH_2=), 125.2 (CH), 124.7 (CH), 123.3 (CH), 44.8 (CH), 44.0 (2 x CH_2), 31.0 (2 x CH_2); **HRMS (ESI)** calcd for $C_{25}H_{24}Cl_2N_3O_4S$ $[M+H]^+$, 532.0859; found, 532.0839.

3,5-Dimethoxy-*N*-{5-[4-(acryloylamino)piperidine-1-sulfonyl]naphthalen-1-yl}benzamide (23n)

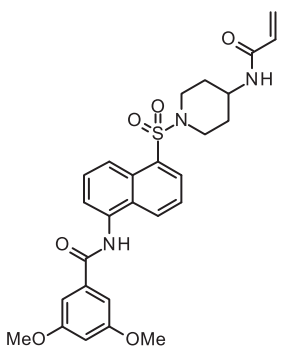

Following general procedure **A - work-up 2** (solvent: DMF; DIPEA (3 eq); flash column chromatography solvent: MeOH/CH_2Cl_2 5:95), the resultant product was precipitated from EtOH to give **23n** as a pale-white solid. **Molecular Formula**: $C_{27}H_{29}N_3O_6S$; **MW**: 523.60 g/mol; **Yield**: 75%; **Mp**: 188-190ºC (EtOH); **^{1}H NMR** (400 MHz, DMSO-*d*$_6$) δ 1.32-1.46 (m, 2H, $CH_{2piperidine}$), 1.75-1.88 (m, 2H, $CH_{2piperidine}$), 2.84-2.95 (m, 2H, $CH_{2piperidine}$), 3.59-3.77 (m, 3H, $CH_{piperidine}$ + $CH_{2piperidine}$), 3.84 (s, 6H, 2 x OCH_3), 5.55 (dd, J = 9.9, 2.4 Hz, 1H, CH_2= cis), 6.05 (dd, J = 17.1, 2.4 Hz, 1H, CH_2= trans), 6.16 (dd, J = 17.1, 9.9 Hz, 1H, CH=), 6.77 (t, J = 2.2 Hz, 1H, H_{arom}), 7.26 (d, J = 2.2 Hz, 2H, H_{arom}), 7.66-7.74 (m, 2H, H_{napht}), 7.76-7.86 (m, 1H, H_{napht}), 8.06 (t, J = 7.6 Hz, 1H, NH), 8.21 (d, J = 7.3 Hz, 1H, H_{napht}), 8.32 (d, J = 8.5 Hz, 1H, H_{napht}), 8.57 (d, J = 8.6 Hz, 1H, H_{napht}), 10.55 (s, 1H, NH); **^{13}C NMR** (101 MHz, DMSO-*d*$_6$) δ 165.9 (C=O), 163.8 (C=O), 160.5 (2 x C), 136.1 (C), 134.8 (C), 133.5 (C), 131.7 (CH), 130.4 (C), 130.1 (CH), 129.8 (CH), 128.8 (C), 127.8 (CH), 125.3 (CH_2=) 125.3 (CH), 124.7 (CH), 123.1 (CH), 105.7 (2 x CH), 103.8 (CH), 55.6 (2 x CH_3), 44.8 (CH), 44.0 (2 x CH_2), 31.0 (2 x CH_2); **HRMS (ESI)** calcd for $C_{27}H_{30}N_3O_6S$ $[M+H]^+$, 524.1850; found, 524.1839.

3,4,5-Trimethoxy-*N*-{5-[4-(acryloylamino)piperidine-1-sulfonyl]naphthalen-1-yl}benzamide (23o)

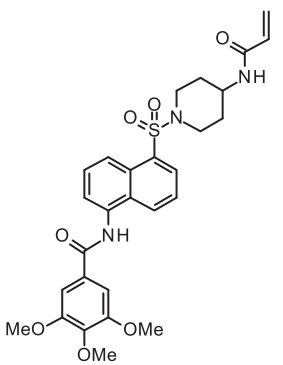

Following general procedure **C - work-up 3** (solvent: DMF; DIPEA (3 eq); flash column chromatography solvent: MeOH/CH_2Cl_2 5:95), the resultant purified product was precipitated from EtOH to give **23o** as a light-yellow solid. **Molecular Formula:** $C_{28}H_{31}N_3O_7S$; **MW**: 553.63 g/mol;

Yield: 52%; **Mp**: 138-140ºC (EtOH); **^{1}H NMR** (400 MHz, DMSO-d_6) δ 1.32-1.46 (m, 2H, $CH_{2piperidine}$), 1.77-1.87 (m, 2H, $CH_{2piperidine}$), 2.84-2.95 (m, 2H, $CH_{2\ piperidine}$), 3.61-3.74 (m, 3H, $CH_{2piperidine}$ + $CH_{piperidine}$), 3.76 (s, 3H, OCH_3), 3.90 (s, 6H, 2 x OCH_3), 5.55 (dd, J = 9.9, 2.4 Hz, 1H, CH_2= cis), 6.05 (dd, J = 17.1, 2.4 Hz, 1H, CH_2= trans), 6.16 (dd, J = 17.1, 9.9 Hz, 1H, CH=), 7.46 (s, 2H, H_{arom}), 7.69-7.76 (m, 2H, H_{napht}), 7.80 (dd, J = 8.6, 7.5 Hz, 1H), 8.07 (d, J = 7.6 Hz, 1H, NH), 8.21 (dd, J = 7.3, 1.0 Hz, 1H, H_{napht}), 8.33 (d, J = 8.5 Hz, 1H, H_{napht}), 8.58 (d, J = 8.7 Hz, 1H, H_{napht}), 10.54 (s, 1H, NH); **^{13}C NMR** (101 MHz, DMSO-d_6) δ 165.7 (C=O), 163.8 (C=O), 152.8 (2 x C), 140.5 (C), 134.9 (C), 133.5 (C), 131.7 (CH), 130.5 (C), 130.1 (CH), 129.9 (CH), 129.1 (C), 128.8 (C), 127.9 (CH), 125.3 (CH + CH_2=), 124.7 (CH), 123.1 (CH), 105.4 (2 x CH), 60.2 (CH_3), 56.1 (2 x CH_3), 44.8 (CH), 44.0 (2 x CH_2), 31.0 (2 x CH_2); **HRMS (ESI)**: calcd for $C_{28}H_{32}N_3O_7S$ $[M+H]^+$, 554.1955; found, 554.1941.

N-{5-[4-(Acryloylamino)piperidine-1-sulfonyl]naphthalen-1-yl}naphthalene-2-carboxamide (23p)

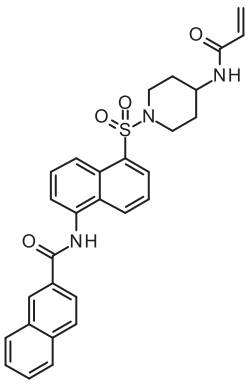

Following general procedure **A - work-up 2** (solvent: DMF; DIPEA (3 eq); flash column chromatography solvent: MeOH/CH_2Cl_2 2-10:90-98), the resultant purified product was precipitated from EtOH to give **23p** as a white solid. **Molecular Formula**: $C_{29}H_{27}N_3O_4S$; **MW**: 513.61 g/mol; **Yield**: 59%; **Mp**: > 210ºC (EtOH); **^{1}H NMR** (300 MHz, DMSO-d_6) δ 1.31-1.48 (m, 2H, $CH_{2piperidine}$), 1.76-1.89 (m, 2H, $CH_{2piperidine}$), 2.85-2.97 (m, 2H, $CH_{2piperidine}$), 3.60-3.81 (m, 3H, $CH_{piperidine}$ + $CH_{2piperidine}$), 5.55 (dd, J = 9.7, 2.6 Hz, 1H, CH_2= cis), 6.04 (dd, J = 17.1, 2.6 Hz, 1H, CH_2= trans), 6.16 (dd, J = 17.1, 9.7 Hz, 1H, CH=), 7.61-7.77 (m, 3H, H_{arom}), 7.77-7.86 (m, 2H, H_{arom}), 8.02-8.17 (m, 5H, H_{arom} + NH), 8.22 (d, J = 6.4 Hz, 1H, H_{arom}), 8.43 (d, *J* = 8.5 Hz, 1H, H_{arom}), 8.53-8.62 (m, 1H, H_{arom}), 8.75 (s, 1H, H_{arom}), 10.78 (s, 1H, NH); **^{13}C NMR** (101 MHz, DMSO-d_6) δ 166.5 (C=O), 163.8 (C=O), 134.9 (C), 134.5 (C), 133.5 (C), 132.2 (C), 131.7 (CH) 131.5 (C), 130.4 (C), 130.1 (CH), 129.9 (CH), 129.1 (CH), 128.9 (C), 128.4 (CH), 128.1 (CH), 128.0 (CH), 127.9 (CH), 127.7 (CH), 126.9 (CH), 125.3 (CH_2=), 125.2 (CH), 124.7 (CH), 124.6 (CH), 123.0 (CH), 44.8 (CH), 44.0 (2 x CH_2), 31.0 (2 x CH_2); **HRMS (ESI)** calcd for $C_{29}H_{28}N_3O_4S$ $[M+H]^+$, 514.1795; found, 514.1772.

N-{5-[4-(Acryloylamino)piperidine-1-sulfonyl]naphthalen-1-yl}benzo[1,3]dioxole-5-carboxamide (23q)

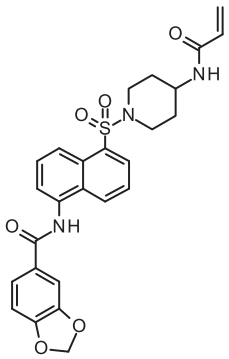

Following general procedure **A - work-up 2** (solvent: DMF; DIPEA (3 eq); flash column chromatography solvent: MeOH/CH_2Cl_2 5:95), the compound **23q** was obtained as a white solid. **Molecular Formula**: $C_{26}H_{25}N_3O_6S$; **MW**: 507.56 g/mol; **Yield**: 56%; **Mp**: > 210ºC; **^{1}H NMR** (400 MHz, DMSO-*d_6*) δ 1.30-1.47 (m, 2H, $CH_{2piperidine}$), 1.73-1.90 (m, 2H, $CH_{2piperidine}$), 2.82-2.97 (m, 2H, $CH_{2piperidine}$), 3.57-3.81 (m, 3H, $CH_{2piperidine}$ + $CH_{piperidine}$), 5.55 (dd, J = 9.9, 2.4 Hz, 1H, CH_2= cis), 6.05 (dd, J = 17.0, 2.4 Hz, 1H, CH_2= trans), 6.16 (dd, J = 17.0, 9.9 Hz, 1H, CH=), 6.17 (s, 2H, CH_2), 7.11 (d, J = 8.1 Hz, 1H, H_{arom}), 7.64 (d, J = 1.6 Hz, 1H, H_{arom}), 7.67-7.82 (m, 4H, H_{napht} + H_{arom}), 8.07 (d, J = 7.5 Hz, 1H, NH), 8.21 (d, J = 7.1 Hz, 1H, H_{napht}), 8.33 (d, J = 8.5 Hz, 1H, H_{napht}), 8.56 (d, J = 8.6 Hz, 1H, H_{napht}), 10.44 (s, 1H, NH); **^{13}C NMR** (101 MHz, DMSO-*d_6*) δ 165.4 (C=O), 163.8 (C=O), 150.3 (C) 147.5 (C), 134.9 (C), 133.5 (C), 131.7 (CH), 130.5 (C), 130.1 (CH), 129.9 (CH), 128.8 (C), 128.0 (C), 127.8 (CH), 125.3 (CH_2=), 125.2 (CH), 124.6 (CH), 123.1 (CH), 122.9 (CH), 108.1 (CH), 107.9 (CH), 101.9 (CH_2), 44.8 (CH), 44.0 (2 x CH_2), 31.0 (2 x CH_2); **HRMS (ESI)** calcd for $C_{26}H_{25}N_3NaO_6S$ $[M+Na]^+$, 530.1356; found, 530.1344.

3-Phenyl-*N*-{5-[4-(acryloylamino)piperidine-1-sulfonyl]naphthalen-1-yl}benzamide (23r)

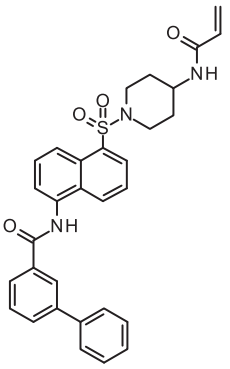

Following general procedure **A - work-up 2** (solvent: DMF; DIPEA (3 eq); flash column chromatography solvent: MeOH/CH_2Cl_2 5:95), the resultant product was precipitated from EtOH to give **23f** as a white solid. **Molecular Formula**: $C_{31}H_{29}N_3O_4S$; **MW**: 539.64 g/mol; **Yield**: 41%; **Mp**: 148-150ºC (EtOH); **^{1}H NMR** (300 MHz, DMSO-*d_6*) δ 1.31-1.48 (m, 2H, $CH_{2piperidine}$), 1.75-1.89 (m, 2H, $CH_{2piperidine}$), 2.82-2.97 (m, 2H, $CH_{2piperidine}$), 3.58-3.81 (m, 3H, $CH_{2piperidine}$ + $CH_{piperidine}$), 5.55 (dd, J = 9.7, 2.6 Hz, 1H, CH_2= cis), 6.04 (dd, J = 17.0, 2.6 Hz, 1H, CH_2= trans), 6.16 (dd, J = 17.0, 9.7 Hz, 1H, CH=), 7.43 (t, J = 7.3 Hz, 1H, H_{arom}), 7.53 (t, J = 7.5 Hz, 2H, H_{arom}), 7.62-7.86 (m, 6H, H_{napht} + H_{arom}), 7.95 (d, J = 7.9 Hz, 1H, H_{arom}), 8.06 (d, J = 7.6 Hz, 2H, NH + H_{arom}), 8.21 (d, J = 6.8 Hz, 1H, H_{napht}), 8.35-8.46 (m, 2H, H_{napht} + H_{arom}), 8.58 (d, J = 7.9 Hz, 1H, H_{napht}), 10.72 (s, 1H, NH); **^{13}C NMR** (101 MHz, DMSO-*d_6*) δ 166.3 (C=O), 163.8 (C=O), 140.4 (C), 139.5 (C), 134.9 (C), 134.8 (C), 133.5 (C), 131.7 (CH), 130.4 (C), 130.1 (CH), 130.0 (CH), 129.9 (CH), 129.3 (CH), 129.1 (2 x CH), 128.9 (C), 127.9 (CH), 127.87 (CH), 127.1 (CH), 126.9 (2 x CH), 126.1 (CH), 125.3 (CH_2=), 125.2 (CH), 124.7 (CH), 123.1 (CH), 44.8 (CH), 44.0 (2 x CH_2), 31.0 (2 x CH_2); **HRMS (ESI)** calcd for $C_{31}H_{30}N_3O_4S$ $[M+H]^+$, 540.1952; found, 540.1935.

4-Phenyl-*N*-{5-[4-(acryloylamino)piperidine-1-sulfonyl]naphthalen-1-yl}benzamide (23s)

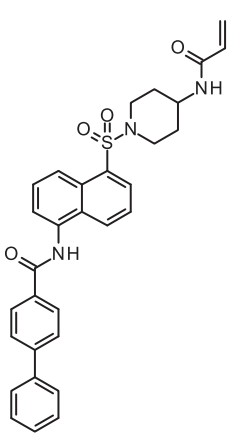

Following general procedure **A - work-up 2** (solvent: DMF; DIPEA (3 eq); before quenching with water; the resulting crude extract was dissolved in CH_2Cl_2 and extracted three times with H_2O. The organic layer was washed with brine, dried over Na_2SO_4, filtrated and the solvent was evaporated under vacuum. Precipitation from MeOH/CH_2Cl_2 3:97), the compound **23s** was obtained as a white solid. **Molecular Formula**: $C_{31}H_{29}N_3O_4S$; **MW**: 539.64 g/mol; **Yield**: 78%; **Mp**: > 210ºC (MeOH/CH_2Cl_2); **^{1}H NMR** (400 MHz, DMSO-*d_6*) δ 1.30-1.49 (m, 2H, $CH_{2piperidine}$), 1.75-1.90 (m, 2H, $CH_{2piperidine}$), 2.81-2.98 (m, 2H, $CH_{2piperidine}$), 3.54-3.82 (m, 3H, $CH_{piperidine}$ + $CH_{2piperidine}$), 5.56 (dd, J = 9.9, 2.3 Hz, 1H, CH_2= cis), 6.06 (dd, J = 17.1, 2.3 Hz, 1H, CH_2= trans), 6.17 (dd, J = 17.1, 9.9 Hz, 1H, CH=), 7.35-7.60 (m, 3H, H_{arom}), 7.65-7.84 (m, 5H, H_{arom} + H_{napht}), 7.90 (d, J = 8.4 Hz, 2H, H_{arom}), 8.08 (d, J = 7.5 Hz, 1H, NH), 8.17-8.25 (m, 3H, H_{napht} + H_{arom}), 8.39 (d, J = 8.5 Hz, 1H, H_{napht}), 8.59 (d, J = 7.8 Hz, 1H, H_{napht}), 10.67 (s, 1H, NH); **^{13}C NMR** (101 MHz, DMSO-*d_6*) δ 166.0 (C=O), 163.8 (C=O), 143.4 (C), 139.1 (C), 134.9 (C), 133.5 (C), 132.9 (C), 131.7 (CH), 130.4 (C), 130.1 (CH), 129.9 (CH), 129.1 (2 x CH), 128.8 (C), 128.6 (2 x CH), 128.2 (CH), 127.8 (CH), 126.9 (2 x CH), 126.7 (2 x CH), 125.3 (CH_2=), 125.2 (CH), 124.6 (CH), 123.1 (CH), 44.8 (CH), 44.0 (2 x CH_2), 31.0 (2 x CH_2); **HRMS (ESI)** calcd for $C_{31}H_{30}N_3O_4S$ $[M+H]^+$, 540.1952; found, 540.1943.

***Tert*-butyl *N*-{1-[5-(3-Aminobenzoylamino)naphthalene-1-sulfonyl]piperidin-4-yl}carbamate (32)**

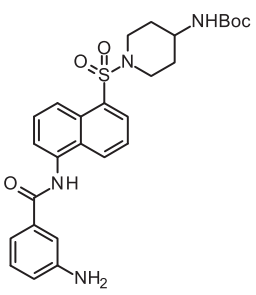

Following general procedure **G**, the compound **32** was obtained as a grey solid. **Molecular Formula:** $C_{27}H_{32}N_4O_5S$; **MW**: 524.63 g/mol; **Yield**: 93%; **Mp**: 130-140ºC; **^{1}H NMR** (300 MHz, DMSO-*d_6*) δ 1.35 (s, 9H, 3 x CH_3), 1.36-1.45 (m, 2H, $CH_{2piperidine}$), 1.70-1.82 (m, 2H, $CH_{2piperidine}$), 2.73-2.87 (m, 2H, $CH_{2piperidine}$), 3.27-3.40 (m, 1H, $CH_{piperidine}$), 3.58-3.69 (m, 2H, $CH_{2piperidine}$), 5.35 (s, 2H, NH_2), 6.76-6.82 (m, 1H, H_{arom}), 6.87 (d, J = 7.4 Hz, 1H, NH), 7.15-7.27 (m, 3H, H_{arom}), 7.64-7.81 (m, 3H, H_{napht}), 8.16, (dd, J = 7.4, 1.0 Hz, 1H, H_{napht}), 8.29 (d, J = 8.5 Hz, 1H, H_{napht}), 8.54 (d, J = 8.4 Hz, 1H, H_{napht}), 10.38 (s, 1H, NH); **LRMS (ESI)**: *m/z* 525.2 $[M+H]^+$.

***Tert*-butyl *N*-(1-{5-[(3-Acetylamino)benzoylamino]naphthalene-1-sulfonyl}piperidin-4-yl)carbamate (33a)**

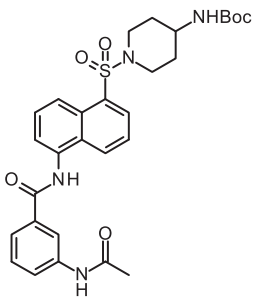

Following general procedure **C - work-up 3** (DIPEA (1.5 eq); flash column chromatography solvent: MeOH/CH_2Cl_2 5:95), the resultant product was precipitated from EtOH to give **33a** as a white solid. **Molecular Formula**: $C_{29}H_{34}N_4O_6S$; **MW**: 566.67 g/mol; **Yield**: 60%; **Mp**: > 210ºC (EtOH); **^{1}H NMR** (300 MHz, DMSO-*d*$_6$) δ 1.34 (s, 9H, 3 x CH_3), 1.37-1.44 (m, 2H, $CH_{2piperidine}$), 1.70-1.82 (m, 2H, $CH_{2piperidine}$), 2.08 (s, 3H, CH_3), 2.74-2.87 (m, 2H, $CH_{2piperidine}$), 3.57-3.70 (m, 2H, $CH_{2piperidine}$), 6.87 (d, J = 7.6 Hz, 1H, NH), 7.50 (t, J = 7.9 Hz, 1H, H_{arom}), 7.66-7.84 (m, 4H, H_{napht}), 7.88 (d, J = 9.0 Hz, 1H, H_{arom}), 8.17 (d, J = 7.6 Hz, 1H, H_{arom}), 8.18 (s, 1H, H_{arom}), 8.32 (d, J = 8.4 Hz, 1H, H_{napht}), 8.56 (d, J = 8.0 Hz, 1H, H_{napht}), 10.16 (s, 1H, NH), 10.58 (s, 1H, NH); **LRMS (ESI)**: *m/z* 567.2 $[M+H]^+$.

***Tert*-butyl *N*-(1-{5-[(3-(Benzoylamino)benzoylamino]naphthalene-1-sulfonyl}piperidin-4-yl)carbamate (33b)**

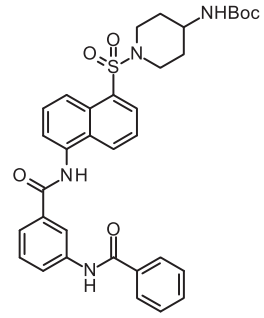

Following general procedure **C - work-up 2** (DIPEA (1.5 eq); no flash column chromatography purification), the compound **33b** was obtained as a beige solid. **Molecular Formula**: $C_{34}H_{36}N_4O_6S$; **MW**: 628.74 g/mol; **Yield**: 99%; **Mp**: 140-142ºC; **^{1}H NMR** (300 MHz, DMSO-*d*$_6$) δ 1.37 (s, 9H, 3 x CH_3), 1.35-1.47 (m, 2H, $CH_{2piperidine}$), 1.69-1.83 (m, 2H, $CH_{2piperidine}$), 2.75-2.86 (m, 2H, $CH_{2piperidine}$), 2.91-3.08 (m, 1H, $CH_{piperidine}$), 3.58-3.70 (m, 2H, $CH_{2piperidine}$), 6.88 (d, J = 7.6 Hz, 1H, NH), 7.50-7.64 (m, 4H, H_{arom}), 7.68-7.83 (m, 3H, H_{napht}), 7.88 (d, J = 8.0 Hz, 1H, H_{arom}), 7.98-8.04 (m, 2H, H_{arom}), 8.09 (dd, J = 8.2, 1.3 Hz, 1H, H_{arom}), 8.18 (dd, J = 7.3, 1.0 Hz, 1H, H_{napht}), 8.34 (d, J = 8.5 Hz, 1H, H_{napht}), 8.44 (t, J = 1.8 Hz, 1H, H_{arom}), 8.56 (d, J = 7.5 Hz, 1H, H_{napht}), 10.49 (s, 1H, NH), 10.62 (s, 1H, NH); **LRMS (ESI)**: *m/z* 629.2 $[M+H]^+$.

***N*-(1-{5-[3-(Acetylamino)benzoylamino]naphthalene-1-sulfonyl}piperidin-4-yl)ammonium trifluoroacetate salt (34a)**

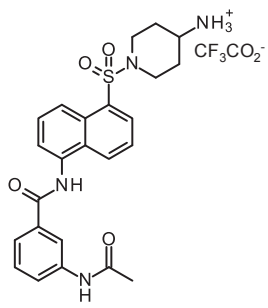

Following general procedure **B**, the compound **34a** was obtained as a pale white solid. **Molecular Formula**: $C_{26}H_{27}F_3N_4O_6S$; **MW:** 580.58 g/mol; **Yield**: 97%; **Mp**: 196-198ºC (washing Et_2O); **^{1}H NMR** (300 MHz, DMSO-*d*$_6$) δ 1.42-1.60 (m, 2H, $CH_{2piperidine}$), 1.89-2.00 (m, 2H, $CH_{2piperidine}$), 2.08 (s, 3H, CH_3), 2.68-2.83 (m, 2H, $CH_{2piperidine}$), 3.05-3.23 (m, 1H, $CH_{piperidine}$), 3.75-3.87 (m, 2H, $CH_{2piperidine}$), 7.50 (t, J = 7.9 Hz, 1H, H_{arom}),

7.66-7.93 (m, 8H, NH_3^+ + H_{arom} + H_{napht}), 8.20 (d, J = 7.6 Hz, 1H, H_{arom}), 8.22 (s, 1H, H_{arom}), 8.33 (d, J = 8.5 Hz, 1H, H_{napht}), 8.56 (d, J = 8.3 Hz, 1H, H_{napht}), 10.17 (s, 1H, NH), 10.60 (s, 1H, NH).

N-(1-{5-[3-(Benzoylamino)benzoylamino]naphthalene-1-sulfonyl}piperidin-4-yl)ammonium trifluoroacetate salt (34b)

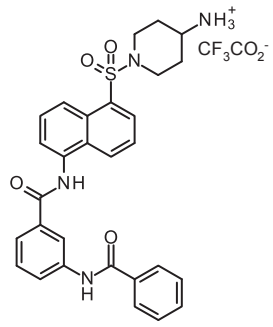

Following general procedure **B**, the compound **34b** was obtained as an orange solid. **Molecular Formula**: $C_{31}H_{29}F_3N_4O_6S$; **MW**: 642.64 g/mol; **Yield**: 100%; **Mp**: 125-127ºC (washing Et_2O); **^{1}H NMR** (300 MHz, DMSO-*d_6*) δ 1.43-1.59 (m, 2H, $CH_{2piperidine}$), 1.88-2.02 (m, 2H, $CH_{2piperidine}$), 2.71-2.84 (m, 2H, $CH_{2piperidine}$), 3.10-3.19 (m, 1H, $CH_{piperidine}$), 3.75-3.88 (m, 2H, $CH_{2piperidine}$), 7.51-7.66 (m, 4H, H_{arom}), 7.71-7.90 (m, 7H, NH_3^+ + H_{arom} + H_{napht}), 7.97-8.03 (m, 2H, H_{arom}), 8.03-8.09 (m, 1H, H_{arom}), 8.21 (d, J = 6.7 Hz, 1H, H_{napht}), 8.36 (d, J = 8.4 Hz, 1H, H_{napht}), 8.47 (s, 1H, H_{arom}), 8.57 (d, J = 8.6 Hz, 1H, H_{napht}), 10.50 (s, 1H, NH), 10.65 (s, 1H, NH).

3-Acetylamino-*N*-{5-[4-(acryloylamino)piperidine-1-sulfonyl]naphthalen-1-yl}benzamide (31a)

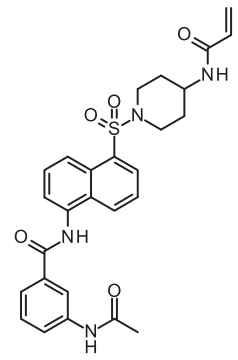

Following general procedure **C - work-up 3** (solvent: CH_2Cl_2 (0.08 M) and DMF (0.234 M), DIPEA (3.7 eq); evaporation of solvents before work-up; flash column chromatography solvent: MeOH/CH_2Cl_2 6:94), the resultant product was precipitated from Et_2O/EtOH to give **31a** as a white solid. **Molecular Formula**: $C_{27}H_{28}N_4O_5S$; **MW**: 520.60 g/mol; **Yield**: 54%; **Mp**: > 210ºC (Et_2O/EtOH); **^{1}H NMR** (300 MHz, DMSO-*d_6*) δ 1.30-1.48 (m, 2H, $CH_{2piperidine}$), 1.72-1.89 (m, 2H, $CH_{2piperidine}$), 2.08 (s, 3H, CH_3), 2.83-2.99 (m, 2H, $CH_{2piperidine}$), 3.57-3.81 (m, 2H, $CH_{piperidine}$ + $CH_{2piperidine}$), 5.55 (dd, J = 9.8, 2.5 Hz, 1H, CH_2= cis), 6.04 (dd, J = 17.1, 2.5 Hz, 1H, CH_2= trans), 6.16 (dd, J = 17.1, 9.8 Hz, 1H, CH=), 7.50 (t, J = 7.9 Hz, 1H, H_{arom}), 7.67-7.84 (m, 4H, H_{napht}), 7.87 (d, J = 8.6 Hz, 1H, H_{arom}), 8.06 (d, J = 7.3 Hz, 1H, NH), 8.19 (s, 1H, H_{arom}), 8.20 (d, J = 7.6 Hz, 1H, H_{arom}), 8.32 (d, J = 8.6 Hz, 1H, H_{napht}), 8.56 (d, J = 8.1 Hz, 1H, H_{napht}), 10.17 (s, 1H, NH), 10.59 (s, 1H, NH); **HRMS (ESI)** calcd for $C_{27}H_{29}N_4O_5S$ $[M+H]^+$, 521.1853; found, 521.1849.

3-Benzoylamino-*N*-{5-[4-(acryloylamino)piperidine-1-sulfonyl]naphthalen-1-yl}benzamide (31b)

Following general procedure **C - work-up 2** (DIPEA (2 eq); no flash column chromatography purification), the compound **31b** was obtained as a beige solid.

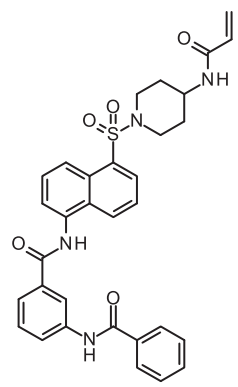

Molecular Formula: $C_{32}H_{30}N_4O_5S$; **MW**: 582.67 g/mol; **Yield**: 62%; **Mp**: 164-166ºC; **^{1}H NMR** (400 MHz, DMSO-*d_6*) δ 1.31-1.49 (m, 2H, $CH_{2piperidine}$), 1.73-1.92 (m, 2H, $CH_{2piperidine}$), 2.80-3.00 (m, 2H, $CH_{2piperidine}$), 3.56-3.81 (m, 3H, $CH_{piperidine}$ + $CH_{2piperidine}$), 5.55 (dd, J = 9.9, 2.2 Hz, 1H, CH_2= cis), 6.05 (dd, J = 17.1, 2.2 Hz, 1H, CH_2= trans), 6.16 (dd, J = 17.1, 9.9 Hz, 1H, CH=), 7.48-7.66 (m, 4H, H_{arom}), 7.68-7.84 (m, 3H, H_{napht}), 7.89 (d, J = 7.7 Hz, 1H, H_{arom}), 7.98-8.14 (m, 4H, NH + H_{arom}), 8.22 (d, J = 7.1 Hz, 1H, H_{napht}), 8.36 (d, J = 8.5 Hz, 1H, H_{napht}), 8.46 (s, 1H, H_{arom}), 8.58 (d, J = 8.2 Hz, 1H, H_{napht}), 10.51 (s, 1H, NH), 10.65 (s, 1H, NH); **^{13}C NMR** (101 MHz, DMSO-*d_6*) δ 166.5 (C=O), 165.7 (C=O), 163.8 (C=O), 139.5 (C), 134.9 (C), 134.5 (C), 134.7 (C), 133.6 (C), 131.8 (CH), 131.7 (CH), 130.4 (C), 130.1 (CH), 129.8 (CH), 128.9 (C), 128.8 (CH), 128.5 (2 x CH), 127.9 (CH), 127.7 (2 x CH), 125.3 (CH_2=), 125.2 (CH), 124.7 (CH), 123.6 (CH), 123.1 (CH), 122.8 (CH), 120.2 (CH), 44.8 (CH), 44.0 (2 x CH_2), 31.0 (2 x CH_2); **HRMS (ESI)** calcd for $C_{32}H_{30}N_4NaO_5S$ $[M+Na]^+$, 605.1829; found, 605.1808.

***Tert*-butyl *N*-(1-{5-[(3,4-Dimethoxybenzoylamino)naphthalene-1-sulfonyl]piperidin-4-yl}methyl)carbamate (38)**

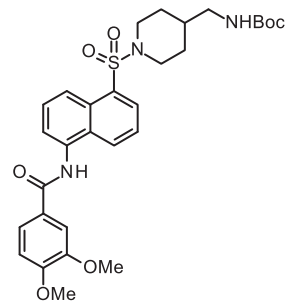

Following general procedure **A - work-up 1** (Solvent: CH_2Cl_2 (0.1 M); DIPEA (1.5 eq); flash column chromatography solvent: EtOAc/CH_2Cl_2 2:8), the compound **38** was obtained as a light-yellow foam. **Molecular Formula**: $C_{30}H_{37}N_3O_7S$; **MW**: 583.70 g/mol; **Yield**: 48%; **^{1}H NMR** (300 MHz, DMSO-*d_6*) δ 0.95-1.13 (m, 2H, CH_2), 1.34 (s, 9H, 3 x CH_3), 1.37-1.48 (m, 1H, $CH_{piperidine}$), 1.58-1.70 (m, 2H, $CH_{2piperidine}$), 2.53-2.66 (m, 2H, $CH_{2piperidine}$), 2.70-2.81 (m, 2H, $CH_{2piperidine}$), 3.68-3.79 (m, 2H, $CH_{2piperidine}$), 3.86 (m, 6H, 2 x OCH_3), 6.83 (t, J = 5.6 Hz, 1H, NH), 7.13 (d, J = 8.5 Hz, 1H, H_{arom}), 7.64-7.81 (m, 5H, H_{napht} + H_{arom}), 8.17 (dd, J = 7.3, 1.0 Hz, 1H, H_{napht}), 8.30 (d, J = 8.5 Hz, 1H, H_{napht}), 8.57 (d, J = 8.4 Hz, 1H, H_{napht}), 10.43 (s, 1H, NH); **LRMS (ESI)**: *m/z* 584.2 $[M+H]^+$.

N-(1-{5-[(3,4-Dimethylbenzoylamino)naphthalene-1-sulfonyl]piperidin-4-yl}methyl)ammonium trifluoroacetate salt (39)

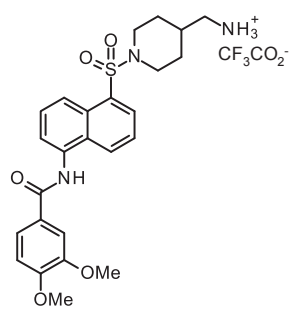

Following general procedure **B**, the compound **39** was obtained as a white solid. **Molecular Formula**: $C_{25}H_{26}F_3N_3O_7S$; **MW**: 569.55 g/mol; **Yield**: 89%; **Mp**: > 210ºC (washing Et_2O); **^{1}H NMR** (300 MHz, DMSO-*d_6*) δ 1.10-1.27 (m, 2H, CH_2), 1.53-1.69 (m, 1H, $CH_{piperidine}$), 1.70-1.81 (m, 2H, $CH_{2piperidine}$), 2.54-

2.65 (m, 2H, $CH_{2piperidine}$), 2.66-2.75 (m, 2H, $CH_{2piperidine}$), 3.74-3.83 (m, 2H, $CH_{2piperidine}$), 3.86 (s, 6H, 2 x OCH_3), 7.13 (d, J = 8.5 Hz, 1H, H_{arom}), 7.61-7.82 (m, 8H, NH_3^+ + H_{napht} + H_{arom}), 8.19 (d, J = 6.4 Hz, 1H, H_{napht}), 8.31 (d, J = 8.4 Hz, 1H, H_{napht}), 8.58 (d, J = 8.5 Hz, 1H, H H_{napht}), 10.45 (s, 1H, NH).

3,4-Dimethoxy-*N*-(5-{4-[(acryloylamino)methyl]piperidine-1-sulfonyl}naphthalen-1-yl)benzamide (35)

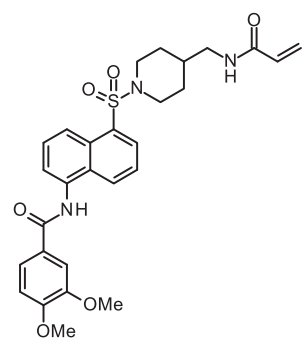

Following general procedure **C - work-up 2** (DIPEA (2.5 eq); flash column chromatography solvent: MeOH/CH_2Cl_2 3-5:95-97), the compound **35** was obtained as a white foam. **Molecular Formula**: $C_{28}H_{31}N_3O_6S$; **MW**: 537.63 g/mol; **Yield**: 74%; **^{1}H NMR** (300 MHz, DMSO-d_6) δ: 1.00-1.19 (m, 2H, CH_2), 1.38-1.57 (m, 1H, $CH_{piperidine}$), 1.60-1.74 (m, 2H, $CH_{2piperidine}$), 2.54-2.67 (m, 2H, $CH_{2piperidine}$), 2.92-3.03 (m, 2H, $CH_{2piperidine}$), 3.69-3.81 (m, 2H, $CH_{2piperidine}$), 3.86 (s, 6H, 2 x OCH_3), 5.55 (dd, J = 9.9, 2.4 Hz, 1H, CH_2= cis), 6.03 (dd, J = 17.0, 2.4 Hz, 1H, CH_2= trans), 6.20 (dd, J = 17.0, 9.9 Hz, 1H, CH=), 7.13 (d, J = 8.6 Hz, 1H, H_{arom}), 7.64-7.81 (m, 5H, H_{napht} + H_{arom}), 8.06 (t, J = 5.7 Hz, 1H, NH), 8.18 (dd, J = 7.3, 1.0 Hz, 1H, H_{napht}), 8.30 (d, J = 8.5 Hz, 1H, H_{napht}), 8.58 (d, J = 8.6 Hz, 1H, H_{napht}), 10.43 (s, 1H, NH); **^{13}C NMR** (101 MHz, DMSO-d_6) δ 165.7 (C=O), 164.6 (C=O), 151.8 (C), 148.4 (C), 135.1 (C), 133.4 (C), 131.7 (CH), 130.5 (C), 130.0 (CH), 129.8 (CH), 128.9 (C), 127.8 (CH), 126.2 (C), 125.2 (CH), 125.1 (CH_2=), 124.6 (CH), 123.0 (CH), 121.3 (CH), 111.1 (CH), 111.0 (CH), 55.7 (CH_3), 55.6 (CH_3), 45.1 (CH_2), 43.5 (2 x CH_2), 35.0 (CH), 29.2 (2 x CH_2); **HRMS (ESI)** calcd for $C_{28}H_{32}N_3O_6S$ $[M+H]^+$, 538.2006; found, 538.1990.

***Tert*-butyl *N*-(2-{4-[5-(3,4-Dimethoxybenzoylamino)naphthalene-1-sulfonyl]piperazin-1-yl}-2-oxoethyl)carbamate (40)**

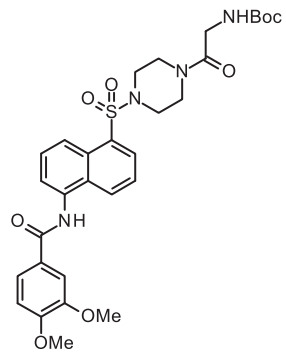

Following general procedure **A - work-up 2** (solvent: DMF (0.4 M); sulfonyl chloride (1.1 eq); DIPEA (1.5 eq); after filtration and the different washing steps, the solid was diluted in CH_2Cl_2 an extracted once with water. The recovered organic layer was then washed twice with saturated aqueous $NaHCO_3$ solution, twice with saturated NaCl solution, dried (Na_2SO_4), filtered and evaporated), the resultant solid was dried/stored (until use) under vacuum over P_2O_5 to give **40** as a white solid. **Molecular Formula:** $C_{30}H_{36}N_4O_8S$; **MW**: 612.69 g/mol; **Yield**: 69%; **Mp**: 174-176ºC (decomposition); **^{1}H NMR** (300 MHz, DMSO-d_6) δ 1.35 (s, 9H, 3 x CH_3), 3.07-3.14 (m, 4H, 2 x $CH_{2piperazine}$), 3.37-3.55 (m, 4H, 2 x $CH_{2piperazine}$), 3.71 (d, J = 6.0 Hz, 2H, CH_2), 3.86 (s, 6H, 2 x OCH_3), 6.70 (t, J = 5.8? Hz, 1H, NH),

7.13 (d, J = 8.4 Hz, 1H, H_{arom}), 7.58-7.87 (m, 5H, H_{napht} + H_{arom}), 8.20 (d, J = 7.3 Hz, 1H, H_{napht}), 8.34 (d, J = 8.3 Hz, 1H, H_{napht}), 8.61 (d, J = 8.0 Hz, 1H, H_{napht}), 10.44 (s, 1H, NH); **LRMS (ESI)**: *m/z* 613.2 $[M+H]^+$.

_N_-[2-(4-{5-[(3,4-Dimethoxybenzoyl)amino]naphthalene-1-sulfonyl}piperazin-1-yl)-2-oxoethyl]ammonium trifluoroacetate salt (41)

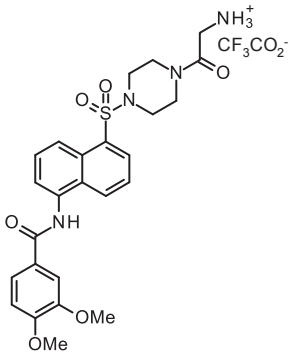

Following general procedure **B**, the compound **41** was obtained as a white solid. **Molecular Formula**: $C_{27}H_{29}F_3N_4O_8S$; **MW**: 626.60 g/mol; **Yield**: 96%; **Mp**: 144-146ºC (washing Et_2O); **^{1}H NMR** (300 MHz, DMSO-d_6) δ 3.07-3.25 (m, 4H, 2 x $CH_{2piperazine}$), 3.35-3.47 (m, 4H, 2 x $CH_{2piperazine}$), 3.52-3.63 (m, 2H, CH_2), 3.86 (s, 6H, 2 x OCH_3), 7.13 (d, J = 8.6 Hz, 1H, H_{arom}), 7.60-7.82 (m, 5H, H_{arom} + H_{napht}), 7.85-8.00 (m, 3H, NH_3^+), 8.21 (d, J = 7.5 Hz, 1H, H_{napht}), 8.34 (d, J = 8.4 Hz, 1H, H_{napht}), 8.63 (d, J = 8.5 Hz, 1H, H_{napht}), 10.48 (s, 1H, NH).

_N_-(5-{4-[2-(acryloylamino)acetyl]piperazine-1-sulfonyl}naphthalen-1-yl)-3,4-dimethoxybenzamide (36)

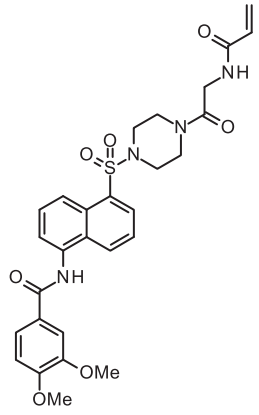

Following general procedure **C - work-up 4** (flash column chromatography solvent: MeOH/CH_2Cl_2 5:95), the compound **36** was obtained as a white foam. **Molecular Formula**: $C_{28}H_{30}N_4O_7S$; **MW**: 566.62 g/mol; **Yield**: 80%; **^{1}H NMR** (400 MHz, DMSO-d_6) δ 3.07-3.20 (m, 4H, 2 x $CH_{2piperazine}$), 3.44-3.56 (m, 4H, 2 x $CH_{2piperazine}$), 3.86 (s, 6H, 2 x OCH_3), 3.99 (d, J = 5.4 Hz, 2H, CH_2), 5.57 (dd, J = 10.2, 2.1 Hz, 1H, CH_2= cis), 6.05 (dd, J = 17.1, 2.1 Hz, 1H, CH_2= trans), 6.33 (dd, J = 17.1, 10.2 Hz, 1H, CH=), 7.13 (d, J = 8.6 Hz, 1H, H_{arom}), 7.66-7.84 (m, 5H, H_{arom} + H_{napht}), 8.15-8.25 (m, 2H, NH + H_{napht}), 8.35 (d, J = 8.5 Hz, 1H, H_{napht}), 8.63 (d, J = 8.6 Hz, 1H, H_{napht}), 10.46 (s, 1H, NH); **^{13}C NMR** (101 MHz, DMSO-d_6) δ 167.0 (C=O), 165.7 (C=O), 164.7 (C=O), 151.9 (C), 148.4 (C), 135.2 (C), 132.3 (C), 131.5 (CH), 130.6 (C), 130.5 (CH), 130.3 (CH), 128.9 (C), 128.1 (CH), 126.2 (C), 125.5 (CH_2=), 125.4 (CH), 124.6 (CH), 122.9 (CH), 121.3 (CH), 111.1 (CH), 111.0 (CH), 55.7 (CH_3), 55.6 (CH_3), 45.5 (CH_2), 45.4 (CH_2), 43.8 (CH_2), 41.0 (CH_2), 40.4 (CH_2); **HRMS (ESI)**: calcd for $C_{28}H_{31}N_4O_7S$ $[M+H]^+$, 567.1908; found, 567.1889.

***Tert*-butyl _N_-({1-[5-(3,4-Dimethoxybenzoylamino)naphthalene-1-sulfonyl]piperidin-4-ylcarbamoyl}methyl)carbamate (42)**

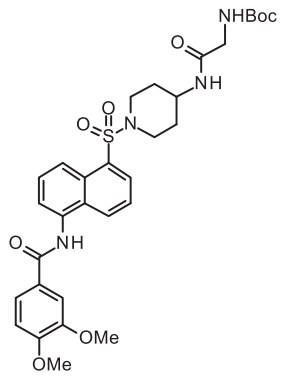

Following general procedure **F** (DIPEA (2.2 eq); acid (1.1 eq), the compound **42** was obtained as a white solid. **Molecular Formula**: $C_{31}H_{38}N_4O_8S$; **MW**: 626.72 g/mol; **Yield**: 66%; **^{1}H NMR** (300 MHz, DMSO-*d_6*) δ 1.35 (s, 9H, 3 x CH_3), 1.64-1.84 (m, 2H, $CH_{2piperidine}$), 1.70-1.82 (m, 2H, $CH_{2piperidine}$), 2.80-2.97 (m, 2H, $CH_{2piperidine}$), 3.44 (d, J = 5.7 Hz, 2H, CH_2), 3.53-3.73 (m, 3H, $CH_{piperidine}$ + $CH_{2piperidine}$), 3.86 (s, 6H, 2 x OCH_3), 6.81 (t, J = 5.7 Hz, 1H, NH), 7.13 (d, J = 8.5 Hz, 1H, H_{arom}), 7.61-7.85 (m, 6H, H_{napht} + H_{arom} + NH), 8.19 (d, J = 7.0 Hz, 1H, H_{napht}), 8.31 (d, J = 8.3 Hz, 1H, H_{napht}), 8.55 (d, J = 8.5 Hz, 1H, H_{napht}), 10.44 (s, 1H, NH); **LRMS (ESI)**: *m/z* 627.2 $[M+H]^+$.

N-({1-[5-(3,4-Dimethoxybenzoylamino)naphthalene-1-sulfonyl]piperidin-4-ylcarbamoyl}methyl)ammonium trifluoroacetate salt (43)

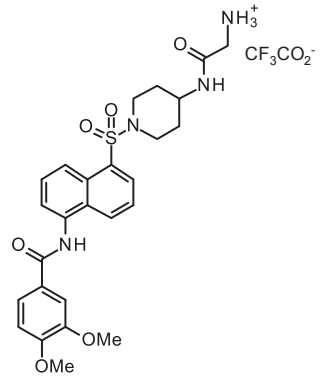

Following general procedure **B**, the compound **43** was obtained as a white solid. **Molecular Formula**: $C_{28}H_{31}F_3N_4O_8S$; **MW**: 640.63 g/mol; **Yield**: 92%; **^{1}H NMR** (300 MHz, DMSO-*d_6*) δ 1.42-1.60 (m, 2H, $CH_{2piperidine}$), 1.74-2.00 (m, 2H, $CH_{2piperidine}$), 2.84-3.04 (m, 2H, $CH_{2piperidine}$), 3.37-3.51 (m, 2H, CH_2), 3.57-3.81 (m, 3H, $CH_{piperidine}$ + $CH_{2piperidine}$), 3.86 (s, 6H, 2 x OCH_3), 7.13 (d, J = 8.5 Hz, 1H, H_{arom}), 7.62-7.88 (m, 6H, H_{arom} + H_{napht} + NH), 7.88-8.05 (m, 3H, NH_3^+), 8.20 (d, J = 7.0 Hz, 1H, H_{napht}), 8.32 (d, J = 8.2 Hz, 1H, H_{napht}), 8.57 (d, J = 8.9 Hz, 1H, H_{napht}), 10.46 (s, 1H, NH).

N-(5-{4-[2-(acryloylamino)acetylamino]piperidine-1-sulfonyl}naphthalen-1-yl]-3,4-dimethoxybenzamide (37)

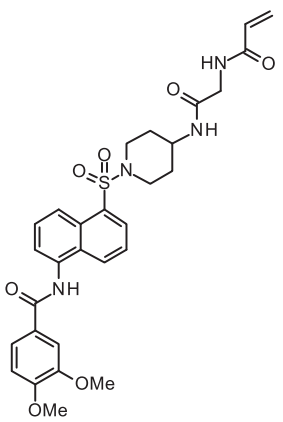

Following general procedure **C - work-up 3** (solvent: DMF (0.1 M); flash column chromatography solvent: MeOH/CH_2Cl_2 5:95), the compound **37** was obtained as a white foam. **Molecular Formula**: $C_{29}H_{32}N_4O_7S$; **MW**: 580.65 g/mol; **Yield**: 50%; **^{1}H NMR** (300 MHz, DMSO-*d_6*) δ 1.29-1.49 (m, 2H, $CH_{2piperidine}$), 1.68-1.88 (m, 2H, $CH_{2piperidine}$), 3.54-3.68 (m, 3H, $CH_{piperidine}$ + $CH_{2piperidine}$), 3.71 (d, J = 5.7 Hz, 2H, CH_2), 3.86 (s, 6H, 2 x OCH_3), 5.59 (dd, J = 10.0, 2.2 Hz, 1H, CH_2= cis), 6.06 (dd, J = 17.1, 2.2 Hz, 1H, CH_2= trans), 6.29 (dd, J = 17.1, 10.0 Hz, 1H, CH=), 7.13 (d, J = 8.5 Hz, 1H, H_{arom}), 7.60-7.84 (m, 5H, H_{arom} + H_{napht}), 7.93 (d, J = 7.3 Hz, 1H, NH), 8.20 (d, J = 7.0 Hz, 1H, H_{napht}), 8.26 (t, J = 5.7 Hz, 1H, NH), 8.31 (d, J

= 8.6 Hz, 1H, H_{napht}), 8.56 (d, J = 8.5 Hz, 1H, H_{napht}), 10.44 (s, 1H, NH); **^{13}C NMR** (101 MHz, DMSO-*d_6*) δ 168.0 (C=O), 165.8 (C=O), 164.8 (C=O), 151.8 (C), 148.4 (C), 135.1 (C), 133.5 (C), 131.6 (CH), 130.6 (C), 130.0 (CH), 129.9 (CH), 128.8 (C), 127.8 (CH), 126.2 (C), 125.4 (CH_2=), 125.3 (CH_2), 124.6 (CH), 122.9 (CH), 121.3 (CH), 111.1 (CH), 111.0 (CH), 55.7 (CH_3), 55.6 (CH_3), 44.9 (CH), 44.0 (2 x CH_2), 41.9 (CH_2), 31.0 (2 x CH_2); **HRMS (ESI)**: calcd for $C_{29}H_{33}N_4O_7S$ $[M+H]^+$, 581.2064; found, 581.2050.

N-(5-{4-[3-(Dimethylamino)propanoylamino]piperidine-1-sulfonyl}naphthalen-1-yl)-3,4-dimethoxybenzamide (45)

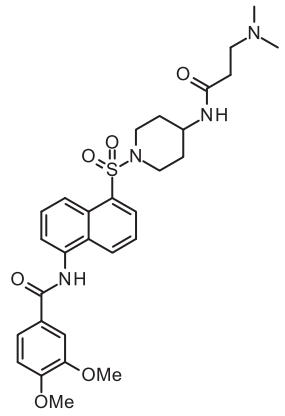

Following general procedure **F**, the compound **45** was obtained as a white solid. **Molecular Formula**: $C_{29}H_{36}N_4O_6S$; **MW**: 568.68 g/mol; **Yield**: 55%; **Mp**: 119-120ºC (washing EtOH); **^{1}H NMR** (300 MHz, DMSO-*d_6*) δ 1.26-1.44 (m, 2H, $CH_{2piperidine}$), 1.70-1.84 (m, 2H, $CH_{2piperidine}$), 2.06 (s, 6H, 2 x CH_3), 2.15 (t, J = 7.3 Hz, 2H, CH_2), 2.43 (t, J = 7.3 Hz, 2H, CH_2), 2.82-2.97 (m, 2H, $CH_{2piperidine}$), 3.52-3.73 (m, 3H, $CH_{piperidine}$ + $CH_{2piperidine}$), 3.86 (s, 6H, 2 x OCH_3), 7.13 (d, J = 8.6 Hz, 1H, H_{arom}), 7.63-7.82 (m, 5 H, H_{napht} + H_{arom}), 7.90 (d, J = 7.4 Hz, 1H, NH), 8.20 (dd, J = 1.0, 7.3 Hz, 1H, H_{napht}), 8.31 (d, J = 8.4 Hz, 1H, H_{napht}), 8.55 (d, J = 8.3 Hz, 1H, H_{napht}), 10.44 (s, 1H, NH); **^{13}C NMR** (101 MHz, DMSO-*d_6*) δ 170.2 (C=O), 165.6 (C=O), 151.8 (C), 148.4 (C), 135.1 (C), 133.5 (C), 130.5 (C), 130.0 (CH), 129.9 (CH), 128.8 (C), 127.8 (CH), 126.2 (C), 125.2 (CH), 124.6 (CH), 122.9 (CH), 121.3 (CH), 111.1 (CH), 111.0 (CH), 55.7 (CH_3), 55.6 (CH_3), 55.1 (CH_2), 44.7 (2 x CH_3), 44.4 (CH), 43.9 (2 x CH_2), 33.5 (CH_2), 31.0 (2 x CH_2); **HRMS (ESI)**: calcd for $C_{29}H_{37}N_4O_6S$ $[M+H]^+$, 569.2428; found, 569.2412.

N-(2-{4-[5-(dimethylamino)naphthalene-1-sulfonyl]piperazin-1-yl}-2-oxoethyl)prop-2-enamide (EB1-155)

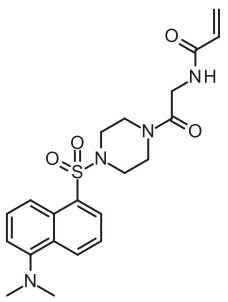

Following general procedure **C-work-up 2** (DIPEA (4 eq); flash column chromatography solvent: EtOAc), the resultant product was precipitated from EtOH to give **EB1-155** as a yellow solid. **Molecular Formula**: $C_{21}H_{26}N_4O_4S$; **MW**: 430.53 g/mol; **Yield**: 45%; **Mp**: 183-185ºC (EtOH), lit. 185-186°C;[118] **^{1}H NMR** (300 MHz, $CDCl_3$) δ 2.88 (s, 6H, 2 x CH_3), 3.16-3.26 (m, 4H, 2 x $CH_{2piperazine}$), 3.42-3.51 (m, 2H, $CH_{2piperazine}$), 3.64-3.72 (m, 2H, $CH_{2piperazine}$), 4.05 (d, J = 4.1 Hz, 2H, CH_2), 5.65 (dd, J = 10.1, 1.6 Hz, 1H, CH_2= cis), 6.13 (dd, J = 17.1, 10.1 Hz, 1H, CH=), 6.27 (dd, J = 17.1, 1.6 Hz, 1H, CH_2= trans), 6.56 (br s, 1H, NH), 7.20 (d, J = 7.0 Hz, 1H, H_{napht}), 7.55 (t, J = 8.0 Hz, 2H, H_{napht}), 8.21 (d, J = 7.4 Hz, 1H, H_{napht}), 8.35 (d, J = 8.8 Hz, 1H, H_{napht}), 8.59 (d,

J = 8.5 Hz, 1H, H_{napht}); **HRMS (ESI)**: calcd for $C_{21}H_{27}N_4O_4S$ $[M+H]^+$, 431.1748; found, 431.1755.

Biochemistry

A. *Preparation and Solubility of inhibitors*

Inhibitor's mother solution at 10 mM in DMSO was prepared and preserved at -20ºC until use. From this solution different concentrations were prepared in the same buffer as employed in the inhibition assay (TRIS-NaCl buffer, pH 8.0). A maximum of 3% DMSO was employed to increase solubility of inhibitors within the assay conditions.

B. *TG crosslinking activity assay*

10 μM of TG-isoform specific biotinylated peptides[151-154] (pepK5 for TG1; pepT26 for TG2; pepF11 for FXIIIa, pre-activated with thrombin; and, pepY25 for TG6) were added to a spermine-coupled 96-well microplate in a 0.1 mL solution containing 40 mM TRIS buffer (pH 8.0), 140 mM NaCl, 5 mM dithiothreitol (DTT), 30 mM $CaCl_2$ and a 0.05% Pluronic F-127 (v/v), were incubated in the presence of the inhibitor/vehicle and the desired TG isoform for 30 min. Microplates were washed three times with a TBS-0.1% Tween-20. Subsequently, 100 μL of Streptavidin-labeled peroxidase (HRP) was added and plates were incubated for 15 min at 37ºC. Then, the microtitterplates were washed three times with TBS-0.1% Tween-20. To visualize TG activity, 100 μL of a 100 mM sodium acetate (pH 6.0) containing 0.2 mg/mL of 3,3',5,5'-tetramethylbenzidine (TMB) and 0.01% (v/v) H_2O_2 were added to each well. Colour development was stopped by adding 100 μL of 0.5N H_2SO_4. Absorbance was measured at 450 nm.

For inhibition purposes, different concentrations of the desired inhibitors were incubated with the enzyme in the same buffer and conditions as described above for the TG activity assay.

Bibliography - Chapter 2

131. Barf, T.; Kaptein, A. Irreversible protein kinase inhibitors: balancing the benefits and risks. *J. Med. Chem*. **2012**, *55*, 6243-6262.

132. Flanagan, M. E.; Abramite, J. A.; Anderson, D. P.; Aulabaugh, A.; Dahal, U. P.; Gilbert, A. M.; Li, C.; Montgomery, J.; Oppenheimer, S. R.; Ryder, T.; Schuff, B. P.; Uccello, D. P.; Walker ,G. S.; Wu, Y.; Brown, M. F.; Chen, J. M.; Hayward, M. M.; Noe, M. C.; Obach, R. S.; Philippe, L.; Shanmugasundaram, V.; Shapiro, M. J.; Starr, J.; Stroh, J.; Che, Y. Chemical and computational methods for the characterization of covalent reactive groups for the prospective design of irreversible inhibitors. *J. Med. Chem*. **2014**, *57*, 10072-10079.

133. Mah, R.; Thomas, J. R.; Shafer C. M. Drug discovery considerations in the development of covalent inhibitors. *Bioorg. Med Chem. Lett.* **2014**, *24*, 33-39.

134. Jöst, C.; Nitsche, C.; Scholz, T.; Roux, L.; Klein, C. D. Promiscuity and selectivity in covalent enzyme inhibition: a systematic study of electrophilic fragments. *J. Med. Chem*., **2014**, *57*, 7590–7599

135. Krippendorff, B. F.; Neuhaus, R.; Lienau, P.; Reichel, A.; Huisinga, W. Mechanism-based inhibition: deriving K(I) and k(inact) directly from time-dependent IC(50) values. *J. Biomol. Screen*. **2009**, *14*, 913-923.

136. Mei, D.; Yin, Y.; Wu, F.; Cui, J.; Zhou, H.; Sun, G.; Jiang, Y.; Feng, Y. Discovery of potent and selective urea-based ROCK inhibitors: exploring the inhibitor's potency and ROCK2/PKA selectivity by 3D-QSAR, molecular docking and molecular dynamics simulations. *Bioorg. Med. Chem*. **2015**, *23*, 2505-2517.

137. Cui, H.; Kamal, Z.; Ai, T.; Xu, Y.; More, S. S.; Wilson, D. J.; Chen, L. Discovery of potent and selective Sirtuin 2 (SIRT2) inhibitors using a fragment-based approach. *J. Med. Med*. **2014**, *57*, 8340-8357.

138. Karki, R.; Song, C.; Kadayat, T. M.; Magar, T. B.; Bist, G.; Shrestha, A.; Na, Y.; Kwon, Y.; Lee, E. S. Topoisomerase I and II inhibitory activity, cytotoxicity, and structure–activity relationship study of dihydroxylated 2,6-diphenyl-4-aryl pyridines. *Bioorg. Med. Chem*. **2015**, *23*, 3638-3654.

139. Wang, F.; Yang, Z.; Liu, Y.; Ma, L.; Wu, Y.; He, L.; Shao, M.; Yu, K.; Wu, W.; Pu, Y.; Nie, C.; Chen, L. Synthesis and biological evaluation of diarylthiazole derivatives as antimitotic and antivascular agents with potent antitumor activity. *Bioorg. Med. Chem.* **2015**, *23*, 3337-3350.

140. Jenkins, T. J.; Guan, B.; Dai, M.; Li, G.; Lightburn, T. E.; Huang, S.; Freeze, B. S.; Burdi, D. F.; Jacutin-Porte, S.; Bennett, R.; Chen, W.; Minor, C.; Ghosh, S.;

Blackburn, C.; Gigstad, K. M.; Jones, M.; Kolbeck, R.; Yin, W.; Smith, S.; Cardillo, D.; Ocain, T. D.; Harriman, G. C. Design, synthesis, and evaluation of naphthalene-sulfonamide antagonists of human CCR8. *J. Med. Chem*. **2007**, *50*, 566-584.

141. Flanagan, M. E.; Abramite, J. A.; Anderson, D. P.; Aulabaugh, A.; Dahal, U. P.; Gilbert, A. M.; Li, C.; Montgomery, J.; Oppenheimer, S. R.; Ryder, T.; Schuff, B. P.; Uccello, D. P.; Walker, G. S.; Wu, Y.; Brown, M. F.; Chen, J. M.; Hayward, M. M.; Noe, M. C.; Obach, R. S.; Philippe, L.; Shanmugasundaram, V.; Shapiro, M. J.; Starr, J.; Stroh, J.; Che, Y. Chemical and computational methods for the characterization of covalent reactive groups for the prospective design of irreversible inhibitors. *J. Med. Chem*. **2014**, *57*, 10072-10079.

142. Dahal, U. P.; Obach, R. S.; Gilbert, A. M. Benchmarking in vitro covalent binding burden as a tool to assess potential toxicity caused by nonspecific covalent binding of covalent drugs. *Chem. Res. Toxicol*. **2013**, *26*, 1739-1745.

143. Nakayama, S.; Atsumi, R.; Takakusa, H.; Kobayashi, Y.; Kurihara, A.; Nagai, Y.; Nakai, D.; Okazaki, O. A zone classification system for risk assessment of idiosyncratic drug toxicity using daily dose and covalent binding. *Drug. Metab. Dispos*. **2009**, *37*, 1970-1977.

144. Albert, A. Chemical aspects of selective toxicity. *Nature* **1958**, *182*, 421-422.

145. Stella, V. Pro-drugs: an overview and definition. *ACS Symposium Series*. Pro-drugs as Novel Drug Delivery Systems. **1975**, *14*, 1-115.

146. Byung-Zun Ahn and Dai-Eun Sok. Michael acceptors as a tool for anticancer drug design. *Curr. Pharm. Des.* **1996**, *2*, 247-262.

147. Rooseboom, M.; Commandeur, J. N.; Vermeulen, N. P. Enzyme-catalyzed activation of anticancer prodrugs. *Pharmacol. Rev*. **2004**, *56*, 53-102.

148. Rautio, J.; Kumpulainen, H.; Heimbach, T.; Oliyai, R.; Oh, D.; Järvinen, T.; Savolainen, J. Prodrugs: design and clinical applications. *Nat. Rev. Drug. Discov*. **2008**. *7*, 255-270.

149. Carmi, C.; Galvani, E.; Vacondio, F.; Rivara, S.; Lodola, A.; Russo, S.; Aiello, S.; Bordi, F.; Costantino, G.; Cavazzoni, A.; Alfieri, R. R.; Ardizzoni, A.; Petronini, P. G.; Mor, M. Irreversible inhibition of epidermal growth factor receptor activity by 3-aminopropanamides. *J. Med. Chem*. **2012**, *55*, 2251-2264.

150. Maresso, A. W.; Wu, R.; Kern, J. W.; Zhang, R.; Janik, D.; Missiakas, D. M.; Duban, M. E.; Joachimiak, A.; Schneewind, O. Activation of inhibitors by sortase triggers irreversible modification of the active site. *J. Biol. Chem*. **2007**, *282*, 23129-23139.

151. Fukui, M.; Kuramoto, K.; Yamasaki, R.; Shimizu, Y.; Itoh, M.; Kawamoto, T.; Hitomi, K. Identification of a highly reactive substrate peptide for

transglutaminase 6 and its use in detecting transglutaminase activity in the skin epidermis. *FEBS J.* **2013**, *280*, 1420-1429.

152. Hitomi, K.; Kitamura, M.; Sugimura, Y. Preferred substrate sequences for transglutaminase 2: screening using a phage-displayed peptide library. *Amino Acids* **2009**, *36*, 619-624.

153. Sugimura, Y.; Hosono, M.; Wada, F.; Yoshimura, T.; Maki, M.; Hitomi, K. Screening for the preferred substrate sequence of transglutaminase using a phage-displayed peptide library: identification of peptide substrates for TGASE 2 and Factor XIIIA. *J. Biol. Chem*. **2006**, *281*, 17699-17706.

154. Sugimura, Y.; Hosono, M.; Kitamura, M.; Tsuda, T.; Yamanishi, K.; Maki, M.; Hitomi, K. Identification of preferred substrate sequences for transglutaminase 1-development of a novel peptide that can efficiently detect cross-linking enzyme activity in the skin. *FEBS J*. **2008**, *275*, 5667-5677.

CHAPTER 3

Indole-based TG2 inhibitors

1. Introduction and context of the work

Based on the encouraging results for the naphthalene-based compounds synthesized in Chapter 2, the synthesis of more potent TG2 inhibitors have been investigated. Once at this point, two aspects have to be taken into account:

1) the *N*-[1-(sulfonyl)piperidin-4-yl)acrylamide moiety was observed as a common factor that helped to considerably increase the inhibitory activity of the compounds. This fact can be observed when naphthalenesulfonamide inhibitors bearing other sulfonyl-acrylamide linkers in their warhead moieties, resulting in a decrease in potency (section 4.1, Chapter 2).

2) based on the high activity over TG2 (but also their good selectivity profile over TG1, TG6, and FXIIIa) of the naphthalene-based inhibitors presented in chapter 2 (**Figure 54**), taken compound **23b** as the lead compound (**Figure 54**), a new approach for the synthesis of new TG2 inhibitors was sighted. The central naphthalene ring for the naphthalene derivatives will be replaced with the aim of improving the activity over TG2 of the new series of compounds, but also their solubility for the biological assays.

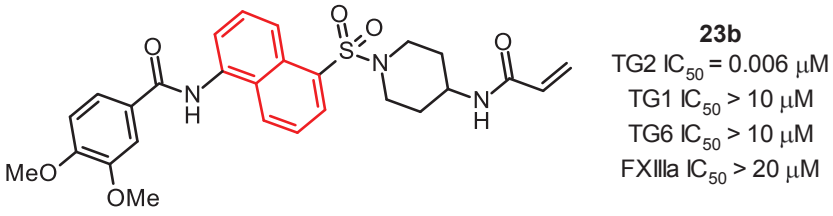

Figure 54. Structure of **23b**, its potency (IC_{50}) over TG2 and its selectivity profile

As it is shown in **Figure 55**, for the new series of TG2 inhibitors, naphthalene was replaced by an indole core. Furthermore, different substitutions at the different positions around the indole were carried out (R_1 and R_2). In addition, piperidineacrylamide and sulfonyl moieties will be preserved within the structures of the compounds herein synthesized

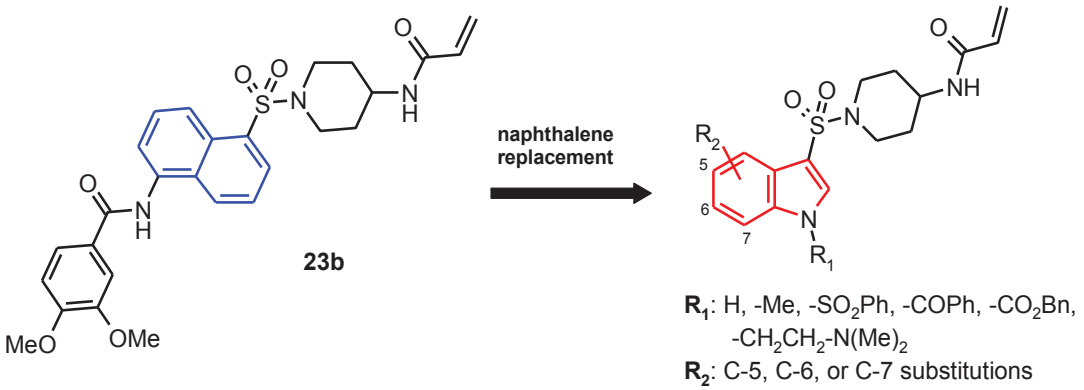

Figure 55. Structure of inhibitor **23b**, and the general structure for the new synthesized indolesulfonamides inhibitors presented in this Chapter. R_1, represents different substitutions on indole nitrogen; and R_2, represents different substitutions from C-5 to C-7 position around the indole

Indoles are probably the most widely distributed heterocyclic compounds in nature having medicinal importance:

1) it takes part on the structure of natural biomolecules like the amino acid tryptophan. (**Figure 56**)

2) indole derivatives isolated from natural sources have been considered good bioactive compounds.[155-158] One of the natural indole derivatives, indole-3-carbinol (see **Figure 56**), found in certain vegetables included in human's diet, has been demonstrated to be beneficial against certain cancers.[159,160]

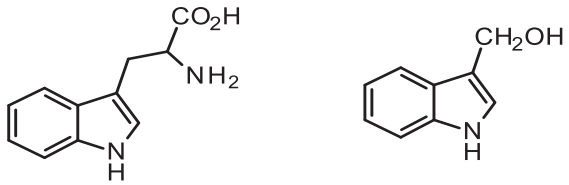

tryptophan indole-3-carbinol

Figure 56. Structure of the natural occurring indolic compounds tryptophan and indole-3-carbinol

3) but also, indole has been widely used as classical scaffold in the development of drugs to treat pathologies such as cancer,[161] AIDS (inhibition of the HIV-1 non-nucleoside reverse retrotranscriptase),…..[162,163]

In this race to synthesize new drugs, indoles have attracted a great deal of attention amongst the scientific community due to their therapeutic uses. With the same main objectives as the last chapter (the synthesis of new, potent and selective inhibitory compounds against TG2), in the next sections the work done for the synthesis of the new indole-3-sulfonamide TG2 inhibitory compounds and their SAR studies will be described.

2. *N*-substituted or not indolesulfonamide derivatives

A series of indolesulfonamide compounds with substituted or not nitrogen atom was first synthesized. This was performed to observe the effect of different substituents at the *N*-1 position of the indole with respect to compounds' activity. The general structure from the compounds synthesized is shown in **Figure 57**, where it can be observed that the *N*-position from the indole underwent alkylation (R = -Me, $-(CH_2)_2-N(Me)_2$), sulfonylation (R = $-SO_2Ph$), acylation (R = -COPh, $-CO_2Bn$), and also was left intact without been substituted (R = H).

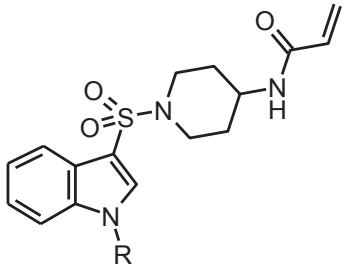

R = H, Me, SO_2Ph, COPh, CO_2Bn, $-(CH_2)_2-N(Me)_2$

Figure 57. General structure of the indolesulfonamide TG2 inhibitors synthesized in this section, and the different substituents introduced at *N*-1 position (R)

2.1. Synthesis of 1-(benzenesulfonyl)indole derivative 47 and 1*H*-indole derivative 48

The strategy for the synthesis of the non substituted indolesulfonamide **48** started from the synthesis of 1-(benzenesulfonyl)indole **51** represented on **Scheme 38**. Starting from the commercially available indole a two-step reaction was carried out in order to protect its nitrogen. Firstly, a deprotonation step using NaH in DMF at 0ºC for 30 minutes, followed by the reaction of the *N*-anion indole with benzene sulfonyl chloride at room temperature, provided **49** in 40% yield.[164] A next chlorosulfonation step was carried out based on the method employed by Janosik et al.[165] Thus, the *N*-protected indole was made to react with chlorosulfonic acid in acetonitrile at 0ºC, then the reaction was left to reach at room temperature, obtaining the resulting sulfonyl chloride **50** in 74% yield. Then, the reaction between sulfonyl chloride **50** and 4-(*N*-Boc-amino)piperidine gave sulfonamide **51** in 81% yield. Deprotection of **51** yielded ammonium salt **52** in quantitative yield. Then, the subsequent acylation of **52** with acryloyl chloride in the presence of the Hünig's base (DIPEA), provided the 1-(benzenesulfonyl)indole derivative **47** in 92% yield. Finally, the SO_2Ph group deprotection was carried out in the presence of $LiOH.H_2O$ to provide 1*H*-indolesulfonamide **48** in 78% yield.

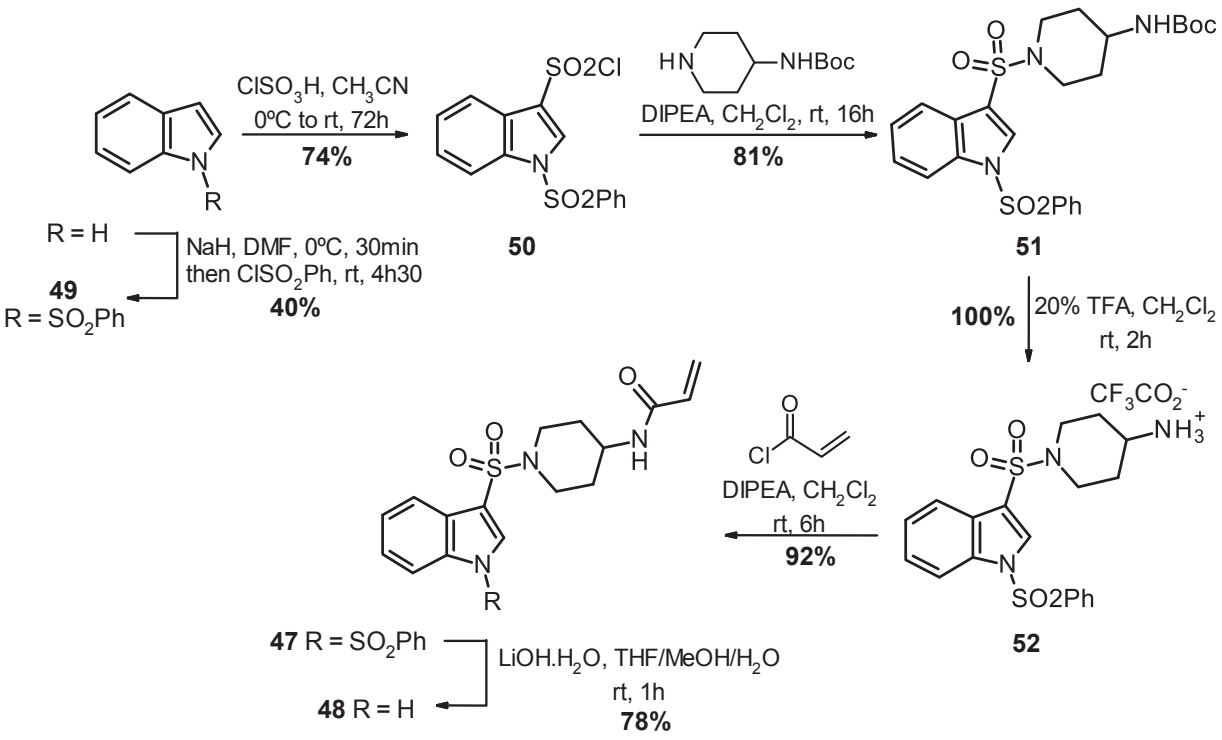

Scheme 38. Synthesis of inhibitors **47** and **48**

2.2. TG transamidation inhibition of 47 and 48

As it shown in **Table 19**, the potencies of indoles **47** and **48** were studied. It should be noticed that the 1*H*-indole **48** is over 2-fold more potent than 1-(benzenesulfonyl)indole **86**. This better potency of **48** compared with compound **47**, can be explained by the fact that benzenesulfonyl is a more bulky moiety, thus being not tolerable at that position within the TG2 active site, or possibly by the fact that the NH group of the indole could form any favorable hydrogen interactions within the active site. As also reported in **Table 19**, both compounds present a good selectivity profile over TG1, TG6 and FXIIIa.

IC_{50} (μM)	TG2	TG1	TG6	FXIIIa
47	0.711 ± 0.003*	> 100	> 50	> 100
48	0.31	> 20	NT	> 20

*Values accompanied by standard deviation were averaged from at least two independent experiments; they were otherwise obtained in a single determination. NT = not tested.

Table 19. TG2 inhibition and TG selectivity of **47** and **48**

2.3. Different *N*-substituted indole inhibitors

2.3.1. Synthesis of the different *N*-substituted indole derivatives 53a-d

For these derivatives, taking the 1-(benzenesulfonyl)indole derivative **51** as the starting material, the obtaining of the key intermediate1*H*-indole **54** was necessary for the synthesis of the different target derivatives **53a-d**. The compound **51** underwent a desulfonylation in the presence of $LiOH.H_2O$ giving the 1*H*-indole **54** in 84% yield (**Scheme 39**).

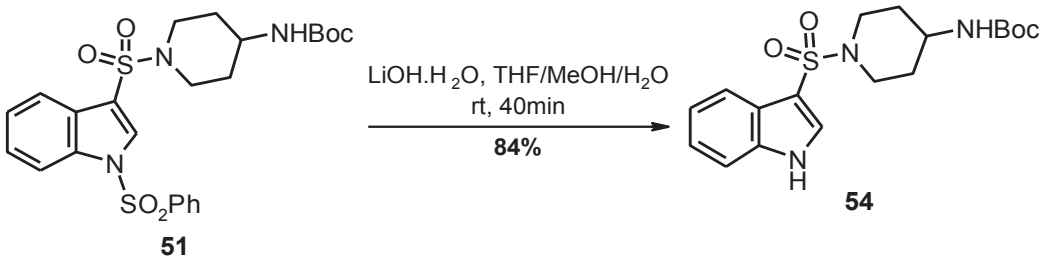

Scheme 39. Synthesis of the 1-(benzenesulfonyl)indole derivative **54**

From **54**, a three step synthesis was carried out in order to obtain the next set of *N*-protected indolesulfonamides (**Scheme 40**). Starting from derivative **54**, different *N*-substitutions, previous deprotonation with NaH in DMF at 0ºC, were performed by reacting with benzyl chloroformate, iodomethane, 2-chloro-*N*,*N*-(dimethyl)ethylamine hydrochloride, or benzoyl chloride in the presence of the Hünig's base, providing the *N*-substituted indoles **55a-d**. Then, deprotection of the *tert*-butoxycarbonyl in TFA provided the different ammonium salts **56a-d**, followed by acylation with acryloyl chloride in the presence of DIPEA to obtain the final compounds **53a-d**. The yields for each of the three steps are shown in **Table 20**. In spite of the low yield obtained for the *N*-Cbz protection of indole **54** (27%), the reaction has not been optimized at this stage of the research.

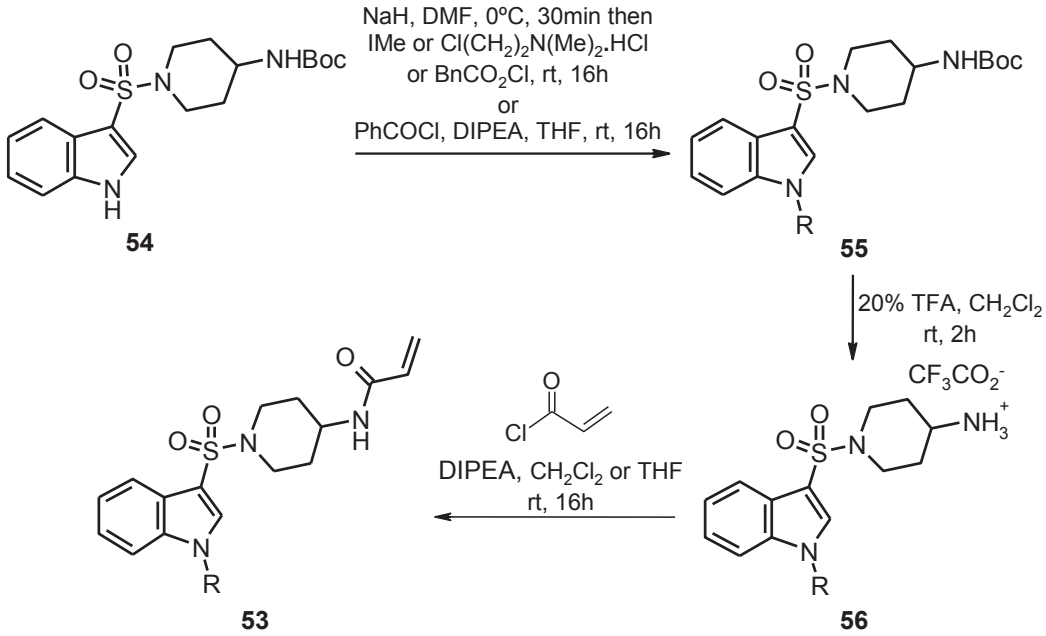

Scheme 40. General synthesis of *N*-substituted inhibitors **53a-d**

R	**55** - Yield (%)	**56** - Yield (%)	**53** - Yield (%)
Me	**55a -** 85	**56a -** 89	**53a -** 59
$(CH_2)_2N(Me)_2$	**55b -** 83	**56b -** 100	**53b-** 52
Cbz	**55c -** 27	**56c -** 93	**53c -** 71
PhCO	**55d -** 100	**56d -** 100	**53d -** 61

Table 20. Isolated yields (%) for compounds **53**, **55** and **56**

2.3.2. TG transamidation inhibition of 53a-d

As it shown in **Table 21**, indole inhibitors with different substituents at the *N*-position were studied. It should be noticed that the Cbz bulky moiety and the methyl group for compounds **53c** and **53a** were the most potent of this serie of derivatives with IC_{50} values of 0.133 and 0.165 μM, respectively. On the contrary, when other bulky groups were introduced (benzenesulfonyl, benzoyl), IC_{50} values decreased up to 5 -fold and 2 -fold for compounds **47** and **53d**, respectively, compared to that of **53c**. This fact highlights the probable importance of the rotable benzyl in the Cbz structure from compound **53c**. Furthermore, lenghthening the alkyl chain with a dimethylethane moiety lead to an almost 2-fold loss of activity when compared to the *N*-methylated derivative **55a**. It can also be highlighted that **53a** is twice potent than the 1*H*-indole inhibitor **48.** Knowing the almost equipotencies observed for compounds **53a** and **53c**, and the fact that the *N*-methylated indole **53a** is more soluble within the biological assays than indole **53c**, the next set of derivatives are will be carried out on a *N*-methylated indolic scaffold.

IC_{50} (μM)	R	TG2	TG1	TG6	FXIIIa
53a	Me	0.165 ± 0.055*	> 50	> 50	> 50
53b	$(CH_2)_2N(Me)_2$	0.315 ± 0.025*	> 50	> 50	> 50
53c	CBz	0.133	> 50	> 50	> 50
53d	PhCO	0.301 ± 0.012*	> 50	> 50	> 50

*Values accompanied by standard deviation were averaged from at least two independent experiments; they were otherwise obtained in a single determination.

Table 21. TG2 inhibition and TG selectivity of **53a-d**

3. Introduction of a benzamide group at C-5, C-6 or C-7 position on indole

In this section, different indole inhibitors with a benzamide group introduced at C-5, C-6, and C-7 positions on indole were investigated (**Figure 58**). In this case, benzamide was the selected substituent owing to the good inhibition results obtained by the 5-(arylamido)naphthalene derivatives **23a-s** synthesized in chapter 2 (Section 8.5; table 12, page **X**). Therefore, in the present section, the synthesis of 5-, 6-, and 7-(benzoylamino)-1-methylindole derivatives, and its activity over TG2 (as well as other TG isoforms), will be described.

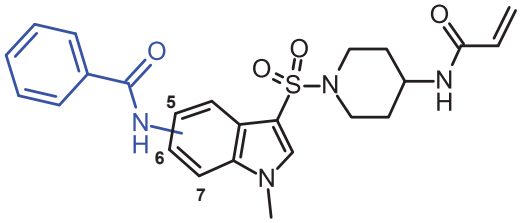

Figure 58. General structure of the 5-,6-, and 7-(benzoylamido)-1-methylindole inhibitors synthesized

3.1. Synthesis of the 5-(benzoylamino)-1-methylindole derivative 57

For the synthesis of 5-(benzoylamino)indole **57**, obtention of the 5-amino derivative **58** was the first objective for the first step of the synthesis (**Scheme 41**). Firstly, starting from the commercially available 5-nitroindole, deprotonation of the amine with NaH in DMF at 0ºC for 30 minutes, followed by treatment with iodomethane provided the 1-methylindole **59** in quantitative yield. Further chlorosulfonation in two steps, sulfonation with the $DMF.SO_3^-$ complex in CH_2Cl_2 at room temperature for 75 minutes followed by chlorination with thionyl chloride at reflux conditions furnished sulfonyl chloride **60**. The $DMF.SO_3^-$ complex was selected this time to be employed as the sulfonating agent, instead of the chlorosulfonic acid, in oder to carry out the reaction under less acidic conditions. After sulfonamide formation in the presence of the 4-(*N*-Boc-amino)piperidine and DIPEA, reduction of the nitro group from compound **61** with iron powder in an ammonium chloride solution was carried out in order to provide amine **58** in 86% yield.

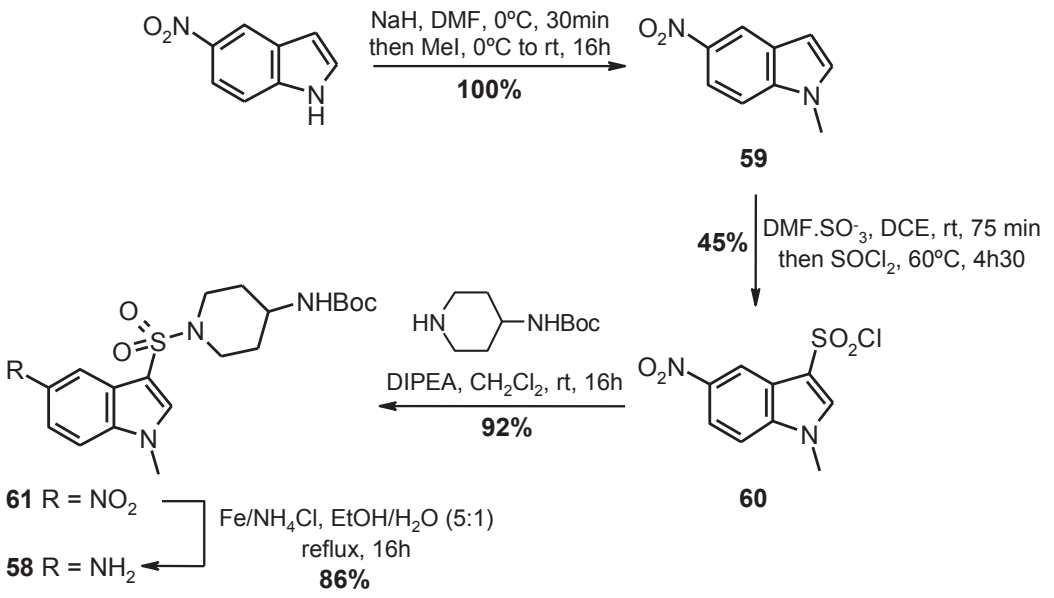

Scheme 41. Synthesis of the 5-amino derivative **58**

Then, as shown in **Scheme 42**, coupling of the amine **58** with benzoyl chloride in CH_2Cl_2 and in the presence of DIPEA furnished benzamide **62** in 76% yield. Then, Boc hydrolysis in acid conditions (TFA), followed by acylation with acryloyl chloride gave the final indole **57** in 33% yield. In spite of the low yield obtained for the acylation reaction to give the final benzamide **57** from the ammonium salt **63**, the reaction was not optimized. The global yield for this 7 step synthesis was 10%.

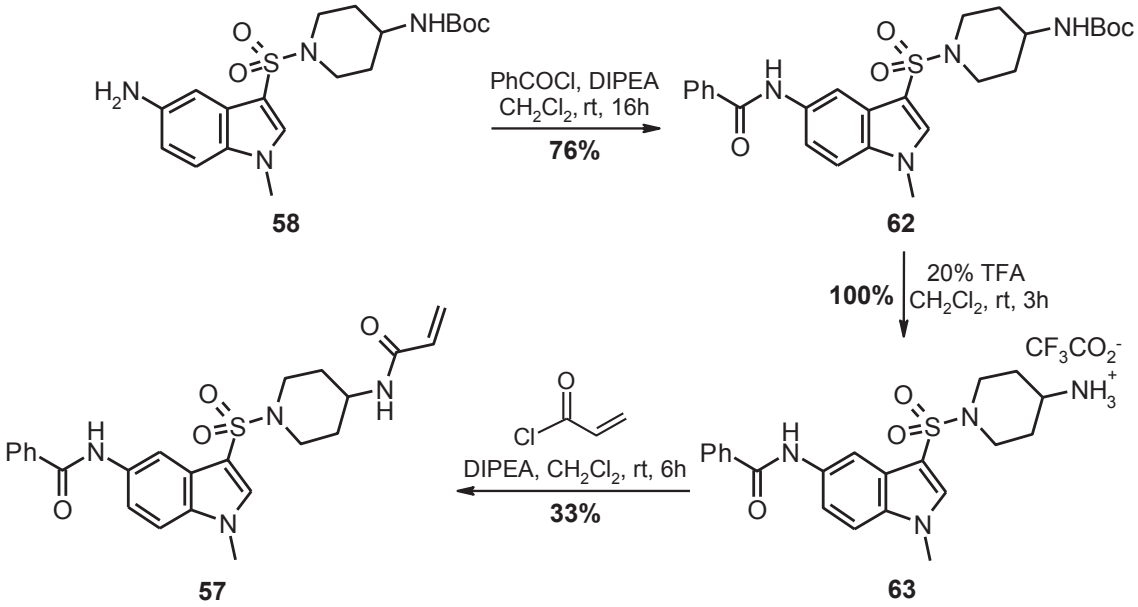

Scheme 42. Synthesis of the 5-(benzoylamino)-1-methylindole inhibitor **57**

3.2. Synthesis of the 6-(benzoylamino)-1-methylindole derivative 64

The synthesis of the 6-(benzoylamino) derivative **64**, was carried out with the intention to compare its TG2 inhibitory activity with the already synthesized 5-(benzoylamino)-1-methylindole **57**, both bearing the same benzamide substituents. Firstly, on the effort to

produce amine **65,** and starting from the commercially available 6-nitroindole, the same synthetic procedure used for the obtaining of aniline **58** (*N*-alkylation, chlorosulfonation, sulfonylation, and nitro group reduction) was employed (**Scheme 43**).

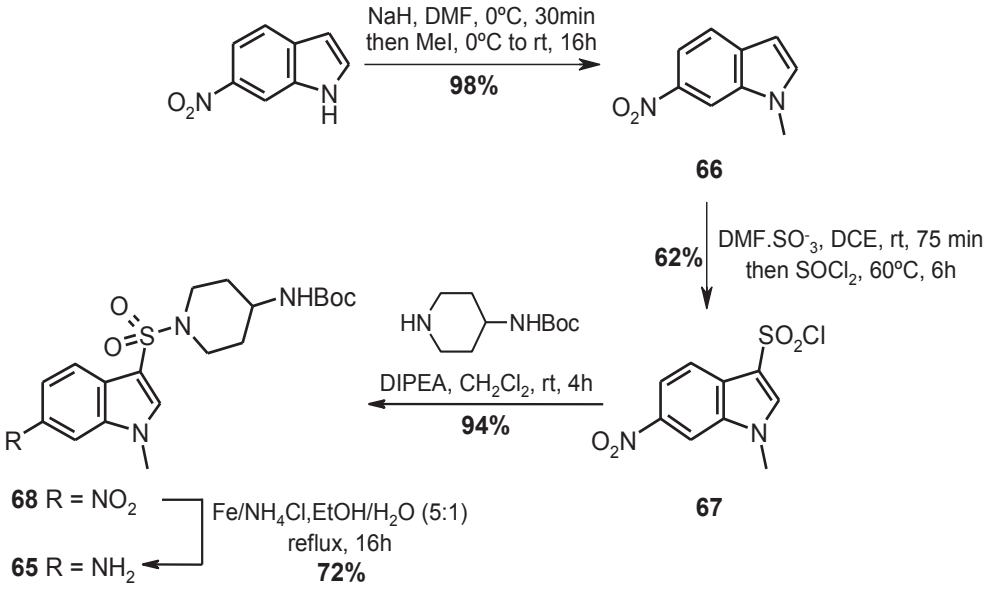

Scheme 43. Synthesis of the 6-amino derivative **65**

From amine **65**, the synthesis of the final compound **64**, as it can be observed in **Scheme 44**, follows the same amine acylation, Boc hydrolysis and acrylamide formation steps as shown previously in **Scheme 42** for the obtaining of **57**. The global yield for the obtaining of the target compound **64** is 21% (7 steps).

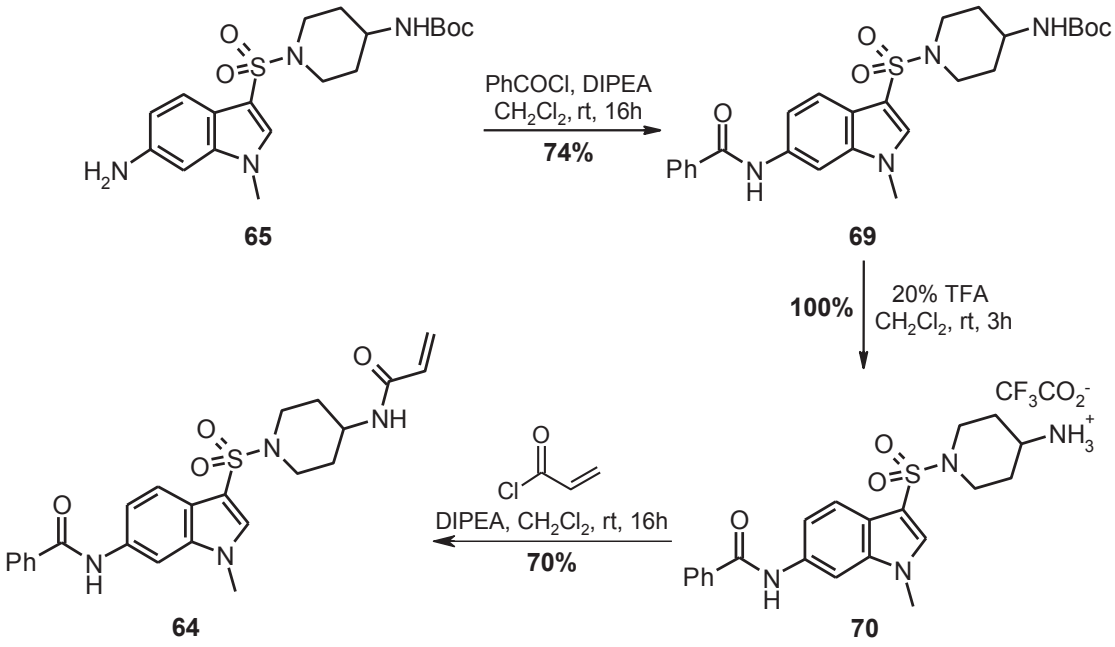

Scheme 44. Synthesis of the 6-(benzoylamino)-1-methylindole inhibitor **64**

3.3. Synthesis of the 7-(benzoylamino)-1-methylindole derivative 71

As it was done for the synthesis of the 5- and 6-(benzoylamino) derivatives **57** and **64**, the same synthesis strategy for the obtaining of the 7-(benzoylamino) derivative **71** was employed. Furthermore, as also described for the first two derivatives **57** and **64**, the obtaining of the key amine intermediate **72** was also performed. Results and conditions for the synthesis of amine **72**, starting from the commercially available 7-nitroindole, are reported in **Scheme 45**.

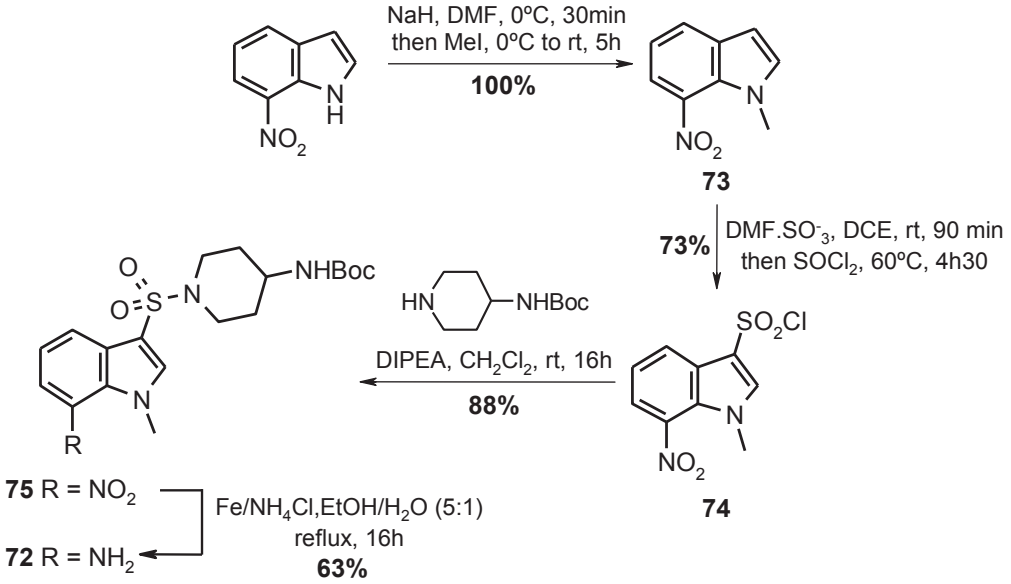

Scheme 45. Synthesis of the 7-amino derivative **72**

In **Scheme 46** the results for the 3 steps followed to obtain the final 7-(benzoylamino)-1-methylindole **71** from amine **72** are presented. The desired indole **71** was obtained from the 7-nitroindole in a global yield of 22% (7 steps).

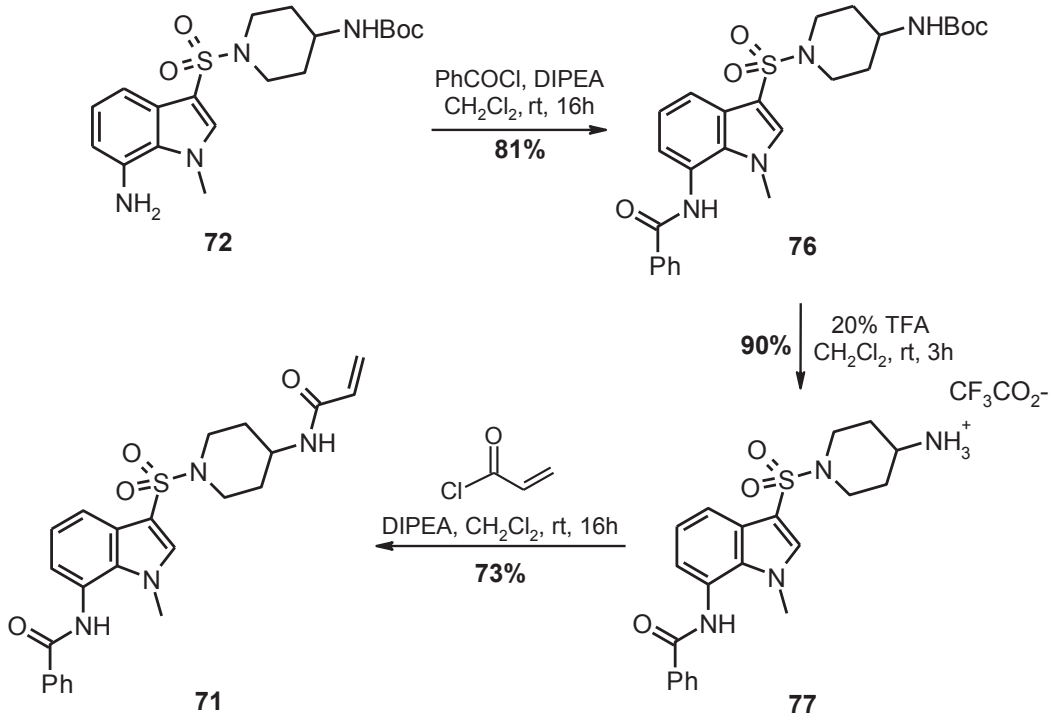

Scheme 46. Synthesis of the 7-(benzoylamino)-1-methylindole inhibitor **71**

3.4. TG transamidation inhibition of 57, 64 and 71

The different benzamides substituted at position C-5, C-6, and C-7 for indolesulfonamides **57**, **64** and **71** were next investigated. As it is shown in **Table 22** benzamide at C-7 position on indole (**71**) resulted in best potencies over TG2 (IC_{50} = 0.092 μM), with potencies of more than 5-times and 28-times regarding benzamide substituted at C-6 (**64**) and C-5 (**57**) positions on indole, respectively. Furthermore, indolesulfonamide **71** also presented a good selectivity profile, with IC_{50} values of > 20, and 20 μM over TG1 and TG6 respectively.

IC_{50} (μM)	Position	TG2	TG1	TG6
57	C-5	0.497	> 20	> 20
64	C-6	0.092 ± 0.001*	> 10	20
71	C-7	0.014 ± 0.001*	> 20	20

*Values accompanied by standard deviation were averaged from at least two independent experiments; they were otherwise obtained in a single determination. NT = not tested.

Table 22. TG2 inhibition and TG selectivity of indolesulfonamides **57**, **64** and **71**

4. Introduction of different amides at C-7 position

Based on the good inhibition results of the substituted benzamide at C-7 position of **71**, the synthesis of a variety of different indole derivatives substituted at the C-7 position in the indole were carried out (**Figure 59**). These derivatives include in their structure at the **R2** position different substituted phenyl groups a more bulky moiety (e.g., adamantane), but also a 3,4-dimethoxybenzyl, and a methyl 3-phenylpropanoate at that position. It can also be observed in **Figure 59** that indole was *N*-methylated (**R1** = Me) (this is the case for the majority of the compounds synthesized here), but also a non *N*-substituted indole (**R1** = H) was synthesized. This 1*H*-indole derivative was synthesized in order to check if indole can form any hydrogen bond with its -NH group that could improve the inhibitory activity of the compounds over TG2.

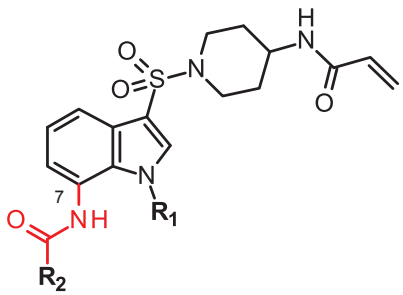

R1 = H, Me
R2 = Ph, 4-MeOPh, 4-ClPh, 3-ClPh, 3-MeOPh, 3,4-diMeOPh, 3-O_2NPh, naphth-2-yl, quinolin-2-yl, adamantan-1-yl, 3,4-diMeOBn, pyridin-3-yl

Figure 59. General structure of the 7-(arylamido)indole TG2 inhibitors from this section, and the different substitutions introduced at R_1 and R_2. R_1, represents a methylation or an Hydrogne at N-1 position; and **R2**, represent the different aryl substituents introduced for the obtaining of the different arylamides

4.1. Synthesis of compounds 78a-k

The synthesis of the final *N*-methylated indoles **78a-k** was performed by means of the same three synthesis step strategy as carried out for the obtaining of the final 1-methylindole **71** (**Scheme 46**). As it can be observed in **Scheme 47,** starting from the already synthesized amine **72**, the same synthesis approach was carried out to give the different final indole derivatives. Firstly, the acylation of the amine **72** with the corresponding acyl chlorides in the presence of DIPEA yielded the different amides **79a-k**, followed by the *N*-Boc deprotection in acid conditions (20% TFA in CH_2Cl_2) furnished the corresponding ammonium salts **80a-k**. Finally, the acylation of the corresponding ammonium salts with acryloyl chloride provided the final *N*-methylated indolesulfonamides **78a-k**. The yields for each of these three synthesis steps are reported in **Table 23**.

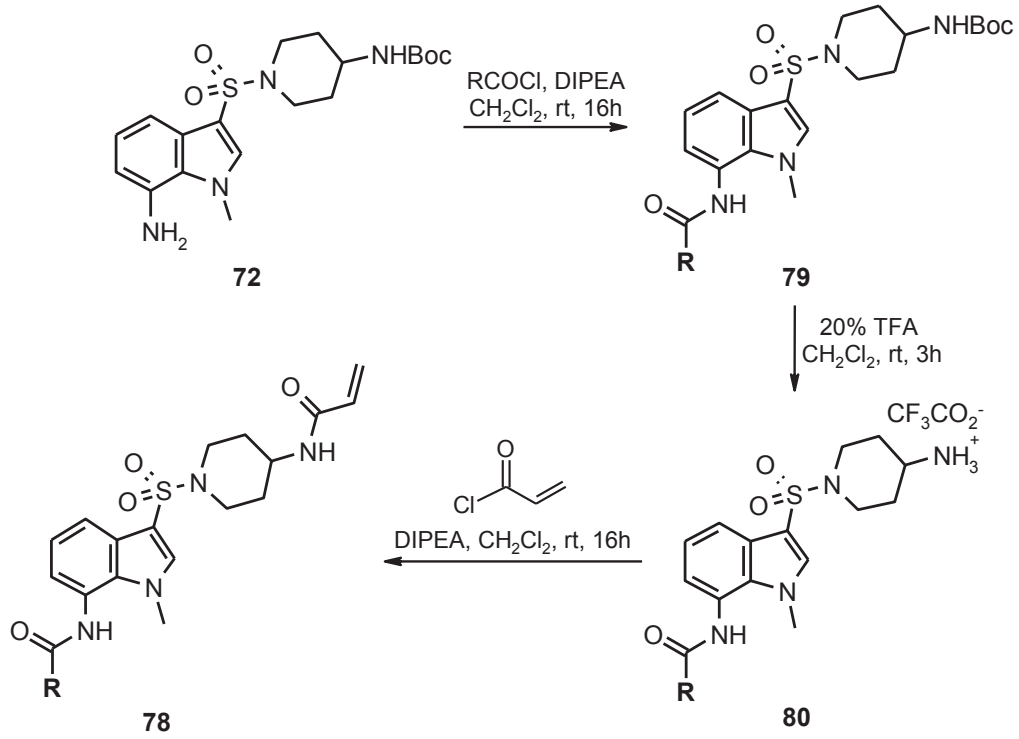

Scheme 47. General synthesis of inhibitors **78a-k**

R	**79** - Yield (%)	**80** - Yield (%)	**78** - Yield (%)
3-MeOPh	**79a -** 77	**80a -** 100	**78a -** 75
3-ClPh	**79b -** 62	**80b -** 97	**78b -** 63
3-O_2NPh	**79c -** 98	**80c -** 100	**78c -** 57
4-MeOPh	**79d -** 67	**80d -** 97	**78d -** 63
4-ClPh	**79e -** 53	**80e -** 93	**78e -** 87
3,4-diMeOPh	**79f -** 88	**80f -** 100	**78f -** 68
3,4-diMeOBn	**79g -** 48	**80g -**100	**78g -** 60
pyridin-3-yl	**79h -** 42	**80h -** 100	**78h -** 43
naphth-2-yl	**79i -** 78	**80i -** 100	**78i -**75
quinolin-2-yl	**79j -** 81	**80j -**100	**78j -** 53
adamantan-1-yl	**79k -** 83	**80k -** 100	**78k -** 65

Table 23. Isolated yields (%) for compounds **78** to **80**

4.2. Synthesis of the 7-(3,4,-dimethoxybenzamido)-1*H*-indole derivative 81

As commented previously, at the beginning of Section 4, a non *N*-methylated indolesulfonamide was also synthesized. The 3,4-dimethoxybenzamide substituent was selected to be compared with the *N*-methyl derivative **78f** in terms of inhibitory activity against TG2. Starting from the commercially available 7-nitroindole, chlorosulfonylation with chlorosulfonic acid in acetonitrile furnished sulfonyl chloride **82** in 80% yield. Then, amine sulfonylation with the 4-(*N*-Boc-amino)piperidine provided nitro compound **83** in 80% yield, followed by the nitro group reduction with iron and NH_4Cl in EtOH/H_2O (5:1) solution for 16h at reflux conditions provided amine **84** in 50% yield (**Scheme 48**).

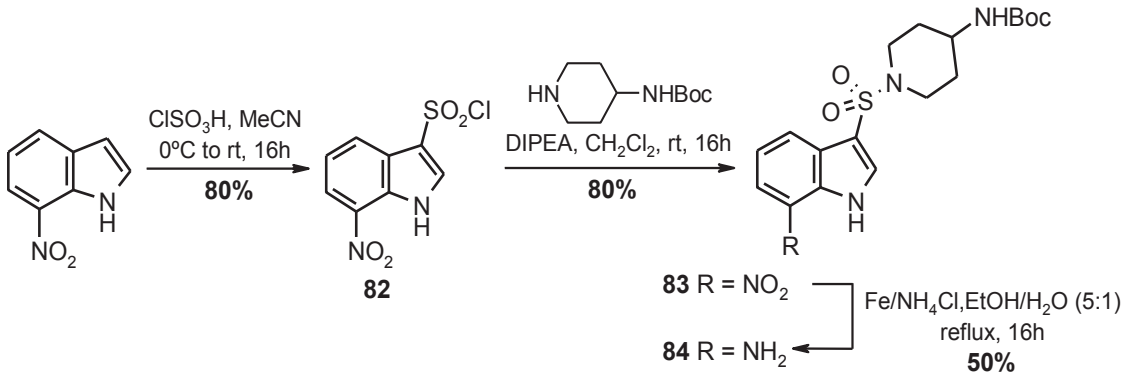

Scheme 48. Synthesis of the 7-amino derivative **84**

From amine **84**, as shown in **Scheme 49**, following the next steps of amine acylation (53%), *N*-Boc deprotection (87%) and acrylation (40%), the final indolesulfonamide **81** was obtained. The global yield for the synthesis of the final indolesulfonamide **81** was 6% (6 steps). As observed in **Scheme 49**, the low yield observed for the obtaining of compounds **85** and **81** (53% and 40% respectively), can be explained by the additional reaction of the NH of both indole starting materials (**84** and **86)** with the corresponding acyl chorides. Although, these possibly formed indole products were not neither isolated nor characterized, and the reaction was not optimized.

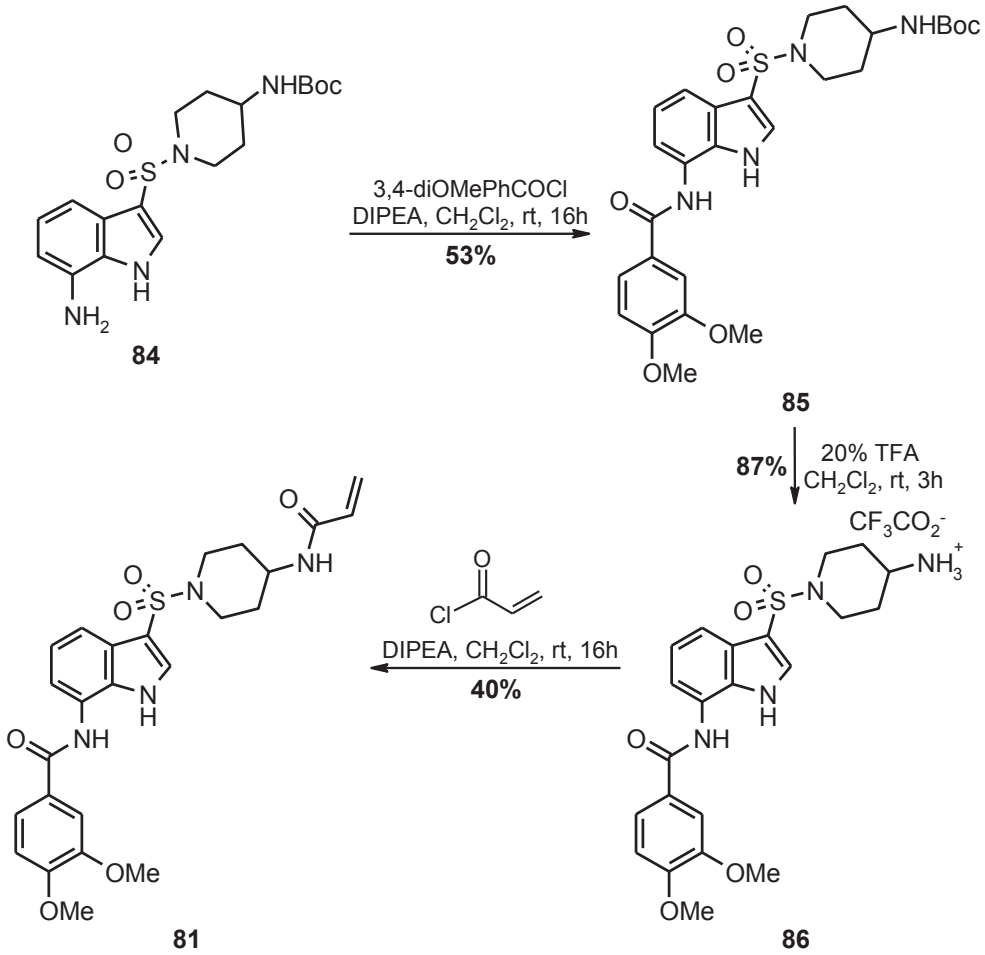

Scheme 49. Synthesis of inhibitor **81**

4.3. TG transamidation inhibition of 78a-k and 81

Structure activity relationship studies for the different 7-(arylamido) derivatives **78a-k**, and **81** are reported in **Table 24**. As it can be observed, compounds bearing a mono o di-substituted benzamides (**78a-f**) improved their potencies against TG2 compared to the non-substituted benzamide (**71**). In addition, Substituted benzamide at *meta* position (**78a-c**) resulted in better potencies than the substituted at *para* position (**78d**, **78e**), up to 52-fold more active against TG2. Moreover, compounds bearing electron withdrawing groups at *meta* position such as chlorine (**78b**), and nitro group (**78c**) resulted in better activities than the electron donating group methoxy (**78a**, **78f**). To compare with the more active compound from the naphthalenesulfonamide serie from **Chapter 2**, compound **23b** (TG2 IC_{50} = 0.006 μM), bearing the same 3,4-diMeOPh moiety, compound **78f** was over 2-fold more active bearing the indolic core. Moreover, the introduction of more bulky substituents such as naphthyl bearing compound **78i** increased drastically the activity of the compound reaching an IC_{50} value bellow 2 nM over TG2 (65% inhibition at 2 nM). In an attempt to do more soluble compounds with a protonable amine in aqueous solution, the 3-pyridyl **78h** was proved no to be so potent as the naphthyl-, the 3-O_2NPh, and 3-ClPh derivatives, compounds **78i**, **78c** and **78b** respectively, with an IC_{50} of 0.015 μM. On the other hand, when an additional

methylene was present, the 3,4-dimethoxybenzyl derivative **78g** resulted in a loss of 17-fold in activity compared to compound **78f**. Free rotation of the sp^3 carbon introduced has therefore not a favorable impact on activity. When nitrogen is free resulting in the 1*H*-indolesulfonamide **81**, a loss of potency of 2.3-fold relative to its 3,4-dimethoxyphenyl *N*-methylated analog **78f** was observed. In terms of selectivity, all newly produced indolesulfonamides have potencies of more than 10 μM over TG1, TG6, and FXIIIa, with the exception of indolesulfonamides **78b-e**, with IC_{50} values for TG6 of 10 μM, < 10 μM (65% inhibition at 10 μM), < 10 μM (56% inhibition at 10 μM), and < 10 μM (60% inhibition at 10 μM), respectively.

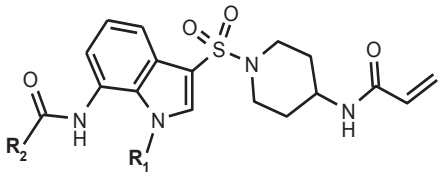

IC_{50} (μM)	R_1	R_2	TG2	TG1	TG6	FXIIIa
71	CH_3	Ph	0.014 ± 0.001*	> 20	20	NT
78a	CH_3	3-MeOPh	0.005	> 10	> 10	> 10
78b	CH_3	3-ClPh	0.002	> 10	10	> 10
78c	CH_3	3-O_2NPh	0.002	> 10	< 10 (65% inhib.)**	> 10
78d	CH_3	4-MeOPh	0.012	> 10	< 10 (56% inhib.)**	> 10
78e	CH_3	4-ClPh	0.009	> 10	< 10 (60% inhib.)**	> 10
78f	CH_3	3,4-diMeOPh	0.0027	> 10	> 10	> 10
78g	CH_3	3,4-diMeOBn	0.044	NT	NT	> 10
78h	CH_3	pyridin-3-yl	0.016	> 10	> 10	NT
78i	CH_3	naphth-2-yl	0.0017	NT	NT	> 10
78j	CH_3	quinolin-2-yl	0.018	NT	NT	> 10
78k	CH_3	adamantan-1-yl	0.042	NT	NT	> 10
81	H	3,4-diMeOPh	0.042	> 10	10	> 10

*Values accompanied by standard deviation were averaged from at least two independent experiments; they were otherwise obtained in a single determination. NT = not tested. **Inhibition at 10 μM.

Table 24. TG2 inhibition and TG selectivity of **78a-k** and **81**

5. Synthesis of different 1-methylindolesulfonamides 87a-d with an inverted amide at the C-7 position

As it can be observed in **Figure 60**, a change in orientation of the amide moiety at the C-7 position on indole was carried out. In order to be compared with compounds **78f, 78g** and **78i**, this amide inversion was performed to know if it is advantageous for the compounds' inhibitory activity over TG2 (but also keeping the good selectivity profile over other TG isoforms tested previously).

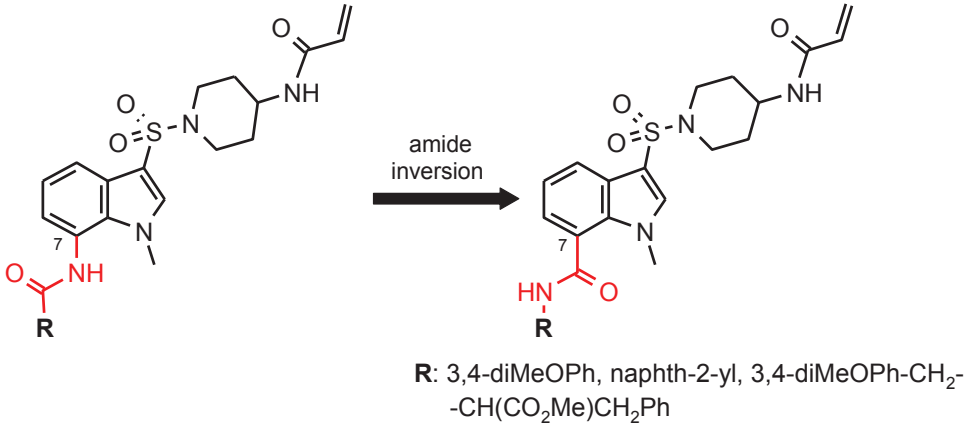

Figure 60. Representation of the amide inversion at C-7 position on indole, the general structure of the compounds synthesized in this section, and the different substituents introduced at R

5.1. Synthesis of 7-substituted inverted amide indoles 87a-d

For the obtaining of derivatives with the inverted amide, different approaches were visualized. The first temptatives to invert the amide are shown in **Scheme 50**. First of all, the synthesis of the methyl ester **88** was performed. This was carried out starting from the commercially available methyl 1*H*-indole-7-carboxylate which underwent methylation by treating it with MeI in DMF to give indole **89** in 100% yield, followed by chlorosulfonation to provide the sulfonyl chloride **90** in 54% yield. Then, subsequent sulfonamide formation with the the 4-(*N*-Boc-amino)piperidine, in the presence of the Hünig's base, furnished sulfonamide **88** in 86% yield.

From compound **88**, and as a first attempt to obtain directly the inverted amide compound, compound **91a** was firstly tried to be synthesized. The ester group from compound **88** was tried to condensate with a big excess of 3,4-dimethoxyaniline in the presence of Me_3Al following the method from Joseph et al.[166] Since condensation failed, the next temptative was the saponification of the ester from compound **88** to subsequently undergone a chlorination to form the desired acyl chloride, which could be coupled to the 3,4-dimethoxyaniline to form the desired inverted amide **91a**.

Saponification of the ester **88** in the presence of $LiOH.H_2O$ in THF/EtOH/H_2O (1.5:1:1) furnished the acid **92** in 96% yield. However, in the next steps, the formation of the desired acyl chloride failed by using oxalyl chloride in DMF as catalyst, since the Boc protecting group was hydrolyzed in acidic conditions (HCl released). These results did

not allow the use of an acyl chloride to further acylate via coupling with the corresponding amines. In conclusion, a different way to address the efforts in the formation of the inverted amide was required.

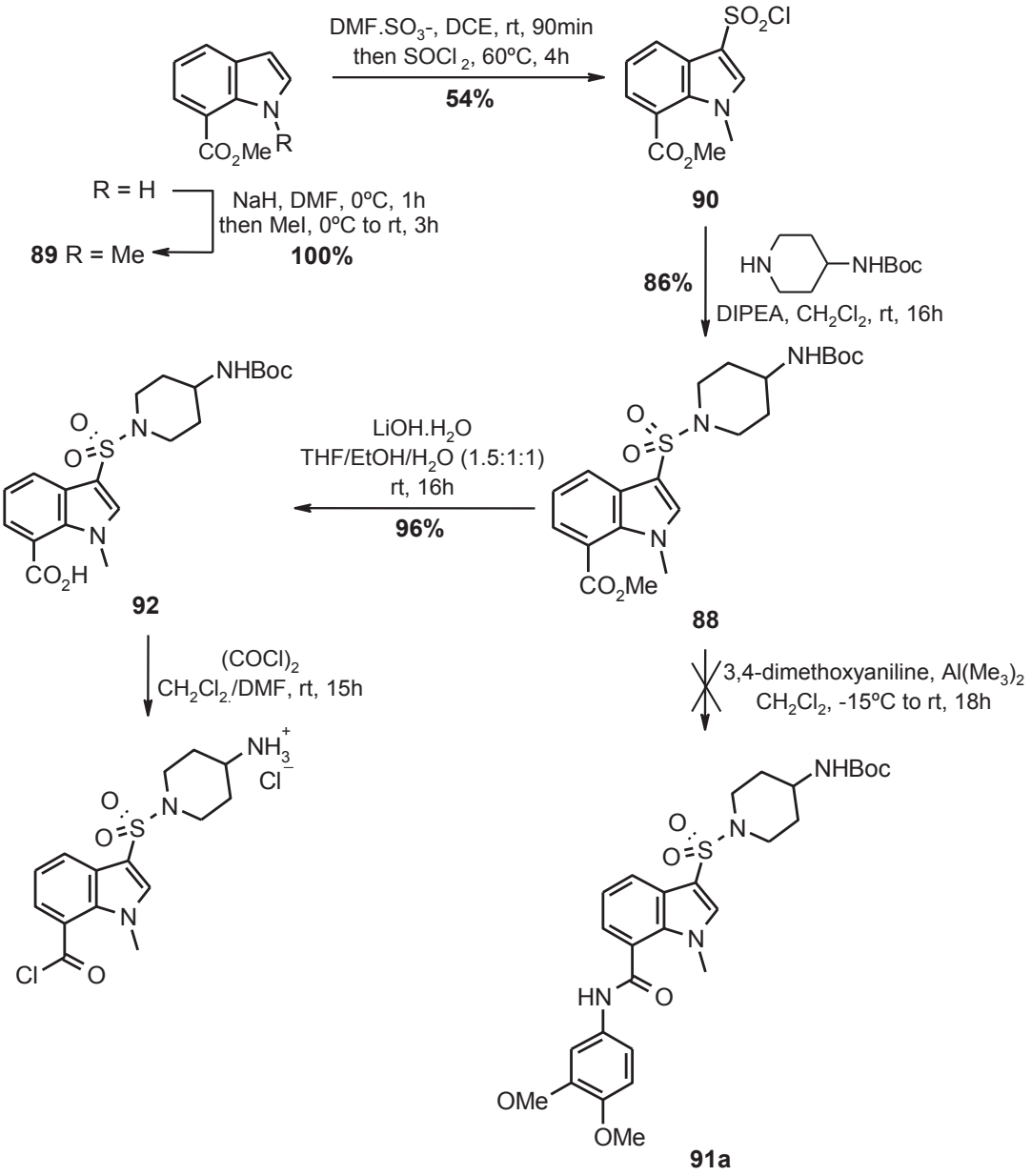

Scheme 50. Representation of the first approach followed for the synthesis of compound **91a**

A different approach to obtain compounds in which the orientation of the amide is inverted, is presented in **Scheme 51**. After saponification of the methyl ester **88**, the acid **92** was coupled to the corresponding amines (3,4-dimethoxyaniline, 3,4-dimethoxybenzylamine, (S)-phenylalanine methyl ester hydrochloride and 2-naphthylamine) in the presence of EDCI and the coupling agent HOBt providing the desired amides **91a-d** (whose orientation has been inverted). Then, the acid deprotection of the amine (20% TFA) followed by the acylation with acryloyl chloride yielded final

indolesulfonamides **87a-d**. The yields for the obtaining of each of the different compounds for the obtaining of final indoles **87a-d** are presented in **Table 25**.

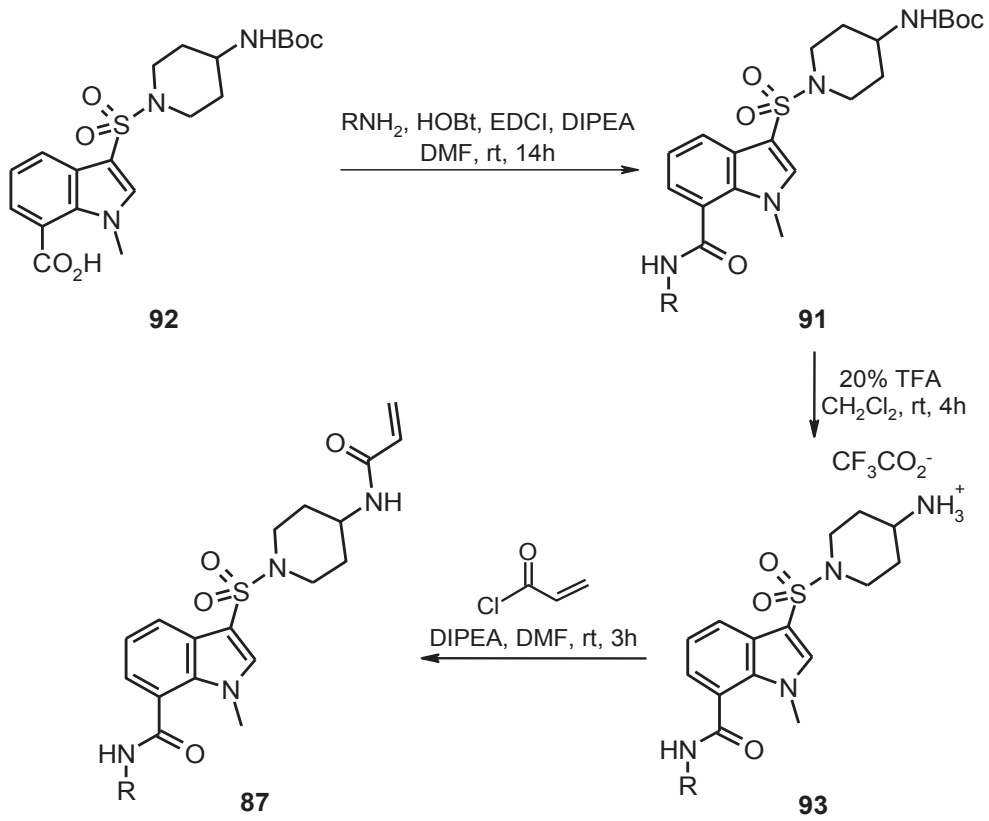

Scheme 51. General synthesis of inhibitors **87a-d**

R	**91** - Yield (%)	**93** - Yield (%)	**87** - Yield (%)
3,4-diMeOPh	**91a** - 73	**93a** - 96	**87a** - 67
3,4-diMeOBn	**91b** - 62	**93b** - 100	**87b** - 46
(*S*) $CH(CO_2Me)CH_2Ph$	**91c** - 46	**93c** - 100	**87c** - 61
naphth-2-yl	**91d** - 35	**93d** - 100	**87d** - 52

Table 25. Isolated yields (%) for compounds **87**, **91** and **93**

5.2. TG transamidation inhibition of 87a-d

When the change in orientation of the amide at C-7 position was studied (**Table 26**), none of the inhibitors were so potent as the non-inversed derivatives with the same substituents at C-7 position. The fact that the corresponding non-inverted amide inhibitors of compounds **87a** and **87d** (compounds **78f** and **78i** respectively) (**Table 24**; page 169), have higher potencies could be explained because of the more available carbonyl group of these non-inverted amides, thus allowing it to form easily some

hydrogen bond interactions. The only compound who was almost equipotent regarding its opposite non-inverted amide was the 3,4-MeOBn substituted amide (**87b**) with a little improvement compared to compound **78g**. This could be explained by the free rotation of the sp^3 carbon between the amide group and the substituent 3,4-diMeOPh in both molecules, therefore not having any improvement on their activity. In the case of derivative **87c**, no signs of activity improvement was observed (IC_{50} = 0.040 μM). These compounds presented a good selectivity profile over the different TG tested.

IC_{50} (μM)	R	TG2	TG1	TG6	FXIIIa
78f	/	0.0027	> 10	> 10	> 10
87a	3,4-diMeOPh	0.007	10	< 10 (61.5% inhib.)*	> 10
87b	3,4-diMeOBn	0.034	NT	NT	> 10
87c	(*S*) $CH(CO_2Me)CH_2Ph$	0.040	NT	NT	> 10
87d	naphth-2-yl	0.012	NT	NT	> 50

Values were obtained in a single determination. NT = not tested. *Inhibition at 10 μM.

Table 26. TG2 inhibition and TG selectivity of **78f**, and **87a-d**

6. Modulation of the warhead on 78f

In this section a new series of analogs of compound **78f** were synthesized. As it can be observed in **Figure 61**, two new moieties were introduced within the warhead's structure, a COC≡CH (**94**) and a $COCH_2CH_3$ (**95**) moieties. On one hand, Prop-2-yn-1-one group introduction will be compared with the acryloyl group regarding its reactivity towards the nucleophilic thiol group from TG2 active site. On the other hand, replacement of acryloyl with the propionyl group, will be used as a negative control in the transamidation assays. Propionyl is expected to have low reactivity, what it means, a much higher IC_{50} value compared to its acryloyl analog **78f**.

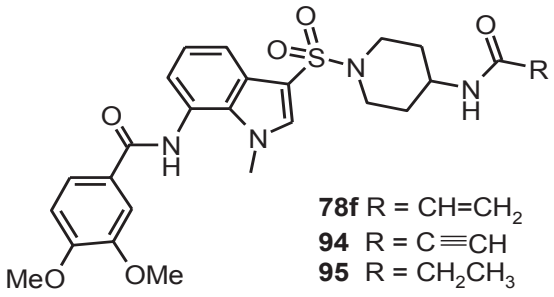

Figure 61. General structure of the analogs of **78f**, compounds **94** and **95**

6.1. Synthesis of 94 and 95

For the synthesis of analogs **94** and **95**, an amide formation, starting from the ammonium salt **80f**, was carried out. As shown in **Scheme 52**, a coupling reaction with propiolic acid provided derivative **94** in 6% yield. On the other hand, amine acylation with propionyl chloride provided derivative **95** in 59% yield. The low yield obtained (6%) for the sythesis of compound **94** can be explained by the low reactivity of the propiolic acid upon the amide formation, observing no complete consumption of the acid by monitoring the reaction by thin layer chromatography. However, the reation has not been optimized.

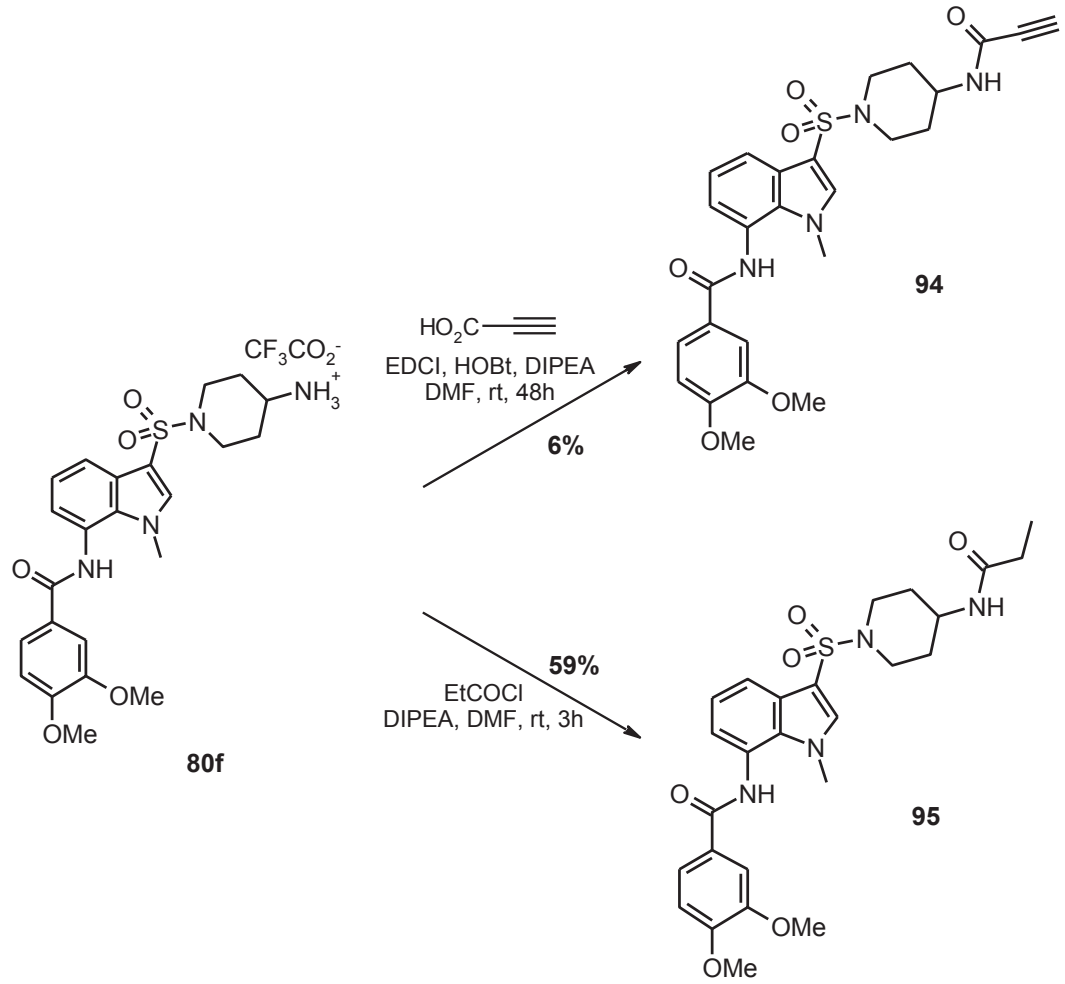

Scheme 52. Synthesis of **94** and **95**

6.2. TG transamidation inhibition of 94 and 95

Regarding the modulations around the warhead moiety, it can be observed in the **Table 27** that propiolamide **94** resulted in a loss of potency of around 172-fold when compared to its acrylamide analog **78f**. This loss of activity of propiolamido analog can be explained by its sp hybridization, this way having a different orientation within the catalytic tunnel of TG2. On the other hand, and as expected, the IC_{50} from the

propionamide analog **95** was superior to 50 μM, explained by a non reaction with the thiol from the active site cysteine of TG2.

IC_{50} (μM)	R	TG2	TG1	TG6	FXIIIa
78f	/	0.0027	> 10	> 10	> 10
94	COC≡CH	0.453	NT	NT	NT
95	$COCH_2CH_3$	> 50	NT	NT	> 300

Values accompanied by standard deviation were averaged from at least two independent experiments; they were otherwise obtained in a single determination. NT = not tested.

Table 27. TG2 inhibition and TG selectivity of **78f**, **94** and **95**

7. Conclusion

In order to improve the activity of the naphthalenesulfonamide **23b** (TG2 IC_{50} = 0.0065 μM), and with the intention of keeping the same good selectivity profile against the other TG isoforms, a wide variety of inhibitors bearing and indole core were successfully synthesized.

Indolesulfonamides substituted at the C-7 position reached the best potencies, with IC_{50} values within the very low nanomolar range for compounds **78b-c**, **78f** (**Table 24**), where *meta*-substituted benzamides and the analog of naphthalenesulfonamide **23b** bearing the 3,4-diMeOPh moiety, were more than twice active over TG2. In the case of compound **78i**, its potency was observed below 2 nM, but with the disadvantage of being the less soluble compound. On the contrary, a change of orientation of the amide was not tolerated, leading to compounds generally less active. This was probably owing to the hydrogen interactions that carbonyl can make inside the active pocket of TG2, being less accessible to favor these interactions in the compounds with the inverted amide (compounds **87a-d**).

To conclude, the objectives from this chapter, which include the development of new potent indole-based TG2 inhibitors, with also presenting a good selectivity profile against the other transglutaminase isoforms, were achieved. As a representative of this chapter, compound **78f,** presenting one of the best activities for TG2 (IC_{50} = 0.0027 μM**),** better selectivity for TG6 than the meta-chloro and meta-nitro derivatives **78b** and **78c** respectively (TG6 IC_{50} > 10 μM) and being a more soluble compound than **78i**, was taken as the lead compound from these new series of indolesulfonamide TG2 inhibitors.

Experimental part - Chapter 3

Organic chemistry synthesis

Generalities

All the reagents, solvents, and conditions employed for the organic synthesis, and characterizations of the compounds described in this chapter, were the same as the ones employed in Chapter 2 (page 112).

General procedures

A. *Indole N-protection*

NaH (1.5 eq) were added to a indole solution (1 eq) in anhydrous DMF (0.281 M) at 0ºC. After 30 minutes in stirring conditions at 0ºC the solution is left to return at room temperature, and benzenesulfonyl chloride, iodomethane, benzyl chloroformate, or 2-chloro-*N*,*N*-dimethylethylamine hydrochloride (1.2 eq) were added. The reaction mixture was left to perform in stirring conditions under argon atmosphere until the starting material was completely consumed (3 to 16 hours). After this time the solvent was evaporated and the crude residue dissolved in CH_2Cl_2 and extracted three times with water, the organic layer washed with saturated aqueous NaCl solution, and dried over Na_2SO_4. Then, the solvent was evaporated and the resulting extracts purified by flash column chromatography (solvent: MeOH in CH_2Cl_2 or PE/EtOAc) to obtain the desired purified product.

B. C-3 *indole chlorosulfonation*

Method 1

To a solution of the indole (1 eq) in anhydrous acetonitrile (0.8 M) was added dropwise chlorosulfonic acid (3 eq) at 0ºC. The solution was allowed to reach room temperature and left to react until completion (from 16 to 72 hours). The resulting mixture was poured into ice/water and extracted three times with chloroform. The combined extracts were washed twice with saturated aqueous $NaHCO_3$ (addition of small amounts of saturated aqueous NaCl solution was sometimes necessary to prevent formation of emulsions), and dried over Na_2SO_4. Removal of the solvent in vacuo gave the final compound.

Method 2

To a $DMF.SO_3^-$ complex (1.2 eq) solution in 1,3-dichloroethane (1M) was added the indole (1 eq) at room temperature. After 90 min thionyl chloride was added (1.2 eq) and the reaction mixture was allowed to perform at 60ºC (reflux) until completion (from 4 to 16 hours). Once the reaction was finished, the solvents were evaporated, and the

resultant crude material precipitated (solvent: CH_2Cl_2) and washed with the same solvent to afford the final sulfonyl chloride.

C. *Indole N-*SO_2Ph *deprotection*

To a solution of the *N*-SO_2Ph-protected indole (1 eq) in THF (0.19 M) at room temperature was added MeOH (0.19 M) and H_2O (0.19 M), followed by the addition of $LiOH.H_2O$ (5 eq). The reaction was left to perform at 0ºC to completion (from 40 to 60 minutes). After this time the solvent was evaporated, the crude material dissolved in CH_2Cl_2 and extracted four times with water, to finally being dried over Na_2SO_4. After evaporation of the solvent, the crude material was crystallized from EtOH and filtered to afford the desired 1*H*-indole. The almost pure solid was also purified by flash column chromatography (solvent: MeOH in CH_2Cl_2) to afford the final 1*H*-indole.

D. *Ester saponification*

To a solution of ester (1 eq), in THF/EtOH/H_2O (1.5:1.0:1.0, 0.072 M) solution was added $LiOH.H_2O$ (2.7 eq). The reaction was left to perform to completion at room temperature (16 hours). After this time, the solvents were evaporated and water was added to the crude material. Then the pH was adjusted to 2, and a white precipitate was formed. T he precipitate was filtered and washed with water to give the desired acid. Then, the product was left to dry under vacuum with P_2O_5 until use.

E. *Boc deprotection*

Addition of trifluoroacetic acid (1/5; v/v) to a solution containing the Boc-protected amine bearing compound dissolved in CH_2Cl_2 (4/5; v/v). Then, the reaction was left to proceed for 2 to 4 hours. Solvent and excess TFA were evaporated under vacuum. The resulting dried residue was precipitated from Et_2O, filtrated, and washed with Et_2O. The final acetate salt was then recovered from the filter, and stored under vacuum with P_2O_5 until use.

F. *Sulfonamide formation*

DIPEA (2 eq) was added to a solution of the amine (1 eq) in CH_2Cl_2 (0.1 M), following by the addition of the corresponding sulfonyl chloride (1.1 eq) on ice-water (0ºC). The reaction was left to react under argon atmosphere at room temperature until completion (4 to 16 hours).

Work-up 1: The reaction mixture was filtrated and the precipitate was washed with CH_2Cl_2.

Work-up 2: The reaction mixture was then extracted three times with water, the recovered organic layer washed with saturated NaCl solution, and dried over Na_2SO_4. Then the solvent was evaporated and the resulting crude product was purified by flash column chromatography (solvent: MeOH in CH_2Cl_2), yielding the desired products.

G. *Acrylamide formation*

To a solution of the amine (1 eq) in solvent (THF or CH_2Cl_2 or DMF; 0,1 M) was added DIPEA (2 eq) at room temperature, followed by the addition of the acyl chloride (1.1 eq) on ice-water (0ºC). After returning to room temperature the reaction mixture was allowed to proceed until completion (from 3 to 16 hours) under argon atmosphere.

Work-up 1 *(THF as solvent)*: THF was removed under vacuum and the resulting crude extract dissolved in CH_2Cl_2 and extracted three times with water. The organic layer was washed with saturated aqueous NaCl solution and dried over Na_2SO_4 before evaporating the solvent again under vacuum. The resulting residue was purified by flash column chromatography (solvent: PE/EtOAc or MeOH/CH_2Cl_2) to yield the desired compound.

Work-up 2 *(CH_2Cl_2 as solvent)*: The reaction mixture was diluted in CH_2Cl_2 and extracted three times with water, the organic layer washed once with saturated aqueous NaCl solution, dried over Na_2SO_4, and the solvent concentrated to dryness. The resulting residue was purified using flash column chromatography (solvent: MeOH/CH_2Cl_2 or PE/EtOAc) to yield the desired compound.

Work-up 3*(DMF as solvent)*: Addition of the reaction mixture (dropwise manner) into a flask containing water. Then, the precipitate formed was filtrated, washed with 1N aqueous HCl solution (2 mL), and washed again with water. The resulting solid was dried under vacuum in P_2O_5, to finally being purified by flash column chromatography (solvent: MeOH/CH_2Cl_2) and/or precipitated (solvents: MeOH, EtOH, MeOH/CH_2Cl_2 or Et_2O).

Work-up 4*(CH_2Cl_2 as solvent)*: Once finished, the reaction mixture was filtrated and the formed precipitate was washed with CH_2Cl_2.

Work-up 5 *(CH_2Cl_2 as solvent)*: Once the reaction was finished, the solvent was evaporated under vacuum, and the resulting crude material filtrated and washed with MeOH or EtOH.

Work-up 6 *(DMF as solvent)*: The solvent was evaporated under vacuum, and the resulting dried crude mixture was diluted in CH_2Cl_2, washed three times with water and once with saturated aqueous NaCl solution. The organic fraction was dried over Na_2SO_4 and the solvent concentrated to dryness. The resulting residue was purified by flash column chromatography (solvent: MeOH/CH_2Cl_2) and/or precipitated (solvents: EtOH, MeOH, or Et_2O).

H. *Nitro reduction*

To a solution of the nitro compound (1 eq) in EtOH/H_2O (5:1) was added iron powder (2.5 eq) at room temperature followed by saturated aqueous NH_4Cl solution (1.4 M). Then, the reaction was allowed to reach 80ºC, and allowed to proceed for 16 h.

Work-up 1: Once the reaction was finished the solvents were evaporated. The crude material dissolved in EtOAc, was extracted three times with water, and dried over

Na_2SO_4 to finally being concentrated to dryness. The crude extracts were then precipitated from MeOH.

Work-up 2: After this time, the reaction mixture was then filtrated through a celite pad with EtOH/EtOAc (1/5, v/v), and concentrated to dryness. The filtrated crude material was then diluted in CH_2Cl_2 and extracted three times with water, washed once with saturated aqueous NaCl solution, and dried over Na_2SO_4. After that, the solvent was evaporated, and the crude extracts were purified by flash column chromatography (solvent: MeOH/CH_2Cl_2) or precipitated (solvents: Et_2O or CH_2Cl_2).

I. *Amide formation*

DIPEA (3 eq) was added to a DMF (0.22 M) solution containing the amine (1.1 eq), carboxylic acid (1 eq), EDCI (1.2 eq), and HOBt (1.2 eq) at 0ºC. Then, the reaction was left at room temperature until completion (from 14 to 48 h).

Work-up 1: the reaction mixture was added in a dropwise manner into a flask containing water. Then, the precipitate formed was filtrated, and washed with water. The resulting solid was dried under vacuum in P_2O_5, to finally being purified by flash column chromatography (solvent: MeOH/CH_2Cl_2). The resulting product was precipitated (solvents: MeOH or Et_2O).

Work-up 2: Once the reaction was finished, the solvent was evaporated under vacuum. The resulting dried crude mixture was diluted in CH_2Cl_2, washed three times with water and once with saturated aqueous NaCl solution. The organic fraction was dried over Na_2SO_4 and the solvent concentrated to dryness. The resulting residue was purified by flash column chromatography (solvent: MeOH/CH_2Cl_2), and the resultant product precipitated from MeOH.

1-(Benzenesulfonyl)indole (49), CAS 40899-71-6

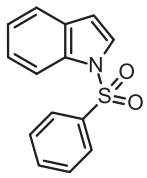

Following general procedure **A** (sulfonyl chloride (1.35 eq), flash column chromatography (solvent: PE/EtOAc 1:1), the resultant solid was precipitated from EtOH to give **49** as a white solid. **Molecular Formula**: $C_{14}H_{11}NO_2S$; **MW**: 257.31 g/mol; **Yield**: 40%; **Mp**: 74-76ºC (EtOH), lit. 75-78°C;[164] **^{1}H NMR** (300 MHz, DMSO-d_6) δ 6.85 (dd, J = 3.7, 0.8 Hz, 1H, H_{indole}), 7.25 (td, J = 7.5, 1.0 Hz, 1H, H_{indole}), 7.35 (td, J = 7.2, 1.1 Hz, 1H, H_{indole}), 7.55-7.64 (m, 3H, H_{indole} + H_{arom}), 7.69 (tt, J = 7.3, 1.7 Hz, 1H, H_{arom}), 7.81 (d, J = 3.7 Hz, 1H, H_{indole}), 7.91-8.01 (m, 3H, H_{indole} + H_{arom}).

1-(Benzenesulfonyl)indole-3-sulfonyl chloride (50), CAS 535930-73-5

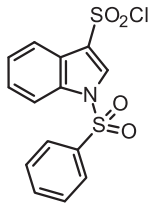

Following general procedure **B - method 1**, the compound **50** was obtained as a white solid. **Molecular Formula**: $C_{14}H_{10}ClNO_4S_2$; **MW**:

355.82 g/mol; **Yield**: 74%; **Mp**: 144-146°C, lit. 144-145°C;[165] **^{1}H NMR** (300 MHz, DMSO-d_6) δ 7.28 (td, J = 7.5, 1.0 Hz, 1H, H_{indole}), 7.36 (td, J = 7.6, 1.3 Hz, 1H, H_{indole}), 7.57-7.66 (m, 3H, H_{indole} + H_{arom}), 7.71 (tt, J = 7.4, 1.7 Hz, 1H, H_{arom}), 7.76 (d, J = 7.1 Hz, 1H, H_{indole}), 7.92 (d, J = 8.2 Hz, 1H, H_{indole}), 8.03 (d, J = 7.7 Hz, 2H, H_{arom}).

Tert-butyl _N_-{1-[1-(Benzenesulfonyl)indole-3-sulfonyl]piperidin-4-yl}carbamate (51)

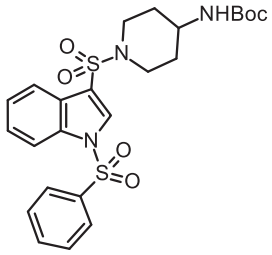

Following general procedure **F - *work-up 2*** (DIPEA (1.5 eq); flash chromatography solvent: MeOH/CH_2Cl_2 1:99), the compound **51** was obtained as a white solid. **Molecular Formula**: $C_{24}H_{29}N_3O_6S_2$; **MW**: 519.63 g/mol; **Yield**: 81%; **Mp**: 165-166°C; **^{1}H NMR** (300 MHz, DMSO-d_6) δ 1.34 (s, 9H, 3 x CH_3), 1.37-1.46 (m, 2H, $CH_{2piperidine}$), 1.67-1.81 (m, 2H, $CH_{2piperidine}$), 2.52-2.60 (m, 2H, $CH_{2piperidine}$), 3.12-3.28 (m, 1H, $CH_{piperidine}$), 3.47-3.60 (m, 2H, $CH_{2piperidine}$), 6.83 (d, J = 7.3 Hz, 1H, NH), 7.41 (td, J = 7.6, 0.9 Hz, 1H, H_{indole}), 7.50 (td, J = 7.5, 1.3 Hz, 1H, H_{indole}), 7.66 (t, J = 7.6 Hz, 2H, H_{arom}), 7.76 (tt, J = 7.4, 1.7 Hz, 1H, H_{arom}), 7.81 (d, J = 7.9 Hz, 1H, H_{indole}), 8.03 (d, J = 8.2 Hz, 1H, H_{indole}), 8.18 (d, J = 7.2 Hz, 2H, H_{arom}), 8.35 (s, 1H, H_{indole}); **LRMS (ESI)**: *m/z* 520.2 $[M+H]^+$.

_N_-{1-[1-(Benzenesulfonyl)indole-3-sulfonyl]piperidin-4-yl}ammonium trifluoroacetate salt (52)

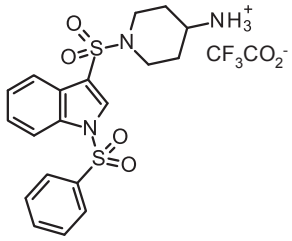

Following general procedure **E**, the compound **52** was obtained as a white solid. **Molecular Formula**: $C_{21}H_{22}F_3N_3O_6S_2$; **MW**: 553.54 g/mol; **Yield**: 100%; **Mp**: 113-116°C (washing Et_2O); **^{1}H NMR** (300 MHz, DMSO-d_6) δ 1.42-1.60 (m, 2H, $CH_{2piperidine}$), 1.86-1.99 (m, 2H, $CH_{2piperidine}$), 2.42-2.47 (m, 2H, $CH_{2piperidine}$), 2.98-3.11 (m, 1H, $CH_{piperidine}$), 3.67-3.81 (m, 2H, $CH_{2piperidine}$), 7.42 (t, J = 7.1 Hz, 1H, H_{indole}), 7.51 (t, J = 7.1 Hz, 1H, H_{indole}), 7.67 (t, J = 7.6 Hz, 2H, H_{arom}), 7.74-7.88 (m, 5H, H_{arom} + NH_3^+ + H_{indole}), 8.03 (d, J = 8.2 Hz, 1H, H_{indole}), 8.19 (d, J = 8.0 Hz, 2H, H_{arom}), 8.39 (s, 1H, H_{indole}).

_N_-{1-[1-(Benzenesulfonyl)indole-3-sulfonyl]piperidin-4-yl}prop-2-enamide (47)

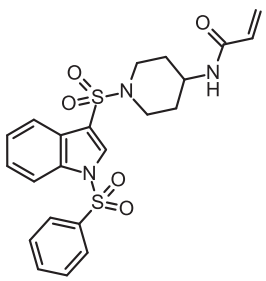

Following general procedure **G-work-up 2** (no flash chromatography purification; to the crude extracts were precipitated from EtOH, then filtered and washed with EtOH), the compound **47** was obtained as a white solid. **Molecular Formula**: $C_{22}H_{23}N_3O_5S_2$; **MW**: 473.57 g/mol; **Yield**: 92%; **Mp**: > 210°C (EtOH); **^{1}H NMR** (300 MHz, DMSO-d_6) δ 1.31-1.49

(m, 2H, $CH_{2piperidine}$), 1.74-1.87 (m, 2H, $CH_{2piperidine}$), 2.53-2.65 (m, 2H, $CH_{2piperidine}$), 3.49-3.66 (m, 3H, $CH_{piperidine}$ + $CH_{2piperidine}$), 5.55 (dd, J = 9.6, 2.7 Hz, 1H, CH_2= cis), 6.03 (dd, J = 17.1, 2.7 Hz, 1H, CH_2= trans), 6.14 (dd, J = 9.6, 17.1 Hz, 1H, CH=), 7.42 (td, J = 7.6, 1.0 Hz, 1H, H_{indole}), 7.50 (td, J = 7.8, 1.1 Hz, 1H, H_{indole}), 7.65 (t, J = 7.6 Hz, 2H, H_{arom}), 7.77 (tt, J = 7.4, 1.5 Hz, 1H, H_{arom}), 7.81 (d, J = 7.7 Hz, 1H, H_{indole}), 8.00 (d, J = 7.4 Hz, 1H, NH), 8.03 (d, J = 8.2 Hz, 1H, H_{indole}), 8.18 (d, J = 7.3 Hz, 2H, H_{arom}), 8.37 (s, 1H, H_{indole}); **^{13}C NMR** (101 MHz, DMSO-*d_6*) δ 163.8 (C=O), 136.1 (C), 135.5 (CH), 134.0 (C), 131.7 (CH), 130.7 (CH), 130.2 (2 x CH), 127.4 (2 x CH), 126.3 (CH), 125.5 (C), 125.2 (CH_2=), 125.0 (CH), 120.9 (CH), 117.8 (C), 113.6 (CH), 44.6 (CH), 44.5 (2 x CH_2), 30.5 (2 x CH_2); **LRMS (ESI)**: *m/z* 474.1 $[M+H]^+$.

N-[1-(1*H*-Indole-3-sulfonyl)piperidin-4-yl]prop-2-enamide (48)

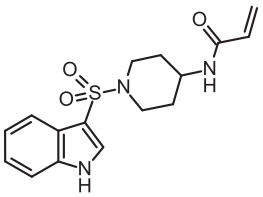

Following general procedure **C** (The crude extracts were purified by flash column chromatography, solvent: MeOH/CH_2Cl_2 3-4:96-97), the resultant product was precipitated from EtOH to give **48** as a white solid. **Molecular Formula**: $C_{16}H_{19}N_3O_3S$; **MW**: 333.40 g/mol; **Yield**: 78%; **Mp**: > 210°C (EtOH); **^{1}H NMR** (300 MHz, DMSO-*d_6*) δ 1.35-1.55 (m, 2H, $CH_{2piperidine}$), 1.74-1.90 (m, 2H, $CH_{2piperidine}$), 2.38-2.48 (m, 2H, $CH_{2piperidine}$), 3.45-3.62 (m, 3H, $CH_{piperidine}$ + $CH_{2piperidine}$), 5.53 (dd, J = 9.8, 2.6 Hz, 1H, CH_2= cis), 6.02 (dd, J = 17.1, 2.6 Hz, 1H, CH_2= trans), 6.15 (dd, J = 17.1, 9.8 Hz, 1H, CH=), 7.19 (td, J = 7.4, 1.2 Hz, 1H, H_{indole}), 7.25 (td, J = 7.5, 1.3 Hz, 1H, H_{indole}), 7.52 (d, J = 7.0 Hz, 1H, H_{indole}), 7.78 (d, J = 7.2 Hz, 1H, H_{indole}), 7.95 (s, 1H, H_{indole}), 8.02 (d, J = 7.2 Hz, 1H, NH), 12.17 (s, 1H, NH); **^{13}C NMR** (101 MHz, DMSO-*d_6*) δ 163.8 (C=O), 136.1 (C), 131.7 (CH), 131.1 (CH), 125.2 (CH_2=), 124.2 (C), 122.9 (CH), 121.4 (CH), 119.4 (CH), 112.7 (CH), 109.0 (C), 44.9 (CH), 44.6 (2 x CH_2), 30.5 (2 x CH_2); **LRMS (ESI)**: *m/z* 334.1 $[M+H]^+$.

Tert-butyl *N*-[1-(1*H*-Indole-3-sulfonyl)piperidin-4-yl]carbamate (54)

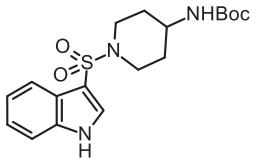

Following general procedure **C** (after filtering the precipitated product, the filtrate was evaporated and purified using flash chromatography; solvent: MeOH/CH_2Cl_2 1:99), the compound **54** was obtained as a white solid. **Molecular Formula**: $C_{18}H_{25}N_3O_4S$; **MW**: 379.47 g/mol; **Yield**: 84%; **Mp**: > 210°C; **^{1}H NMR** (300 MHz, DMSO-*d_6*) δ 1.32 (s, 9H, 3 x CH_3), 1.37-1.49 (m, 2H, $CH_{2piperidine}$), 1.69-1.81 (m, 2H, $CH_{2piperidine}$), 2.32-2.45 (m, 2H, $CH_{2piperidine}$), 3.08-3.22 (m, 1H, $CH_{piperidine}$), 3.44-3.56 (m, 2H, $CH_{2piperidine}$), 6.82 (d, J = 7.3 Hz, 1H, NH), 7.19 (td, J = 7.4, 1.1 Hz, 1H, H_{indole}), 7.25 (td, J = 7.5, 1.3 Hz, 1H, H_{indole}), 7.51 (d, J = 7.6 Hz, 1H, H_{indole}), 7.77 (d, J = 7.5 Hz, 1H, H_{indole}), 7.93 (s, 1H, H_{indole}), 12.16 (s, 1H, NH); **LRMS (ESI)**: *m/z* 380.2 $[M+H]^+$.

Benzyl 3-[4-(*Tert*-butoxycarbonylamino)piperidine-1-sulfonyl]indole-1-carboxylate (55c)

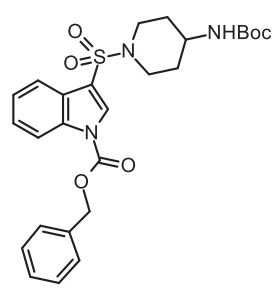

Following general procedure **A** (DMF (0.1 M); flash column chromatography solvent: PE/EtOAc 7:3), the resultant product was product was precipitated from EtOH to give **55c** as a white solid. **Molecular Formula**: $C_{26}H_{31}N_3O_6S$; **MW**: 513.61 g/mol; **Yield**: 27%; **Mp**: 208-210°C (EtOH); **^{1}H NMR** (300 MHz, DMSO-*d_6*) δ 1.33 (s, 9H, 3 x CH_3), 1.34-1.48 (m, 2H, $CH_{2piperidine}$), 1.67-1.83 (m, 2H, $CH_{2piperidine}$), 2.55-2.70 (m, 2H, $CH_{2piperidine}$), 3.15-3.30 (m, 1H, $CH_{piperidine}$), 3.47-3.62 (m, 2H, $CH_{2piperidine}$), 5.53 (s, 2H, CH_2), 6.82 (d, J = 7.4 Hz, 1H, NH), 7.36-7.53 (m, 5H, H_{indole} + H_{arom}), 7.58 (dd, J = 8.0, 1.6 Hz, 2H, H_{arom}), 7.85 (d, J = 7.4 Hz, 1H, H_{indole}), 8.13 (s, 1H, H_{indole}), 8.18 (d, J = 8.2 Hz, 1H, H_{indole}); **LRMS (ESI)**: *m/z* 514.2 $[M+H]^+$.

***Tert*-butyl *N*-[1-(1-Methylindole-3-sulfonyl)piperidin-4-yl]carbamate (55a)**

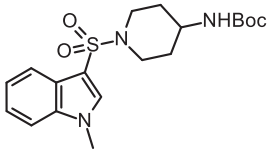

Following general procedure **A** (solvent: DMF (0.1 M); flash column chromatography solvent: MeOH/CH_2Cl_2 1-2:98-99), the compound **55a** was obtained as a white foam. **Molecular Formula**: $C_{19}H_{27}N_3O_4S$; **MW**: 393.50 g/mol; **Yield**: 85%; **^{1}H NMR** (300 MHz, DMSO-*d_6*) δ 1.33 (s, 9H, 3 x CH_3), 1.35-1.50 (m, 2H, $CH_{2piperidine}$), 1.69-1.81 (m, 2H, $CH_{2piperidine}$), 2.33-2.45 (m, 2H, $CH_{2piperidine}$), 3.07-3.24 (m, 1H, $CH_{piperidine}$), 3.43-3.55 (m, 2H, $CH_{2piperidine}$), 3.88 (s, 3H, CH_3), 6.82 (d, J = 7.6 Hz, 1H, NH), 7.24 (td, J = 7.5, 1.1 Hz, 1H, H_{indole}), 7.32 (td, J = 7.6, 1.2 Hz, 1H, H_{indole}), 7.59 (d, J = 8.2 Hz, 1H, H_{indole}), 7.78 (d, J = 7.7 Hz, 1H, H_{indole}), 8.00 (s, 1H, H_{indole}); **LRMS (ESI)**: *m/z* 394.2 $[M+H]^+$.

***Tert*-butyl *N*-(1-{1-[2-(Dimethylamino)ethyl]indole-3-sulfonyl}piperidin-4-yl)carbamate (55b)**

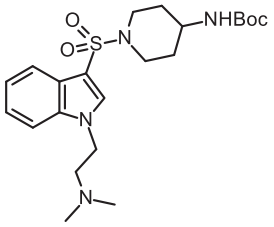

Following general procedure **A** (solvent: DMF (0.1M); the reaction was maintained at 95ºC until completion; flash chromatography solvent: MeOH/CH_2Cl_2 5-10:90-95), the compound **55b** was obtained as a white solid. **Molecular Formula**: $C_{22}H_{34}N_4O_4S$; **MW**: 450.59 g/mol; **Yield**: 83%; **Mp**: 130-132°C; **^{1}H NMR** (300 MHz, DMSO-*d_6*) δ 1.33 (s, 9H, 3 x CH_3), 1.35-1.51 (m, 2H, $CH_{2piperidine}$), 1.67-1.82 (m, 2H, $CH_{2piperidine}$), 2.17 (s, 6H, 2 x CH_3), 2.29-2.43 (m, 2H, $CH_{2piperidine}$), 2.63 (t, J = 6.2 Hz, 2H, CH_2), 3.05-3.20 (m, 1H, $CH_{piperidine}$), 3.43-3.55 (m, 2H, $CH_{2piperidine}$), 4.36 (t, J = 6.2 Hz, 2H, CH_2), 6.81 (d, J = 6.7 Hz, 1H, NH), 7.22 (td, J = 7.5, 1.0 Hz, 1H, H_{indole}), 7.30 (td, J = 7.6, 1.2 Hz, 1H, H_{indole}), 7.66 (d, J = 8.1 Hz, 1H, H_{indole}), 7.78 (d, J = 7.5 Hz, 1H, H_{indole}). 8.01 (s, 1H, H_{indole}); **LRMS (ESI)**: *m/z* 451.2 $[M+H]^+$.

***Tert*-butyl *N*-{[1-(1-Benzoyl)indole-3-sulfonyl]piperidin-4-yl]}carbamate (55d)**

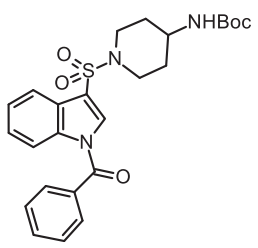

Following general procedure **G - work-up 1** (flash chromatography solvent: MeOH/CH_2Cl_2 1:99), the compound **55d** was obtained as a white solid. **Molecular Formula**: $C_{25}H_{29}N_3O_5S$; **MW**: 483.59 g/mol; **Yield**: 100%; **Mp**: > 210°C; **^{1}H NMR** (300 MHz, DMSO-d_6) δ 1.33 (s, 9H, 3 x CH_3), 1.35-1.48 (m, 2H, $CH_{2piperidine}$), 1.68-1.82 (m, 2H, $CH_{2piperidine}$), 2.57-2.70 (m, 2H, $CH_{2piperidine}$), 3.17-3.30 (m, 1H, $CH_{piperidine}$), 3.47-3.61 (m, 2H, $CH_{2piperidine}$), 6.83 (d, J = 6.9 Hz, 1H, NH), 7.47 (td, J = 7.5, 1.2 Hz, 1H, H_{indole}), 7.55 (td, J = 7.7, 1.4 Hz, 1H, H_{indole}), 7.66 (t, J = 7.4 Hz, 2H, H_{arom}), 7.72-7.80 (m, 2H, H_{indole} + H_{arom}), 7.82-7.93 (m, 3H, H_{indole} + H_{arom}), 8.31 (d, J = 7.7 Hz, 1H, H_{indole}); **LRMS (ESI)**: *m/z* 484.2 $[M+H]^+$.

***N*-{[1-(1-Benzyloxycarbonyl)indole-3-sulfonyl]piperidin-4-yl}ammonium trifluoroacetate salt (56c)**

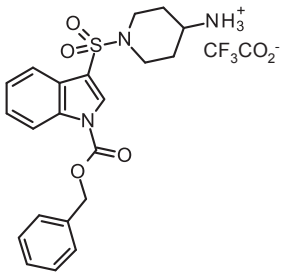

Following general procedure **E**, the compound **56c** was obtained as a white solid. **Molecular Formula**: $C_{23}H_{24}F_3N_3O_6S$; **MW**: 527.51 g/mol; **Yield**: 93%; **Mp**: 192-194°C (washing Et_2O); **^{1}H NMR** (300 MHz, DMSO-d_6) δ 1.42-1.61 (m, 2H, $CH_{2piperidine}$), 1.85-1.99 (m, 2H, $CH_{2piperidine}$), 2.53-2.62 (m, 2H, $CH_{2piperidine}$), 2.94-3.11 (m, 1H, $CH_{piperidine}$), 3.67-3.80 (m, 2H, $CH_{2piperidine}$), 5.53 (s, 2H, CH_2), 7.36-7.54 (m, 5H, H_{indole} + H_{arom}), 7.58 (dd, J = 7.8, 1.6 Hz, 2H, H_{arom}), 7.83 (s, 3H, NH_3^+), 7.86 (d, J = 8.1 Hz, 1H, H_{indole}), 8.17 (s, 1H, H_{indole}), 8.19 (d, J = 8.8 Hz, 1H, H_{indole}).

***N*-[1-(1-Methylindole-3-sulfonyl)piperidin-4-yl]ammonium trifluoroacetate salt (56a)**

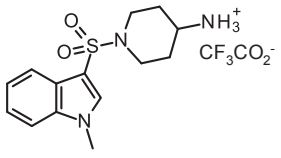

Following general procedure **E**, the compound **56a** was obtained as a white solid. **Molecular Formula**: $C_{16}H_{20}F_3N_3O_4S$; **MW**: 407.41 g/mol; **Yield**: 89%; **Mp**: 195-197°C (washing Et_2O); **^{1}H NMR** (300 MHz, DMSO-d_6) δ 1.44-1.64 (m, 2H, $CH_{2piperidine}$), 1.84-1.97 (m, 2H, $CH_{2piperidine}$), 2.28-2.41 (m, 2H, $CH_{2piperidine}$), 2.91-3.09 (m, 1H, $CH_{piperidine}$), 3.61-3.77 (m, 2H, $CH_{2piperidine}$), 3.89 (s, 3H, CH_3), 7.25 (td, J = 7.5, 1.0 Hz, 1H, H_{indole}), 7.33 (td, J = 7.6, 1.1 Hz, 1H, H_{indole}), 7.60 (d, J = 8.2 Hz, 1H, H_{indole}), 7.79 (d, J = 7.7 Hz, 1H, H_{indole}), 7.83 (s, 3H, NH_3^+), 8.04 (s, 1H, H_{indole}).

***N*-(1-{1-[(2-Dimethylamino)ethyl]indole-3-sulfonyl}piperidin-4-yl)ammonium trifluoroacetate salt (56b)**

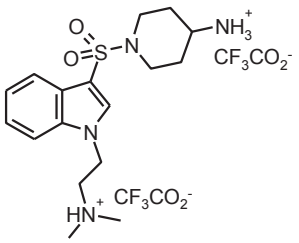

Following general procedure **E**, the compound **56b** was obtained as a white solid. **Molecular Formula**: $C_{21}H_{28}F_6N_4O_6S$; **MW**: 578.52 g/mol; **Yield**: 100%; **Mp**: > 210°C (washing Et_2O); **^{1}H NMR** (300 MHz, DMSO-*d*$_6$) δ 1.46-1.65 (m, 2H, $CH_{2piperidine}$), 1.87-1.99 (m, 2H, $CH_{2piperidine}$), 2.29-2.43 (m, 2H, $CH_{2piperidine}$), 2.87 (s, 6H, 2 x CH_3), 2.93-3.07 (m, 1H, $CH_{piperidine}$), 3.49-3.63 (m, 2H, CH_2), 3.64-3.77 (m, 2H, $CH_{2piperidine}$), 4.67 (t, J = 7.0 Hz, 2H, CH_2), 7.29 (td, J = 7.3, 1.0 Hz, 1H, H_{indole}), 7.38 (td, J = 7.7, 1.1 Hz, 1H, H_{indole}), 7.74 (d, J = 8.2 Hz, 1H, H_{indole}), 7.82 (d, J = 7.7 Hz, 1H, H_{indole}), 7.84-8.02 (m, 3H, NH_3^+), 8.14 (s, 1H, H_{indole}), 9.95 (s, 1H, NH^+).

_N_-[1-(1-Benzoylindole-3-sulfonyl)piperidin-4-yl]ammonium trifluoroacetate salt (56d)

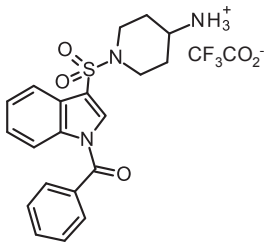

Following general procedure **E**, the compound **56d** was obtained as a white solid. **Molecular Formula**: $C_{22}H_{22}F_3N_3O_5S$; **MW**: 497.49 g/mol; **Yield**: 100 %; **Mp**: 204-206°C (washing Et_2O); **^{1}H NMR** (300 MHz, DMSO-*d*$_6$) δ 1.42-1.59 (m, 2H, $CH_{2piperidine}$), 1.86-1.98 (m, 2H, $CH_{2piperidine}$), 2.54-2.62 (m, 2H, $CH_{2piperidine}$), 2.97-3.13 (m, 1H, $CH_{piperidine}$), 3.66-3.77 (m, 2H, $CH_{2piperidine}$), 7.49 (td, J = 7.5, 1.3 Hz, 1H, H_{indole}), 7.55 (td, J = 7.7, 1.4 Hz, 1H, H_{indole}), 7.66 (t, J = 7.4 Hz, 2H, H_{arom}), 7.73-7.94 (m, 8H, NH_3^+ + H_{arom} + H_{indole}), 8.30 (d, J = 7.6 Hz, 1H, H_{indole}).

Benzyl 3-[4-(Acryloylamino)piperidine-1-sulfonyl]indole-1-carboxylate (53c)

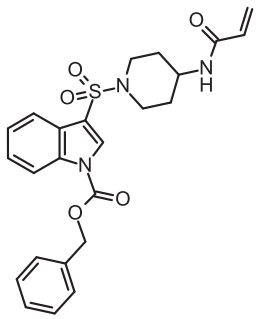

Following general procedure **G - work-up 2** (flash column chromatography solvent: PE/EtOAc 7:3), the resultant product was precipitated from MeOH/CH_2Cl_2 (5:95) to give **53c** as a white solid. **Molecular Formula**: $C_{24}H_{25}N_3O_5S$; **MW**: 467.54 g/mol; **Yield**: 71%; **Mp**: > 210°C (MeOH/CH_2Cl_2); **^{1}H NMR** (300 MHz, DMSO-*d*$_6$) δ 1.34-1.51 (m, 2H, $CH_{2piperidine}$), 1.76-1.88 (m, 2H, $CH_{2piperidine}$), 2.60-2.71 (m, 2H, $CH_{2piperidine}$), 3.52-3.68 (m, 3H, $CH_{piperidine}$ + $CH_{2piperidine}$), 5.53 (s, 2H, CH_2), 5.55 (dd, J = 9.8, 2.6 Hz, 1H, CH_2= cis), 6.02 (dd, J = 17.0, 2.6 Hz, 1H, CH_2= trans), 6.14 (dd, J = 17.0, 9.8 Hz, 1H, CH=), 7.36-7.54 (m, 5H, H_{indole} + H_{arom}), 7.58 (dd, J = 7.9, 1.6 Hz, 2H, H_{arom}), 7.86 (d, J = 7.6 Hz, 1H, H_{indole}), 8.01 (d, J = 7.3 Hz, 1H, NH), 8.15 (s, 1H, H_{indole}), 8.18 (d, J = 8.0 Hz, 1H, H_{indole}); **^{13}C NMR** (101 MHz, DMSO-*d*$_6$) δ 163.8 (C=O), 149.6 (C=O), 134.8 (C), 131.7 (CH), 130.3 (CH), 128.7 (CH), 128.6 (4 x CH), 126.0 (CH), 125.4 (C), 125.2 (CH_2=), 124.4 (CH), 120.5 (CH), 116.6 (C), 115.2 (CH), 69.4 (CH_2), 44.6 (CH), 44.5 (2 x CH_2), 30.6 (2 x CH_2); **LRMS (ESI)**: *m/z* 468.2 $[M+H]^+$.

***N*-[1-(1-Methylindole-3-sulfonyl)piperidin-4-yl]prop-2-enamide (53a)**

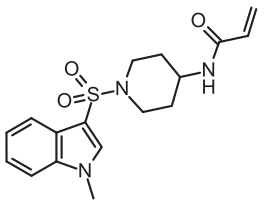

Following general procedure **G - work-up 2** (no flash column chromatography purification. The crude extracts were precipitated from EtOH), the compound **53a** was obtained as a white solid. **Molecular Formula**: $C_{17}H_{21}N_3O_3S$; **MW**: 347.43 g/mol; **Yield**: 59%; **Mp**: > 210°C (EtOH); **^{1}H NMR** (300 MHz, DMSO-*d*$_6$) δ 1.36-1.54 (m, 2H, $CH_{2piperidine}$), 1.74-1.89 (m, 2H, $CH_{2piperidine}$), 2.37-2.48 (m, 2H, $CH_{2piperidine}$), 3.47-3.59 (m, 3H, $CH_{piperidine}$ + $CH_{2piperidine}$), 3.89 (s, 3H, CH_3), 5.53 (dd, J = 9.8, 2.6 Hz, 1H, CH_2= cis), 6.02 (dd, J = 17.0, 2.6 Hz, 1H, CH_2= trans), 6.15 (dd, J = 17.0, 9.8 Hz, 1H, CH=), 7.24 (td, J = 7.5, 1.1 Hz, 1H, H_{indole}), 7.32 (td, J = 7.6, 1.2 Hz, 1H, H_{indole}), 7.60 (d, J = 8.2 Hz, 1H, H_{indole}), 7.80 (d, J = 7.6 Hz, 1H, H_{indole}). 8.02 (s, 1H, H_{indole}), 8.03 (d, J = 7.1 Hz, 1H, NH); **^{13}C NMR** (101 MHz, DMSO-*d*$_6$) δ 163.8 (C=O), 136.7 (C), 134.6 (CH), 131.7 (CH), 125.2 (CH_2=), 124.5 (C), 122.9 (CH), 121.7 (CH), 119.5 (CH), 111.2 (CH), 107.7 (C), 44.8 (CH), 44.6 (2 x CH_2), 33.2 (CH_3), 30.5 (2 x CH_2); **LRMS (ESI)**: *m/z* 348.1 $[M+H]^+$.

***N*-(1-{1-[2-(Dimethylamino)ethyl]indole-3-sulfonyl}piperidin-4-yl)prop-2-enamide (53b)**

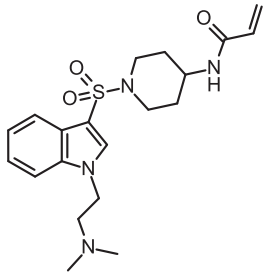

Following general procedure **G - work-up 2** (flash column chrommatography solvent: MeOH/CH_2Cl_2 1:9). The resultant product was precipitated from EtOH to give **53b** as a white solid. **Molecular Formula**: $C_{20}H_{28}N_4O_3S$; **MW**: 404.53 g/mol; **Yield**: 100%; **Mp**: 179-180°C (EtOH); **^{1}H NMR** (300 MHz, DMSO-*d*$_6$) δ 1.35-1.54 (m, 2H, $CH_{2piperidine}$), 1.73-1.88 (m, 2H, $CH_{2piperidine}$), 2.33-2.47 (m, 2H, $CH_{2piperidine}$), 2.50 (s, 6H, 2 x CH_3), 2.64 (t, J = 6.2 Hz, 2H, CH_2), 3.44-3.60 (m, 3H, $CH_{piperidine}$ + $CH_{2piperidine}$), 4.37 (t, J = 6.2 Hz, 2H, CH_2), 5.53 (dd, J = 9.8, 2.6 Hz, 1H, CH_2= cis), 6.02 (dd, J = 17.0, 2.6 Hz, 1H, CH_2= trans), 6.15 (dd, J = 17.0, 9.8 Hz, 1H, CH=), 7.22 (t, J = 7.1 Hz, 1H, H_{indole}), 7.35 (t, J = 7.1 Hz, 1H, H_{indole}), 7.66 (d, J = 8.1 Hz, 1H, H_{indole}), 7.79 (d, J = 7.8 Hz, 1H, H_{indole}), 8.02 (d, J = 7.0 Hz, 1H, NH), 8.03 (s, 1H, H_{indole}); **LRMS (ESI)**: *m/z* 405.2 $[M+H]^+$.

***N*-[1-(1-Benzoylindole-3-sulfonyl)piperidin-4-yl]prop-2-enamide (53d)**

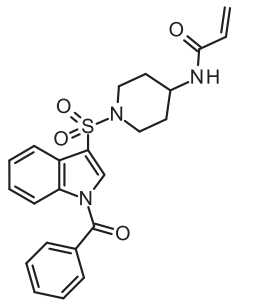

Following general procedure **G - work-up 1** (DIPEA (2.5 eq); flash column chromatography solvent: MeOH/CH_2Cl_2 2:98), the compound **53d** was obtained as a white solid. **Molecular Formula**: $C_{23}H_{23}N_3O_4S$; **MW**: 437.51 g/mol; **Yield**: 61%; **Mp**: > 210°C; **^{1}H NMR** (300 MHz, DMSO-*d*$_6$) δ 1.32-1.52 (m, 2H, $CH_{2piperidine}$), 1.75-1.90 (m, 2H, $CH_{2piperidine}$), 2.60-2.75 (m, 2H, $CH_{2piperidine}$), 3.51-3.71 (m, 3H, $CH_{piperidine}$ + $CH_{2piperidine}$), 5.54 (dd,

J = 9.8, 2.5 Hz, 1H, CH_2= cis), 6.03 (dd, J = 17.1, 2.5 Hz, 1H, CH_2= trans), 6.15 (dd, J = 17.1, 9.8 Hz, 1H, CH=), 7.48 (td, J = 7.5, 1.2 Hz, 1H, H_{indole}), 7.54 (td, J = 7.7, 1.4 Hz, 1H, H_{indole}), 7.65 (t, J = 7.4 Hz, 2H, H_{arom}), 7.71-7.81 (m, 1H, H_{arom}), 7.78 (s, 1H, H_{indole}), 7.86 (d, J = 7.2 Hz, 2H, H_{arom}), 7.90 (d, J = 8.0 Hz, 1H, H_{indole}), 8.03 (d, J = 7.2 Hz, 1H, NH), 8.31 (d, J = 8.0 Hz, 1H, H_{indole}); **LRMS (ESI)**: *m/z* 438.1 $[M+H]^+$.

1-Methyl-5-nitroindole (59), CAS 29906-67-0

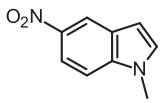

Following general procedure **A** (no flash column chromatography purification), the compound **59** was obtained as a yellow solid. **Molecular Formula**: $C_9H_8N_2O_2$; **MW**: 176.17 g/mol; **Yield**: 100%; **Mp**: 163-165°C (lit. 170-172°C);[167] **^{1}H NMR** (300 MHz, DMSO-*d*$_6$) δ 3.88 (s, 3H, CH_3), 6.74 (d, J = 3.2 Hz, 1H, H_{indole}), 7.60 (d, J = 3.2 Hz, 1H, H_{indole}), 7.65 (d, J = 9.0 Hz, 1H, H_{indole}), 8.04 (dd, J = 9.0, 2.3 Hz, 1H, H_{indole}), 8.57 (d, J = 2.3 Hz, 1H, H_{indole}).

1-Methyl-5-nitroindole-3-sulfonyl chloride (60),[168] CAS 312300-36-0

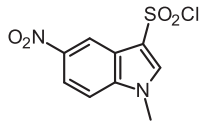

Following general procedure **B - method 2**, the compound **60** was obtained as a dark-orange solid. **Molecular Formula**: $C_9H_7ClN_2O_4S$; **MW**: 274.68 g/mol; **Yield**: 45%; **Mp**: 172-174°C (washing CH_2Cl_2); **^{1}H NMR** (300 MHz, DMSO-*d*$_6$) δ 3.84 (s, 3H, CH_3), 7.62 (dd, J = 9.0, 0.3 Hz, 2H, H_{indole}), 7.64 (s, 1H, H_{indole}), 8.05 (dd, J = 9.0, 2.3 Hz, 1H, H_{indole}), 8.70 (d, J = 2.3 Hz, 1H, H_{indole}).

***Tert*-butyl *N*-[1-(1-Methyl-5-nitroindole-3-sulfonyl)piperidin-4-yl]carbamate (61)**

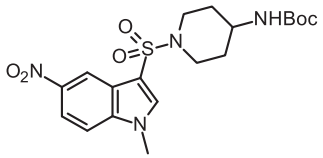

Following general procedure **F - work-up 1**, the compound **61** was obtained as a white solid. **Molecular Formula**: $C_{19}H_{26}N_4O_6S$; **MW**: 438.50 g/mol; **Yield**: 92%; **Mp**: > 210°C (washing CH_2Cl_2); **^{1}H NMR** (300 MHz, DMSO-*d*$_6$) δ 1.33 (s, 9H, 3 x CH_3), 1.36-1.51 (m, 2H, $CH_{2piperidine}$), 1.68-1.83 (m, 2H, $CH_{2piperidine}$), 2.41-2.47 (m, 2H, $CH_{2piperidine}$), 3.11-3.27 (m, 1H, $CH_{piperidine}$), 3.42-3.57 (m, 2H, $CH_{2piperidine}$), 3.97 (s, 3H, CH_3), 6.82 (d, J = 7.0 Hz, 1H, NH), 7.86 (d, J = 9.1 Hz, 1H, H_{indole}), 8.20 (dd, J = 9.1, 2.3 Hz, 1H, H_{indole}), 8.32 (s, 1H, H_{indole}), 8.63 (d, J = 2.3 Hz, 1H, H_{indole}); **LRMS (ESI)**: *m/z* 439.2 $[M+H]^+$.

***Tert*-butyl *N*-[1-(5-Amino-1-methylindole-3-sulfonyl)piperidin-4-yl]carbamate (58)**

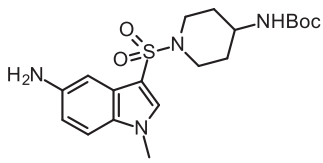

Following general procedure **H - work up 2** (NH_4Cl (0.227 M); no flash chromatography purification. The crude residue was precipitated from Et_2O), the compound **58** was obtained as a light pink solid. **Molecular Formula**:

$C_{19}H_{28}N_4O_4S$; **MW**: 408.52 g/mol; **Yield**: 86%; **Mp**: 112-114°C (Et_2O); **^{1}H NMR** (300 MHz, DMSO-*d_6*) δ 1.33 (s, 9H, 3 x CH_3), 1.36-1.49 (m, 2H, $CH_{2piperidine}$), 1.69-1.82 (m, 2H, $CH_{2piperidine}$), 2.31-2.48 (m, 2H, $CH_{2piperidine}$), 3.09-3.24 (m, 1H, $CH_{piperidine}$), 3.39-3.50 (m, 2H, $CH_{2piperidine}$), 3.76 (s, 3H, CH_3), 4.94 (s, 2H, NH_2), 6.65 (dd, J = 8.7, 2.0 Hz, 1H, H_{indole}), 6.83 (d, J = 7.2 Hz, 1H, NH), 6.94 (d, J = 2.0 Hz, 1H, H_{indole}), 7.23 (d, J = 8.7 Hz, 1H, H_{indole}), 7.73 (s, 1H, H_{indole}); **LRMS (ESI)**: *m/z* 409.2 $[M+H]^+$.

Tert-butyl *N*-{1-[5-(Benzoylamino)-1-methylindole-3-sulfonyl]piperidin-4-yl}carbamate (62)

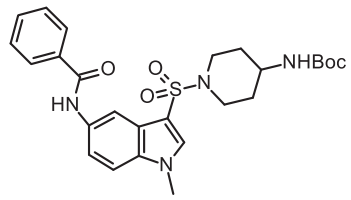

Following general procedure **G - work-up 4**, the compound **62** was obtained as a white solid. **Molecular Formula**: $C_{26}H_{32}N_4O_5S$; **MW**: 512.62 g/mol; **Yield**: 76%; **Mp**: > 210°C (washing CH_2Cl_2); **^{1}H NMR** (300 MHz, DMSO-*d_6*) δ 1.33 (s, 9H, 3 x CH_3), 1.36-1.52 (m, 2H, $CH_{2piperidine}$), 1.71-1.84 (m, 2H, $CH_{2piperidine}$), 2.37-2.45 (m, 2H, $CH_{2piperidine}$), 3.09-3.25 (m, 1H, $CH_{piperidine}$), 3.44-3.58 (m, 2H, $CH_{2piperidine}$), 3.88 (s, 3H, CH_3), 6.83 (d, J = 7.0 Hz, 1H, NH), 7.48-7.64 (m, 4H, H_{arom} + H_{indole}), 7.78 (dd, J = 9.0, 1.8 Hz, 1H, H_{indole}), 7.98 (s, 1H, H_{indole}), 7.95-8.02 (m, 2H, H_{arom}), 8.25 (d, J = 1.8 Hz, 1H, H_{indole}), 10.29 (s, 1H, NH); **LRMS (ESI)**: *m/z* 513.2 $[M+H]^+$.

N-{1-[5-(Benzoylamino)-1-methylindole-3-sulfonyl]piperidin-4yl}ammonium trifluoroacetate salt (63)

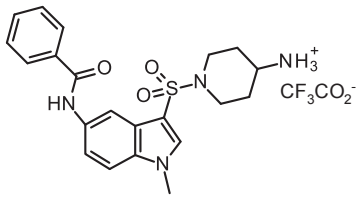

Following general procedure **E**, the compound **63** was obtained as a pale white solid. **Molecular Formula**: $C_{23}H_{25}F_3N_4O_5S$; **MW**: 526.53 g/mol; **Yield**: 100%; **Mp**: > 210°C (washing Et_2O); **^{1}H NMR** (300 MHz, DMSO-*d_6*) δ 1.48-1.65 (m, 2H, $CH_{2piperidine}$), 1.87-1.99 (m, 2H, $CH_{2piperidine}$), 2.32-2.45 (m, 2H, $CH_{2piperidine}$), 2.93-3.12 (m, 1H, $CH_{piperidine}$), 3.63-3.74 (m, 2H, $CH_{2piperidine}$), 3.88 (s, 3H, CH_3), 7.49-7.64 (m, 4H, H_{arom} + H_{indole}), 7.75 (dd, J = 8.3, 1.7 Hz, 1H, H_{indole}), 7.84 (s, 3H, NH_3^+), 7.99 (dd, J = 8.3, 1.7 Hz, 2H, H_{arom}), 8.01 (s, 1H, H_{indole}), 8.28 (d, J = 1.7 Hz, 1H, H_{indole}), 10.31 (s, 1H, NH).

N-{1-Methyl-3-[4-(acryloylamino)piperidine-1-sulfonyl]indol-5-yl}benzamide (57)

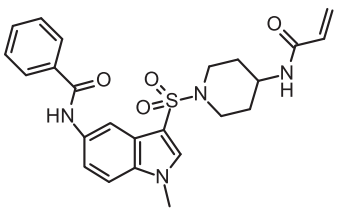

Following general procedure **G - work-up 2** (DIPEA (2.5 eq); flash column chromatography solvent: MeOH/CH_2Cl_2 3:97). The resultant product was precipitated from MeOH, filtered, and washed with MeOH to give **57** as a white solid. **Molecular Formula**: $C_{24}H_{26}N_4O_4S$; **MW**: 466.55 g/mol; **Yield**: 33%; **Mp**: > 210°C (MeOH); **^{1}H NMR** (300

MHz, DMSO-d_6) δ 1.38-1.57 (m, 2H, $CH_{2piperidine}$), 1.76-1.96 (m, 2H, $CH_{2piperidine}$), 2.54-2.59 (m, 2H, $CH_{2piperidine}$), 3.47-3.64 (m, 3H, $CH_{piperidine}$ + $CH_{2piperidine}$), 3.88 (s, 3H, CH_3), 5.53 (dd, J = 9.8, 2.5 Hz, 1H, CH_2= cis), 6.02 (dd, J = 17.0, 2.5 Hz, 1H, CH_2= trans), 6.15 (dd, J = 17.0, 9.8 Hz, 1H, CH=), 7.49-7.63 (m, 4H, H_{arom} + H_{indole}), 7.78 (dd, J = 8.9, 1.9 Hz, 1H, H_{indole}), 7.99 (dd, J = 7.3, 1.6 Hz, 2H, H_{arom}), 8.00 (s, 1H, H_{indole}), 8.03 (d, J = 7.5 Hz, 1H, NH), 8.26 (d, J = 1.9 Hz, 1H, H_{indole}), 10.30 (s, 1H, NH); **^{13}C NMR** (101 MHz, DMSO-d_6) δ 165.3 (C=O), 163.8 (C=O), 135.1 (C), 134.9 (CH), 133.8 (C), 133.6 (C), 131.7 (CH), 131.5 (CH), 128.4 (2 x CH), 127.7 (2 x CH), 125.2 (CH_2=), 124.5 (C), 117.4 (CH), 111.1 (CH), 111.0 (CH), 107.6 (C), 44.9 (CH), 44.6 (2 x CH_2), 33.3 (CH_3), 30.5 (2 x CH_2); **HRMS (ESI)** calcd for $C_{24}H_{27}N_4O_4S$ $[M+H]^+$, 467.1748; found, 467.1740.

1-Methyl-6-nitroindole (66), CAS 99459-48-0

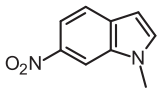

Following general procedure **A** (no flash column chromatography purification), the compound **66** was obtained as a brown solid. **Molecular Formula**: $C_9H_8N_2O_2$; **MW**: 176.17 g/mol; **Yield**: 98%; **Mp**: 73-75°C (lit. 78-80°C);[167] **^{1}H NMR** (300 MHz, DMSO-d_6) δ 3.93 (s, 3H, CH_3), 6.64 (dd, J = 3.0, 0.8 Hz, 1H, H_{indole}), 7.73 (d, J = 8.7 Hz, 1H, H_{indole}), 7.76 (d, J = 3.0 Hz, 1H, H_{indole}), 7.91 (dd, J = 8.7, 2.0 Hz, 1H, H_{indole}), 8.48 (d, J = 2.0 Hz, 1H, H_{indole}).

1-Methyl-6-nitroindole-3-sulfonyl chloride (67)

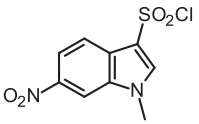

Following genral procedure **B - method 2**, the compound **67** was obtained as an orange solid. **Molecular Formula**: $C_9H_7ClN_2O_4S$; **MW**: 274.68 g/mol; **Yield**: 62%; **Mp**: 148-150°C (washing CH_2Cl_2); **^{1}H NMR** (300 MHz, DMSO-d_6) δ 3.89 (s, 3H, CH_3), 7.78 (s, 1H, H_{indole}), 7.90 (d, J = 8.7 Hz, 1H, H_{indole}), 7.95 (dd, J = 8.7, 2.0, Hz, 1H, H_{indole}), 8.43 (d, J = 2.0 Hz, 1H, H_{indole}).

***Tert*-butyl *N*-[1-(1-Methyl-6-nitroindole-3-sulfonyl)piperidin-4-yl]carbamate (68)**

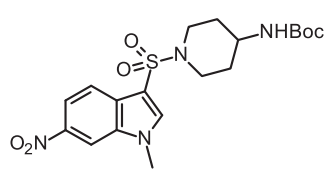

Following general procedure **F - work-up 2** (flash column chromatography solvent: MeOH/CH_2Cl_2 2-3:97-98), the compound **68** was obtained as a white-salmon solid. **Molecular Formula**: $C_{19}H_{26}N_4O_6S$; **MW**: 438.50 g/mol; **Yield**: 94%; **Mp**: > 210°C; **^{1}H NMR** (300 MHz, DMSO-d_6) δ 1.33 (s, 9H, 3 x CH_3), 1.37-1.49 (m, 2H, $CH_{2piperidine}$), 1.63-1.81 (m, 2H, $CH_{2piperidine}$), 2.40-2.44 (m, 2H, $CH_{2piperidine}$), 3.19-3.27 (m, 1H, $CH_{piperidine}$), 3.44-3.56 (m, 2H, $CH_{2piperidine}$), 4.02 (s, 3H, CH_3), 6.82 (d, J = 7.5 Hz, 1H, NH), 7.96 (d, J = 8.9 Hz, 1H, H_{indole}), 8.12 (dd, J = 8.9, 2.0 Hz, 1H, H_{indole}), 8.39 (s, 1H, H_{indole}), 8.63 (d, J = 2.0 Hz, 1H, H_{indole}); **LRMS (ESI)**: *m/z* 439.2 $[M+H]^+$.

***Tert*-butyl *N*-[1-(6-Amino-1-methylindole-3-sulfonyl)piperidin-4-yl]carbamate (65)**

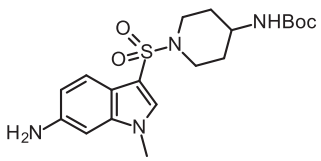

Following general procedure **H - work-up 2** (NH_4Cl (0.34 M); flash column chromatography solvent: $MeOH/CH_2Cl_2$ 3:97), the compound **65** was obtained as a brown foam. **Molecular Formula**: $C_{19}H_{28}N_4O_4S$; **MW**: 408.52 g/mol; **Yield**: 72%; **^{1}H NMR** (300 MHz, DMSO-d_6) δ 1.33 (s, 9H, 3 x CH_3), 1.36-1.48 (m, 2H, $CH_{2piperidine}$), 1.68-1.80 (m, 2H, $CH_{2piperidine}$), 2.29-2.41 (m, 2H, $CH_{2piperidine}$), 3.06-3.22 (m, 1H, $CH_{piperidine}$), 3.40-3.51 (m, 2H, $CH_{2piperidine}$), 3.69 (s, 3H, CH_3), 5.14 (s, 2H, NH_2), 6.56 (s, 1H, H_{indole}), 6.58 (d, J = 7.8 Hz, 1H, H_{indole}), 6.82 (d, J = 7.5 Hz, 1H, NH), 7.40 (d, J = 7.8 Hz, 1H, H_{indole}), 7.61 (s, 1H, H_{indole}); **LRMS (ESI)**: *m/z* 409.2 $[M+H]^+$.

***Tert*-butyl *N*-{1-[6-(benzoylamino)-1-methylindole-3-sulfonyl]piperidin-4-yl}carbamate (69)**

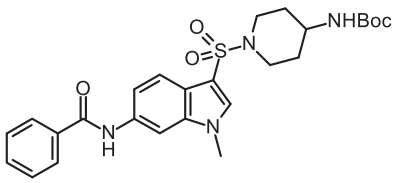

Following general procedure **G-work-up 2** (DIPEA (1.5 eq); flash column chromatography solvent: $MeOH/CH_2Cl_2$ 3:97). The resultant product was precipitated from MeOH to give **69** as a white solid. **Molecular Formula**: $C_{26}H_{32}N_4O_5S$; **MW**: 512.62 g/mol; **Yield**: 74%; **Mp**: > 210°C (MeOH); **^{1}H NMR** (300 MHz, DMSO-d_6) δ 1.33 (s, 9H, 3 x CH_3), 1.37-1.51 (m, 2H, $CH_{2piperidine}$), 1.69-1.83 (m, 2H, $CH_{2piperidine}$), 2.34-2.46 (m, 2H, $CH_{2piperidine}$), 3.09-3.26 (m, 1H, $CH_{piperidine}$), 3.44-3.58 (m, 2H, $CH_{2piperidine}$), 3.86 (s, 3H, CH_3), 6.83 (d, J = 6.5 Hz, 1H, NH), 7.48-7.65 (m, 4H, H_{arom} + H_{indole}), 7.73 (d, J = 8.6 Hz, 1H, H_{indole}), 7.95-8.03 (m, 3H, H_{indole} + H_{arom}), 8.22 (d, J = 1.5 Hz, 1H, H_{indole}), 10.39 (s, 1H, NH); **LRMS (ESI)**: *m/z* 513.2 $[M+H]^+$.

***N*-{1-[6-(Benzoylamino)-1-methylindole-3-sulfonyl]piperidin-4-yl}ammonium trifluoroacetate salt (70)**

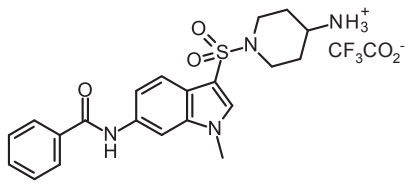

Following general procedure **E**, the compound **70** was obtained as a white solid. **Molecular Formula**: $C_{23}H_{25}F_3N_4O_5S$; **MW**: 526.53 g/mol; **Yield**: 100%; **Mp**: > 210°C (washing Et_2O); **^{1}H NMR** (300 MHz, DMSO-d_6) δ 1.45-1.64 (m, 2H, $CH_{2piperidine}$), 1.87-1.99 (m, 2H, $CH_{2piperidine}$), 2.29-2.42 (m, 2H, $CH_{2piperidine}$), 2.93-3.09 (m, 1H, $CH_{piperidine}$), 3.61-3.75 (m, 2H, $CH_{2piperidine}$), 3.86 (s, 3H, CH_3), 7.49-7.64 (m, 4H, H_{arom} + H_{indole}), 7.74 (d, J = 8.6 Hz, 1H, H_{indole}), 7.83 (s, 3H, NH_3^+), 7.95-8.03 (m, 3H, H_{indole} + H_{arom}), 8.21 (d, J = 1.4 Hz, 1H, H_{indole}), 10.40 (s, 1H, NH).

***N*-{1-Methyl-3-[4-(acryloylamino)piperidine-1-sulfonyl]indol-6-yl}benzamide (64)**

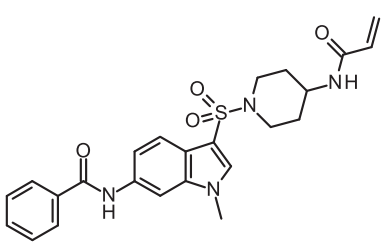

Following general procedure **G-work-up 2** (flash column chromatography solvent: $MeOH/CH_2Cl_2$ 3-4/96-97), the resultant product was precipitated from EtOH to give **64** as a white solid. **Molecular Formula**: $C_{24}H_{26}N_4O_4S$; **MW**: 466.55 g/mol; **Yield**: 70%; **Mp**: > 210°C (EtOH); **^{1}H NMR** (300 MHz, DMSO-*d*$_6$) δ 1.36-1.55 (m, 2H, $CH_{2piperidine}$), 1.76-1.89 (m, 2H, $CH_{2piperidine}$), 2.43-2.47 (m, 2H, $CH_{2piperidine}$), 3.47-3.64 (m, 3H, CH_{piper} + $CH_{2piperidine}$), 3.86 (s, 3H, CH_3), 5.54 (dd, J = 9.8, 2.6 Hz, 1H, CH_2= cis), 6.02 (dd, J = 17.0, 2.6 Hz, 1H, CH_2= trans), 6.15 (dd, J = 17.0, 9.8 Hz, 1H, CH=), 7.49-7.64 (m, 4H, H_{arom} + H_{indole}), 7.74 (d, J = 8.6 Hz, 1H, H_{indole}), 7.96-8.0 (m, 4H, NH + H_{indole} + H_{arom}), 8.22 (d, J = 1.3 Hz, 1H, H_{indole}), 10.40 (s, 1H, NH); **^{13}C NMR** (101 MHz, DMSO-*d*$_6$) δ 165.5 (C=O), 163.8 (C=O), 136.7 (C), 135.1 (C), 135.0 (C), 134.4 (CH), 131.7 (CH), 131.6 (CH), 128.4 (2 x CH), 127.6 (2 x CH), 125.2 (CH_2=), 120.9 (C), 119.5 (CH), 116.1 (CH), 107.8 (C), 102.4 (C), 44.8 (CH), 44.6 (2 x CH_2), 33.2 (CH_3), 30.5 (2 x CH_2); **HRMS (ESI)** calcd for $C_{24}H_{27}N_4O_4S$ $[M+H]^+$, 467.1748; found, 467.1733.

1-Methyl-7-nitroindole (73), CAS 101489-23-0

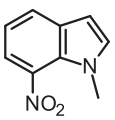

Following general procedure **A** (no flash column chromatography purification), the compound **73** was obtained as a yellow solid. **Molecular Formula**: $C_9H_8N_2O_2$; **MW**: 176.17 g/mol; **Yield**: 100%; **Mp**: 51°C (Lit. 48 °C);[170] **^{1}H NMR** (300 MHz, DMSO-*d*$_6$) δ 3.79 (s, 3H, CH_3), 6.72 (d, J = 3.2 Hz, 1H, H_{indole}), 7.19 (t, J = 7.8 Hz, 1H, H_{indole}), 7.55 (d, J = 3.2 Hz, 1H, H_{indole}), 7.81 (dd, J = 7.8, 0.7 Hz, 1H, H_{indole}), 7.96 (dd, J = 7.8, 1.0 Hz, 1H, H_{indole}); **^{13}C NMR** (101 MHz, DMSO-*d*$_6$) δ 136.1 (C), 134.6 (CH), 133.1 (C), 127.0 (CH), 126.6 (C), 119.1 (CH), 118.4 (CH), 102.2 (CH), 36.6 (CH_3).

1-Methyl-7-nitroindole-3-sulfonyl chloride (74)

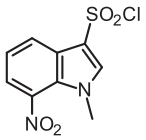

Following general procedure **B - method 2**, the compound **74** was obtained as a light-yellow solid. **Molecular Formula**: $C_9H_7ClN_2O_4S$; **MW**: 274.68 g/mol; **Yield**: 79%; **Mp**: 58-60ºC (washing CH_2Cl_2); **^{1}H NMR** (300 MHz, DMSO-*d*$_6$) δ 3.74 (s, 3H, CH_3), 7.22 (t, J = 7.9 Hz, 1H, H_{indole}), 7.59 (s, 1H, H_{indole}), 7.81 (dd, J = 7.9, 0.7 Hz, 1H, H_{indole}), 8.17 (dd, J = 7.9, 1.1 Hz, 1H, H_{indole}); **^{13}C NMR** (101 MHz, $CDCl_3$) δ 138.1 (CH), 137.7 (C), 127.7 (C), 127.1 (C), 125.8 (CH), 123.2 (CH), 122.2 (CH), 120.0 (C), 39.1 (CH_3).

***Tert*-butyl *N*-[1-(1-Methyl-7-nitroindole-3-sulfonyl)piperidin-4-yl]carbamate (75)**

Following general procedure **F - work-up 2** (no flash column chromatography purification; instead, the crude extracts were concentrated to dryness, and precipitated

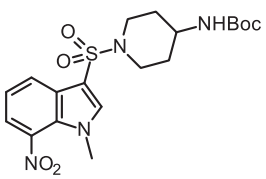

from EtOH), the compound **75** was obtained as a light-yellow solid. **Molecular Formula**: $C_{19}H_{26}N_4O_6S$; **MW**: 438.50 g/mol; **Yield**: 86%; **Mp**: > 210°C (EtOH); **^{1}H NMR** (300 MHz, DMSO-*d*$_6$) δ 1.33 (s, 9H, 3 x CH_3), 1.35-1.50 (m, 2H, $CH_{2piperidine}$), 1.69-1.82 (m, 2H, $CH_{2piperidine}$), 2.52-2.58 (m, 2H, $CH_{2piperidine}$), 3.14-3.28 (m, 1H, $CH_{piperidine}$), 3.43-3.56 (m, 2H, $CH_{2piperidine}$), 3.88 (s, 3H, CH_3), 6.83 (d, J = 7.8 Hz, 1H, NH), 7.41 (t, J = 7.9 Hz, 1H, H_{indole}), 7.96 (dd, J = 7.9, 0.9 Hz, 1H, H_{indole}), 8.18 (dd, J = 7.9, 0.9 Hz, 1H, H_{indole}), 8.27 (s, 1H, H_{indole}); **^{13}C NMR** (101 MHz, DMSO-*d*$_6$) δ 154.7 (C), 138.9 (CH), 136.9 (C), 128.5 (C), 127.0 (C), 125.7 (CH), 121.3 (CH) 120.5 (CH), 109.9 (C), 77.6 (C), 45.8 (CH), 44.4 (2 x CH_2), 37.4 (CH_3), 30.7 (2 x CH_2), 28.2 (3 x CH_3); **LRMS (ESI)**: *m/z* 439.1 $[M+H]^+$, 461.2 $[M+Na]^+$.

Tert-butyl *N*-[1-(7-Amino-1-methylindole-3-sulfonyl)piperidin-4-yl]carbamate (72)

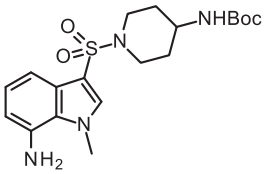

Following general procedure **H - work up 2** (NH_4Cl (0.245 M); no flash column chromatography purification; the crude extract was precipitated from CH_2Cl_2), the compound **72** was obtained as a light-grey solid. **Molecular Formula**: $C_{19}H_{28}N_4O_4S$; **MW**: 408.52 g/mol; **Yield**: 63%; **Mp**: 186-190°C (CH_2Cl_2); **^{1}H NMR** (300 MHz, DMSO-*d*$_6$) δ 1.33 (s, 9H, 3 x CH_3), 1.36-1.48 (m, 2H, $CH_{2piperidine}$), 1.67-1.82 (m, 2H, $CH_{2piperidine}$), 2.30-2.43 (m, 2H, $CH_{2piperidine}$), 3.08-3.23 (m, 1H, $CH_{piperidine}$), 3.40-3.51 (m, 2H, $CH_{2piperidine}$), 4.13 (s, 3H, CH_3), 5.08 (s, 2H, NH_2), 6.52 (d, J = 6.7 Hz, 1H, H_{indole}), 6.82 (d, J = 7.1 Hz, 1H, NH), 6.87 (t, J = 7.7 Hz, 1H, H_{indole}), 7.06 (dd, J = 8.1, 0.9 Hz, 1H, H_{indole}), 7.74 (s, 1H, H_{indole}); **^{13}C NMR** (101 MHz, DMSO-*d*$_6$) δ 154.7 (C), 135.9 (C), 135.0 (CH), 126.8 (C), 126.7 (C), 122.6 (CH), 109.5 (CH) 109.0 (CH), 107.1 (q), 77.6 (C), 46.2 (CH), 44.6 (2 x CH_2), 36.8 (CH_3), 30.7 (2 x CH_2), 28.2 (3 x CH_3); **LRMS (ESI)**: *m/z* 409.1 $[M+H]^+$, 431.2 $[M+Na]^+$.

Tert-butyl *N*-{1-[7-(Benzoylamino)-1-methylindole-3-sulfonyl]piperidin-4-yl}carbamate (76)

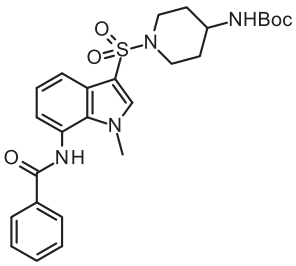

Following general procedure **G - work-up 4**, the compound **76** was obtained as a white solid. **Molecular Formula**: $C_{26}H_{32}N_4O_5S$; **MW**: 512.62 g/mol; **Yield**: 81%; **Mp**: > 210°C (washing CH_2Cl_2); **^{1}H NMR** (300 MHz, DMSO-*d*$_6$) δ 1.34 (s, 9H, 3 x CH_3), 1.37-1.53 (m, 2H, $CH_{2piperidine}$), 1.71-1.86 (m, 2H, $CH_{2piperidine}$), 2.38-2.47 (m, 2H, $CH_{2piperidine}$), 3.13-3.28 (m, 1H, $CH_{piperidine}$), 3.45-3.57 (m, 2H, $CH_{2piperidine}$), 3.95 (s, 3H, CH_3), 6.85 (d, J = 7.5 Hz, 1H, NH), 7.17 (d, J = 7.0 Hz, 1H, H_{indole}), 7.25 (t, J = 7.7 Hz, 1H, H_{indole}), 7.52-7.67 (m, 3H, H_{arom}), 7.76 (dd, J = 7.9, 1.0 Hz, 1H, H_{indole}), 7.98 (s, 1H,

H_{indole}), 8.03 (d, J = 7.5 Hz, 2H, H_{arom}), 10.37 (s, 1H, NH); **LRMS (ESI)**: *m/z* 513.2 $[M+H]^+$.

N-{1-[7-(Benzoylamino)-1-methylindole-3-sulfonyl]piperidin-4-yl}ammonium trifluoroacetate salt (77)

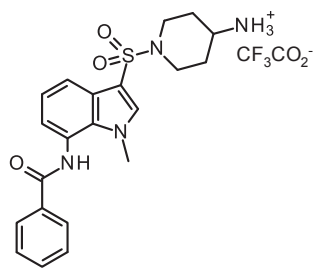

Following general procedure **E**, the compound **77** was obtained as a white solid. **Molecular Formula**: $C_{23}H_{25}F_3N_4O_5S$; **MW**: 526.53 g/mol; **Yield**: 90%; **Mp**: > 210°C (washing Et_2O); **^{1}H NMR** (300 MHz, DMSO-*d*$_6$) δ 1.48-1.66 (m, 2H, $CH_{2piperidine}$), 1.89-2.02 (m, 2H, $CH_{2piperidine}$), 2.33-2.45 (m, 2H, $CH_{2piperidine}$), 3.00-3.17 (m, 1H, $CH_{piperidine}$), 3.65-3.78 (m, 2H, $CH_{2piperidine}$), 3.95 (s, 3H, CH_3), 7.17 (d, J = 7.2 Hz, 1H, H_{indole}), 7.75 (t, J = 7.7 Hz, 1H, H_{indole}), 7.52-7.68 (m, 3H, H_{arom}), 7.77 (dd, J = 7.9, 0.8 Hz, 1H, H_{indole}), 7.85 (s, 3H, NH_3^+), 8.01 (s, 1H, H_{indole}), 8.03 (d, J = 7.7 Hz, 2H, H_{arom}), 10.39 (s, 1H, NH).

N-{1-Methyl-3-[4-(acryloylamino)piperidine-1-sulfonyl]indol-7-yl}benzamide (71)

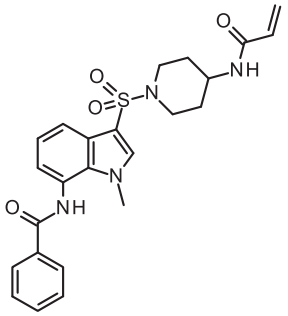

Following general procedure **G - work-up 3** (flash column chromatography solvent: MeOH/CH_2Cl_2 3:97), the resultant product was precipitated from MeOH to give **71** as a white solid. **Molecular Formula**: $C_{24}H_{26}N_4O_4S$; **MW**: 466.55 g/mol; **Yield**: 70%; **Mp**: > 210°C (MeOH); **^{1}H NMR** (300 MHz, DMSO-*d*$_6$) δ 1.39-1.56 (m, 2H, $CH_{2piperidine}$), 1.78-1.92 (m, 2H, $CH_{2piperidine}$), 2.54-2.65 (m, 2H, $CH_{2piperidine}$), 3.45-3.68 (m, 3H, $CH_{piperidine}$ + $CH_{2piperidine}$), 3.96 (s, 3H, CH_3), 5.54 (dd, J = 9.8, 2.5 Hz, 1H, CH_2= cis), 6.03 (dd, J = 17.1, 2.5 Hz, 1H, CH_2= trans), 6.17 (dd, J = 17.1, 9.8 Hz, 1H, CH=), 7.17 (d, J = 6.7 Hz, 1H, H_{indole}), 7.26 (t, J = 7.7 Hz, 1H, H_{indole}), 7.52-7.68 (m, 3H, H_{arom}), 7.77 (dd, J = 8.0, 1.1 Hz, 1H, H_{indole}), 8.00 (s, 1H, H_{indole}), 8.03 (d, J = 7.3 Hz, 2H, H_{arom}), 8.05 (d, J = 6.5 Hz, 1H, NH), 10.37 (s, 1H, NH); **^{13}C NMR** (101 MHz, DMSO-*d*$_6$) δ 167.1 (C=O), 163.8 (C=O), 136.2 (CH), 134.0 (C), 132.7 (C), 131.9 (CH), 131.7 (CH), 128.7 (2 x CH), 127.7 (2 x CH), 126.7 (C), 125.2 (CH_2=), 123.7 (CH), 123.4 (C), 121.9 (CH), 118.6 (CH), 108.1 (C), 44.7 (CH), 44.5 (2 x CH_2), 35.7 (CH_3), 30.5 (2 x CH_2); **HRMS (ESI)** calcd for $C_{24}H_{27}N_4O_4S$ $[M+H]^+$, 467.1748; found, 467.1726.

Tert-butyl *N*-{1-[7-(3,4-Dimethoxybenzoylamino)-1-methylindole-3-sulfonyl]piperidin-4-yl}carbamate (79f)

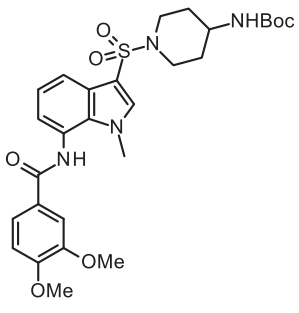

Following general procedure **G - work-up 4**, the compound **79f** was obtained as a white solid. **Molecular Formula**:

$C_{28}H_{36}N_4O_7S$; **MW**: 572.67 g/mol; **Yield**: 88%; **Mp**: 160-164°C (washing CH_2Cl_2); **^{1}H NMR** (300 MHz, DMSO-*d_6*) δ 1.34 (s, 9H, 3 x CH_3), 1.38-1.52 (m, 2H, $CH_{2piperidine}$), 1.71-1.85 (m, 2H, $CH_{2piperidine}$), 2.36-2.45 (m, 2H, $CH_{2piperidine}$), 3.11-3.25 (m, 1H, $CH_{piperidine}$), 3.45-3.57 (m, 2H, $CH_{2piperidine}$), 3.84 (s, 6H, 2 x OCH_3), 3.94 (s, 3H, CH_3), 6.85 (d, J = 6.7 Hz, 1H, NH), 7.12 (d, J = 8.4 Hz, 1H, H_{arom}), 7.16 (d, J = 7.4 Hz, 1H, H_{indole}), 7.25 (t, J = 7.7 Hz, 1H, H_{indole}), 7.60 (d, J = 1.8 Hz, 1H, H_{arom}), 7.69 (dd, J = 8.4, 1.8 Hz, 1H, H_{arom}), 7.75 (dd, J = 8.0, 0.6 Hz, 1H, H_{indole}), 7.97 (s, 1H, H_{indole}), 10.22 (s, 1H, NH); **^{13}C NMR** (101 MHz, DMSO-*d_6*) δ 166.4 (C=O), 154.8 (C=O), 151.8 (C), 148.5 (C), 136.2 (CH), 132.7 (C), 126.7 (C), 126.0 (C), 123.7 (C), 123.6 (CH), 121.9 (CH), 121.0 (CH), 118.4 (CH), 111.1 (CH), 110.9 (CH), 108.0 (C), 77.6 (C), 55.7 (CH_3), 55.6 (CH_3), 46.1 (CH), 44.6 (2 x CH_2), 35.7 (CH_3), 30.8 (2 x CH_2), 28.2 (3 x CH_3); **LRMS (ESI)**: *m/z* 573.2 $[M+H]^+$, 595.2 $[M+Na]^+$.

Tert-butyl *N*-{1-[7-(3-Methoxybenzoylamino)-1-methylindole-3-sulfonyl]piperidin-4-yl}carbamate (79a)

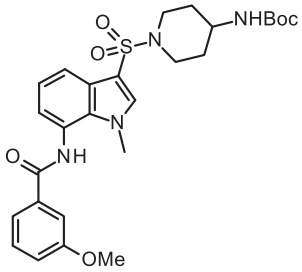

Following general procedure **G - work-up 2** (The crude extracts were precipitated, filtrated and washed with EtOH. The mother waters were also purified by means of flash column chromatography, solvent: MeOH in CH_2Cl_2 3:97), the resultant product was precipitated from EtOH to give **79a** as a white solid. **Molecular Formula**: $C_{27}H_{34}N_4O_6S$; **MW**: 542.66 g/mol; **Yield**: 77%; **Mp**: > 210°C (EtOH); **^{1}H NMR** (300 MHz, DMSO-*d_6*) δ 1.39 (s, 9H, 3 x CH_3), 1.37-1.52 (m, 2H, $CH_{2piperidine}$), 1.70-1.85 (m, 2H, $CH_{2piperidine}$), 2.38-2.47 (m, 2H, $CH_{2piperidine}$), 3.13-3.27 (m, 1H, $CH_{piperidine}$), 3.46-3.56 (m, 2H, $CH_{2piperidine}$), 3.84 (s, 3H, OCH_3), 3.94 (s, 3H, CH_3), 6.84 (d, J = 6.5 Hz, 1H, NH), 7.17 (d, J = 7.2 Hz, 1H, H_{indole}), 7.19 (dd, J = 7.9, 1.7 Hz, 1H, H_{arom}), 7.25 (t, J = 7.7 Hz, 1H, H_{indole}), 7.48 (t, J = 7.9 Hz, 1H, H_{arom}), 7.56 (s, 1H, H_{arom}), 7.61 (d, J = 7.9 Hz, 1H, H_{arom}), 7.73 (dd, J = 8.0, 0.9 Hz, 1H, H_{indole}), 7.98 (s, 1H, H_{indole}), 10.35 (s, 1H, NH); **LRMS (ESI)**: *m/z* 543.2 $[M+H]^+$.

Tert-butyl *N*-{1-[7-(3-Chlorobenzoylamino)-1-methylindole-3-sulfonyl]piperidin-4-yl}carbamate (79b)

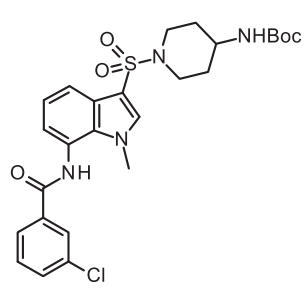

Following general procedure **G - work-up 2** (The crude extracts were precipitated, filtrated and washed with EtOH. The mother waters were also purified by means of flash column chromatography, solvent: MeOH in CH_2Cl_2 2:98), the resultant product was precipitated from EtOH to give **79b** as a white solid. **Molecular Formula**: $C_{26}H_{31}ClN_4O_5S$; **MW**: 547.07 g/mol; **Yield**: 62%; **Mp**: > 210°C (EtOH); **^{1}H NMR** (300 MHz, DMSO-*d_6*) δ 1.34 (s, 9H, 3 x CH_3), 1.38-1.52 (m, 2H, $CH_{2piperidine}$), 1.72-

1.84 (m, 2H, $CH_{2piperidine}$), 2.37-2.47 (m, 2H, $CH_{2piperidine}$), 3.11-3.28 (m, 1H, $CH_{piperidine}$), 3.45-3.57 (m, 2H, $CH_{2piperidine}$), 3.94 (s, 3H, CH_3), 6.84 (d, J = 6.8 Hz, 1H, NH), 7.17 (d, J = 7.2 Hz, 1H, H_{indole}), 7.25 (t, J = 7.7 Hz, 1H, H_{indole}), 7.61 (t, J = 7.8 Hz, 1H, H_{arom}), 7.71 (d, J = 7.8 Hz, 1H, H_{arom}), 7.77 (dd, J = 7.9, 1.1 Hz, 1H, H_{indole}), 7.98 (s, 1H, H_{indole}), 7.99 (d, J = 7.8 Hz, 1H, H_{arom}), 8.06 (s, 1H, H_{arom}), 10.49 (s, 1H, NH); **^{13}C NMR** (126 MHz, DMSO-*d_6*) δ 165.7 (C=O), 154.8 (C=O), 136.2 (CH), 136.0 (C), 133.5 (C), 132.5 (C), 131.7 (CH), 130.7 (CH), 127.5 (CH), 126.7 (C), 126.4 (CH), 123.5 (CH), 123.0 (C), 121.9 (CH), 118.7 (CH), 108.2 (C), 77.6 (C), 46.0 (CH), 44.5 (2 x CH_2), 35.6 (CH_3), 30.8 (2 x CH_2), 28.2 (3 x CH_3); **LRMS (ESI)**: *m/z* 569.2 $[M+Na]^+$.

Tert-butyl *N*-{1-[7-(3-Nitrobenzoylamino)-1-methylindole-3-sulfonyl]piperidin-4-yl}carbamate (79c)

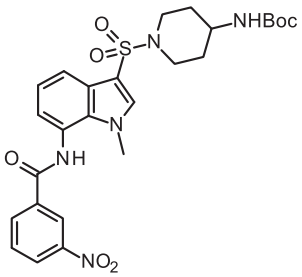

Following general procedure **G - work-up 2** (flash column chromatography solvent: MeOH in CH_2Cl_2 2:98) the resultant product was precipitated from Et_2O to give **79c** as a light yellow solid. **Molecular Formula**: $C_{26}H_{31}N_5O_7S$; **MW**: 557.62 g/mol; **Yield**: 98%; **Mp**: 145-147°C (Et_2O); **^{1}H NMR** (300 MHz, DMSO-*d_6*) δ 1.34 (s, 9H, 3 x CH_3), 1.36-1.53 (m, 2H, $CH_{2piperidine}$), 1.71-1.85 (m, 2H, $CH_{2piperidine}$), 2.39-2.47 (m, 2H, $CH_{2piperidine}$), 3.13-3.28 (m, 1H, $CH_{piperidine}$), 3.45-3.59 (m, 2H, $CH_{2piperidine}$), 3.94 (s, 3H, CH_3), 6.85 (d, J = 7.2 Hz, 1H, NH), 7.22 (d, J = 6.9 Hz, 1H, H_{indole}), 7.27 (t, J = 7.6 Hz, 1H, H_{indole}), 7.78 (dd, J = 7.8, 1.3 Hz, 1H, H_{indole}), 7.89 (t, J = 8.0 Hz, 1H, H_{arom}), 7.99 (s, 1H, H_{indole}), 8.43-8.53 (m, 2H, H_{arom}), 8.85 (t, J = 1.8 Hz, 1H, H_{arom}), 10.75 (s, 1H, NH); **^{13}C NMR** (101 MHz, DMSO-*d_6*) δ 165.1 (C=O), 154.8 (C=O), 148.0 (C), 136.3 (CH), 135.4 (C), 134.0 (CH), 132.5 (C), 130.5 (CH), 126.8 (C), 126.5 (CH), 123.5 (CH), 122.8 (C), 122.5 (CH), 121.9 (CH), 118.9 (CH), 108.2 (C), 77.6 (C), 46.0 (CH), 44.5 (2 x CH_2), 35.6 (CH_3), 30.8 (2 x CH_2), 28.2 (3 x CH_3); **LRMS (ESI)**: *m/z* 558.2 $[M+H]^+$.

Tert-butyl *N*-{1-[7-(4-Methoxybenzoylamino)-1-methylindole-3-sulfonyl]piperidin-4-yl}carbamate (79d)

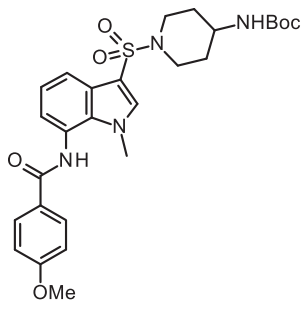

Following general procedure **G - work-up 2** (flash column chromatography solvent: MeOH/CH_2Cl_2 2-3:97-98) the resultant product was precipitated from MeOH to give **79d** as a white solid. **Molecular Formula**: $C_{27}H_{34}N_4O_6S$; **MW**: 542.65 g/mol; **Yield**: 67%; **Mp**: > 210°C (MeOH); **^{1}H NMR** (300 MHz, DMSO-*d_6*) δ 1.34 (s, 9H, 3 x CH_3), 1.39-1.53 (m, 2H, $CH_{2piperidine}$), 1.71-1.85 (m, 2H, $CH_{2piperidine}$), 2.38-2.47 (m, 2H, $CH_{2piperidine}$), 3.12-3.27 (m, 1H, $CH_{piperidine}$), 3.45-3.57 (m, 2H, $CH_{2piperidine}$), 3.85 (s, 3H, CH_3, OCH_3), 3.93 (s, 3H, CH_3),

6.85 (d, J = 8.2 Hz, 1H, NH), 7.09 (d, J = 8.9 Hz, 2H, H_{arom}), 7.15 (dd, J = 7.5, 1.1 Hz, 1H, H_{indole}), 7.24 (t, J = 7.7 Hz, 1H, H_{indole}), 7.75 (dd, J = 8.1, 1.1 Hz, 1H, H_{indole}), 7.96 (s, 1H, H_{indole}), 8.01 (d, J = 8.9 Hz, 2H, H_{arom}), 10.21 (s, 1H, NH); **LRMS (ESI)**: *m/z* 543.2 $[M+H]^+$.

***Tert*-butyl *N*-{1-[7-(4-Chlorobenzoylamino)-1-methylindole-3-sulfonyl]piperidin-4-yl}carbamate (79e)**

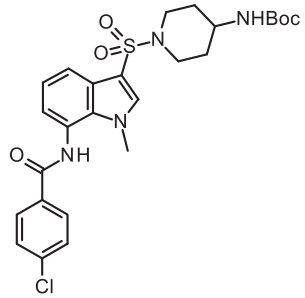

Following general procedure **G - work-up 2** (flash column chromatography solvent: MeOH/CH_2Cl_2 3:97), the resultant product was precipitated from PE/EtOH (few drops of EtOH) to give **79e** as a white solid. **Molecular Formula**: $C_{26}H_{31}ClN_4O_5S$; **MW**: 547.07 g/mol; **Yield**: 53%; **Mp**: > 210°C (PE/EtOH); **^{1}H NMR** (300 MHz, DMSO-d_6) δ 1.34 (s, 9H, 3 x CH_3), 1.37-1.52 (m, 2H, $CH_{2piperidine}$), 1.71-1.84 (m, 2H, $CH_{2piperidine}$), 2.38-2.47 (m, 2H, $CH_{2piperidine}$), 3.11-3.27 (m, 1H, $CH_{piperidine}$), 3.45-3.58 (m, 2H, $CH_{2piperidine}$), 3.93 (s, 3H, CH_3), 6.84 (d, J = 7.1 Hz, 1H, NH), 7.17 (d, J = 7.0 Hz, 1H, H_{indole}), 7.25 (t, J = 7.7 Hz, 1H, H_{indole}), 7.65 (d, J = 8.6 Hz, 2H, H_{arom}), 7.76 (dd, J = 7.9, 1.0 Hz, 1H, H_{indole}), 7.98 (s, 1H, H_{indole}), 8.04 (d, J = 8.6 Hz, 2H, H_{arom}), 10.44 (s, 1H, NH); **LRMS (ESI)**: *m/z* 569.2 $[M+Na]^+$.

***Tert*-butyl *N*-{1-[7-(Pyridine-3-carbonylamino)-1-methylindole-3-sulfonyl]piperidin-4-yl}carbamate (79h)**

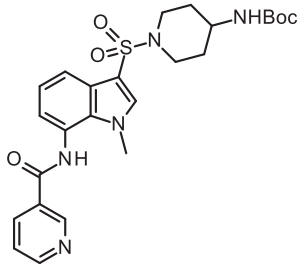

Following general procedure **G - work-up 3** (solvents: CH_2Cl_2 (0.1 M) and DMF (0.183 M); after completion of the reaction, evaporation of CH_2Cl_2 and pouring the remaining reaction mixture in DMF into a flask containing water. The precipitate formed was filtrated, the resulting solid washed with water and dried under vacuum with P_2O_5; flash column chromatography solvent: MeOH/CH_2Cl_2 5:95), the compound **79h** was obtained as a white solid. **Molecular Formula**: $C_{25}H_{31}N_5O_5S$; **MW**: 513.61 g/mol; **Yield**: 42%; **Mp**: 165-167°C; **^{1}H NMR** (300 MHz, DMSO-d_6) δ 1.34 (s, 9H, 3 x CH_3), 1.37-1.52 (m, 2H, $CH_{2piperidine}$), 1.72-1.84 (m, 2H, $CH_{2piperidine}$), 2.42-2.50 (m, 2H, $CH_{2piperidine}$), 3.13-3.27 (m, 1H, $CH_{piperidine}$), 3.45-3.57 (m, 2H, $CH_{2piperidine}$), 3.96 (s, 3H, CH_3), 6.85 (d, J = 6.7 Hz, 1H, NH), 7.21 (t, J = 6.4 Hz, 1H, H_{indole}), 7.26 (t, J = 7.7 Hz, 1H, H_{indole}), 7.61 (dd, J = 7.8, 4.8 H, 1H, H_{pyr}), 7.77 (dd, J = 7.8, 1.2 Hz, 1H, H_{indole}), 7.99 (s, 1H, H_{indole}), 8.36 (dt, J = 7.8, 1.7 Hz, 1H, H_{pyr}), 8.81 (dd, J = 4.8, 1.7 Hz, 1H, H_{pyr}), 9.19 (d, J = 1.7 Hz, 1H, H_{pyr}); **LRMS (ESI)**: *m/z* 514.2 $[M+H]^+$.

***Tert*-butyl *N*-{1-[7-(Naphthalene-2-carbonylamino)-1-methylindole-3-sulfonyl]piperidin-4-yl}carbamate (79i)**

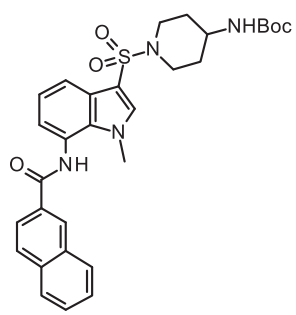

Following general procedure **G - work-up 4** (the resulting solid was purified by flash column chromatography, solvent: MeOH/CH_2Cl_2 2:98), the compound **79i** was obtained as a white solid. **Molecular Formula**: $C_{30}H_{34}N_4O_5S$; **MW**: 562.68 g/mol; **Yield**: 78%; **Mp**: 130-135°C; **^{1}H NMR** (300 MHz, DMSO-*d_6*) δ 1.34 (s, 9H, 3 x CH_3), 1.33-1.55 (m, 2H, $CH_{2piperidine}$), 1.72-1.86 (m, 2H, $CH_{2piperidine}$), 2.40-2.59 (m, 2H, $CH_{2piperidine}$), 3.12-3.32 (m, 1H, $CH_{piperidine}$), 3.45-3.60 (m, 2H, $CH_{2piperidine}$), 3.99 (s, 3H, CH_3), 6.86 (d, J = 7.3 Hz, 1H, NH), 7.22 (d, J = 6.7 Hz, 1H, H_{indole}), 7.28 (t, J = 7.6 Hz, 1H, H_{indole}), 7.60-7.76 (m, 2H, H_{napht}), 7.78 (dd, J = 7.8, 1.2 Hz, 1H, H_{napht}), 8.00 (s, 1H, H_{indole}), 8.15-8.02 (m, 4H, H_{indole} + H_{napht}), 8.66 (s, 1H, H_{napht}), 10.55 (s, 1H, NH); **LRMS (ESI)**: *m/z* 563.2 $[M+H]^+$, 585.2 $[M + Na]^+$.

Tert-butyl _N_-{1-[7-(3,4-(Dimethoxyphenylacetylamino)-1-methylindole-3-sulfonyl]piperidin-4-yl}carbamate (79g)

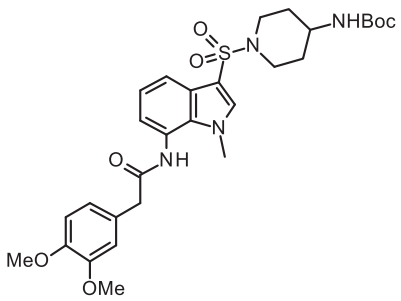

Following general procedure **G - work-up 2** (flash column chromatography solvent: MeOH/CH_2Cl_2 2:98), the resultant product was precipitated from Et_2O to give **79g** as a white solid. **Molecular Formula**: $C_{29}H_{38}N_4O_7S$; **MW**: 586.70 g/mol; **Yield**: 48%; **Mp**: 130-135°C (Et_2O); **^{1}H NMR** (300 MHz, DMSO-*d_6*) δ 1.32 (s, 9H, 3 x CH_3), 1.30-1.50 (m, 2H, $CH_{2piperidine}$), 1.69-1.82 (m, 2H, $CH_{2piperidine}$), 2.30-2.60 (m, 2H, $CH_{2piperidine}$), 3.10-3.28 (m, 1H, $CH_{piperidine}$), 3.41-3.54 (m, 2H, $CH_{2piperidine}$), 3.32 (s, 2H, CH_2), 3.72 (s, 3H, OCH_3), 3.73 (s, 3H, OCH_3), 3.75 (s, 3H, CH_3), 6.82 (d, J = 6.2 Hz, 1H, NH), 6.86-6.97 (m, 2H, H_{arom}), 6.99 (d, J = 1.5 Hz, 1H, H_{arom}), 7.03 (d, J = 7.4 Hz, 1H, H_{indole}), 7.17 (t, J = 7.7 Hz, 1H, H_{indole}), 7.67 (d, J = 7.7 Hz, 1H, H_{indole}), 7.87 (s, 1H, H_{indole}), 9.90 (s, 1H, NH); **LRMS (ESI)**: *m/z* 587.2 $[M+H]^+$.

Tert-butyl _N_-(1-{7-[(Adamantan-1-yl)carbonylamino]-1-methylindole-3-sulfonyl}piperidin-4-yl)carbamate (79k)

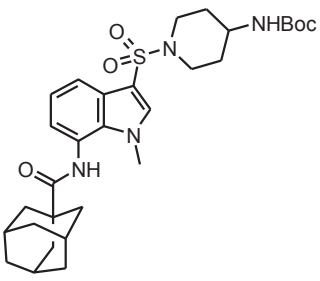

Following general procedure **G - work-up 5**, the resultant dried residue was precipitated from MeOH, filtrated, and precipitated from MeOH, to give **79k** as a light-orange solid. **Molecular Formula**: $C_{30}H_{42}N_4O_5S$; **MW**: 570.74 g/mol; **Yield**: 83%; **Mp**: > 210°C (MeOH); **^{1}H NMR** (300 MHz, DMSO-*d_6*) δ 1.33 (s, 9H, 3 x CH_3), 1.31-1.51 (m, 2H, $CH_{2piperidine}$), 1.66-1.84 (m, 8H, $CH_{2piperidine}$ + $H_{adamant}$), 1.90-2.00 (m, 6H, $H_{adamant}$), 2.00-2.10 (m, 3H, $H_{adamant}$), 2.31-2.55 (m, 2H, $CH_{2piperidine}$), 3.08-3.25 (m, 1H, $CH_{piperidine}$), 3.44-3.55 (m, 2H, $CH_{2piperidine}$), 3.92 (s, 3H, CH_3), 6.83 (d, J =

6.2 Hz, 1H, NH), 6.96 (d, J = 7.7 Hz, 1H, H_{indole}), 7.18 (t, J = 7.7 Hz, 1H, H_{indole}), 7.69 (d, J = 7.7 Hz, 1H, H_{indole}), 7.94 (s, 1H, H_{indole}), 9.33 (s, 1H, NH); **LRMS (ESI)**: *m/z* 571.3 $[M+H]^+$.

***Tert*-butyl *N*-{1-[7-(Quinoline-2-carbonylamino)-1-methylindole-3-sulfonyl]piperidin-4-yl}carbamate (79j)**

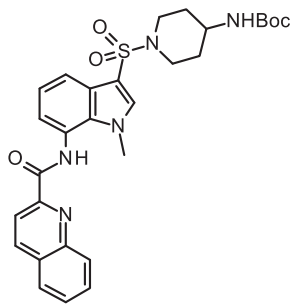

Following general procedure **G - work-up 4** (the resulting solid was purified by flash column chromatography, solvent: MeOH/CH_2Cl_2 2:98), the compound **79j** was obtained as a light-yellow solid. **Molecular Formula**: $C_{29}H_{33}N_5O_5S$; **MW**: 563.67 g/mol; **Yield**: 81%; **Mp**: > 210°C; **^{1}H NMR** (300 MHz, DMSO-d_6) δ 1.34 (s, 9H, 3 x CH_3), 1.32-1.57 (m, 2H, $CH_{2piperidine}$), 1.70-1.87 (m, 2H, $CH_{2piperidine}$), 2.32-2.67 (m, 2H, $CH_{2piperidine}$), 3.10-3.30 (m, 1H, $CH_{piperidine}$), 3.45-3.60 (m, 2H, $CH_{2piperidine}$), 4.10 (s, 3H, CH_3), 6.85 (d, J = 7.4 Hz, 1H, NH), 7.27 (t, J = 7.7 Hz, 1H, H_{indole}), 7.42 (d, J = 7.3 Hz, 1H, H_{indole}), 7.75 (d, J = 7.4 Hz, 1H, H_{indole}), 7.78 (dt, J = 8.0, 1.0 Hz, 1H, H_{quinol}), 7.93 (dt, J = 8.3, 1.4 Hz, 1H, H_{quinol}), 8.00 (s, 1H, H_{indole}), 8.15 (d, J = 7.8 Hz, 1H, H_{quinol}), 8.22 (d, J = 8.3 Hz, 1H, H_{quinol}), 8.26 (d, J = 8.4 Hz, 1H, H_{quinol}), 8.66 (d, J = 8.4 Hz, 1H, H_{quinol}), 11.05 (s, 1H, NH); **LRMS (ESI)**: *m/z* 564.2 $[M+H]^+$.

***N*-{1-[7-(3,4-Dimethoxybenzoylamino)-1-methylindole-3-sulfonyl]piperidin-4-yl}ammonium trifluoroacetate salt (80f)**

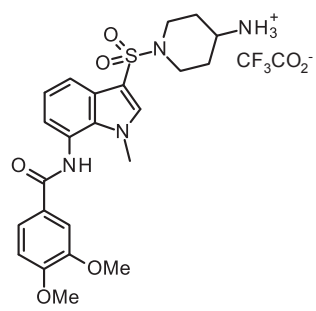

Following general procedure **E**, the compound **80f** was obtained as a white solid. **Molecular Formula**: $C_{25}H_{29}F_3N_4O_7S$; **MW**: 586.58 g/mol; **Yield**: 100%; **Mp**: 158-160°C (washing Et_2O); **^{1}H NMR** (300 MHz, DMSO-d_6) δ 1.48-1.66 (m, 2H, $CH_{2piperidine}$), 188-2.01 (m, 2H, $CH_{2piperidine}$), 2.32-2.45 (m, 2H, $CH_{2piperidine}$), 2.98-3.15 (m, 1H, $CH_{piperidine}$), 3.65-3.77 (m, 2H, $CH_{2piperidine}$), 3.84 (s, 6H, 2 x OCH_3), 3.93 (s, 3H, CH_3), 7.12 (d, J = 8.5 Hz, 1H, H_{arom}), 7.16 (d, J = 7.2 Hz, 1H, H_{indole}), 7.26 (t, J = 7.7 Hz, 1H, H_{indole}), 7.59 (d, J = 2.0 Hz, 1H, H_{arom}), 7.67 (dd, J = 8.3, 1.9 Hz, 1H, H_{arom}), 7.76 (dd, J = 7.9, 0.8 Hz, 1H, H_{indole}), 7.84 (s, 3H, NH_3^+), 8.00 (s, 1H, H_{indole}), 10.24 (s, 1H, NH).

***N*-{1-[7-(3-Methoxybenzoylamino)-1-methylindole-3-sulfonyl]piperidin-4-yl}ammonium trifluoroacetate salt (80a)**

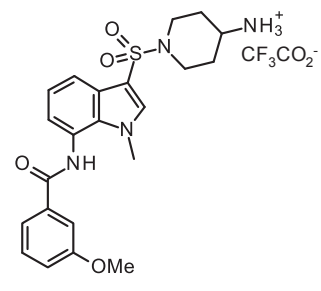

Following general procedure **E**, the compound **80a** was obtained as a white solid. **Molecular Formula**:

$C_{24}H_{27}F_3N_4O_6S$; **MW**: 556.55 g/mol; **Yield**: 100%; **Mp**: > 210°C (washing Et_2O); **^{1}H NMR** (300 MHz, DMSO-*d_6*) δ 1.48-1.67 (m, 2H, $CH_{2piperidine}$), 1.89-2.01 (m, 2H, $CH_{2piperidine}$), 2.33-2.46 (m, 2H, $CH_{2piperidine}$), 2.98-3.15 (m, 1H, $CH_{piperidine}$), 3.64-3.77 (m, 2H, $CH_{2piperidine}$), 3.84 (s, 3H, CH_3, OCH_3), 3.95 (s, 3H, CH_3), 7.17 (d, J = 7.9 Hz, 1H, H_{indole}), 7.19 (dd, J = 8.1, 1.7 Hz, 1H, H_{arom}), 7.26 (t, J = 7.7 Hz, 1H, H_{indole}), 7.48 (t, J = 7.9 Hz, 1H, H_{arom}), 7.56 (s, 1H, H_{arom}), 7.61 (d, J = 7.4 Hz, 1H, H_{arom}), 7.70 (dd, J = 7.8, 1.0 Hz, 1H, H_{indole}), 7.84 (br s, 3H, NH_3^+), 8.01 (s, 1H, H_{indole}), 10.37 (s, 1H, NH).

N-{1-[7-(3-Chlorobenzoylamino)-1-methylindole-3-sulfonyl]piperidin-4-yl}ammonium trifluoroacetate salt (80b)

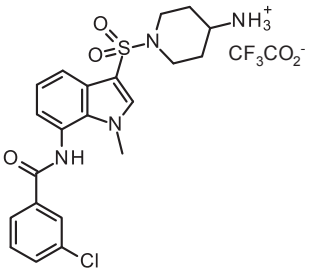

Following general procedure **E**, compound **80b** was obtained as a white solid. **Molecular Formula**: $C_{23}H_{24}ClF_3N_4O_5S$; **MW**: 560.97 g/mol; **Yield**: 97%; **Mp**: > 210°C (washing Et_2O); **^{1}H NMR** (300 MHz, DMSO-*d_6*) δ 1.48-1.66 (m, 2H, $CH_{2piperidine}$), 1.89-2.01 (m, 2H, $CH_{2piperidine}$), 2.34-2.46 (m, 2H, $CH_{2piperidine}$), 2.98-3.17 (m, 1H, $CH_{piperidine}$), 3.64-3.77 (m, 2H, $CH_{2piperidine}$), 3.94 (s, 3H, CH_3), 7.17 (d, J = 7.2 Hz, 1H, H_{indole}), 7.27 (t, J = 7.8 Hz, 1H, H_{indole}), 7.62 (t, J = 7.9 Hz, 1H, H_{arom}), 7.72 (d, J = 9.0 Hz, 1H, H_{arom}), 7.78 (dd, J = 7.9, 1.1 Hz, 1H, H_{indole}), 7.84 (br s, 3H, NH_3^+), 7.98 (d, J = 7.8 Hz, 1H, H_{arom}), 8.01 (s, 1H, H_{indole}), 8.06 (s, 1H, H_{arom}), 10.51 (s, 1H, NH).

N-{1-[7-(3-Nitrobenzoylamino)-1-methylindole-3-sulfonyl]piperidin-4-yl}ammonium trifluoroacetate salt (80c)

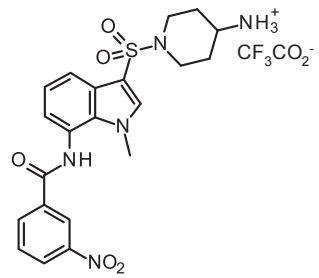

Following general procedure **E**, compound **80c** was obtained as a pale white solid. **Molecular Formula**: $C_{23}H_{24}F_3N_5O_7S$; **MW**: 571.53 g/mol; **Yield**: 100%; **Mp**: > 210°C (washing Et_2O); **^{1}H NMR** (300 MHz, DMSO-*d_6*) δ 1.48-1.66 (m, 2H, $CH_{2piperidine}$), 1.87-2.02 (m, 2H, $CH_{2piperidine}$), 2.33-2.46 (m, 2H, $CH_{2piperidine}$), 2.99-3.17 (m, 1H, $CH_{piperidine}$), 3.65-3.78 (m, 2H, $CH_{2piperidine}$), 3.95 (s, 3H, CH_3), 7.22 (d, J = 6.9 Hz, 1H, H_{indole}), 7.29 (t, J = 7.7 Hz, 1H, H_{indole}), 7.80 (dd, J = 7.8, 1.0 Hz, 1H, H_{indole}), 7.86 (br s, 3H, NH_3^+), 7.90 (t, J = 8.0 Hz, 1H, H_{arom}), 8.03 (s, 1H, H_{indole}), 8.42-8.54 (m, 2H, H_{arom}), 8.84 (t, J = 1.8 Hz, 1H, H_{arom}), 10.78 (s, 1H, NH).

N-{1-[7-(4-Methoxybenzoylamino)-1-methylindole-3-sulfonyl]piperidin-4-yl}ammonium trifluoroacetate salt (80d)

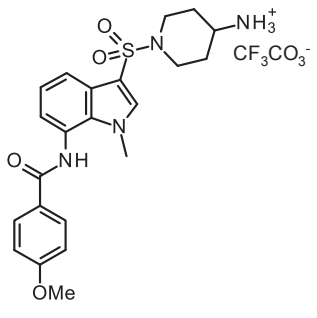

Following general procedure **E**, the compound **80d** was obtained as a white solid. **Molecular Formula**: $C_{24}H_{27}F_3N_4O_6S$; **MW**: 556.55 g/mol; **Yield**: 99%; **Mp**: >

210°C (washing Et_2O); **^{1}H NMR** (300 MHz, DMSO-*d_6*) δ 1.48-1.66 (m, 2H, $CH_{2piperidine}$), 1.89-2.01 (m, 2H, $CH_{2piperidine}$), 2.32-2.46 (m, 2H, $CH_{2piperidine}$), 2.99-3.15 (m, 1H, $CH_{piperidine}$), 3.65-3.77 (m, 2H, $CH_{2piperidine}$), 3.85 (s, 3H, OCH_3), 3.92 (s, 3H, CH_3), 7.10 (d, J = 8.9 Hz, 2H, H_{arom}), 7.15 (d, J = 7.3 Hz, 1H, H_{indole}), 7.25 (t, J = 7.7 Hz, 1H, H_{indole}), 7.76 (dd, J = 8.1, 0.9 Hz, 1H, H_{indole}), 7.84 (br s, 3H, NH_3^+), 8.00 (s, 1H, H_{indole}), 8.01 (d, J = 8.9 Hz, 2H, H_{arom}), 10.23 (s, 1H, NH).

N-{1-[7-(4-Chlorobenzoylamino)-1-methylindole-3-sulfonyl]piperidin-4-yl}ammonium trifluoroacetate salt (80e)

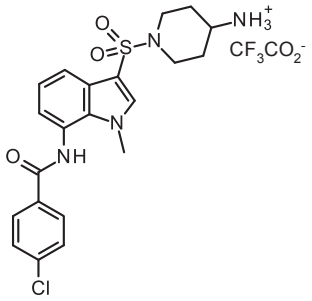

Following general procedure **E**, the compound **80e** was obtained as a white-salmon coloured solid. **Molecular Formula**: $C_{23}H_{24}ClF_3N_4O_5S$; **MW**: 560.97 g/mol; **Yield**: 93%; **Mp**: > 210°C (washing Et_2O); **^{1}H NMR** (300 MHz, DMSO-*d_6*) δ 1.48-1.65 (m, 2H, $CH_{2piperidine}$), 1.86-2.02 (m, 2H, $CH_{2piperidine}$), 2.34-2.46 (m, 2H, $CH_{2piperidine}$), 3.00-3.14 (m, 1H, $CH_{piperidine}$), 3.65-3.77 (m, 2H, $CH_{2piperidine}$), 3.93 (s, 3H, CH_3), 7.17 (d, J = 7.3 Hz, 1H, H_{indole}), 7.26 (t, J = 7.7 Hz, 1H, H_{indole}), 7.66 (d, J = 8.6 Hz, 2H, H_{arom}), 7.78 (dd, J = 7.9, 0.8 Hz, 1H, H_{indole}), 7.82 (br s, 3H, NH_3^+), 8.01 (s, 1H, H_{indole}), 8.04 (d, J = 8.6 Hz, 2H, H_{arom}), 10.47 (s, 1H, NH).

N-{1-[7-(Pyridin-3-carbonylamino)-1-methylindole-3-sulfonyl]piperidin-4-yl}ammonium trifluoroacetate salt (80h)

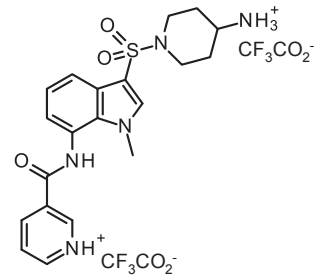

Following general procedure **E**, the compound **80h** was obtained as a light-grey coloured solid. **Molecular Formula**: $C_{24}H_{25}F_6N_5O_7S$; **MW**: 641.54 g/mol; **Yield**: 100%; **Mp**: 190-192°C (washing Et_2O); **^{1}H NMR** (300 MHz, DMSO-*d_6*) δ 1.50-1.69 (m, 2H, $CH_{2piperidine}$), 1.89-2.02 (m, 2H, $CH_{2piperidine}$), 2.35-2.46 (m, 2H, $CH_{2piperidine}$), 2.98-3.15 (m, 1H, $CH_{piperidine}$), 3.64-3.77 (m, 2H, $CH_{2piperidine}$), 3.97 (s, 3H, CH_3), 7.20 (d, J = 7.0 Hz, 1H, H_{indole}), 7.28 (t, J = 7.7 Hz, 1H, H_{indole}), 7.64-7.76 (m, 1H, H_{pyr}), 7.79 (dd, J = 7.8, 1.2 Hz, 1H, H_{indole}), 7.91-8.00 (m, 4H, H_{pyr} + NH_3^+), 8.03 (s, 1H, H_{indole}), 8.42-8.61 (m, 1H, H_{pyr}), 8.81-8.91 (m, 1H, H_{pyr}), 9.21-9.33 (m, 1H, H_{pyr}), 10.66-10.89 (m, 1H, NH).

N-{1-[7-(Naphthalen-2-carbonylamino)-1-methylindole-3-sulfonyl]piperidin-4-yl}ammonium trifluoroacetate salt (80i)

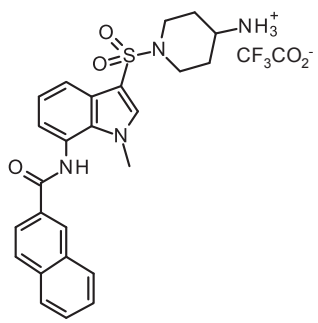

Following general procedure **E**, the compound **80i** was obtained as a light-yellow solid. **Molecular Formula**: $C_{27}H_{27}F_3N_4O_5S$; **MW**: 576.59 g/mol; **Yield**: 100%; **Mp**: > 210°C (washing Et_2O); **^{1}H NMR** (300 MHz, DMSO-*d_6*) δ

1.73-1.43 (m, 2H, $CH_{2piperidine}$), 1.88-2.04 (m, 2H, $CH_{2piperidine}$), 2.35-2.59 (m, 2H, $CH_{2piperidine}$), 3.00-3.21 (m, 1H, $CH_{piperidine}$), 3.66-3.79 (m, 2H, $CH_{2piperidine}$), 3.99 (s, 3H, CH_3), 7.22 (d, J = 6.8 Hz, 1H, H_{indole}), 7.29 (t, J = 7.7 Hz, 1H, H_{indole}), 7.60-7.72 (m, 2H, H_{napht}), 7.79 (d, J = 6.8 Hz, 1H, H_{napht}), 7.80-7.93 (br s, 3H, NH_3^+),8.03 (s, 1H, H_{indole}), 8.04-8.15 (m, 4H, H_{indole} + H_{napht}), 8.66 (s, 1H, H_{napht}), 10.57 (s, 1H, NH).

_N_-{1-[7-(3,4-Dimethoxyphenylacetylamino)-1-methylindole-3-sulfonyl]piperidin-4-yl}ammonium trifluoroacetate salt (80g)

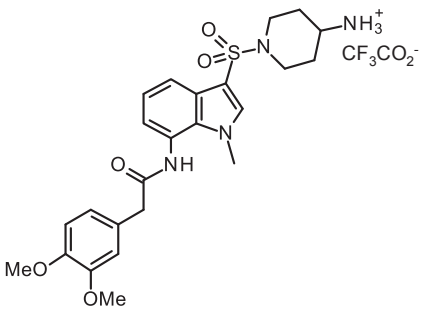

Following general procedure **E**, the compound **80g** was obtained as a grey solid. **Molecular Formula**: $C_{26}H_{31}F_3N_4O_7S$; **MW**: 600.61 g/mol; **Yield**: 100%; **Mp**: 120-123°C (washing Et_2O); **^{1}H NMR** (300 MHz, DMSO-*d_6*) δ 1.47-1.64 (m, 2H, $CH_{2piperidine}$), 1.87-2.00 (m, 2H, $CH_{2piperidine}$), 2.33-2.42 (m, 2H, $CH_{2piperidine}$), 2.93-3.11 (m, 1H, $CH_{piperidine}$), 3.63-3.75 (m, 2H, $CH_{2piperidine}$), 3.75 (s, 9H, CH_3 + 2 x OCH_3), 4.44 (d, J = 5.9 Hz, 2H, CH_2), 6.87-6.95 (m, 2H, H_{arom}), 6.99 (s, 1H, H_{arom}), 7.27 (t, J = 7.3 Hz, 1H, H_{indole}), 7.33 (dd, J = 7.3, 1.3 Hz, 1H, H_{indole}), 7.84 (br s, 3H, NH_3^+), 7.89 (dd, J = 6.1, 1.4 Hz, 1H, H_{indole}), 8.06 (s, 1H, H_{indole}), 9.14 (t, J = 6.1 Hz, 1H, NH).

_N_-(1-{7-[(Adamantan-1-yl)carbonylamino]-1-methylindole-3-sulfonyl}piperidin-4-yl)ammonium trifluoroacetate salt (80k)

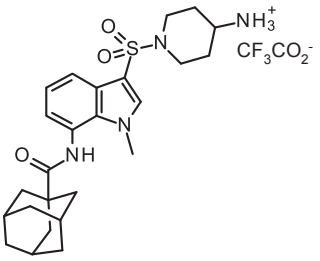

Following general procedure **E**, the compound **80k** was obtained as a pale orange solid. **Molecular Formula**: $C_{27}H_{35}F_3N_4O_5S$; **MW**: 584,65 g/mol; **Yield**: 100%; **Mp**: > 210°C (washing Et_2O); **^{1}H NMR** (300 MHz, DMSO-*d_6*) δ 1.47-1.64 (m, 2H, $CH_{2piperidine}$), 1.65-1.80 (m, 6H, $H_{adamant}$), 1.87-2.00 (m, 8H, $CH_{2piperidine}$ + $H_{adamant}$), 2.00-2.10 (m, 3H, $H_{adamant}$), 2.31-2.45 (m, 2H, $CH_{2piperidine}$), 2.98-3.20 (m, 1H, $CH_{piperidine}$), 3.63-3.76 (m, 2H, $CH_{2piperidine}$), 3.92 (s, 3H, CH_3), 6.96 (d, J = 7.4 Hz, 1H, H_{indole}), 7.19 (t, J = 7.7 Hz, 1H, H_{indole}), 7.70 (d, J = 7.5 Hz, 1H, H_{indole}), 7.84 (br s, 3H, NH_3^+), 7.97 (s, 1H, H_{indole}), 9.35 (s, 1H, NH).

_N_-{1-[7-(Quinolin-2-carbonylamino)-1-methylindole-3-sulfonyl]piperidin-4-yl}ammonium trifluoroacetate salt (80j)

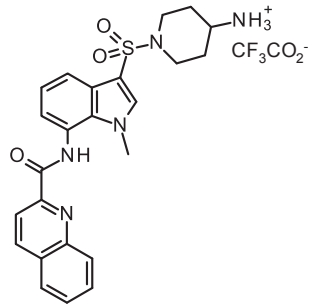

Following general procedure **E**, the compound **80j** was obtained as a yellow solid. **Molecular Formula**: $C_{26}H_{26}F_3N_5O_5S$; **MW**: 577.58 g/mol; **Yield**: 100%; **Mp**: >

210°C (washing Et_2O); **^{1}H NMR** (300 MHz, DMSO-d_6) δ 1.47-1.67 (m, 2H, $CH_{2piperidine}$), 1.86-2.04 (m, 2H, $CH_{2piperidine}$), 2.38-2.47 (m, 2H, $CH_{2piperidine}$), 2.97-3.18 (m, 1H, $CH_{piperidine}$), 3.64-3.79 (m, 2H, $CH_{2piperidine}$), 4.09 (s, 3H, CH_3), 7.29 (t, J = 7.8 Hz, 1H, H_{indole}), 7.41 (d, J = 7.4 Hz, 1H, H_{indole}), 7.73-7.82 (m, 2H, H_{indole} + H_{quinol}), 7.83-7.98 (m, 4H, H_{quinol} + NH_3^+), 8.03 (s, 1H, H_{indole}), 8.15 (d, J = 7.6 Hz, 1H, H_{quinol}), 8.19-8.29 (m, 2H, H_{quinol}), 8.66 (d, J = 8.4 Hz, 1H, H_{quinol}), 11.06 (s, 1H, NH).

3,4-Dimethoxy-*N*-{3-[4-(acryloylamino)piperidine-1-sulfonyl]-1-methylindol-7-yl}benzamide (78f)

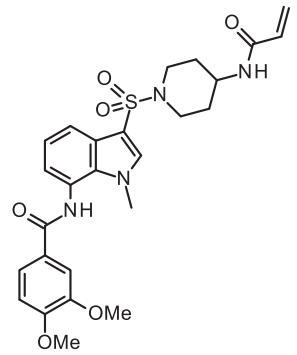

Following general procedure **G - work-up 3** (flash column chromatography solvent: MeOH/CH_2Cl_2 5:95 (solid deposition in MeOH), the resultant product was precipitated from MeOH to give **78f** as a white solid. **Molecular Formula**: $C_{26}H_{30}N_4O_6S$; **MW**: 526.60 g/mol; **Yield**: 68%; **Mp**: 154-156°C (MeOH); **^{1}H NMR** (300 MHz, DMSO-d_6) δ 1.39-1.57 (m, 2H, $CH_{2piperidine}$), 1.78-1.92 (m, 2H, $CH_{2piperidine}$), 2.53-2.61 (m, 2H, $CH_{2piperidine}$), 3.46-3.66 (m, 3H, $CH_{piperidine}$ + $CH_{2piperidine}$), 3.84 (s, 6H, 2 x OCH_3), 3.94 (s, 3H, CH_3), 5.54 (dd, J = 9.8, 2.5 Hz, 1H, CH_2= cis), 6.04 (dd, J = 17.1, 2.5 Hz, 1H, CH_2= trans), 6.17 (dd, J = 17.1, 9.8 Hz, 1H, CH=), 7.12 (d, J = 8.5 Hz, 1H, H_{arom}), 7.16 (d, J = 6.7 Hz, 1H, H_{indole}), 7.25 (t, J = 7.7 Hz, 1H, H_{indole}), 7.61 (d, J = 1.8 Hz, 1H, H_{arom}), 7.68 (dd, J = 8.4, 2.0 Hz, 1H, H_{arom}), 7.76 (dd, J = 8.1, 1.0 Hz, 1H, H_{indole}), 7.99 (s, 1H, H_{indole}), 8.05 (d, J = 7.2 Hz, 1H, NH), 10.22 (s, 1H, NH); **^{13}C NMR** (101 MHz, DMSO-d_6) δ 166.4 (C=O), 163.8 (C=O), 151.8 (C), 148.5 (C), 136.2 (CH), 132.7 (C), 131.7 (CH), 126.7 (C), 126.0 (C), 125.2 (CH_2=), 123.7 (C), 123.6 (CH), 121.9 (CH), 121.0 (CH), 118.4 (CH), 111.1 (CH), 110.9 (CH), 108.0 (C), 55.7 (CH_3), 55.6 (CH_3), 44.7 (CH), 44.5 (2 x CH_2), 35.6 (CH_3), 30.5 (2 x CH_2); **HRMS (ESI)** calcd for $C_{26}H_{31}N_4O_6S$ $[M+H]^+$, 527.1959; found, 527.1937.

3-Methoxy-*N*-{3-[4-(acryloylamino)piperidine-1-sulfonyl]-1-methylindol-7-yl}benzamide (78a)

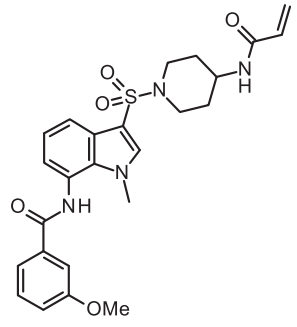

Following general procedure **G-work-up 3** (flash column chromatography solvent: MeOH/CH_2Cl_2 5:95 (solid deposition in MeOH), the resultant product was precipitated from MeOH to give **78a** as a white solid. **Molecular Formula**: $C_{25}H_{28}N_4O_5S$; **MW**: 496.58 g/mol; **Yield**: 75%; **Mp**: > 210°C (MeOH); **^{1}H NMR** (300 MHz, DMSO-d_6) δ 1.40-1.56 (m, 2H, $CH_{2piperidine}$), 1.78-1.91 (m, 2H, $CH_{2piperdine}$), 2.53-2.61 (m, 2H, $CH_{2piperidine}$), 3.44-3.66 (m, 3H, $CH_{piperidine}$ + $CH_{2piperidine}$), 3.84 (s, 6H, OCH_3), 3.95 (s, 3H, CH_3), 5.54 (dd, J = 9.8, 2.6 Hz, 1H, CH_2=

cis), 6.04 (dd, J = 17.0, 2.6 Hz, 1H, CH_2= trans), 6.17 (dd, J = 17.0, 9.8 Hz, 1H, CH=), 7.17 (d, J = 7.1 Hz, 1H, H_{indole}), 7.19 (dd, J = 8.2, 1.9 Hz, 1H, H_{arom}), 7.26 (t, J = 7.7 Hz, 1H, H_{indole}), 7.48 (t, J = 7.9 Hz, 1H, H_{arom}), 7.57 (s, 1H, H_{arom}), 7.61 (d, J = 7.5 Hz, 1H, H_{arom}), 7.77 (dd, J = 7.9, 1.1 Hz, 1H, H_{indole}), 8.00 (s, 1H, H_{indole}), 8.05 (d, J = 7.3 Hz, 1H, NH), 10.37 (s, 1H, NH); **^{13}C NMR** (101 MHz, DMSO-*d_6*) δ 166.8 (C=O), 163.8 (C=O), 159.4 (C), 136.3 (CH), 135.3 (C), 132.7 (C), 131.7 (CH), 129.8 (CH), 126.7 (C), 125.2 (CH_2=), 123.7 (CH), 123.4 (C), 122.0 (CH), 119.8 (CH), 118.6 (CH), 117.7 (CH), 112.9 (CH) , 108.1 (C), 55.4 (CH_3), 44.7 (CH), 44.5 (2 x CH_2), 35.7 (CH_3), 30.5 (2 x CH_2); **HRMS (ESI)** calcd for $C_{25}H_{29}N_4O_5S$ $[M+H]^+$, 497.1853; found, 497.1833.

3-Chloro-*N*-{3-[4-(acryloylamino)piperidine-1-sulfonyl]-1-methylindol-7-yl}benzamide (78b)

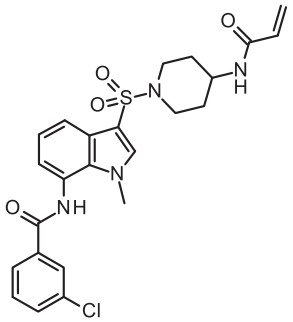

Following general procedure **G - work-up 3** (flash column chromatography solvent: MeOH/CH_2Cl_2 2-3:97-98 (solid deposition in MeOH/CH_2Cl_2), the resultant product was precipitated from MeOH to give **78b** as a white solid. **Molecular Formula**: $C_{24}H_{25}ClN_4O_4S$; **MW**: 501.00 g/mol; **Yield**: 63%; **Mp**: > 210°C (MeOH); **^{1}H NMR** (300 MHz, DMSO-*d_6*) δ 1.39-1.56 (m, 2H, $CH_{2piperidine}$), 1.79-1.91 (m, 2H, $CH_{2piperidine}$), 2.54-2.62 (m, 2H, $CH_{2piperidine}$), 3.45-3.67 (m, 3H, $CH_{piperidine}$ + $CH_{2piperidine}$), 3.94 (s, 3H, CH_3), 5.54 (dd, J = 9.8, 2.5 Hz, 1H, CH_2= cis), 6.03 (dd, J = 17.1, 2.5 Hz, 1H, CH_2= trans), 6.17 (dd, J = 17.1, 9.8 Hz, 1H, CH=), 7.18 (d, J = 7.1 Hz, 1H, H_{indole}), 7.26 (t, J = 7.7 Hz, 1H, H_{indole}), 7.61 (t, J = 7.8 Hz, 1H, H_{arom}), 7.72 (d, J = 8.5 Hz, 1H, H_{arom}), 7.78 (dd, J = 7.9, 1.1 Hz, 1H, H_{indole}), 7.99 (d, J = 7.5 Hz, 1H, H_{arom}), 8.00 (s, 1H, H_{indole}), 8.02 (d, J = 6.8 Hz, 1H, NH), 8.06 (s, 1H, H_{arom}), 10.50 (s, 1H, NH); **^{13}C NMR** (101 MHz, DMSO-*d_6*) δ 165.8 (C=O), 163.8 (C=O), 136.3 (CH), 136.0 (C), 133.5 (C), 132.6 (C), 131.8 (CH), 131.7 (CH), 130.7 (CH), 127.5 (CH), 126.8 (C), 126.4 (CH), 125.2 (CH_2=), 123.6 (CH), 123.1 (C), 121.9 (CH), 118.7 (CH), 108.1 (C), 44.7 (CH), 44.5 (2 x CH_2), 35.6 (CH_3), 30.5 (2 x CH_2); **HRMS (ESI)** calcd for $C_{24}H_{25}ClN_4NaO_4S$ $[M+Na]^+$, 523.1177; found, 523.1156.

3-Nitro-*N*-{3-[4-(acryloylamino)piperidine-1-sulfonyl]-1-methylindol-7-yl}benzamide (78c)

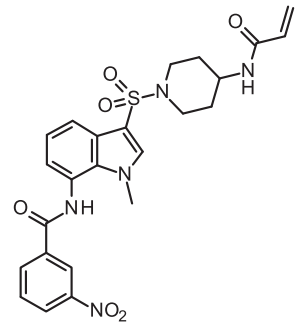

Following general procedure **G - work-up 3** (flash column chromatography solvent: MeOH/CH_2Cl_2 2-3:97-98 (solid deposition in MeOH/CH_2Cl_2), the resultant product was precipitated from MeOH to give **78c** as a white solid. **Molecular Formula**: $C_{24}H_{25}N_5O_6S$; **MW**: 511.55 g/mol; **Yield**: 57%; **Mp**: 160-163°C (MeOH); **^{1}H NMR** (300 MHz, DMSO-*d_6*) δ 1.40-1.58 (m, 2H, $CH_{2piperidine}$), 1.80-1.92 (m,

2H, $CH_{2piperidine}$), 2.54-2.66 (m, 2H, $CH_{2piperidine}$), 3.46-3.68 (m, 3H, $CH_{piperidine}$ + $CH_{2piperidine}$), 3.94 (s, 3H, CH_3), 5.54 (dd, J = 9.8, 2.5 Hz, 1H, CH_2= cis), 6.03 (dd, J = 17.1, 2.5 Hz, 1H, CH_2= trans), 6.17 (dd, J = 17.1, 9.8 Hz, 1H, CH=), 7.22 (d, J = 6.7 Hz, 1H, H_{indole}), 7.28 (t, J = 7.6 Hz, 1H, H_{indole}), 7.79 (dd, J = 7.7, 1.2 Hz, 1H, H_{indole}), 7.89 (t, J = 7.9 Hz, 1H, H_{arom}), 8.01 (s, 1H, H_{indole}), 8.06 (d, J = 7.3 Hz, NH), 8.44-8.54 (m, 2H, H_{arom}), 8.85 (t, J = 1.8 Hz, 1H, H_{arom}), 10.76 (s, 1H, NH); **^{13}C NMR** (101 MHz, DMSO-*d_6*) δ 165.1 (C=O) 163.8 (C=O), 148.0 (C), 136.4 (CH), 135.4 (C), 134.1 (CH), 132.5 (C), 131.7 (CH), 130.5 (CH), 126.8 (C), 126.5 (CH), 125.2 (CH_2=), 123.5 (CH), 122.9 (C), 122.5 (CH), 122.0 (CH), 118.9 (CH), 108.9 (C), 44.7 (CH), 44.5 (2 x CH_2), 35.6 (CH_3), 30.5 (2 x CH_2); **HRMS (ESI)** calcd for $C_{24}H_{26}N_5O_6S$ $[M+H]^+$, 512.1598; found, 512.1590.

4-Methoxy-*N*-{3-[4-(acryloylamino)piperidine-1-sulfonyl]-1-methylindol-7-yl}benzamide (78d)

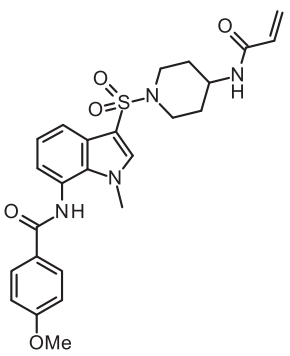

Following general procedure **G - work-up 3** (flash column chromatography solvent: MeOH/CH_2Cl_2 5:95 (solid deposition in MeOH/CH_2Cl_2), the compound **78d** was obtained as a white solid. **Molecular Formula**: $C_{25}H_{28}N_4O_5S$; **MW**: 496.58 g/mol; **Yield**: 63%; **Mp**: > 210°C; **^{1}H NMR** (300 MHz, DMSO-*d_6*) δ 1.38-1.56 (m, 2H, $CH_{2piperidine}$), 1.79-1.91 (m, 2H, $CH_{2piperidine}$), 2.54-2.66 (m, 2H, $CH_{2piperidine}$), 3.45-3.67 (m, 3H, $CH_{piperidine}$ + $CH_{2piperidine}$), 3.85 (s, 3H, OCH_3), 3.93 (s, 3H, CH_3), 5.54 (dd, J = 9.9, 2.5 Hz, 1H, CH_2= cis), 6.03 (dd, J = 17.1, 2.5 Hz, 1H, CH_2= trans), 6.17 (dd, J = 17.1, 9.9 Hz, 1H, CH=), 7.10 (d, J = 8.8 Hz, 2H, H_{arom}), 7.15 (dd, J = 7.4, 0.9 Hz, 1H, H_{indole}), 7.25 (t, J = 7.7 Hz, 1H, H_{indole}), 7.76 (dd, J = 7.9, 1.0 Hz, 1H, H_{indole}), 7.98 (s, 1H, H_{indole}), 8.01 (d, J = 8.8 Hz, 2H, H_{arom}), 8.05 (d, J = 7.3 Hz, 1H, NH), 10.23 (s, 1H, NH); **^{13}C NMR** (101 MHz, DMSO-*d_6*) δ 166.5 (C=O), 163.8 (C=O), 162.1 (C), 136.2 (CH), 132.8 (C), 131.7 (CH), 129.6 (2 x CH), 126.7 (C), 126.0 (C), 125.2 (CH_2=), 123.7 (C + CH), 121.9 (CH), 118.4 (CH), 113.9 (2 x CH), 108.1 (C), 55.5 (CH_3), 44.7 (CH), 44.5 (2 x CH_2), 35.6 (CH_3), 30.5 (2 x CH_2); **HRMS (ESI)** calcd for $C_{25}H_{29}N_4O_5S$ $[M+H]^+$, 497.1853; found, 497.1844.

4-Chloro-*N*-{3-[4-(acryloylamino)piperidine-1-sulfonyl]-1-methylindol-7-yl}benzamide (78e)

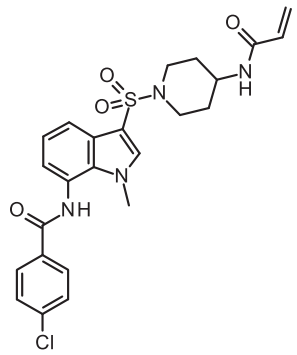

Following general procedure **G - work-up 3** (flash column chromatography solvent: MeOH/CH_2Cl_2 5:95 (solid deposition in MeOH/CH_2Cl_2), the compound **78e** was obtained as a white solid. **Molecular Formula**: $C_{24}H_{25}ClN_4O_4S$; **MW**: 501.00 g/mol; **Yield**: 87%; **Mp**: > 210°C; **^{1}H NMR** (300 MHz, DMSO-*d_6*) δ 1.39-1.57 (m, 2H, $CH_{2piperidine}$), 1.77-1.92 (m, 2H,

$CH_{2piperidine}$), 2.54-2.66 (m, 2H, $CH_{2piperidine}$), 3.46-3.67 (m, 3H, $CH_{piperidine}$ + $CH_{2piperidine}$), 3.94 (s, 3H, CH_3), 5.54 (dd, J = 9.8, 2.5 Hz, 1H, CH_2= cis), 6.03 (dd, J = 17.1, 2.5 Hz, 1H, CH_2= trans), 6.17 (dd, J = 17.1, 9.8 Hz, 1H, CH=), 7.17 (dd, J = 7.4, 0.8 Hz, 1H, H_{indole}), 7.25 (t, J = 7.7 Hz, 1H, H_{indole}), 7.65 (d, J = 8.5 Hz, 2H, H_{arom}), 7.77 (dd, J = 8.1, 1.1 Hz, 1H, H_{indole}), 8.00 (s, 1H, H_{indole}), 8.05 (d, J = 8.6 Hz, 2H, H_{arom} + NH), 10.45 (s, 1H, NH); **^{13}C NMR** (101 MHz, DMSO-*d_6*) δ 166.1 (C=O), 163.8 (C=O), 136.8 (C), 136.3 (CH), 132.7 (C), 132.6 (C), 131.7 (CH), 129.6 (2 x CH), 128.8 (2 x CH), 126.8 (C), 125.2 (CH_2=), 123.6 (CH), 123.2 (C), 122.0 (CH), 118.7 (CH), 108.1 (C), 44.7 (CH), 44.5 (2 x CH_2), 35.7 (CH_3), 30.5 (2 x CH_2); **HRMS (ESI)** calcd for $C_{24}H_{25}ClN_4NaO_4S$ $[M+Na]^+$, 523.1177; found, 523.1164.

N-{3-[4-(Acryloylamino)piperidine-1-sulfonyl]-1-methylindol-7-yl}pyridine-3-carboxamide (78h)

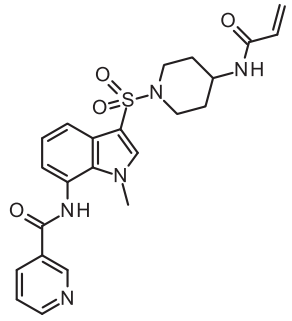

Following general procedure **G - work-up 2** (DIPEA (3.5 eq); flash column chromatography, solvent: MeOH/CH_2Cl_2 5-10:90-95), the compound **78h** was obtained as a white solid. **Molecular Formula**: $C_{23}H_{25}N_5O_4S$; **MW**: 467.54 g/mol; **Yield**: 43%; **Mp**: 188-190°C; **^{1}H NMR** (300 MHz, DMSO-*d_6*) δ 1.39-1.58 (m, 2H, $CH_{2piperidine}$), 1.79-1.91 (m, 2H, $CH_{2piperidine}$), 2.54-2.67 (m, 2H, $CH_{2piperidine}$), 3.44-3.67 (m, 3H, $CH_{piperidine}$ + $CH_{2piperidine}$), 3.97 (s, 3H, CH_3), 5.54 (dd, J = 9.8, 2.5 Hz, 1H, CH_2= cis), 6.03 (dd, J = 17.1, 2.5 Hz, 1H, CH_2= trans), 6.16 (dd, J = 17.1, 9.8 Hz, 1H, CH=), 7.20 (d, J = 6.7 Hz, 1H, H_{indole}), 7.27 (t, J = 7.7 Hz, 1H, H_{indole}), 7.62 (dd, J = 8.0, 4.8 H, 1H, H_{pyr}), 7.79 (dd, J = 7.8, 1.2 Hz, 1H, H_{indole}), 8.01 (s, 1H, H_{indole}), 8.05 (d, J = 7.3 Hz, 1H, NH), 8.37 (dt, J = 8.0, 1.9 Hz, 1H, H_{pyr}), 8.81 (dd, J = 4.8, 1.5 Hz, 1H, H_{pyr}), 9.20 (d, J = 1.6 Hz, 1H, H_{pyr}), 10.58 (s, 1H, NH); **^{13}C NMR** (101 MHz, DMSO-*d_6*) δ 165.7 (C=O), 163.8 (C=O), 152.5 (CH), 148.7 (CH), 136.3 (CH), 135.5 (CH), 132.5 (C), 131.7 (CH), 129.6 (C), 126.8 (C), 125.2 (CH_2=), 123.8 (CH), 123.6 (CH), 122.9 (C), 122.0 (CH), 118.8 (CH), 108.1 (C), 44.7 (CH), 44.5 (2 x CH_2), 35.7 (CH_3), 30.5 (2 x CH_2); **HRMS (ESI)** calcd for $C_{23}H_{26}N_5O_4S$ $[M+H]^+$, 468.1700; found, 468.1682.

N-{3-[4-(Acryloylamino)piperidine-1-sulfonyl]-1-methylindol-7-yl}naphthalene-2-carboxamide (78i)

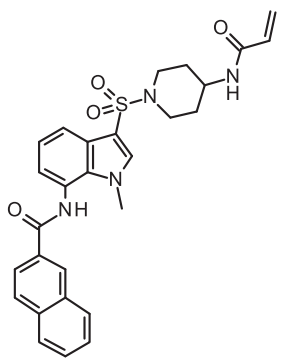

Following general procedure **G - Work-up 3** (flash column chromatography, solvent: MeOH/CH_2Cl_2 2:98), the resultant product was precipitated from MeOH to give **78i** as a white solid. **Molecular Formula**: $C_{28}H_{28}N_4O_4S$; **MW**: 516.61 g/mol; **Yield**: 75%; **Mp**: 176-178ºC (MeOH); **^{1}H NMR** (300 MHz, DMSO-*d_6*) δ 1.57-1.39 (m, 2H, $CH_{2piperidine}$), 1.95-1.76 (m, 2H,

$CH_{2piperidine}$), 2.68-2.37 (m, 2H, $CH_{2piperidine}$), 3.70-3.45 (m, 3H, $CH_{piperidine}$ + $CH_{2piperidine}$), 3.99 (s, 3H, CH_3), 5.55 (dd, J = 9.8, 2.5 Hz, 1H, CH_2= cis), 6.03 (dd, J = 17.1, 2.5 Hz, 1H, CH_2= trans), 6.18 (dd, J = 17.1, 9.8 Hz, 1H, CH=), 7.22 (d, J = 7.1 Hz, 1H, H_{indole}), 7.28 (t, J = 7.6 Hz, 1H, H_{indole}), 7.73-7.60 (m, 2H, H_{napht}), 7.79 (d, J = 6.9 Hz, 1H, H_{napht}), 8.01 (s, 1H, H_{indole}), 8.15-8.00 (m, 5H, NH + H_{indole} + H_{napht}), 8.67 (s, 1H, H_{napht}), 10.56 (s, 1H, NH); **^{13}C NMR** (101 MHz, DMSO-*d_6*) δ 167.2 (C=O), 163.9 (C=O), 136.3 (CH), 134.4 (C), 132.7 (C), 132.2 (C), 131.7 (CH), 131.3 (C), 129.1 (CH), 128.3 (2 x CH), 128.0 (CH), 127.7 (CH), 127.0 (CH), 126.8 (C), 125.2 (CH_2=), 124.3 (CH), 123.6 (CH), 123.5 (C), 122.0 (CH), 118.6 (CH), 108.1 (C), 44.7 (CH), 44.5 (2 x CH_2), 35.7 (CH_3), 30.6 (2 x CH_2); **HRMS (ESI)** calcd for $C_{28}H_{29}N_4O_4S$ $[M+H]^+$, 517.1904; found, 517.1891.

N-{1-[7-(3,4-Dimethoxyphenylacetylamino)-1-methylindole-3-sulfonyl]piperidin-4-yl}acrylamide (78g)

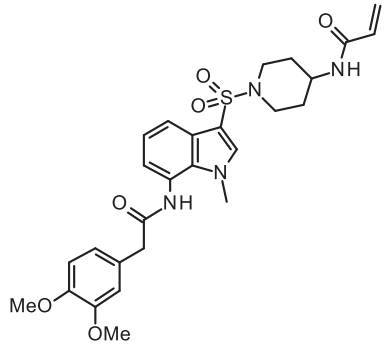

Following general procedure **G - Work-up 3** (flash column chromatography, solvent: MeOH/CH_2Cl_2 5:95), the resultant product was precipitated from MeOH to give **78g** as a white solid **Molecular Formula**: $C_{27}H_{32}N_4O_6S$; **MW**: 540.63 g/mol; **Yield**: 60%; **Mp**: 126-128°C (MeOH); **^{1}H NMR** (300 MHz, DMSO-*d_6*) δ 1.55-1.36 (m, 2H, $CH_{2piperidine}$), 1.90-1.72 (m, 2H, $CH_{2piperidine}$), 2.67-2.33 (m, 2H, $CH_{2piperidine}$), 3.85-3.35 (m, 3H, $CH_{piperidine}$ + $CH_{2piperidine}$), 3.62 (s, 2H, CH_2), 3.73 (s, 3H, OCH_3), 3.74 (s, 3H, OCH_3), 3.76 (s, 3H, CH_3), 5.53 (dd, J = 9.8, 2.5 Hz, 1H, CH_2= cis), 6.02 (dd, J = 17.1, 2.5 Hz, 1H, CH_2= trans), 6.16 (dd, J = 17.1, 9.8 Hz, 1H, CH=), 6.98-6.85 (m, 2H, H_{arom}), 7.00 (s, 1H, H_{arom}), 7.17 (d, J = 7.5 Hz, 1H, H_{indole}), 7.18 (t, J = 7.7 Hz, 1H, H_{indole}), 7.69 (d, J = 8.1 Hz, 1H, H_{indole}), 7.89 (s, 1H, H_{indole}), 8.03 (d, 1H, NH), 9.91 (s, 1H, NH); **^{13}C NMR** (101 MHz, DMSO-*d_6*) δ 171.1 (C=O), 163.8 (C=O), 148.5 (C), 147.7 (C), 136.1 (CH), 132.3 (C), 131.7 (CH), 127.9 (C), 126.7 (C), 125.2 (CH_2=), 123.3 (C), 123.2 (CH), 121.8 (CH), 121.3 (CH), 118.3 (CH), 113.0 (CH), 111.8 (CH), 107.9 (C), 55.5 (CH_3), 55.4 (CH_3), 44.7 (CH), 44.4 (2 x CH_2), 42.4 (CH_2), 35.5 (CH_3), 30.5 (2 x CH_2); **HRMS (ESI)** calcd for $C_{27}H_{32}N_4NaO_4S$ $[M+Na]^+$, 563.1935; found, 563.1913.

N-{3-[4-(Acryloylamino)piperidine-1-sulfonyl]-1-methylindol-7-yl}adamantane-1-carboxamide (78k)

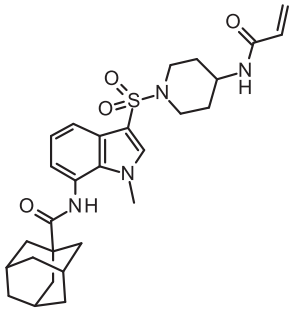

Following general procedure **G - work-up 5**, the resultant dried residue was precipitated from MeOH and filtered to give **78k** as a light-orange solid. **Molecular Formula**: $C_{28}H_{36}N_4O_4S$; **MW**: 524.67 g/mol; **Yield**: 65%; **Mp**: > 210°C

(MeOH); **^{1}H NMR** (300 MHz, DMSO-*d*$_6$) δ 1.51-1.38 (m, 2H, $CH_{2piperidine}$), 1.78-1.65 (m, 6H, $H_{adamant}$), 1.90-1.78 (m, 2H, $CH_{2piperidine}$), 2.00-1.90 (m, 6H, $H_{adamant}$), 2.10-2.00 (m, 3H, $H_{adamant}$), 2.60-2.41 (m, 2H, $CH_{2piperidine}$), 3.68-3.43 (m, 2H, $CH_{piperidine}$ + $CH_{2piperidine}$), 3.93 (s, 3H, CH_3), 5.54 (dd, J = 9.8, 2.5 Hz, 1H, CH_2= cis), 6.03 (dd, J = 17.1, 2.5 Hz, 1H, CH_2= trans), 6.16 (dd, J = 17.1, 9.8 Hz, 1H, CH=), 6.96 (d, J = 7.4 Hz, 1H, H_{indole}), 7.19 (t, J = 7.9 Hz, 1H, H_{indole}), 7.70 (d, J = 7.9 Hz, 1H, H_{indole}), 7.96 (s, 1H, H_{indole}), 8.05 (d, J = 7.4 Hz, 1H, NH), 9.33 (s, 1H, NH); **^{13}C NMR** (101 MHz, DMSO-*d*$_6$) δ 177.6 (C=O), 163.8 (C=O), 136.1 (CH), 132.8 (C), 131.7 (CH), 126.6 (C), 125.2 (CH_2=), 124.0 (C), 123.8 (CH), 121.8 (CH), 118.2 (CH), 107.9 (C), 44.7 (CH), 44.4 (2 x CH_2), 40.4 (C), 38.6 (3 x CH_2), 36.1 (3 x CH_2), 36.0 (CH_3), 30.5 (2 x CH_2), 27.7 (3 x CH); **HRMS (ESI)** calcd for $C_{28}H_{36}N_4NaO_4S$ $[M+Na]^+$, 547.2349; found, 547.2350.

N-{3-[4-(Acryloylamino)piperidine-1-sulfonyl]-1-methylindol-7-yl}quinoline-2-carboxamide (78j)

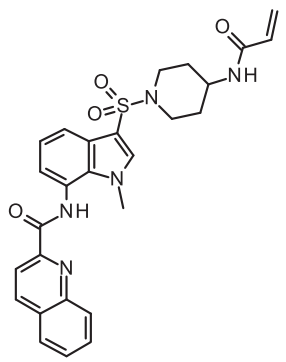

Following general procedure **G - work-up 6** (flash column chromatography solvent: MeOH/CH_2Cl_2 2:98), the resultant product was precipitated from MeOH to give **78j** as a yellow solid. **Molecular Formula**: $C_{27}H_{27}N_5O_4S$; **MW**: 517.60 g/mol; **Yield**: 53%; **Mp**: > 210°C (MeOH); **^{1}H NMR** (300 MHz, DMSO-*d*$_6$) δ 1.59-1.40 (m, 2H, $CH_{2piperidine}$), 1.93-1.78 (m, 2H, $CH_{2piperidine}$), 2.65-2.40 (m, 2H, $CH_{2piperidine}$), 3.68-3.46 (m, 2H, $CH_{piperidine}$ + $CH_{2piperidine}$), 4.10 (s, 3H, CH_3), 5.55 (dd, J = 9.8, 2.4 Hz, 1H, CH_2= cis), 6.03 (dd, J = 17.1, 2.4 Hz, 1H, CH_2= trans), 6.17 (dd, J = 17.1, 9.8 Hz, 1H, CH=), 7.28 (t, J = 7.8 Hz, 1H, H_{indole}), 7.43 (d, J = 7.0 Hz, 1H, H_{indole}), 7.77 (d, J = 8.1 Hz, 1H, H_{indole}), 7.77 (dt, J = 8.2, 0.9 Hz, 1H, H_{quinol}), 7.93 (dt, J = 8.3, 1.3 Hz, 1H, H_{quinol}), 8.02 (s, 1H, H_{indole}), 8.06 (d, J = 7.2 Hz, 1H, NH), 8.15 (d, J = 7.8 Hz, 1H, H_{quinol}), 8.22 (d, J = 8.3 Hz, 1H, H_{quinol}), 8.27 (d, J = 8.4 Hz, 1H, H_{quinol}), 8.68 (d, J = 8.5 Hz, 1H, H_{quinol}), 11.06 (s, 1H, NH); **^{13}C NMR** (101 MHz, DMSO-*d*$_6$) δ 164.1 (C=O), 163.8 (C=O), 149.7 (C), 146.1 (C), 138.2 (CH), 136.2 (CH), 131.8 (C), 131.7 (CH), 130.8 (CH), 129.5 (CH), 129.1 (C), 128.5 (CH), 128.2 (CH), 126.8 (C), 125.2 (CH_2=), 123.5 (C), 122.1 (CH), 121.9 (CH), 118.9 (CH), 118.1 (CH), 107.9 (C), 44.8 (CH), 44.5 (2 x CH_2), 36.2 (CH_3), 30.5 (2 x CH_2); **HRMS (ESI)** calcd for $C_{27}H_{28}N_5O_4S$ $[M+H]^+$, 518.1857; found, 518.1836.

7-Nitro-1*H*-indole-3-sulfonyl chloride (82), CAS 132745-01-8

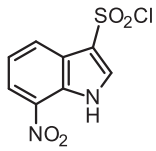

Following general procedure **B - method 1**, the compound **82** was obtained as a yellow solid. **Molecular Formula**: $C_8H_5ClN_2O_4S$; **MW**: 260.65 g/mol; **Yield**: 80%; **Mp**: 168-170°C (Lit. 172-173°C);[170] **^{1}H NMR** (300 MHz, DMSO-*d*$_6$) δ 7.27 (t, J = 7.9 Hz, 1H, H_{indole}), 7.43 (d, J

= 2.1 Hz, 1H, H_{indole}), 8.11 (dd, J = 8.1, 0.7 Hz, 1H, H_{indole}), 8.24 (d, J = 7.7 Hz, 1H, H_{indole}), 11.76 (d, J = 2.1 Hz, 1H, NH).

Tert-butyl *N*-[1-(7-Nitro-1*H*-indole-3-sulfonyl)piperidin-4-yl]carbamate (83)

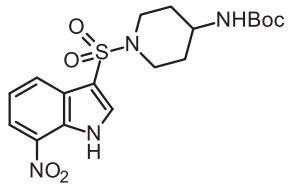

Following general procedure **F - work-up 1**, the compound **83** was obtained as a yellow solid. **Molecular Formula**: $C_{18}H_{24}N_4O_6S$; **MW**: 424.47 g/mol; **Yield**: 80%; **Mp**: > 210°C (washing CH_2Cl_2); **^{1}H NMR** (300 MHz, DMSO-*d*$_6$) δ 1.32 (s, 9H, 3 x CH_3), 1.35-1.48 (m, 2H, $CH_{2piperidine}$), 1.69-1.81 (m, 2H, $CH_{2piperidine}$), 2.41-2.46 (m, 2H, $CH_{2piperidine}$), 3.12-3.27 (m, 1H, $CH_{piperidine}$), 3.44-3.57 (m, 2H, $CH_{2piperidine}$), 6.81 (d, J = 7.4 Hz, 1H, NH), 7.46 (t, J = 7.9 Hz, 1H, H_{indole}), 8.01 (s, 1H, H_{indole}), 8.27 (dd, J = 8.0, 2.2 Hz, 2H, H_{indole}), 12.81 (s, 1H, NH); **LRMS (ESI)**: *m/z* = 425.1 $[M+H]^+$.

Tert-butyl *N*-[1-(7-Amino-1*H*-indole-3-sulfonyl)piperidin-4-yl]carbamate (84)

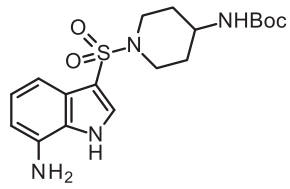

Following general procedure **H - work-up 1** (NH_4Cl (0.259 M), the compound **84** was obtained as a yellow solid. **Molecular Formula**: $C_{18}H_{26}N_4O_4S$; **MW**: 394.49 g/mol; **Yield**: 50%; **Mp**: > 210°C (washing MeOH); **^{1}H NMR** (300 MHz, DMSO-*d*$_6$) δ 1.33 (s, 9H, 3 x CH_3), 1.36-1.49 (m, 2H, $CH_{2piperidine}$), 1.66-1.82 (m, 2H, $CH_{2piperidine}$), 2.29-2.43 (m, 2H, $CH_{2piperidine}$), 3.05-3.24 (m, 1H, $CH_{piperidine}$), 3.41-3.56 (m, 2H, $CH_{2piperidine}$), 5.29 (s, 2H, NH_2), 6.43 (d, J = 7.2 Hz, 1H, H_{indole}), 6.82 (d, J = 7.0 Hz, 1H, NH), 6.88 (t, J = 7.6 Hz, 1H, H_{indole}), 6.99 (d, J = 7.8 Hz, 1H, H_{indole}), 7.86 (s, 1H, H_{indole}), 11.72 (s, 1H, NH); **LRMS (ESI)**: *m/z* = 395.2 $[M+H]^+$.

Tert-butyl *N*-[1-{7-[(3,4-Dimethoxybenzoyl)amino]-1*H*-indol-3-sulfonyl}piperidine-4-yl]carbamate (85)

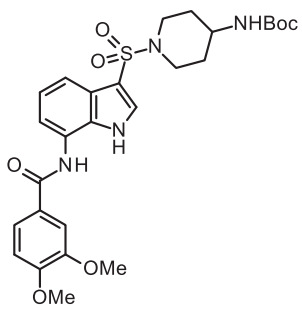

Following general procedure **G - work-up 3** (solvents: CH_2Cl_2 (0.1 M) and DMF (0.86 M); no flash column chromatography), the resultant solid was precipitated from MeOH/CH_2Cl_2 (5:95) to give **85** as a light-yellow solid. **Molecular Formula**: $C_{27}H_{34}N_4O_7S$; **MW**: 558.65 g/mol; **Yield**: 53%; **Mp**: 155-157°C (MeOH/CH_2Cl_2); **^{1}H NMR** (300 MHz, DMSO-*d*$_6$) δ 1.33 (s, 9H, 3 x CH_3), 1.37-1.52 (m, 2H, $CH_{2piperidine}$), 1.70-1.84 (m, 2H, $CH_{2piperidine}$), 2.32-2.47 (m, 2H, $CH_{2piperidine}$), 3.07-3.25 (m, 1H, $CH_{piperidine}$), 3.46-3.59 (m, 2H, $CH_{2piperidine}$), 6.84 (d, J = 7.3 Hz, 1H, NH), 7.12 (d, J = 8.5 Hz, 1H, H_{arom}), 7.20 (t, J = 7.8 Hz, 1H, H_{indole}), 7.42 (d, J = 7.2 Hz, 1H, H_{indole}), 7.62 (d, J = 2.1 Hz, 1H, H_{arom}), 7.67 (d, J = 9.0 Hz, 1H, H_{arom}), 7.70 (dd, J = 8.3, 2.0 Hz, 1H,

H_{indole}), 7.92 (d, J = 2.2 Hz, 1H, H_{indole}), 10.14 (s, 1H, NH), 11.95 (d, J = 2.2 Hz, 1H, NH); **LRMS (ESI)**: *m/z* = 559.2 $[M+H]^+$.

_N_-{1-[7-(3,4-Dimethoxybenzoyl)amino-1_H_-indole-3-sulfonyl]piperidin-4-yl}ammonium trifluoroacetate salt (86)

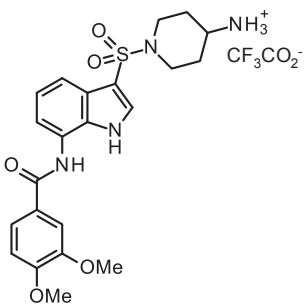

Following general procedure **E**, the compound **86** was obtained as a yellow solid. **Molecular Formula**: $C_{24}H_{27}F_3N_4O_7S$; **MW**: 572.55 g/mol; **Yield**: 87%; **Mp**: 180-183°C (washing Et_2O); **^{1}H NMR** (300 MHz, DMSO-d_6) δ 1.47-1.65 (m, 2H, $CH_{2piperidine}$), 1.87-2.01 (m, 2H, $CH_{2piperidine}$), 2.29-2.42 (m, 2H, $CH_{2piperidine}$), 2.96-3.12 (m, 1H, $CH_{piperidine}$), 3.66-3.78 (m, 2H, $CH_{2piperidine}$), 3.85 (s, 6H, 2 x OCH_3), 7.12 (d, J = 8.5 Hz, 1H, H_{arom}), 7.22 (t, J = 7.8 Hz, 1H, H_{indole}), 7.39 (d, J = 7.3 Hz, 1H, H_{indole}), 7.61 (d, J = 2.0 Hz, 1H, H_{arom}), 7.66 (d, J = 8.0 Hz, 1H, H_{arom}), 7.70 (dd, J = 8.5, 2.0 Hz, 1H, H_{indole}), 7.84 (br s, 3H, NH_3^+), 7.94 (d, J = 3.0 Hz, 1H, H_{indole}), 10.17 (s, 1H, NH), 11.98 (d, J = 3.0 Hz, 1H, NH).

3,4-Dimethoxy-_N_-{3-[4-(acryloylamino)piperidine-1-sulfonyl]-1_H_-indol-7-yl}benzamide (81)

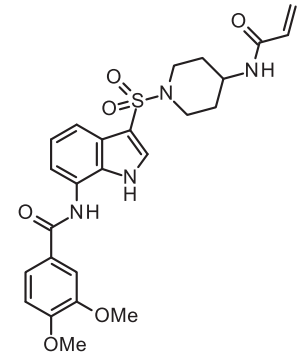

Following general procedure **G - work-up 3** (flash column chromatography solvent: MeOH/CH_2Cl_2 7:93), the compound **81** was obtained as a light-yellow solid. **Molecular Formula**: $C_{25}H_{28}N_4O_6S$; **MW**: 512.58 g/mol; **Yield**: 40%; **Mp**: > 210°C; **^{1}H NMR** (300 MHz, DMSO-d_6) δ 1.38-1.55 (m, 2H, $CH_{2piperidine}$), 1.77-1.9 (m, 2H, $CH_{2piperidine}$), 2.54-2.66 (m, 2H, $CH_{2piperidine}$), 3.45-3.65 (m, 3H, $CH_{piperidine}$ + $CH_{2piperidine}$), 3.85 (s, 6H, 2 x OCH_3), 5.54 (dd, J = 9.8, 2.5 Hz, 1H, CH_2= cis), 6.02 (dd, J = 17.1, 2.5 Hz, 1H, CH_2= trans), 6.16 (dd, J = 17.1, 9.8 Hz, 1H, CH=), 7.12 (d, J = 8.5 Hz, 1H, H_{arom}), 7.21 (t, J = 7.8 Hz, 1H, H_{indole}), 7.42 (d, J = 7.3 Hz, 1H, H_{indole}), 7.62 (d, J = 2.0 Hz, 1H, H_{arom}), 7.65 (d, J = 7.5 Hz, 1H, H_{arom}), 7.70 (dd, J = 8.4, 2.0 Hz, 1H, H_{indole}), 7.94 (d, J = 2.9 Hz, 1H, H_{indole}), 8.04 (d, J = 7.4 Hz, 1H, NH), 10.17 (s, 1H, NH), 11.98 (d, J = 2.9 Hz, 1H, NH); **^{13}C NMR** (101 MHz, DMSO-d_6) δ 165.1 (C=O), 163.8 (C=O), 151.7 (C), 148.3 (C), 131.7 (CH), 130.8 (CH), 130.3 (C), 126.6 (C), 125.6 (C), 125.2 (CH_2=), 124.3 (C), 121.5 (CH), 121.4 (CH), 117.8 (CH), 116.4 (CH), 111.3 (CH), 110.9 (CH), 109.4 (C), 55.7 (CH_3), 55.6 (CH_3), 44.8 (CH), 44.6 (2 x CH_2), 30.5 (2 x CH_2); **HRMS (ESI)** calcd for $C_{25}H_{29}N_4O_6S$ $[M+H]^+$, 513.1802; found, 513.1787.

Methyl 1-Methylindole-7-carboxylate (89),[171] CAS 167479-21-2

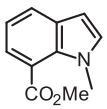

Following general procedure **A** (flash column chromatography solvent: PE/EtOAc 9:1), the compound **89** was obtained as a yellow oil. **Molecular Formula**: $C_{11}H_{11}NO_2$; **MW**: 189.21g/mol; **Yield**: 100%; **^{1}H NMR** (300 MHz, DMSO-*d*$_6$) δ 3.89 (s, 3H, CH_3), 3.97 (s, 3H, CH_3), 6.55 (d, J = 3.1 Hz, 1H, H_{indole}), 7.06 (d, J = 3.1 Hz, 1H, H_{indole}), 7.10 (t, J = 7.6 Hz, 1H, H_{indole}), 7.67 (dd, J = 7.6, 1.1 Hz, 1H, H_{indole}), 7.77 (dd, J = 7.6, 1.1 Hz, 1H, H_{indole}).

Methyl 3-(Chlorosulfonyl)-1-methylindole-7-carboxylate (90),[172] CAS 1158209-68-7

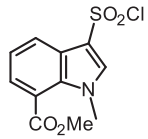

Following general procedure **B - method 2** (solvent: DCE (0.733 M); the resultant dried residue was dissolved in EtOAc/CH_2Cl_2 1:1, and purified by using flash column chromatography, solvent: EtOAc), the compound **90** was obtained as a brown solid. **Molecular Formula**: $C_{11}H_{11}NO_2$; **MW**: 287.71 g/mol; **Yield**: 54%; **Mp**: 125-127°C; **^{1}H NMR** (300 MHz, DMSO-*d*$_6$) δ 4.00 (s, 3H, CH_3), 4.02 (s, 3H, CH_3), 7.43 (t, J = 7.8 Hz, 1H, H_{indole}), 7.86 (dd, J = 7.6, 1.1 Hz, 1H, H_{indole}), 7.88 (s, 1H, H_{indole}), 8.21 (dd, J = 8.0, 1.2 Hz, 1H, H_{indole}).

Methyl 3-[4-(*Tert*-butoxycarbonylamino)piperidine-1-sulfonyl]-1-methylindole-7-carboxylate (88)

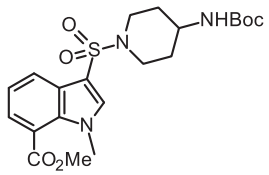

Following general procedure **F - work-up 2** (flash column chromatography solvent: MeOH/CH_2Cl_2 1-2:98-99), the resultant product was precipitated from EtOH to give **88** as a white solid. **Molecular Formula**: $C_{21}H_{29}N_3O_6S$; **MW**: 451.63 g/mol; **Yield**: 86%; **Mp**: 185-187°C (EtOH); **^{1}H NMR** (300 MHz, DMSO-*d*$_6$) δ 1.33 (s, 9H, 3 x CH_3), 1.35-1.50 (m, 2H, $CH_{2piperidine}$), 1.70-1.81 (m, 2H, $CH_{2piperidine}$), 2.38-2.47 (m, 2H, $CH_{2piperidine}$), 3.12-3.28 (m, 1H, $CH_{piperidine}$), 3.42-3.54 (m, 2H, $CH_{2piperidine}$), 3.88 (s, 3H, CH_3), 3.93 (s, 3H, CH_3), 6.83 (d, J = 7.6 Hz, 1H, NH), 7.32 (t, J = 7.7 Hz, 1H, H_{indole}), 7.64 (dd, J = 7.4, 1.1 Hz, 1H, H_{indole}), 8.03 (dd, J = 8.0, 1.2 Hz, 1H, H_{indole}), 8.04 (s, 1H, H_{indole}); **LRMS (ESI)**: *m/z* 474.2 $[M+Na]^+$.

3-[4-(*Tert*-butoxycarbonylamino)piperidine-1-sulfonyl]-1-methylindole-7-carboxylic acid (92)

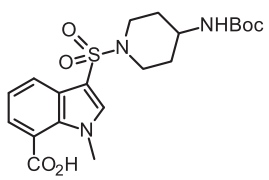

Following general procedure **D**, the compound **92** was obtained as a white solid. **Molecular Formula**: $C_{20}H_{27}N_3O_6S$; **MW**: 437.51 g/mol; **Yield**: 96%; **Mp**: > 210ºC; **^{1}H NMR** (300 MHz, DMSO-*d*$_6$) δ 1.33 (s, 9H, 3 x CH_3), 1.36-1.50 (m, 2H, $CH_{2piperidine}$), 1.68-1.83 (m, 2H, $CH_{2piperidine}$), 2.36-2.47 (m, 2H, $CH_{2piperidine}$), 3.12-3.26 (m, 1H, $CH_{piperidine}$), 3.42-3.55 (m, 2H, $CH_{2piperidine}$), 3.84 (s, 3H, CH_3), 6.83 (d, J = 7.6 Hz, 1H, NH), 7.30 (t, J = 7.8 Hz, 1H, H_{indole}), 7.64 (dd, J = 7.4,

1.0 Hz, 1H, H_{indole}), 8.00 (dd, J = 8.1, 1.0 Hz, 1H, H_{indole}), 8.09 (s, 1H, H_{indole}), 13.39 (br s, 1H, CO_2H); **LRMS (ESI)**: *m/z* 438.0 $[M+H]^+$.

***Tert*-butyl *N*-{1-[7-(3,4-Dimethoxyphenylcarbamoyl)-1-methylindole-3-sulfonyl]piperidin-4-yl}carbamate (91a)**

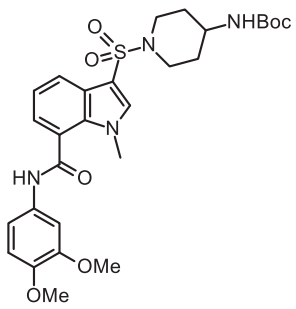

Following general procedure **I -work-up 1** (flash column chromatography solvent: MeOH/CH_2Cl_2 4-5:95-96), the resultant product was precipitated from MeOH to give **91a** as a white solid. **Molecular Formula**: $C_{28}H_{36}N_4O_7S$; **MW**: 572.67 g/mol; **Yield**: 73%; **Mp**: 203-205°C (MeOH); **^{1}H NMR** (300 MHz, DMSO-d_6) δ 1.34 (s, 9H, 3 x CH_3), 1.52-1.37 (m, 2H, $CH_{2piperidine}$), 1.85-1.71 (m, 2H, $CH_{2piperidine}$), 2.60-2.38 (m, 2H, $CH_{2piperidine}$), 3.25-3.10 (m, 1H, $CH_{piperidine}$), 3.59-3.47 (m, 2H, $CH_{2piperidine}$), 3.75 (s, 6H, 2 x OCH_3), 3.85 (s, 3H, CH_3), 6.85 (d, J = 7.2 Hz, 1H, NH), 6.95 (d, J = 8.9 Hz, 1H, H_{arom}), 7.32 (t, J = 7.3 Hz, 1H, H_{indole}), 7.33 (d, J = 10.9 Hz, 1H, H_{arom}), 7.43 (dd, J = 3.8, 1.0 Hz, 1H, H_{indole}), 7.44 (s, 1H, H_{arom}), 7.95 (dd, J = 8.1, 1.1 Hz, 1H, H_{arom}), 8.09 (s, 1H, H_{indole}), 10.53 (s, 1H, NH); **LRMS (ESI)**: *m/z* 573.2 $[M+H]^+$, 595.2 $[M+Na]^+$.

***Tert*-butyl *N*-{1-[7-(3,4-Dimethoxybenzylcarbamoyl)-1-methylindole-3-sulfonyl]piperidin-4-yl}carbamate (91b)**

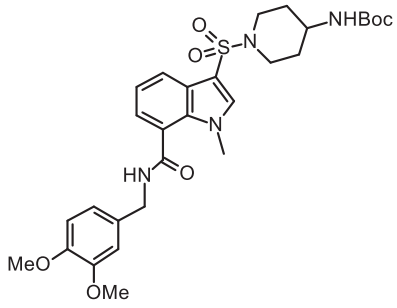

Following general procedure **I - work-up 1** (flash column chromatography solvent: MeOH in CH_2Cl_2 5:95), the resultant product was precipitated from MeOH to give **91b** as a white solid. **Molecular Formula**: $C_{29}H_{38}N_4O_7S$; **MW**: 586.70 g/mol; **Yield**: 62%; **Mp**: 161-163°C (MeOH); **^{1}H NMR** (300 MHz, DMSO-d_6) δ 1.33 (s, 9H, 3 x CH_3), 1.50-1.33 (m, 2H, $CH_{2piperidine}$), 1.82-1.70 (m, 2H, $CH_{2piperidine}$), 2.50-2.36 (m, 2H, $CH_{2piperidine}$), 3.25-3.10 (m, 1H, $CH_{piperidine}$), 3.56-3.44 (m, 2H, $CH_{2piperidine}$), 3.74 (s, 6H, 2 x OCH_3), 3.75 (s, 3H, CH_3), 4.44 (d, J = 5.9 Hz, 2H, CH_2), 6.53 (d, J = 7.1 Hz, 1H, NH), 6.97-6.88 (m, 2H, H_{arom}), 7.00 (s, 1H, H_{arom}), 7.35 (t, J = 7.3 Hz, 1H, H_{indole}), 7.31 (dd, J = 7.2, 1.4 Hz, 1H, H_{indole}), 7.88 (dd, J = 9.1, 1.4 Hz, 1H, H_{indole}), 8.02 (s, 1H, H_{indole}), 9.12 (t, J = 6.0 Hz, 1H, NH); **LRMS (ESI)**: *m/z* 587.2 $[M+H]^+$.

Methyl (2S)-2-({3-[4-(*Tert*-butoxycarbonylamino)piperidine-1-sulfonyl]-1-methylindole-7-carbonyl}amino)-3-phenylpropanoate (91c)

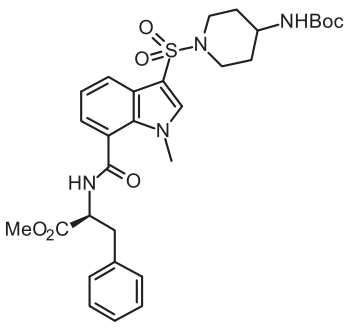

Following general procedure **I** – **work-up 1** (flash column chromatography solvent: MeOH/CH_2Cl_2 5:95), the resultant product was precipitated from Et_2O to give **91c** as a white solid. **Molecular Formula**: $C_{30}H_{38}N_4O_7S$; **MW**: 598.71 g/mol; **Yield**: 46%; **Mp**: 155-157°C (Et_2O); **^{1}H NMR** (300 MHz, DMSO-d_6) δ 1.33 (s, 9H, 3 x CH_3), 1.50-1.33 (m, 2H, $CH_{2piperidine}$), 1.82-1.68 (m, 2H, $CH_{2piperidine}$), 2.51-2.32 (m, 2H, $CH_{2piperidine}$), 2.99 (dd, J = 13.8, 11.0 Hz, 1H, CH_2), 3.24 (dd, J = 13.8, 4.5 Hz, 1H, CH_2), 3.28-3.10 (m, 1H, $CH_{piperidine}$), 3.51 (s, 3H, CH_3), 3.55-3.40 (m, 2H, $CH_{2piperidine}$), 3.71 (s, 3H, CH_3), 4.87-4.75 (m, 1H, CH), 6.82 (d, J = 7.2 Hz, 1H, NH), 7.07 (dd, J = 7.2, 1.0 Hz, 1H, H_{indole}), 7.38-7.20 (m, 6H, H_{arom} + H_{indole}), 7.87 (dd, J = 8.2, 1.1 Hz, 1H, H_{indole}), 7.99 (s, 1H, H_{indole}), 9.16 (d, J = 8.2 Hz, 1H, NH); **LRMS (ESI)**: *m/z* 599.2 $[M+H]^+$.

Tert-butyl *N*-{1-[1-methyl-7-(naphth-2-ylcarbamoyl)indole-3-sulfonyl]piperidin-4-yl}carbamate (91d)

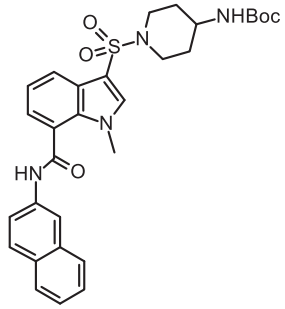

Following general procedure **I - work-up 2** (flash column chromatography solvent: MeOH in CH_2Cl_2 1:99), the resultant product was precipitated from MeOH, to give **91d** as a white solid. **Molecular Formula**: $C_{30}H_{34}N_4O_5S$; **MW**: 562.68 g/mol; **Yield**: 35%; **Mp**: > 210°C (MeOH); **^{1}H NMR** (300 MHz, DMSO-d_6) δ 1.34 (s, 9H, 3 x CH_3), 1.53-1.35 (m, 2H, $CH_{2piperidine}$), 1.88-1.71 (m, 2H, $CH_{2piperidine}$), 2.55-2.35 (m, 2H, $CH_{2piperidine}$), 3.28-3.10 (m, 1H, $CH_{piperidine}$), 3.59-3.47 (m, 2H, $CH_{2piperidine}$), 3.88 (s, 3H, CH_3), 6.85 (d, J = 7.3 Hz, 1H, NH), 7.36 (t, J = 7.3 Hz, 1H, H_{indole}), 7.57-7.41 (m, 3H, H_{napht}), 7.75 (dd, J = 8.9, 1.9 Hz, 1H, H_{napht}), 7.89 (dd, J = 7.8, 3.1 Hz, 1H, H_{indole}), 7.92 (d, J = 9.2 Hz, 1H, H_{napht}), 7.97 (d, J = 8.1 Hz, 1H, H_{napht}), 8.12 (s, 1H, H_{indole}), 8.51 (s, 1H, H_{napht}), 10.92 (s, 1H, NH); **LRMS (ESI)**: *m/z* 563.2 $[M+H]^+$.

N-{1-[7-(3,4-Dimethoxyphenylcarbamoyl)-1-methylindole-3-sulfonyl]piperidin-4-yl}ammonium trifluoroacetate salt (93a)

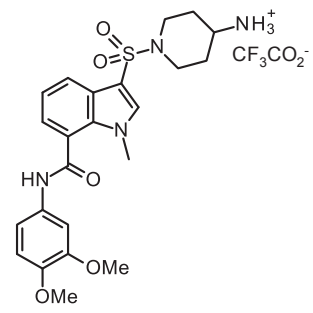

Following general procedure **E**, the compound **93a** was obtained as a white- salmon coloured solid. **Molecular Formula**: $C_{25}H_{29}F_3N_4O_7S$; **MW**: 586.58 g/mol; **Yield**: 96%; **Mp**: > 210°C (washing Et_2O); **^{1}H NMR** (300 MHz, DMSO-d_6) δ 1.47-1.65 (m, 2H, $CH_{2piperidine}$), 1.87-2.01 (m, 2H, $CH_{2piperidine}$), 2.30-2.44 (m, 2H, $CH_{2piperidine}$), 2.96-3.12 (m, 1H, $CH_{piperidine}$), 3.64-3.73 (m, 2H, $CH_{2piperidine}$), 3.75 (s, 6H, 2 x OCH_3), 3.85 (s, 3H, CH_3), 6.95 (d, J = 8.8 Hz, 1H, H_{arom}),

7.33 (t, J = 7.6 Hz, 1H, H_{indole}), 7.34 (d, J = 8.8 Hz, 1H, H_{arom}), 7.42 (d, J = 2.4 Hz, 1H, H_{arom}), 7.45 (dd, J = 8.0, 1.0 Hz, 1H, H_{indole}), 7.83 (br s, 3H, NH_3^+), 7.95 (dd, J = 8.0, 1.0 Hz, 1H, H_{indole}), 8.13 (s, 1H, H_{indole}), 10.55 (s, 1H, NH).

N-{1-[7-(3,4-Dimethoxybenzylcarbamoyl)-1-methylindole-3-sulfonyl]piperidin-4-yl}ammonium trifluoroacetate salt (93b)

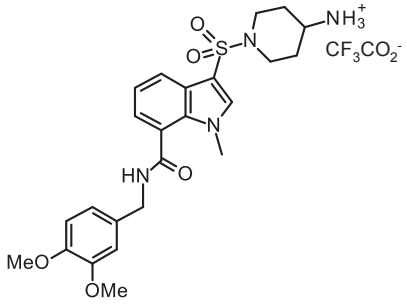

Following general procedure **E**, the compound **93b** was obtained as a light-orange solid. **Molecular Formula**: $C_{26}H_{31}F_3N_4O_7S$; **MW**: 600.61 g/mol; **Yield**: 100%; **Mp**: 112-115°C (washing Et_2O); **^{1}H NMR** (300 MHz, DMSO-d_6) δ 1.64-1.47 (m, 2H, $CH_{2piperidine}$), 2.00-1.87 (m, 2H, $CH_{2piperidine}$), 2.42-2.33 (m, 2H, $CH_{2piperidine}$), 3.11-2.93 (m, 1H, $CH_{piperidine}$), 3.75-3.63 (m, 2H, $CH_{2piperidine}$), 3.75 (s, 9H, CH_3 + 2 x OCH_3), 4.44 (d, J = 5.9 Hz, 2H, CH_2), 6.95-6.87 (m, 2H, H_{arom}), 6.99 (s, 1H, H_{arom}), 7.27 (t, J = 7.3 Hz, 1H, H_{indole}), 7.33 (dd, J = 7.3, 1.3 Hz, 1H, H_{indole}), 7.84 (d, J = 5.7 Hz, 1H, NH_3^+),7.89 (dd, J = 6.1, 1.5 Hz, 1H, H_{indole}), 8.06 (s, 1H, H_{indole}), 9.14 (t, J = 6.1 Hz, 1H, NH).

[1-(7-{[(1S)-1-benzyl-2-methoxy-2-oxoethyl]carbamoyl}-1-methylindole-3-sulfonyl)piperidin-4-yl]ammonium trifluoroacetate salt (93c)

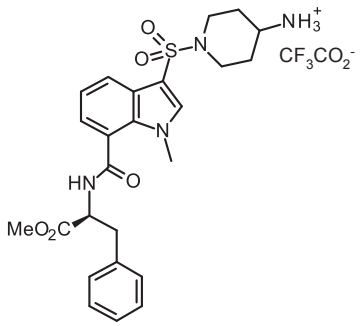

Following general procedure **E**, the compound **93c** was obtained as an orange salt solid. **Molecular Formula**: $C_{27}H_{31}F_3N_4O_7S$; **MW**: 612.62 g/mol; **Yield**: 80%; **^{1}H NMR** (300 MHz, DMSO-d_6) δ 1.63-1.45 (m, 2H, $CH_{2piperidine}$), 1.98-1.85 (m, 2H, $CH_{2piperidine}$), 2.60-2.41 (m, 2H, $CH_{2piperidine}$), 3.00 (dd, J = 13.6, 11.16 Hz, 1H, CH_2), 3.15-2.93 (m, 1H, $CH_{piperidine}$), 3.24 (dd, J = 13.6, 4.4 Hz, 1H, CH_2), 3.50 (s, 3H, CH_3), 3.72 (s, 3H, CH_3), 3.80-3.58 (m, 2H, $CH_{2piperidine}$), 4.88-4.75 (m, 1H, CH),7.10 (d, J = 6.5 Hz, 1H, H_{indole}), 7.37-7.20 (m, 6H, H_{arom} + H_{indole}), 7.82 (d, J = 3.6 Hz, 3H, NH_3^+),7.88 (dd, J = 8.1, 0.8 Hz, 1H, H_{indole}), 8.02 (s, 1H, H_{indole}), 9.18 (d, J = 8.2 Hz, 1H, NH).

N-{1-[1-Methyl-7-(naphth-2-ylcarbamoyl)indole-3-sulfonyl]piperidin-4-yl}ammonium trifluoroacetate salt (93d)

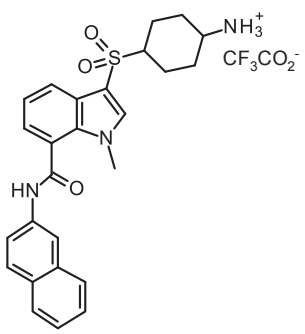

Following general procedure **E**, the compound **93d** was obtained as a grey solid. **Molecular Formula**: $C_{27}H_{27}F_3N_4O_5S$; **MW**: 576.59 g/mol; **Yield**: 100%; **Mp**: > 210°C (washing Et_2O); **^{1}H NMR** (300 MHz, DMSO-d_6) δ

1.66-1.46 (m, 2H, $CH_{2piperidine}$), 2.01-1.86 (m, 2H, $CH_{2piperidine}$), 2.55-2.30 (m, 2H, $CH_{2piperidine}$), 3.13-2.96 (m, 1H, $CH_{piperidine}$), 3.79-3.60 (m, 2H, $CH_{2piperidine}$), 3.88 (s, 3H, CH_3), 7.37 (t, J = 7.3 Hz, 1H, H_{indole}), 7.59-7.41 (m, 3H, H_{napht}), 7.75 (dd, J = 8.8, 1.8 Hz, 1H, H_{napht}), 7.95-7.80 (m, 4H, NH_3^+ + H_{indole}), 7.93 (d, J = 9.1 Hz, 1H, H_{napht}), 7.98 (d, J = 8.1 Hz, 1H, H_{napht}), 8.15 (s, 1H, H_{indole}), 8.51 (s, 1H, H_{napht}),10.93 (s, 1H, NH).

N-(3,4-Dimethoxyphenyl)-1-methyl-3-[4-(acryloylamino)piperidine-1-sulfonyl]indole-7-carboxamide (87a)

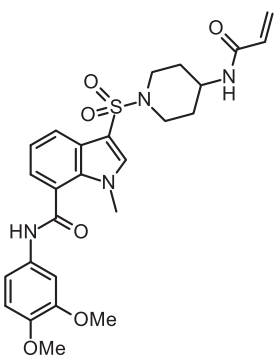

Following general procedure **G - work-up 3** (flash column chromatography solvent: MeOH/CH_2Cl_2 3-5:95-97), the resultant product was precipitated from Et_2O to give **87a** as a white-salmon coloured solid. **Molecular Formula**: $C_{26}H_{30}N_4O_6S$; **MW**: 526.60 g/mol; **Yield**: 67%; **Mp**: 145-147°C (Et_2O); **^{1}H NMR** (300 MHz, DMSO-d_6) δ 1.39-1.56 (m, 2H, $CH_{2piperidine}$), 1.78-1.90 (m, 2H, $CH_{2piperidine}$), 2.53-2.60 (m, 2H, $CH_{2piperidine}$), 3.49-3.64 (m, 3H, $CH_{piperidine}$ + $CH_{2piperidine}$), 3.75 (s, 6H, 2 x OCH_3), 3.85 (s, 3H, CH_3), 5.54 (dd, J = 9.8, 2.5 Hz, 1H, CH_2= cis), 6.03 (dd, J = 17.0, 2.5 Hz, 1H, CH_2= trans), 6.16 (dd, J = 17.0, 9.8 Hz, 1H, CH=), 6.95 (d, J = 8.8 Hz, 1H, H_{arom}), 7.32 (t, J = 7.7 Hz, 1H, H_{indole}), 7.33 (d, J = 8.4 Hz, 1H, H_{arom}), 7.43 (dd, J = 6.5, 1.0 Hz, 1H, H_{indole}), 7.44 (d, J = 2.4 Hz, 1H, H_{arom}), 7.95 (dd, J = 8.0, 1.0 Hz, 1H, H_{indole}), 8.05 (d, J = 7.4 Hz, 1H, NH), 8.11 (s, 1H, H_{indole}), 10.53 (s, 1H, NH); **HRMS (ESI)** calcd for $C_{26}H_{31}N_4O_6S$ $[M+H]^+$, 527.1959; found, 527.1956.

N-(3,4-Dimethoxybenzyl)-1-methyl-3-[4-(acryloylamino)piperidine-1-sulfonyl]indole-7-carboxamide (87b)

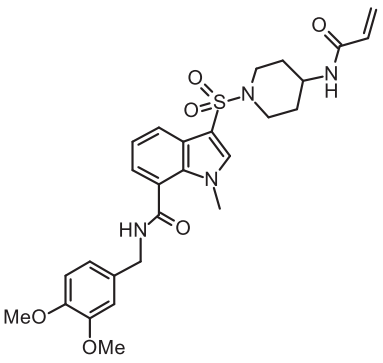

Following general procedure **G - work-up 6** (flash column chromatography solvent: MeOH/CH_2Cl_2 5:95), the resultant product was precipitated from Et_2O to give **87b** as a white solid. **Molecular Formula**: $C_{27}H_{32}N_4O_6S$; **MW**: 540.63 g/mol; **Yield**: 46%; **Mp**: 155-157°C (Et_2O); **^{1}H NMR** (300 MHz, DMSO-d_6) δ 1.58-1.47 (m, 2H, $CH_{2piperidine}$), 1.90-1.77 (m, 2H, $CH_{2piperidine}$), 2.62-2.41 (m, 2H, $CH_{2piperidine}$), 3.65-3.45 (m, 2H, $CH_{piperidine}$ + $CH_{2piperidine}$), 3.74 (s, 6H, 2 x OCH_3), 3.75 (s, 3H, CH_3), 4.45 (d, J = 5.9 Hz, 2H, CH_2), 5.54 (dd, J = 9.8, 2.5 Hz, 1H, CH_2= cis), 6.02 (dd, J = 17.0, 2.5 Hz, 1H, CH_2= trans), 6.15 (dd, J = 17.0, 9.8 Hz, 1H, CH=), 6.97-6.88 (m, 2H, H_{arom}), 7.00 (s, 1H, H_{arom}), 7.27 (t, J = 7.3 Hz, 1H, H_{indole}), 7.32 (dd, J = 7.3, 1.6 Hz, 1H, H_{indole}), 7.89 (dd, J = 7.6, 1.6 Hz, 1H, H_{indole}), 8.03 (d, J = 7.2 Hz, 1H, NH), 8.04 (s, 1H, H_{indole}),9.13 (t, J = 5.7 Hz, 1H, NH); **^{13}C NMR** (101 MHz,

DMSO-d_6) δ 167.3 (C=O), 163.8 (C=O), 148.6 (C), 147.8 (C), 136.4 (CH), 132.4 (C), 131.7 (CH), 131.6, 125.9 (C), 125.2 (CH_2=), 123.5 (C), 122.6 (CH), 121.1 (CH), 121.0 (CH), 119.7 (CH), 111.7 (CH), 111.5 (CH), 108.2 (C), 55.5 (CH_3), 55.4 (CH_3), 44.7 (CH), 44.5 (2 x CH_2), 42.6 (CH_2), 35.9 (CH_3), 30.5 (2 x CH_2); **HRMS (ESI)** calcd for $C_{26}H_{31}N_4O_6S$ $[M+H]^+$, 541.2115; found, 541.2100.

Methyl (2S)-2-({1-Methyl-3-[4-(acryloylamino)piperidine-1-sulfonyl]indole-7-carboxamide-3-phenylpropanoate (87c)

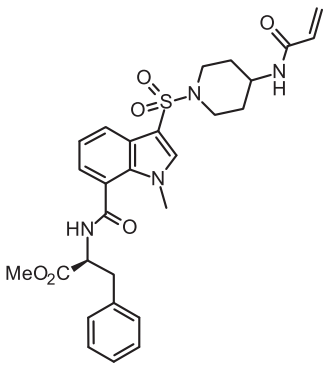

Following general procedure **G- work-up 6** (flash column chromatography solvent: MeOH/CH_2Cl_2 2:98), the resultant product was precipitated from Et_2O to give **87c** as a white solid. **Molecular Formula**: $C_{28}H_{32}N_4O_6S$; **MW**: 552.64 g/mol; **Yield**: 61%; **Mp**: 128-130°C (Et_2O); **^{1}H NMR** (300 MHz, DMSO-d_6) δ 1.54-1.35 (m, 2H, $CH_{2piperidine}$), 1.89-1.74 (m, 2H, $CH_{2piperidine}$), 2.62-2.31 (m, 2H, $CH_{2piperidine}$), 3.00 (dd, J = 13.8, 11.3 Hz, 1H, CH_2), 3.24 (dd, J = 13.8, 4.5 Hz, 1H, CH_2), 3.52 (s, 3H, CH_3), 3.64-3.40 (m, 3H, $CH_{piperidine}$ + $CH_{2piperidine}$), 3.71 (s, 3H, CH_3), 4.87-4.75 (m, 1H, CH), 5.53 (dd, J = 9.8, 2.6 Hz, 1H, CH_2= cis), 6.02 (dd, J = 17.1, 2.6 Hz, 1H, CH_2= trans), 6.15 (dd, J = 17.1, 9.8 Hz, 1H, CH=), 7.08 (d, J = 7.2 Hz, 1H, H_{indole}), 7.39-7.18 (m, 6H, H_{arom} + H_{indole}), 7.89 (d, J = 8.1 Hz, 1H, H_{indole}), 8.01 (s, 1H, H_{indole}), 8.02 (d, J = 8.1 Hz, 1H, NH), 9.16 (d, J = 8.1 Hz, 1H, NH); **^{13}C NMR** (101 MHz, DMSO-d_6) δ 171.9 (CO), 167.4 (C=O), 163.8 (C=O), 137.6 (C), 136.4 (CH), 132.2 (C), 131.7 (CH), 129.2 (2 x CH), 128.3 (2 x CH), 126.6 (CH), 125.9 (C), 125.2 (CH_2=), 122.7 (C), 122.6 (CH), 121.2 (CH), 121.0 (CH), 108.2 (C), 53.8 (CH), 52.2 (CH_3), 44.7 (CH), 44.5 (2 x CH_2), 36.2 (CH), 35.5 (CH_3), 30.5 (2 x CH_2); **HRMS (ESI)** calcd for $C_{28}H_{33}N_4O_6S$ $[M+H]^+$, 553.2115; found, 553.2079.

1-Methyl-*N*-(naphth-2-yl)-3-[4-(acryloylamino)piperidine-1-sulfonyl]indole-7-carboxamide (87d)

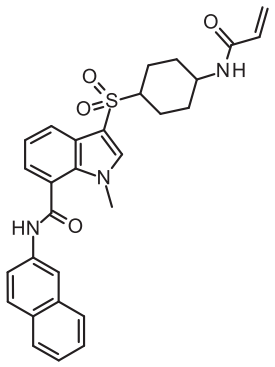

Following general procedure **G - work-up 6** (The resulting extracts were crystallized from MeOH), the compound **87d** was obtained as a white solid. **Molecular Formula**: $C_{28}H_{28}N_4O_4S$; **MW**: 516.61 g/mol; **Yield**: 52%; **Mp**: 157-158°C (MeOH); **^{1}H NMR** (300 MHz, DMSO-d_6) δ 1.57-1.39 (m, 2H, $CH_{2piperidine}$) 1.57-1.39 (m, 2H, $CH_{2piperidine}$), 1.91-1.78 (m, 2H, $CH_{2piperidine}$), 2.60-2.32 (m, 2H, $CH_{2piperidine}$), 3.64-3.49 (m, 3H, $CH_{piperidine}$ + $CH_{2piperidine}$), 3.88 (s, 3H, CH_3), 5.55 (dd, J = 9.8, 2.5 Hz, 1H, CH_2= cis), 6.03 (dd, J = 17.1, 2.5 Hz, 1H, CH_2= trans), 6.17 (dd, J = 17.1, 9.8 Hz, 1H, CH=),7.36 (t, J = 7.5 Hz, 1H, H_{indole}), 7.56-7.41 (m, 3H,

H_{napht}), 7.75 (dd, J = 8.8, 1.9 Hz, 1H, H_{napht}), 7.89 (dd, J = 8.0, 3.1 Hz, 1H, H_{indole}), 7.93 (d, J = 9.2 Hz, 1H, H_{napht}), 7.99 (d, J = 8.7 Hz, 1H, H_{napht}), 8.06 (d, J = 7.7 Hz, 1H, NH), 8.14 (s, 1H, H_{indole}), 8.52 (s, 1H, H_{napht}), 10.92 (s, 1H, NH); **^{13}C NMR** (101 MHz, DMSO-*d_6*) δ 166.2 (C=O), 163.9 (C=O), 136.6 (CH), 136.5 (C), 133.4 (C), 132.2 (C), 131.7 (CH), 130.1 (C), 128.5 (CH), 127.5 (2 x CH), 126.6 (CH), 126.1 (C), 125.3 (CH_2=), 125.0 (CH), 123.4 (C), 122.9 (CH), 121.5 (CH), 121.3 (CH), 120.4 (CH), 116.0 (CH), 108.4 (C), 44.8 (CH), 44.6 (2 x CH_2), 36.0 (CH_3), 30.6 (2 x CH_2); **HRMS (ESI)** calcd for $C_{28}H_{29}N_4O_4S$ $[M+H]^+$, 517.1904; found, 517.1888.

3,4-Dimethoxy-*N*-{1-methyl-3-[4-(prop-2-ynoylamino)piperidine-1-sulfonyl]indol-7-yl}benzamide (94)

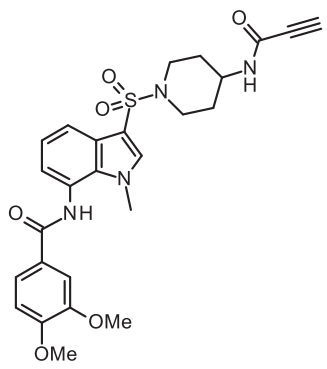

Following general procedure **I - work-up2** (flash column chromatography solvent: MeOH/CH_2Cl_2 5:95), the resultant product was precipitated from MeOH, to give **94** as an orange solid. **Molecular Formula**: $C_{26}H_{28}N_4O_6S$; **MW**: 524.59 g/mol; **Yield**: 6%; **Mp**: 170°C (MeOH); **^{1}H NMR** (300 MHz, DMSO-*d_6*) δ 1.59-1.35 (m, 2H, $CH_{2piperidine}$), 1.86-1.70 (m, 2H, $CH_{2piperidine}$), 2.68-2.35 (m, 2H, $CH_{2piperidine}$), 3.62-3.26 (m, 3H, $CH_{piperidine}$ + $CH_{2piperidine}$), 3.84 (s, 3H, CH_3, OCH_3), 3.85 (s, 3H, OCH_3), 3.94 (s, 3H, CH_3), 4.11 (s, 1H, CH), 7.12 (d, J = 8.5 Hz, 1H, H_{arom}), 7.16 (d, J = 7.0 Hz, 1H, H_{indole}), 7.25 (t, J = 7.7 Hz, 1H, H_{indole}), 7.61 (s, 1H, H_{arom}), 7.68 (d, J = 8.5 Hz, 1H, H_{arom}), 7.75 (d, J = 7.5 Hz, 1H, H_{indole}), 7.98 (s, 1H, H_{indole}), 8.73 (d, J = 7.5 Hz, 1H, NH), 10.22 (s, 1H, NH); **HRMS (ESI)** calcd for $C_{26}H_{29}N_4O_6S$ $[M+H]^+$, 525.1802; found, 525.1812.

3,4-Dimethoxy-*N*-{1-methyl-3-[4-(propanoylamino)piperidine-1-sulfonyl]indol-7-yl}benzamide (95)

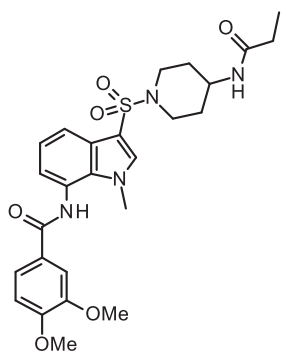

Following general procedure **G - Work-up 3** (flash column chromatography solvent: MeOH/CH_2Cl_2 5:95), the resultant product was precipitated from MeOH to give **95** as a white solid. **Molecular Formula**: $C_{26}H_{32}N_4O_6S$; **MW**: 528.62 g/mol; **Yield**: 68%; **Mp**: > 210°C (MeOH); **^{1}H NMR** (300 MHz, DMSO-*d_6*) δ 0.93 (t, J = 7.6 Hz, 1H, CH_3), 1.52-1.32 (m, 2H, $CH_{2piperidine}$), 1.86-1.72 (m, 2H, $CH_{2piperidine}$), 2.01 (q, J = 7.6 Hz, 2H, CH_2), 2.62-2.34 (m, 2H, $CH_{2piperidine}$), 3.59-3.35 (m, 3H, $CH_{piperidine}$ + $CH_{2piperidine}$), 3.84 (s, 3H, OCH_3), 3.85 (s, 3H, OCH_3), 3.94 (s, 3H, CH_3), 7.12 (d, J = 8.7 Hz, 1H, H_{arom}), 7.16 (d, J = 7.3 Hz, 1H, H_{indole}), 7.25 (t, J = 7.7 Hz, 1H, H_{indole}), 7.61 (d, J = 1.9 Hz, 1H, H_{arom}), 7.68 (dd, J = 8.1, 1.9 Hz, 1H, H_{arom}), 7.72 (d, J = 7.5 Hz, 1H, NH), 7.76 (d, J = 7.5 Hz, 1H, H_{indole}), 7.98 (s, 1H, H_{indole}), 10.22 (s, 1H, NH); **^{13}C NMR** (101 MHz, DMSO-*d_6*) δ 172.2 (C=O),

166.4 (C=O), 151.8 (C), 148.5 (C), 136.2 (CH), 132.7 (C), 126.7 (C), 126.0 (C), 123.7 (C), 123.6 (CH), 121.9 (CH), 121.0 (CH), 118.4 (CH), 111.1 (CH), 110.9 (CH), 108.0 (C), 55.7 (CH_3), 55.6 (CH_3), 44.6 (CH + 2 x CH_2), 35.7 (CH_3), 30.7 (2 x CH_2), 28.4 (CH_2), 9.89 (CH_3); **HRMS (ESI)** calcd for $C_{26}H_{33}N_4O_6S$ $[M+H]^+$, 529.2115; found, 529.2087.

Biochemistry

A. *Preparation and solubility of inhibitors*

Inhibitor's mother solution at 10 mM in DMSO was prepared and preserved at -20ºC until use. From this solution different concentrations were prepared in the same buffer as employed in the inhibition assay (TRIS-NaCl buffer, pH 8.0). A maximum of 3% DMSO was employed to increase solubility of inhibitors within the assay conditions.

B. *TG crosslinking activity assay*

With regard to the measurement of the transamidation activity for the transglutaminases tested in this chapter, and the IC_{50} determination for each compound, conditions and techniques employed were also the same as performed in chapter 2.

Bibliography - Chapter 3

155. Longeon, A.; Copp, B. R.; Quévrain, E.; Roué, M.; Kientz, B.; Cresteil, T.; Petek, S.; Debitus, C.; Bourguet-Kondracki, M. L. Bioactive indole derivatives from the south pacific marine sponges *Rhopaloeides odorabile* and *Hyrtios sp*. *Mar. Drugs* **2011**, *9*, 879-888.

156. Li, J. L.; Huang, L.; Liu, J.; Song, Y.; Gao, J.; Jung, J. H.; Liu, Y.; Chen, G. Acetylcholinesterase inhibitory dimeric indole derivatives from the marine actinomycetes Rubrobacter radiotolerans. *Fitoterapia* **2015**, *102*, 203-207.

157. Manivasagan, P.; Kang, K. H.; Sivakumar, K.; Li-Chan, E. C.; Oh, H. M.; Kim, S. K. Marine actinobacteria: an important source of bioactive natural products. *Environ. Toxicol. Pharmacol*. **2014**, *38*, 172-188.

158. Khan, N.; Mukhtar, H. Dietary agents for prevention and treatment of lung cancer. *Cancer. Lett*. **2015**, *359*, 155-164.

159. Aggarwal, B. B.; Ichikawa, H. Molecular targets and anticancer potential of indole-3-carbinol and its derivatives. *Cell Cycle* **2005**, *4*, 1201-1215.

160. Ahmad, A.; Sakr, W. A.; Rahman, K. M. Anticancer properties of indole compounds: mechanism of apoptosis induction and role in chemotherapy. *Curr. Drug. Targets* **2010**, *11*, 652-66.

161. Biersack, B.; Schobert, R. Indole compounds against breast cancer: recent developments. *Curr. Drug. Targets* **2012**, *13*, 1705-19.

162. Piscitelli, F.; Coluccia, A.; Brancale, A.; La Regina, G.; Sansone, A.; Giordano, C.; Balzarini, J.; Maga, G.; Zanoli, S.; Samuele, A.; Cirilli, R.; La Torre, F.; Lavecchia, A.; Novellino, E.; Silvestri, R. Indolylarylsulfones bearing natural and unnatural amino acids. Discovery of potent inhibitors of HIV-1 non-nucleoside wild type and resistant mutant strains reverse transcriptase and coxsackie B4 virus. *J. Med. Chem*. **2009**, *52*, 1922-1934.

163. Zhao, Z.; Wolkenberg, S. E.; Sanderson, P. E.; Lu, M.; Munshi, V.; Moyer, G.; Feng, M.; Carella, A. V.; Ecto, L. T.; Gabryelski, L. J.; Lai, M. T.; Prasad, S. G.; Yan, Y.; McGaughey, G. B.; Miller, M. D.; Lindsley, C. W.; Hartman, G. D.; Vacca, J. P.; Williams, T. M. Novel indole-3-sulfonamides as potent HIV non-nucleoside reverse transcriptase inhibitors (NNRTIs). *Bioorg. Med. Chem. Lett*. **2008,** *18*, 554-559.

164. Conway, S. C.; Gribble, G. W. Synthesis of 1-(phenylsulfonyl)indole-3-yl trifluoromethanesulfonate. *Heterocycles* **1990**, *30*, 627-633.

165. Janosik, T.; Shirani, H.; Wahlström, N.; Malky, I.; Stensland, B.; Bergman, J. Efficient sulfonation of 1-phenylsulfonyl-1*H*-pyrroles and 1-phenylsulfonyl-1*H*-

indoles using chlorosulfonic acid in acetonitrile. *Tetrahedron* **2006**, *62*, 1699–1707.

166. Joucla, L.; Popowycz, F.; Olivier, L.; Meijer, L.; Joseph, B. Access to paullone analogues by intramolecular Heck reaction. *Helv. Chim. Acta* **2007**, *90*, 753-763.

167. Tolnai, G. L.; Ganss, S.; Brand, J. P.; and Waser, J. C2-selective direct alkynylation of indoles. *Org*. *Lett*. **2013**, 15, 112-115.

168. Qun, Li; Sham, H.; Steiner, B. A.; Gwaltney, S. L.; II; Barr, K. J.; Imade, H. M.; Rosenberg, S.; Woods, K. W. Preparation of sulfonamides as cell proliferation inhibitors. **2000**, WO 2000/073264; *Chem*. *Abstr*., **134**, 29308.

169. Davis, P. D.; Hill, C. H.; Lawton, G.; Nixon, J. S.; Wilkinson, S. E.; Hurst, S. A.; Keech, E.; Turner, S. E. Inhibitors of protein kinase C. 1. 2,3-Bisarylmaleimides. *J. Med. Chem*. **1992**, *35*, 177-184.

170. Adel Hamed M. M.; Buyanov, V. N.; Zhigachev, V. E.; Kurkovskaya, L. N.; Suvorov, N. N. Indole derivatives. 136. 4-, 5-, 6-, and 7-Nitro-3-indolesulfonic chlorides and sulfonamides. *Chem*. *Heterocycl*. *Compd*. **1990**, *26*, 1116-1120.

171. Masafumi, K.; Atsuyuki, K.; Kazuhiro, N.; Akira, M.; Tsuyoshi, N.; Naohitio. O. Synthesis and biological activity of *N*-(aminoiminomethyl)-1*H*-indole carboxamide derivatives as Na^+/H^+ exchanger inhibitors. *Chem*. *Pharm*. *Bull*. **1999**, *47*, 1538-1548.

172. Hebeisen, P.; Kitas, E. A.; Minder, R. E.; Mohr, P.; Wessel, H. P. Preparation of aminothiazole derivatives as fructose-1,6-bisphosphatase inhibitors for treating diseases such as diabetes. **2009**, WO 2009/068467, *Chem*. *Abstr*., **150**, 563821.

CHAPTER 4

Mechanism of inhibition of lead compounds

1. Optimization of a continuous TG2-GDH coupled enzymatic assay

The methodology employed for the characterization of the enzyme kinetics for compounds bearing an acrylamide warhead herein synthesized, was the continuous GDH-coupled enzymatic assay as described in the introduction of this dissertation.[82,84] The coupled reaction of TG2 and GDH is described in the **Scheme 10** (page 38). First of all, the methodology was optimized and validated to define the kinetic Michaelis-Menten constants (V_{max}, K_m, k_{cat}) of the TG2 in this assay. The conditions employed are described in the next paragraphs.

1.1. Optimization and validation of the GDH-coupled assay conditions

Based on the GDH-linked assay previously described from the works of Day et al.[82] and Klöck et al.,[84] water was chosen as the acyl acceptor substrate. Herein, the *N*,*N*-dimethylcasein (DMC) was selected as the acyl donor substrate for the TG2, instead of Cbz-Gln-Gly, owing to its lower K_m values for TG reviewed in the literature. The DMC K_m values were 10^{-3} to 10^{-4}-times lower compared to those of Cbz-Gln-Gly for the different TG2 kinetic methods reported.[173] The determination of the TG2 kinetic parameters using this methodology was investigated.

First of all, different conditions were studied in order to obtain the best reaction rate (v, μM min^{-1}) as possible for the development of this kinetic measurement in a microtiter plate measurement system. Different concentrations for the reactants/reagents for both coupled enzymatic reactions were analyzed (variations of the reaction mixture components: α-ketoglutarate (α-KG), NADH, GDH, DMC, and TG2). Regarding the conditions for the GDH reaction within the enzymatic assay, different variations of the reactant/reagents, ranging from 44.4 to 57.1 mM (α-KG), from 555 to 238 μM (NADH), and from 11.11 to 4.76 U/mL (GDH), were studied. On the other hand, regarding the TG2 reaction, the TG2 acyl donor substrate assayed concentrations ranged from 222 to 190 μM of DMC. The initial rate (v, μM min^{-1}) values were measured as the slope of the progress curve after some minutes of reaction's latence time (slope was taken aproximatively from 10 to 40 min) once TG2 was added to the reaction mixture (see **Graph 1)**. At the end, increasing TG2 concentrations from 0.047 μM, to 0.190 μM (4.1-fold increase of TG2) resulted in the higher initial reaction rates compared with the non-TG2 assay (background).

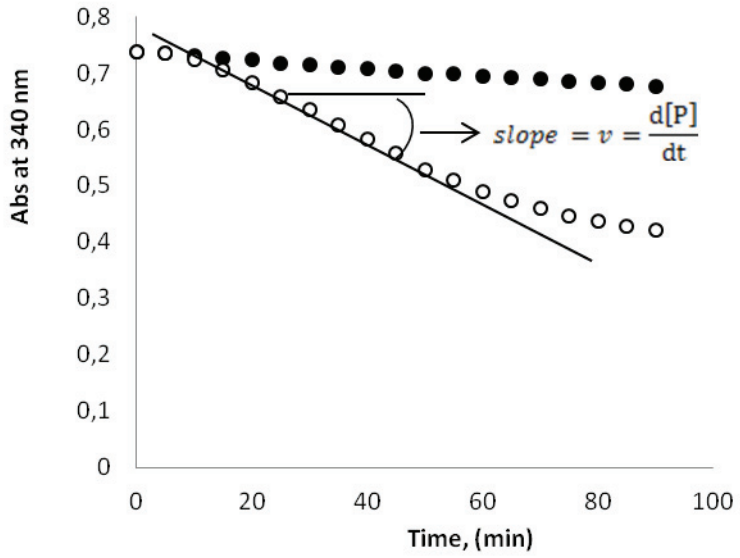

Graph 1. Progression curve of the enzymatic kinetic assay showing the blank and the TG2 positive control of the assay. Slope values, as observed, where normally taken after 15 to 40 min of the TG2 addition, after a period of reaction latence of some min. (●) no TG2 in the reaction mixture (blank); (○) TG2 positive control (0.190 µM TG2). Assays were perfromed in 200 mM MOPS buffer (pH 7.1) at 36ºC

After assaying and testing the different conditions for the assay, the standarized conditions to perform the kinetic assay are as follows: 200 mM MOPS buffer (pH 7.1), 4 mM $CaCl_2$, 57.1 mM α-ketoglutarate, 238 µM NADH, 4.76 Units/mL GDH (0.499 Units), 190 µM or 19 µM *N*,*N*-dimethylcasein and 0.190 µM TG2 for a final volume of 105 µL per well. The reaction was started after the addition of the TG2 at 36ºC. The decrease in absorbance owing to the oxidation of the NADH was monitored at 340nm.

1.2. Measuring the kinetic Michaelis-Menten kinetic constants: V_{max}, K_m, and k_{cat}

Under the optimized conditions, the kinetic Michaelis-Menten parameters were obtained. After measuring the initial enzymatic reaction rate for different concentrations of DMC, K_m and V_{max} values were calculated by linearizing the Michaelis-Menten equation using the Eadie-Hofstee and the Hanes-Woolf plots. The graph representing the Michaelis-Menten hyperbolic curve for different substrate concentrations is shown in **Graph 2**. The selected DMC concentrations employed to plot the Michaelis-Menten hyperbole were 19, 50, 100 and 190 µM.

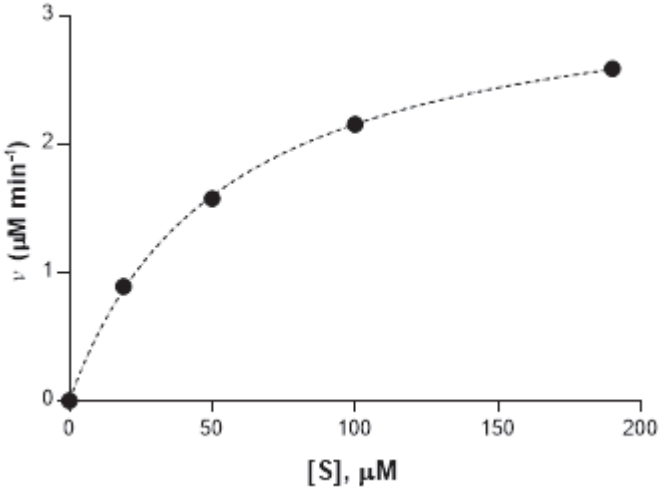

Graph 2. Michaelis-Menten plot for TG2 using DMC as substrate. Initial rates (v) measured from 15 to 40 min after addition of TG2 (0.190 μM) to the reaction mixture at 36ºC in 200 mM MOPS buffer (pH 7.1). Dashed lines are fitted to a hyperbola (R^2> 0.99)

The data and the plotting for the determination of the K_m and V_{max} values by means of the Eadie-Hofstee and the Hanes-Woolf plots are shown **Graphs 3** and **4**, where the reaction rate of the assay comes determined by following equations (12) and (13), for the Eadie-Hofstee and the Hanes-Woolf plots respectively.

$$v = -K_m \frac{v}{[S]} + V_{max} \qquad (12)$$

$$\frac{[S]}{v} = \frac{1}{V_{max}}[S] + \frac{K_m}{V_{max}} \qquad (13)$$

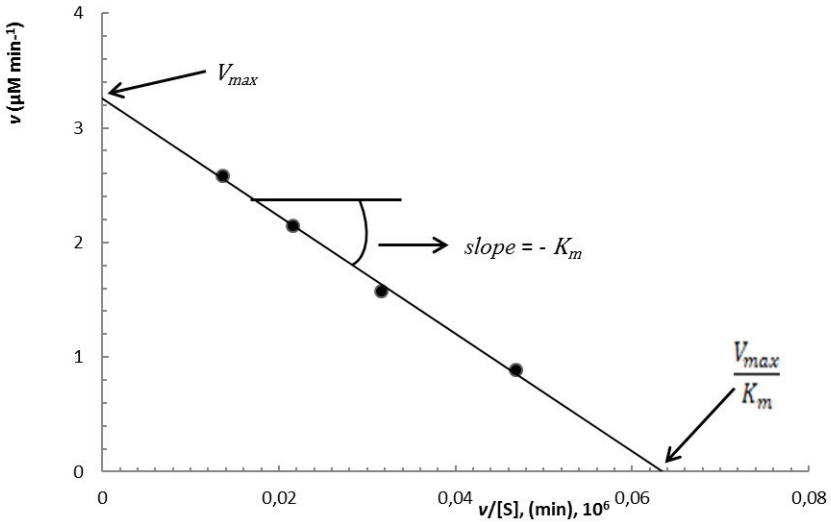

Graph 3. Eadie-Hofstee plot where V_{max} is equal to the value from intercept of the line with y-axis; and, K_m is given as the absolute value from the slope of the linear equation described as $v = -51.289 \frac{v}{[S]} + 3.257$; $R^2 = 0.996$

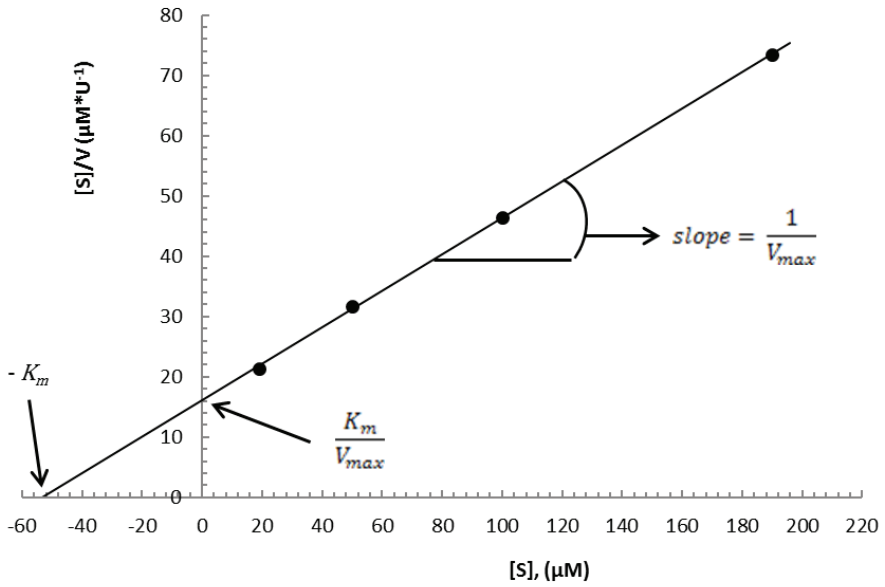

Graph 4. Hanes-Woolf plot. K_m is given as the absolute value of the intercept of the line with x-axis; and, V_{max} being equal to $\frac{1}{slope}$; the linear regression equation is described as $\frac{[S]}{v} = 0.302\,[S] + 16.088$; $R^2 = 0.999$

The K_m and V_{max} values obtained for both methods are shown in **Table 28**.

Method	K_m (µM)	V_{max} (µM min^{-1})
Eadie-Hofstee Plot	51.7	3.26
Hanes-Wolf Plot	52	3.31
Mean ± S.D.	51.85 ± 0.15	3.28 ± 0.025

Table 28. K_m and the V_{max} values obtained from the Eadie-Hofstee and the Hanes-Wolf plots. K_m and V_{max} values are also expressed as the mean ± S.D (n=2). of both values calculated by the two different plot analysis

Knowing V_{max} and initial enzyme concentration $[E_0]$ values, k_{cat} (turnover rate) can be calculated from the equation (14), where $[E_0]$ is the initial enzyme concentration. Substituting V_{max} and $[E_0]$ on equation (14) k_{cat} gives a value of 17 min^{-1}.

$$V_{max} = k_{cat}\,[E_0] \qquad (14)$$

To conclude it is observed that DMC tighly bound to TG2 because of its lower K_m value (51.85 µM ± 0.15) compared to the carbobenzyloxy-L-glutamylglycine and the DMPDA whose K_m values fall within the mM range (K_m values of 6.8 mM and 2.4 mM respectively). On the contrary, K_m values for the 4-(*N*-carbobenzyloxy-L-phenylalanylamino)butyric acid coumarin-7-yl ester (CbzGBC) and *N*-Cbz-L-glutamyl(-*p*-nitrophenylester)glycine (*N*-Cbz-L-Glu(*p*-nitrophenylester)Gly) esters (from coumarin- and *p*-nitrophenyl-based kinetic assays) fall in the micromolar range

with lower values of 9 μM and 20 μM respectively. Furthermore, the turnover rate (herein k_{cat} of 17.26 min^{-1}) is identical to that obtained by using also water as the acyl acceptor when Cbz-Gln-Gly was employed as the acyl donors (k_{cat} of 17 ± 0.6 min^{-1}). This does not occur in the case of the coumarin-based fluorimetric assay and the *p*-nitrophenyl-based assay, whose k_{cat} are higher with values of 78 ± 5 min^{-1} and 54.6 min^{-1} respectively. Owing to their low K_m and k_{cat} values, the synthesis of the esters above could be of great interest. However, because of their hard and time-consuming synhesis they have been discarded to be used at this point of the work.

1.3. Validation of the of the assay: inter-assay repeatability

To evaluate the reproducibility of the assay, the initial rate values (v) for same TG2 concentration (0.190 μM) from several measurements from independent assays were obtained for two different concentrations of DMC, 19 and 190 μM respectively. This two DMC concentrations were selected for being values below and above the K_m observed for this method. The standard deviation (S.D.), the mean, and the coefficient of variation (C.V.) were calculated (see **Table 29**) to check the inter-assay variability of the method. It can be observed C.V.values are not higher than 8.62 % and 4.33 % for the initial rate (v) values for the 19 and 190 μM of DMC assayed respectively. These C.V. results, knowing that C.V. values less than 20% in interassay experiments, and under the same experiment conditions are aceptable for analytical assays,[174] demonstrate a good inter-assay repeatibility of the method.

	190 μM DMC (μM min^{-1})	19 μM DMC (μM min^{-1})
Mean	2.64	1.04
S.D.	0.11	0.09
C.V. (%)	4.33	8.62

Table 29. Different initial rate (v) values measured for at least three independent kinetic mesurements for the two DMC selected concentrations (19 and 190 μM). v values were averaged and both their S.D. and C.V. were calculated

2. Inhibition study of derivatives 23b, 78f and reference X

In this section the kinetic studies for **23b**, **78f** and the reference inhibitor **X** from the work of Prime et al.[112] (see **Figure 62**) were analyzed using the methodology herein described. All these compounds have in common the reactive acrylamide moiety, a Michael acceptor such as some α-unsaturated carbonyl derivatives which were reported as irreversible "covalent" modifiers of the active site thiol of cysteine proteases.[73]

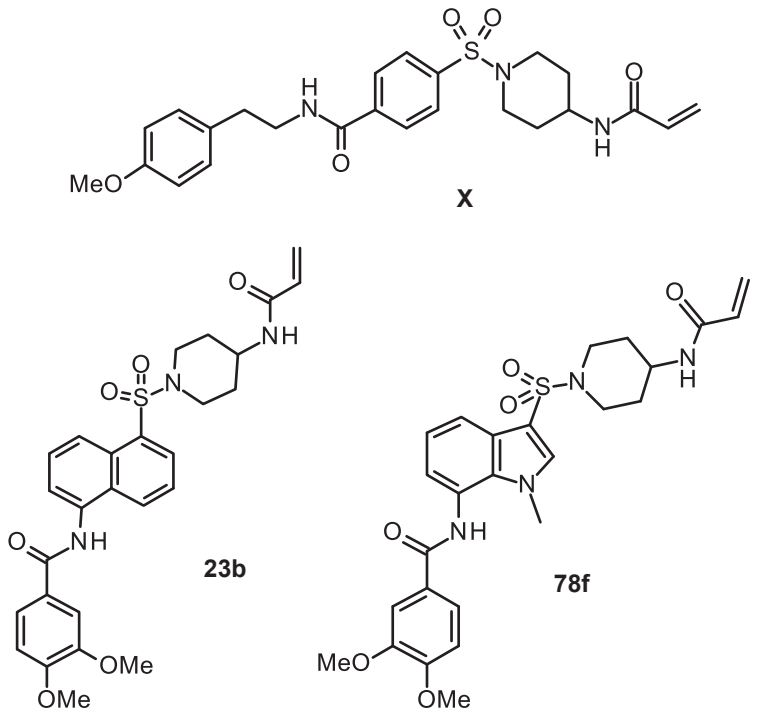

Figure 62. Structure of the three TG2 inhibitors herein studied. All compounds are bearing an acrylamide electrophilic warhead

2.1. Inhibition study of 23b

Kinetic studies for **23b** (see **Figure 62**) were firstly performed at two different concentrations of DMC (below and above K_m), without preliminary incubation of the inhibitor with the enzyme. The inhibitory concentrations assayed of **23b** ranged from 0.01 to 1 μM. Assaying two DMC concentrations will provide the possibility to measure the K_I of the inhibitor using a Dixon plot.[175,176] Dixon plots is an alternative method to measure the K_I dissociation constant of inhibition by plotting $1/v$ *vs.* [I], where a family of intersecting lines for different substrate concentrations is observed for competitive and no competitive inhibition, but not for uncompetitive inhibition (see **Figure 63**). Single reciprocal plots of $1/v$ *vs.* [I] for the different class of reversible inhibition are described in the next equations (15), (16), and (17):

Competitive inhibition Dixon plot equation:

$$\frac{1}{v} = \left(\frac{Km}{K_I V_{max}\,[S]}\right)[\mathrm{I}] + \left(\frac{K_m}{[S]} + 1\right)\frac{1}{V_{max}} \qquad (15)$$

Non-competitive inhibition Dixon plot equation:

$$\frac{1}{v} = \left(\frac{1}{K_I V_{max}}\right)\left(\frac{K_m}{[S]} + 1\right)[\mathrm{I}] + \left(\frac{K_m}{[S]} + 1\right)\frac{1}{V_{max}} \qquad (16)$$

Uncompetitive inhibition Dixon plot equation:

$$\frac{1}{v} = \left(\frac{1}{K_I V_{max}}\right)[\mathrm{I}] + \left(\frac{K_m}{[S]} + 1\right)\frac{1}{V_{max}} \qquad (17)$$

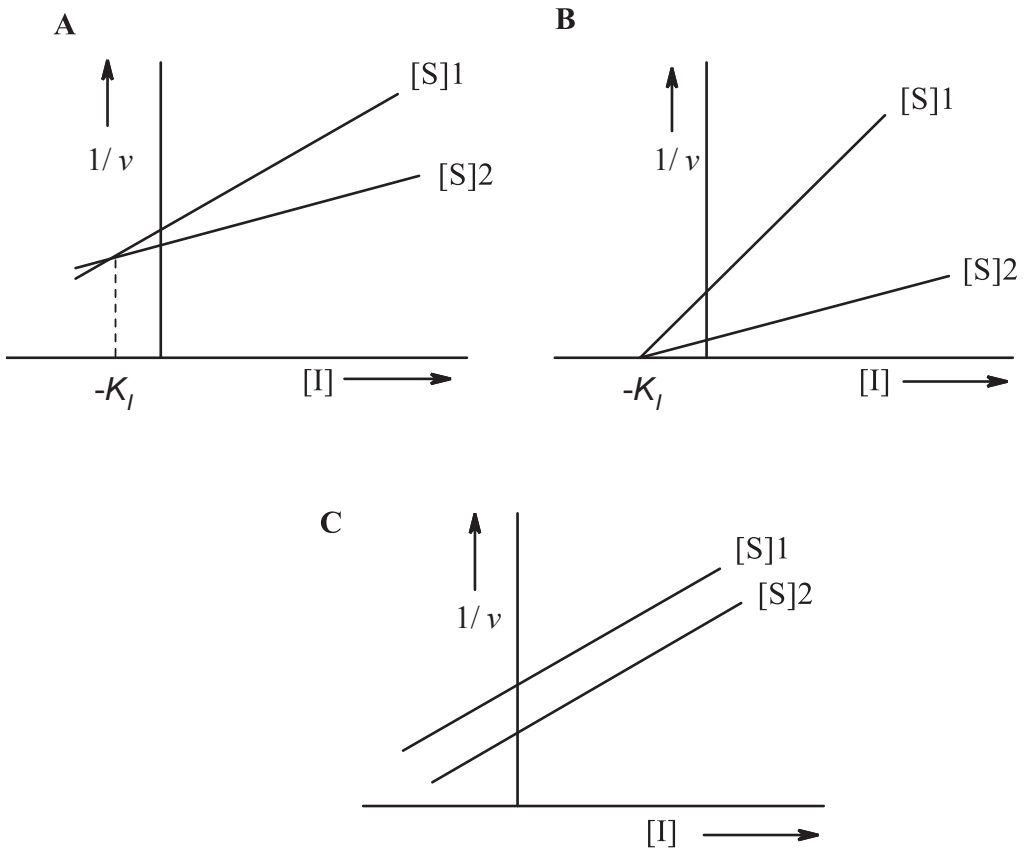

Figure 63. Dixon plots for $1/v$ *vs.* [I] (e.g., two substrate concentrations represented as [S]1 and [S]2 in the graphs) for the different modes of inhibition; **A**. Dixon plot for competitive inhibition. It corresponds to equation (15); **B**. Dixon plot for non-competitive pure inhibition. It corresponds to equation (16); **C**. Dixon plot for uncompetitive inhibition. It corresponds to equation (17)

In a first attempt to measure the TG2 inhibition kinetics, two concentrations of DMC, below and above the K_m (9.8 μM and 190 μM) were analyzed in the presence of different concentrations of compound **23b**. Data from the observed initial rate values (v) against the inhibitor concentrations tested are represented in **Graph 5**. This plot, for both DMC concentrations, did not follow a linear behavior. This is indicative of the possible formation of reversible enzyme-inhibitor complexes, EI and/or ESI.

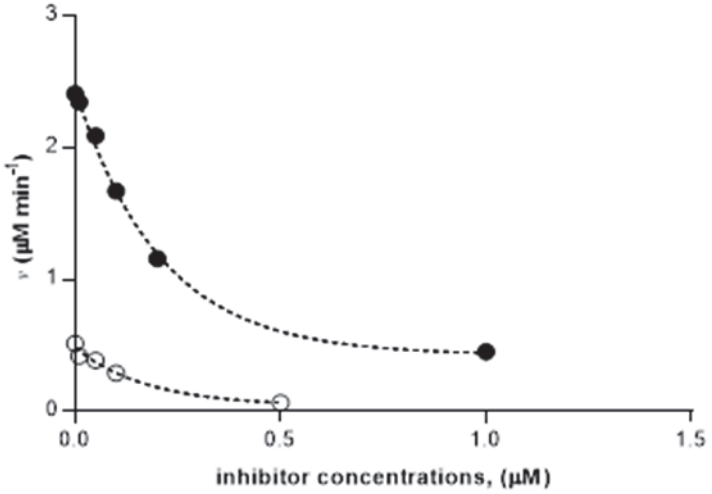

Graph 5. Plot of *v* values *vs.* [I] for both DMC concentrations (9.8 and 190 μM) assayed for **23b**. (●) 190 μM of DMC; (○) 9.8 μM of DMC (dashed lines are drawn for the eyes)

The initial rate (*v*) data obtained for each inhibitor concentration was used to perform a Dixon plot (see **Graph 6**). Therefore, initial rate values for each inhibitor concentration, at both of the concentrations of DMC assayed (190 and 9.8 μM), were linearized and the dissociation constant K_I have been calculated as the intersection of the two lines. The obtained K_I value was 0.052 μM.

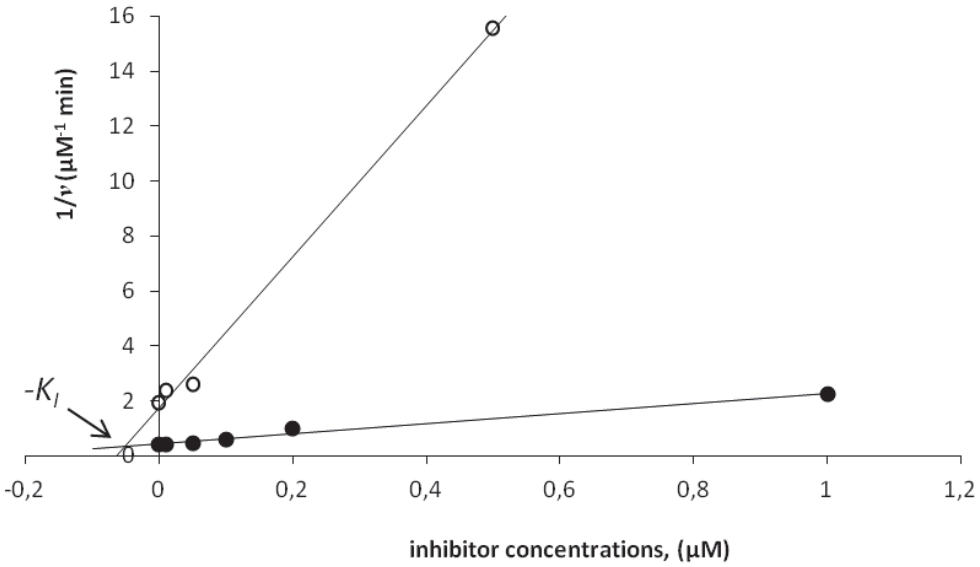

Graph 6. Dixon plot where $\frac{1}{v}$ values were plotted against the different inhibitor concentrations for compound **23b**. A Dixon competitive inhibition model is observed (see **A**, **Figure 84**), corresponding to equation (15). (●) $\frac{1}{v}$ values *vs.* [I] for 190 μM of DMC whose linear regression equation is expressed as $\frac{1}{v} = 1.806\,[\mathrm{I}] + 0.448$, with an $R^2 = 0.981$; (○) $\frac{1}{v}$ values *vs.* [I] for 9.8 μM of DMC whose linear regression equation is expressed as $\frac{1}{v} = 27.448\,[\mathrm{I}] + 1.776$, with an $R^2 = 0.996$

This preliminary kinetic for compound **23b**, suggested that this TG2 inhibitor follows a competitive reversible inhibition mode of action.

As a second approach to confirm if TG2 can be inactivated irreversibly, or not, a further inactivating chemical step was carried out. For this purpose, the enzyme was preincubated with the inhibitor at different period of times (15, 30 and 90 minutes) at 36ºC. The selected concentrations of the inhibitor to perform the assay were 0.05, 0.1 and 0.2 μM. Once the different preincubation times were ended, the remaining components of the assay mixture, including the DMC as the glutamine donor, were added to the enzyme-inhibitor solution to start the enzymatic assay. The initial reaction rates (v) obtained for each for each preincubation assay, at the different concentrations of inhibitor, were plotted against the different inhibitor concentrations employed (see **Graph 7**). It can be observed in **Graph 7** that v values *vs.* inhibitor concentration, [I] for the different preincubation experiments follow a linear regression tendency.

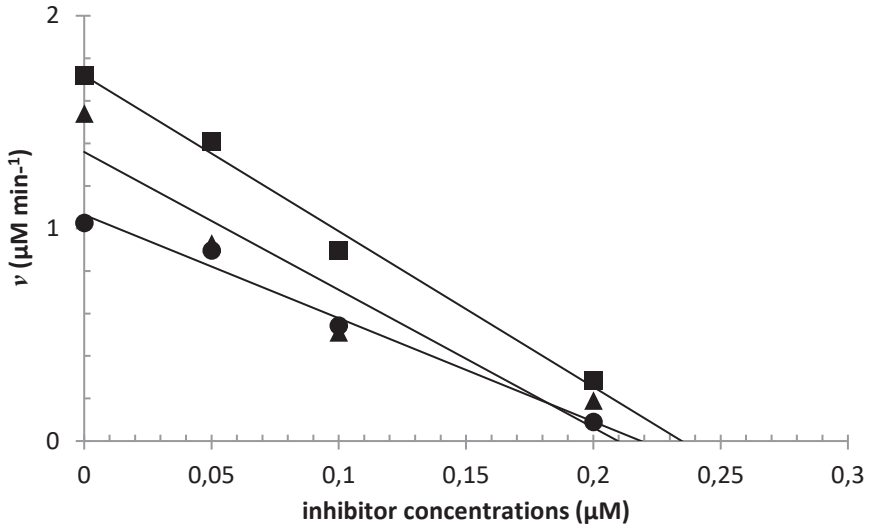

Graph 7. Plot of v values *vs.* [I] after different preincubation times (15, 30, and 90 min) at 36ºC for compound **23b**. Linear regression equation is referred as $v = b[I] + a$, where b and a correspond to the slope and the intercept with the y-axis respectively. (■) v values after 15 min of preincubation. Linear regression equation is expressed as $v = -7.320\,[I] + 1.718$, with an $R^2 = 0.989$; (▲) v values after 30 min of preincubation. Linear regression equation is expressed as $v = -6.483\,[I] + 1.359$, with an $R^2 = 0.902$.; (●) v values after 90 min of preincubation. Linear regression equation is expressed as $v = -4.863\,[I] + 1.064$, with an $R^2 = 0.984$

An approximation of the stoichiometry of the interaction of compound **23b** with the TG2 was also studied. To do this, inhibitor concentrations, [I], found from **Graph 7** when the tendency line intercepts the x-axis for the different preincubation times, were compared with the initial enzyme concentration, [E_0]. The x-intercept of [I] were found to be between 0.21 and 0.235 μM, while [E_0] is 0.19 μM. These values suggest the probable interaction of one (may be two) molecules of inhibitor with the TG2 (concentration values for [E_0] and [I] are above the same micromolar range). The need of more inhibitor concentrations would be of great value to obtain a more reliable estimation of this interaction.

Moreover, in order to obtain the rate of inactivation of the irreversible step, k_{inact} (see **Scheme 84**), the decrease in TG2 activity at each inhibitor concentrations, after preincubations of 15, 30 and 90 minutes, was studied. To obtain the constant rate of the exponential decay of TG2 activity as a function of time (k_{obs}), a monoexponential decay corresponding to the remaining TG2 activity at the different time at 36ºC was determined using equation (7), for each inhibitor concentration assayed. Representation of the rate (v) for the different inhibitor concentrations and the different preincubation times are presented in **Graph 8**.

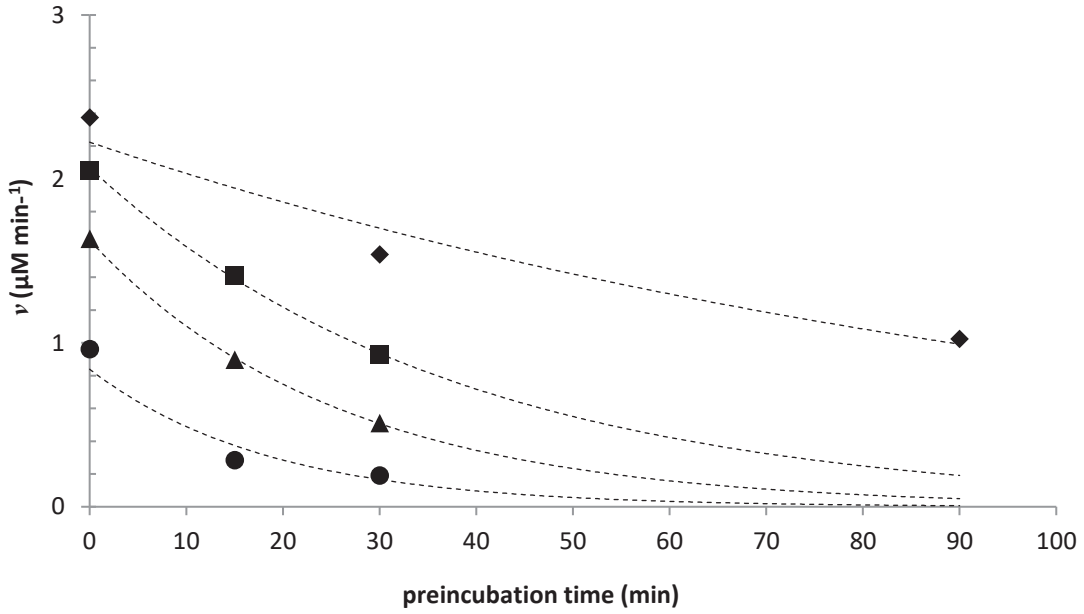

Graph 8. Plot of v values for the different concentrations of compound **23b** *vs.* the different preincubation times (15, 30 and 90 min). (♦) no inhibitor; (■) 0.05 μM of inhibitor; (▲) 0.1 μM of inhibitor; (●) 0.2 μM of inhibitor (dashed lines represent the exponential decay of TG2 activity)

The decay in TG2 activity was then transformed into a linear trend by converting TG2 activity values into their natural logarithm, ln(A), being A the TG2 residual activity at a certain time (%) (see **Graph 9**). Then k_{obs}, which is defined in equation (18), is the slope ($-k_{obs}$) of the linearized TG2 monoexponential decay.

$$\ln (A) = -k_{obs}\, t + A_0 \qquad (18)$$

In equation (18), A is the residual TG2 activity; A_0 is the initial TG2 activity (intercepting the y-axis); and, t is the preincubation time for each of the inhibitor concentrations.

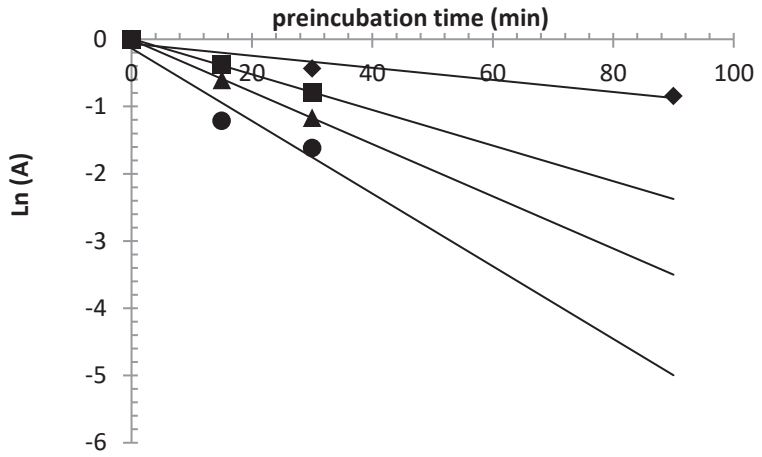

Graph 9. Linearized TG2 residual activity, at the different preincubation times (from no preincubation to 30 min preincubation period). (♦) Ln(A) values without inhibitor. Linear regression equation is expressed as $\mathrm{Ln\,(A)} = -0.009\,\mathrm{t} - 0.0656$, with an $R^2 = 0.957$; (■) Ln(A) values at 0.05 µM of inhibitor. Linear regression equation is expressed as $\mathrm{Ln\,(A)} = -0.0265\,\mathrm{t} + 0.0071$, with an $R^2 = 0.999$; (▲) Ln(A) values at 0.1 µM of inhibitor. Linear regression equation is expressed as $\mathrm{Ln\,(A)} = -0.0388 - 0.0064$, with an $R^2 = 0.999$; (●) Ln(A) values at 0.2 µM of inhibitor Linear regression equation is expressed as $\mathrm{Ln\,(A)} = -0.054\,\mathrm{t} - 0.1349$, with an $R^2 = 0.923$

Values of the k_{obs} constants were used to fit a double reciprocal plot as described previously[73,91,177] using the equation (19), which is the linearized form of equation (6). Kinetic parameters K_I and k_{inact} have been calculated by plotting $1/k_{obs}$ against 1/[I].

$$\frac{1}{k_{obs}} = \frac{1}{k_{inact}} + \frac{K_I}{k_{inact}} \cdot \frac{1}{[\mathrm{I}]} \quad (19)$$

Both, the double reciprocal plotting of $1/k_{obs}$ and 1/[I] and the kinetic parameters obtained are shown in **Graph 10** and **Table 30** respectively.

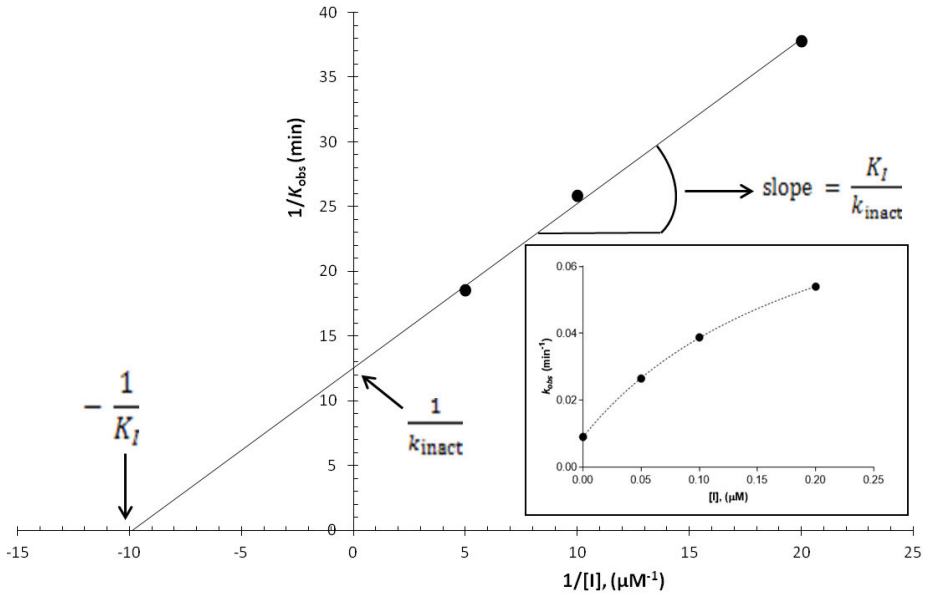

Graph 10. Double reciprocal plot of k_{obs} *vs.* concentration of inhibitor, [I]. The equation of the linear regression is expressed as $\frac{1}{k_{obs}} = 1.2690 \frac{1}{[I]} + 12.537$; $R^2 = 0.997$. The inset shows the k_{obs} plotted against the different inhibitor concentrations employed for the preincubation assay (0, 0.05, 0.100, and 0.200 μM). Dashed line is fitted to an hyperbole ($R^2 > 0.999$)

Parameter	Observed values
k_{inact}	0.080 min^{-1}
K_I	0.100 μM
k_{inact}/K_I	800,000 M^{-1} min^{-1}

Table 30. TG2 inhibition kinetic parameters (k_{inact}, K_I, and k_{inact}/K_I) for compound **23b** obtained from the double reciprocal plot (see **Graph 10**)

It can be observed that the value of the dissociation constant K_I calculated from this plot falls also within a similar submicromolar range compared to that calculated by the DIXON plot (K_I = 0.052 μM). Values of 0.052 μM and 0.100 μM, respectively, were obtained. This K_I values are within the nanomolar range indicating a good binding affinity of TG2 for the inhibitor on forming the reversible EI complex compared with the existent TG2 inhibitors assayed to date (see **Section 2**) whose K_I values are not lower than 0.070 μM. Regarding the efficiency for the reactivity of the compound **23b** on inactivating TG2, the second-order rate k_{inact}/K_I (herein 800,000 M^{-1} min^{-1}) demonstrates a good efficiency of the TG2 inactivation (the value exceeds 10^5 M^{-1} min^{-1}). It is among the most potent/reactive TG2 irreversible inhibitors to date (see **Section 2**). Compounds **XX** from the work of Hausch et al.,[86] and compound **XI** from the work of de Macédo et al.[113] showed high k_{inact}/K_I values higher than 10^6 M^{-1} min^{-1} ($2.9\ 10^6$ and $3.0\ 10^6$ M^{-1} min^{-1} respectively), showing similar affinity for TG2 within the same nanomolar range with K_I values of 0.150 μM and 0.070 μM, respectively, relative to compound **23b**.

2.2. Inhibition study of 78f

TG2 kinetic studies were carried out with indole **78f** (see **Figure 76**) at DMC concentrations of 190 and 22 μM. Initial rate (v) values obtained at the two different concentrations of DMC are represented in **Graph 11**, where the inhibitor concentration herein assayed were 0.01, 0.05, 0.1 and 0.2 μM.

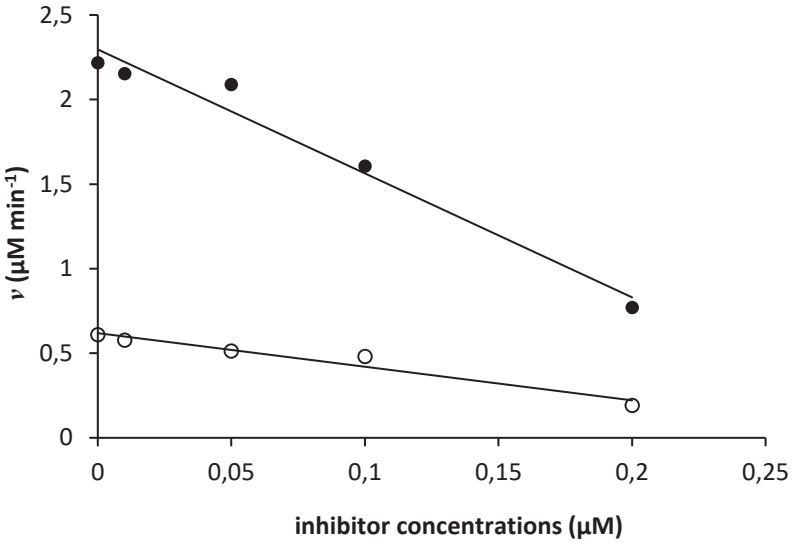

Graph 11. Initial rate (v) values for the different concentrations of compound **78f** assayed at two DMC concentrations (22 and 190 μM). Linear regression equation is referred as $v = b[I] + a$, where b and a correspond to the slope and the intercept at the y-axis respectively. (●) 190 μM of DMC. Linear regression equation is expressed as $v = -7.327\,[I] + 2.296$, with an $R^2 = 0.972$; (○) 22 μM of DMC. Linear regression equation is expressed as $v = -1.986\,[I] + 0.619$, with an $R^2 = 0.953$

Then, initial rate value data were assayed to be linearized, and $\frac{1}{v}$ values were plotted against the different inhibitor concentrations (see **Graph 12**), as done for compound **23b**. However, in this case, it is not possible to have a linear behavior as in the case of compound **23b**, showing that the system does not follow a reversible mechanism. It could be concluded that inhibitor **78f** follows a non-reversible inactivation mechanism.

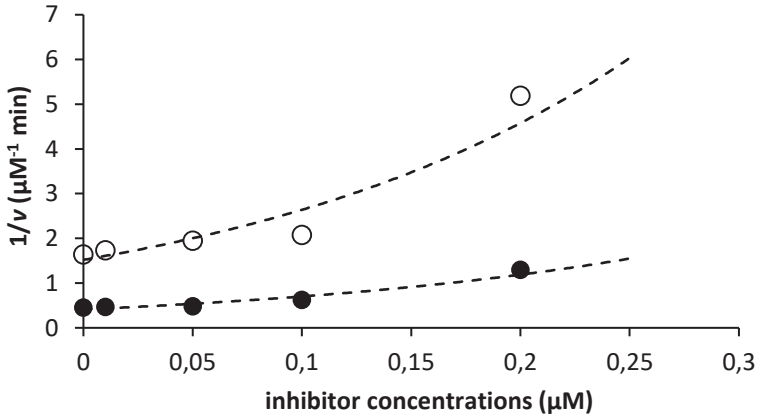

Graph 12. Plot of $1/v$ values against the different inhibitor concentrations of compound **78f**. (●) 190 μM of DMC; (○) 22 μM of DMC (dashed lines are drawn for the eyes)

As a second approach to confirm if TG2 can be inactivated irreversibly, the enzyme was also preincubated with the inhibitor at different time points (15, 30 and 102 minutes) at 36ºC with different concentrations of the inhibitor (0.0095, 0.047 and 0.095 μM). The initial reaction rates (v) obtained for each preincubation assay, at the different

concentrations of inhibitor, were also plotted against the different inhibitor concentrations used (see **Graph 13**), following a linear regression tendency.

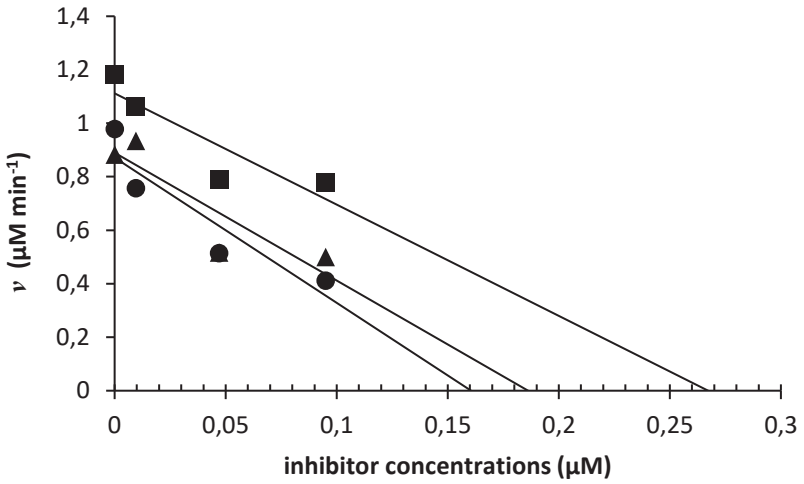

Graph 13. Plot of *v* values *vs.* inhibitor concentrations after different preincubation times (15, 30 and 90 min) at 36ºC for compound **78f**. Linear regression equation is referred as $v = \mathrm{b[I]} + \mathrm{a}$, where b and a correspond to the slope and the intercept with the y-axis respectively. (■) *v* values after 15 min of preincubation. Linear regression equation is expressed as $v = -4.161\,[\mathrm{I}] + 1.112$, with an $R^2 = 0.793$; (▲) *v* values after 30 min of preincubation. Linear regression equation is expressed as $v = -4.779\,[\mathrm{I}] + 0.889$, with an $R^2 = 0.787$.; (●) *v* values after 90 min of preincubation. Linear regression equation is expressed as $v = -5.429\,[\mathrm{I}] + 0.871$, with an $R^2 = 0.850$

The stoichiometry of compound **78f** for its interaction with the TG2 active site followed the same tendency as for compound **23b** (see **Graph 7**). As shown in **Graph 13**, the intersection of *v* with the x-axis found for the different preincubation times (x-axis intercept values were found from 0.16 to 0.26 μM) for the same [E_0] employed (0.19 μM) also suggest the probable interaction of one molecule of inhibitor with the TG2.

Representation of the *v* values for the different inhibitor concentrations for the different preincubation plotted against the different preincubation times are represented in **Graph 14**. As done previously for compound **23b**, in order to obtain the kinetic parameters (K_I and k_{inact}) for the irreversible mechanism of action, monoexponential decay of the rate values for each of the inhibitor's concentration taken after 0, 15, 30 and 102 minutes of preincubation at 36ºC were also studied in order to obtain the residual activity of TG2.

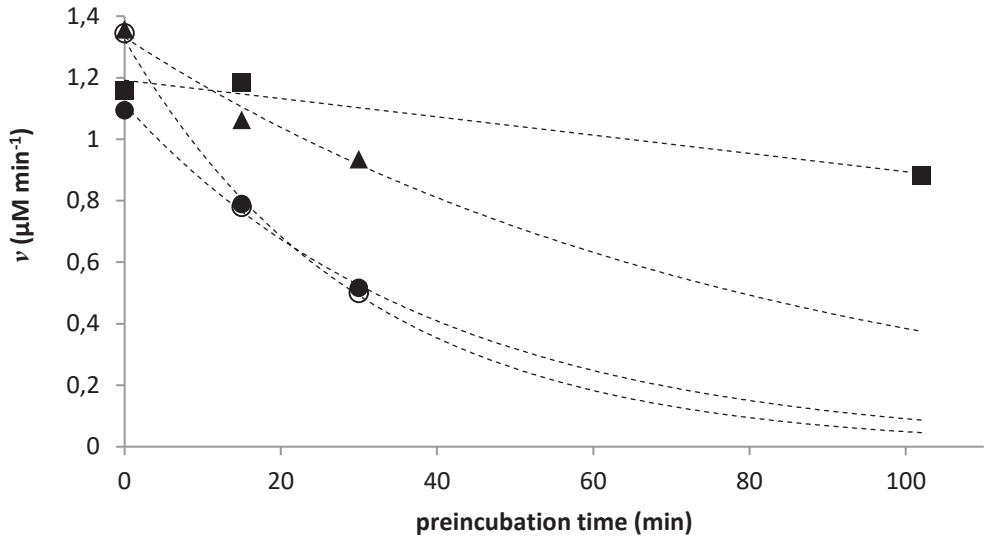

Graph 14. Plot of *v* values for the different inhibitor concentrations for compound **78f** *vs*. the different preincubation times (15, 30 and 102 min). (■) 0 μM of inhibitor; (▲) 0.0095 μM of inhibitor; (●) 0.047 μM of inhibitor; (○) 0.095 μM of inhibitor (dashed lines represent the exponential decay of TG2 activity)

The exponential decay in TG2 activity for the different inhibitor concentrations along the different preincubation times was also confirmed (**Graph 15**), were k_{obs} values against the different inhibitor concentrations will be obtained as the slope ($-k_{obs}$) from the linearized TG2 monoexponential activity decay, as defined by equation (18).

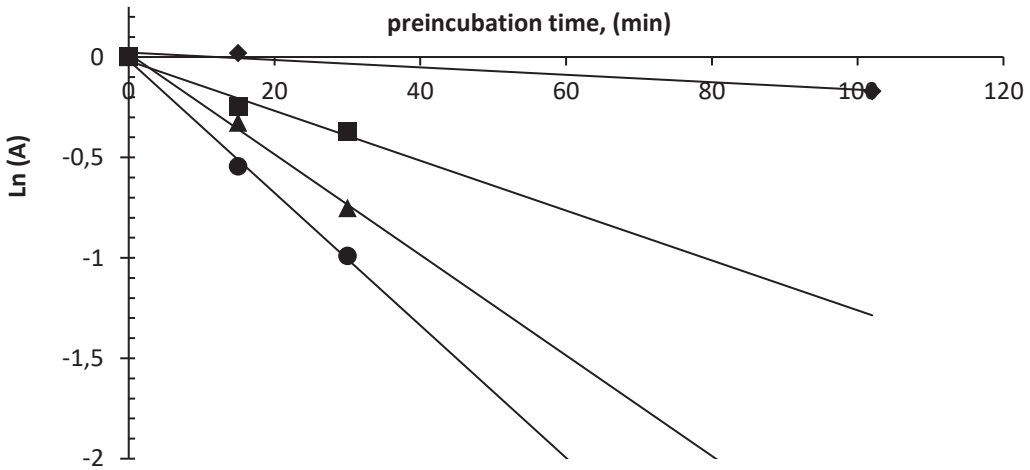

Graph 15. Linearized TG2 residual activity, at the different preincubation times (from no preincubation to 30 min preincubation period). (♦) Ln(A) values without inhibitor. Linear regression equation is expressed as $\mathrm{Ln}\,(A) = -0.0018\,t + 0.0222$, with an $R^2 = 0.946$; (■) Ln(A) values at 0.0095 μM of inhibitor. Linear regression equation is expressed as $\mathrm{Ln}\,(A) = -0.0124\,t - 0.0193$, with an $R^2 = 0.969$; (▲) Ln(A) values at 0.047 μM of inhibitor. Linear regression equation is expressed as $\mathrm{Ln}\,(A) = -0.025\,t + 0.0163$, with an $R^2 = 0.994$; (●) Ln(A) values at 0.095 μM of inhibitor Linear regression equation is expressed as $\mathrm{Ln}\,(A) = -0.033\,t - 0.0167$, with an $R^2 = 0.996$

k_{obs} Values were also used to fit a double reciprocal plot of $1/k_{obs}$ and 1/[I] (**Graph 16**) in order to obtain the kinetic parameters (K_I, k_{inact}, and k_{inact}/K_I) which are presented in **Table 31**.

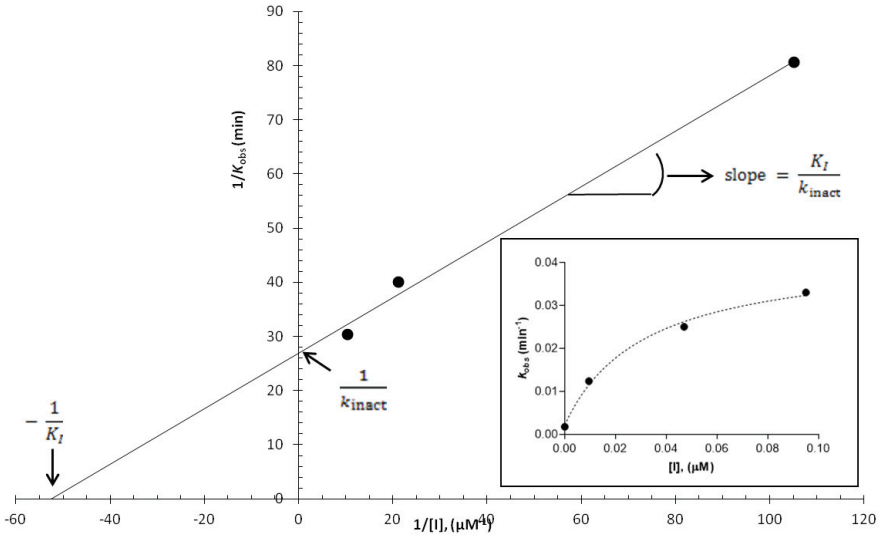

Graph 16. Double reciprocal plot of k_{obs} *vs.* concentration of inhibitor, [I]. The equation of the linear regression is expressed as $\frac{1}{k_{obs}} = 0.513\ \frac{1}{[I]} + 26.863$; $R^2 = 0.994$. The inset shows the K_{obs} plotted against the different inhibitor concentrations employed for the preincubation assay (0.0095, 0.047 and 0.095 μM). Dashed line is fitted to an hyperbole ($R^2 = 0.995$)

Parameter	Observed values
k_{inact}	0.037 min^{-1}
K_I	0.020 μM
k_{inact}/K_I	1,850,000 M^{-1} min^{-1}

Table 31. TG2 inhibition kinetic parameters (k_{inact}, K_I, and k_{inact}/K_I) for compound **78f** obtained from the double reciprocal plot (see **Graph 16**)

It can be observed that the binding affinity of TG2 for compound **78f** (K_I = 0.020 μM) is smaller than the one found for compound **23b** (K_I = 0.052-0.100 μM). Compared with the existent TG2 inhibitors assayed to date (see **Section 2**) whose K_I values, as in the case of compound **XI**[113] are not lower than 0.070 μM, this new synthesized inhibitor also showed a better affinity for TG2. Comparing the efficiency for the reactivity of compound **78f** on inactivating TG2, the second-order rate k_{inact}/K_I parameter (herein 1,850,000 M^{-1} min^{-1}) demonstrated a better efficiency on the TG2 inactivation than compound **23b** (800,000 M^{-1} min^{-1}), being among the most potent/reactive TG2 irreversible inhibitors to date.

2.3. Inhibition study of reference piperidine acrylamide X.

Kinetic studies were also carried out for the TG2 inhibitoin with the 4-aminopiperidine compound of reference, compound **X** (see **Figure 62**). As performed for the other two compounds herein studied inhibition was also carried at DMC concentrations of 48 μM and 190 μM. In this case, initial rate (v) values (see **Graph 17**) did not follow a linear regression when plotting them against the different inhibitor concentrations assayed (0.1, 0.2, 0.5 and 2 μM). This suggests an equilibrium denoted by the formation of the reversible EI and/or ESI complex, therefore existing an equilibrium where the K_I dissociation constant can be measured. To study the dissociation constant K_I the initial rate values were linearized and the K_I was observed at the intercept point from both lines. The Dixon plot is shown in **Graph 18**, where the observed K_I value is 0.190 μM for this compound.

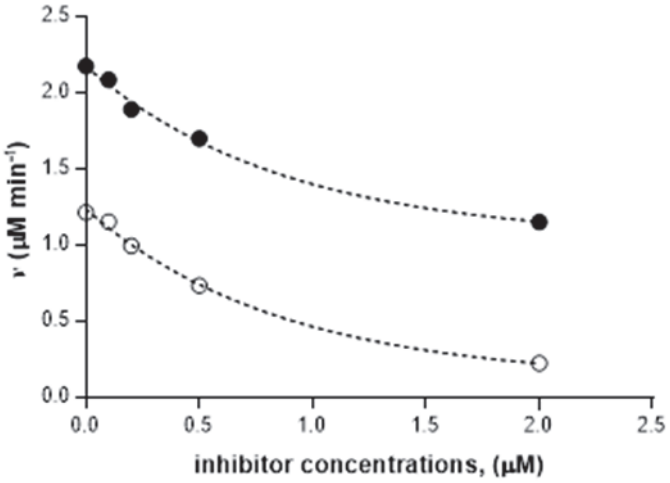

Graph 17. Initial rate (v) values for the different concentrations of compound **X** assayed at the two DMC concentrations (48 and 190 μM). (●) 190 μM of DMC; (○) 48 μM of DMC. A nonlinear regression tendency is shown, suggesting an equilibrium given by the formation of the reversible EI complex (dashed lines are drawn for the eyes)

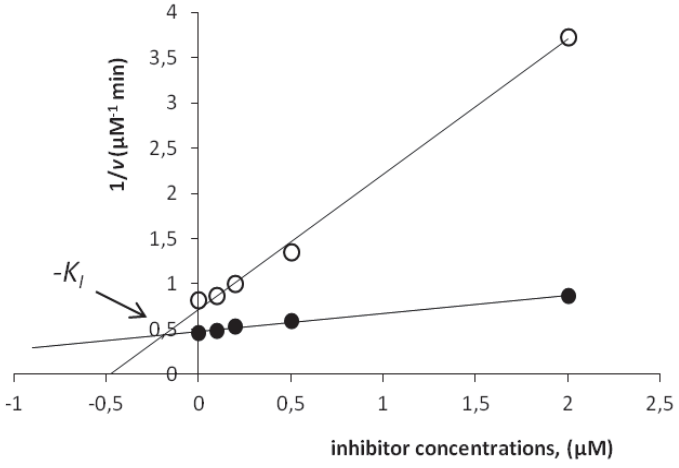

Graph 18. Dixon plot where $\frac{1}{v}$ values were plotted against the different inhibitor concentrations. A Dixon competitive inhibition model is observed (see **A**, **Figure 88**). (●) $\frac{1}{v}$ values *vs.* [I] for 190 μM of

DMC whose linear regression equation is expressed as $\frac{1}{v} = 0.198\,[I] + 0.472$, with an $R^2 = 0.992$; (○) $\frac{1}{v}$ values *vs.* [I] for 48 μM of DMC whose linear regression equation is expressed as $\frac{1}{v} = 1.492\,[I] + 0.718$, with an $R^2 = 0.996$

The same preincubation experience at 36ºC of TG2 in the presence of different concentrations of inhibitor **X** (0, 0.095, 0.190 and 0.47 μM) at different preincubation times (0, 15, 30 and 90 min), as done for compounds **23b** and **78f**, was also carried out. The irreversible kinetic parameters obtained are presented in **Table 32**.

Parameter	Observed Values
k_{inact}	0.018 min^{-1}
K_I	0.182 μM
k_{inact}/K_I	100,000 M^{-1} min^{-1}

Table 32. TG2 inhibition kinetic parameters (k_{inact}, K_I, and k_{inact}/K_I) for compound **X** obtained from the double reciprocal plot

In conclusion, linearized data in **Graph 18** suggest a reversible mode of inhibition for compound of reference **X** for the formation of the EI complex. In addition, further preincubation studies to study its irreversible mode of action confirmed its irreversibility. As shown in **Table 32**, K_I and k_{inact}/K_I values were lower than those values found for compounds **23b** and **78f**, thus indicating lower affinity for TG2 but also less efficiency on inactivating TG2.

3. Study of the chemical modification of Cys277 of TG2 by inhibitors 23b and 78f

In order to verify that the newly produced TG2 inhibitors **23b** and **78f**, covalently modify the TG2 active site residue Cys277, His-tagged recombinant human TG2 (rhTG2) was incubated in the presence of inhibitor, digested with trypsin, and analyzed by means of LC-MS/MS.

The His-tagged rhTG2 protein amino acid sequence employed is shown below:

MAHHHHHHAEELVLERCDLELETNGRDHHTADLCREKLVVRRGQPFWLTLHF
EGRNYQASVDSLTFSVVTGPAPSQEAGTKARFPLRDAVEEGDWTATVVDQQD
CTLSLQLTTPANAPIGLYRLSLEASTGYQGSSFVLGHFILLFNAWCPADAVYLDS
EEERQEYVLTQQGFIYQGSAKFIKNIPWNFGQFQDGILDICLILLDVNPKFLKNA
GRDCSRRSSPVYVGRVGSGMVNCNDDQGVLLGRWDNNYGDGVSPMSWIGSV
DILRRWKNHGCQRVKYGQCWVFAAVACTVLRCLGIPTRVVTNYNSAHDQNS
NLLIEYFRNEFGEIQGDKSEMIWNFHCWVESWMTRPDLQPGYEGWQALDPTPQ
EKSEGTYCCGPVPVRAIKEGDLSTKYDAPFVFAEVNADVVDWIQQDDGSVHKS
INRSLIVGLKISTKSVGRDEREDITHTYKYPEGSSEEREAFTRANHLNKLAEKEE

TGMAMRIRVGQSMNMGSDFDVFAHITNNTAEEYVCRLLLCARTVSYNGILGPE
CGTKYLLNLTLEPFSEKSVPLCILYEKYRDCLTESNLIKVRALLVEPVINSYLLAE
RDLYLENPEIKIRILGEPKQKRKLVAEVSLQNPLPVALEGCTFTVEGAGLTEEQK
TVEIPDPVEAGEEVKVRMDLVPLHMGLHKLVVNFESDKLKAVKGFRNVIIGPA

In the TG2 sequence above, it can be observed the hexaHis-tag (highlighted in blue), and the expected proteolytic sequence (highlighted in yellow) which includes the active site Cys277 (in bold red).

His-tagged rhTG2 was firstly incubated with each of the new inhibitors **23b** and **78f**. Then, protein Cysteines were modified by reacting with iodoacetamide (carbamidomethylated), and the entire protein digested with Trypsin. Once His-tagged rhTG2 was digested with trypsin, the amino acid sequence, the percentage of protein coverage, the mass (MH^+), and the TG2 modifications for some aminoacids of the corresponding peptidic sequences of interest (including the active site Cys277), were investigated. It has to be mentioned that the work performed regarding both the tryptic digestion of the enzyme and the LC-MS/MS analysis herein presented, has benefited from the facilities and expertise of the Protein Science Facility of the SFR biosciences Lyon (UMS3444/US8).

In the case of the trypsin digestion for the His-tagged rhTG2 incubated with inhibitor **23b**, the protein was identified with a coverage of 63.4%. In **Table 33**, the tryptic fragment of interest containing Cys277 (VKYGQC_{277}WVFAAVAC_{285}TVLR), the corresponding amino acid modifications, and its mass (MH^+) are presented. In this table, it could be observed that the tryptic peptide of interest containing the Cys277 (2013 Da) has been modified in the Cys277 with the inhibitor **23b** (523.18 Da), but also presenting a carbamidomethylation in Cys285 (57.02 Da). The expected overall mass (Da) for this peptidic fragment corresponded with the observed masses found after MS analysis (2594.66 Da; MH^+).

Fragment amino acid sequence	Amino acid modifications	Mass (MH^+; Da)
VKYGQC_{277}WVFAAVAC_{285}TVLR	C_{277} (+**23b**) C_{285} (Carbamidomethylation; CAM)	2594.66

Table 33. The modifications and the mass (MH^+) of the tryptic fragment VKYGQC_{277}WVFAAVAC_{285}TVLR containing the active site Cys277 of the TG2 active site

Then, to confirm that the tryptic fragment of 2594.66 Da (precursor ion of interest) detected in the first MS analysis corresponds to the sequence of the Cys277-modified TG2, this peptide was then fragmented and analyzed by MS/MS. The resulting y and b peaks (**Figure 64**), derived from the fragmentation of this peptide, were successfully assigned to the amino acid sequence of the Cys277-covalently modified TG2 peptide fragment VKYGQC_{277}WVFAAVAC_{285}TVLR. From 8 to 12 of the 17 possible y and b

peaks confirmed the observed modified peptide sequence. Therefore, it can be concluded that the active site Cys277 of TG2 was modified by compound **23b**.

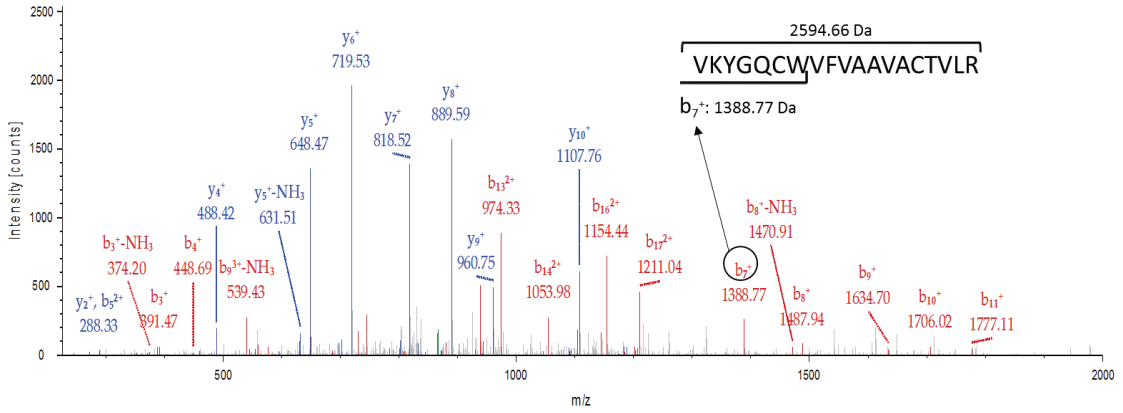

Figure 64. The 2594.66 Da peptidic fragment analysis by MS/MS for the inhibited TG2 sample with compound **23b**, showing the identified y and b peaks. The $b7^+$ peak (1388.77 Da) provided the identity of the peptide fragment with the covalent adduct on Cys277

Concerning the protein analysis for the His-tagged rhTG2 incubated with inhibitor **78f**, the protein was identified with a coverage of 60.23%. In this case, in **Table 34** can be observed two fragments of interests, both with their corresponding amino acid modifications, and their calculated masses (MH^+), as done previously for inhibitor **23b**. The expected mass for both tryptic fragments without any modification are 2013 Da and 1786 Da, corresponding with the amino acid sequences VKYGQC$_{277}$WVF-AAVAC$_{285}$TVLR (18 amino acids, 2012 Da) and YGQC$_{277}$WVFAAVAC$_{285}$TVLR (16 aminoacids; 1786 Da), respectively. After MS analysis, it can be observed that both fragments contained a modified active site Cys277 forming an adduct with inhibitor **78f** (526.18 Da), but also including a carbamidomethylation (57.02 Da) in Cys285. The expected overall mass (Da) for both modified fragments corresponded with the observed masses by MS analysis.

Fragment aminoacid sequence	Aminoacid modifications	Mass (MH^+; Da)
VKYGQC$_{277}$WVFAAVAC$_{285}$TVLR	C$_{277}$ (+**78f**) C$_{285}$ (Carbamidomethylation; CAM)	2597.66
YGQC$_{277}$WVFAAVAC$_{285}$TVLR	C$_{277}$ (+**78f**) C$_{285}$ (Carbamidomethylation; CAM)	2370.44

Table 34. The modifications and the mass (MH^+) of the tryptic fragments VKYGQC$_{277}$WVFAAVAC$_{285}$TVLR and YGQC$_{277}$WVFAAVAC$_{285}$TVLR, both containing the active site Cys277 of the TG2 active site

In addition, both selected parental ions (for both amino acid sequences; VKYGQC$_{277}$WVFAAVAC$_{285}$TVLR and YGQC$_{277}$WVFAAVAC$_{285}$TVLR) were also fragmented and analyzed by MS/MS spectrometry. The obtained y and b peaks were also being correctly assigned to the expected amino acid sequence of both fragments, with a modified Cys277 by compound **78f**, and also a carbamidomethylated Cys285. In **Figure 65**, the MS/MS spectra for the 2597.66 Da (**A**) and the 2370.44 Da (**B**) fragments are shown. In this case, it can also be concluded that Cys277 of the TG2 active site was also modified by compound **78f**.

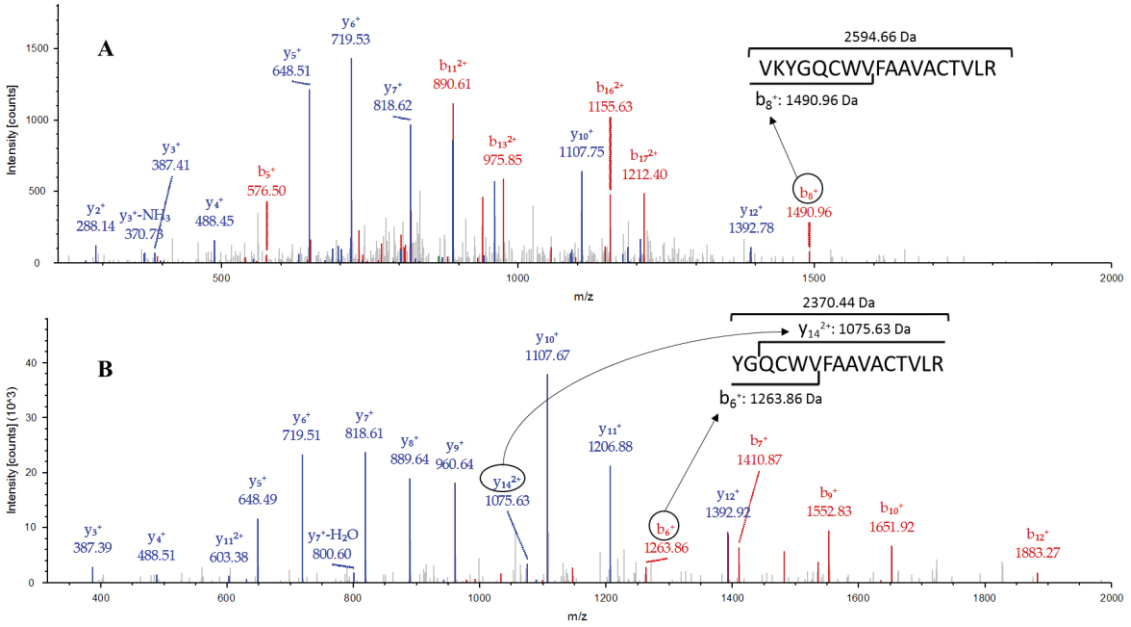

Figure 65. The 2597.66 Da (**A**) and the 2370.44 Da (**B**) peptidic fragments analysis by MS/MS for the inhibited TG2 samples with compound **78f**, showing the identified y and b peaks. The b_8+ peak (1490.96 Da) provided the identity of the peptide fragment with the covalent adduct on Cys277 for the fragment of 2594.66 Da (**A**); and either b_8^+ or y_{14}^{2+} peaks also provided, for the 2370.44 Da sequence, the identity of the modified peptidic fragment by the covalent adduct on Cys277 (**B**)

Furthermore, it was noteworthy that no other Cysteine from the protein was detected to be modified for any of the inhibitors assayed during the analysis of the LC-MS/MS (data not shown).

4. Conclusion

GDH linked assay has been adapted, optimized, and validated to measure the inhibition of TG2. Inhibitors **23b** and **78f** have been demonstrated to have an exponential time-dependent inactivation of the enzyme. K_I and k_{inact}/K_I values were indicative of a strong binding to the TG2, and also a good efficiency of inactivation of TG2.

On the other hand, the compound **78f** have shown a faster formation of the non irreversible complex EI owing to the linearity of the initial rate (v) against the inhibitor concentration [I], suggesting that reversible enzyme-inhibitor complex EI possibly underwent a first-order kinetic reaction, owing to the inactivation of the enzyme by the

inhibitor forming the EI* inactivated complex. Furthermore, at both substrate concentrations assayed, $1/v$ values *vs.* [I] did not fit to a Dixon competitive plot to estimate the K_I, giving a clue for the irreversible mode of inactivation of TG2 of this inhibitor. After the different time preincubation experiences, the results showed that this compound has better efficiency on inactivating TG2 than compound **23b**, but also better affinity (K_I) value.

On the contrary, reference compound **X** whose initial rate (v) values against inhibitor concentration [I] were not linear, $1/v$ values *vs.* [I] fitted to a competitive Dixon plot model, suggesting a reversible competitive mode of inhibition. Furthermore, K_I was estimated (K_I = 0.190 μM) and showed a lower affinity compared to **23b** and **78f** because of its K_I 3.6-fold superior than that found for compound **23b**, and 9.5-fold higher relative to compound **78f**. In addition, its efficiency on inhibiting TG2 (k_{inact}/K_I = 0.10 μM^{-1} min^{-1}) resulted lower than those obtained for compound **23b** and compound **78f** (see **Table 35**).

Parameter	**23b**	**78f**	**X**
k_{inact}	0.080 min^{-1}	0.037 min^{-1}	0.018 min^{-1}
K_I	0.052-0.100 μM	0.020 μM	0.182-0.190 μM
k_{inact}/K_I	800,000 μM^{-1} min^{-1}	1,850,000 μM^{-1} min^{-1}	100,000 μM^{-1} min^{-1}

Table 35. Summary of TG2 inhibition kinetic parameters (k_{inact}, K_I, and k_{inact}/K_I) obtained for compounds **23b**, **78f** and **X**

Finally, confirming the irreversible mechanism biochemically concluded in this chapter, the new synthesized compounds **23b** and **78f** were found to chemically modify specifically the Cys277 from the TG2 active site by LC-MS/MS.

Experimental part - Chapter 4

Generalities

General assay reagents (*N*,*N*-dimethylcasein, α-ketoglutarate, NADH, MOPS, $CaCl_2$) were purchased by Sigma-Aldrich. Recombinant TG2 (rhTG2) was purchased form Covalab R&D (Lyon, France).

All enzymatic assays were performed in a Greiner 96 Flat Bottom Transparent Polystyrol microtitter plates. Kinetic measurements were carried out at 340 nm wavelenght in a Infinite M-200 Tecan device (Salzburg, Austria).

All inhibitors herein assayed were stored at -20ºC in DMSO (1 mM solution). This solution was allowed to reach room temperature before each experiment.

The different data obtained was analyzed by using excel (Microsoft©) and GraphPad prism 7 (GraphPad Software, Inc.) softwares.

Standard TG2 kinetic assay

The deamidation TG2 activity was assayed in a volume of 105 µL containing 200 mM MOPS buffer (pH 7.1), 4 mM $CaCl_2$, 57.1 mM α-ketoglutarate, 238 µM NADH, 47.6 mU/mL GDH (7.125 Units), with different concentrations of *N*,*N*-dimethylcasein (19, 50, 100 and 190 µM DMC), and 0.19 µM rhTG2 (TG2 specific activity was 5 297 U/mg according to supplier's data sheet (opr-0036, Covalab R&D, Lyon, France), where TG2 activity was determined by measuring the rate of fluorescence after rhTG2-catalyzed monodansylcadaverine incorporation into *N*,*N*-dimethylcasein; and U is defined as the increase in fluorescence intensity of 1 a.u./min). The kinetic assays were initiated by the addition of the rhTG2. The consumption of NADH was observed at 36ºC as the decreased in absorbance at 340 nm, and the raw slopes were converted into rates using the extinction coefficient of the NADH ($\varepsilon = 6220\ M^{-1}\ cm^{-1}$) and a light path of 0.3 cm.

All the obtained rate values from this kinetic assay were corrected by the blank (assay without TG2).

For the corresponding Blank assay the rhTG2 solution was replaced with the same volume of MOPS buffer.

TG2 inhibition assays

A. *General inhibition kinetic measurements*

To solution mixture containing MOPS buffer (pH 7.1), 4 mM $CaCl_2$, 57.1 mM α-ketoglutarate, 238 µM NADH, 4.76 mU/mL GDH (0.499 Units), and 19 or 190 µM of

N,*N*-dimethylcasein was added 5 µL of a solution containing inhibitor (at ≤ 0.3% DMSO per well, v/v) at the different final concentrations per well as employed for kinetic studies described in the section 4 from this chapter. Thereafter, the assay was initiated by the addition of rhTG2 to obtain the same final concentration of 0.19 µM per well at 36ºC. The reaction rates were measured from the slopes as did for the standard TG2 kinetic assay.

B. *Preincubation inhibition assays*

rhTG2 (0.19 µM) was preincubated with different concentrations of the inhibitor for 15, 30 and 90 min (or 15, 30 and 102 min as in the case of compounds **X** and **78f**) independently. After this time, the assay was initiated by addition of the remaining assay solution at the same final concentrations as performed for the general inhibition kinetic measurements. Kinetic runs started when *N*,*N*-dimethylcasein (190 µM at the final concentration in the assay) was added to the reaction mixture.

TG2-inhibitor incubation for tryptic digestion

To 5 µg of TG2 in 45 µL of a MOPS buffer (200 Mm, 5 Mm $CaCl_2$, pH 7.1) solution were added 5 µL of inhibitor (0.400 µM of final concentration), and the reaction was left at 37ºC for 1 h. Then, the reaction was freezed prior to LC-MS/MS analysis.

Bibliography - Chapter 4

173. Pietsch, M.; Wodtke, R.; Pietzsch, J.; Löser, R. Tissue transglutaminase: an emerging target for therapy and imaging. *Bioorg. Med. Chem. Lett*. **2013**, *23*, 6528-6543.

174. Estimating precision, repeatability, and reproducibility from Gaussian and non-Gaussian data: a mixed models approach. *J. Appl. Stat*. **2010**, *30*, 1729-1747.

175. Dixon, M. The determination of enzyme inhibitor constants. *Biochem. J*. **1953**, *55*, 170–171.

176. Butterworth, P. J. The use of Dixon plots to study enzyme inhibition. *Biochim. Biophys. Acta*. **1972**, *289*, 251-253.

177. Rajashekhar, B.; Fitzpatrick, P. F.; Colombo, G.; Villafranca, J. J. Synthesis of several 2-substituted 3-(p-hydroxyphenyl)-1-propenes and their characterization as mechanism-based inhibitors of dopamine beta-hydroxylase. *J. Biol. Chem*. **1984**, *259*, 6925-6930.

CHAPTER 5

Inhibition studies in biological samples

1. Introduction and objectives

In this chapter, implementation of different TG2 inhibition studies for some of the compounds synthesized in cell/tissue extracts, in cell culture, and in post-mortem brain tissues samples are described as a part of my secondment period work within the TRANSPATH project (Marie Curie Actions, ITN). This secondment period was performed in the department of Anatomy and Neurosciences at the VU University Medical Center (Amsterdam, The Netherlands). A selection of the most potent TG2 inhibitory compounds herein synthesized, and one of the synthesized prodrugs from a selection of these compounds were tested (see **Figure 67**). Furthermore, several studies of cell viability in different cell line cultures were also carried out in order to test the toxicity of the compounds.

First of all, as shown in **Figure 66**, previous efforts were addressed to study the potency values (IC_{50}) for some compounds in cell and tissue extracts, in a less complex non-living cellular environment. In addition, and as mentioned in the paragraph above, cell viability studies were required to subsequently perform different inhibition studies in a living cellular environment. Inhibitory compounds used as reference in this study are compounds **X**, **EB1-155**, and **Z006** (Zedira, GmbH).

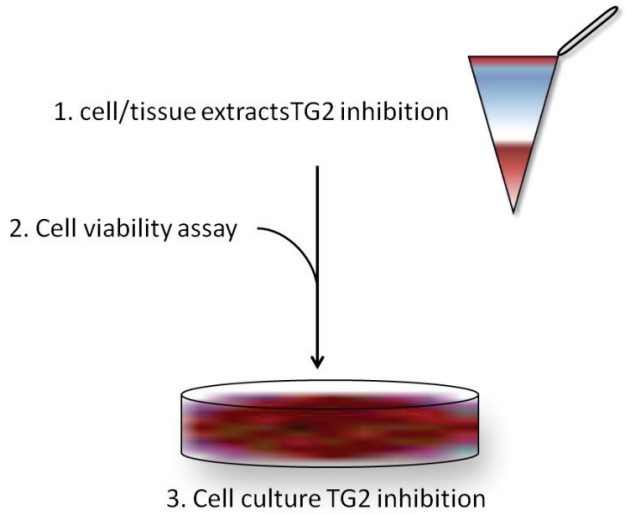

Figure 66. Representation of the different steps followed for the TG2 inhibition assays carried out in this chapter

Finally, the main objectives in this chapter are:

1. Determination of the inhibitory efficacy of the TG2 inhibitors in *in situ* cell culture assay's, using different cell lines
2. Evaluation the toxicity of the inhibitory compounds tested in different cell cultures
3. Study the inhibition of some of the compounds at a cellular level (and with different cell lines)

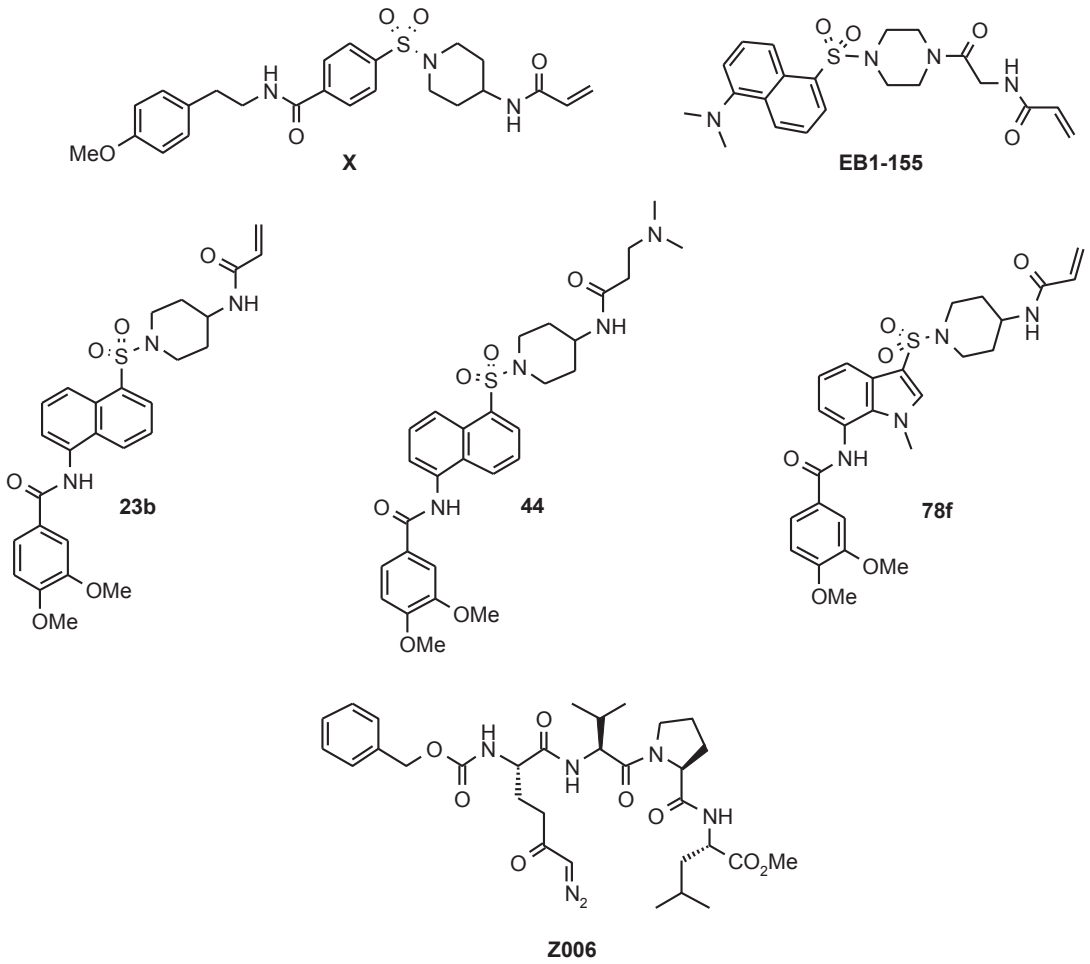

Figure 67. Structure of the TG2 inhibitors used in the different assays carried out in this chapter

2. TG2 inhibition in tissue and cell extracts

To demonstrate the efficacy of a selection of TG2 inhibitors in a cellular and tissue context, the TG2 inhibitors were tested using different cell cultures and tissue samples. Cell lysates were prepared from the culturing of neurovascular smooth muscle cells (vSMCs), human astrocytes (HAS), and neuroblastoma cell (SH-S5Y5) lines. SH-SY5Y cells were employed as a neurodegenerative disease-like culture model[67] (e.g. Parkinson's disease) in which TG2 was found to be implicated. Astrocytes were also used in a cellular model for neuroinflammation and neurodegeneration,[178] and neurovascular smooth muscle cells, which constitutively express TG2, were used as a model for degeneration in cerebral amyloid angiopathy.[179] In addition, TG2 inhibition studies were carried out in lysates from human embryonic kidney (HEK 293T AD) cells transfected with TG2 Val (HEK TG2Val cells; Valine at position 224), as described by Kanchan et al.[180] this TG2 variant has been described to have increased enzymatic activity and Ca^{+2} sensitivity in comparison with the recombinant human TG2 (rhTG2), with a glycine at the same position, which has been used so far in this dissertation for the SAR analysis of the compounds produced (for HEK TG2Val cell lysates inhibition

data was courtesy of Éva Sivadó, PhD student at the Cancer Research Center of Lyon, France).

On the other hand, tissue extracts, were prepared from different mouse tissues from an EAE (experimental autoimmune encephalomyelitis) mouse model for multiple sclerosis.

Furthermore, as different proteins and molecules are present in the different prepared cell and tissue extracts, determining the IC_{50} values of these inhibitory compounds would be of great value to know at which level the different cellular components (e.g., proteins) interfere with the inhibitory activity of the compounds herein studied. **Figure 68** shows the different steps carried out to measure the TG2 activity of the different cell lysates. Once the cell culture was at an optimal confluence, lysates were prepared, the proteins were quantified followed by the TG2 titration for different dilutions of the lysates/extracts. Therefore, the inhibition on the cell lysates for the different inhibitory compounds was carried out at a fixed TG2 concentration for each of the samples. Mouse tissue extracts were prepared by Navina Chrobok (PhD student, department of anatomy and neuroscience, VUMC University, Amsterdam).

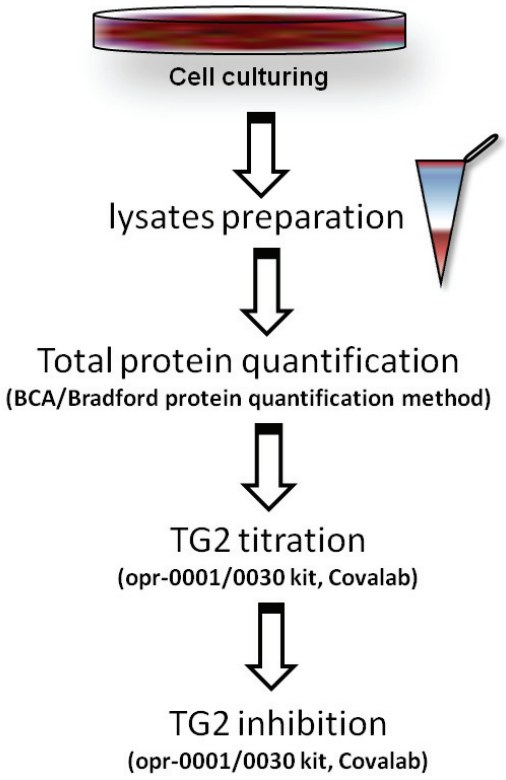

Figure 68. Schematic representation of the different steps for the preparation of the cell/tissue extracts until the measurement of their TG2 inhibition. TG2 activity in neurovascular smooth muscle cells (vSMCs), human astrocytes (HAS), and neuroblastoma (SH-S5Y5) cell extracts was measured with the opr-0001 TG kit (Covalab, France). On the contrary the opr-0030 TG2 specific kit (Covalab, France) was used to measure the TG2 activity for the HEK TG2Val cell protein extracts

2.1. TG2 inhibition in cell lysates.

TG2 inhibition in protein lysates obtained for the different cell line and TG2 concentrations are shown in **Table 36**.

	vSMCs	HAS	SH-SY5Y	HEK TG2Val
[protein], (μg/50 μL)	10	10	0.25	0.90
[TG2], (μg/mL)	0.034	0.087	0.097	0.030

Table 36. Values of protein and TG2 activity measurements by employing the BCA protein measurement kit and the Opr-0001 TG crosslinking kit (Covalab, France), respectively. Values for the different cell lysates (vSMCs, HAS, SH-SY5Y, and HEK TG2Val cells) are shown

At the TG2 concentrations used, inhibition tests were performed in a 96-well microtiter plate, using the opr-0001 TG transamidation kit from Covalab (France). As observed in the inhibition results from **Table 36**, results from prodrug **44**, clearly demonstrated the lowest potency value from all the compounds tested. This might be explained by the fact that bearing a 3-(*N,N*-dimethylamino)-*N*-methylpropanamide warhead moiety makes it less reactive. On the other hand, naphthalenesulfonamides **23b** demonstrated higher potencies in vSMCs lysates when compared with reference compounds **X** and **Z006**. Regarding inhibition in HAS and SH-SY5Y lysates, activity of compound **23b** was 4.31- and 2.28-fold higher than observed for compound **Z006**. On the other hand, TG2 inhibition in HEK TG2Val protein lysates demonstrated that compound **23b** showed an increase of 37.5- and 4.7-fold in activity compared to compounds of references, **X** and **EB1-155**, respectively.

IC_{50} TG2 (μM)	vSMCs	HAS	SH-SY5Y	HEK TG2Val
EB1-155	NT	NT	NT	0.0168
23b	0.09 ± 0.045	0.13 ± 0.0005	0.057	0.0036
44	NT	> 5	> 5	NT
X	2.3 ± 0.015	NT	NT	0.135
Z006	0.44 ± 0.005	0.56 ± 0.0015	0.13	NT

Values accompanied by standard deviation were averaged from at least two independent experiments in triplicates; they were otherwise obtained in a single determination. NT = not tested.

Table 37. TG2 lysates inhibition for the different cellular lysates (from vSMCs, HAS, SH-SY5Y, and HEKVal cell lines). In the case of HEKVal, cell lysates correspond to lysates obtained after three days of incubation of cells with different concentrations of inhibitor

2.2. TG2 inhibition in tissue extracts

In collaboration with Navina Chrobok (PhD student, department of Anatomy and Neurosciences, VU University Medical Center, Amsterdam) different tissue extracts from an EAE mouse model for multiple sclerosis (MS) were used to study TG2 inhibition with the synthesized naphthalene **23b**, and also with the indole **78f**. These compounds were also compared with the reference **X** within the assays. Inhibition results for TG2 in highly diluted tissue extracts are shown in **Table 38**. TG2 concentration values used within the assays are 0.084 and 0.110 µg/mL for liver extracts 1 and 2, respectively.

IC_{50} (µM)	**X**	**23b**	**78f**
Liver extract 1	0.1	0.072	< 0.010 (65 % inhib)*
Liver extract 2	0.68	0.064	< 0.010 (57 % inhib)*

* Inhibition at 0.010 µM.

Table 38. IC_{50} results (µM) are shown for **X**, **23b** and **78f** in two different liver tissue extracts

Independently from the tissue extract, indole **78f** demonstrated the highest activity when compared to the other compounds (see **Table 38**). Reference compound **13** in any case demonstrated less potent for the compounds tested herein.

3. Toxicity of the inhibitory compounds in cell culture

To determine toxicity of the inhibitors in cell culture systems, a variety of cellular viability assays and cell lines were used. As shown in **Figure 69,** different cell cultures were treated with inhibitors using different incubation times. After the incubation periods, toxicity was measured using a panel of cellular viability and toxicity assays. These methods are described below.

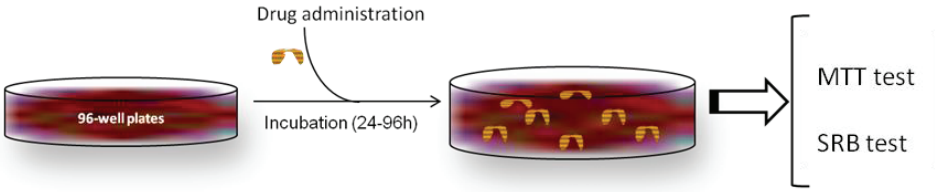

Figure 69. Schematic representation of the cell viability studies. After culturing the cells until appropriate growth, inhibitors were administered and cultured for different periods of time (24-96 h). Then different methods for measuring the cell viability were employed

3.1. Cell viability of vSMCs and SH-SY5Y cells

3.1.1. MTT test

The MTT test is based in the mitochondrial activity of the cells. This test is based on the 3-(4,5-dimethylthiazol-2-yl)-2,5-diphenyltetrazolium bromide (MTT) which will be transformed to its MTT formazan by the mitochondrial dehydrogenases.[181,182]

The vSMCs and SH-SY5Y cell cultures were incubated for 96 and 24 hours, respectively, with increasing inhibitor concentrations, ranging from 0.01 to 100 µM, and with increasing concentrations of the vehicle (DMSO) proportions, from 0.0003% to 3% DMSO. Toxicity results after 4 days of incubation of vSMCs cells with the different inhibitors (see **Graph 19)** showed almost no apparent toxicity up to 10 µM for all the inhibitors. On the contrary, results for the vehicle (DMSO) were analyzed at the same proportions used to dissolve these compounds, showing a cytotoxic effect for the cells when administered at a 3% in culture (see **Graph 20**). Moreover, when comparing both inhibitor and DMSO toxicity results, that toxicity seems to come from the different vehicle proportions used to dissolve the different inhibitors, and not from the inhibitors themselves.

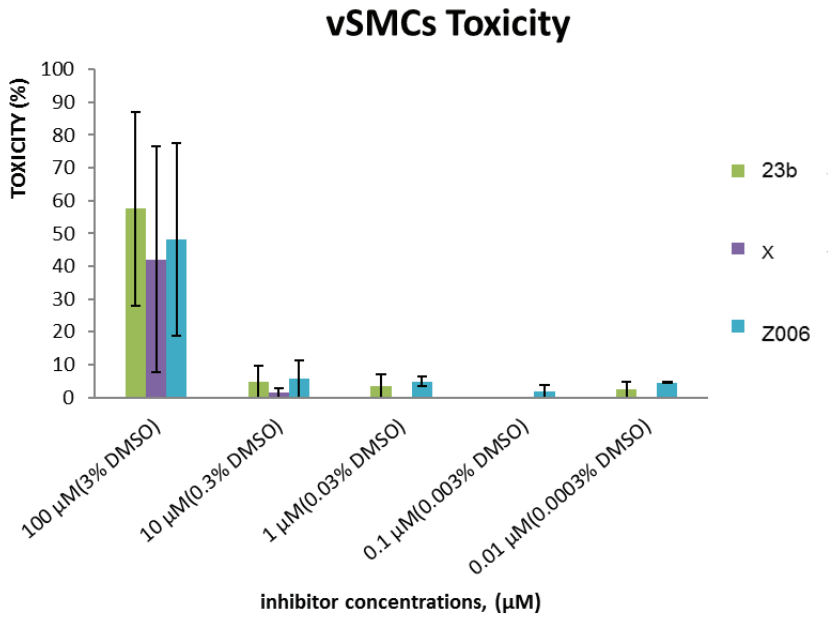

Graph 19. Inhibitors toxicity results in vSMCs culture after 4 days' incubation with the different concentrations of inhibitors dissolved in different proportions of vehicle (DMSO) in the culture medium. Results were averaged from at least two different separated assays ± S.D. The experiments were performed in triplicate

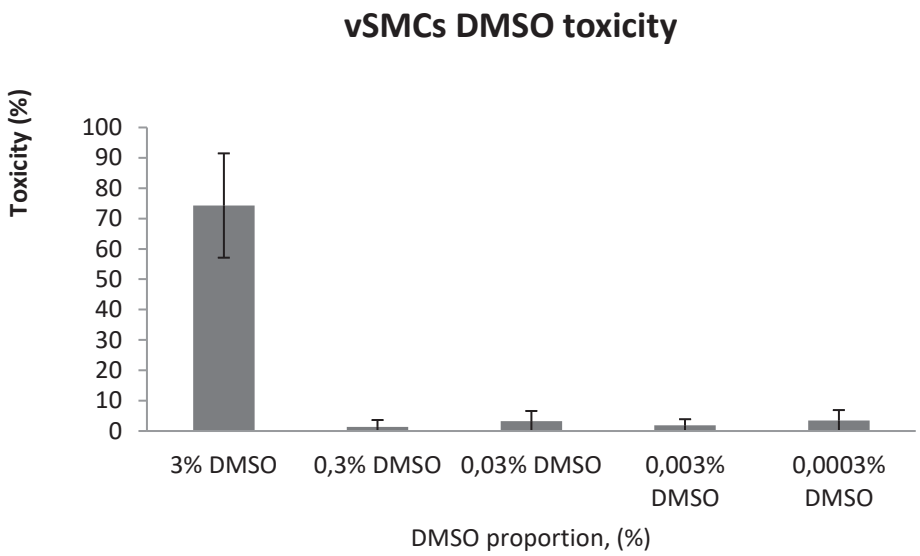

Graph 20. Vehicle (DMSO) toxicity results in vSMCs culture after 4 days incubation at different vehicle proportions (%, v/v) in the culture medium. Results were averaged from at least two different separated assays ± S.D. The experiments were performed in triplicate

Analysis of the toxicity found in SH-SY5Y cell culture for 24 hours (see **Graph 21**), demonstrated that the compounds showed no toxicity to the cells also up to 10 µM of inhibitor. These results, compared to the vehicle (DMSO) toxicity results shown in **Graph 22,** highlight the fact that 3% DMSO is toxic for the cells, again demonstrating that cell toxicity is caused by the vehicle and not by the inhibitors.

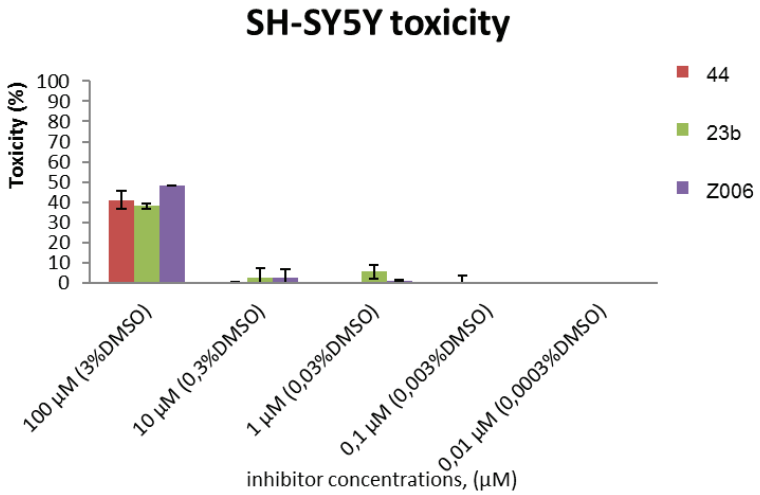

Graph 21. Inhibitors toxicity results in retinoic acid (RA) SH-SY5Y cell culture after 1-day incubation with the different concentrations of inhibitors dissolved in different proportions of vehicle (DMSO) in the culture medium. Results were averaged from at least two different separated assays ± S.D. The experiments were performed in triplicate

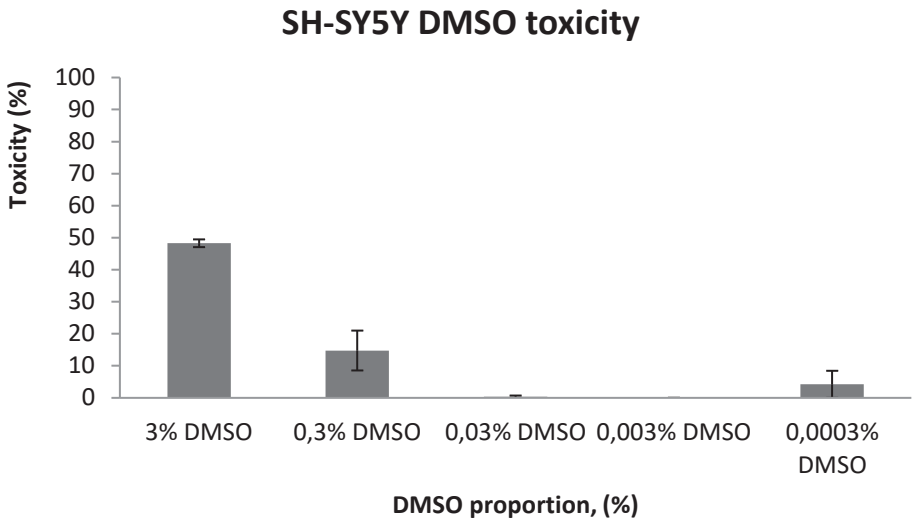

Graph 22. Vehicle (DMSO) toxicity results in retinoic acid (RA) SH-SY5Y cell culture after 1-day incubation at different vehicle proportions (%, v/v) in the culture medium. Results were averaged from at least two different separated assays ± S.D. The experiments were performed in triplicate

3.1.2. SRB test

In addition to the mitochondrial activity results obtained from the MTT assay, the sulforhodamine B (SRB) colorimetric test, which is based on the measurement of the total cellular protein content, was used. This assay relies on the ability of the SRB to bound protein content of cells that have been fixed culture plates with Trifluoroacetic acid (TFA). This results from the fact that SRB contains two sulfonic groups that binds basic amino acid residues under mild acidic conditions.[183]

Using this method, toxicity is shown in **Graph 23**. Similar to the MTT assay, toxicity was absent using up to 10 μM of inhibitors. Again, when observed the cytotoxicity induced by the different vehicle (DMSO) proportions used to dissolve the different inhibitor's in solution (see **Graph 24**), DMSO seems to be the cause of the toxicity but not the compounds.

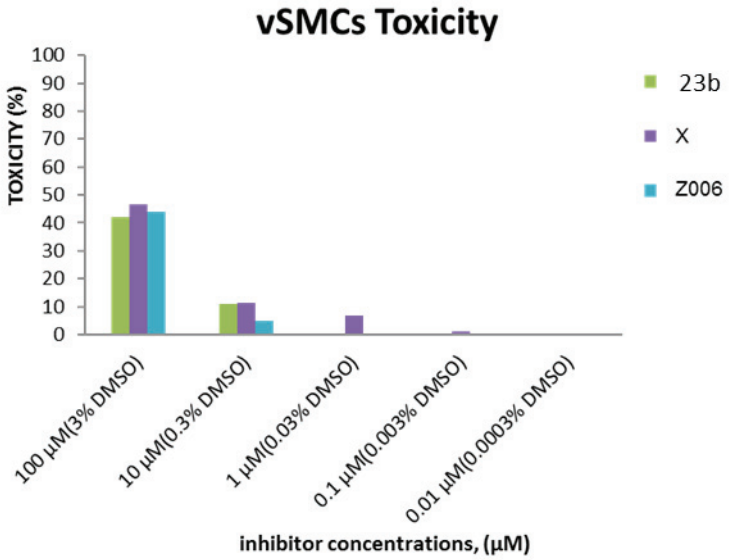

Graph 23. Inhibitors toxicity results in vSMCs culture after 4 days' incubation with the different concentrations of inhibitors dissolved in different proportions of vehicle (DMSO) in the culture medium. The experiment was performed in triplicate

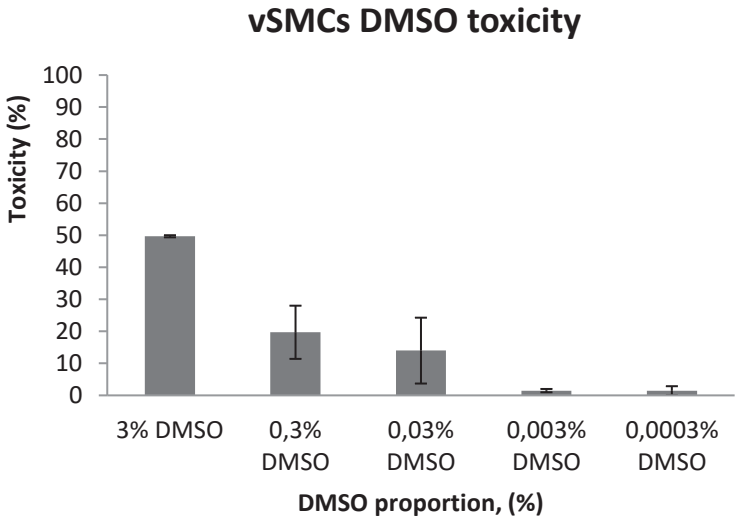

Graph 24. Vehicle (DMSO) toxicity results in vSMCs culture after 4 days' incubation at different vehicle proportions (%, v/v) in the culture medium. Results were averaged from at least two different separated assays ± S.D. The experiments were performed in triplicate

4. TG2 inhibition in cell culture

4.1. *in situ* TG2 activity in cell culture models (BAP incorporation assay)

As a measurement of cellular TG2 activity, the methodology here is based on the incorporation of biotinamido pentylamine (BAP) into cellular proteins. This method was originally described by Zhang et al.,[184] and modified by Verhaar et al. (see **Figure 70**),[67] and is based on the detection of TG2-mediated covalent incorporation of the amine donor BAP into cellular proteins following activation of transamidation activity

by a rise in intracellular Ca^{2+} concentration as a result of exposure of the cells to Ca^{2+} ionophore A23187.

By using this cellular BAP incorporation assay, the *in situ* TG2 inhibition in different cell cultures was analyzed for different inhibitor concentrations after the incubation of the cells with the amine donor (BAP) prior to the addition of the A23187 Ca^{2+} ionophore.

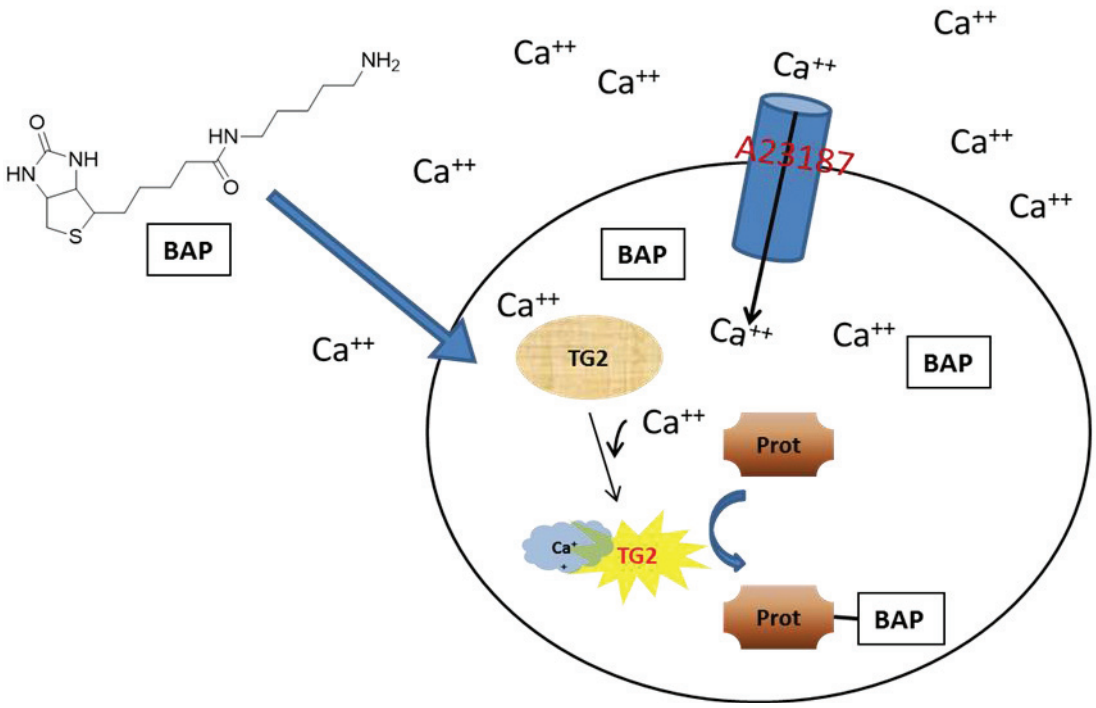

Figure 70. Schematic overview of cellular determination of TG2 activity, as described in experimental section (*in situ* TG2 activity). Upon cellular stimulation with calcium ionophore A23187, the cellular Ca^{2+} concentration is increased and TG2 is activated resulting in the incorporation of BAP into proteins

The compound **23b** was diluted at different concentrations using the methodology described above in a vSMCs cell culture. Potency achieved by inhibiting the cellular TG2 activity resulted in an *in situ* TG2 inhibition with a low IC_{50} of approximately **0.030 µM** (see **Graph 25**).

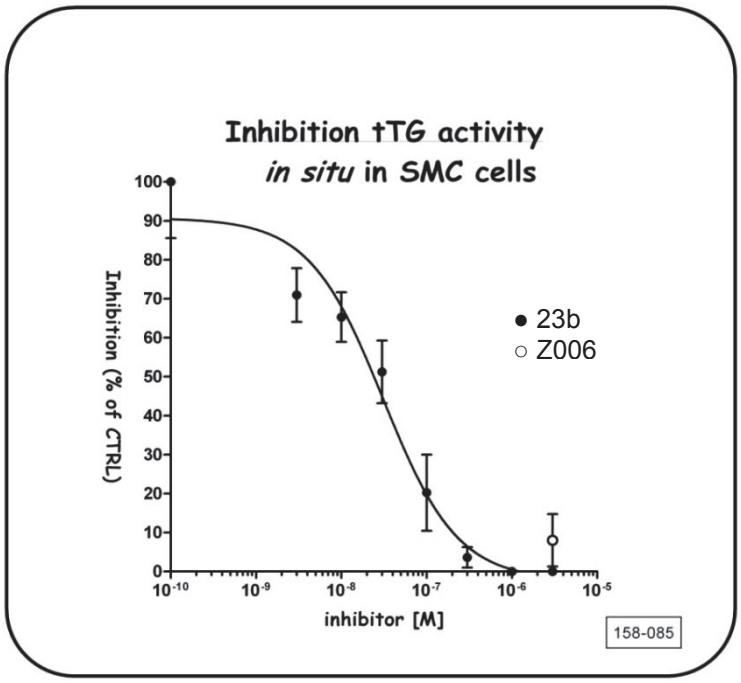

Graph 25. vSMCs *in situ* TG2 activity. The cellular concentration–response curves of **23b** was determined by measuring TG2 activity in vSMCs cells in the presence of increasing inhibitor concentrations. Cellular TG activity in cells treated with A23187 (10 μM, 45min) was defined as maximum activity and set to 100%. TG2 activity in the presence of inhibitors was plotted on a log-scale with Graphpad Prism5. Data is expressed as percentage of maximum TG2 activity. Background correction was performed as described in the experimental part. All experiments were performed three times in triplicate and data are depicted as mean ± SEM (graph courtesy of Department of Anatomy and Neurosciences, VU University Medical Center, Amsterdam). (Note: results were confirmed by Kees Jongenelen Department of Anatomy and Neurosciences, VU University Medical Center, Amsterdam)

In addition, preliminary inhibition studies were carried out in order to check potencies of some of the inhibitors synthesized in other cellular models. Preliminary results on inhibiting cellular TG2 were carried out in HAS and SH-SY5Y cell cultures using the same BAP incorporation assay as performed in the vSMCs described above. Regarding HAS cell culture (see **Graph 26**), approximate IC_{50} values obtained for compounds **23b**, **44** and **Z006** are reported in **Table 39**. At a maximal concentration of 5μM of **23b** TG2 activity seemed to be 100% inhibited. On the contrary, cellular TG2 activity was found to be maximal at 0.5 μM for compounds **Z006**, not being effective at this concentration.

Compound	IC_{50} (μM)
23b	0.74
44	0.96
Z006	3.8

Table 39. IC_{50} results (μM) are shown for **23b**, **44** and **Z006** for the *in situ* TG2 activity in HAS

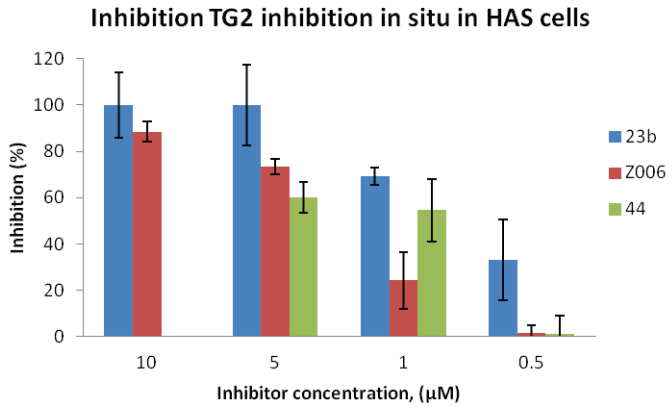

Graph 26. HAS *in situ* TG2 activity. The cellular TG2 inhibition (%) of the compounds described above were determined by measuring TG2 activity in HAS cells in the presence of decreasing inhibitor concentrations. Cellular TG activity in cells treated with A23187 (10 µM, 45min) was defined as maximum activity and set to 100% regarding the non-ionophore induced TG2 activity. Data is expressed as percentage of TG2 inhibition. Background correction was performed as described in the experimental part. The experiment was performed in triplicate and bars represent mean values ± SD

Furthermore, a preliminary study of *in situ* TG2 inhibition in SH-SY5Y cells, as previously performed by Verhaar et al.,[67] was carried out for compounds **23b**, **Z006** and the prodrug **44** (see **Graph 27**). An approximate IC_{50} was found at **0.880 µM**, which was similar to potencies found in a reference study[67] ($IC_{50} \approx 0.700$ µM). Prodrug **44** was not effective below concentrations of 10 µM. One explanation could be that the prodrugs need more than 30 minutes of incubation in a cellular context to be activated into their respective active compound. Furthermore, the highest TG2 inhibition by compound **23b** was found using 0.5 µM, which might be caused by the poor solubility of compound **23b** in the culture medium at the different corresponding vehicle proportions.

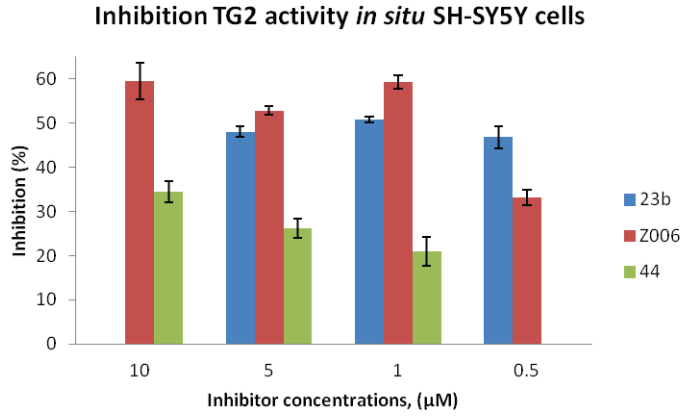

Graph 27. SH-SY5Y *in situ* TG2 activity. The cellular TG2 inhibition (%) of the compounds described above were determined by measuring TG2 activity in RA differentiated SH-SY5Y cells in the presence of decreasing inhibitor concentrations. Cellular TG2 activity in cells treated with A23187 (10 µM, 45min) was defined as maximum activity and set to 100%. Data is expressed as percentage of TG2 inhibition. Background correction was performed as described in experimental section. The experiment was performed in triplicate and bars represent mean values ± SD

In a macrophages cell line, the similar cellular TG2 activity assay was performed. An IC_{50} value of approximately 0.7 µM was found for compound **23b** in this cell model (see **Graph 28**). As for compound **EB1-155**, potencies were found to be superior to 100 µM (see **Graph 29**), the highest concentration assayed in this macrophage cell model.

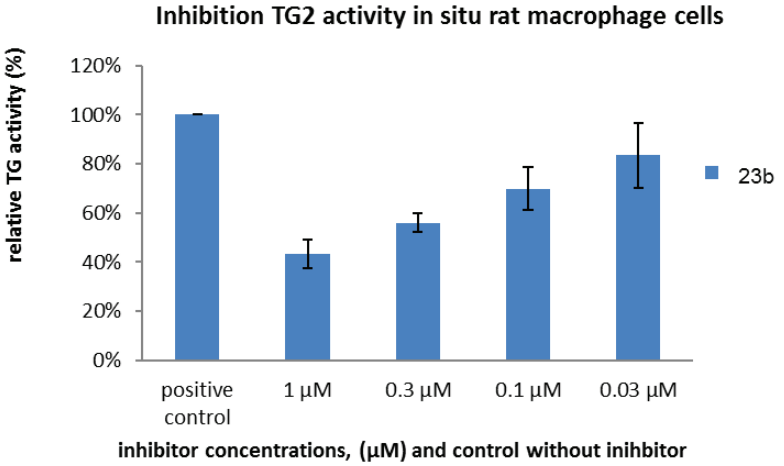

Graph 28. Rat macrophages *in situ* TG2 activity assay. The cellular TG2 activity (%) in the presence of compound **23b** was determined by measuring TG2 activity of rat macrophages in the presence of decreasing inhibitor concentrations. Cellular TG2 activity in cells treated with A23187 (10 µM, 45min) was defined as maximum activity and set to 100%. Data is expressed as percentage of maximum TG2 activity. The experiment was performed in triplicate and bars represent mean values ± SEM (data courtesy of Navina Chrobok, PhD student, department of anatomy and neuroscience, VUMC university, Amsterdam)

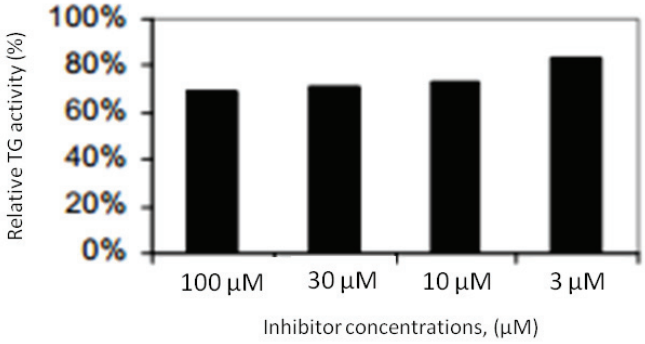

Graph 29. Rat macrophages *in situ* TG2 activity assay. The cellular TG2 activity (%) in the presence of compound **EB1-155** was determined by measuring TG2 activity of rat macrophages in the presence of decreasing inhibitor concentrations. Cellular TG2 activity in cells treated with A23187 (10 µM, 45min) was defined as maximum activity and set to 100%. Data is expressed as percentage of maximum TG2 activity (graph courtesy of Navina Chrobok, PhD student, department of anatomy and neuroscience, VUMC university, Amsterdam)

5. Conclusion

Newly produced compound **23b** turned out to be the most potent inhibitor in the cell lysates studied, even better than compounds **X**, **Z006**, used as references in this study. In the case of the liver tissue extracts indole compound **78f** seemed to be the most effective in tissue extracts, with IC_{50} values bellow 10 nM. Furthermore, toxicity studies revealed that all compounds tested have no apparent toxicity when treating vSMCs, SH-SY5Y cells (after 96 and 24 hours of treatment with inhibitors, respectively) when used at 10 μM of inhibitors.

Moreover, cellular TG2 inhibition results showed that compound **23b** has potencies values in the low micromolar range in all the cell cultures tested. In addition, in comparison with compounds **Z006** and **EB1-155**, used as reference, compound **23b** showed better efficacy on inhibiting cellular TG2.

Experimental part - Chapter 5

Cell culture

A. *vSMCs cell culture*

Human smooth muscle cells (SMCs, Sciencell Research Laboratories, Sanbio, Uden, The Netherlands) were cultured at 37°C under 5% CO_2 in air in a 1:1 mixture of Dulbecco's modified Eagle's medium (DMEM; PAA Laboratories, Pasching, Austria) and F10 nutrient mixture (Gibco Life technologies, Blijswijk, The Netherlands) containing 50% fetal calf serum (FCS), 1/100 non-essential amino acids (Gibco Life technologies), 2.5 mM L-glutamine, 1% growth supplement (ScienCell) and 1% penicillin/streptomycin. Cells were plated in black 96-wells plates or 6-wells plates (Nunc, VWR Amsterdam, The Netherlands) and grown until near-confluence.

B. *HAS cell culture*

Human astrocytes were cultured at 37ºC, under 5% CO_2 in air in a medium consisted of Dulbecco's modified Eagle's medium (DMEM)-F10 (Gibco, Life Technologies, Breda, The Netherlands), supplemented with 10% v/v heat-inactivated fetal calf serum (FCS) (Gibco), 2 mM L-glutamine (Sigma-Aldrich), and 1% penicillin/streptomycin. Cells were plated in 96-well plates or 6-well plates (Nunc, VWR Amsterdam, The Netherlands) and grown until near-confluence.

C. *SH-SY5Y cell culture*

SH-SY5Y cells were cultured at 37ºC, under 5% CO_2 in air in a1:1mixture of Eagle's minimum essential medium and Ham's F12 nutrient mixture, containing 10% FBS, 2.5mM L-glutamine, 1/100 non-essential aminoacids and 1 mM sodium pyruvate. Cells were plated in 12-well plates (25,000 cells/cm^2). After 24h, the medium was removed and replaced by cell culture medium containing 3% FBS and 20 mM retinoic acid (RA) (Sigma). Six days after retinoic acid (RA) administration, cells were used for cellular TG2 activity measurements.

TG2 activity assay in cell/tissue extracts

Cell culture medium was removed and cells washed twice with cold phosphate buffered saline (PBS) and sonicated (Branson sonifier, Danbury, CT, USA) in 1.5 mL ice-cold homogenizing buffer (TBS containing a 1:1000 proportion of aprotinin, leupeptin and pepstatin-A protease inhibitors). The protein of lysates was determined using the BCA assay. TG2 titration for lysates were performed using the TG transamidation kit opr-0001 from Covalab R&D, (France, Lyon) following the manufacturers operational

procedure. Inhibitors assayed were prepared at 0.1 M in a 100% DMSO as stock solutions kept at -20ºC. Various concentrations of TG2 inhibitors herein synthesized (compound (**13**) and **Z006** (Zedira, GmbH) were used as references) or DMSO vehicle were added together with diluted protein lysates to the assay.

Cellular TG2 activity assay

For cellular TG2 activity measurements, incorporation of BAP into proteins was determined in SH-SY5Y cells, human astrocytes (HAS), and neurovascular smooth muscle cells (vSMCs) as described previously.[69] All cells incubation steps were performed at 37°C and under 5% CO_2 in air. Cells were washed once with phosphate buffered saline (PBS), and incubated thereafter for 4 h with culture media containing 1 mM BAP. Subsequently, without changing medium, the cells were preincubated for 30 min with the TG2 inhibitors (dissolved in dimethylsulfoxide (DMSO) as 0.1 mM stock solutions) prior to addition of 10 mM of the Ca2+ ionophore A23187 (Sigma) for 40 min, or, depending on the experiment. The cells were then carefully washed twice with cold PBS and sonicated (Branson sonifier, Danbury, CT, USA) in 400 µL ice-cold homogenizing buffer (50 mM Tris, 150 mM NaCl, pH 7.4, containing 1 mM EDTA, 0.1 mM phenylmethylsulphonyl fluoride (PMSF) and 1 µg/mL of aprotinin/pepstatin). The protein concentrations of the lysates were determined with the BCA assay and either immediately used for detection of TG2 activity, or stored at -20°C. The use of frozen samples did not affect any of the results in the following detection method (data not shown).

For detection of TG2 activity, 96-well Maxisorp plates were incubated with 50 µl of coating buffer (50 mM Tris, 150 mM NaCl, 5 mM EGTA, 5 mM EDTA, pH 7.4), followed by 1 µg of cell lysate and incubated overnight at 4ºC. After this step, 200 µL of incubation buffer (50 mM Tris-Cl, 80 mM NaCl, 2.5% BSA, 0.01% sodium dodecyl sulfate (SDS) and 0.01% Tween-20, pH 7.4) was added. Incubation was continued for 2 h at 37ºC. After this period, wells were washed three times with 200 µL washing buffer (50 mM Tris-Cl, 80 mM NaCl, 0.5% BSA, 0.01% Tween-20; pH 7.4), followed by incubation with 100 µl of 0.1 µg/ml streptavidin coupled to streptavidin conjugated poly-horseradish peroxidase (Poly-HRP, Sanquin), diluted in wash buffer over 1 hour at room temperature (RT). Subsequently, wells were washed three times with washing buffer and incubated in a 0.6 mg/mL OPD-solution (6 mg/mL OPD, 35 mM citric acid, 50 mM Na_2HPO_4, pH 5.0) containing 0.01% hydrogen peroxide for 30 min at RT. The reaction was stopped by adding 1 M H_2SO_4. Absorbance was measured on a microplate reader (SPECTRAmax250, Molecular Devices, USA) at a wavelength of 490 nm and was corrected for background, which was defined as the absorbance in cellular extracts obtained from experiments where BAP had been omitted from the culture medium.

Cell viability assays

A. *MTT toxicity test*

Under normal growth conditions, SH-SY5Y cells and vSMC cells were cultured in 96-well cell culture plates (Nunc). A final concentration of 0.5 mg/mL MTT was added to each well and was allowed to incubate for 45 min at 37ºC under 5% CO_2 in air. Thereafter, the medium was removed and replaced by 150 µL of DMSO to which 0.5% (v/v) FBS had been added. After formazan solubilization by vibration on a plate shaker, the absorbance of each well was measured at 540 nm using the SPECTRAmax 250 microplate reader. Absorbance data were calculated by subtracting the mean of background readings obtained from identical incubations in the absence of cells.

B. *SRB toxicity test*

Under normal growth conditions vSMC cells were cultured in 96-well plates (Nunc). Medium was removed and cells fixed with 25 µL of a cold 50% TCA solution in 200 µL culture medium. Plates were emptied and gently washed 5-times with water before incubation for 15 min with 50 µL of a 0.4% SRB solution at RT. Plates were again emptied, washed 4-times with 200 µL 1% acetic acid, and left to air dry for 3 h. After Addition of unbuffered 10 mM TRIS solution and homogenation, the plate was read at 540 nm. Absorbance data were calculated by subtracting the mean of background readings obtained from identical incubations in the absence of cells.

Bibliography - Chapter 5

178. van Strien, ME.; Brevé, J. J.; Fratantoni, S.; Schreurs, M. W.; Bol, J. G.; Jongenelen, C. A.; Drukarch, B.; van Dam, A. M. Astrocyte-derived tissue transglutaminase interacts with fibronectin: A role in astrocyte adhesion and migration? *PLoS One*. **2011**, *6*, e25037.

179. Blaise, R.; Mateo, V.; Rouxel, C.; Zaccarini, F.; Glorian, M.; Béréziat, G.; Golubkov, V. S.; Limon, I. Wild-type amyloid beta 1-40 peptide induces vascular smooth muscle cell death independently from matrix metalloprotease activity. *Aging Cell.* **2012**, *11*, 384-393.

180. Kanchan, K.; Ergülen, E.; Király, R.; Simon-Vecsei, Z.; Fuxreiter, M.; Fésüs, L. Identification of specific one amino acid change in recombinant human transglutaminase 2 in regulating its activity and calcium sensitivity. *Biochem. J.* **2013**, *455*, 261-272.

181. Kasugai, S.; Hasegawa, N.; Ogura, H. A simple in vito cytotoxicity test using the MTT (3-(4,5)-dimethylthiazol-2-yl)-2,5-diphenyl tetrazolium bromide) colorimetric assay: analysis of eugenol toxicity on dental pulp cells (RPC-C2A). *Jpn J. Pharmacol*. **1990**, *52*, 95-100.

182. Mosmann, T. Rapid colorimetric assay for cellular growth and survival: application to proliferation and cytotoxicity assays. *J. Immunol. Methods* **1983**, *65*, 55-63.

183. Vichai, V.; Kirtikara, K. Sulforhodamine B colorimetric assay for cytotoxicity screening. *Nat. Protoc*. **2006**, *1*, 1112-1116.

184. Zhang, J.; Lesort, M.; Guttmann, R. P.; Johnson G.V. Modulation of the in situ activity of tissue transglutaminase by calcium and GTP. *J. Biol. Chem*. **1998**, *273*, 2288-2295.

GENERAL CONCLUSION AND FUTURE PERSPECTIVES

General conclusion

A wide range of inhibitory compounds (naphthalene- indole-based compounds) have been successfully synthesized against tissue transglutaminase (TG2). These new TG2 inhibitors have been proved to inhibit TG2 cross-linking activity at the low nanomolar range, but also presenting a good selectivity profile against other transglutaminase isoforms tested (TG1, TG6 and FXIIIa).

Regarding activity over TG2 (IC_{50}), and within the same test conditions employed in this work, potencies reached in *in vitro* TG2 cross-linking assay measurements (Covalab R&D, Lyon, France) overcome those of the compounds employed as reference in this work (Compounds **X** and **EB1-155**), even presenting the same 4-amino piperidine-based warhead (as in the case of compound **X**). Improved IC_{50} values were as well observed in terms of IC_{50} for the different TG2 inhibition in tissue or cell extracts. The newly produced compounds also showed more efficacy on inhibiting TG2 in cell culture inhibition studies, also presenting no toxicity up to 10 μM of concentration in cell culture for two of the three cell lines studied.

Regarding the TG2 kinetic analysis, naphthalene **23b**, and indole **78f** inhibitors has been demonstrated to have an exponential time-dependent irreversible inactivation of TG2, demonstrating a high efficiency on inactivating TG2 (k_{inact}/K_I values over 100,000 M^{-1} min^{-1} for both inhibitors). Furthermore, both compounds showed better efficiency on TG2 inactivation (better k_{inact}/K_I), but also a better affinity for TG2 (K_I) than the reference compound **X** bearing the same 4-aminopiperidine warhead structure. Irreversible covalent modification of active site Cys277of TG2 by **23b** and **78f** was also demonstrated by LC-MS/MS analysis, thus confirming the irreversible mechanism of action found by enzymology.

Future perspectives

Owing to the improved activity over TG2 obtained by the indole-based compounds compared with the naphthalene-based compounds (retaining the same selectivity profile for other transglutaminases), a new perspective in the synthesis of new compounds can be glimpsed. As presented in **Figure 71** pharmacomodulation of the indolic core would be of interest in order to reach new drug candidates for inhibiting TG2.

As shown in **Figure 71**, different substitutions would be implemented at 4-, 5-, or 6-positions on indole (R_1). For example, the bromination can be performed on **78f** to

reach 6-bromo or 4,6-dibromo indole derivatives (work in progress). From the 6-bromo derivative, palladium coupling reactions (Stille, Suzuki-Miyaura, Heck and Sonogashira reactions), will provide a large set of 6-substituted 7-(arylamido)-1-methylindole derivatives.

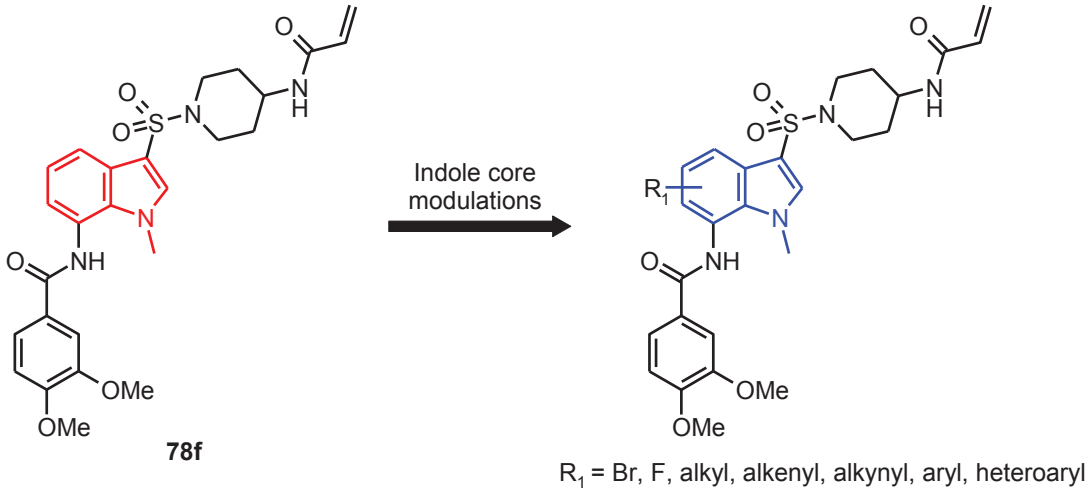

Figure 71. Schematic representation of the indole core pharmacomodulations based on the lead compound **78f**, where different substituents (R_1) could be introduced in order to obtain different substituted 7-(arylamido)-1-methylindole derivatives